Naval Command,
Control and Ocean
Surveillance Center RDT&E Division San Diego, CA
92152-5001

Technical Document 2891
December 1995

Proceedings of the Electromagnetic Propagation Workshop

R. Paulus

19960429 037

Approved for public release; distribution is unlimited.

DTIC QUALITY INSPECTED 1

DISCLAIMER NOTICE

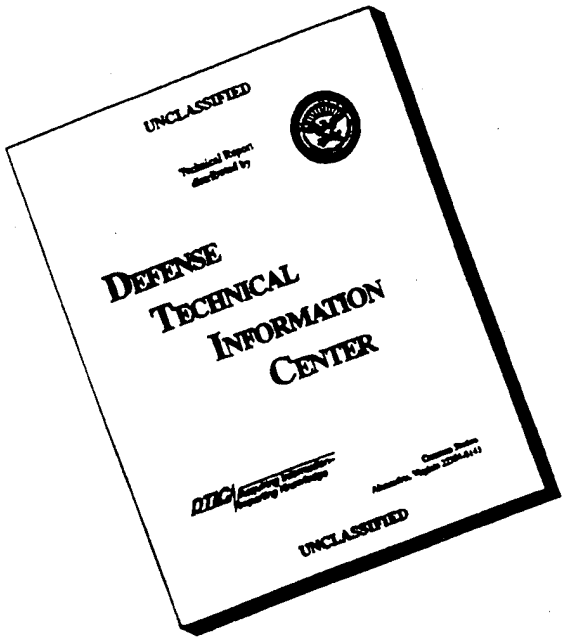

THIS DOCUMENT IS BEST QUALITY AVAILABLE. THE COPY FURNISHED TO DTIC CONTAINED A SIGNIFICANT NUMBER OF PAGES WHICH DO NOT REPRODUCE LEGIBLY.

Technical Document 2891
December 1995

Proceedings of the Electromagnetic Propagation Workshop

R. Paulus

NAVAL COMMAND, CONTROL AND OCEAN SURVEILLANCE CENTER
RDT&E DIVISION
San Diego, California 92152-5001

K. E. EVANS, CAPT, USN
Commanding Officer

R. T. SHEARER
Executive Director

ADMINISTRATIVE INFORMATION

The work detailed in this Proceedings of the Electromagnetic Propagation Workshop was compiled in response to interest by the Space and Naval Warfare Systems Command (PMW–175) and Naval Sea Systems Command (PED USW ASTD–E), and under the auspices of the Office of the Director, Defense Research and Engineering (ODDRE). The Workshop was organized by NRaD and hosted by Johns Hopkins University Applied Physics Laboratory. The computer data files of these exhibits are also approved for public release.

R. Paulus
Code 883

WFP

INTRODUCTION

In response to interest by the Space and Naval Warfare Systems Command (PMW-175) and Naval Sea Systems Command (PEO USW ASTO-E) and under the auspices of the Office of the Director, Defense Research and Engineering (ODDRE), an Electromagnetic Propagation Workshop was organized by NRaD and hosted by Johns Hopkins University Applied Physics Laboratory 18 to 20 July 1995. The workshop provided a forum to present and compare tropospheric electromagnetic propagation models and to examine the means to provide required environmental inputs, emphasizing military tactical applications in the 100 MHz to 20 GHz frequency range. The intent was to inform the military user community of current capabilities and provide a technical exchange between model developers. Topics specifically addressed at the workshop included:

- Service Perspective
- Operational Needs
- Direct/Remote Sensing of the Propagation Environment
- Meteorological models
- Refractive Variability
- Refractive Structure Characterization
- Propagation Models
- Sample Case Comparisons

The workshop attracted over 100 participants, including participation by all services and 6 allied countries.

This document is a compilation of workshop proceedings based on material supplied by the presenters. The workshop itself is an extension of previous conferences/symposia, including an ODDRE tri-service workshop [1], a conference on microwave propagation in the marine atmospheric boundary layer sponsored by the AEGIS Program Office of the Naval Sea Systems Command [2], recent conferences sponsored by NATO Advisory Group for Aerospace Research and Development (AGARD) [3-6], and a VHF/UHF community conference sponsored by the Naval Security Group [7].

The final pages of the Introduction provide information on the organization and attendance of the workshop. The proceedings is organized in the same manner as the agenda below. Session I is an overview of the DOD coordinated Technology Area for Battlespace Environments that includes the meteorological and electromagnetic (EM) propagation areas discussed in the workshop. Session II presents operational requirements for and applications of EM propagation assessment systems. Session III presents various means to provide the environmental input to the EM propagation models. Session IV describes the propagation models developed by several different researchers and Session V is a comparison of model outputs for 10 selected sample cases that are typically of interest for operational assessment. After each presentation, questions from the participants for the speaker are included. Session VI is a panel discussion

summarizing the workshop and discussing future directions by addressing three issues brought up in the course of the workshop:

- What features/characteristics are needed in an operational assessment system and how does that differ from a research system?
- Do models need to be improved?
- Are benchmarks needed?

REFERENCES

[1] "Proceedings of the Technical Exchange and Coordination Workshop on Environmental Support for C^2I/Tactical Decision Aids," Naval Ocean Systems Center Technical Document 780, January 1985.

[2] "Proceedings: Conference on Microwave Propagation in the Marine Boundary Layer," Naval Environmental Prediction Research Facility Technical Report TR 89-02, January 1989

[3] "Operational Decision Aids for Exploiting or Mitigating Electromagnetic Propagation Effects," AGARD CP 453, September 1989.

[4] "Remote Sensing of the Propagation Environment," AGARD CP 502, February 1992.

[5] "Multiple Mechanism Propagation Paths (MMPPs): Their Characterization and Influence on System Design," AGARD CP 543, July 1994.

[6] "Propagation Assessment in Coastal Environments," AGARD CP 567, February 1995.

[7] "Beyond Line-of-Sight Conference," University of Texas Applied Research Laboratories, August 1994.

OFFICE OF THE DIRECTOR OF
DEFENSE RESEARCH AND ENGINEERING
WASHINGTON, DC 20301-3030

April 25, 1995

MEMORANDUM FOR CHIEF OF STAFF OF THE ARMY (DAMI-POI)
CHIEF OF NAVAL OPERATIONS (N096)
CHIEF OF STAFF OF THE AIR FORCE (AF/XOW)

SUBJECT: Electromagnetic Propagation Workshop

As presented to me by CDR Dave Markham, PMW-175, I fully endorse the plans to conduct a tri-service workshop during 18-20 July to inform the military user community of our current capabilities in electromagnetic propagation assessment relevant to military tactical applications.

The unclassified workshop being organized by the Naval Command, Control and Ocean Surveillance Center's Research, Development, Test and Evaluation Division is an important undertaking because of the recent shift in military emphasis to regional conflicts and joint operations in the littoral. Hosting the workshop at the Johns Hopkins University Applied Physics Laboratory in nearby Laurel, Maryland will allow full participation by Washington-based headquarters and systems command staff. I also expect participation by some NATO country scientists, engineers, and military personnel. I encourage wide dissemination of the attached announcement.

Bradley P. Smith
Captain, U.S. Navy
Assistant for Enviromental Sciences

cc: RADM Gaffney, CNMOC
COL Misciasci, AWS

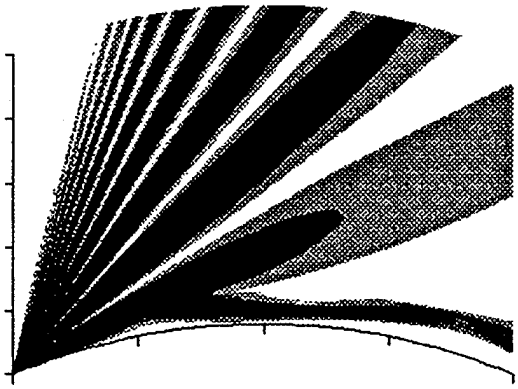

ELECTROMAGNETIC PROPAGATION WORKSHOP
July 18-20, 1995

Sponsored by
Office of the Director, Defense Research and Engineering

Cosponsored by:
Space and Naval Warfare Systems Command
Naval Sea Systems Command

Organized by:
Naval Command, Control and Ocean Surveillance Center
Research, Development, Test and Evaluation Division
San Diego, California

Hosted by:
Johns Hopkins University
Applied Physics Laboratory
Laurel, Maryland

This workshop will provide a forum to present and compare tropospheric EM propagation models and the means to provide the required environmental inputs, emphasizing military tactical applications in the 100 MHz to 20 GHz frequency range. The intent is to inform the military user community of current capabilities and provide a technical exchange between model developers. The workshop will examine propagation mechanisms (multipath, diffraction, tropospheric scatter, ducting), effects of antenna patterns, polarization, surface roughness, and variable terrain, and the means to provide the refractive input data. Specific topics include:

- Service Perspective
- Operational Needs
- Direct/Remote Sensing of the Propagation Environment
- Meteorological models
- Refractive Variability
- Refractive Structure Characterization
- Propagation Models
- Sample Case Comparisons

Participation by all services and interested NATO countries is encouraged; the workshop is unclassified. Submit abstracts (1-3 pages) for prospective presentations by 15 May and include **Title, Author(s) Name, Address, Telephone Number, and E-mail Address**. Presenters will be requested to provide reproducible black and white copies of their presentation graphics for inclusion in a workshop proceedings. In addition, EM propagation model presentations require electronic submission of model output results for at least 1 sample case, a summary of which is attached.

For further information or submission of abstracts **(by 15 May)** contact:

R PAULUS
NCCOSC RDTE DIV 543
49170 PROPAGATION PATH
SAN DIEGO CA 92152-7385

email: paulus@nosc.mil
voice: (619) 553-1424
fax: (619) 553-1417
DSN prefix: 553-

SYNOPSIS OF SAMPLE CASES

The following 10 sample cases will be used to compare the various models presented at the workshop. These cases are not benchmarks, and the models will not be ranked or graded based on the results presented. All cases assume an omnidirectional antenna, a smooth sea and horizontal polarization unless otherwise stated. The last 4 cases include a real mixed sea and terrain path with heights up to 244 m. Hard copies of coverage diagrams are desired. ASCII files of one-way propagation factor versus receiver height, range, or time of assessment are required for one or more cases, to be supplied by 15 June, 1995. A complete description of the sample cases is available from the workshop organizers.

Sample Case 1.
The environment is a strong surface-based duct, frequency is 3 GHz, transmitter antenna height is 25 m, and polarization is vertical. Receiver heights to 5 km and ranges to 250 km are required.

Sample Case 2.
The environment is a 13 m evaporation duct, frequency is 10 GHz, and the transmitter antenna is 25 m above the sea. The antenna pattern is a "sin(x)/x" pattern with a beamwidth of 2 degrees and an elevation angle of 1 degree. Receiver heights to 100 m and ranges to 100 km are required.

Sample Case 3.
The environment is a 20 m evaporation duct over a wind-roughened sea surface. The frequency is 10 GHz and the transmitter height is 25 m above the sea. The wind speed is 10 m/s. Receiver heights to 100 m and ranges to 100 km are required.

Sample Case 4.
The environment is a range-dependent surface-based duct that rises to a low elevated duct. The frequency is 3300 MHz and the transmitter antenna height is 30 m above sea level. Receiver heights to 1000 m and ranges to 200 km are required.

Sample Case 5.
The environment is a combined surface-based and elevated duct. Frequency is 450 MHz and the transmitter antenna height is 9 km. Receiver heights to 10 km and ranges to 400 km are required.

Sample Case 6.
Same environment as Case 1. The frequency is 10 GHz and the transmitter antenna is 1000 m above the sea. Receiver heights to 1500 m and ranges to 100 km are required.

Sample Case 7.
Same environment as Case 1, but over terrain. Frequency is 10 GHz and transmitter antenna is 1000 m above sea level. Receiver heights to 1500 m and ranges to 100 km are required.

Sample Case 8.
Environment is a standard atmosphere over the terrain path. Frequency is 3 GHz and transmitter antenna is 10 m above local terrain. Receiver heights to 500 m and ranges to 100 km are required.

Sample Case 9.
Same environment as Case 1, but over terrain. Frequency is 3 GHz and transmitter antenna is 10 m above local terrain. Receiver heights to 500 m and ranges to 100 km are required.

Sample Case 10.
Environments are 43 measured refractivity profiles over 10 days over the terrain path. Frequency is 127.75 MHz, the polarization is vertical, the transmitter antenna is 9.1 m above local ground level, and the receiver antenna is 30.5 m above mean sea level. Range is 100.35 km.

EM PROPAGATION WORKSHOP ATTENDANCE LIST
PARSONS AUDITORIUM
JULY 18-20, 1995

Dave Alessio
Naval Research Laboratory
Code 5330
Washington, DC 20375-5336
Tel: (202) 767-1362
Fax: (202) 767-6172
alessio@radar.nrl.navy.mil

Kenneth Anderson
NCCOSC RDTE DIV 543
53560 Hull St
San Diego CA 92152-5001
Tel: (619) 553-1420
Fax: (619) 553-1417
kenn@nosc.mil

CDR H. G. Bancroft III, US Navy
Deputy Chief, METOC Branch (SOJ3-OW)
HQ US Special Operations Command
7701 Tampa Point Blvd
MacDill AFB, FL 33621-5323
Tel/Fax: (813) 828-2519
bancrohj@hqsocom.af.mil

Amalia Barrios
NCCOSC RDTE DIV 543
53560 Hull St
San Diego CA 92152-5001
Tel: (619) 553-1429
Fax: (619) 553-1417
barrios@nosc.mil

David F. Bassett
Army Research Laboratory
Survivability/Lethality Analysis Directorate
Aberdeen Proving Ground, MD 21005-5068
AMSRL-SL-1
Bldg 433
Tel: (410) 278-8624
Fax: (410) 278-7254
dbassett@arl.mil

1LT Giancarlo E. Bautista
Air Force Information Warfare Center
102 Hall Blvd Ste 342
San Antonio, TX 78243-7020
Tel: (210) 977-2706
Fax: (210) 977-2145

Tom Bell
Naval Weapons Center
Code 418200D (C2186)
NAWCWPNS/CL
China Lake, CA
Tel: (619) 927-1250
Fax: (619) 939-2062
bellt@scfe.chinalake.navy.mil

Melvin Benham
NSWC/DD
Tel: (540) 663-7893

David W. Blood
Applied Research Laboratory, Penn State University
PO Box 330, State College, PA 16804
Tel: (814) 863-9916
Fax: (814) 863-8783

Donald Boyer
Naval Surface Warfare Center
Dahlgren Division
Code N24
17320 Dahlgren Road
Dahlgren, VA 22448-5100
Tel: (703)663-1908
Fax: (703)663-1221
dboyer@relay.nswc.navy.mil

James K. Breakall
Applied Research Lab
PO Box 30
State College, PA 16804
Tel: (814) 863-8600
Fax: (814) 863-8783
jkb@arlvax.arl.psu.edu

John Briski
IIT Research Institute
185 Admiral Cochrane Drive
Annapolis, MD 21401
Tel: (410) 573-7742
Fax: (410) 573-7760

Charles B. Brooks
Naval Research Laboratory
Code 5707
4555 Overlook Ave., SW
Washington, DC 20375-5339
Tel: (202) 767-2133
Fax: (202) 767-6767

Dr. Stephen Burk
Naval Research Laboratory
Marine Meteorology Division
Monterey, CA 93943-5502
Tel: (408) 656-4797
Fax: (408) 656-4769
burk@nrlmry.navy.mil

Gary Bust
Applied Research Laboratories the University of Texas at Austin
PO Box 8029
Austin, TX 78713-8029
Tel: (512) 835-3623
Fax: (512) 835-3808
gbust@arlut.utexas.edu

John Campbell
Naval Research Laboratory
Stennis Space Center, MS
Tel: (601) 688-5440
Fax: (601) 688-5049

Robert W. Chiu
USARL/SLAD/EWD
AMSRL-SL-EM
White Sands Missile Range, NM 88002-5513
Tel: (505) 678-5238
Fax: (505) 678-6172
rchiu@arl.mil

Clair Chua
Naval Research Laboratory
Effectiveness of Naval Electronic Warfare Systems
Washington, DC 20375
Tel: (202) 767-2483
Fax: (202) 767-6767
chua@enews.nrl.navy.mil

Chris Diamond
Naval Oceanographic Office
ATTN: Code N541
1002 Balch Blvd
Stennis Space Ctr., MS 39522-5001
Tel: (601) 688-5895
Fax: (601) 688-4569

Dalcio K. Dacol
Naval Research Laboratory
Code 7145
Washington, DC 2035-5350
Rel: (202) 767-3173
dacol@abyss.nrl.navy.mil

Kenneth L. Davidson
Department of Meteorology
589 Dyer Road, Room 254
Naval Postgraduate School
Monterey, CA 93934-5114
Tel: (408) 656-2563
Fax: (408) 656-3061
davidson@nps.navy.mil

L. Samuel Ditman
Naval Surface Warfare Center, White Oak
Code B42
10,901 New Hampshire Ave
Silver Spring, MD 20903-5000
Tel: (301) 394-3458
Fax: (301) 394-4657

John C. Eidson
MIT Lincoln Laboratory
244 Wood Street
Lexington, MA 02173-9108
Tel: (617) 981-3520
Fax: (617) 981-6095

David L. Eppink
JSC/IITRI
185 Admiral Cochrane Drive
Annapolis, MD 21401
Tel: (410) 573-7599
Fax: (410) 573-7760

Dr. Stephen Fast
The Applied Research Laboratories at the University of Texas-Austin
PO Box 8029, Austin, TX 78713-8029
Tel: (512) 835-3034
Fax: (512) 835-3100

Greg Gentry
Estimation and Signal Processing Group
Systems Research and Technology Department
Naval Surface Warfare Center
Dahlgren Division
Code B32
17320 Dahlgren Road
Dahlgren, VA 22448-5100
Tel: (703) 663-6464
Fax: (703) 663-6468
ggentry@godsend.nswc.navy.mi

Dr. Edward Harrison (CAPT, USN(Ret))
Computer Sciences Corporation
AP #2, Suite 4000
2611 Jefferson Davis Highway
Arlington, VA 22202-4016
Tel: (703) 418-8534
Fax: (703) 418-4972

Claude Hattan
NCCOSC RDTE DIV 543
53560 Hull St
San Diego CA 92152-5001
Tel: (619) 553-1427
Fax: (619) 553-1417
hattan@nosc.mil

Roger A. Helvey
Naval Air Warfare Center Weapons Division
521 9th Street
Point Mugu, CA 93042-5001
Tel: (805) 989-8383
Fax: (805) 989-4817

Herbert Hitney
NCCOSC RDTE DIV 543
53560 Hull St
San Diego CA 92152-5001
Tel: (619) 553-1428
Fax: (619) 553-1417
herb@nosc.mil

Julie A. Huffman
Appied Research Laboratory
PO Box 30
State College, PA 16804
Tel: (814) 865-7312
Fax: (814) 863-8783

Giuseppe Izzi
Naval Undersea Warfare Center Division
1176 Howell Street
Newport RI 02841-1708
Tel: (401) 841-3952
Fax: (401) 841-1315

Prof. Ramakrishna Janaswamy
Code EC/Js
NAVAL POSTGRADUATE SCHOOL
Monterey CA 93943
Tel: (408) 656-3217
Fax: (408) 656-2760
janaswam@nps.navy.mil

David G. Kenney
ITT Research Institute
185 Admiral Cochrane Dr.
Annapolis, MD 21401
Tel: (410) 573-7371
Fax: (410) 573-7344

Phil Kerr
DoD Joint Spectrum Center (JSC)
120 Worthington Basin
Annapolis, MD 21402-5064
Tel: (410) 293-2556
Fax: (410) 293-2631

Glenn Kronschnabl
Applied Research Laboratories the University of Texas at Austin
PO Box 8029
Austin, TX 78713-8029
Tel: (512) 835-3623
Fax: (512) 835-3808

H. Sang Lee
Science & Engineering Services, Inc.
4014 Blackburn Lane
Burtonsville, MD 20866
Tel: (301) 989-1896
Fax: (301) 421-4137

Dr. Menachem Levitas
Technology Service Corporation
Washington Division
962 Wayne Ave
Silver Spring, MD 20910
Tel: (301) 565-2970
Fax: (301) 565-0673

Daniel B. Lysak
Applied Research Laboratory, Penn State University
PO Box 330, State College, PA 16804
Tel: (814) 863-7773
Fax: (814) 863-8783

Keith A. Lysiak
Applied Research Lab
PO Box 30
State College, PA 16804
Tel: (814) 863-7303
Fax: (814) 863-8783

CDR David G. Markham, USN
COMSPAWARSYSCOM (PMW 175)
Crystal Park #5, Suite 301
2451 Crystal Drive
Arlington, VA 22245-5200
Tel: (703) 602-7039
Fax: (703) 602-1535

Lee U. Martin
Code 5348
Naval Research Laboratory
Washington, DC 20375-5320
Tel: (202) 404-8844
Fax: (202) 404-8687

Diana McCammon
Applied Research Laboratory
Pennsylvania State University
State College, PA 16804
Tel: (814) 863-4159
Fax: (814) 863-8783

William McIntrye
Effectiveness of Naval Electronics Warfare Systems (ENEWS)
Naval Research Laboratory
4555 Overlook Ave SW
Washington, DC 20376
Tel: (202) 767-2897
Fax: (202) 767-6767
mac@enews.nrl.navy.mil

CDR Denis M. Meanor
Chief of Naval Operations (N096)
3450 Massachusetts Ave., NW
US Naval Observatory Bldg 1
Washington, DC 20392-5421

Richard Meidenbauer
IITRI
185 Admiral Cochrane Drive
Annapolis, MD 21401
Tel: (410) 573-7500
Fax: (410) 573-7634

Scott E. Metker
Appied Research Laboratory
PO Box 30
State College, PA 16804
Tel: (814) 865-7312
Fax: (814) 863-8783

Walter Dale Meyer
Headquarters Air Weather Service/XOXT
102 West Losey Street, Room 105
Scott AFB, IL 62225-5206
Tel: (618) 256-5631 ext 444
Fax: (618) 256-6306
meyerw@hqaws.safb.af.mil

LT David Milot
NAVLANTMETOCCEN
9141 Third Ave
Norfolk, VA 23511-2394
Tel: (804) 444-3770
Fax: (804) 444-4479

Eric L. Mokole (Code 5340)
Naval Research Laboratory
4555 Overlook Ave., SW
Washington, DC 20375-5336
Tel: (202) 404-8844
Fax: (202) 404-8687

Anthony Notari
Science & Engineering Services, Inc.
4014 Blackburn Lane
Burtonsville, MD 20866
Tel: (301) 989-1896
Fax: (301) 421-4137

Richard Paulus
NCCOSC RDTE DIV 543
53560 Hull St
San Diego CA 92152-5001
Tel: (619) 553-1424
Fax: (619) 553-1417
paulus@nosc.mil

Michael J. Pastore
Integrated Performance Decisions (IPD)
60 Garden Ct. Road
Suite 210
Monterey, CA 93940
Tel: (408) 375-2729
Fax: (408) 375-2707
pastore@cc.atinc.com

Wayne Patterson
Office of Naval Research ONR 322AM
800 North Quincy St.
Arlington VA 22217-5660
Tel: (703) 696-7042
Fax: (703) 696-3390
patterw@onrhq.onr.navy.mil

Steven W. Payne
Naval Research Laboratory
Marine Meteorology Division
7 Grace Hopper Avenue
Monterey, CA 93943-5502
Tel: (408) 656-4758
Fax: (408) 656-4314

Mary Peters
Naval Research Laboratory
Code 7420
4555 Overlook Ave SW
Washington, DC 20375-5350
Tel: (202) 767-2024
Fax: (202 767-0167
mary.peters@nrl.navy.mil

C. Russell Philbrick
Applied Research Laboratory, Penn State University
PO Box 330, State College, PA 16804
Tel: (814) 863-7682
Fax: (814) 863-8783

Timothy Politowicz
Naval Research Laboratory
Code 8124
4555 Overlook Avenue
Washington, DC 20375-5354
Tel: (202) 767-1998
Fax: (202) 767-6611

James R. Rapp
Director
US Army Research Laboratory
ATTTN: AMSRL-WT-WE
Aberdeen Proving Ground, MD 21005-5066
Tel: (410) 278-3156
Fax: (410) 278-9078

Dr. Juergen Richter
NCCOSC RDTE DIV 54
53560 Hull St
San Diego CA 92152-5001
Tel: (619) 553-3053
Fax: (619) 553-3058
richter@nosc.mil

Homer L. Riggins
JSC/IITRI
185 Admiral Cochrane Drive
Annapolis, MD 21401
Tel: (410) 573-7555
Fax: (410) 573-7760

Ted Rogers
NCCOSC RDTE DIV 543
53560 Hull St
San Diego CA 92152-5001
Tel: (619) 553-1424
Fax: (619) 553-1417
trogers@nosc.mil

Jay S. Rosenthal
Naval Air Warfare Center Weapons Division
521 9th Street
Point Mugu, CA 93042-5001
Tel: (805) 989-7893
Fax: (805) 989-4817

Frank Ryan
NCCOSC RDTE Div.
53560 Hull Street
San Diego, CA 92152-5001
Tel: (619) 553-3099
Fax: (619) 553-4317

S. N. Samaddar (Code 5340)
Naval Research Laboratory
4555 Overlook Ave., SW
Washington, DC 20375-5336
Tel: (202) 404-8844
Fax: (202) 404-8687

Lauree R. Shampine
MIT Lincoln Laboratory
244 Wood Street
Lexington, MA 02173-9108
Tel: (617) 981-2516
Fax: (617) 981-2780

Dr. William J. Stachnik
Office of Naval Research
800 North Qunicy Street
Arlington, VA 22217-5660
Tel: (703) 696-1438
Fax: (703) 696-1331/2611

Janet Stapleton
NSWC/DD Code F42
Dahlgren, VA 22448
Tel: (703) 663-4018
Fax: (703) 663-7419

William T. Thompson
Naval Research Laboratory
Marine Meteorology Division
7 Grace Hopper Ave.
Monterey, CA 93943
Tel: (408) 656-4733
Fax: (408) 656-4769
thompson@nrlmry.navy.mil

Paul R. Tiedeman, PEO(USW)ASTO-E
2531 Jefferson Davis Highway
Arlington, VA 22242-5169
Tel: (202) 602-3087 ext.460
Fax: (202) 602-5152

Dr. Matthew J. Vanderhill
MIT/Lincoln Laboratory
244 Wood Street
Lexington, MA 02173-9108
Tel: (617) 981-2854
Fax: (617) 981-2780

Mel Wagstaff
Planning Systems Incorporated PSI
PSI Science Center
115 Christian Lane
Slidell, LA 70458
Tel: (504) 649-0450
Fax: (504) 649-0480
STU: (504) 649-5978

Dr. John Walters
Naval Research Laboratory
Code 5330
Washington, DC 20375-5336
Tel: (202) 767-1362
Fax: (202) 767-6172

Douglas H. Werner
Applied Research Lab
PO Box 30
State College, PA 16804
Tel: (814) 863-7187
Fax: (814) 863-8783
dhw@arlvax.arl.psu.edu

Thomas M. Willey
Department of Defense
Joint Spectrum Center
120 Worthington Basin
Annapolis, MD 21402-5064
Tel: (410) 293-2326
Fax: (410) 293-9809
willey@jsc.mil

Dave Williams
Naval Undersea Warfare Center
Naval Undersea Warfare Center Detachment
ATTN: Code 61, D. Williams
New London, CT 06320
Tel: (202) 440-4384
Fax: (202) 440-6099

LCDR Zdenka S. Willis, USN
COMNAVAIRSYSCOM (AIR-4.5M)
1421 Jefferson Davis Highway
Arlington, VA 22243-5120

D. Keith Wilson
Penn State, Dept of Meteorology
503 Walker Bldg.,
University Park, PA 16801
Tel: (814) 865-3533
Fax: (814) 865-3663

Matthew T. Woitowicz, Mail Stop 127-106
Lockheed Martin-Government Electronic Systems
199 Borton Landing Road
PO Box 1027,
Moorestown, NJ 08057-3075
Tel: (609) 722-4752
Fax: (609) 722-4888
mwoitowi@motown.ge.com

LCDR James Zmyslo, USN
Naval Information Warfare Activity
3801 Nebraska Ave., NW
Washington, DC 20393
Tel: (202) 764-0604
Fax: (202) 764-0329

APL Personnel:
Johns Hopkins University Applied Physics Laboratory
Johns Hopkins Road
Laurel, MD 20723

Phone (301) 953-5000

Name	Extension
Lee Dantzler	5387
Don A Day	5465
Dan Dockery	5461
Dennis Donahue	6258
Pete Econ	5612
Richard Farrell	6229
David Freund	6260
Richard Giannola	5964
Julius Goldhirsh	5042
Gerry Konstanzer	7518
James Kuttler	6222
Morris London	4309
Dennis Moy	4715
Fred Newman	5075
Alfred Randall	8285
John Rowland	8660
Russ Rzemien	8924
Bob Spangler	6955
Basil Stoyanov	6261
Al Tomko	7568
Gregg Tornatore	6366
Mike Thomas	4414

FOREIGN VISITORS

CDR Simon Bevan -Royal Navy
SOIN3(METOC)
Commander in Chief Fleet Staff
Eastbury Park
Northwood
MIDDX, HA63HP
UNITED KINGDOM
Tel: UK 01923-837360
Fax: UK 01923-837455
Fleet@Fwoc.demon.co.uk.

Dr. Gary H. Brooke
Numerical Decisions Group, Inc
947 Fort St. Suite 8A
Victoria, BC Canada V8V 3K3
Tel: (604) 380-7983
Fax: (604) 380-7249

Dr K.H. Craig
Rutherford Appleton Laboratory
Chilton
Didcot
OX11 0QX
U.K.
Tel: +44 1235 445134
Fax: +44 1235 446140
ken.craig@rl.ac.uk

Catherine Giannilevigne
Ministere de la Defense
Delegation Generale pour l'Armement
Direction des Constructions Navales
Center technique des Systemes
Navals:DGA/DCN/CTSN/LSA/RAD
BP 28
83800 TOULON Naval - FRANCE
Tel: (33) 94 11 40 47 or (33) 94 96 88 44
Fax: (33) 94 06 88 69

Michael Kindler
IABG
EinsteinstraBe 20
85521 Ottobrunn
Germany
Tel: +49 89-6088-2666
Fax: +49 89-6088-3992

Dr Mireille F. Levy
Signal Science Ltd and Rutherford Appleton Laboratory
Chilton, Didcot, Oxfordshire OX11 0QX, U.K.
Tel: +44 1235 446522
Fax: +44 1235446140
m.levy@rl.ac.uk

FOREIGN VISITORS cont'd

Mr. David Lewis -Staff of CINCFLEET
SOIN3(METOC)
Commander in Chief Fleet Staff
Eastbury Park
Northwood
MIDDX, HA63HP
UNITED KINGDOM
Tel: UK 01923-837360
Fax: UK 01923-837455
Fleet@Fwoc.demon.co.uk.

Eric Mandine
Universite de TOULON
Laboratorie Modelisation et
Signal/ETMA/MNC
BP 132 - 83957 LA GARDE - FRANCE
Tel: (33) 94 14 24 80-
Fax: (33) 94 14 24 48
mcpel@isitv.fr

Sherman Marcus
RAFAEL
Dept. 88
P.O. Box 2250
Haifa, Israel
Tel: 972-4-229387
Fax: 972-4-794875

M. H. Vogel
TNO Physics and Electronics Laboratory
Oude Waelsdorperweg 63
PO Box 96864
2509 JG The Hague
The Netherlands
Tel: 070 326 42 21
Fax: 070 328 09 61

Electromagnetic Propagation Workshop

Parsons Auditorium, Building 1
Johns Hopkins University Applied Physics Laboratory

18 July 1995
0800-0830 Check-in and Registration
0830-0845 Welcoming Remarks - Dr. G. Smith, JHU/APL
0845-0915 Keynote Address/Introduction - CAPT B. Smith, OSD/DDR&E
0915-0930 Administrative Remarks

0930-1000 Session I. Overview

0930-1000 Richter, J.H., "Technology Area Plan for Battlespace Environments - Atmospheric Effects"
1000-1020 Break

1020-1600 Session II. Operational Requirements and Applications

Chair: CDR Dave Markham, SPAWAR PMW-175

1020-1040 Meanor, D., CDR, Navy and Marine Corps Requirements
1040-1100 Brown, D.R., Army Requirements
1100-1120 Robinson, C., LCOL, Joint Spectrum Center Brief
1120-1140 Bevan, S.,CDR, "The Development of an Environmental Electromagnetic Modelling System (EEMS) for the UK Royal Navy"
1140-1200 Craig, K.H. and M.F. Levy, "The UK Environmental EM Modelling System (EEMS)"
1200-1300 Lunch
1300-1320 Konstanzer, G.C., "SEAWASP AN/SPY-1B Tactical Decision Aid"
1320-1340 Vogel, M.H., "Decision Tool for Optimal Deployment of Radar Systems"
1340-1400 Lott, G.K., CDR, S.E. Paluszek, D. Brant, "RF Mission Planner"
1400-1420 Markham, D.G., CDR, "Navy METOC Systems"
1420-1440 Tiedeman, P.R., "SPP ADM"
1440-1500 Break
1500-1520 Lin, C.C. and J.P. Reilly, "Application of Propagation Models to Terrain Clutter and Target Masking Viewed by a Shipboard Radar"
1520-1540 Marcus, S.W., "Backscatter from Parabolic Equations: Fact or Fantasy"
1540-1600 Meyer, D., Air Force Requirements

19 July 1995

0800-1200 Session III. Environmental Inputs for Propagation Models

Chair: Dr. Steve Burk, NRL Monterey

0800-0820 Rogers, L.T., "Effects of the Variability of Atmospheric Refractivity"
0820-0840 Burk, S.D. and W.T. Thompson, "Modeling Mesoscale Refractivity Structure During the VOCAR Experiment"
0840-0900 Thompson, W.T. and S.D. Burk, "Variations in Atmospheric Refractivity Induced by Coastal Mesoscale Processes"
0900-0920 Rogers, L.T., "Radio Remote Sensing of Refractivity by Combinatorial Optimization"
0920-0940 Boyer, D.D., F.J. Ryan, and G. Gentry, "Remote Environmental Sensing Techniques Based on Inverse Scattering of Electromagnetic Waves"
0940-1000 Anderson, K.D., "The GPS Sounder - A Technique to Infer Tropospheric Refractivity Profiles from Low Elevation Angle Measurements of GPS Signals"
1000-1020 Break
1020-1040 Philbrick, C.R. and D.B. Lysak, Jr., "Lidar Atmospheric Profile Sensor (LAPS): Remote Sensing of Atmospheric Properties"
1040-1100 Blood, D.W., "Measurements of Tropospheric Refractivity Provide Environmental Input to EM Wave Propagation Analysis/Prediction"
1100-1120 Rowland, J.R., "SEAWASP Automated Environmental Assessment Instrumentation"
1120-1140 Davidson, K.L. and C.H. Wash, "Shipboard and Satellite Sensing of Refractive Conditions"
1140-1200 Helvey, R.A., "Persistence of Refractive Layering in Isentropic Coordinates"
1200-1300 Lunch

1300-1640 Session IV. EM Propagation Model Descriptions

Chair: Dr. Ken Craig, Signal Science Ltd and RAL, UK

1300-1320 Hattan,C.P., "Standard EM Propagation Model"
1320-1340 Anderson, K.D., "MLAYER, A Multilayer Waveguide Computer Program for Propagation Analysis"
1340-1400 Dockery, G.D., "Description of the Tropospheric Electromagnetic Parabolic Equation Routine (TEMPER)
1400-1420 Kuttler, J.R. and G.D. Dockery, "Description and Performance of a New Impedance Boundary Algorithm in TEMPER"
1420-1440 Hitney, H.V., "Radio Physical Optics Model"
1440-1500 Break
1500-1520 Eppink, D. and H. Riggins, "Propagation Analysis Using TIREM"
1520-1540 Barrios, A.E., "Capabilities and Limitations of the Terrain Parabolic Equation Model (TPEM)"

1540-1600 Ryan, F.J., "VTRPE: A Variable Terrain Electromagnetic Propagation Model for Littoral Environments"
1600-1620 Levy, M.F. and K.H. Craig, "The EEMS Hybrid PE Models for Fast Propagation Assessment"
1620-1640 Marcus, S.W., "The IFDG Package for Propagation Predictions in an Inhomogeneous Troposphere over Irregular Terrain"

20 July 1995

0800-0840 Session IV. EM Propagation Model Descriptions (cont)

0800-0820 Mandine, E., M.C. Pelissier, and C. Giannilevigne, "Radar Propagation in a Turbulent Atmosphere: A Random Profiles Generator"
0820-0840 Kenney, D.G., "Accelerated-Intermediate-Region Propagation Model"

0840-1150 Session V. Propagation Sample Cases

Chairman: Dr. Gary Brooke, NDG, Canada

0840-0900 Brooke, G.H. and E.S. Holmes, "Towards Benchmark Solutions for EM Tropospheric Propagation Problems"
0900-0920 Fast, S.A., "A Comparison of Electromagnetic Wave Propagation Software Using Standard Terrain Cases"
0920-1150 Sample Case Comparisons
1150-1300 Lunch

1300-1430 Session VI. Summary and Future Directions

Panel: CDR Dave Markham, Paul Tiedeman, Gary Brooke, Steve Burk, Jim Kuttler, and Rich Paulus

SESSION I. OVERVIEW

"Technology Area Plan for Battlespace Environments"

Dr. Juergen Richter
NCCOSC RDTE DIV 54
53560 Hull St
San Diego CA 92152-5001
Tel: (619) 553-3053
Fax: (619) 553-3058
richter@nosc.mil

Science and Technology Program
Technical Review

BATTLESPACE ENVIRONMENTS TECHNOLOGY AREA

ATMOSPHERIC EFFECTS TECHNOLOGY EFFORT

21 June 1995

Dr. Juergen Richter
U.S. Naval Command, Control & Ocean Surveillance Center

Code54 — Ocean & Atmospheric Sciences Division

OUTLINE

- TAXONOMY
- BACKGROUND
- TECHNOLOGY OBJECTIVES
- ACCOMPLISHMENTS
- PLANS
- SUMMARY

TAXONOMY

Sub-Area: Lower Atmosphere Environment
Technology Effort: Atmospheric Effects
POC: Dr. Juergen Richter (619) 553-3053

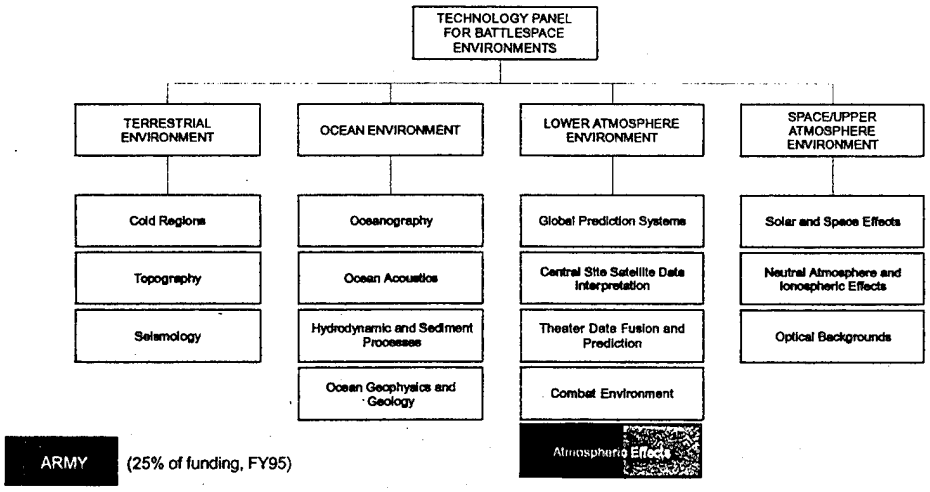

ARMY (25% of funding, FY95)

NAVY (31% of funding, FY95)

AIR FORCE (44% of funding, FY95)

BACKGROUND

Sub-Area: Lower Atmosphere Environment
Technical Effort: Atmospheric Effects
POC: Dr. Juergen Richter (619) 553-3053

- For **systems affected by the lower atmosphere**, provide ***real time*** assessment for operational use, and a ***simulation*** capability for planning, training and development
- Principal Performers:
  - ARL
  - NCCOSC
  - PL/GP
- Primary Customers:
  - CECOM, DMSO
  - Naval Meteorology and Oceanography Command, Space and Naval Warfare Systems Command
  - Air Combat Command, AWS, Space and Missile Center, Electronic Systems Center
- FY94 - In-House: 42%
  - Contract: 58%

TECHNOLOGY OBJECTIVES

Sub-Area: Lower Atmosphere Environment
Technical Effort: Atmospheric Effects
POC: Dr. Juergen Richter (619) 553-3053

- **EM/EO/ACOUSTIC PROPAGATION MODELS**
- **TACTICAL DECISION AIDS**
- **SENSING TECHNIQUES**
- **SIMULATION**

ACCOMPLISHMENTS

Sub-Area: Lower Atmosphere Environment
Technical Effort: Atmospheric Effects
POC: Dr. Juergen Richter (619) 553-3053

- **EM/EO/ACOUSTIC PROPAGATION**
  - *ACOUSTIC MODELS AND VALIDATION*
  - *EM PROPAGATION MODELS*
  - *EO TRANSMISSION AND RADIANCE MODELS*
- **TACTICAL DECISION AIDS**
  - *IWEDA, WIDA, ACT/EOS, EOTDA*
- **REMOTE SENSING**
  - *GPS, VOCAR, BALLISTIC WINDS*
- **SIMULATION**
  - *CSSM, VISIBILITY, BEAMS, SMOKE*

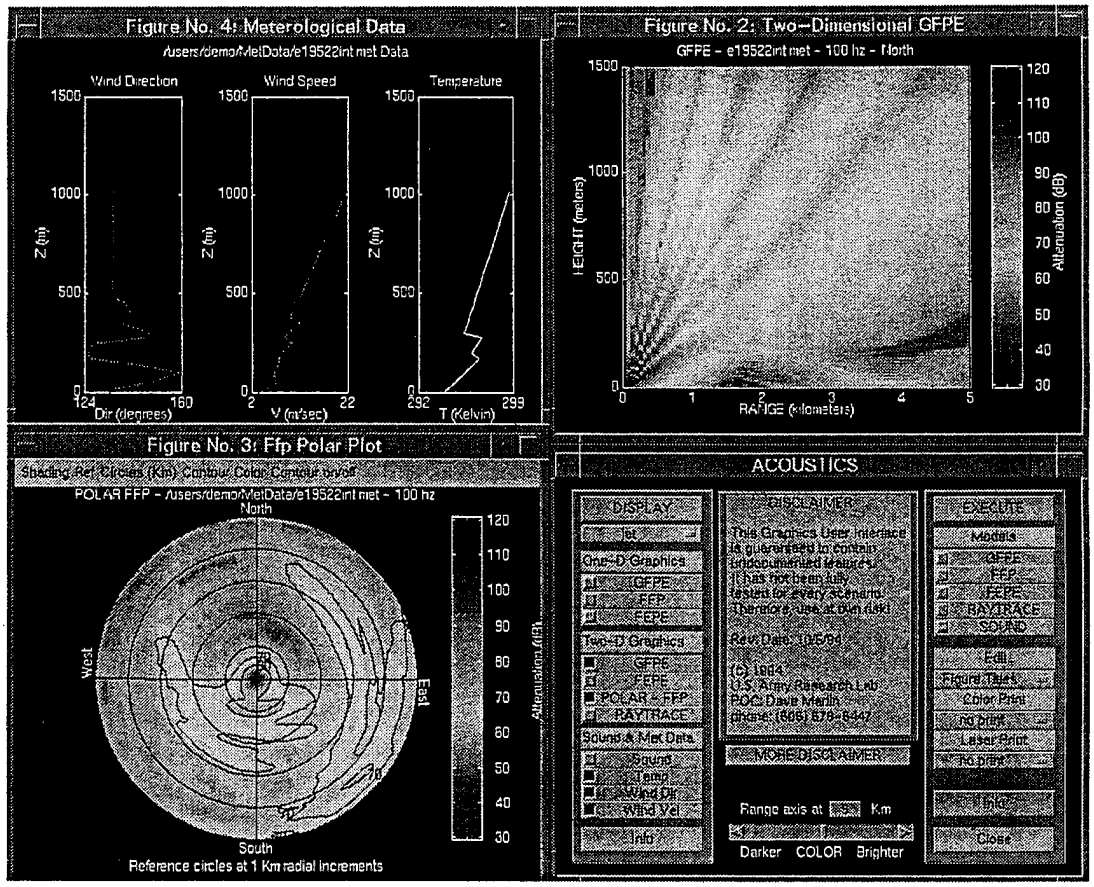
Figure No. 4: Meterological Data
/users/demo/MetData/e19522int.met Data
Wind Direction
Wind Speed
Temperature
Z (ft)
Dir (degrees)
V (mi'sec)
T (Kelvin)
Figure No. 2: Two-Dimensional GFPE
GFPE - e19522int.met - 100 hz - North
HEIGHT (meters)
RANGE (kilometers)
Attenuation (dB)
Figure No. 3: Ffp Polar Plot
POLAR FFP - /users/demo/MetData/e19522int.met - 100 hz
North
South
East
West
Reference circles at 1 Km radial increments
ACOUSTICS
DISPLAY
DISCLAIMER
EXECUTE
One-D Graphics
Two-D Graphics
Sound & Met Data
MORE DISCLAIMER
Range axis at Km
Darker COLOR Brighter
Models
Print
Close

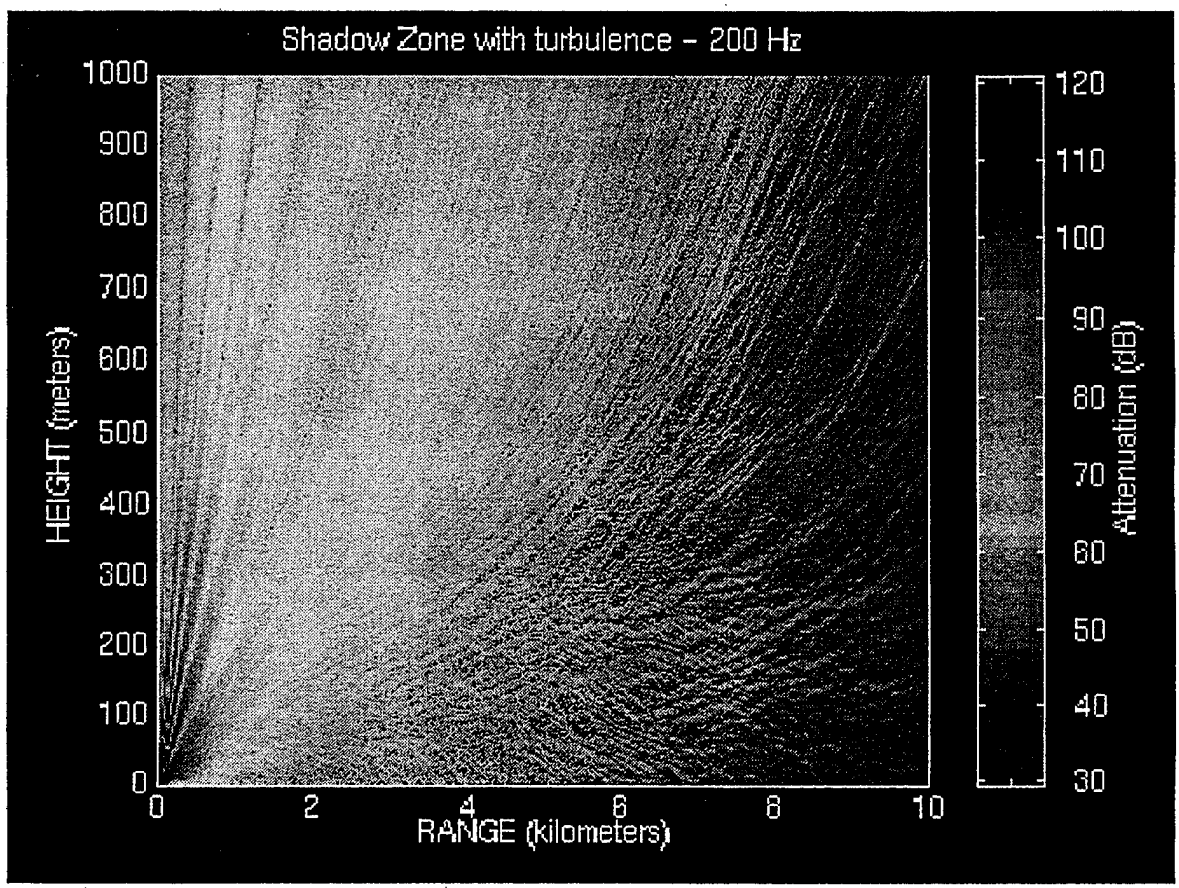
Shadow Zone with turbulence - 200 Hz
HEIGHT (meters)
RANGE (kilometers)
Attenuation (dB)

BATTLEFIELD
ENVIRONMENT
DIRECTORATE

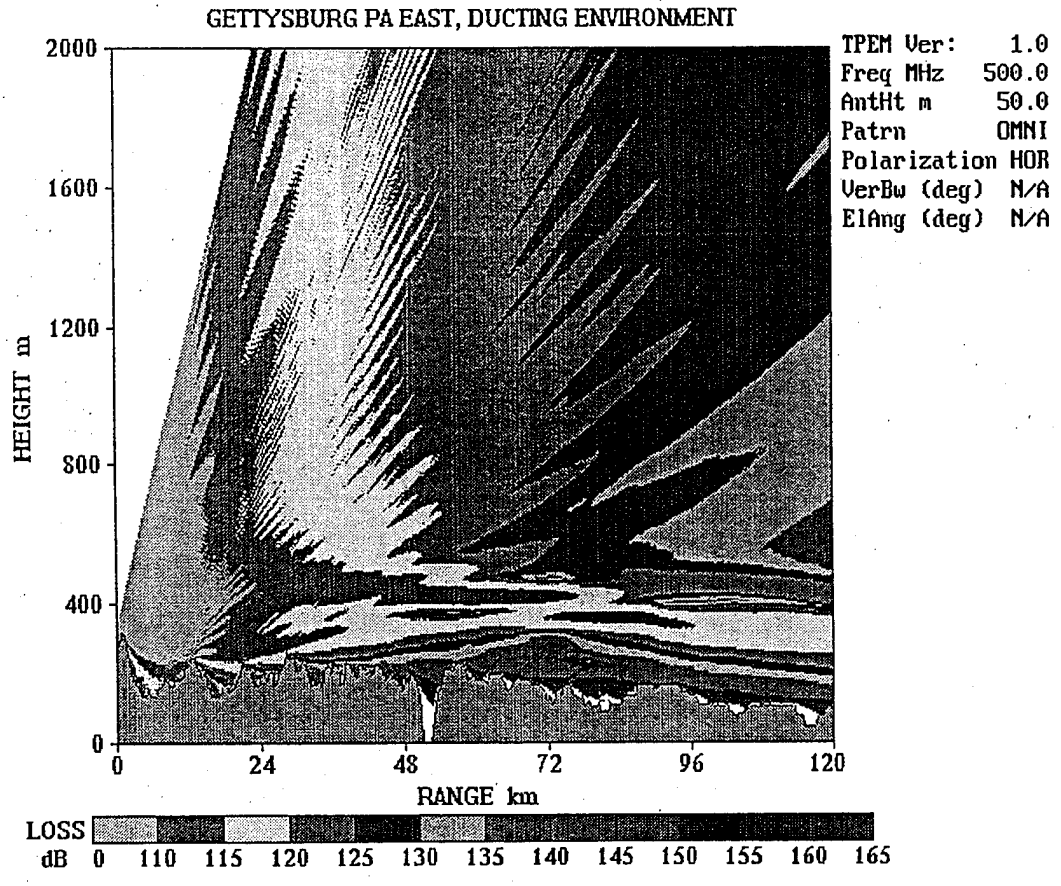
GETTYSBURG PA EAST, DUCTING ENVIRONMENT
TPEM Ver: 1.0
Freq MHz 500.0
AntHt m 50.0
Patrn OMNI
Polarization HOR
VerBw (deg) N/A
ElAng (deg) N/A
HEIGHT m
2000
1600
1200
800
400
0
0
24
48
72
96
120
RANGE km
LOSS
dB 0 110 115 120 125 130 135 140 145 150 155 160 165

SERVICE PARTICIPATION EXAMPLE

LOWER ATMOSPHERIC TRANSMISSION/RADIANCE CODES

AIR FORCE - NAVY - ARMY PROGRAM

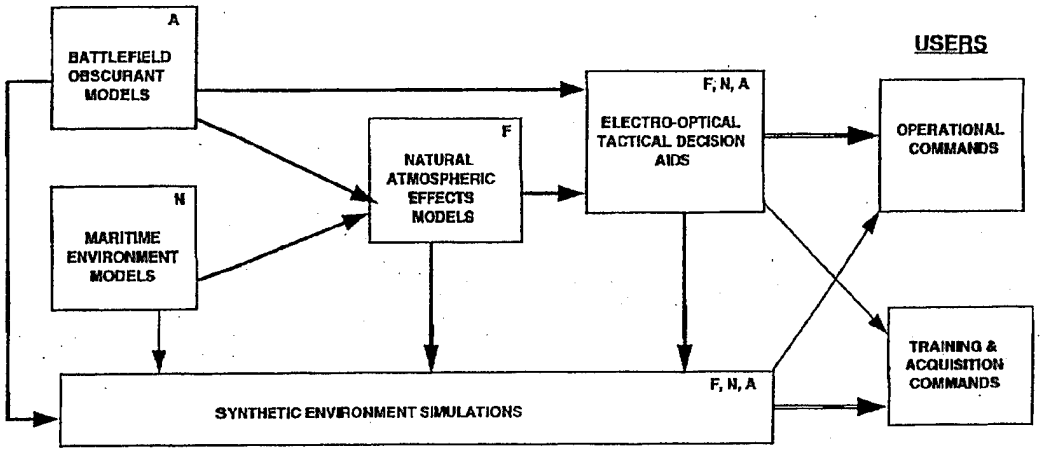

ATMOSPHERIC TRANSMISSION AND RADIANCE MODELS

MODTRAN

- LTE Thermal Emission
- Solar and Thermal Multiple Scattering
- Band Model Radiation Transport
- Wavelength > 0.2 microns (2 cm^{-1} Resolution)
- Incorporated in E-O TDA's

MOSART

- LOS Paths Within Atmosphere and Intersecting Earth's Surface
- Extensive Set of Global Databases
- Incorporated in BMDO/NRL Synthetic Scene Generation Model
- Incorporated in DMSO E^2DIS

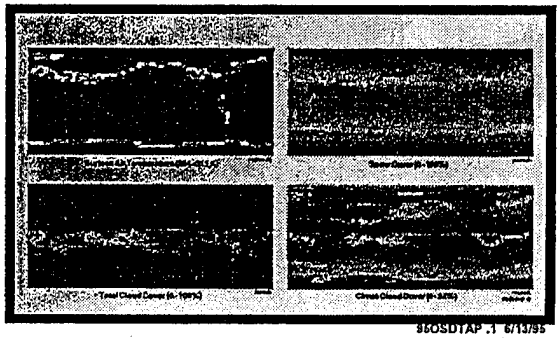

ATMOSPHERIC TRANSMISSION AND RADIANCE MODELS

Accomplishments

- Upgraded MODTRAN Band Models and Cloud/Rain Models
- Completed MOSART Atmospheric Effects Database Generator/Interpolator for E²DIS

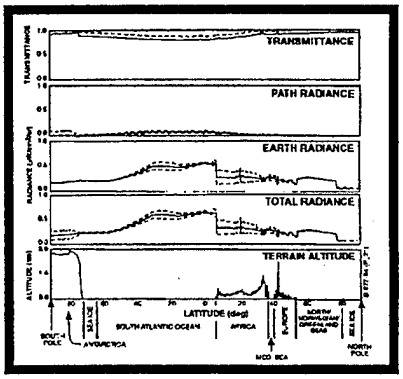

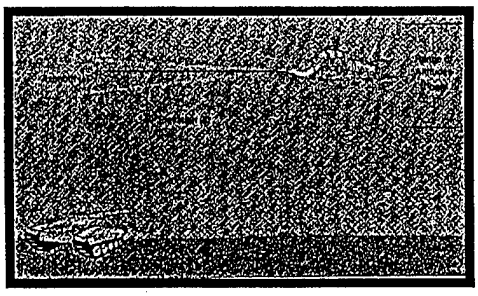

Plans

- Incorporate Multiple/Finite Clouds
- Upgrade Multiple Scattering
- Develop Stand-Alone Climatological Module for Common Accessibility by Transmission and Radiance Codes

95OSDTAP .2 6/13/95

ACCOMPLISHMENTS

Sub-Area: Lower Atmosphere Environment
Technical Effort: Atmospheric Effects
POC: Dr. Juergen Richter (619) 553-3053

- **EM/EO/ACOUSTIC PROPAGATION**
  - *ACOUSTIC MODELS AND VALIDATION*
  - *EM PROPAGATION MODELS*
  - *EO TRANSMISSION AND RADIANCE MODELS*
- **TACTICAL DECISION AIDS**
  - *IWEDA, WIDA, ACT/EOS, EOTDA*
- **REMOTE SENSING**
  - *GPS, VOCAR, BALLISTIC WINDS*
- **SIMULATION**
  - *CSSM, VISIBILITY, BEAMS, SMOKE*

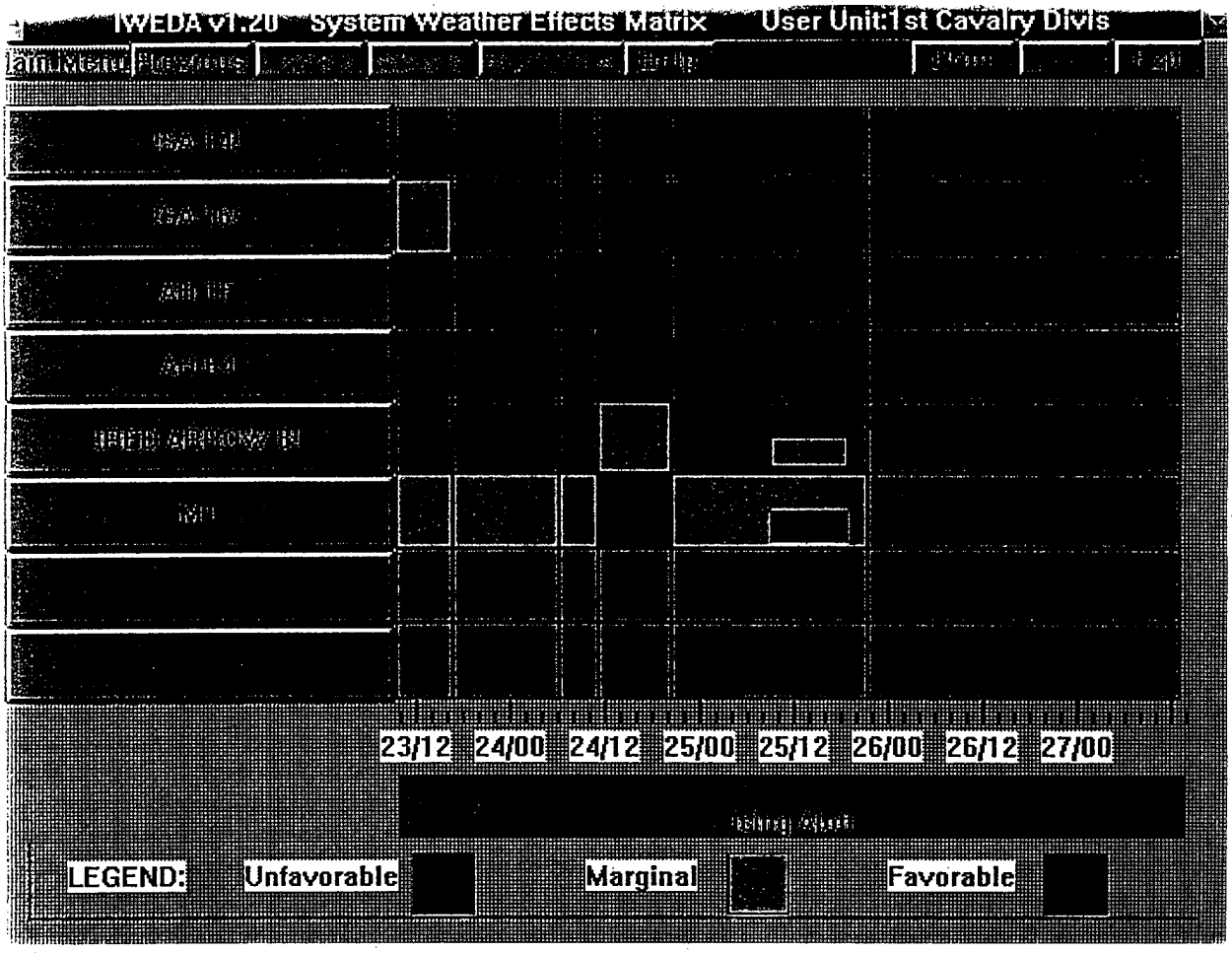
IWEDA v1.20 System Weather Effects Matrix User Unit:1st Cavalry Divis
23/12
24/00
24/12
25/00
25/12
26/00
26/12
27/00
LEGEND:
Unfavorable
Marginal
Favorable

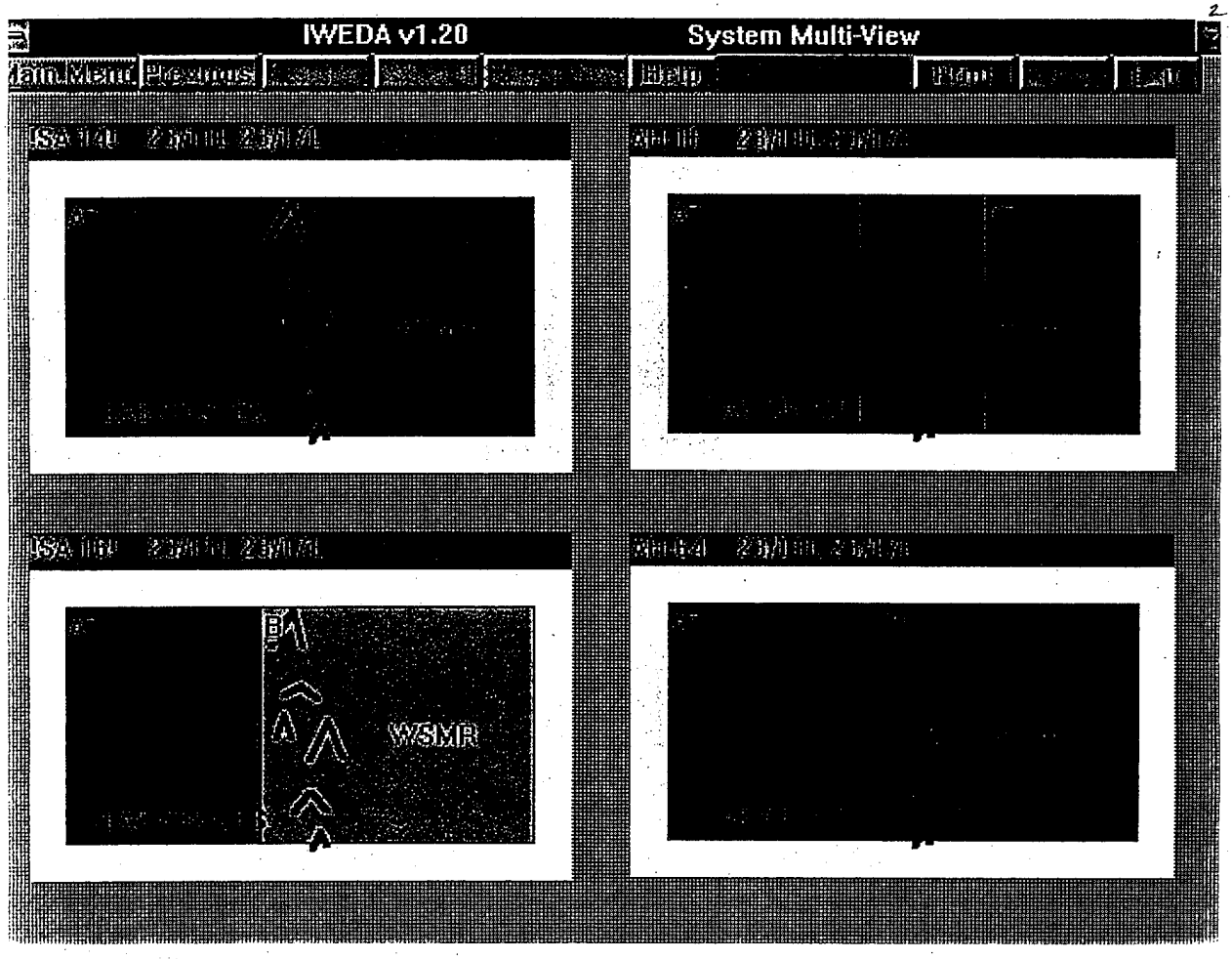
IWEDA v1.20
System Multi-View
Help
WSMR

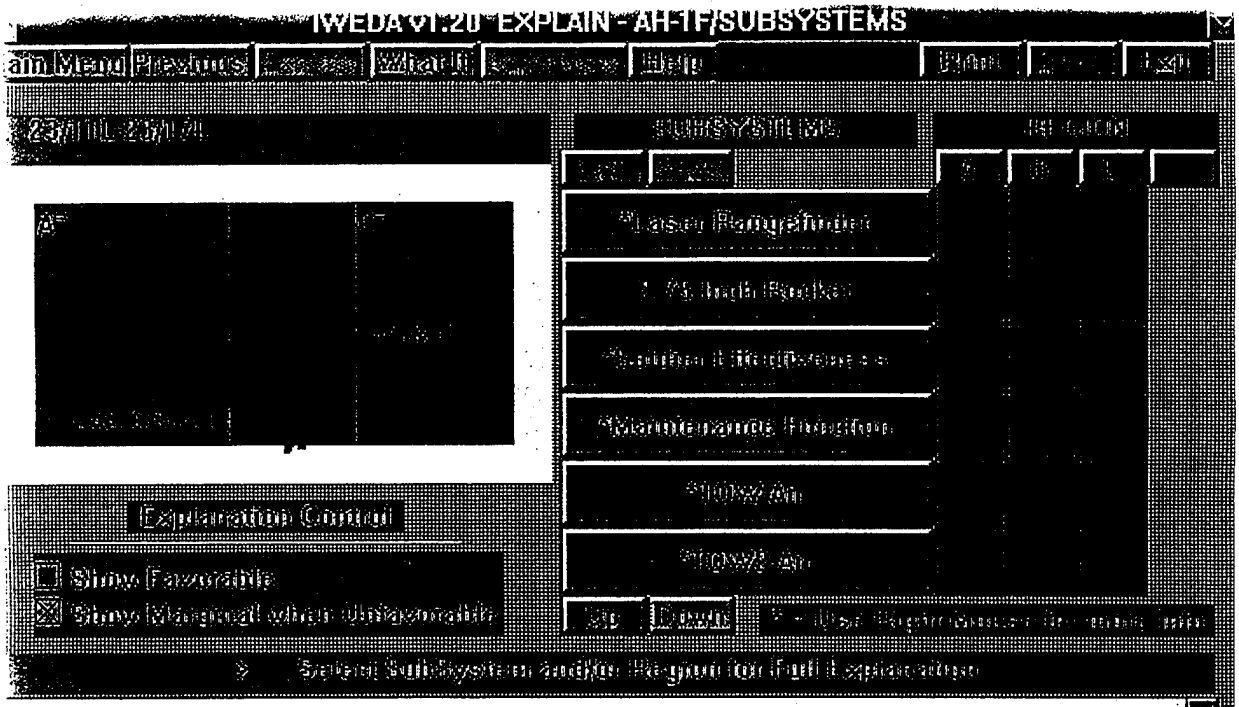

TOW-Air: Unfavorable conditions in Region B

Unfavorable Borderline impact on TOW-Air Performance/Effectiveness due to a prevailing forecast value of Icing Intensity = Light. A decrease in Icing Intensity to None will result in a marginal condition. Any occurrence of icing may cause the missile to freeze to the rails and make firing very difficult.

SERVICE PARTICIPATION EXAMPLE

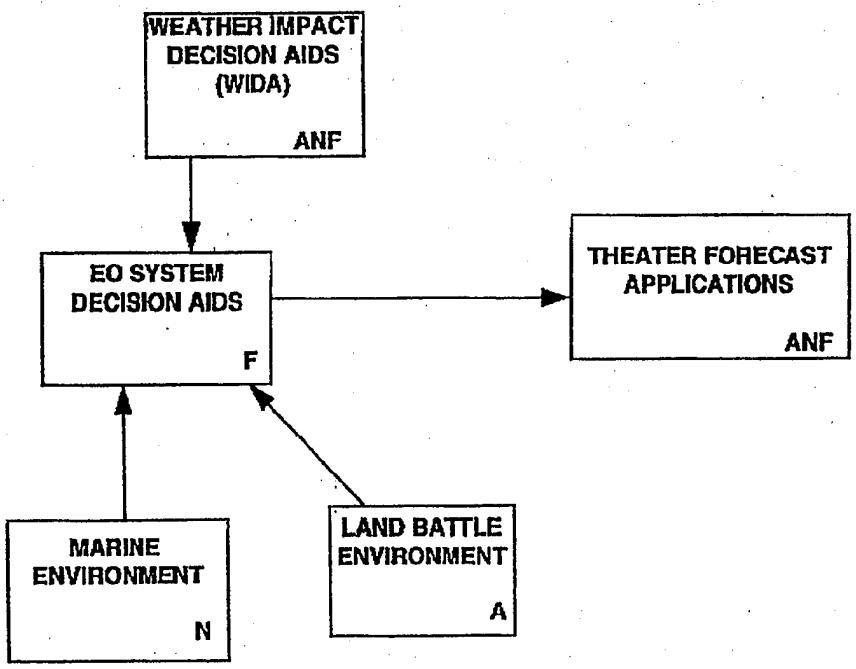

WEATHER IMPACT DECISION AID
WIDA

Weather Impact Decision Aids

WIDA

Annual Tri-Service Meeting

NRaD Facilities
San Diego
28-29 March 1995

The Air Force's Phillips Laboratory, Geophysics Directorate (PL/GP)
Advanced Weather Systems (PE63707F) Program Office (GPAA)
29 Randolph Rd. Hanscom AFB MA 01731-3010

WIDAGPSD.DOC

ACT/EOS

Air Combat Targeting/Electro-Optical Simulation

- Develop Electro-Optical(EO) Weather Impact Decision Aids for Use in DoD Combat Mission Planning Systems
  - -- Allow Mission Planners to Automatically Include Impact of Weather in Choosing Weapons and Times Over Target(TOT)
    - --- Rapid Application of Air Power(RAAP)
    - --- Automated Planning System(APS)
    - --- Wing Command and Control System(WCCS)
    - --- Force Level Execution System(FLEX)
- Provide EO Sensor Scene Simulation for Air Crew Situational Awareness Prior to Mission Execution
  - --- Air Force Mission Support System (AFMSS)

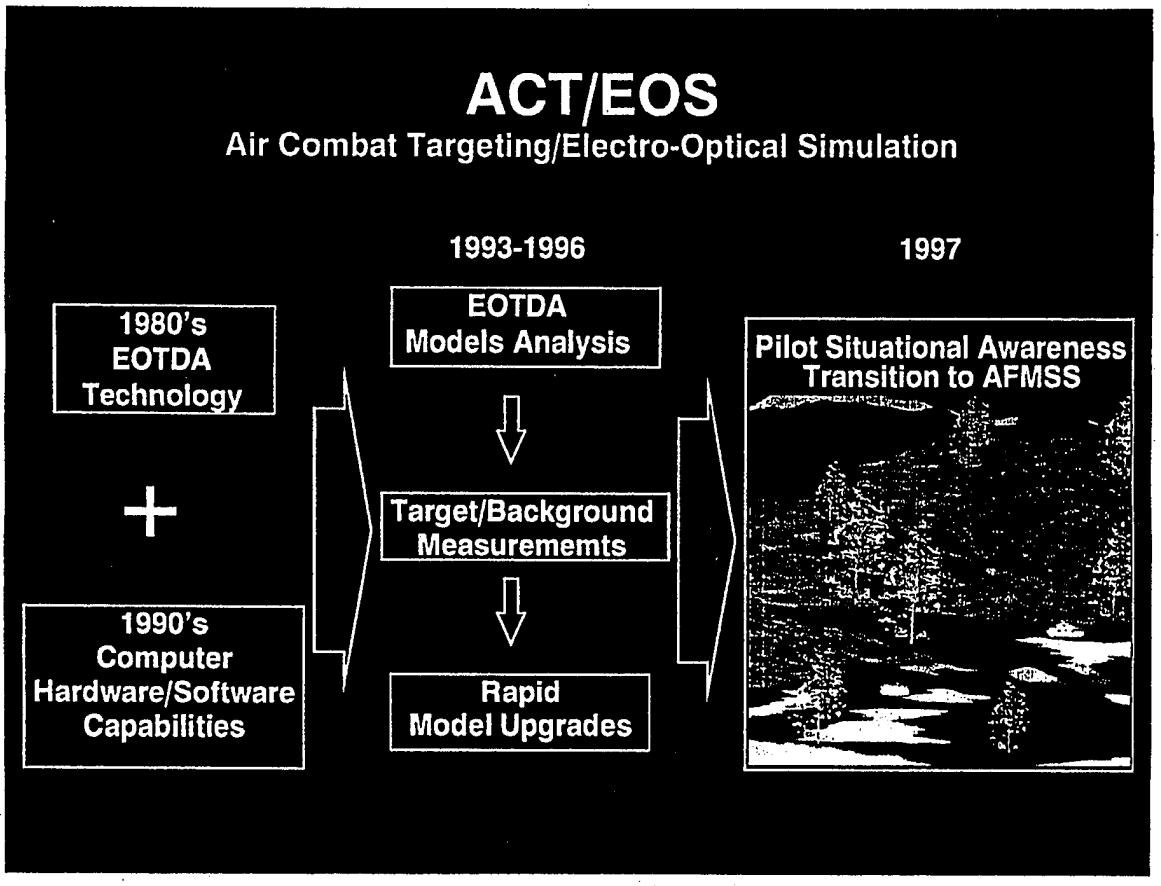

ACCOMPLISHMENTS

Sub-Area: Lower Atmosphere Environment
Technical Effort: Atmospheric Effects
POC: Dr. Juergen Richter (619) 553-3053

- **EM/EO/ACOUSTIC PROPAGATION**
  - *ACOUSTIC MODELS AND VALIDATION*
  - *EM PROPAGATION MODELS*
  - *EO TRANSMISSION AND RADIANCE MODELS*
- **TACTICAL DECISION AIDS**
  - *IWEDA, WIDA, ACT/EOS, EOTDA*
- **REMOTE SENSING**
  - *GPS, VOCAR, BALLISTIC WINDS*
- **SIMULATION**
  - *CSSM, VISIBILITY, BEAMS, SMOKE*

GPS Sounder

The Concept of the Inversion Technique

Hitney, H.V., Modelling Tropospheric Ducting Effects on Satellite-to-Ground Paths, AGARD CP-543, Oct. 1993

Anderson, K.D., Tropospheric Refractivity Profiles Inferred From Low-Elevation Angle Measurements of GPS Signals, AGARD CP-567, Sept. 1994

Received Signal

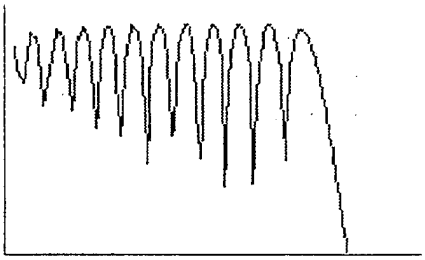

Time/Range/Angle

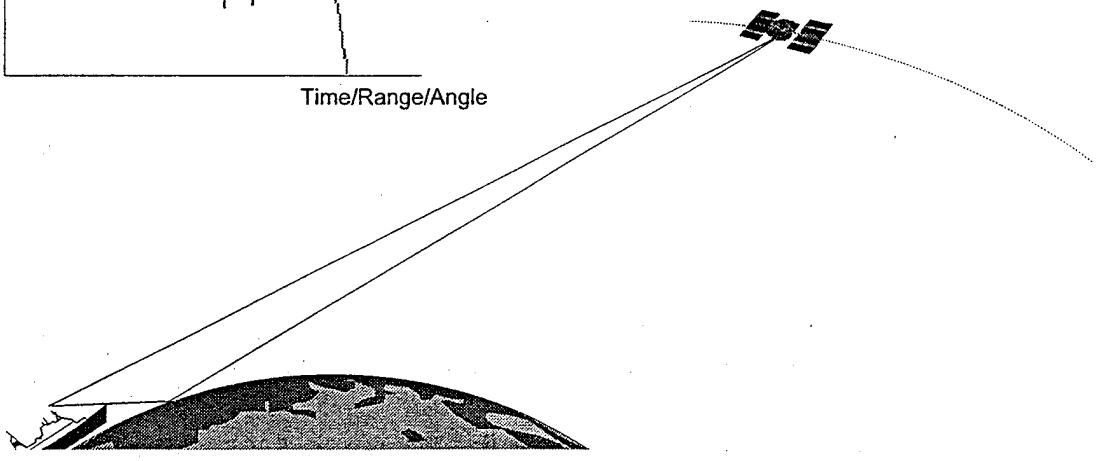

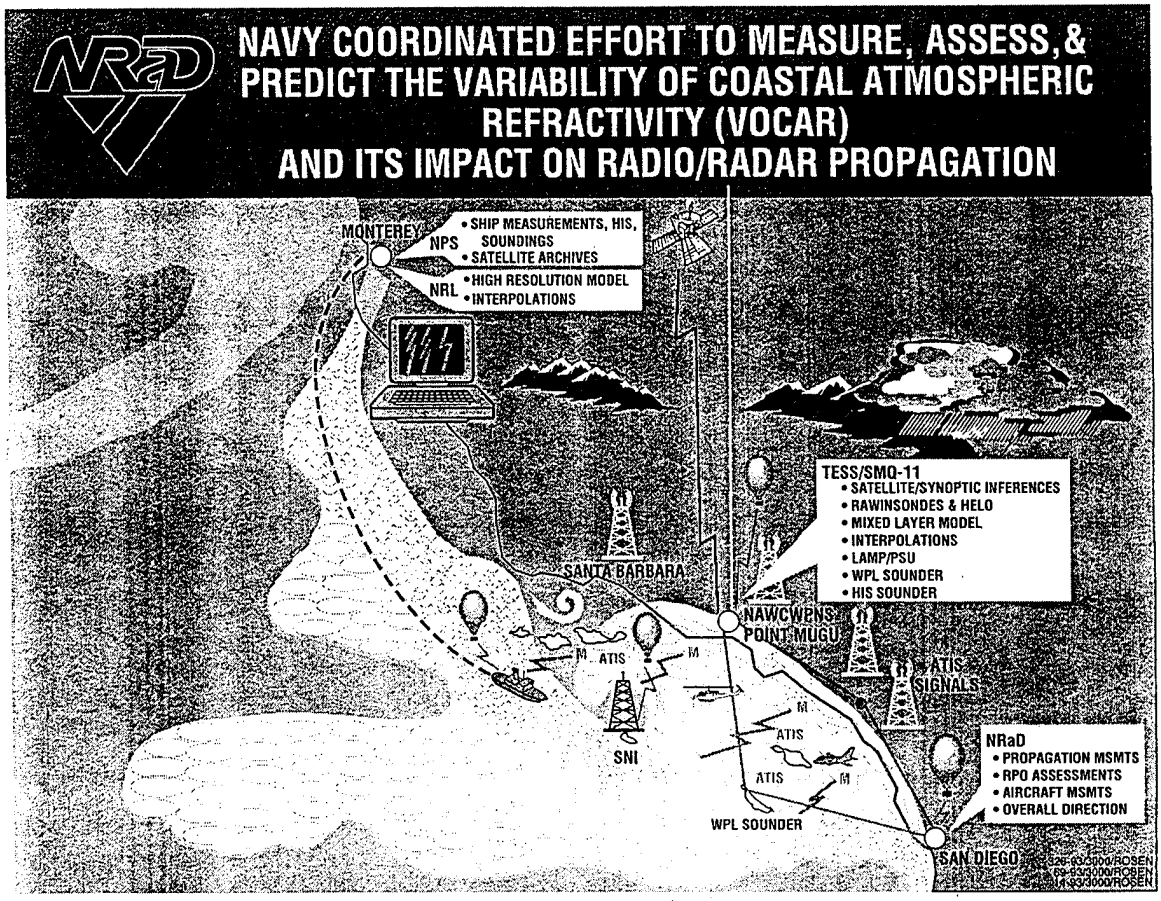
NAVY COORDINATED EFFORT TO MEASURE, ASSESS, & PREDICT THE VARIABILITY OF COASTAL ATMOSPHERIC REFRACTIVITY (VOCAR) AND ITS IMPACT ON RADIO/RADAR PROPAGATION
MONTEREY
NPS • SHIP MEASUREMENTS, HIS, SOUNDINGS • SATELLITE ARCHIVES
NRL • HIGH RESOLUTION MODEL • INTERPOLATIONS
TESS/SMQ-11 • SATELLITE/SYNOPTIC INFERENCES • RAWINSONDES & HELO • MIXED LAYER MODEL • INTERPOLATIONS • LAMP/PSU • WPL SOUNDER • HIS SOUNDER
SANTA BARBARA
NAWCWPNS POINT MUGU
ATIS SIGNALS
ATIS
SNI
WPL SOUNDER
NRaD • PROPAGATION MSMTS • RPO ASSESSMENTS • AIRCRAFT MSMTS • OVERALL DIRECTION
SAN DIEGO

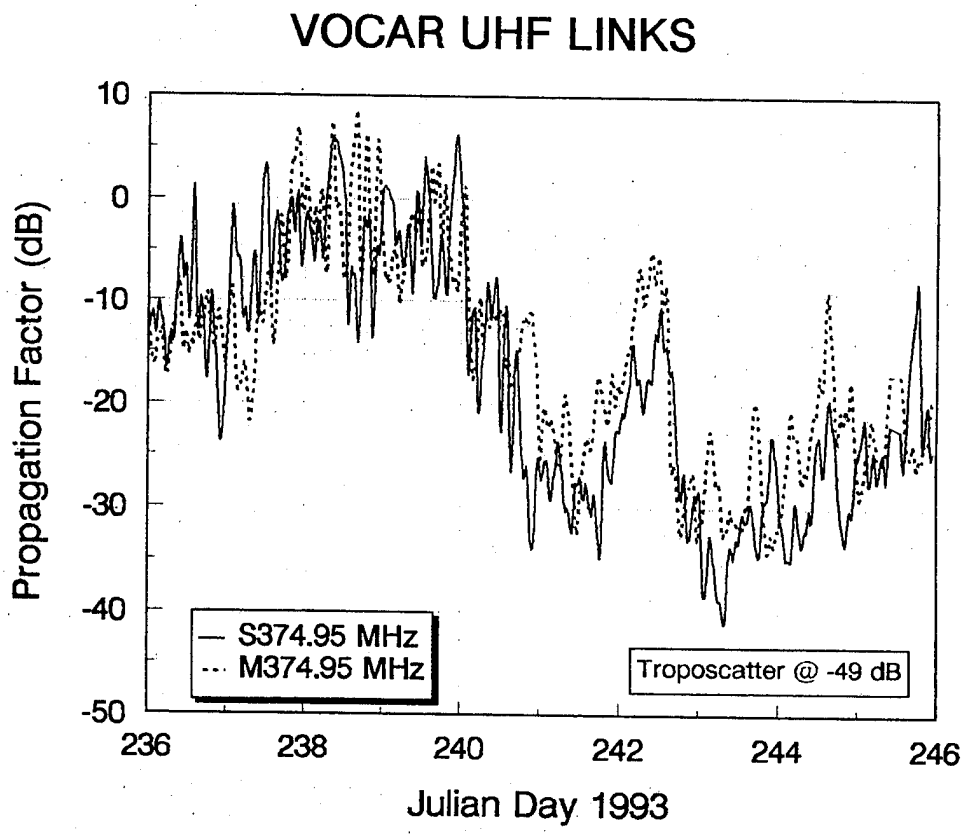
VOCAR UHF LINKS
Propagation Factor (dB)
10
0
-10
-20
-30
-40
-50
236
238
240
242
244
246
Julian Day 1993
S374.95 MHz
M374.95 MHz
Troposcatter @ -49 dB

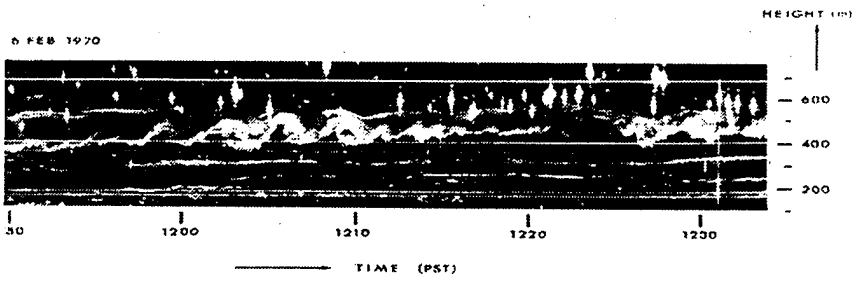

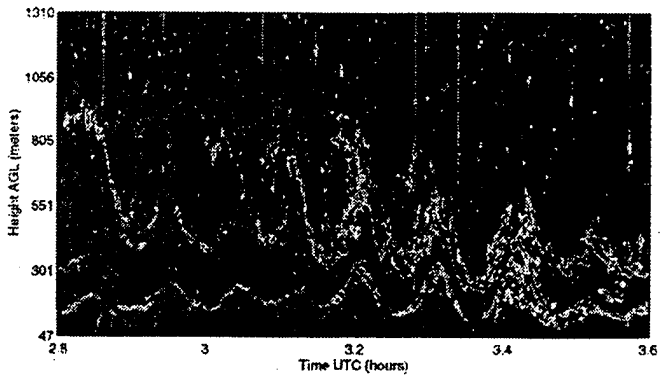

Plate 3. FMCW radar record showing low-level waves on October 26, 1992.

ACCOMPLISHMENTS

Sub-Area: Lower Atmosphere Environment
Technical Effort: Atmospheric Effects
POC: Dr. Juergen Richter (619) 553-3053

- **EM/EO/ACOUSTIC PROPAGATION**
  - *ACOUSTIC MODELS AND VALIDATION*
  - *EM PROPAGATION MODELS*
  - *EO TRANSMISSION AND RADIANCE MODELS*
- **TACTICAL DECISION AIDS**
  - *IWEDA, WIDA, ACT/EOS, EOTDA*
- **REMOTE SENSING**
  - *GPS, VOCAR, BALLISTIC WINDS*
- **SIMULATION**
  - *CSSM, VISIBILITY, BEAMS, SMOKE*

CLOUD SCENE SIMULATION MODEL (CSSM)

- **Physics-Based Empirical Model**
  - Fractal-derived cloud shapes
  - Multi-dimensional (3 spatial and 1 temporal)
  - Multi cloud types (stratiform, cirriform, cumuliform)
  - Convection physics for cumuliform cloud types
- **Future Development**
  - Add orographic effects on cloud formation
  - Implement integrated rain model
  - Add precipitation model
  - Add drop size distributions
  - Add IR and u-wave radiative parameterizations

Sample CSSM Output Fields

Stratus Layer

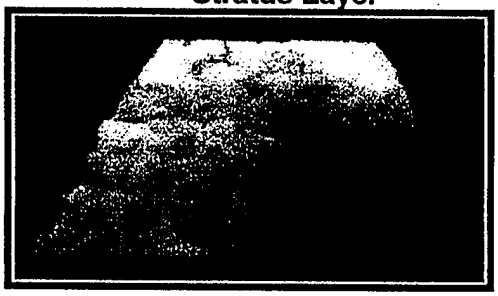

Cirrus Layer

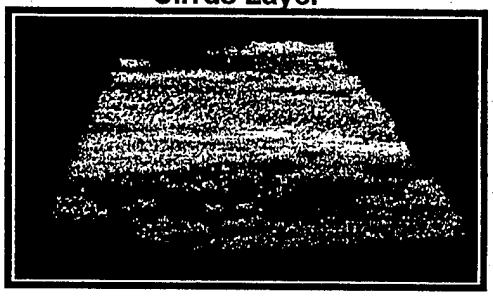

Cumulus Layer

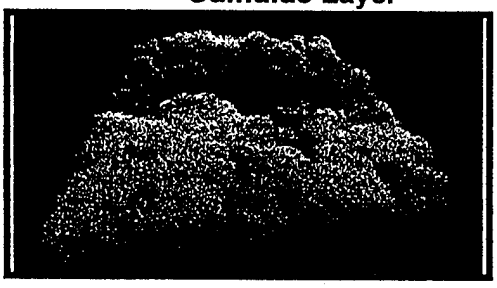

Stratocumulus Layer

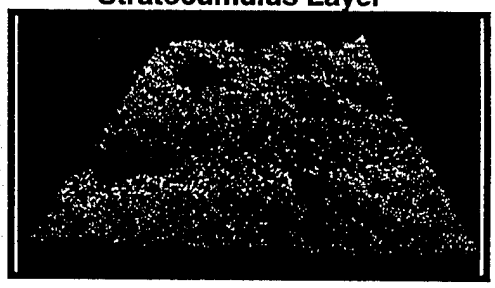

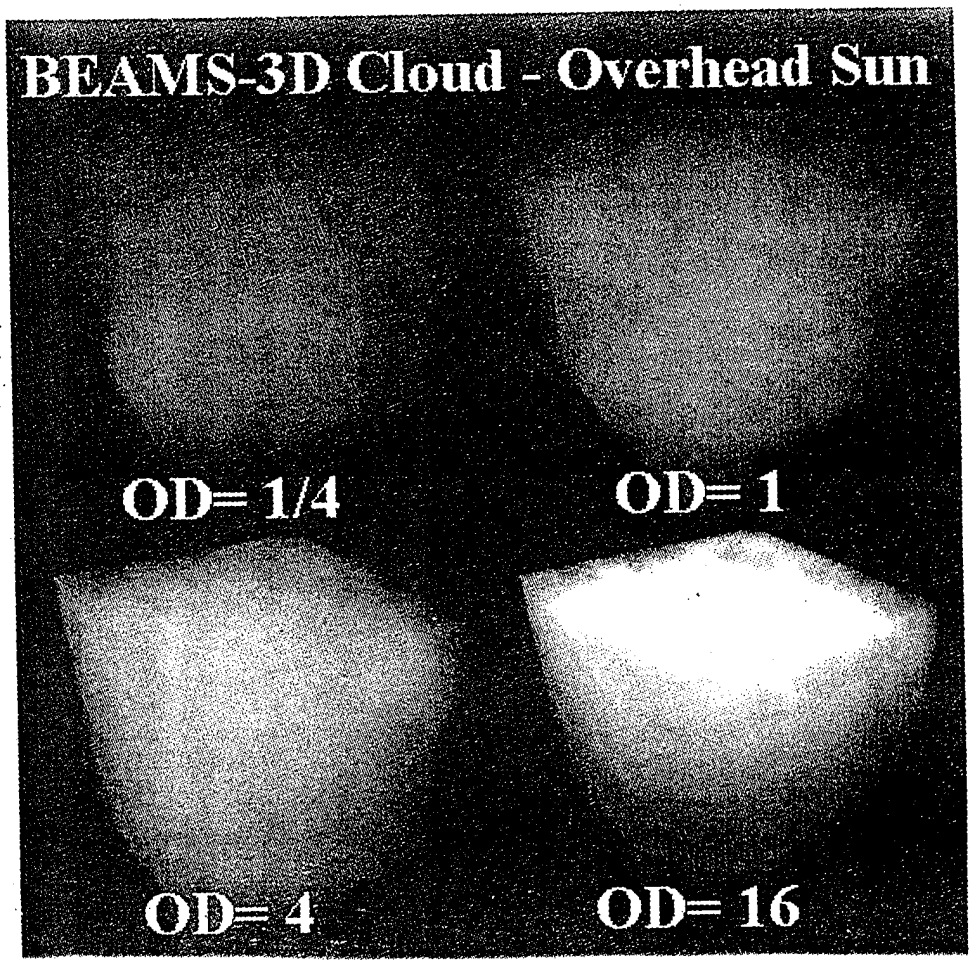
BEAMS-3D Cloud - Overhead Sun
OD= 1/4
OD= 1
OD= 4
OD= 16

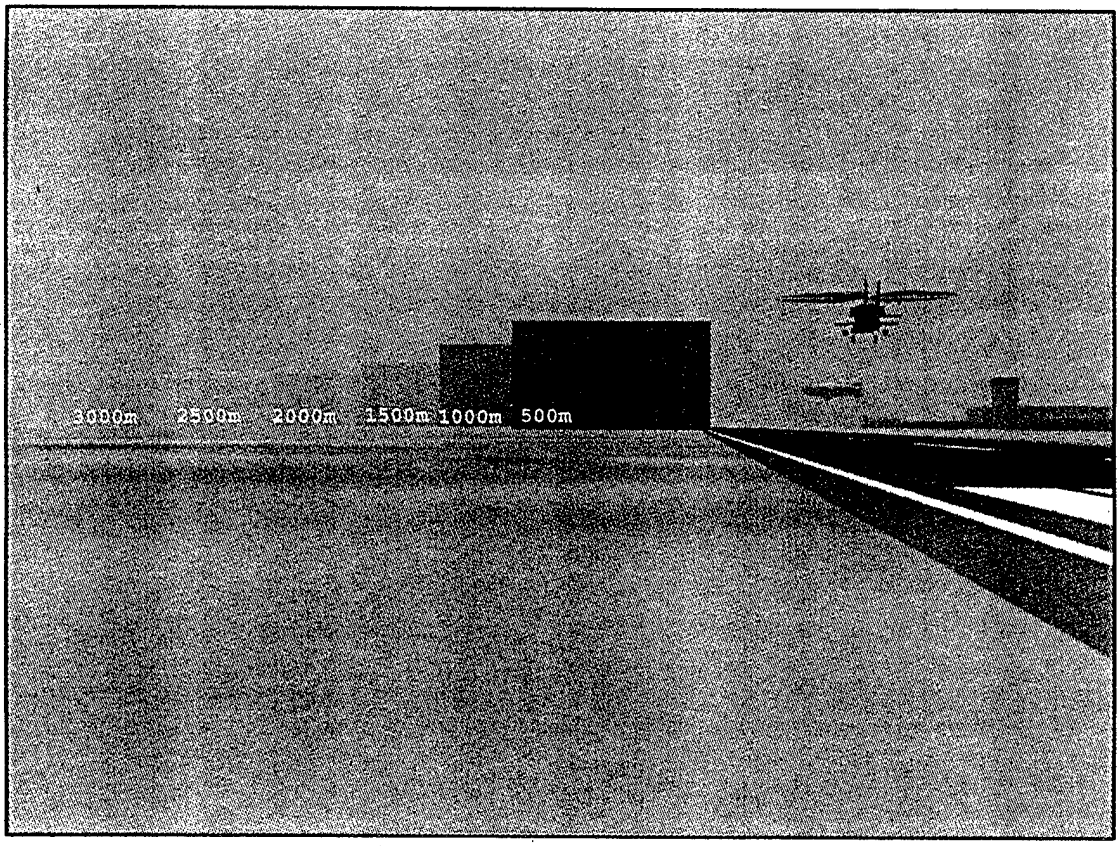
3000m 2500m 2000m 1500m 1000m 500m

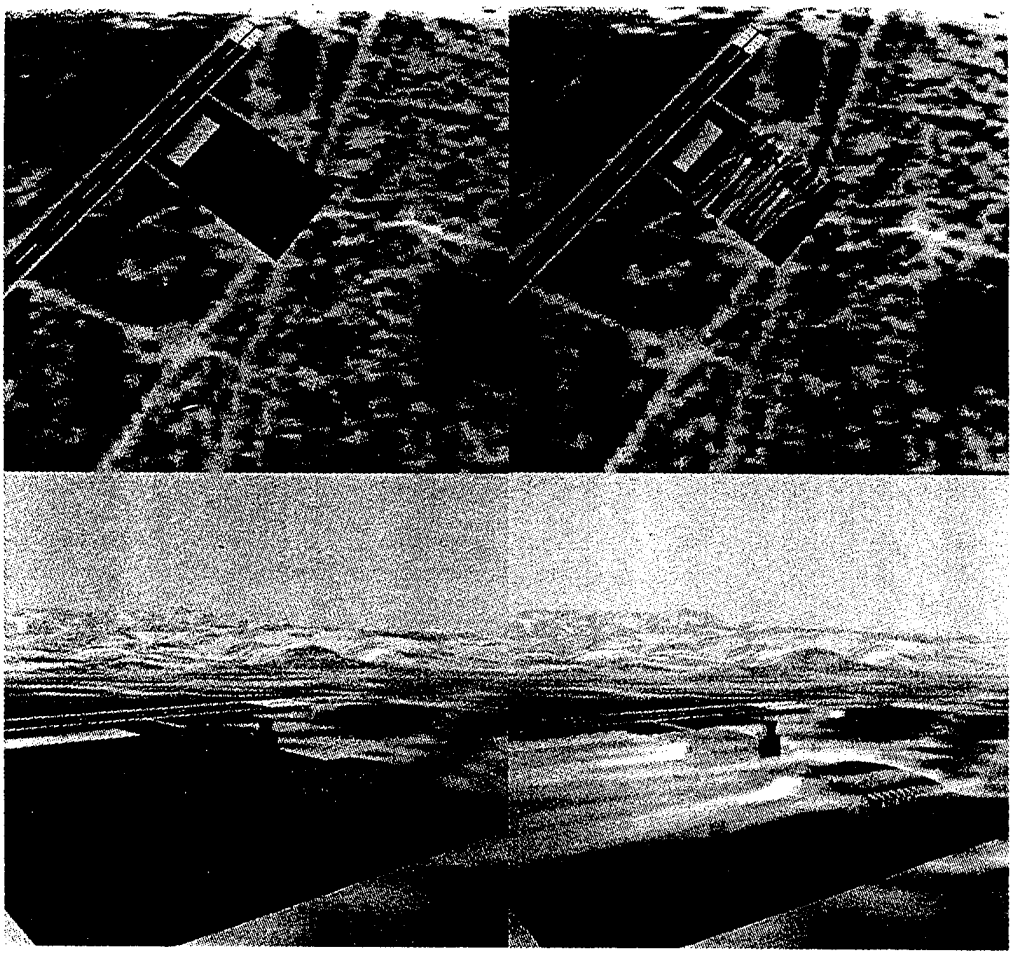

PLANS

Sub-Area: Lower Atmosphere Environment
Technical Effort: Atmospheric Effects
POC: Dr. Juergen Richter (619) 553-3053

EM/EO/ACOUSTIC PROPAGATION

- *EM MODELS (TERRAIN, SCATTERING, WORKSHOP)*
- *TRANSMISSION MODELS (PARTIAL CLOUDS, IMPROVED MULTIPLE SCATTERING AND RADIATIVE TRANSFER ROUTINES, GLOBAL CLIMATOLOGIES AND TERRAIN SPECIFICATIONS)*
- *ACOUSTIC PROPAGATION (COMPLEX TERRAIN AND SURFACE ROUGHNESS MODELS)*

TACTICAL DECISION AIDS

- *ACOUSTIC PROPAGATION TDA*
- *WIDA, ACT/EOS*
- *EOTDA*
- *TESS/NITES/C4I SYSTEMS*

PLANS

Sub-Area: Lower Atmosphere Environment
Technical Effort: Atmospheric Effects
POC: Dr. Juergen Richter (619) 553-3053

REMOTE SENSING

- *RADIO REFRACTIVITY*
- *AIRBORNE BALLISTIC WINDS LIDAR DEMO*
- *ABL TURBULENCE MEASUREMENTS AND MODELING*
- *LIDAR DETECTION OF CBW AGENTS*

SIMULATION

- *MODEL PHYSICS DEVELOPMENT AND INTEGRATION*
- *DEMONSTRATION OF BEAMS AND BLIRP MODELS TO DMSO AND STRICOM*

SUMMARY

Sub-Area: Lower Atmosphere Environment
Technical Effort: Atmospheric Effects
POC: Dr. Juergen Richter (619) 553-3053

- **EXCELLENT TRISERVICE COORDINATION**
  - *ATMOSPHERIC TRANSMISSION PLAN*
  - *EOTDA, WIDA*
  - *EM PROPAGATION*
- **EXCELLENT COORDINATION OF SIMULATION EFFORT THROUGH DMSO**
- **FULL SPECTRUM INTEGRATED PROGRAM**

Dr. Juergen Richter, "Technology Area Plan for Battlespace Environments - Atmospheric Effects"

DISCUSSION

S. MARCUS

Does ARL include 3D effects in their models in order to account for wind speeds and gradients not in the plane of incidence? If so, can these be applied to the em problem?

AUTHOR'S REPLY

Dr. D. Brown responded to this question - ARL showed 2D model results because of the relative maturity of those models; we are developing full 3D models in recognition of the issues you raise. Our newest ARL employee, Dr. Keith Wilson, also is attending this workshop, and is an acoustics modeler. Any detailed questions I invite you to address to him.

SESSION II. OPERATIONAL REQUIREMENTS AND APPLICATIONS

Chair: CDR D. Markham

Navy and Marine Corps Requirements

CDR Denis M. Meanor
Chief of Naval Operations (N096)
3450 Massachusetts Ave., NW
US Naval Observatory Bldg 1
Washington, DC 20392-5421

Navy Requirements for EM Modeling

CDR Denis Meanor
CNO (N096)

Littoral Warfare

- Threat
- Near shore and overland problem
- Range dependent environment

Recent CinC Concerns

- COMUSNAVCENT - 1993
  - Cruise missiles, low flying aircraft, periscopes
  - SHAREM 110 R&D demonstration
- CINCPACFLT, CINCLANTFLT - 1992
  - Atmospheric refractivity forecasting system
  - Real time data, over land, optimize sensing and weapons systems

emreq.ppT

Consolidated Command Technology Issues

- Dec 1994 - CINCLANTFLT, CINCPACFLT, CINCUSNAVEUR, CINCUSNAVCENT
- Littoral Warfare / Surveillance / SEW
  - Ship self defense
  - Theater missile defense
  - Improved EM/EO sensor prediction
  - Battlegroup cooperative engagement
  - Ship to shore communications

emreq.ppT

Navy Systems

- Operation Requirements Documents having EM issues:
  - Surveillance and targeting
  - Mission planning
  - Defensive countermeasures
  - Anti-ship missile and ship self defense
  - Command and control aircraft

Summary

- Documented needs and requirements
- Overwater and overland predictions
- Characterizing terrain effects
- Measuring clutter and signal loss
- Critical ship and aircraft employment

Army Requirements

Dr. Douglas R. Brown
U.S. Army Research Laboratory
Battlefield Environment Directorate
WSMR, NM 88002-5501

Army Requirements for Radio Frequency Propagation Modeling

For the

Electromagnetic Modeling Workshop

Presented by

Dr. Douglas R. Brown
U.S. Army Research Laboratory
Battlefield Environment Directorate
WSMR, NM 88002-5501

Army Agencies Consulted

U. S. Army Research Laboratory (ARL)
Battlefield Environment Directorate (BED)
Sensors Directorate (SD)

Army Research Office (ARO)

Corps of Engineers Cold Regions Research and Engineering Lab

Space & Strategic Defense Command (SSDC)

Army Space (ARSPACE)

Communications & Electronics Command (CECOM)

Outline of Presentation

Army Propagation Modeling Environment

"Boundary Layer" Propagation

Polarimetric Propagation

Extended Surface Scattering

Volumetric Scattering

Army Propagation Modeling Environment

JDL Reliance: Army relies upon the Navy R&D for E&M Propagation Modeling

Wavelenghts of Interest:

High: Infrared

Moderate: NMMW, Visual

Low: Ultraviolet, Radio

Focus: on battlescale, in lower atmosphere, and lower...

Boundary Layer Propagation

Definition:

Atmosphere: That part coupled convectively to the earth's surface

Terrain: That part of the earth above the saturated soil level

Polarimetric Propagation: Weather Effects

Non-Polarized propagation effects modeled adequately, although SSDC is interested in NMMW refraction effects.

Weather Effects:

Need improved snow models that account for major snow crystal habits and water content. Caution: characterization of falling snow in equivalent or worse condition.

Need improved models of scattering by rain/hail for remote sensing of precipitation intensity

Polarimetric Propagation: Countermeasures

MMW Countermeasure Smokes/Chaff

Need models of resonant extinction by irregular dielectric fibers, metallic flakes;

Need models that predict orientation of particles coupled to realistic atmospheric turbulence.

Design of frequency selective obscurants requires both of the above capabilities.

Application: radar discrimination of targets, reduction of false alarm rates

Extended Surface Scattering

Effects: Normal incidence enhanced backscatter, low grazing angle backscatter

Need better understanding of underlying scattering mechanisms

Effect: Scattering from lossy dielectric surfaces with 2-D roughness

Need models to predict the scattering from such surfaces in near real time

Volumetric Scattering

NMMW Applications: Snow pack, vegetation

Need models that predict the scatter as a function of diurnal and seasonal changes

Application: Target acquisition radar, communications

Below 1 Ghz: Inhomogeneous stratified soil

Need models that predict the subsurface scattered signal for ground penetrating radars

Application: Buried mine detection, structures detection

Summary

Army EM Propagation needs focus on:

1. Battlefield Boundary Layer domains,
2. NMMW Polarimetric Propagation,
3. Surface and volume scattering,

and rely upon Navy R&D for propagation models.

Dr. Douglas Brown, "Army Requirements"

DISCUSSION

D. BLOOD

Scale and grid sizes of needed measurements?

AUTHOR'S REPLY

100s of meters to 1 meter - atmospheric
1 - 10s of meters - subsurface
~ 1 km - climatological

Joint Spectrum Center Brief

LCOL C. Robinson, USMC

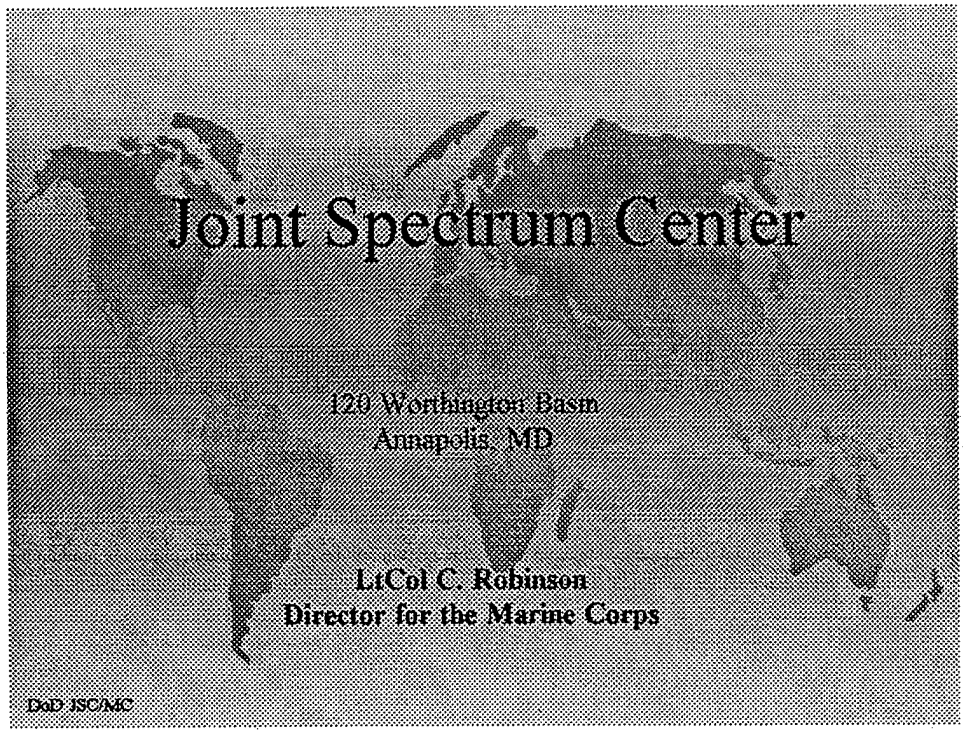
Joint Spectrum Center
120 Worthington Basin
Annapolis, MD
LtCol C. Robinson
Director for the Marine Corps
DoD JSC/MC

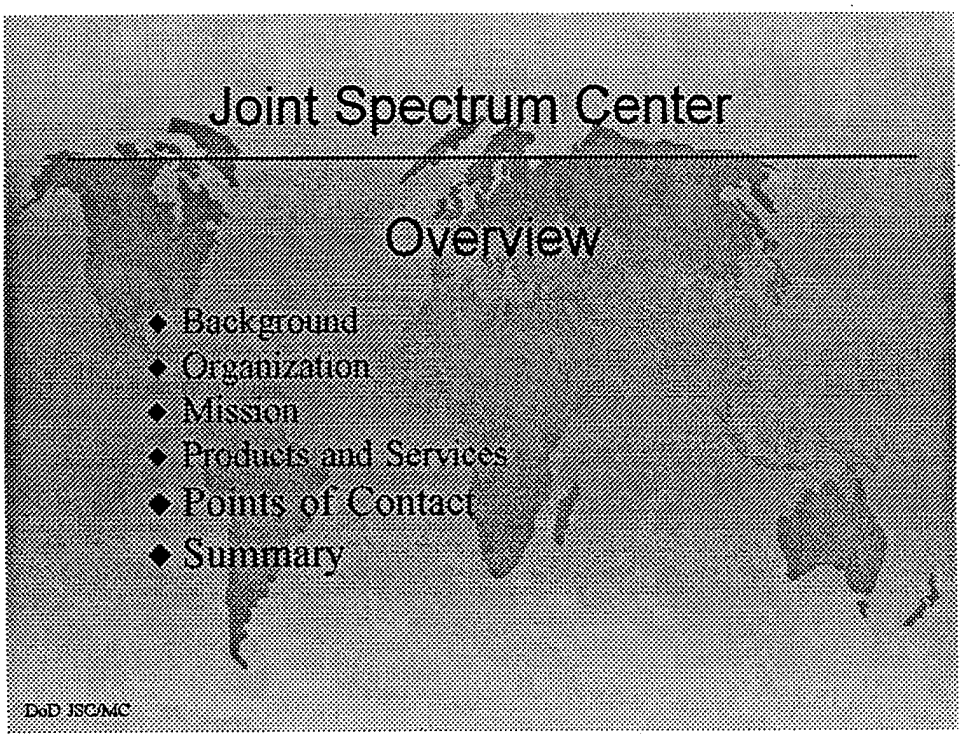
Joint Spectrum Center
Overview
◆ Background
◆ Organization
◆ Mission
◆ Products and Services
◆ Points of Contact
◆ Summary
DoD JSC/MC

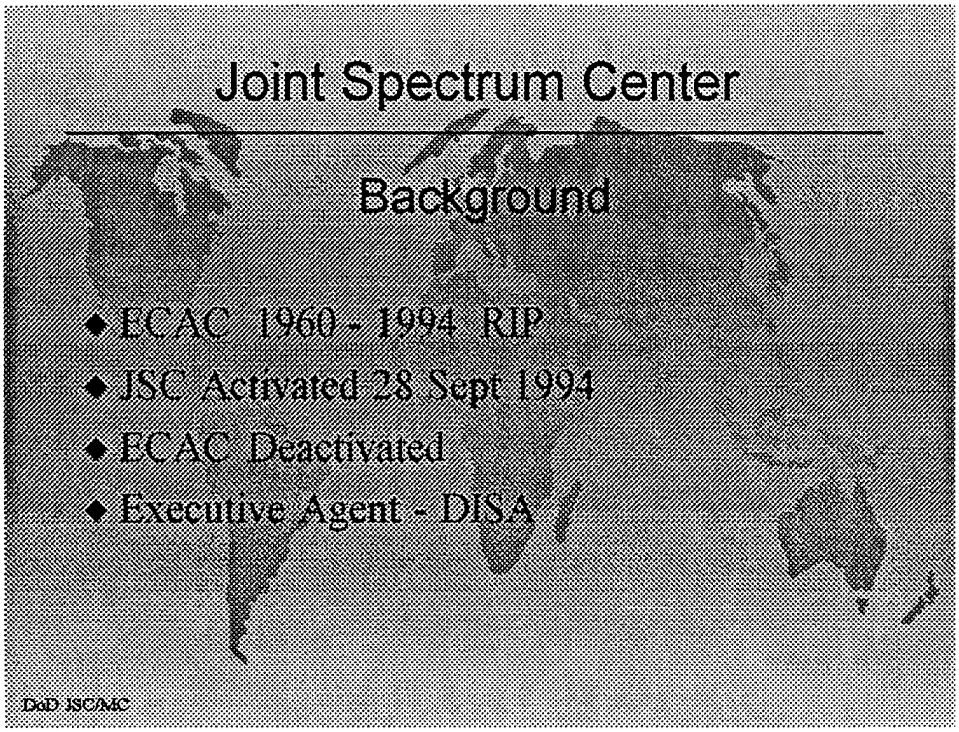

Joint Spectrum Center

Functional Organization Chart

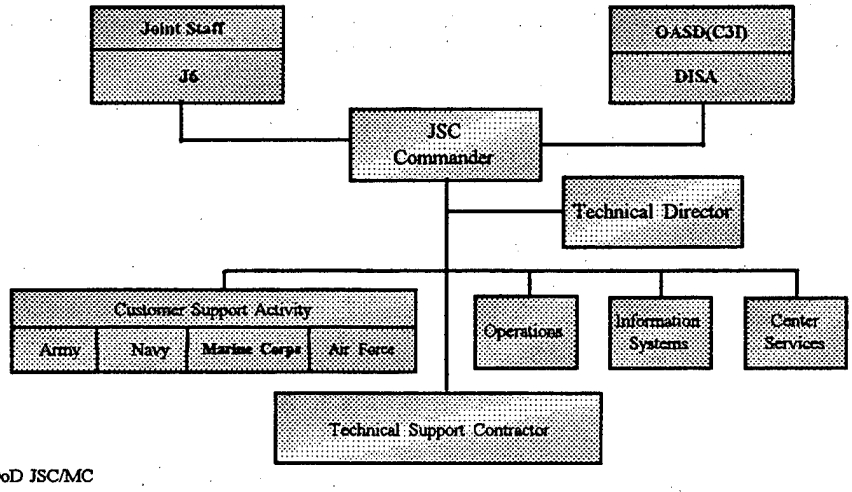

DoD JSC/MC

Joint Spectrum Center

Composition*

Type	Personnel
Officers	11
Enlisted	7 or 8
Civilians	37
Contractor Support	500+

* Per Frequency Panel Con Ops, 26 May 1995

DoD JSC/MC

Joint Spectrum Center

Mission

To ensure the DoD's effective use of the Electromagnetic spectrum in support of national security and military objectives

(The Joint Spectrum Center serves as the Department of Defense focal point for electromagnetic spectrum management matters in support of the Unified Commands, Military Departments and Defense Agencies in planning, acquisition, training, and operations.)

DoD JSC/MC

Joint Spectrum Center
Mission Priorities
◆ Operational Support to Warfighter
◆ Information Systems
◆ Spectrum Management and Use
◆ EM Environmental Effects
DoD JSC/MC

Joint Spectrum Center
PRODUCTS and SERVICES
◆ Frequency Allocation and Assignment Support
◆ Spectrum Planning/Interference Resolution
◆ Spectrum Management Regulations and Policy
◆ Area Studies
◆ Joint Training and E3
◆ E3 Modeling, Simulation and Analysis
◆ Information Systems
DoD JSC/MC

Area Study Content

- Telecommunications
- Geography
- Climate
- Population/ language
- Transportation
- Economy
- Government/ Defense

DoD JSC/MC

Joint Spectrum Center

Data Base Overview

Frequency Assignment

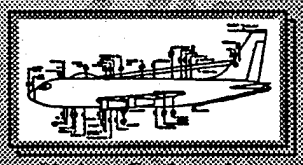

Platform Configuration

Equipment Characteristics

Geographic & Geophysical

Tactical Data (TO &E)

Scenario & Deployment

DoD JSC/MC

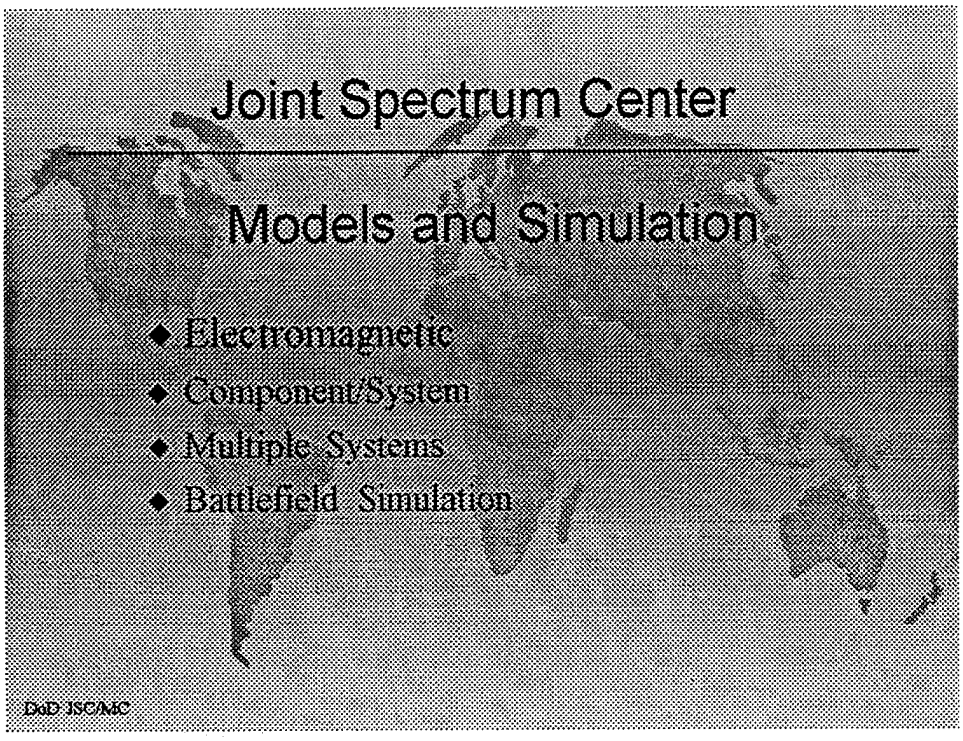
Joint Spectrum Center
Models and Simulation
◆ Electromagnetic
◆ Component/System
◆ Multiple Systems
◆ Battlefield Simulation
DoD JSC/MC

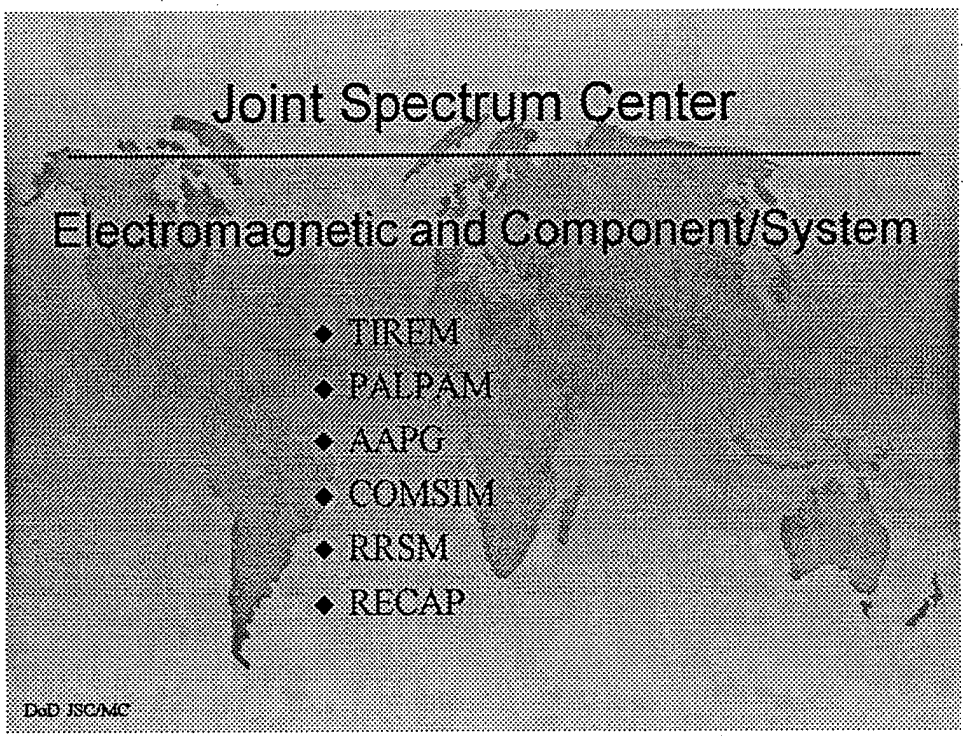
Joint Spectrum Center
Electromagnetic and Component/System
◆ TIREM
◆ PALPAM
◆ AAPG
◆ COMSIM
◆ RRSM
◆ RECAP
DoD JSC/MC

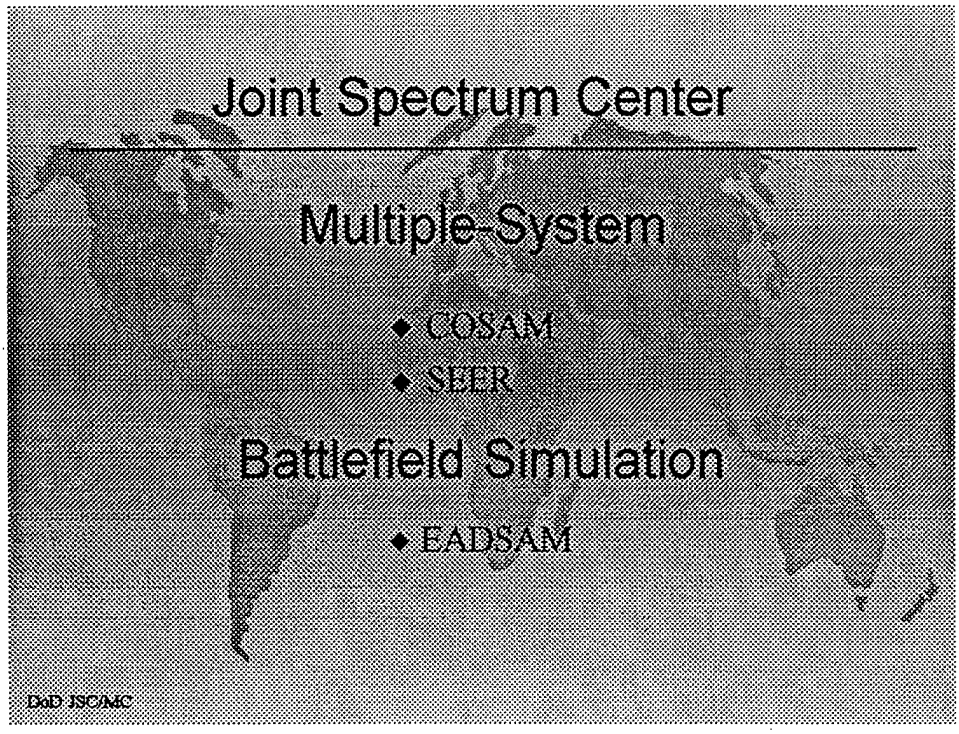
Joint Spectrum Center
Multiple-System
◆ COSAM
◆ SEER
Battlefield Simulation
◆ EADSAM
DoD JSC/MC

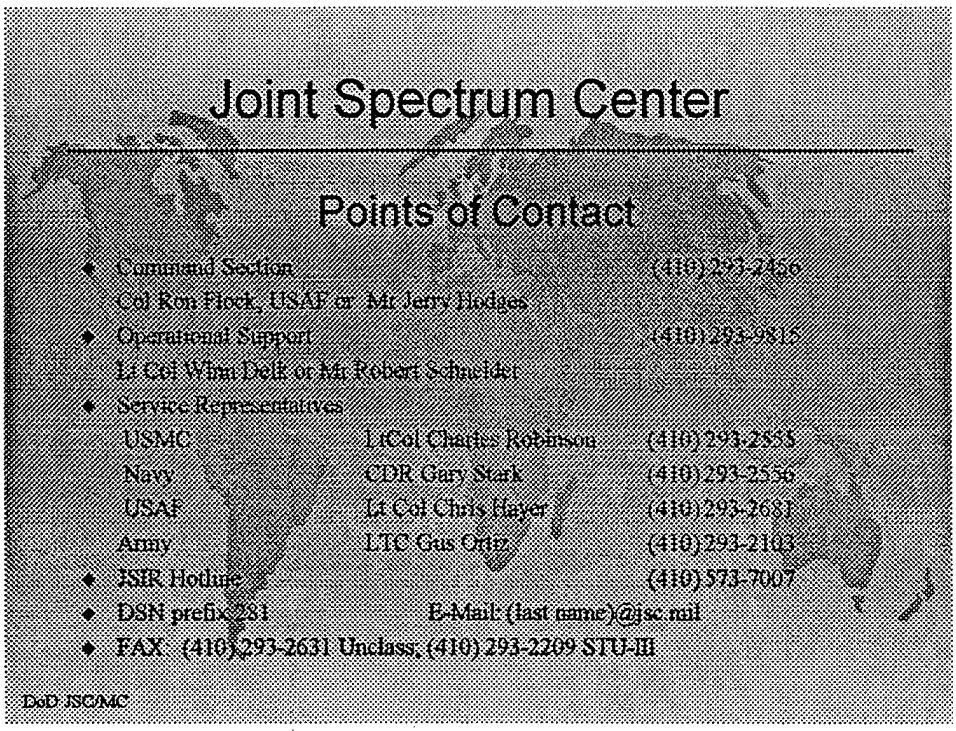
Joint Spectrum Center
Points of Contact
◆ Command Section (410) 293-2456
Col Ron Flock, USAF or Mr Jerry Hodges
◆ Operational Support (410) 293-9815
Lt Col Wini Delf or Mr Robert Schneider
◆ Service Representatives
USMC LtCol Charles Robinson (410) 293-2533
Navy CDR Gary Stark (410) 293-2556
USAF Lt Col Chris Hayer (410) 293-2681
Army LTC Gus Ortiz (410) 293-2103
◆ JSIR Hotline (410) 573-7007
◆ DSN prefix 281 E-Mail: (last name)@jsc.mil
◆ FAX: (410) 293-2631 Unclass; (410) 293-2209 STU-III
DoD JSC/MC

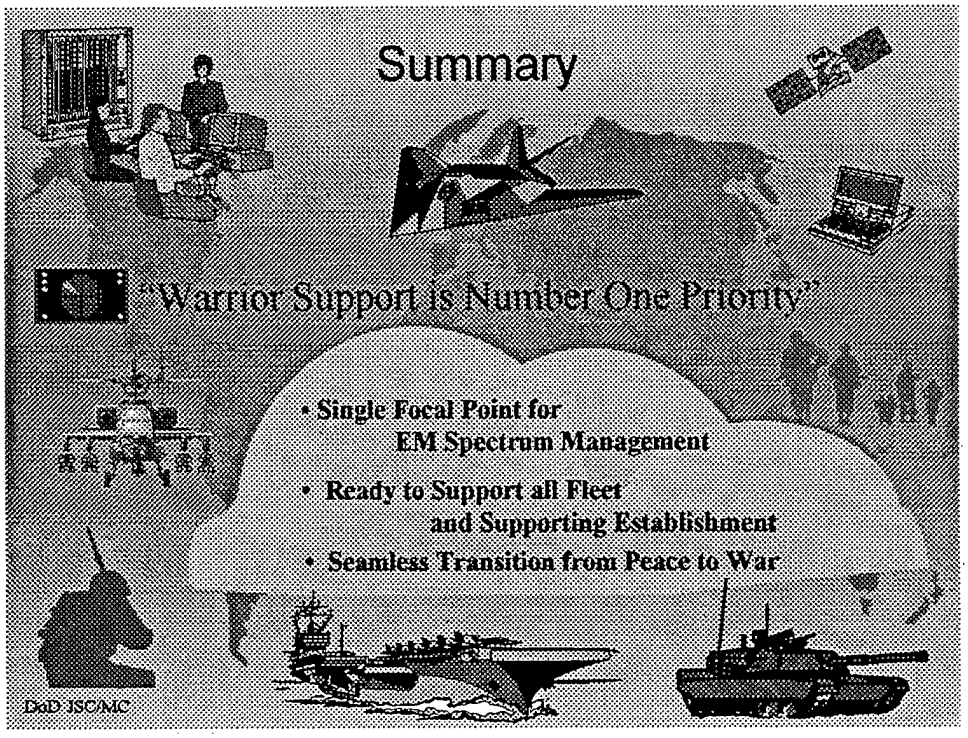
Summary
"Warrior Support is Number One Priority"
• Single Focal Point for
EM Spectrum Management
• Ready to Support all Fleet
and Supporting Establishment
• Seamless Transition from Peace to War
DoD JSC/MC

Joint Spectrum Center
Marine Corps Directorate
◆ LtCol Charles Robinson - Director
◆ Mr Frank Tushoph - Deputy Director
◆ Mrs Judith Rmgler - Secretary
DoD JSC/MC

THE DEVELOPMENT OF AN ENVIRONMENTAL ELECTRO-MAGNETIC MODELLING SYSTEM (EEMS) FOR THE UK ROYAL NAVY

CDR Simon Bevan, RN
David Lewis
Commander in Chief Fleet Staff
Eastbury Park
Northwood
Middlesex HA63HP
United Kingdom
Tel: UK 01923-837360
Fax: UK 01923-837455
email: fleet@fwoc.demon.co.uk

The Royal Navy strategy for developing EEMS exploits recent developments in EM modelling and tactical display techniques to provide operational support in a timely manner. This paper will describe the three phase approach adopted to develop EEMS for RN service.

The emphasis for the first phase has been to make the propagation algorithms more computationally efficient incorporating a range-independent hybrid (PE/raytrace) model which includes terrain. The second phase will focus on developing the fast algorithms required to process elevated antenna propagation-loss (>5000 ft), range dependency and a prototype human computer interface. The final phase will add a communications application and complete the system integration which includes the incorporation of the tactical display system.

The availability of environmental, sensor and threat information is essential. Current radar performance prediction does not consider target speed, aerial rotation rate or operator performance - the factors which define the actual dynamic situation that determines the tactical radar range. Work is progressing towards integrating these key aspects into EEMS to enhance the display of tactical data. The tactical display module uses Blip-Scan techniques to transform the path-loss along a threat profile to a cumulative frequency distribution of probability of target injection into the command decision information system versus range. from which other tactical data can be derived.

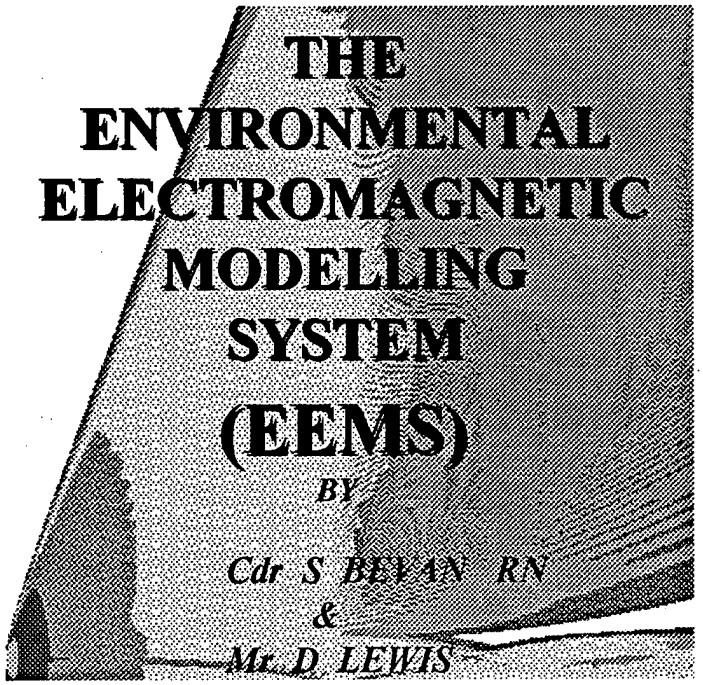

"The Royal Navy's Replacement For The Integrated Refractive Effects Prediction System (IREPS)."

THE AIM OF EEMS:

* THE IREPS REPLACEMENT
* BENEFIT FROM IMPROVED MODELLING
* A REAL-TIME SYSTEM
* IMPROVED TACTICAL ADVICE

EEMS COMPONENTS:

* RADAR PROPAGATION MODEL
* TACTICAL DISPLAYS
* HF COMMS MODEL
* LINKS TO TERRAIN DATABASE
* EO TACTICAL DECISION AID

DEVELOPMENT PHASES:

* PHASE 1 (Jul 95)
  - PROTOTYPE RADAR PROP'N MODEL
  - DEVELOPMENT OF TACTICAL DISPLAYS

* PHASE 2 (Est end 95)
  - ENHANCEMENTS TO RADAR MODEL
  - PROTOTYPE HCI

* PHASE 3 (Est mid 96)
  - HF COMMS MODEL
  - FINAL INTEGRATION

PRESENTATION OUTLINE:

* CONCEPTS FOR RADAR PROPAGATION MODEL DEVELOPMENT

* TACTICAL DISPLAYS

* MEASURES OF EFFECTIVENESS

* PLATFORM STATIONING

* PLANNED DEVELOPMENT

RADAR PROPAGATION:

* ACCURACY vs TIME
  - MORE ACCURATE THAN IREPS
  - OPERATE IN REAL-TIME
  - ACCEPT TERRAIN DATA
  - CONSIDER ELEVATED ANTENNAS
  - RANGE DEPENDENT

* TWO APPROACHES

* RESULTS
  - BOTH GIVE TIMELY RESULTS
  - FUNDAMENTAL IS Hi-Fi
  - PC-PEM (6 Hrs), EEMS (<40 Secs)

RANGE DEPENDENCY:

* ENVIRONMENT DATA (MET):
  - LAND BASED RADIO-SONDE
  - RN AUASS AFLOAT
  - NUMERICAL WEATHER PRODUCTS
  - SURFACE OBSERVATIONS

* ENVIRONMENT DATA (TERRAIN):
  - DIGITAL TERRAIN ELEVATION DATA
  - VECTOR PRODUCT FORMAT

RANGE DEPENDENT PROFILE:

* AUTOMATIC (Interpolation)
  - NWP OUTPUT (17 km Spacing 31 levels, 11 levels < 1500m)
  - DTED / VPF

* MANUAL (Step)
  - AUASS
  - AUASS / LAND ASCENT

TACTICAL DISPLAYS:

* VERTICAL COVERAGE DISPLAYS
  - PATH-LOSS PROFILE
  - SUBJECTIVE ASSESSMENT

* POST PROCESSING ROUTINES
  - PREDICTIVE DETECTION RANGES OF AIRBORNE TARGETS IN OPERATIONAL REGIMES (PREDATOR)
  - PREDATOR RADAR MODEL (PRAM)
  - OBJECTIVE ASSESSMENT
  - RADAR OPERATOR & EQUIPMENT

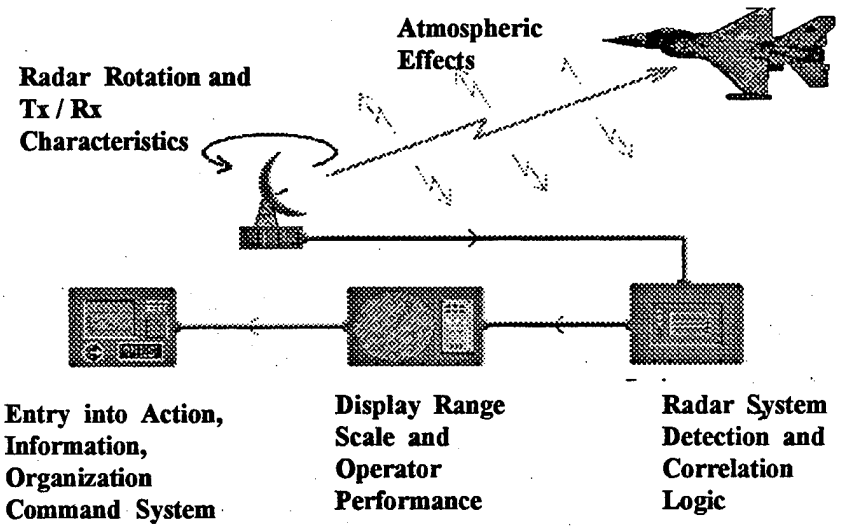

TDRSS:

(TARGET DETECTION RANGE SOFTWARE SUITE)

* PRAM
  - CONVERTS PATH-LOSS TO P(Detection)
  - CALCULATES CONTINUOUS CURVE

* PREDATOR
  - CONSIDERS THE DYNAMIC SITUATION
    * RADAR ROTATION
    * TARGET SPEED
    * DETECTION LOGIC
  - TACTICAL RADAR RANGE
  - PLATFORM STATIONING

MEASURE OF EFFECTIVENESS:

* PROBABILITY OF DETECTION

"The Range for a given probability a static target will be illuminated and provide a paint on the operator's display."

* TACTICAL RADAR RANGE

"The range for a given probability that a valid contact is recognized by the operator and injected into the tactical command system."

PROBABILITY OF DETECTION:

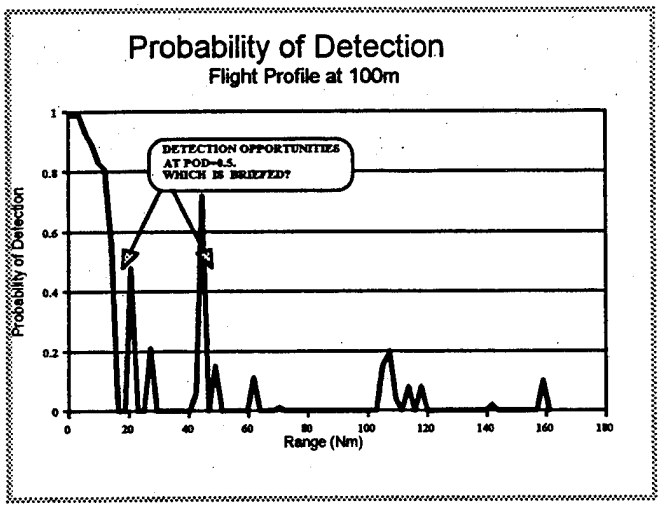

PREDATOR:

* USES FLIGHT TRAJECTORY PATH-LOSS

* ADDS SCENARIO DYNAMICS
  - RADAR ROTATION RATE
  - VALID CONTACT CRITERIA (n OUT OF m)
  - OPERATOR EFFICIENCY
  - OPERATOR DELAYS
  - RADAR RANGE SCALES
  - TARGET SPEED

TACTICAL RADAR RANGE:

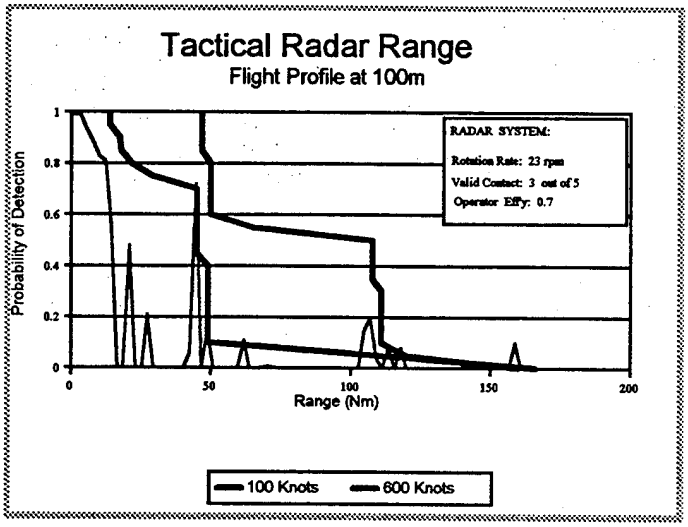

INBOUND TARGET:

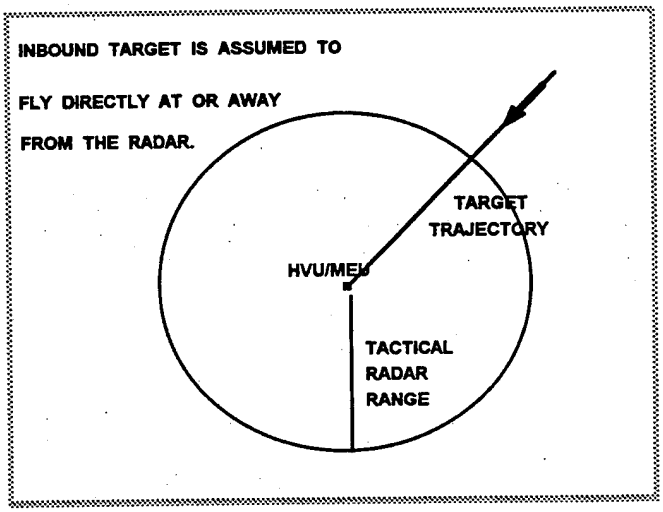

CROSSING TARGETS:

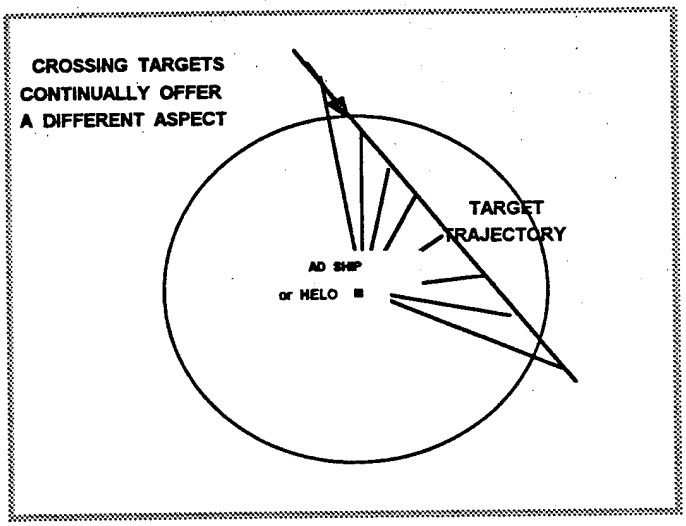

DEVELOPMENTS IN TDRSS:

* CROSSING MODELS:
  - TARGET RCS POLAR DIAGRAM
  - TARGET RANGE AND BEARING
* INITIAL PROTOTYPE DEVELOPED
* TRACKING PROBABILITY?
* STATIONING TACTICAL DECISION AID

EEMS SUMMARY

1. RANGE DEPENDENT MODELS
2. TACTICAL PLANNING FOR ABOVE WATER WARFARE
3. FURTHER DEVELOPMENTS TO SUPPORT:
   - HF COMMS, EO AND TERRAIN DATA HANDLING
   - FULL RANGE DEPENDENCY
   - PLATFORM STATIONING

The UK Environmental EM Modelling System (EEMS)

K.H. Craig and M.F. Levy
Signal Science Ltd and Rutherford Appleton Laboratory
U.K.

A new operational EM propagation forecasting system is being developed for the Royal Navy in the UK. The requirement is for fast computation, modelling of both oversea and overland propagation (with emphasis on the littoral region), integration of various sources of meteorological data (surface, radiosonde, mesoscale model output), and various output options to support more specialised tactical decision aids.

The system has several components:

(1) Radar, system and meteorological parameter editors to simplify the entry, validation and display of the necessary environmental and system data. These will also provide the necessary interfaces to GIS terrain and clutter databases, and to mesoscale model output.

(2) The propagation module, that uses an efficient parabolic equation/ray optics hybrid model for sea/terrain propagation. The module includes deterministic modelling of atmospheric refraction and ducting, terrain diffraction and gaseous absorption.

(3) Output and display modules. These include the normal vertical coverage diagram and path loss versus range and height displays, and provide an interface to the tactical decision aids, such as PREDATOR.

The system is windows based and is initially being developed for use on PC systems. However the architecture and software are designed to be easily ported to other windows-based hardware and operating systems. The EEMS prototype will be demonstrated at the Workshop. The first fully operational version should be installed by the end of this year.

The UK Environmental EM Modelling System (EEMS)

K.H. Craig and M.F. Levy
Signal Science Ltd
and
Rutherford Appleton Laboratory
U.K.

SSL/RAL

Development of PE-based Propagation Tools

- Assessment tools
  - PCPEM (1989)
  - FDPEM (1991)
- Nearshore EM Propagation Study (94/95)
- Operational tools
  - EEMS Phase 1 (Jul 95)
  - EEMS Phases 2/3 (mid 96)

SSL/RAL

Assessment v Operational Requirements

- Assessment Tool
  - System design
  - Trials analysis
  - Off-line analysis
  - Accuracy
  - "Expert" user
  - Simple interface is adequate
- Operational Tool
  - Tactical decision aid
  - Real-time results
  - Speed
  - "Non-expert" user
  - High quality data integration/display

SSL/RAL

PCPEM

- Assessment tool
- Pure split-step parabolic equation
- Overwater propagation only
- Several marine environment atmospheric models (including 2-dimensional profiles)
- Slow (PC + transputer) for
  - large domains
  - large beamwidths
  - high frequencies

SSL/RAL

```
                    PCPEM FIELD GENERATOR
        Version 2.1  -  Copyright (c) Signal Science Ltd 1989,1990

 Output filename                                  pem.fld
 Antenna parameters
 Range/height parameters
 Refractivity option                        * 1D evap duct by met params
 FFT/Beamwidth selection                    * Automatic
 Ground type                                * Sea water
 Roughness type                             * Wind speed
 Millimetre wave absorption parameters

 Sea temperature                  C      15.000
 Air temperature                  C      15.000
 Relative humidity                %      90.000
 Wind speed                       m/s    10.000
 Sea level pressure               mb     1013.250
 Height of measurements           m      10.000

                  Parameter limits
                  0.0          50.000

 F1:run  F2 run+display  F3:loop  F4:batch  F5:defaults  F8:config  F10:quit
```

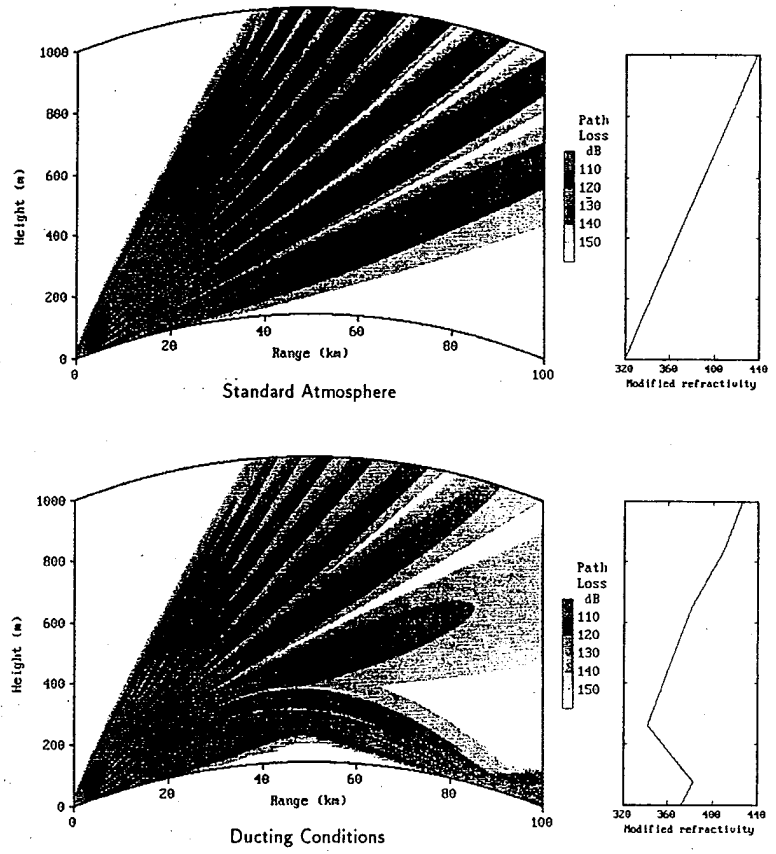

Electromagnetic Coverage Diagrams

FDPEM

- Assessment tool
- Pure finite difference parabolic equation
- Terrain propagation (diffraction)
- 1- and 2-dimensional numerical refractivity profiles
- Very slow (PC + Transputer) for
  - large domains
  - large beamwidths
  - high frequencies

SSL/RAL

EEMS Propagation Model Phase 1 Requirements

- Prototype radar propagation model
  - demonstrate speed (hybrid algorithms)
  - only surface ships and AEW helicopters required
  - nearshore operations - terrain capability essential
- Prototype user interface
  - support for propagation "engine"
  - ease data input (especially met data)

SSL/RAL

EEMS Propagation Engine

- Hybrid propagation model
  - Vertical parabolic equation
  - Horizontal parabolic equation
  - Ray optics
  - Fast execution (standalone PC)
- Overwater/nearshore/inland capability
  - Evaporation duct model and upper air data
  - Terrain masking/diffraction

SSL/RAL

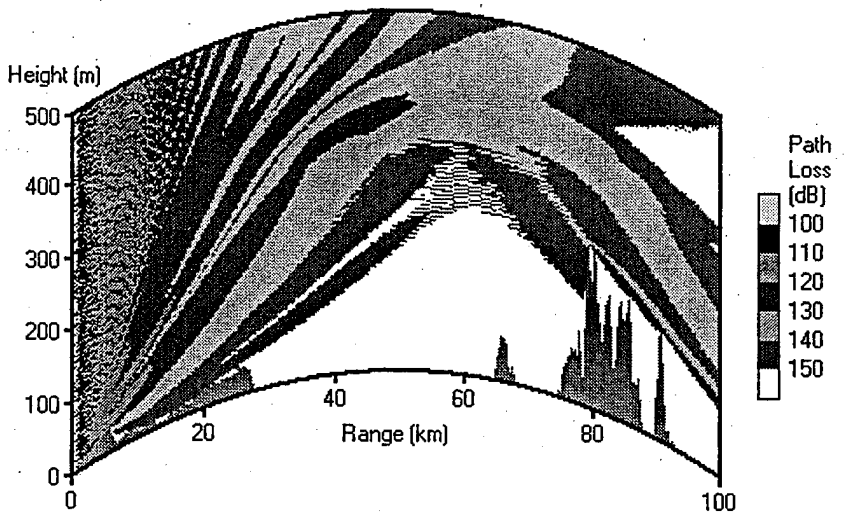

EEMS Execution times

	3 GHz	10 GHz
Surface radar	< 10 s	< 10 s
Helicopter AEW (3000 ft)	3 m	8 m
[Phase 2	15 s	15 s]
E-3 (30,000 ft)	30 m	> 1 h
[Phase 2	< 1 m	< 1m]

SSL/RAL

EEMS Structure

- EEMS Engine
  - Can incorporate any propagation model (eg EEMS, RPO)
- EEMS Tools
  - Met data and system editors
  - Coverage diagram displays
  - Path loss displays
  - Links to PREDATOR
- Windows based and portable
  - support for PCs and UNIX workstations

SSL/RAL

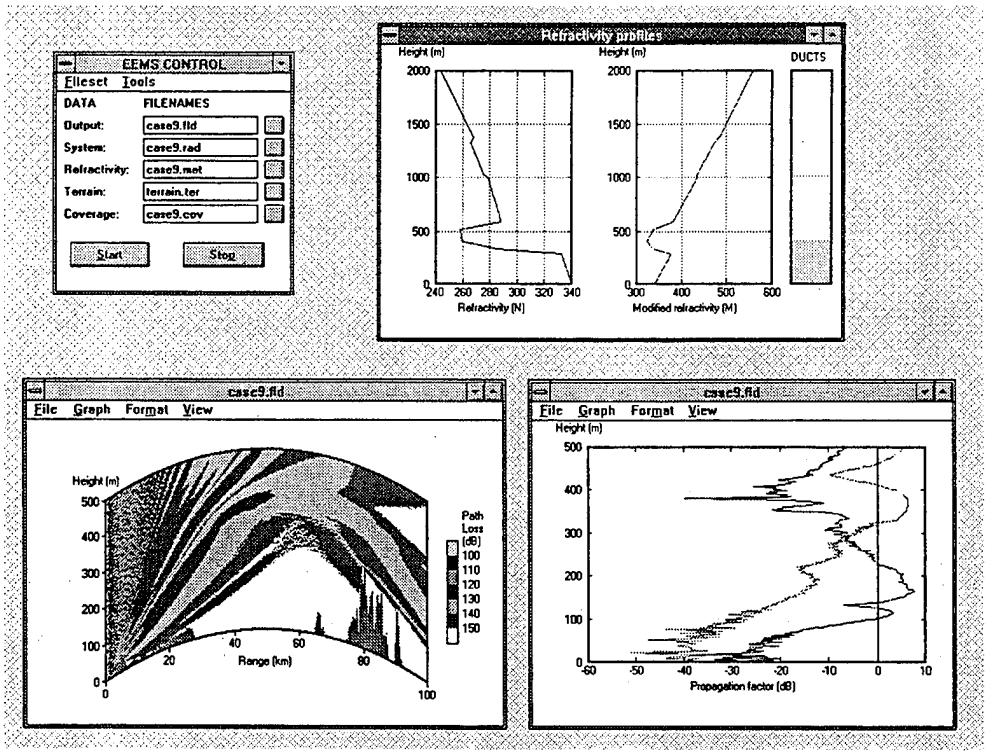

Meteorological Data (Phase 1)

- Manual entry via Met editor
- Upper air data (1D)
  - WMO TEMP code
  - P/T/RH or N/M ascents
  - k-factor
- Evaporation duct (1D)
  - Surface parameters (Battaglia model)
  - Duct height
- Profile merging

SSL/RAL

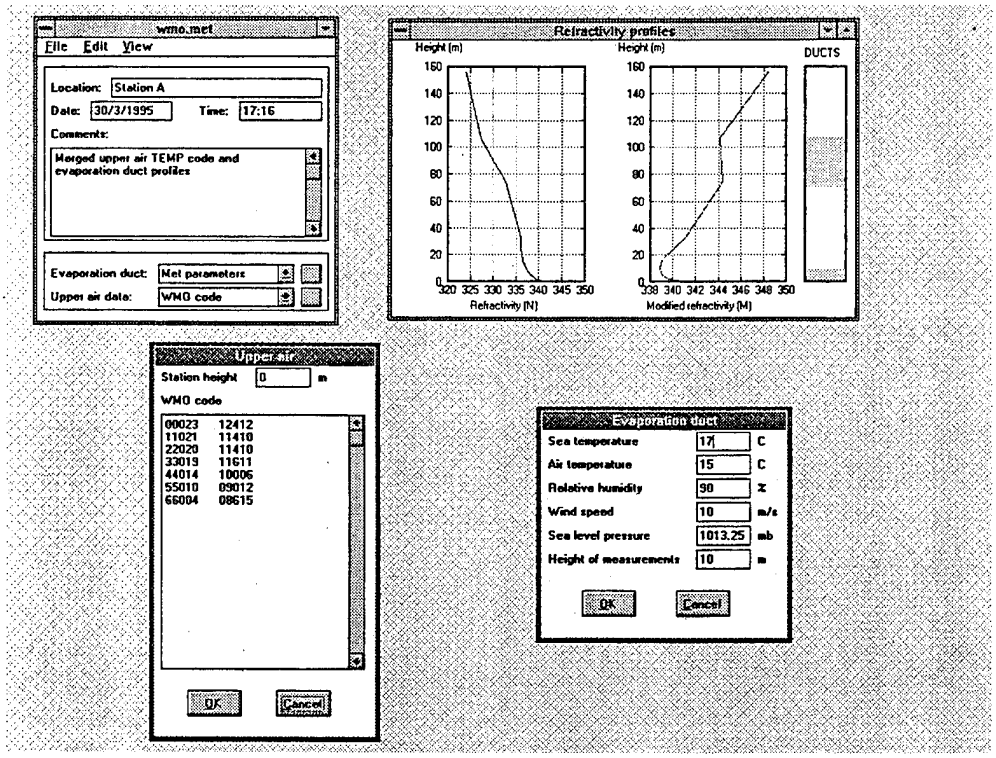

Meteorological Data (Phase 2/3)

- 2/3D capability
- Link to numerical weather model gridded data
- Coastal zone models

SSL/RAL

System Data

- Phase 1
  - Basic RF system and antenna parameters
  - Definition of radar search domain
- Phase 2
  - Radar detection and target parameters

SSL/RAL

Terrain data

- Phase 1
  - File input (prepared off-line; FDPEM format)
  - Assumes perfectly conducting, smooth ground
- Phase 2
  - Surface roughness, electrical parameters
- Phase 3
  - Links to GIS/terrain (and clutter?) database
  - Radar clutter modelling

SSL/RAL

EEMS Displays

- Coverage diagrams
- Path loss displays

Loss type	Trajectories
path loss	horizontal
propagation factor	vertical
field strength	ground-following
	user-defined (PREDATOR)

SSL/RAL

Attack profiles

- Blue line
  - constant level approach: 100m
- Green line
  - initial approach: 500m
  - final approach: 100m

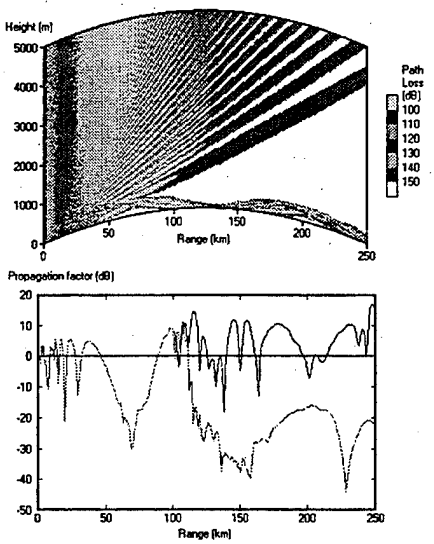

Validation

- PCPEM
  - RN trials: used for forecasting during Gulf hostilities in 1991
  - RAL/MRF airborne trials
  - Overwater path data 3-94GHz (NATO Panel 3/RSG8 of AC 243)
- FDPEM
  - Extensive testing on UK diffraction path data (including terrain cover data)
- Extensive model intercomparisons

SSL/RAL

EEMS Propagation Model Conclusions

- Phase 1 completed
  - Includes both terrain and meteorology for naval nearshore operations
  - Fast hybrid propagation algorithms demonstrated
  - Prototype user interface developed
- Phase 2/3
  - Extend fast hybrid algorithms to high antennas
  - Enhance interfaces (user and database)
  - More "engines" (eg HF comms/groundwave, RPO)
  - Port model to other computing environments

SSL/RAL

Dr. Ken Craig, "The UK Environmental EM Modelling System (EEMS)"

DISCUSSION

M. PASTORE
Have there been any sensitivity studies done in littoral areas to understand the temporal/spatial environmental inputs required to obtain valid propagation model output?

AUTHOR'S REPLY
We have not looked at this specifically for littoral regions. Ted Rogers' talk tomorrow on the VOCAR results addresses your question.

K. ANDERSON
Can you describe how you merge the surface and mixed layers?

AUTHOR'S REPLY
The method is empirical, not meteorologically-based. The merging aims to provide a smooth transition from the evaporation duct profile to the upper air data, at a height some way above the evaporation duct height. The exception is when a surface-based ducting layer exists; in this case the model ignores any evaporation duct entered. (It is assumed that the surface duct will dominate over any evaporation duct effects; in any case the evaporation duct model is likely to be questionable under strongly stable conditions.)

D. DOCKERY
How are you determining stability for the purpose of deciding whether to include an evaporation duct in the refractivity profile? Also, are you allowing for the simultaneous presence of surface-based and evaporative ducts?

AUTHOR'S REPLY
See answer to K. Anderson's question.

H. HITNEY
Does your PE model account for terrain that begins at zero range?

AUTHOR'S REPLY
The PE model itself will cope with terrain at zero length. The difficulty is with the ray optics part of the hybrid model. The Phase 1 model is only intended for emitters located over the sea (although it of course handles terrain remote from the emitter; for surface emitters, 1-2 km of flat surface "starter" seems to be adequate). This limitation should be removed in Phase 2.

SEAWASP AN/SPY-1B TACTICAL DECISION AID

Gerald C. Konstanzer
Johns Hopkins University Applied Physics Laboratory
Johns Hopkins Road
Laurel, MD 20723
(301)953-7518
G_C_Konstanzer@aplmail.jhuapl.edu

The Johns Hopkins University Applied Physics Laboratory (JHU/APL) is tasked by the AEGIS Shipbuilding Program (PMS-400) to lead the development of a prototype tactical decision aid for in situ assessment of radar and weapon system capability. The system under development is called SEAWASP (Shipboard Environmental Assessment & Weapon System Performance). SEAWASP is initially being designed to assist the AN/SPY-1B Radar System Controller (RSC) in understanding the impacts of selected radar doctrine and prevailing environmental conditions on AN/SPY-1B performance. To do this, SEAWASP processes environmental measurements, computes propagation factors and AN/SPY-1B firm track ranges, and presents radar performance estimates to the RSC via an interactive graphical user interface. Developmental versions of SEAWASP's environmental assessment subsystem have been field tested on AEGIS cruisers five times; the full system, which includes the radar performance assessment capability, has been to sea twice. As the system matures, optimal radar doctrine recommendations will be generated automatically and other aspects of weapon system performance, such as engageability, will be addressed. This presentation will describe the various elements of SEAWASP and discuss results indicating SEAWASP's capability to accurately predict observed AN/SPY-1B firm track performance.

SHIPBOARD ENVIRONMENTAL ASSESSMENT/ WEAPON SYSTEM PERFORMANCE (SEAWASP) AN/SPY-1B TACTICAL DECISION AID

18 JULY 1995

ELECTROMAGNETIC PROPAGATION WORKSHOP

OUTLINE:

- BACKGROUND
- SYSTEM DESCRIPTION
- AT-SEA TESTS CG 71, 68, 73, 70
- FUTURE PLAN

PROBLEM

- OPTIMIZATION OF COMBAT SYSTEM ASSETS INCREASINGLY IMPORTANT:

  -TREND IN ASCM DEVELOPMENT TOWARD INCREASED SPEEDS, DECREASED ALTITUDES & CROSS SECTIONS.

  -ASCM DETECTION RANGES SIGNIFICANTLY IMPACTED BY ENVIRONMENTAL CONDITIONS.

  -VARIABLE, CLUTTERED ENVIRONMENTS IN LITTORAL REGIONS SIGNIFICANTLY AFFECT DETECTION RANGES.

  -TIME-ENERGY RESOURCES BECOME INCREASINGLY LIMITED AS NEW ROLES FOR RADAR ARE DEFINED.

- CURRENT DOCTRINE SET WITH LIMITED ENVIRONMENTAL INFORMATION, WITHOUT FULLY KNOWING IMPACTS ON TARGET DETECTIBILITY.

AT-SEA SUPPORT

- 10 YEAR EXPERIENCE MAKING *IN SITU* SYSTEM PERFORMANCE PREDICTIONS IN SUPPORT OF FLEET EXERCISES AND SYSTEM DEVELOPMENT EFFORTS.
  - ENVIRONMENTAL SENSORS DEVELOPMENT
  - ENVIRONMENTAL CHARACTERIZATION
  - PROPAGATION ANALYSIS
  - WEAPON SYSTEM PERFORMANCE MODELS

- HELICOPTERS, ROCKETSONDES, AND/OR SURFACE SENSORS
  - -TERRIER SPG-55B TEST (OCT 84)
  - -14 AEGIS VANDAL (ER) EXERCISES (APR 85 - SEP 93)
  - -MK-92/TERRIER PR EXERCISES (SEP - OCT 86)
  - -USN/FGN MISSILE EXERCISES (MAY 87 - 92)
  - -NTU OPEVAL (APR 88)
  - -TARTAR DT (NOV 89)
  - -SPY-1B DT/OT/TVT (NOV 89 - FEB 90)
  - -CEC DT (AUG 90, FEB - JUNE 94)
  - -SM2 BLK III DT/OT (JUL 91 - AUG 91)
  - -MK-92 DT (OCT 90 - JAN 91)
  - -SETT PROGRAM (DEC 92)
  - -DDG-51 CSSQT/DT/OT (OCT 91-JAN 92)
  - -TERRIER/TARTAR TOMAHAWK EXERCISES (APR 91 - SEP 91)
  - -TERRIER DESERT SHIELD/STORM UPGRADE OPEVAL (SEP 90)

- AGREEMENT BETWEEN OBSERVED TRACK RANGE AND CALCULATED 90% FIRM TRACK RANGE FOR VANDAL(ER) TARGETS BETTER THAN 10% WHEN MEASUREMENTS TIMELY.

APPROACH

- DEVELOP PROTOTYPE TO DEMONSTRATE TECHNOLOGIES AND DEFINE REQUIREMENTS FOR AN AEGIS TACTICAL DECISION AID (TDA):
  - SHIPBOARD ENVIRONMENTAL ASSESSMENT/ WEAPON SYSTEM PERFORMANCE (SEAWASP)
  - BUILD ON CAPABILITIES DEVELOPED FOR POST-EXERCISE ANALYSIS
  - PERIODICALLY, AUTOMATICALLY UPDATE DISPLAYS OF RADAR PERFORMANCE ASSESSMENTS FOR OPERATOR SELECTED SETTINGS AND THREATS
  - SUGGEST OPTIMAL SETTINGS FOR EXISTING ENVIRONMENTAL CONDITIONS
  - DETERMINE SM-2 ENGAGEMENT CAPABILITIES/LIMITATIONS

SEAWASP CONFIGURATIONS

- AUTOMATED ENVIRONMENTAL DATA ACQUISITION SYSTEM

- USS CAPE ST GEORGE (CG 71) CSSQT	- 13 DAYS, SEP 93
- USS ANZIO (CG 68) CEC DTIIA	- 10 DAYS, APR 94
- USS ANZIO (CG 68) CEC DTIIA	- 9 DAYS, JUN 94

- INTERIM CONFIGURATION

- USS PORT ROYAL (CG 73) CSSQT	- 19 DAYS, OCT 94
- USS LAKE ERIE (CG 70) SHAREM 110	- 13 DAYS, FEB 95

- BASELINE 1 CONFIGURATION

- USS ANZIO (CG 68) DEPLOYMENT	- MID 1996
- USS CAPE ST GEORGE (CG 71) DEPLOYMENT	- MID 1996

- BASELINE 2 CONFIGURATION

-AEGIS BASELINE 6 PHASE II

CG 71 / CG 68 OVERVIEW

AUTOMATED ENVIRONMENTAL DATA ACQUISITION SYSTEM

SEP 93, CG 71, 13 DAYS, AFWTF/VACAPES

- FIRST SHIPBOARD TEST.
- COMPUTED AN/SPY-1 PROPAGATION FACTOR BASED ON ENVIRONMENTAL MEASUREMENTS.

APR 94, CG 68, 10 DAYS, VACAPES

- IMPROVEMENTS FROM CG 71 LESSONS LEARNED.
- FIRST TEST OF MET HELO DOWNLINK CAPABILITY.

JUN 94, CG 68, 9 DAYS, AFWTF

- IMPROVEMENTS FROM CG 68 LESSONS LEARNED.
- COMPARE WITH MET DATA FROM INSTRUMENTED BOAT.

SEAWASP AUTOMATED ENVIRONMENTAL DATA ACQUISITION SYSTEM

(CG 71, CG 68)

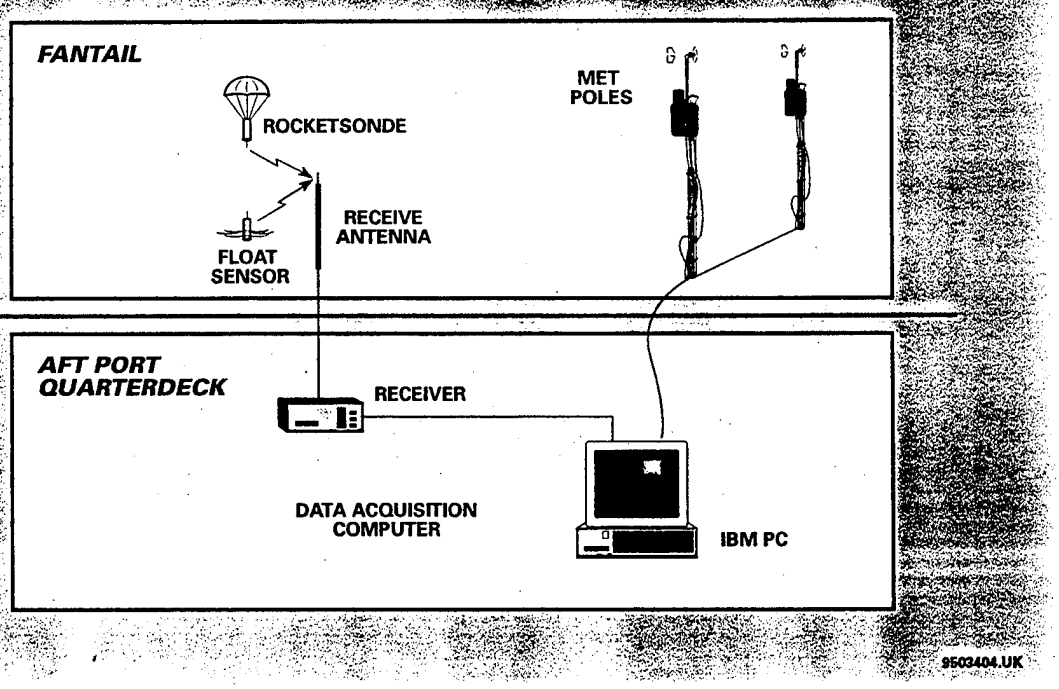

SEAWASP ENVIRONMENTAL SENSORS

- METEOROLOGICAL POLES: 1 HZ RATE
  - PORT SIDE
    - TEMPERATURE (9 m)
    - HUMIDITY (9 m)
    - RELATIVE WIND DIRECTION
    - RELATIVE WIND SPEED
  - STARBOARD
    - TEMPERATURE (9 m)
    - HUMIDITY (9 m)
    - RELATIVE WIND DIRECTION
    - RELATIVE WIND SPEED
    - GPS LATITUDE AND LONGITUDE
    - COMPASS HEADING
    - IR WATER TEMPERATURE
    - PRESSURE
- ROCKETSONDE: 0.5 HZ RATE, 2KFT MAX ALT, 7-10 FT RES
  - -TEMPERATURE
  - HUMIDITY
  - PRESSURE
- SURFACE FLOAT: 0.5 HZ RATE, 15 - 30 MIN LIFE SPAN
  - -TEMPERATURE (2 cm)
  - HUMIDITY (2 cm)
  - PRESSURE
  - WATER TEMPERATURE

METEOROLOGICAL EQUIPMENT

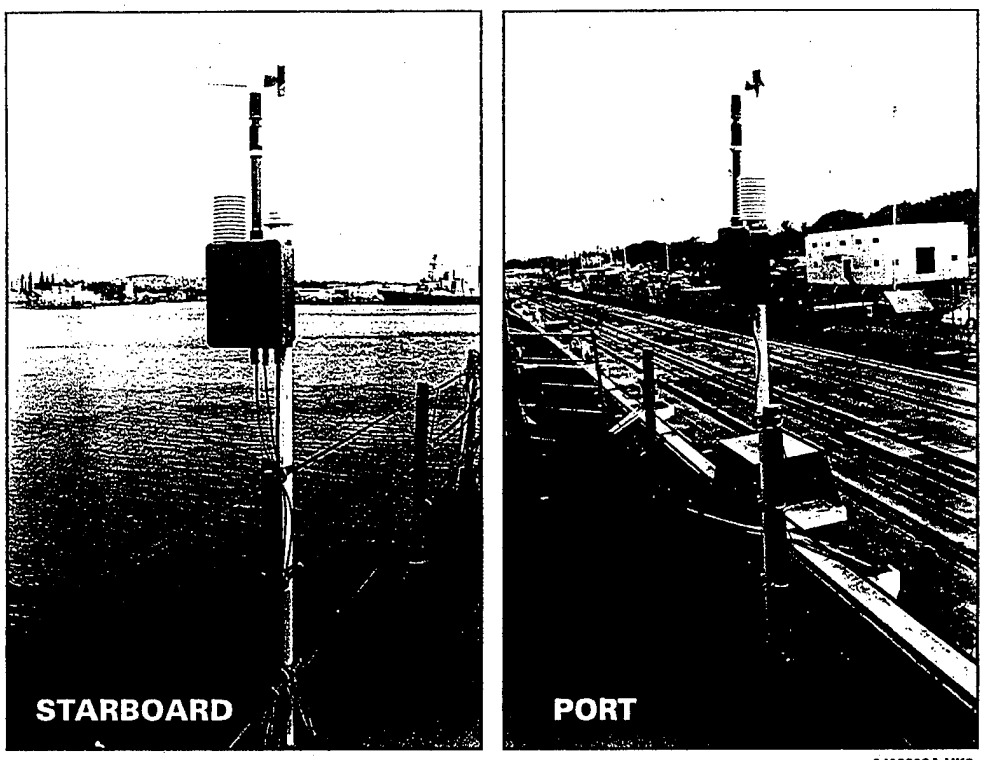

9406686A.UK2

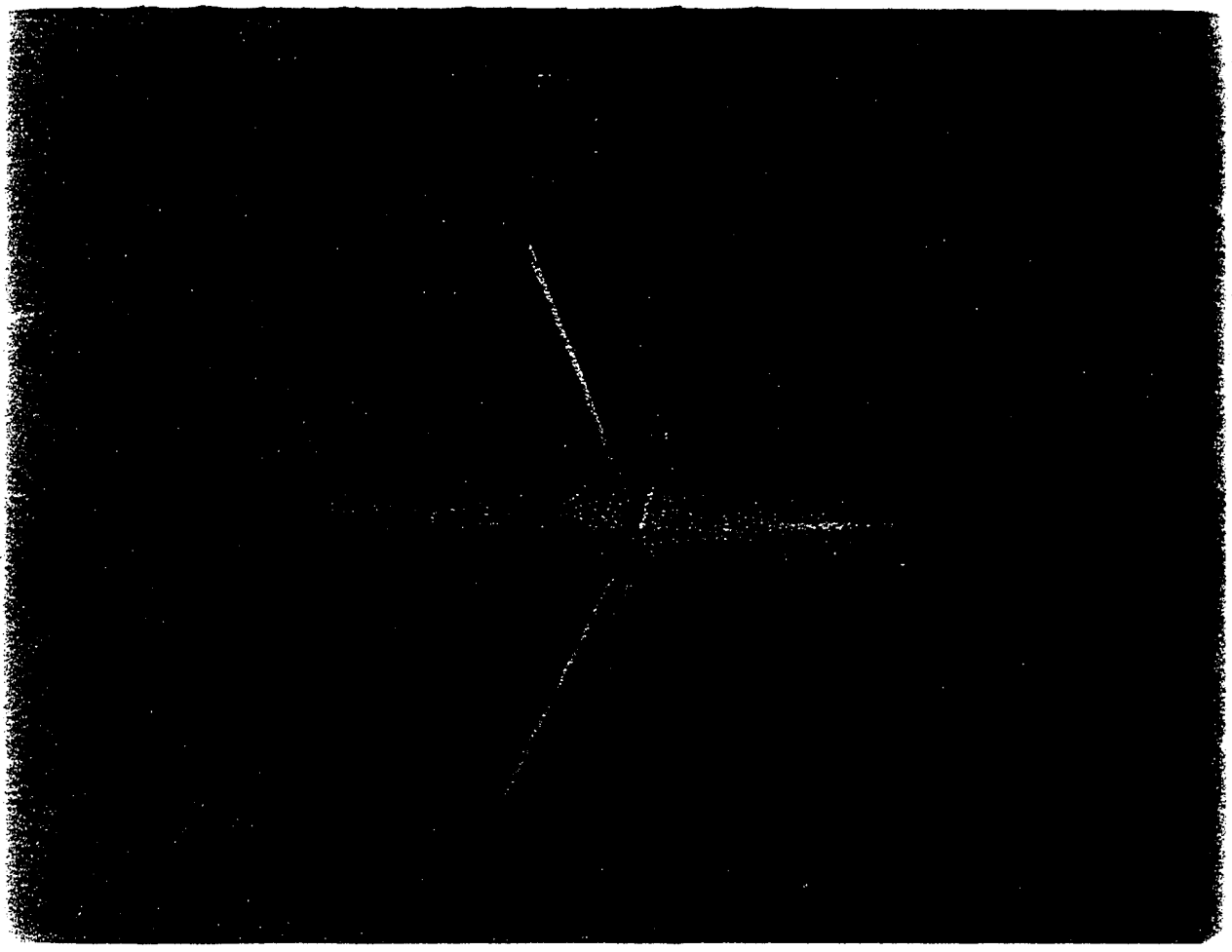

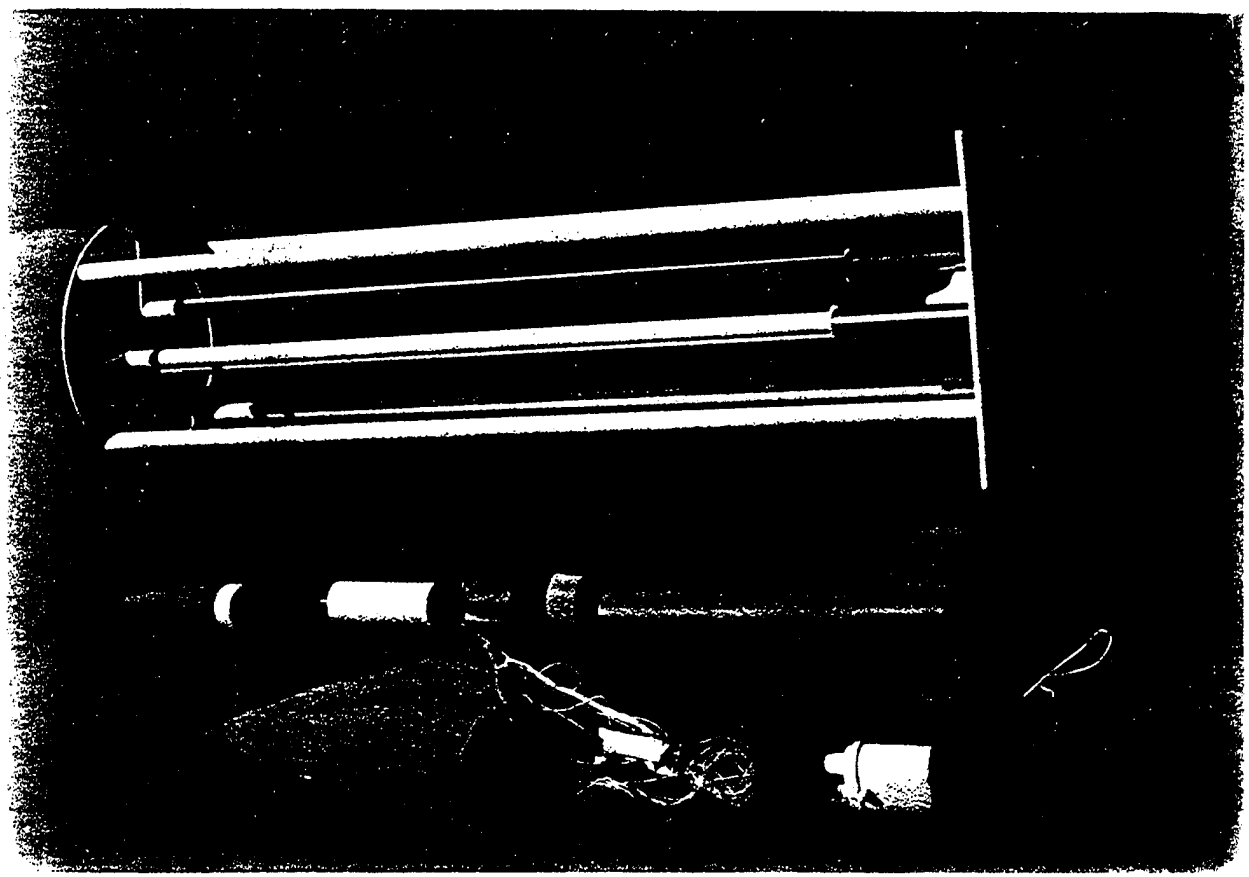

SEAWASP ENVIRONMENTAL CHARACTERIZATION

- PROCESSED MET POLE DATA: 5 MIN AVERAGE; REJECT DATA CORRUPTED BY SHIP AIRWAKE
  - AVG TEMPERATURE (9 m)
  - AVG HUMIDITY (9 m)
  - TRUE WIND DIRECTION
  - TRUE WIND SPEED
  - AVG WATER TEMPERATURE
  - AVG PRESSURE
  - GPS LATITUDE AND LONGITUDE
- SURFACE FLOAT:
  - AVG TEMPERATURE (2 cm)
  - AVG HUMIDITY (2 cm)
  - AVG PRESSURE
  - AVG WATER TEMPERATURE
- PROCESSED EVAP DUCT MODELING:
  - MODIFIED CONSTANT VIRTUAL TEMPERATURE
  - SURFACE MEASUREMENT MODEL
  - PAULUS' IREPS MODEL
- PROCESSED ROCKETSONDE:
  - FILTERED MODIFIED REFRACTIVITY PROFILE
  - MERGED WITH MODELED EVAPORATION DUCT

CG 73/CG 70 OVERVIEW

SEAWASP INTERIM CONFIGURATION

OCT 94, CG 73, 19 DAYS, PMRF

- FIRST TEST OF AUTOMATED RADAR PERFORMANCE PREDICTION AND TACTICAL DISPLAY SYSTEM.
- EXCELLENT AGREEMENT BETWEEN SEAWASP AND OBSERVED AN/SPY-1B PERFORMANCE.
- FEEDBACK ON EASE-OF-USE & TACTICAL SIGNIFICANCE OF DISPLAYS.
- TEST MAJOR UPGRADE OF DATA ACQUISITION H/W, S/W, AND MODELS.
- DEMO METEOROLOGICAL SATELLITE PICTURES DOWNLINK CAPABILITY.

FEB 95, CG 70, 14 DAYS, ARABIAN GULF / GULF OF OMAN

- FIRST TEST IN TACTICALLY SIGNIFICANT REGION
- AGREEMENT BETWEEN SEAWASP AND OBSERVED AN/SPY-1B PERFORMANCE APPEARED GOOD - VALIDATION ON-GOING.
- CONTRIBUTE ROCKETSONDE DATA TO METOC DATA BASE.

SEAWASP INTERIM CONFIGURATION

(CG 70, CG 73)

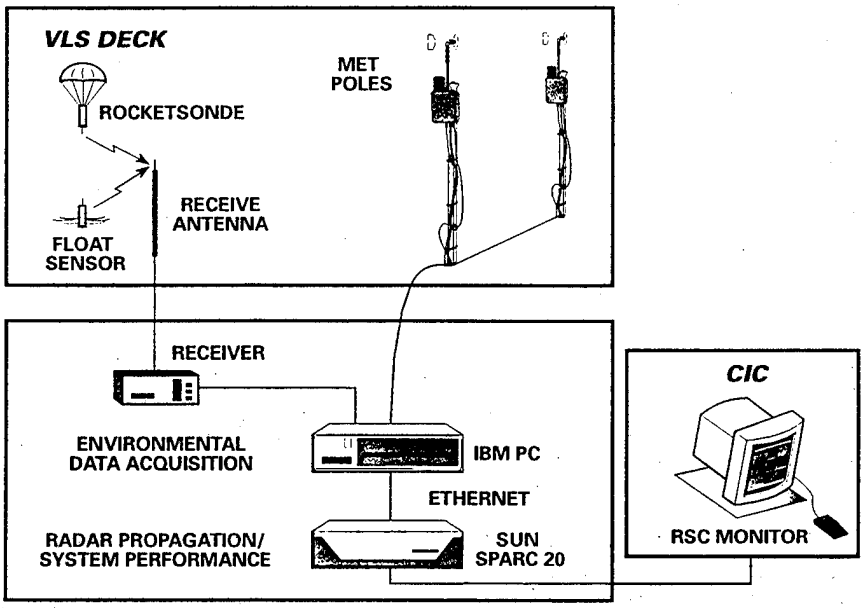

9500193A.UK

SEAWASP AN/SPY-1B PERFORMANCE ASSESSMENT

- TEMPER EM PROPAGATION PROGRAM:
  - SEAWASP ENVIRONMENTAL CHARACTERIZATION
  - AN/SPY-1B PARAMETERS
  - PROPAGATION FACTOR WITH MULTIPATH, DIFFRACTIVE, REFRACTIVE EFFECTS
- SEAWASP FIRMTRACK PROGRAM:
  - TEMPER PROPAGATION FACTOR
  - POWER
  - SENSITIVITY
  - CLEAR/ECM AHS SEARCH PATTERNS
  - PHASED ARRAY GAINS/LOSSES
  - STC FENCE DEPTH
  - HORIZON AND AH SEARCH FRAME TIMES
  - FULL TTT, TRACK MAINTAINANCE, AND DROP-TRACK LOGIC
  - SWERLING 2 TARGET FLUCTUATIONS
  - TARGET DOPPLER LOSS
  - CUMULATIVE DISTRIBUTION CALCULATION
- SEAWASP MAN-MACHINE INTERFACE:
  - OPERATOR-SELECTABLE RADAR PARMETERS
  - OPERATOR-SELECTABLE THREAT LIBRARY
  - AUTOMATED & OPERATOR INITIATED FT ASSESSMENTS
  - SINGLE THREAT & BEARING SLICE FT ASSESSMENTS

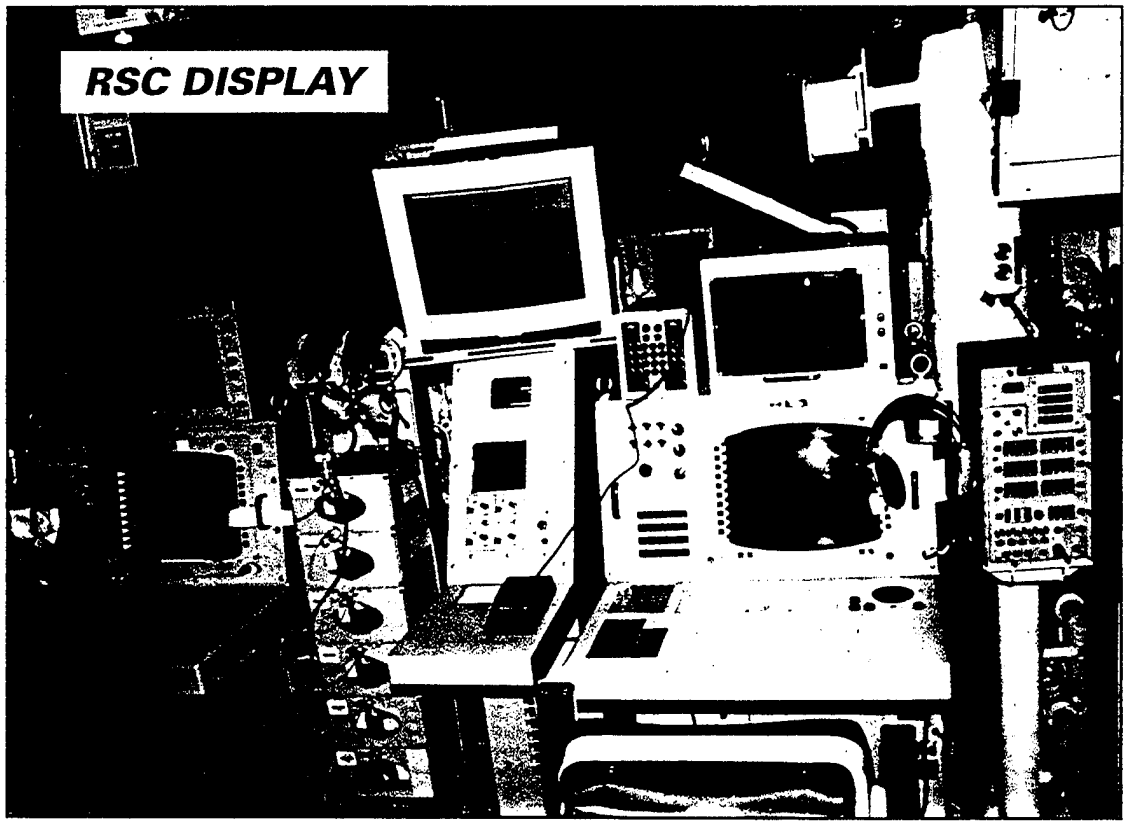

9406684.UK2

SEAWASP MAN MACHINE INTERFACE (MMI)

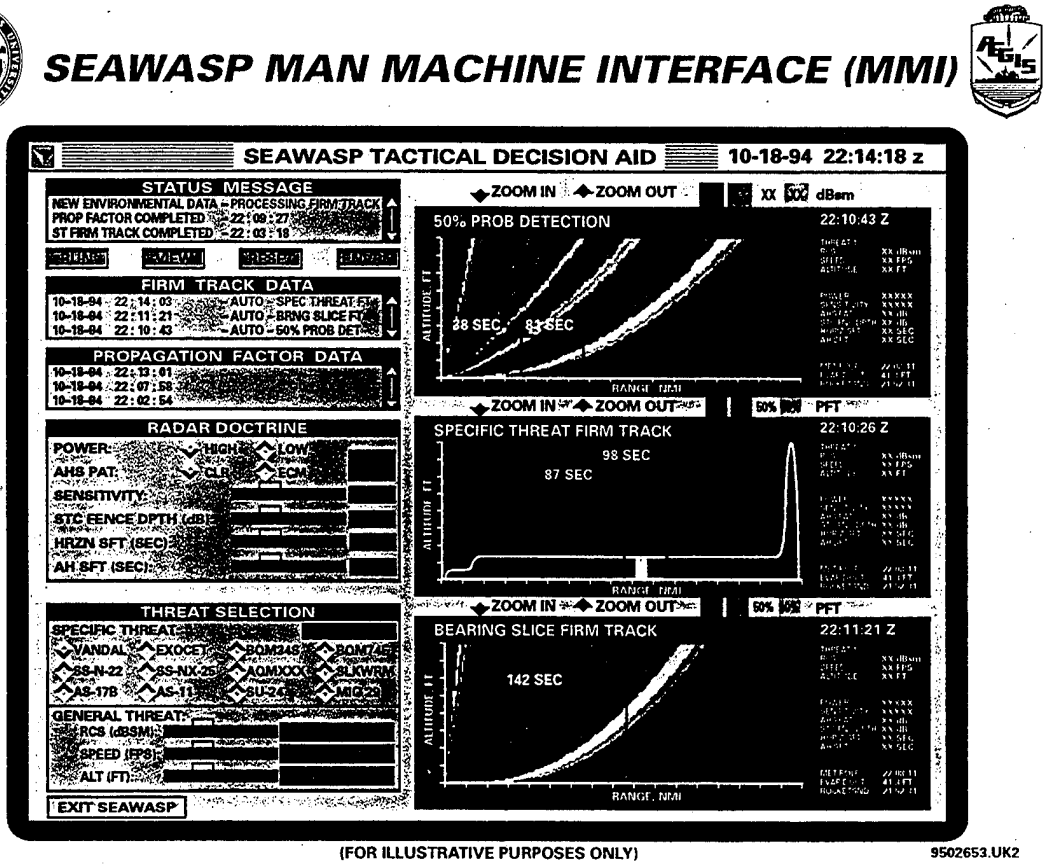

(FOR ILLUSTRATIVE PURPOSES ONLY)

9502653.UK2

CG 73 FIRM TRACK COMPARISON

PERCENT DIFFERENCE BETWEEN SEAWASP CALCULATED PROBABILITIES OF FIRM TRACK (P_{FT}) AND ACTUAL FIRM TRACK RANGES				
TARGET	SEAWASP MEASURED		STANDARD ATMOSPHERE	
	P_{FT} = 90%	10%	P_{FT} = 90%	10%
LOW, SUB	2.4	4.9	28.0	21.3
LOW, SUPER	7.3	9.7	57.6	52.8
LOW, SUB	7.8	7.9	41.0	36.2

- ALL OTHER PRESENTATIONS WERE HIGH ALTITUDE OR ECM EVENTS

PRELIMINARY CG 70 FIRM TRACK COMPARISON *

PERCENT DIFFERENCE BETWEEN SEAWASP CALCULATED PROBABILITIES OF FIRM TRACK (P_{FT}) AND ACTUAL FIRM TRACK RANGES		
TARGET	SEAWASP MEASURED	
	P_{FT} = 90%	10%
400 FT, SUB	6.2	3.1
400 FT, SUB	5.8	2.5
400 FT, SUB	0.1	5.0
600 FT, SUB	9.4	1.9
100 FT, SUB	16.4	9.1
100 FT, SUB	11.2	23.8
100 FT, SUB	21.8	14.4
100 FT, SUB	2.0	6.4

* CASES SHOWN FOR RAIDS WHEN MEASUREMENT DATA WERE TIMELY. VERIFICATION OF SEAWASP RESULTS AND A/C ALTITUDES IN PROGRESS. ACTUAL FIRM TRACK RANGES HAVE BEEN VERFIED.

SEAWASP BASELINE 1.0 CONFIGURATION

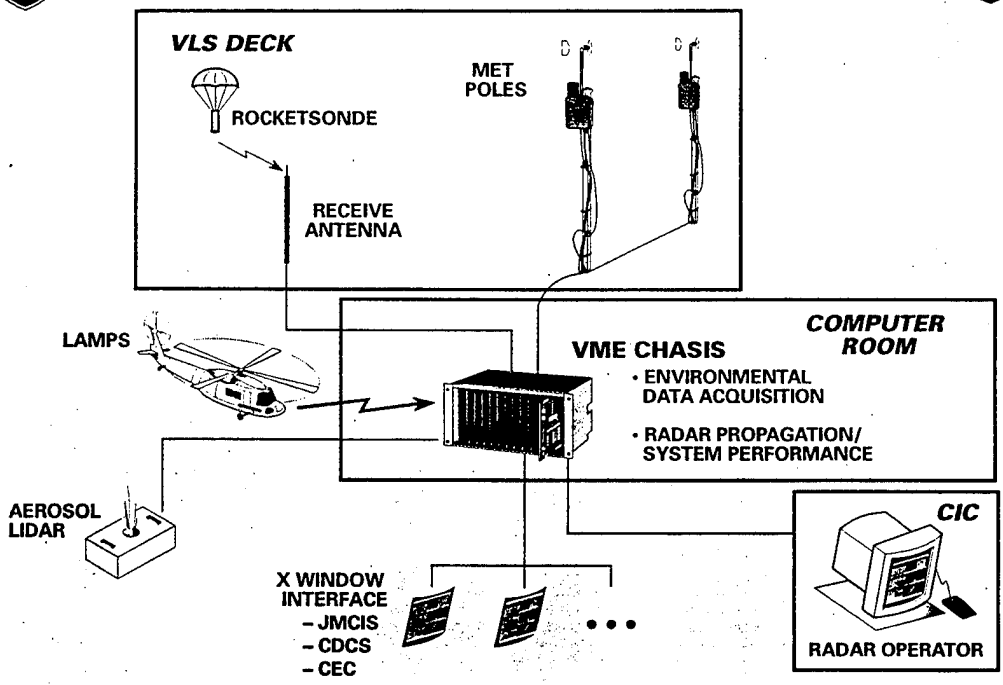

9500194A.UK

NEAR TERM PLANNED IMPROVEMENTS

- TEST CDCS INTEGRATION.
- SHIFT TO VME HARDWARE CONFIGURATION.
- IMPROVE TACTICAL DISPLAY:
  EXPANDED THREAT LIBRARY, ENVIRONMENTAL INFO SUMMARY
- INCORPORATE LESSONS LEARNED FROM ONGOING ENVIRONMENTAL DATA COLLECTS.
- SEAWASP FIRM TRACK UPGRADES:
  ECM, INTERIM SEA CLUTTER, HIGH ALTITUDE & CROSSING TARGETS
- IMPROVE AUTOMATED OPERATIONS & SPEED.
- INTEGRATE ADDITIONAL ENVIRONMENTAL DATA SOURCES:
  AEROSOL LIDAR, MET HELICOPTER, SATELLITE
- INTEGRATE TERRAIN SHADOWING/TARGET VISIBILITY BASED ON MEASURED ENVIRONMENT.
- CONTINUE IMPROVING EVAPORATION DUCT MODEL FOR ULTRA LOW HUMIDITY (GOO) CONDITONS.
- INTEGRATE NAVY STANDARD PROPAGATION MODEL (RPO).

SEAWASP BASELINE 2.0 CONFIGURATION

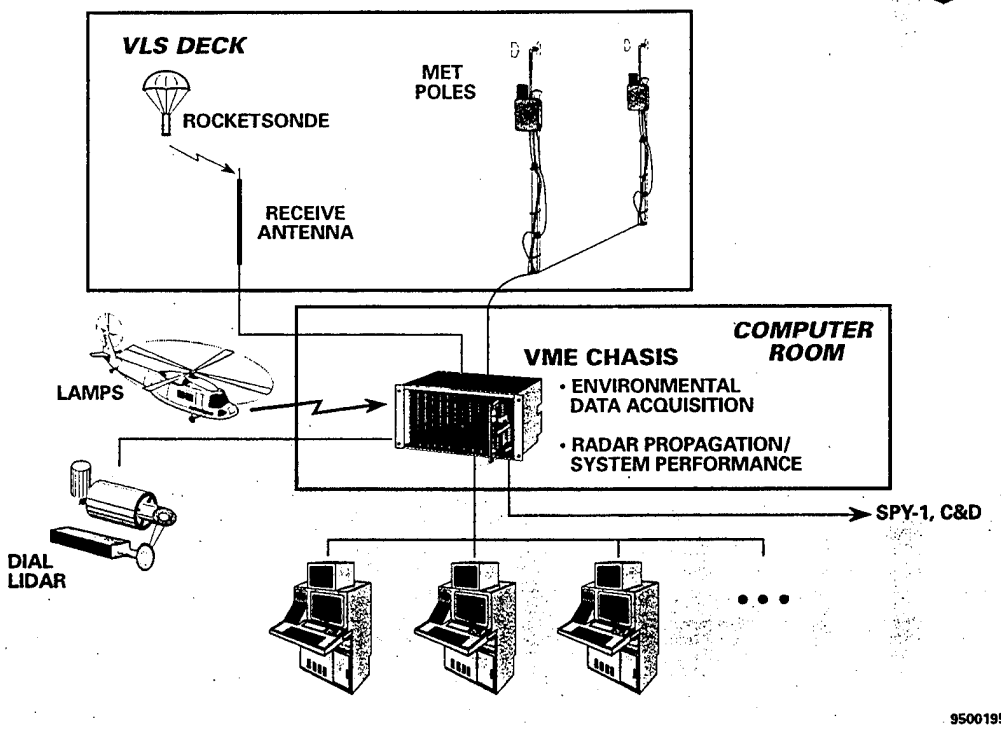

FAR TERM PLAN

- INTERFACE FOR SPY PARAMETERS (RADAR DOCTRINE, CLUTTER MAP, SPECIAL WAVEFORMS, ETC.)
- PROVIDE AUTOMATED DOCTRINE RECOMMENDATIONS.
- INCLUDE LAND AND SEA CLUTTER EFFECTS IN FIRM TRACK CALCULATIONS.
- INCLUDE SM-2 PERFORMANCE INFORMATION.
- INCORPORATE DIAL LIDAR TO CHARACTERIZE ENVIRONMENT IN 3-D NEAR SHIP.
- DEVELOP ATMOSPHERIC MODELING OF ENVIRONMENT TO AUGMENT SHIPBOARD SENSORS (E.G. OVER LAND)

SCHEDULE

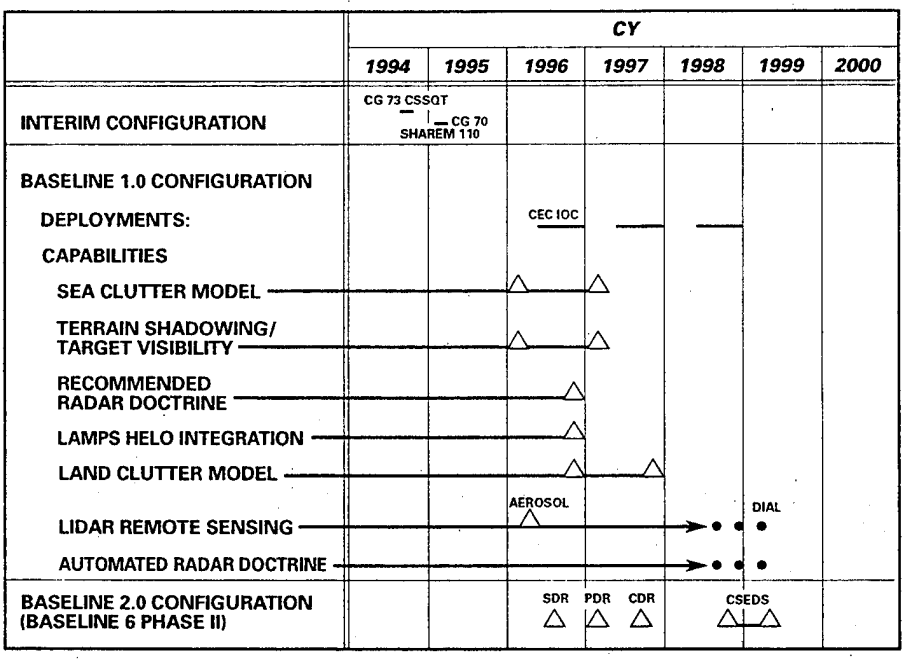

9500196A.UK

DECISION TOOL FOR OPTIMAL DEPLOYMENT OF RADAR SYSTEMS

by M.H. VOGEL
TNO Physics and Electronics Laboratory
P.O, Box 96564
2509 the Hague
the Netherlands

Phone: 31 70 326 42 21 ext. 491
Fax : 31 70 328 09 61

ABSTRACT of paper to be presented at the workshop

In many cases, a radar operator has more than one radar system at his disposal in order to search for approaching targets. These systems may differ largely with respect to transmitted power, antenna gain, frequency, polarisation, noise figure and signal processing. Further, for each radar system, the operator can choose some parameters like pulse repetition frequency. pulse length, frame time, etc. Which radar system and which set of parameters will yield the largest possibility of detection depends heavily on the actual propagation conditions (ducting!), on the target that is expected (altitude. velocity), and on the clutter from the environment.

TNO-FEL has developed a computer program called PARADE that, provided with a set of radar parameters and actual meteorological conditions, calculates coverage diagrams as a function of range and altitude. The program can also compute detection probabilities as a function of range and altitude for a given target radar cross section. Some examples will be shown, displaying the capabilities of PARADE. PARADE is currently being extended to a Decision Tool, which can advise the operator which radar system to use and which parameters to select.

In the future, it is the intention of TNO-FEL to extend PARADE with more sophisticated models for propagation and for clutter computation. A terrain database will be a very useful extension. Further, it will be investigated whether the Decision Tool can be extended with firing doctrines for semi active missiles. For all this, calculation speed is essential. This will give radar operators as well as commanders a very powerful tool which will increase platform survivability.

Decision tool for optimal deployment of radar systems

by
M.H. Vogel
TNO Physics and Electronics Laboratory

959809/V1

Radar operator can often select

- frequency
- polarisation
- pulse length and pulse repetition frequency (PRF)
- staggering of several PRF's
- frame time
- power

Selection is dependent on environment and expected target.

959809/V2

Expected targets

- fighters (many altitudes and speeds possible)
- sea-skimming missiles (both subsonic and supersonic)
- high diving missiles

959809/V3

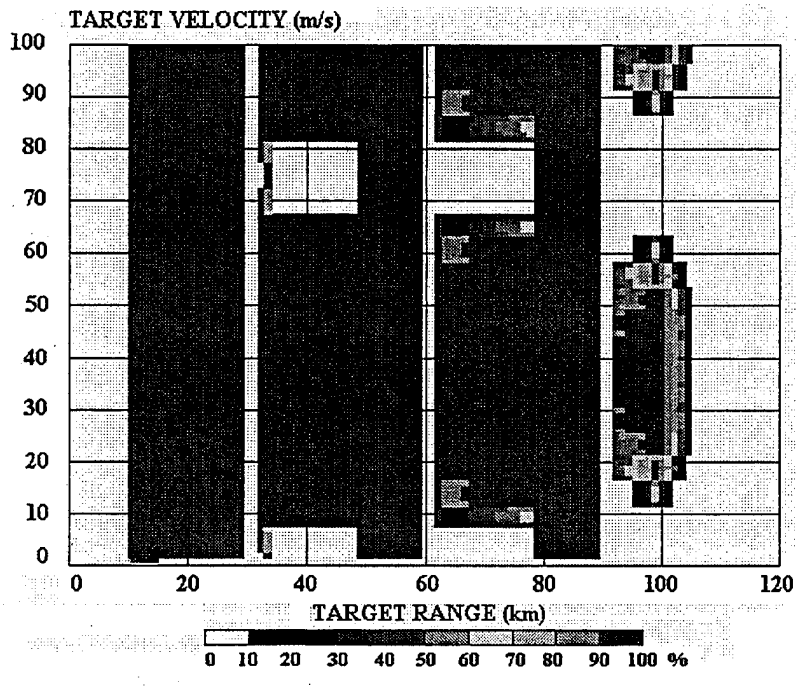

Multipath

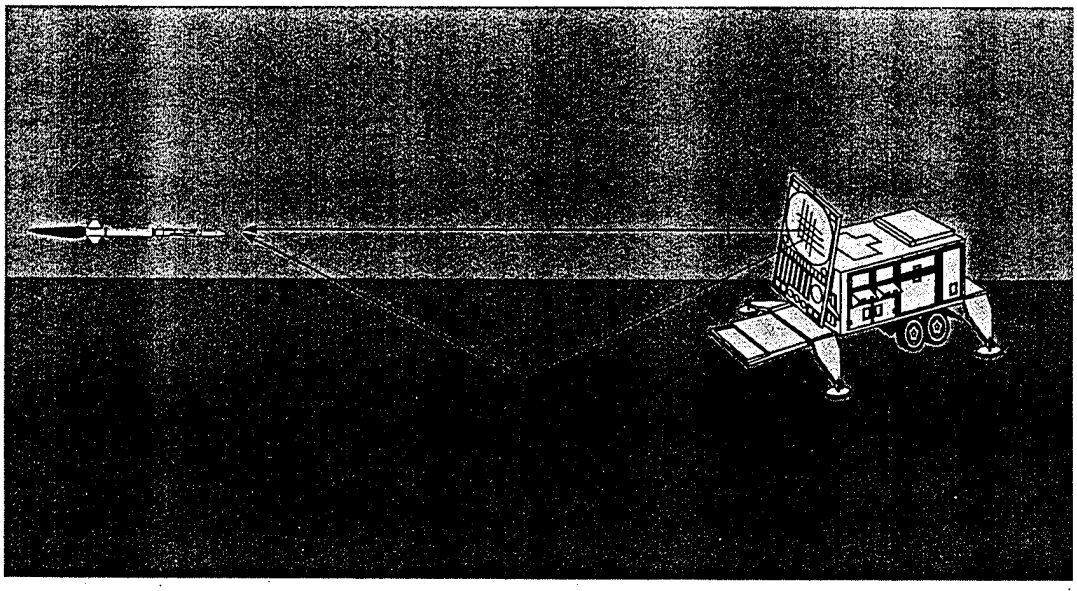

959809/V7

Evaporation Duct Height

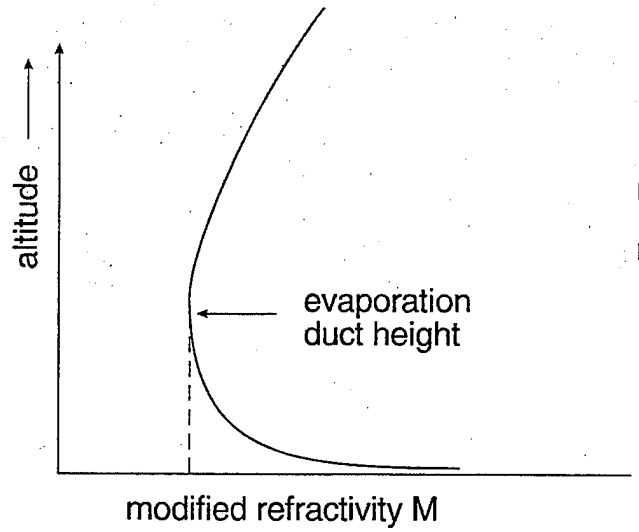

- the height at which M-gradient=0
- dependent on
  - ✓ sea water temperature
  - ✓ air temperature,
  - ✓ relative humidity
  - ✓ wind speed

93/1662

Refractivity conditions

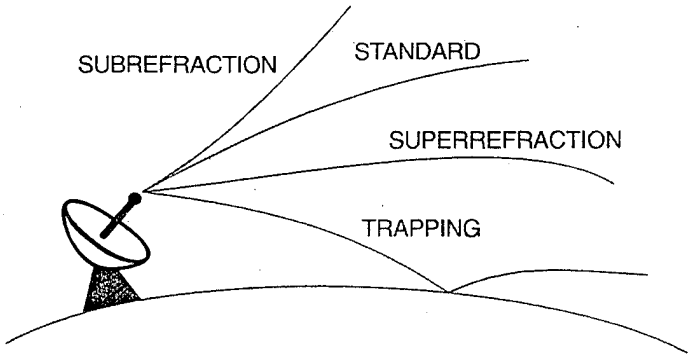

	N-gradient		M-gradient	
Trapping	<-157	N/km	≤0	M/km
Superrefractive	-157 to -79	N/km	0 to 79	M/km
Normal	-79 to 0	N/km	79 to 157	M/km
Subrefractive	>0	N/km	>157	M/km

93/1662

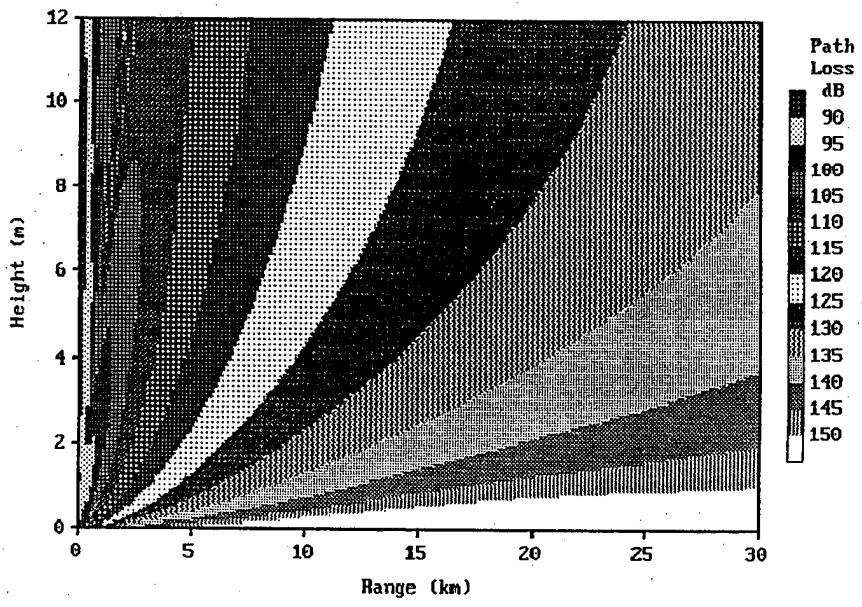

Frequency 3 GHz, Duct height 20 m.

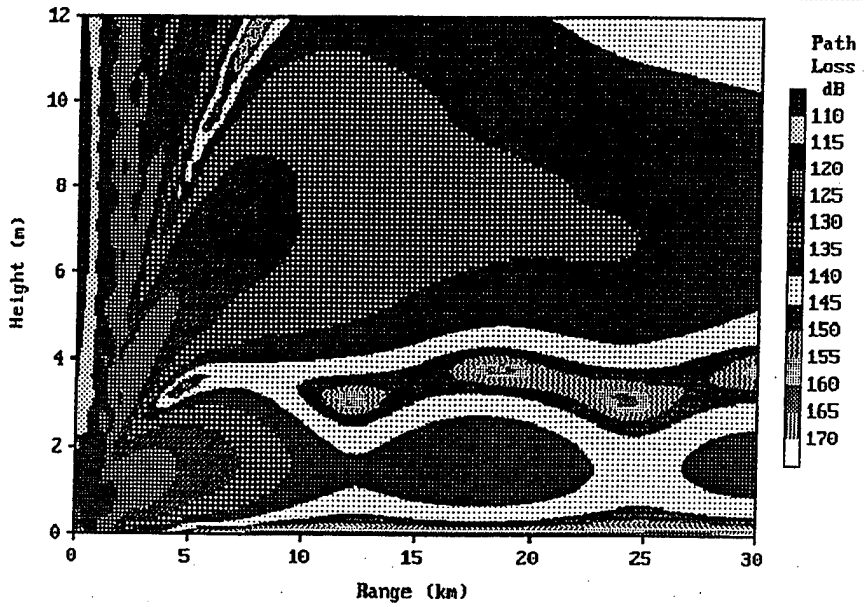

Frequency 16 GHz, Duct height 20 m.

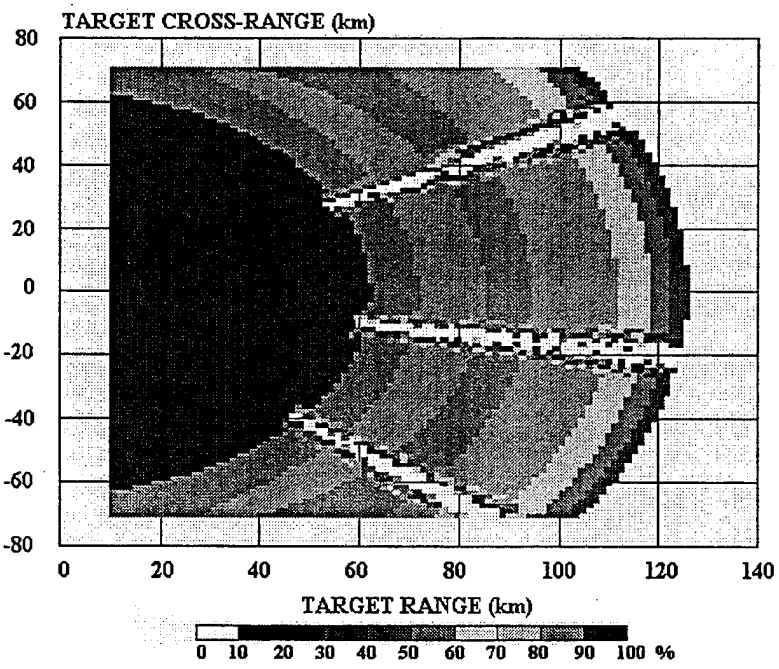

Decision Tool will run on a PC on board by the end of 1995.

It contains models of

- transmitter
- receiver front end
- antenna
- signal processor
- propagation
- clutter
- jamming
- target

S950118/V1

Given

- the meteorological conditions,
- the presence of jammers,
- the expected class of targets,
- the radar parameters selected by the operator,

the Decision Tool informs the radar operator about the detection possibilities.

This assists the operator to select the optimum radar parameters.

959809/V4

In the future, given

- the meteorological conditions,
- the presence of jammers,
- the expected class of targets,

the Decision Tool tells the radar operator which parameters to select.

959809/V5

Future extensions

- infrared systems
- propagation over land and over rough sea
- land clutter
- high-resolution clutter

959809/V6

RF MISSION PLANNER - A JMCIS TOOL

G.K. Lott, S.E. Paluszek, D. Brant
Code EC/lt
Naval Postgraduate School
Monterey, CA 93943
(408) 656-3798
lott@ece.nps.navy.mil

Abstract:

The authors present the current development status of a new, multi-propagation-model planning tool. The software is being developed at the Applied Research Laboratory, The University of Texas at Austin, for the Naval Information Warfare Activity.

The planning tool is designed to operate on a TAC-3 or TAC-4 workstation (HP 9000/755 or later). System design includes integration as a segment of the Joint Maritime Command Information System (JMCIS), and it uses the Navy's Unified Build software. The system specifications call for the final product in mid 1997.

The system uses a geographically oriented approach to specifying and viewing propagation model results. There are many models to choose from, initially including:

Danbolt-Lucus (HF),
GR wave,
TIREM,
VTRPE,
RPO, &
F Factor.

There are plans to incorporate a number of other models, such as ASAPS, GELTI.

Features include the integration of visualization tools, digital mapping, rule-based model selection, presentation of model results as stochastic values, and estimation of defined mission success in geographical context. A mission success visualization tool, called the Lott Plot, permits the user to see the effects on mission success caused by receiver sensitivity, signal-to-noise ratio, channel occupancy, and noise floor.

(Editor's note: CDR Lott was unable to attend; LCDR Zmyslo, Naval Information Warfare Activity, provided a description of RF Mission Planner)

Navy METOC Systems

CDR David G. Markham, USN
COMSPAWARSYSCOM (PMW 175)
Crystal Park #5, Suite 301
2451 Crystal Drive
Arlington, VA 22245-5200
Tel: (703) 602-7039
Fax: (703) 602-1535

METOC SYSTEMS

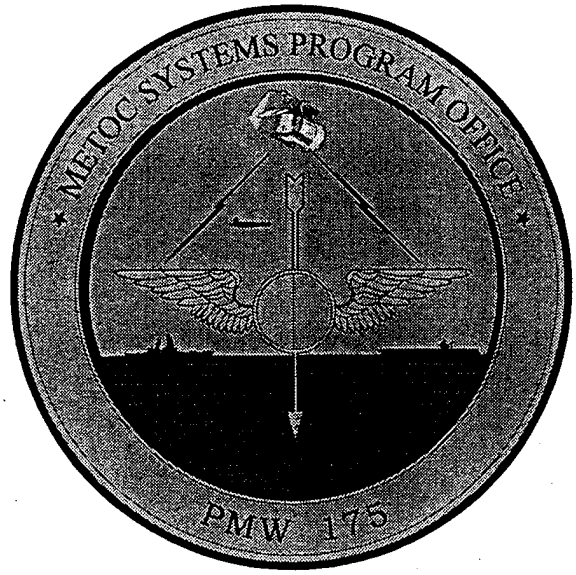

CDR David Markham

18 July 1995

METOC SYSTEMS OUTLINE

- Overview
- TESS(3)/NODDES
- NITES
- USMC METMF Replacement
- Sensors
- EM/EO Support System

OVERVIEW

NAVAL METEOROLOGY AND OCEANOGRAPHY ORGANIZATION

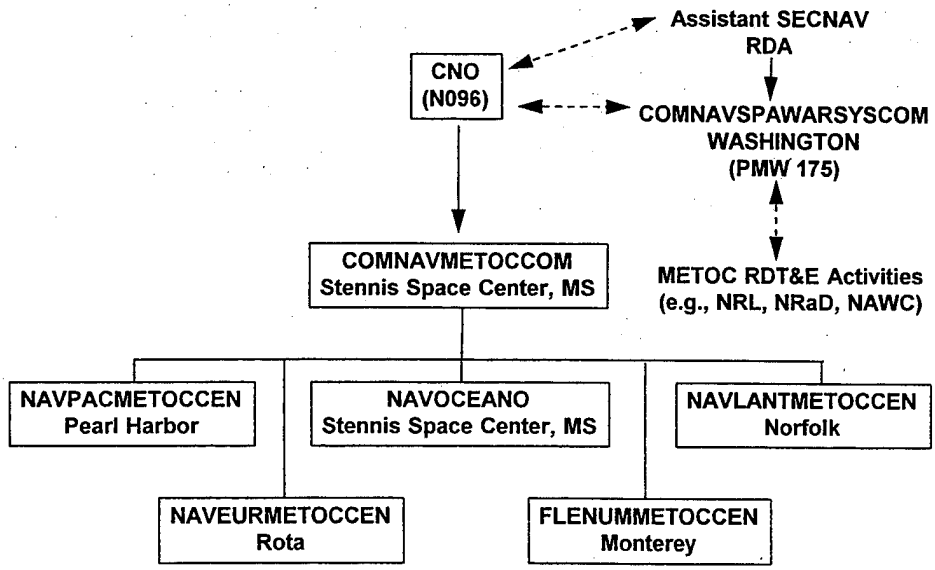

PMW 175 MISSION

- Development, acquisition and life cycle support of meteorological and oceanographic (METOC) sensing, receiving, storing, processing, distribution and display systems
- Development, and transition of applications software for both large scale and tactical computers
- Navy's METOC Systems Integrator/Architect

PMW 175 PROGRAMS...

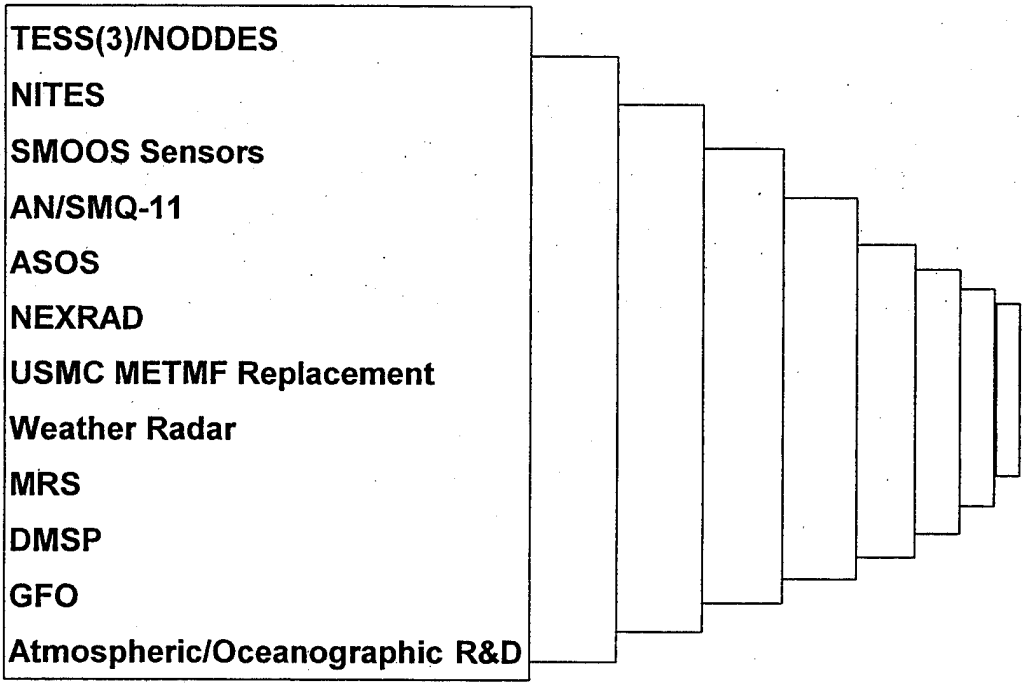

METOC SUPPORT

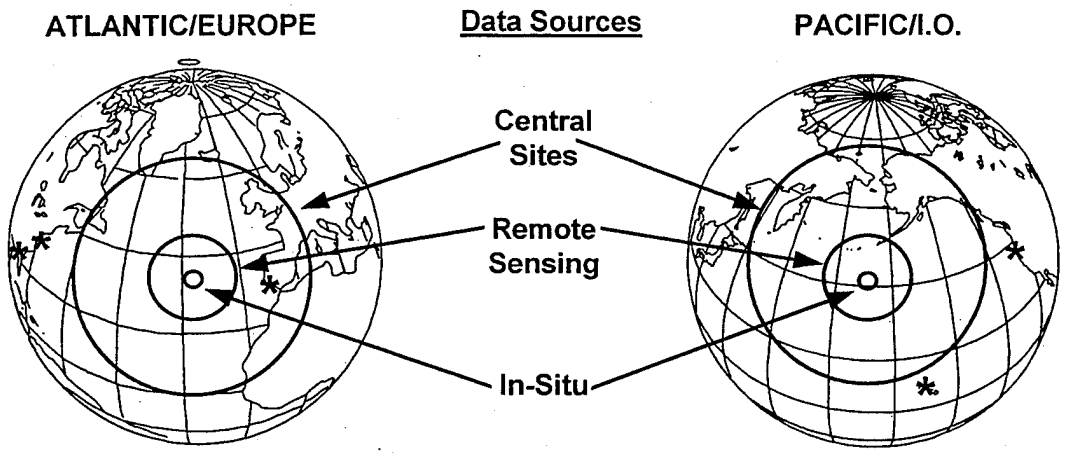

CENTRAL SITE/ THEATER CENTER	SATELLITE BASED	IN-SITU
Direct input to TESS(3) 2- and 3-dimensional grid fields Coarse spatial resolution (10s-100s NMs) Fixed update times Low time resolution (6-12 hrs) To ~ 4,000 NM (near global/theater coverage)	Direct input to TESS(3) 2-dimensional imagery Low spatial resolution (NMs-10s NMs) Fixed update times Low time resolution (6-12 hrs) To ~ 1,200 NM (synoptic scale coverage)	Direct input to TESS(3) and some weapon/sensor systems Point measurements/profiles High resolution (10s to 100s yards) Updated as required High time resolution (mins-10s mins) To ~ 200 NM (mesoscale coverage)

METOC SUPPORT CONCEPT OF OPERATIONS

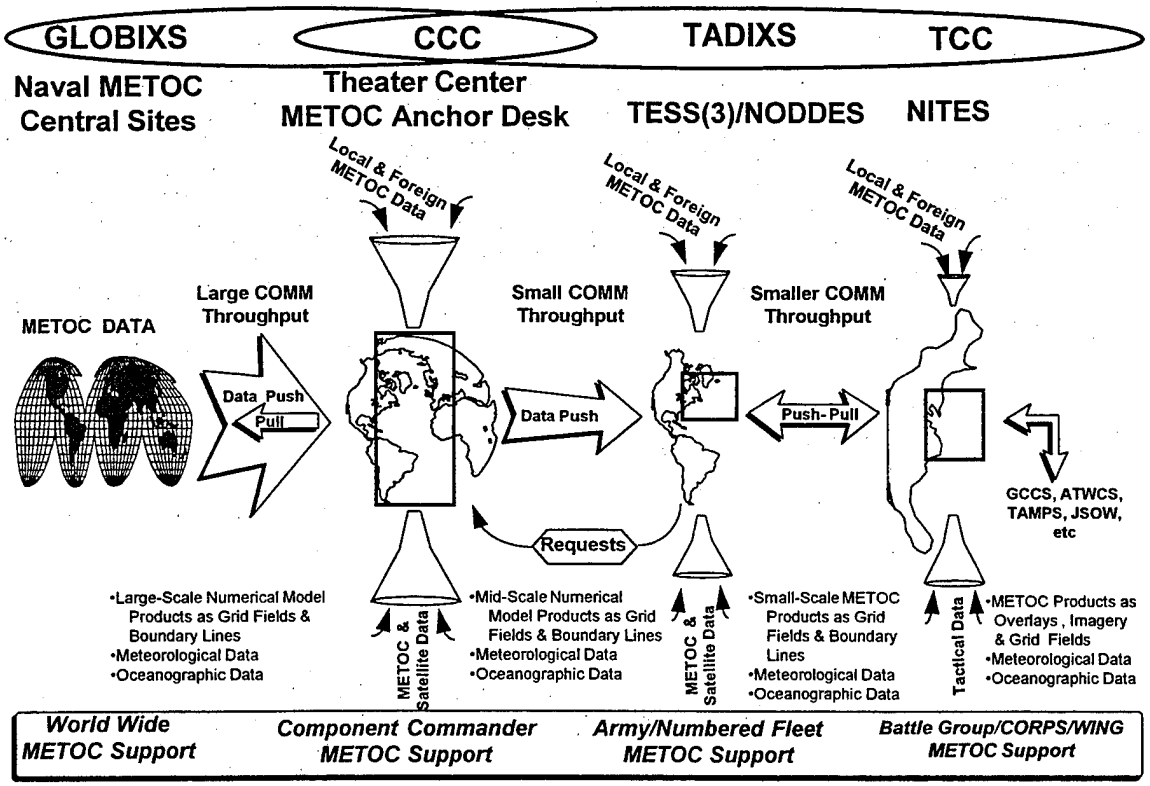

METOC SUPPORT ARCHITECTURE

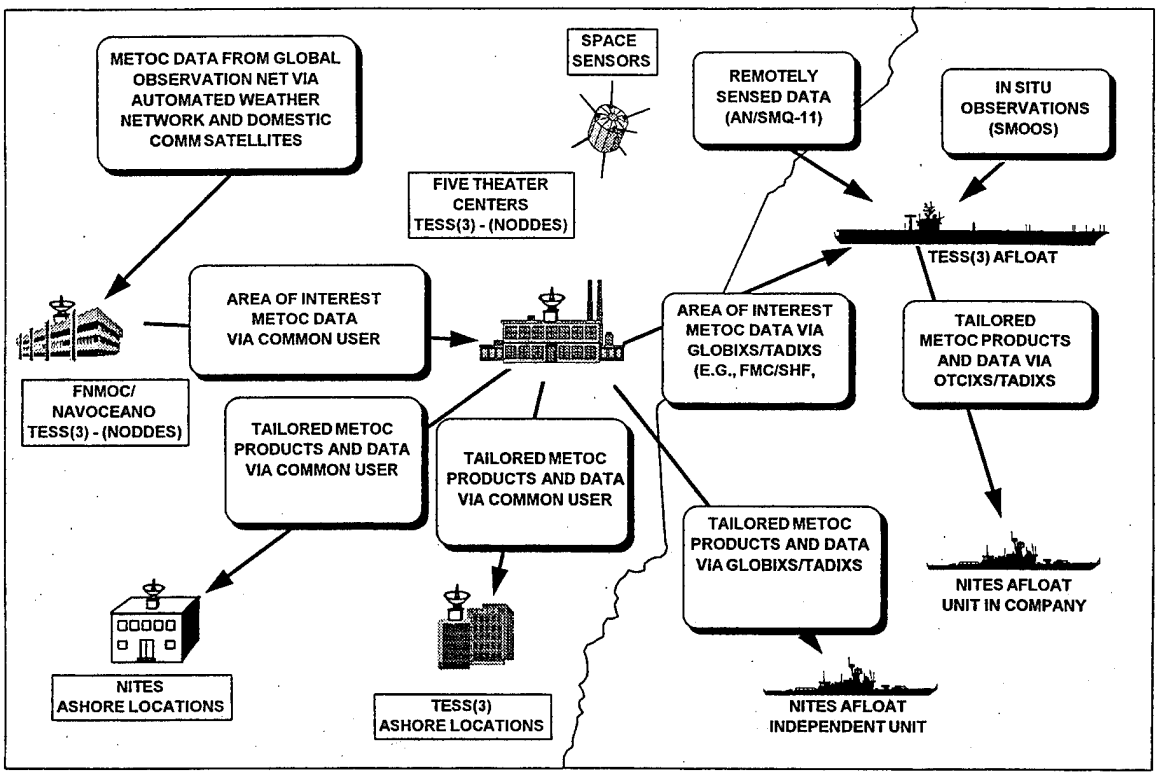

TESS(3)/NODDES

Tactical Environmental Support System

Navy Oceanographic Data Distribution and Expansion System

TESS(3)/NODDES...

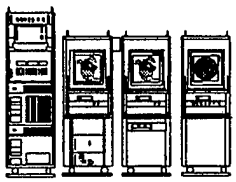

AN/UMK-3(V)1

- Computer-based interactive METOC data receiving, storing, processing, display and distribution system
- Secure, responsive and robust
- Cornerstone of tactical METOC support afloat and ashore
- Critical element of command and control architecture

TESS(3) AFLOAT VARIANT ATTRIBUTES

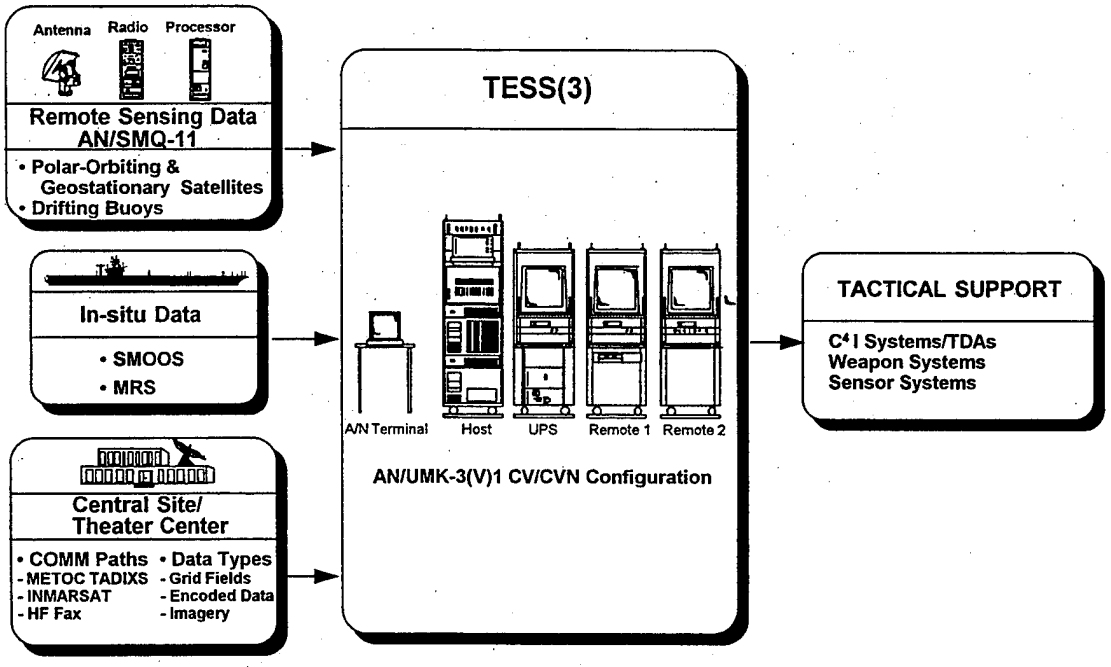

NITES

Navy Integrated Tactical Environmental Subsystem

NITES...

TAC-3

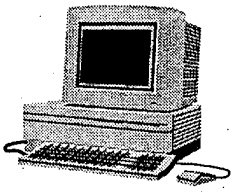

- **Software segment in Joint Maritime Command Information System (JMCIS)**
- **METOC information to non-TESS(3) ships**
- **Tailored data/products to support C4I weapon & sensor systems**
- **Critical interface for management and distribution of METOC information from Anchor Desk/TESS(3)**

NITES VARIANTS

- **NITES**
  - **Classified System**
  - **Afloat**
    - ✦ Some Surface Ships & Submarines
    - ✦ Non-TESS Platforms
  - **Non-Oceanographer Software Configuration**
- **MOSS**
  - **Classified System**
  - **Portable**
  - **Afloat & Ashore**
  - **Oceanographer Software Configuration**
- **TRWS**
  - **Classified System**
  - **Oceanographer Software Configuration**
  - **Afloat**
    - ✦ TESS Platforms
    - ✦ In METOC Division Space
  - **Ashore**
    - ✦ METOC Anchor Desk
    - ✦ Other TESS and Some Non-TESS sites

USMC METMF REPLACEMENT

USMC Meteorological Mobile Facility Replacement

USMC METMF REPLACEMENT...

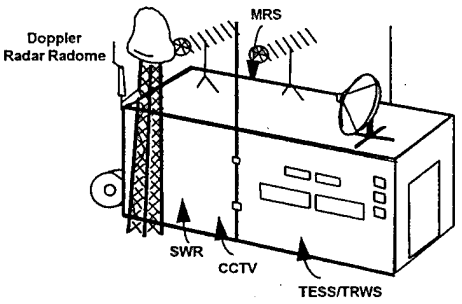

- Deployable USMC METOC support system
- Increased mission responsibility (MEF CE, GCE, CSSE and ACE)
- Downsized METMF footprint to one shelter

USMC METMF CAPABILITIES

- Increased processing capacity
- Automated to fullest extent
- Interoperable within Component and JTF
- Full range of weather support
- Direct satellite readout

SENSORS

Shipboard Meteorological and Oceanographic Observing System (SMOOS)

Small combatant sensors

Other new sensors

Current SMOOS Sensors...

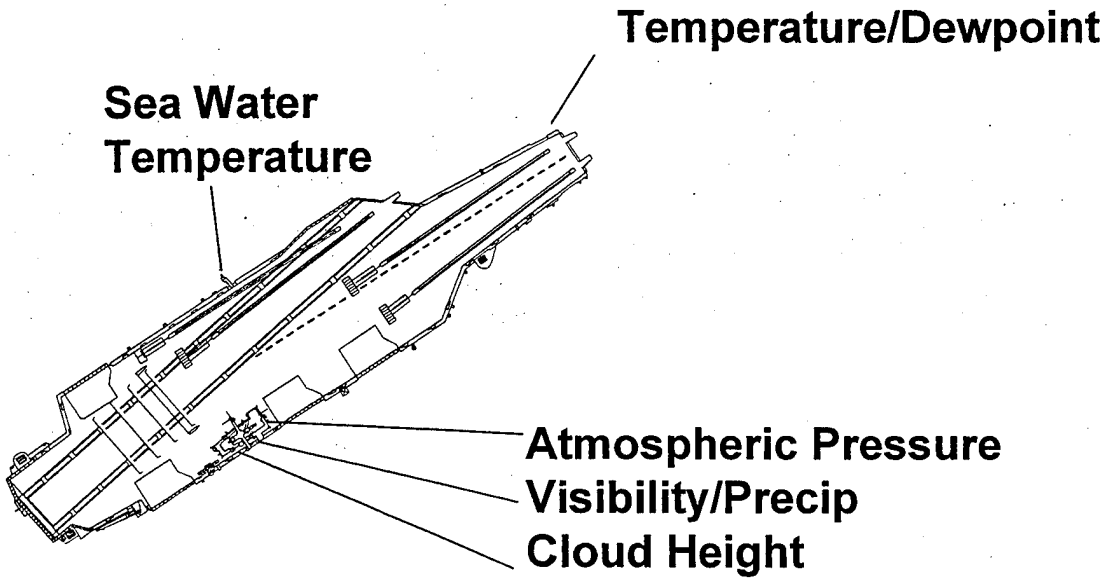

- Collocated with TESS on major combatants (30% complete)
- Processes, stores and transmits data to TESS(3)

FUTURE SMOOS SENSORS...

LIDAR Profiler (temp, humidity, wind)

Passive Water Vapor Profiler

Ship Mounted Radiometer (sea surface temp)

Nephelometer (boundary layer aerosols)

Vertical sounder for aerosol sampling

LIDAR ATMOSPHERIC PROFILE SENSOR (LAPS)

- Temperature and humidity sounder development by ARL/PSU
- Wind sounder development by Coherent Technologies, Inc.
- R&D version of ARL system tested at Point Mugu, JUL - OCT 1993
- Prototype of ARL system demo at Penn State, MAY 1995; sea trials scheduled for FY96 (NAVO ship)
- Combined system planned for FY98-99

SMALL COMBATANT SENSORS...

- Cost
- Durability
- Accuracy
- Resolution
- RF interference
- Measurement techniques

R/V Point Sur

SENSOR INTERCOMPARISON...

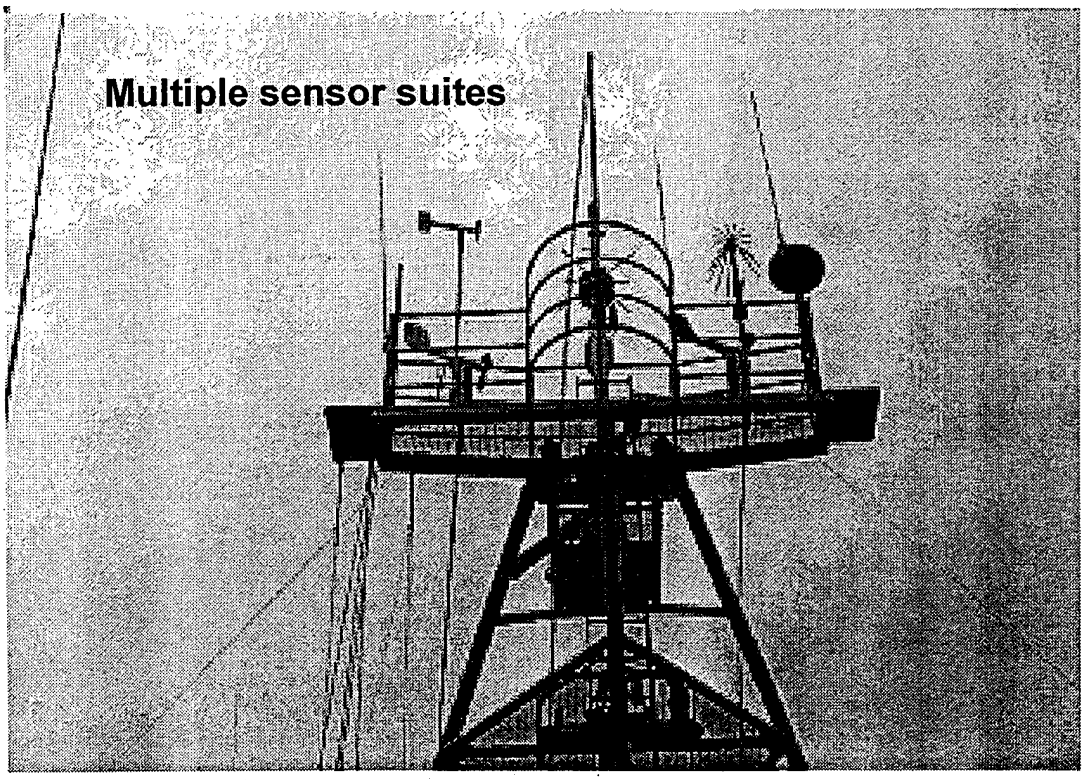

OTHER NEW SENSORS...

- Dropsonde
- Rocketsonde
- Projectile sonde
- UAV with complete METOC sensor package
- Automated buoys (moored and drifting)
- Expendable surf zone buoys (swimmer deployed)

EM/EO SUPPORT SYSTEM

EM/EO SUPPORT SYSTEM...

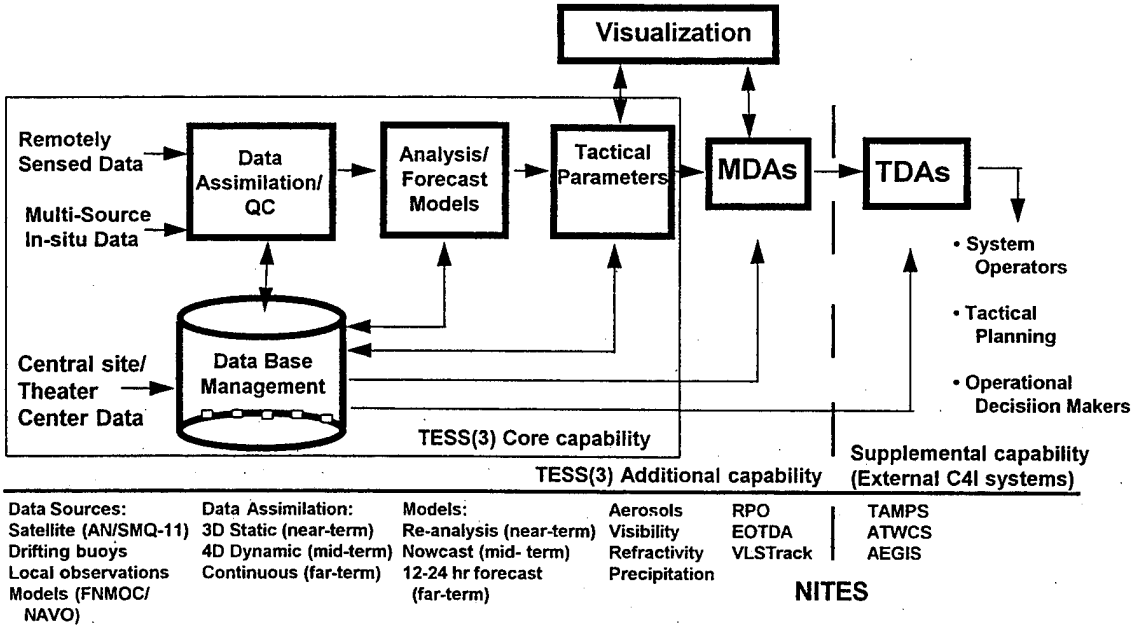

SHAREM 110 DEMO CONOPS

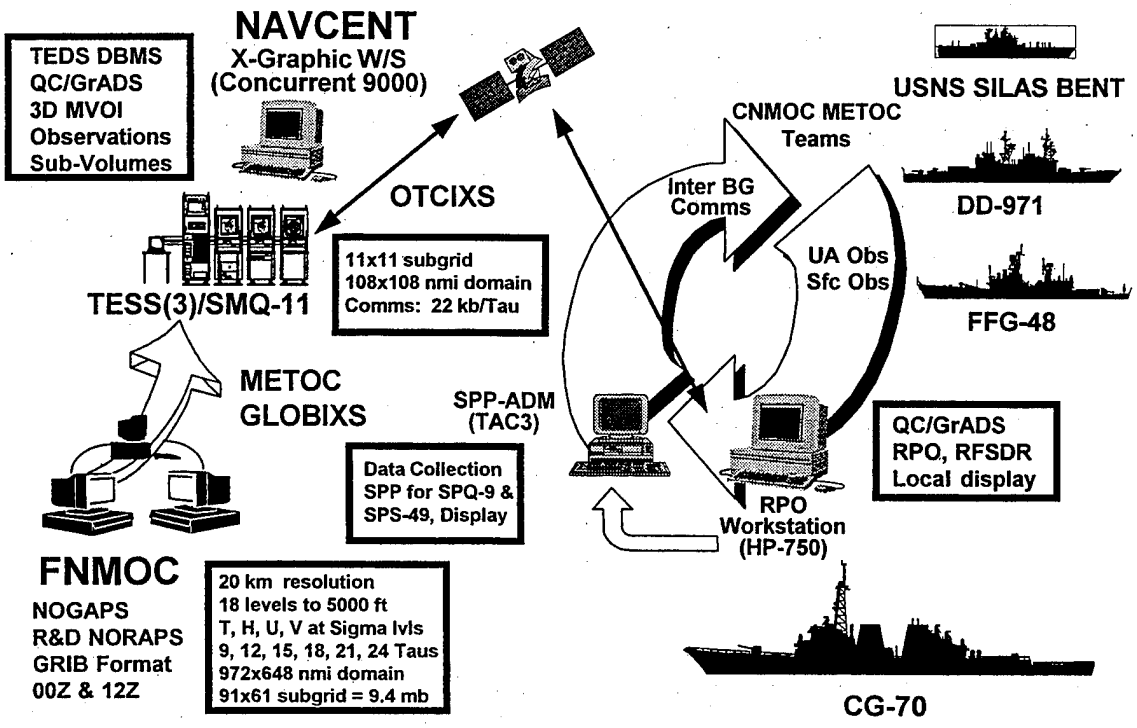

SHAREM 110 DEMO AREA

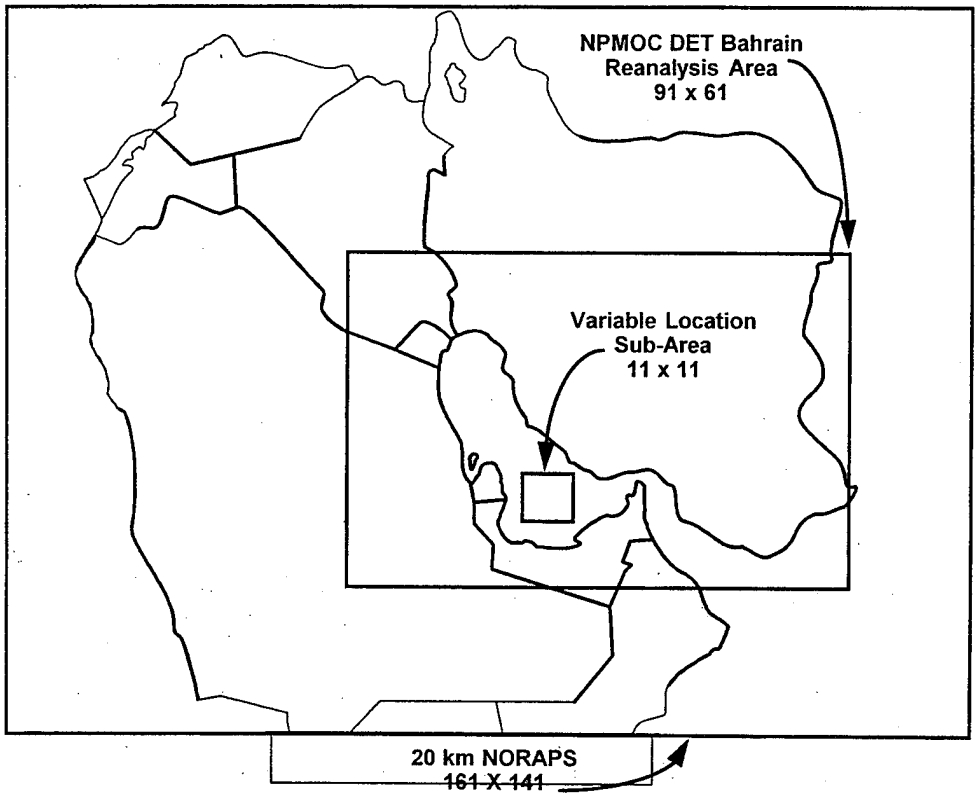

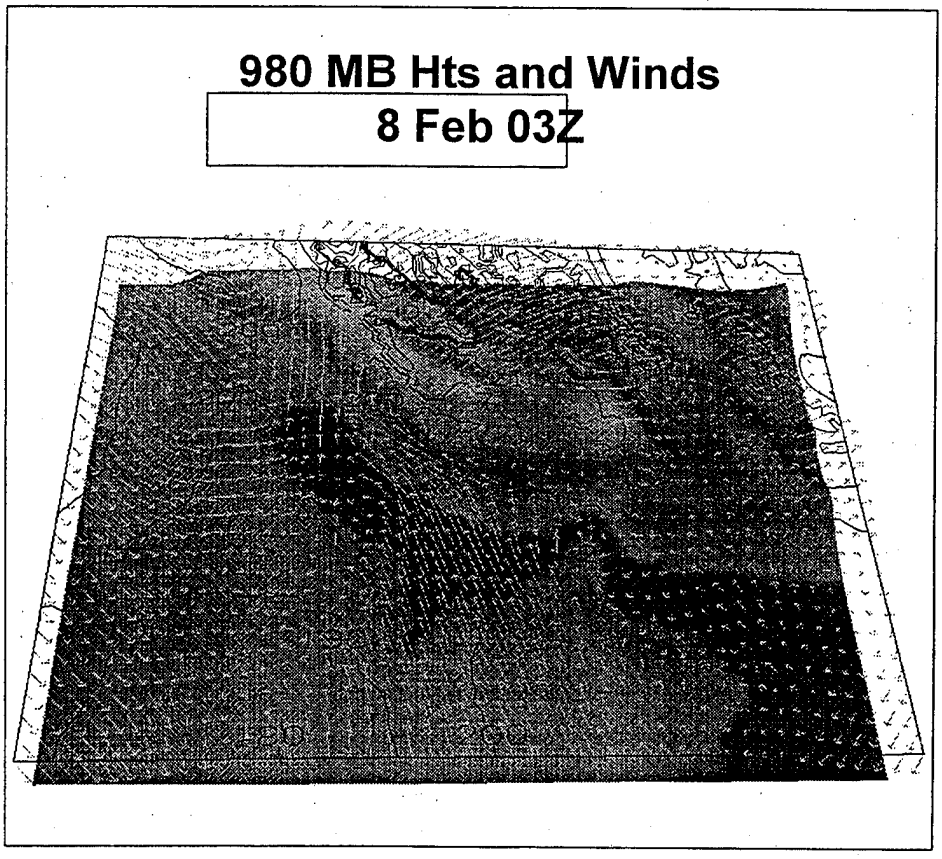

980 MB Hts and Winds
290K Dew Point Temperature Isosurface
8 Feb 03Z

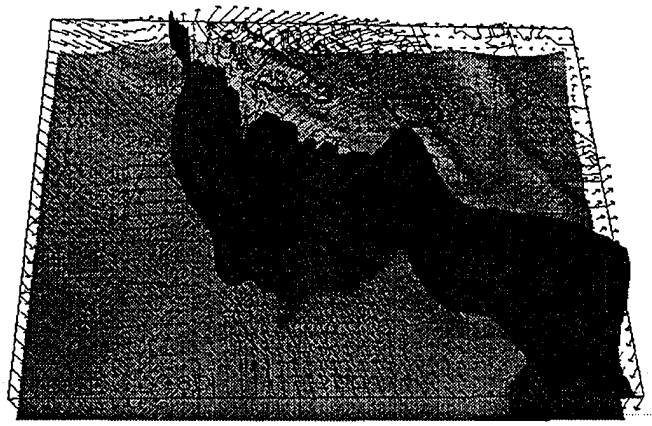

SPP ADM

Paul R. Tiedeman, PEO(USW)ASTO-E
2531 Jefferson Davis Highway
Arlington, VA 22242-5169
Tel: (202) 602-3087 ext.460
Fax: (202) 602-5152

Mr. Paul Tiedeman, "SPP-ADM"

DISCUSSION

R. PAULUS

Are SHAREM exercises to continue on for the next few years?

AUTHOR'S REPLY

SHAREM exercises will continue. The specific role/use of the surface ship ADM (acoustic & non-acoustic) during these exercises will be worked out with SWDG (Surface Warfare Development Group) over the next few months.

Application of Propagation Models to Terrain Clutter and Target Masking Viewed by a Shipboard Radar.

C. C. Lin and J. P. Reilly
The Johns Hopkins University Applied Physics Laboratory
Johns Hopkins Road
Laurel, Maryland 20723-6099
Telephone: (301)953-5000
email: christopher.lin@aplmail.jhuapl.edu
email: patrick.reilly@aplmail.jhuapl.edu

Abstract

In this paper, a site-specific approach is presented to characterize terrain and target visibility and terrain clutter as seen by a shipboard radar in a coastal environment. The method takes into account the location of the ship, the particular terrain topography, the radar parameters, and the propagation effect. The method incorporates refractive index models of the atmosphere surrounding the radar, an optical ray-trace model, an electromagnetic parabolic equation model, and a data base of terrain elevations.

Both terrain shadowing and clutter can be simulated. The method can accommodate atmospheric data that varies in three dimensions, if such detailed information is available. The model can accommodate the interaction of terrain and meteorology. Alternatively, less detailed atmospheric inputs may be used, such as with a stratified atmosphere assumption. Site specific terrain contours are described through the DTED data base, which is provided by the Defense Mapping Agency.

The model is configured with varying degrees of complexity. Relatively simple, but fast methods of calculation are provided via programs designated *TEVIR-I* and *TEVIR-II*. TEVIR I computes terrain and target shadowing, where the propagation can be represented as straight line propagation over a round earth with an equivalent earth radius factor. Atmospheric profiles fitting this category can be represented by a constant gradient of the index of refraction versus height. The "standard atmosphere" is one example fitting into this category. TEVIR II also determines terrain and target shadowing, but with arbitrary atmospheric inputs. TEVIR-II computes terrain visibility using a geometric ray-tracing method.

The RADSCAT method is a higher fidelity method that employs the electromagnetic parabolic equation program TEMPER to calculate the propagation factor. The TEMPER method includes a perfectly absorbing terrain boundary. RADSCAT includes both refraction and diffraction effects, and can simulate terrain shadowing and backscatter. This method can also accept refractivity that varies in three dimensions. Whereas the RADSCAT method provides much more detailed information, it is also takes much more time to execute as compared with the TEVIR methods.

Variations in atmospheric refractivity can significantly alter patterns of terrain clutter and shadowing. The effects will depend structure of atmospheric refractivity, as well as terrain relief. With a surface-based duct for instance, it is possible to markedly increase the density of directly illuminated terrain, or to greatly extend the range extent over which strong clutter is returned. The paper provides several examples to illustrate these effects. These examples will include sample cases provided by the Electromagnetic Propagation Workshop Organizers as applied to the littoral environment.

The RADSCAT and TEVIR models were compared with radar measurements taken off the west coast of the U.S. from an S-band radar. The correspondence between measured and simulated clutter is very good for radar cells that contain at least a portion of directly illuminated terrain, i.e., a land mass that is not

completely in shadow. This correspondence is evident in the geographic patterns and statistical distribution of clutter returns in both northern Washington and southern California. Although the terrain has similar mountainous relief in the two locations, the composition of the terrain is quite different. In the measurement area of northern Washington, the terrain is forested, with little cultural development. In southern California, the terrain is semi-arid, with significant cultural development present, particularly along the coast. Despite the differences in terrain composition, the clutter returns on directly illuminated surfaces were similar in the two locations.

Illumination of terrain within shadowed regions occurs via diffraction, which is automatically accounted for in the TEMPER model. In these shadowed regions, the model predicts generally lower clutter strengths as compared with measurements. In this paper we discuss several hypotheses that might explain the discrepancy. Primary considerations include: (a) smearing due to platform motion during the measurement interval, (b) inadequate representation of diffraction, (c) multiple scattering effects, (d) data collection response dynamics.

Although the simulated patterns of strong clutter correspond very well to measurements, there was approximately a 4% discrepancy in the range to geographic features. We are investigating the possibility of timing errors in the measurements, or of errors in the simulation.

Future improvements in the model will incorporate the *Digital Feature Analysis Data* (DFAD) data base of terrain composition. This data base, also published by the Defense Mapping Agency, indicates features such as vegetation, structures, roads, bridges, power lines, etc. With such data, it is possible to better predict backscatter, and the effects of both natural and cultural features.

Application of Propagation Models to Terrain Clutter and Target Masking Viewed by a Shipboard Radar

18 July 1995

C. C. Lin
J. P. Reilly
The Johns Hopkins University Applied Physics Laboratory

Electromagnetic Propagation Workshop

OBJECTIVES

- **Predict Illuminated / Shadowed Areas**
  - Target Visibility Map
  - Terrain Visibility Map
- **Predict Land Clutter**
  - Radar Performance Analysis
  - Radar System Design
- **Real-Time Application**
  - Interface with Real-time Tactical Decision Aid
  - Incorporate Real-time Refractivity Data

OUTLINE

- Approach
- Terrain / Target Masking Model
- Terrain Clutter Model
- Model Verification
- Considerations for Real-Time Application
- Summary

Electromagnetic Propagation Workshop

APPROACH

- Access DMA Map Data
  - DTED (Terrain Elevations)
  - DFAD (Terrain Features)
- Develop Ray-Trace Method for Illumination & Shadowing
- Adapt TEMPER Propagation Model (F^4)
  - More Accurate Than Ray Tracing
  - Calculation within Shadow Zones (Diffraction)
- Develop Land Clutter Prediction Models ($\sigma_o F^4$)
- Validate with Shipboard Radar Measurement

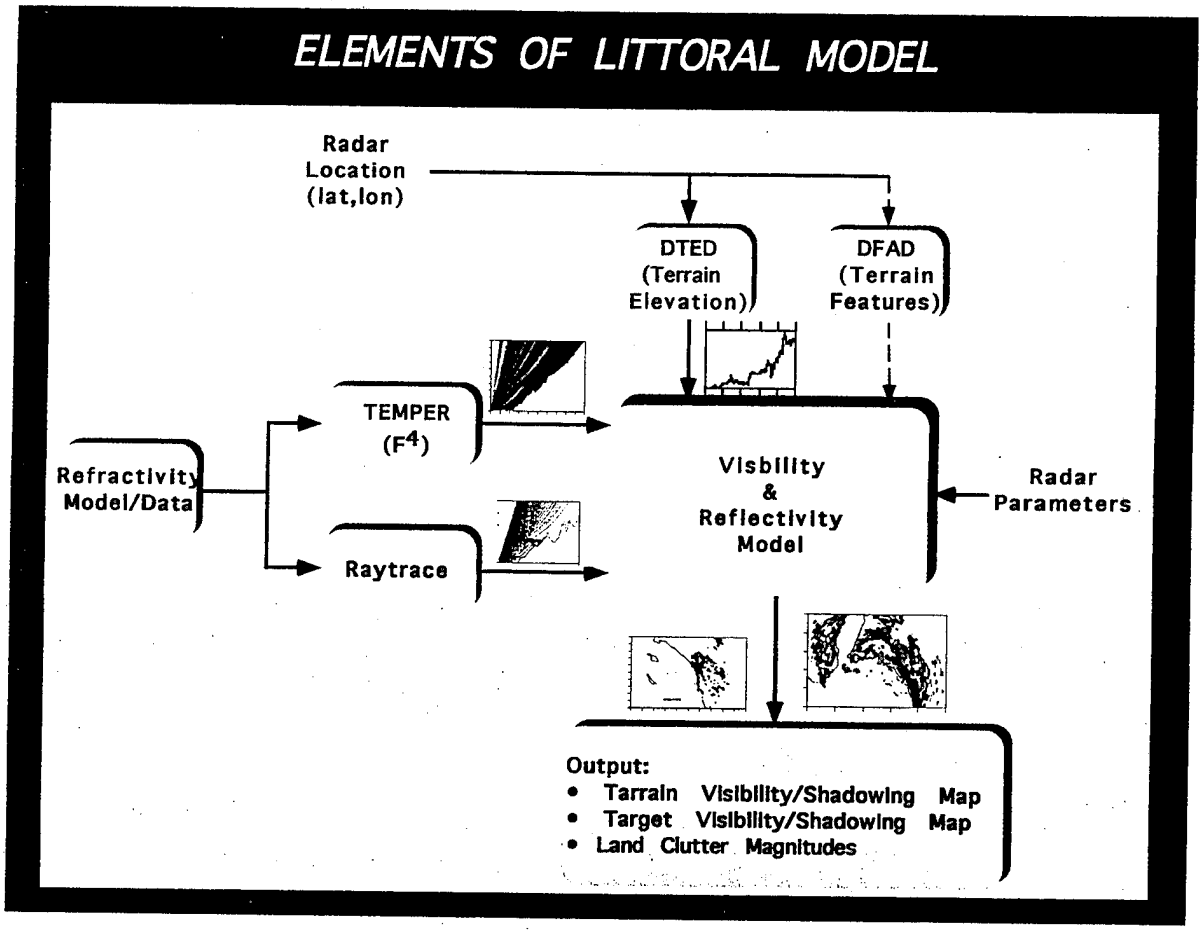
ELEMENTS OF LITTORAL MODEL
Radar Location (lat,lon)
DTED (Terrain Elevation)
DFAD (Terrain Features)
TEMPER (F^4)
Refractivity Model/Data
Raytrace
Visbility & Reflectivity Model
Radar Parameters
Output:
• Tarrain Visibility/Shadowing Map
• Target Visibility/Shadowing Map
• Land Clutter Magnitudes

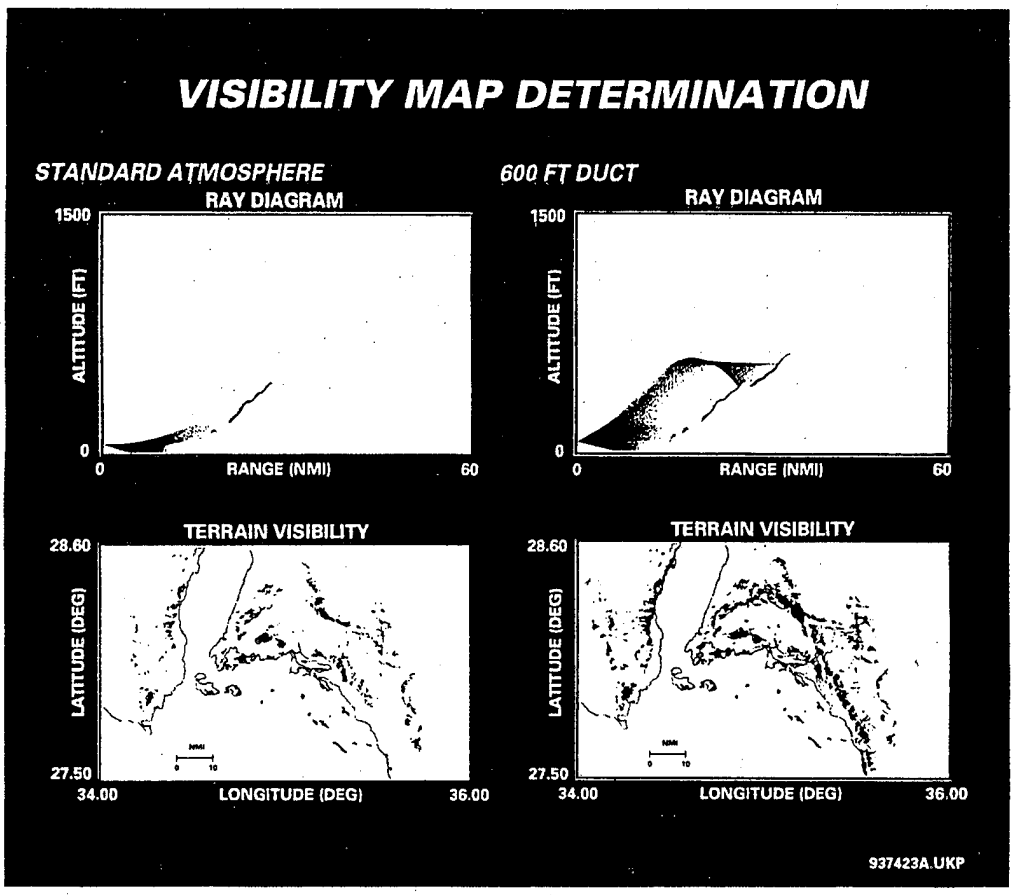
VISIBILITY MAP DETERMINATION
STANDARD ATMOSPHERE
600 FT DUCT
RAY DIAGRAM
1500
ALTITUDE (FT)
0
RANGE (NMI)
60
TERRAIN VISIBILITY
28.60
LATITUDE (DEG)
27.50
34.00
LONGITUDE (DEG)
36.00
937423A.UKP

VISIBILITY DIAGRAM

RADAR HEIGHT = 62 FT

TARGET ALTITUDE = 150 FEET ABOVE TERRAIN/SEA

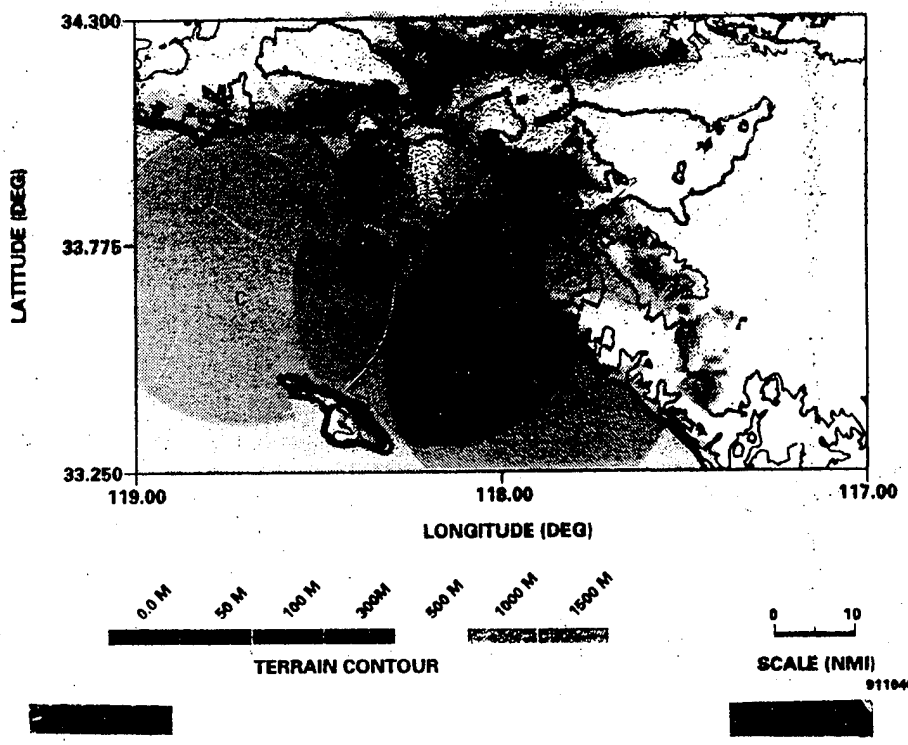

911046.UKO

ONE-WAY PROPAGATION FACTOR USING TEMPER, S-BAND

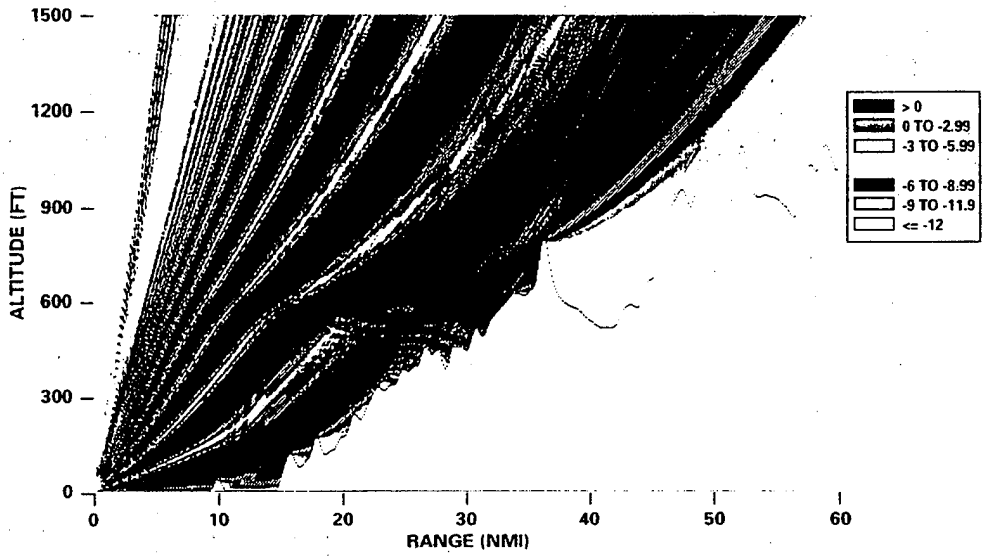

937425A.UKP

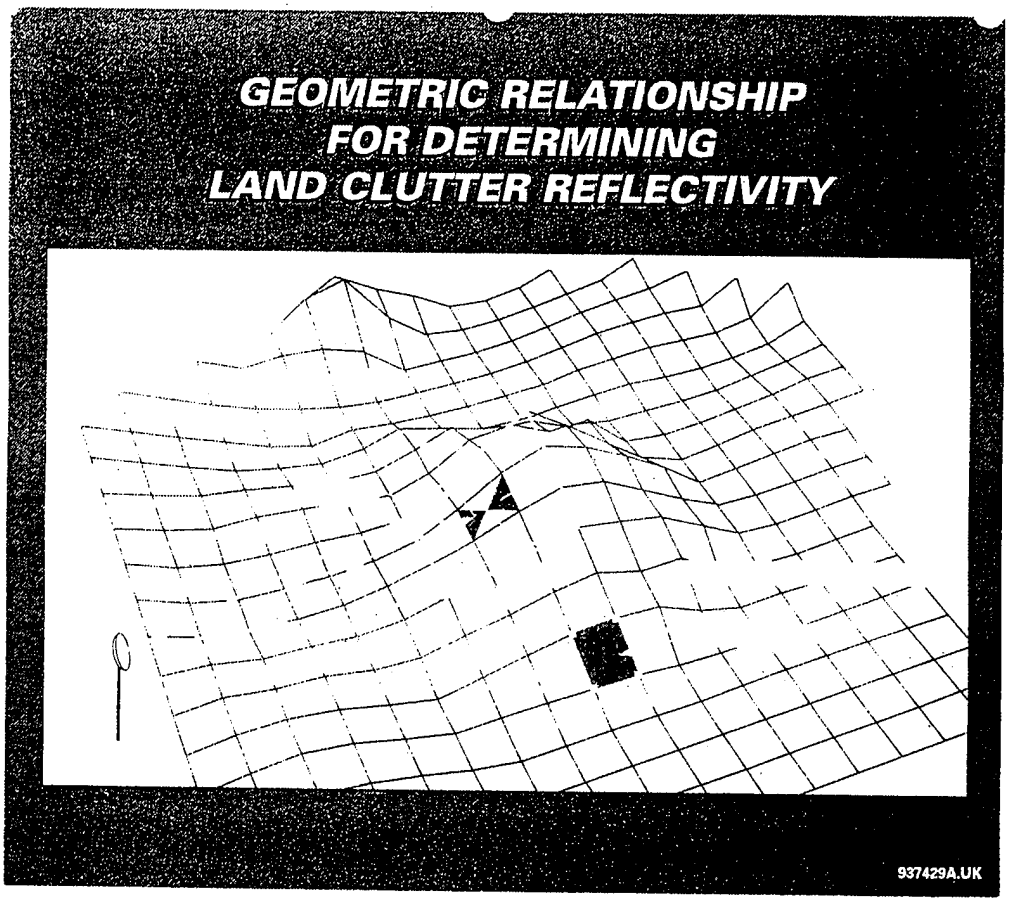

Constant-γ Land Clutter Model

$$\sigma_{oi} = \gamma \sin \psi_i \qquad \gamma = \gamma_r \left(\frac{f}{f_r}\right)^{1/2} \qquad \sigma_o = \frac{1}{n}\sum_{1}^{n} \sigma_{oi}$$

σ_{oi} = Reflectivity of DTED Facet
σ_o = Clutter Reflectivity of Radar Cell
γ = Clutter Reflectivity Constant
γ_r = Reference Constant
ψ_i = Grazing Angle on ith Facet
f = Radar Frequency
f_r = Reference Frequency
n = Number of DTED Facets in Radar Cell

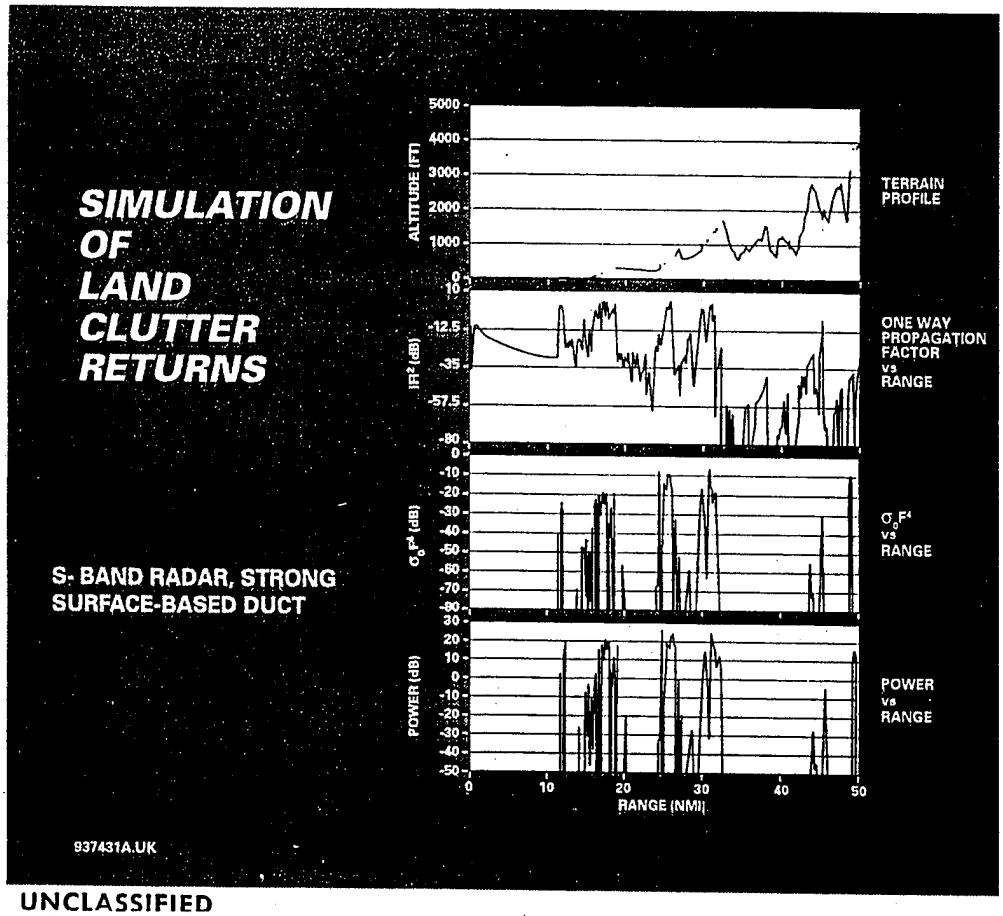

UNCLASSIFIED

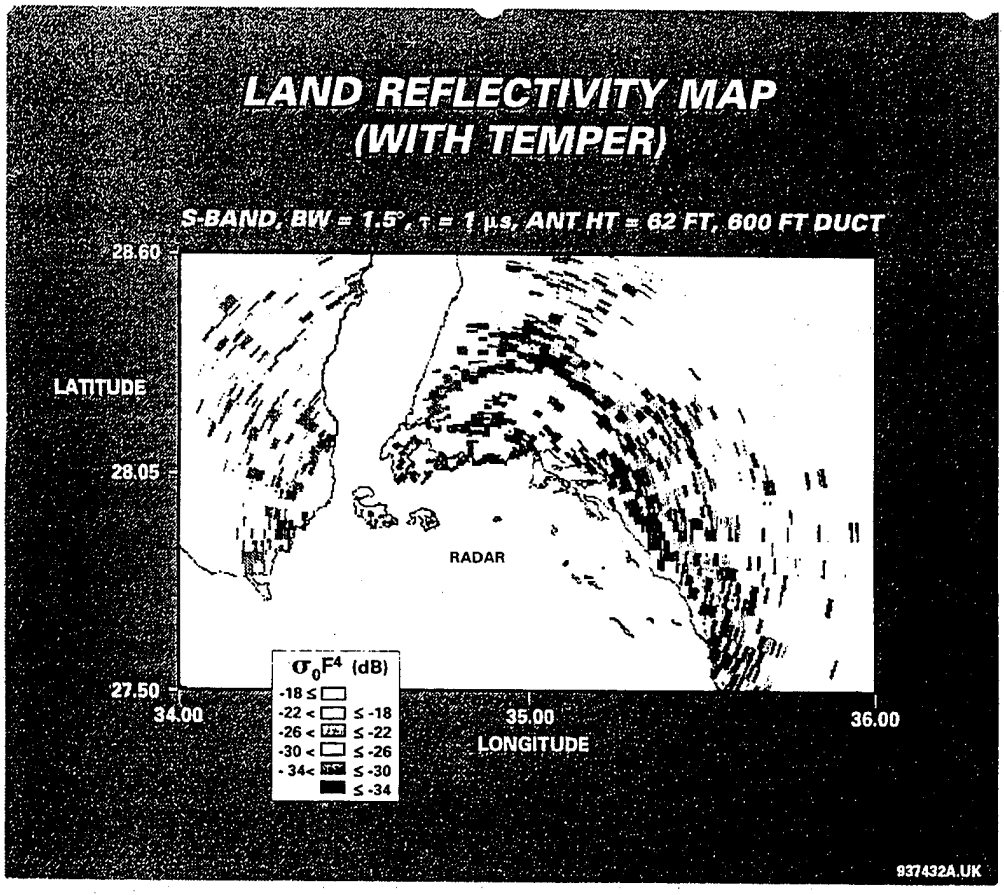

USS CALIFORNIA (CGN 36) DATA COLLECT

DATA COLLECTED DURING NTU DT

- MAY 1993 (OLYMIC PENINSULA, WASHINGTON): FORESTED, HIGH RELIEF
- JUNE 1993 (CAMP PENDLETON, SO. CALIFORNIA): SEMI ARID, CULTURED, HIGH RELIEF

SPS-48E RADAR MEASUREMENTS

- S-BAND, $\tau = 3\mu s$, ANT H = 120 FT, BW = 1.6°, R_u = 150 nmi
- MEASURED DYNAMIC RANGE > 100dB

HELICOPTER REFRACTIVITY

- PROVIDED BY AEGIS PROGRAM

937768.UK

MEASURED CLUTTER REFLECTIVITY SOUTHERN CALIFORNIA

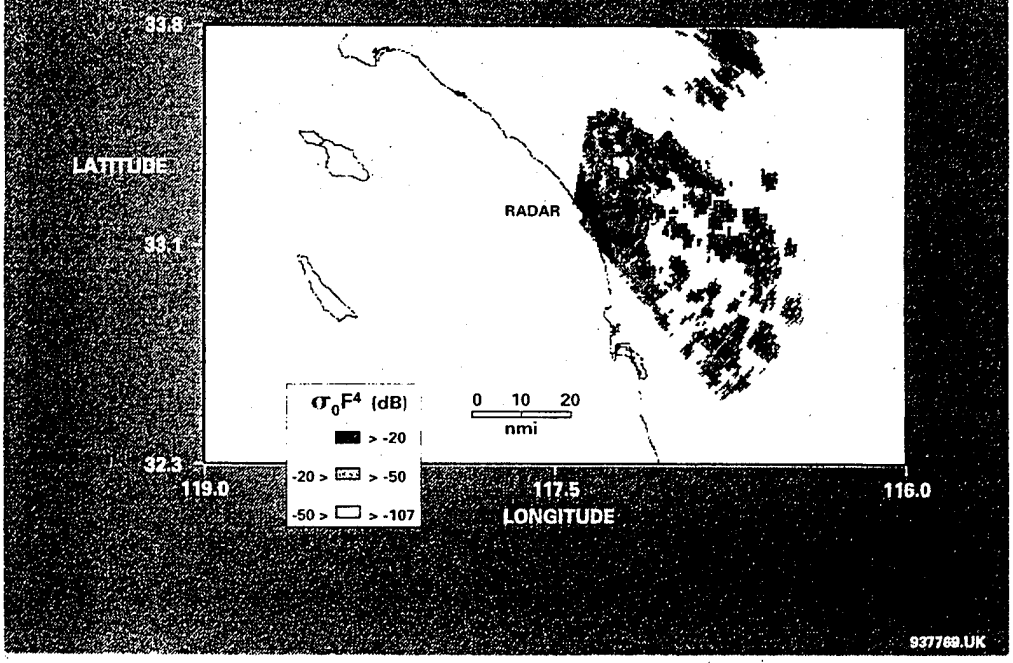

937769.UK

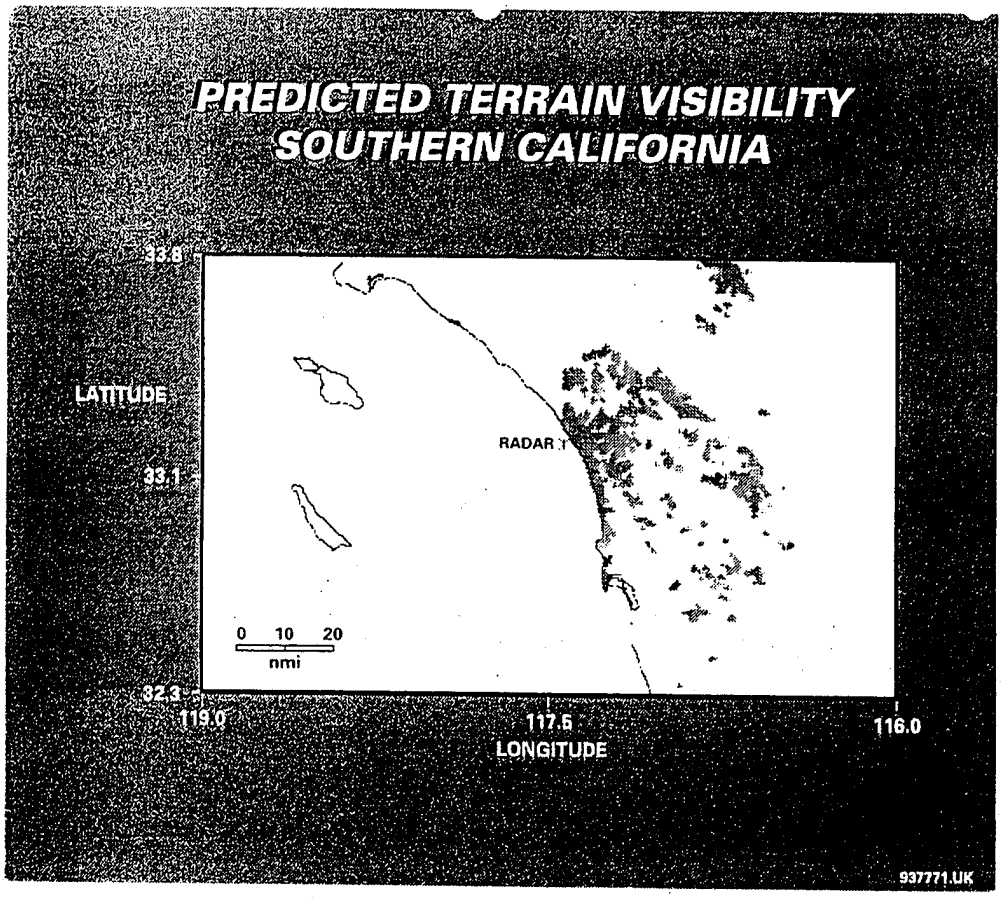

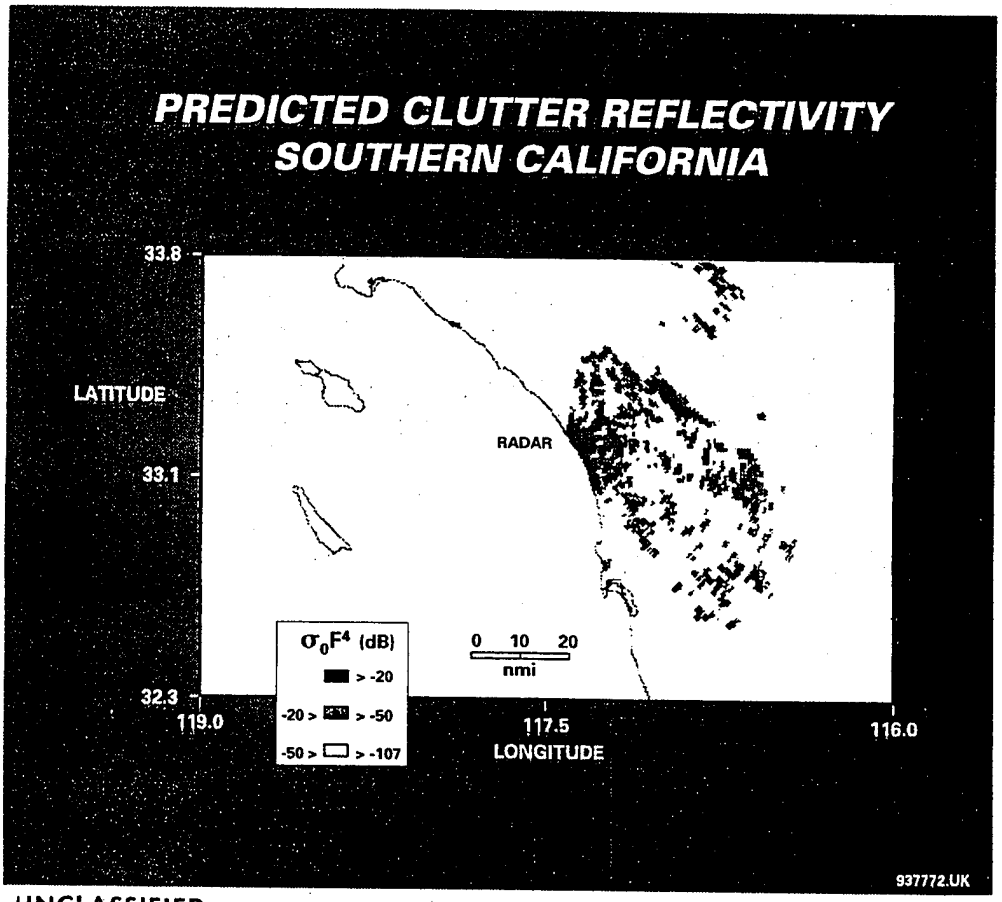

F2A-94-4-NNR
Page 22

UNCLASSIFIED

CUMULATIVE DISTRIBUTION OF MEASURED AND MODELED $\sigma_o F^4$, SIDELOBE EFFECT

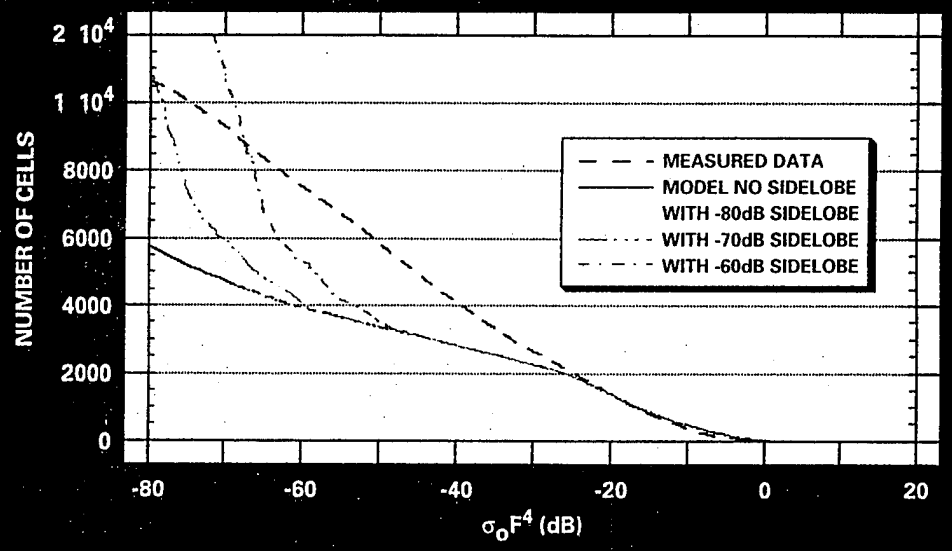

9500931.UK

LAND CLUTTER MEASUREMENT FROM ILLUMINATED TERRAIN vs MODEL

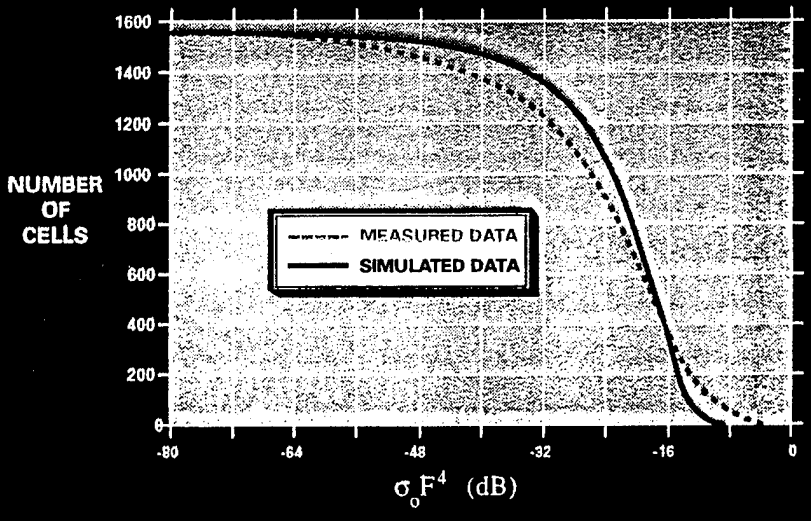

9404554.UK

Model Simplification Approach

(A) Using 0° Incident Angle to Determine Grazing Angle

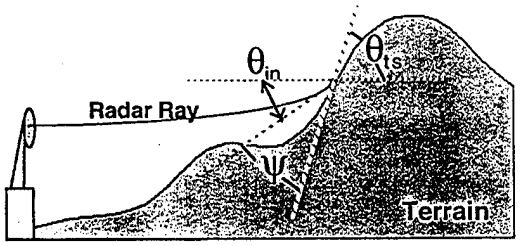

$$\psi = \theta_{ts} - \theta_{in} \xrightarrow{\theta_{in}=0} \psi \approx \theta_{ts}$$

where ψ = Grazing Angle
θ_{ts} = Terrain Slope
θ_{in} = Incident Angle

(B) Using One Slice Terrain Profile to Determine Land Clutter within a Beamwidth

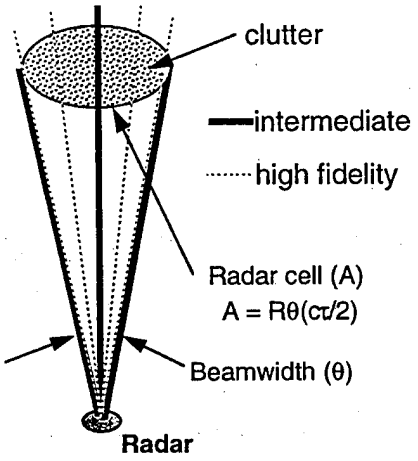

Electromagnetic Propagation Workshop

Raytrace Vs 0° Incident Angle

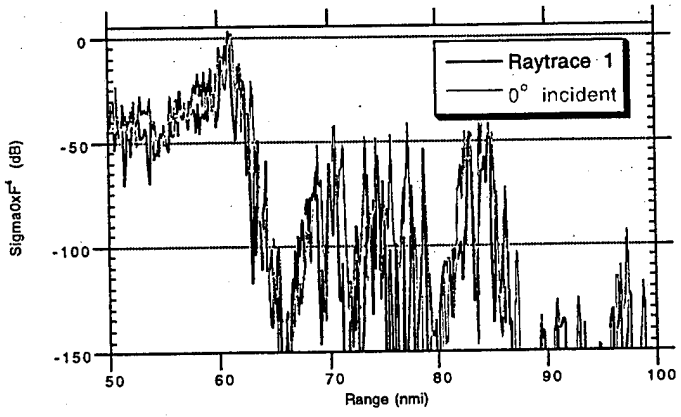

1 Slice Vs. 5 Slices within a 1.5° Beamwidth

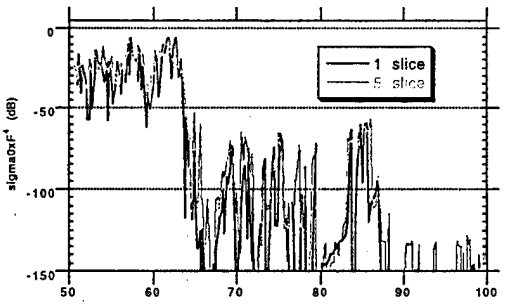

1 Slice Vs. 5 Slices within a 3° Beamwidth

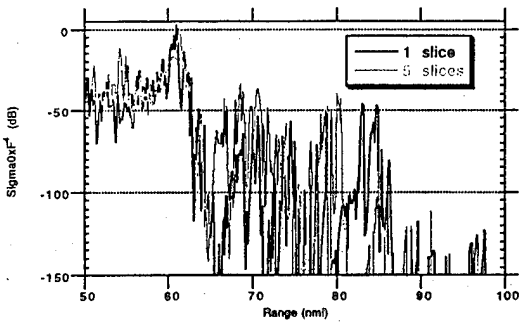

Electromagnetic Propagation Workshop

SUMMARY

- **Terrain Masking Model has Excellent Prediction of Illuminated/Shadowed Regions**
- **Clutter Model has Good Prediction of Clutter Magnitude on Directly Illuminated Terrain**
- **Clutter Model Underestimates of Clutter Magnitudes on Shadowed Terrain**
- **Terrain Masking has been Implemented in Tactical Decision System**
- **Model Simplification has a Good Potential for Real-Time Application**

FURTHER WORK

- Additional Verification
- Diffraction Zone Improvement
- Short Pulse Model
- Incorporated DFAD
- Real-Time Applications

Mr. Chris Lin, "Application of Propagation Models to Terrain Clutter and Target Masking Viewed by a Shipboard Radar

DISCUSSION

M. LEVY

1) Why do you use the PE field at the "first" point above the ground level to calculate clutter?
2) Can the method be applied to sea clutter?

AUTHOR'S REPLY

Mr. Dan Dockery responded to this question:
1) Terrain is implemented in TEMPER by truncating the field at each range at the terrain height. For this reason, there is not necessarily a mesh point precisely at the terrain boundary. Taking the first point above the boundary works well since we are not actually enforcing a boundary condition at the terrain height.

2) The above method will not work for sea clutter because reflections are important and a formal boundary condition is enforced at the surface. Recall that the incident field is the quantity needed in clutter calculations.

S. MARCUS

How does your characterization of clutter using reflectivity jive with the work at Lincoln Labs which claims that the main contribution to clutter is from discretes such as telephone poles, silos, etc.?

AUTHOR'S REPLY

By my understanding, Lincoln Lab characterizes land clutter based on empirical data. Most of the data were measured at positive depression angles (*i.e.* looking down). However, our problem has a low elevation angle (*i.e.* looking up). So far, we don't know how to compare our model with their work, and just began the process of understanding each other.

J. SEELEY

What is meant by "real-time" application of clutter model and why not use measured data instead of a model?

AUTHOR'S REPLY

"Real-time" implies run time of the application; it is too difficult in SPY to extract actual clutter information.

BACKSCATTER FROM PARABOLIC EQUATIONS: FACT OR FANTASY?

Sherman W. Marcus
RAFAEL
P.O.Box 2250
Haifa, Israel
email: mernav@techunix.technion.ac.il

Parabolic equations (PE) have recently found wide use in propagation predictions in complex environments and over irregular boundaries [1-4]. Although the PE is an approximation to the governing Helmholtz equation, it can in principle be made as accurate as desired for calculating forward scatter. It is an irrefutable mathematical fact, however, that PE solutions cannot account for backscatter.

The question then arises: Can the PE solution, which is based only on forward scatter, be used in a subsequent procedure for computing backscatter? This idea has been applied to underwater acoustic reverberation calculations, wherein ocean inhomogeneities scatter energy backwards as well as forwards. In such a case, the PE solution is marched to a given distance, and the solution there is used as an initial condition to march the solution in the backward direction [5]. Although this procedure might suffice for the acoustic reverberation problem, the potential sources of backscatter in the electromagnetic propagation problem are quite different. Although such scattering sources might include sudden changes in atmospheric refractivity, they are more likely to be characterized by sudden changes in the terrain.

The determination of scattering from solid boundary discontinuities is not at all new. Indeed, the geometrical theory of diffraction was developed to account for such discontinuities. A basic method for considering backscatter is Kirchoff's approximation, in which the field on the surface of a scatterer is assumed to be that of the incident wave over the illuminated portion of the body. Once the field is known on the surface, standard integration techniques, such as that based on Green's theorem, can be used to obtain the scattered field everywhere else. It would therefore appear plausible to use this same principle for computing backscatter from forward propagation. That is, consider the forward scatter solution along some bounding surface as an incident field. Then, integrate this surface field to obtain solutions at any points of interest within the propagation medium, including points at backward locations.

Forward scatter versions of this procedure have been employed previously. A Green's function version was used implicitly to confine the PE grid to a region near the ground

that is bounded above by a horizontal reference plane located above all terrain irregularities [1]. An integral transform version has been used explicitly to determine the fields above this reference plane [6]. The Green's function method can also be used to compute the fields above the reference plane. When the PE Green's function is used, it would provide results that are essentially identical to those presented in Reference 6, and only forward scatter would be included. But there is no inherent reason to limit implementation to the PE Green's function. If, instead, the Green's function for the elliptic Helmholtz equation is used, then the ôincidentö fields along the reference plane can be continued in both the forward and backward directions into the region above this plane.

For the scheme cited above, although a solution is being obtained of an equation that has the capability of providing both forward and backscatter information, the amount of backscatter included would be limited. This is because the solution is based on the fields on the reference plane, and these fields only contain forward scatter information. However, as the reference plane is lowered and approaches the ground-based source of the potential backscatter, the horizontal change in the field magnitude along the ground near this source would become more pronounced. If the integration is performed over the surface itself, a first order approximation of backscatter would be obtained.

Results obtained using this method will be presented for backscatter effects from the following types of discontinuities:

1. Horizontal ground over which the ground properties vary (e.g. land-sea-land).

2. A bend in an atmospheric duct.

3. A ground obstacle.

REFERENCES

[1] Marcus, S.W., "A hybrid (finite difference - surface Green's function) method for computing transmission losses in an inhomogeneous atmosphere over irregular terrain", IEEE Trans. Antennas Propagat., Vol. 40, No. 12, Dec. 1992.

[2] Barrios, A. E., "A terrain parabolic equation model for propagation in the Troposphere", IEEE Trans. Antennas Propagat., Vol. 42, No. 1, Jan. 1994.

[3] G. D. Dockery, "Modelling electromagnetic wave propagation in the troposphere using the parabolic equation", IEEE Trans. Antennas Propagat., vol. AP-36, no. 10, pp. 1464-1470, Oct. 1988.

[4] K. H. Craig and M. F. Levy, "Parabolic equation modelling of the effects of multipath and ducting on radar systems", IEE Proc.-F, Vol. 138, No. 2, Apr. 1991.

[5] F. D. Tappert, "The parabolic approximation method", in Wave Propagation and Underwater Acoustics., J.B. Keller and J.S. Papadakis, Eds., New York: Springer-Verlag, 1977.

[6] M. Levy, "Horizontal parabolic equation solution of radio wave propagation problems on large domains", IEEE Trans. Antennas Propagat., Vol. 43, No. 2, pp. 137-144, Feb. 1995.

BACKSCATTER FROM PARABOLIC EQUATIONS:

FACT or *FANTASY*

Kirchoff Approximation

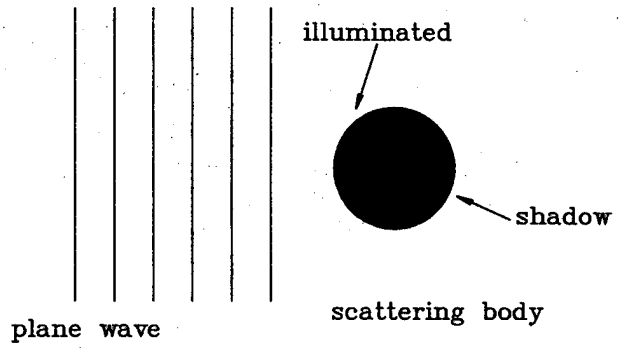

scattered field from integral over field on surface
surface field = incident field

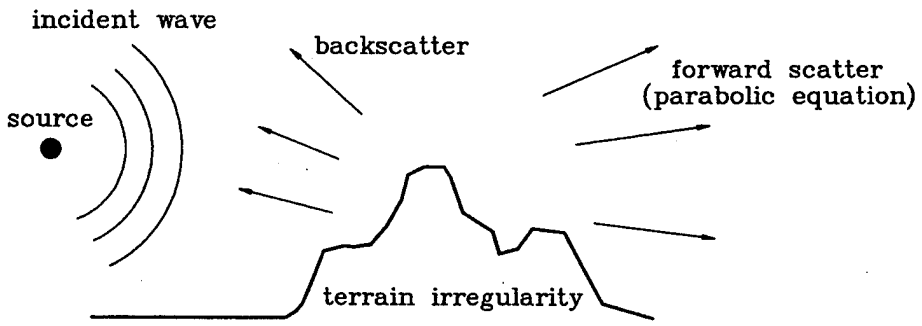

Scattering from terrain irregularity.

With parabolic equation, terrain has no effect on calculations in backward direction.

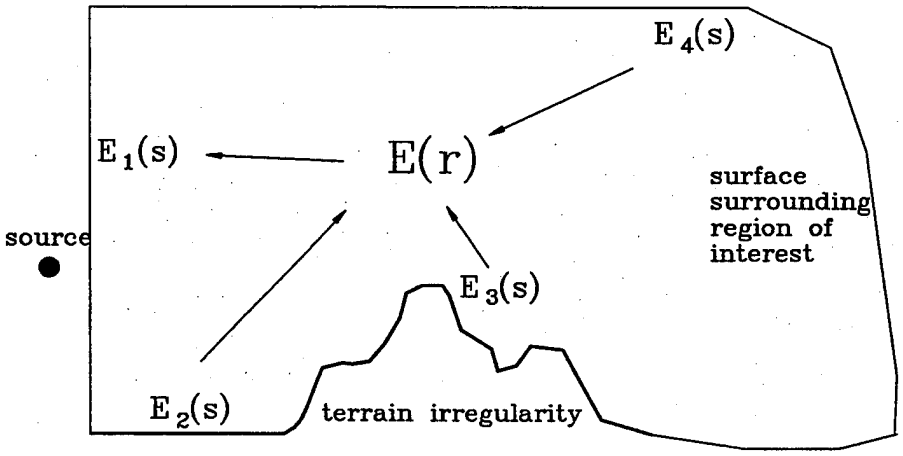

Solution of elliptic differential equation for E(r) using Green's theorem.
E(r) within region can be found in terms of E(s) and its normal derivative along surface.

E(s) ?????

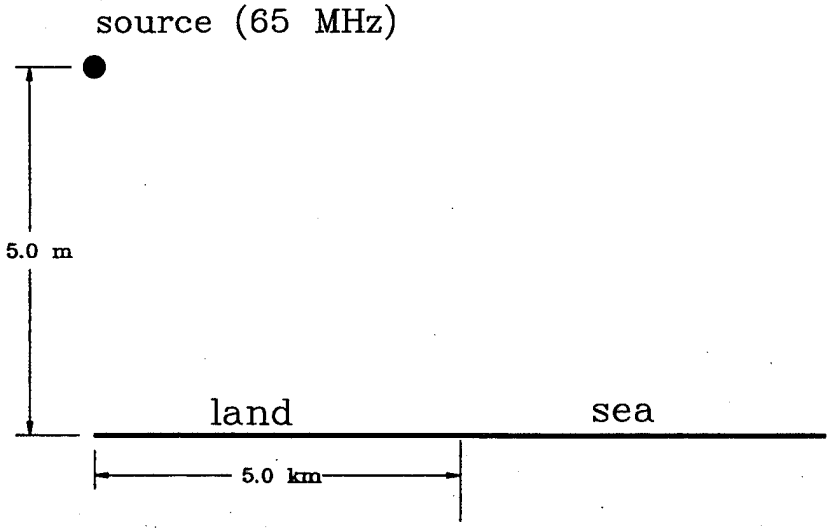

Mixed path configuration used for backscatter predictions.

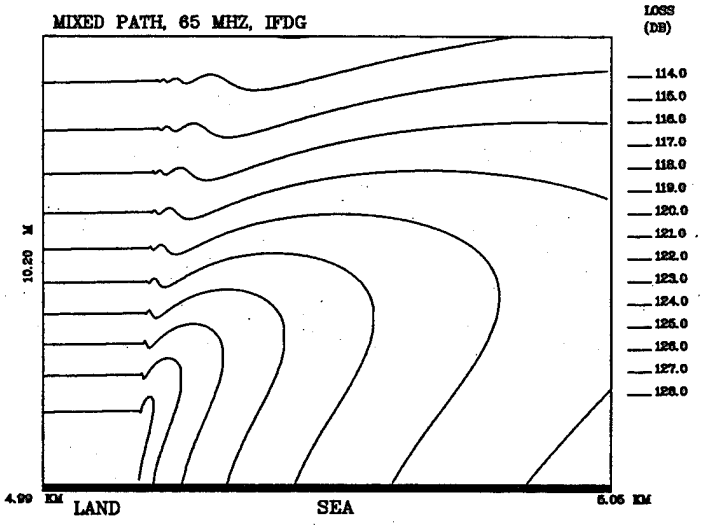

Equi-path loss contour plot for propagation over mixed path, frequency = 65 MHz, vertical polarization, transmitter height = 5 m. Results were obtained using the IFDG method.

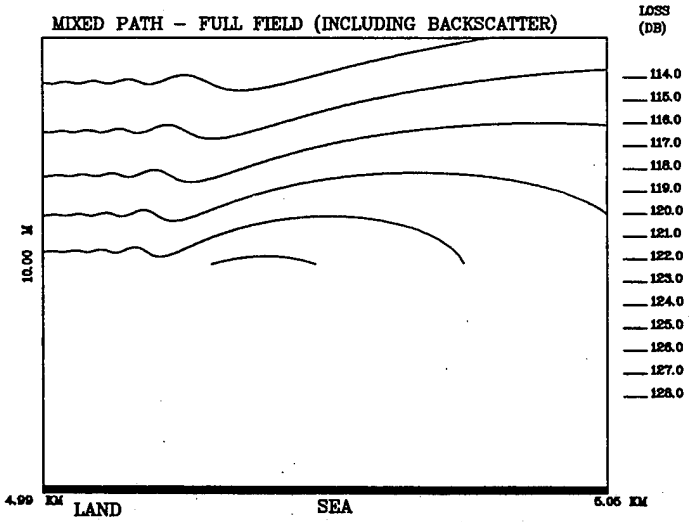

Field due to propagation over mixed path, frequency = 1 GHz, vertical polarization, transmitter height = 5 m. Predictions obtained from BSCAT model.

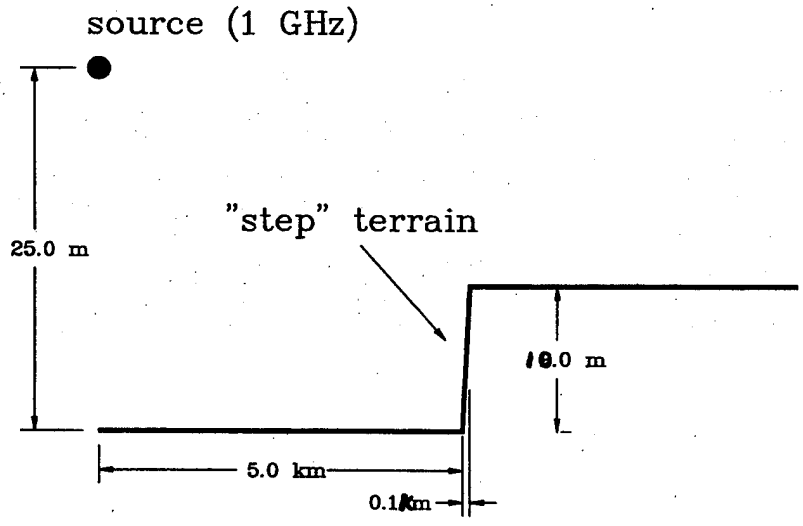

Step terrain configuration used for backscatter predictions.

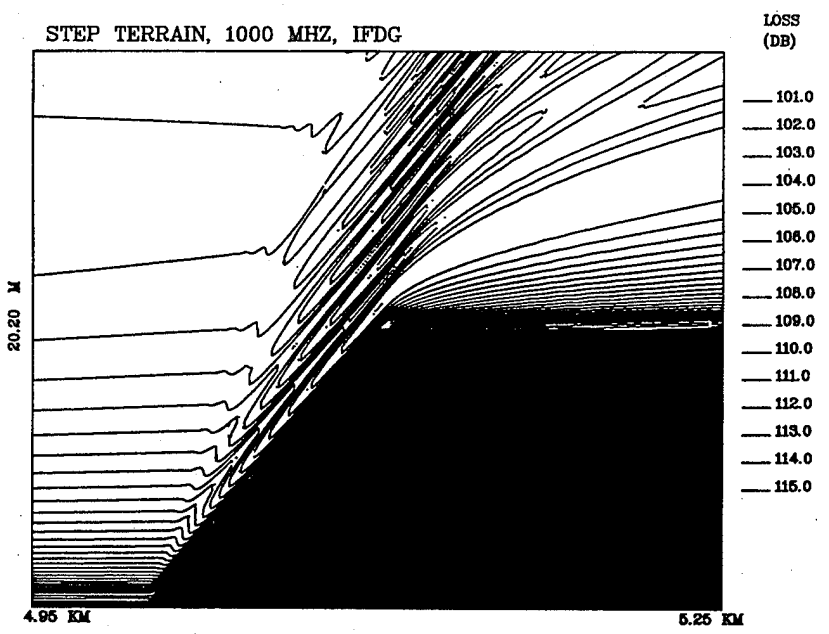

Equi-path loss contour plot for propagation over step-terrain, frequency = 1 GHz, vertical polarization, transmitter height = 25 m. Results were obtained using the IFDG method.

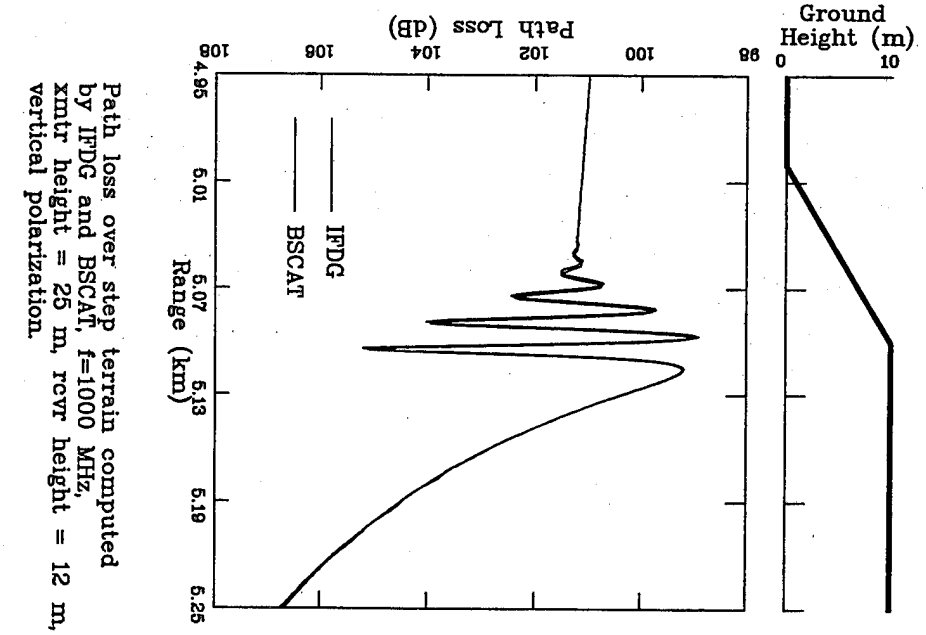

Path loss over step terrain computed by IFDG and BSCAT, f=1000 MHz, xmtr height = 25 m, rcvr height = 12 m, vertical polarization.

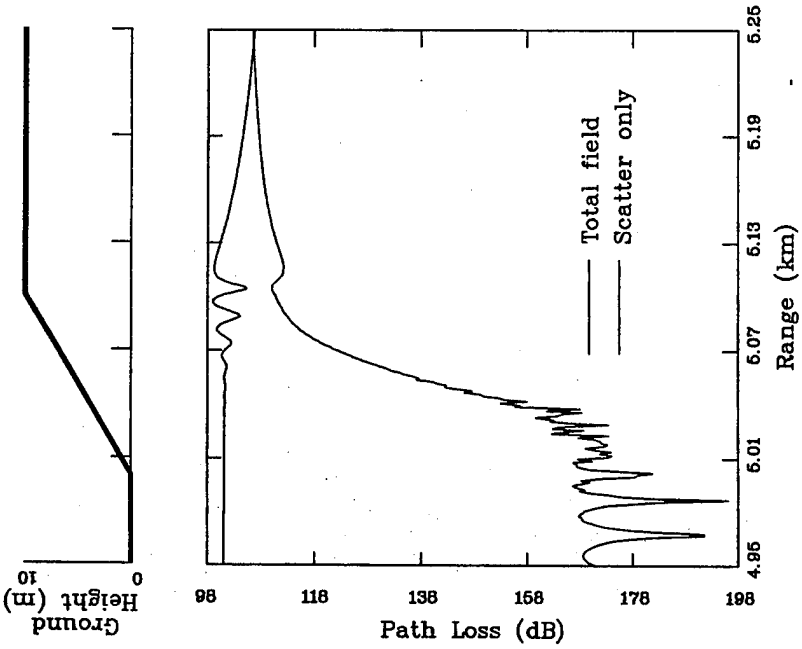

Total field and scattered field computed by BSCAT due to step terrain, f=1 GHz, xmtr height = 25 m, rcvr height = 12 m, vertical polarization.

RADAR CLUTTER

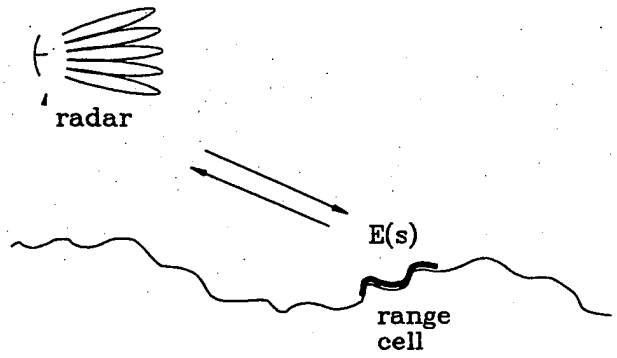

Illuminated terrain patch as a source of backscatter.

Dr. Sherman Marcus, "Backscatter from Parabolic Equations: Fact or Fantasy?"

DISCUSSION

M. LEVY
Can this method cope with a ducting environment?

AUTHOR'S REPLY
Not without major revision.

G. BROOKE
Have you considered comparing your results with those generated using two-way PE methods from underwater acoustics?

AUTHOR'S REPLY
It is not clear to me that backscatter from a terrain irregularity in the em case is comparable to the volumetric scattering in the underwater acoustic case. If such an analogy is valid, however, then comparisons can be performed in the future.

R. JANASWAMY
You are comparing two solutions, one based on PE and the second based on Green's function with surface current based on the solution of PE. You would expect them to agree. How about comparing your second solution to an exact solution?

Comment: Backscattering will become important in situations involving multiple scattering, for example in the region between two hills. The solution will require a 'true backscattered' field.

AUTHOR'S REPLY
Although no quantitative comparisons have been performed yet, the qualitative behavior of the scattered field has been observed to behave as expected: the scattered field from a point slope discontinuity behaves like an effective source.

A more precise backscattered field can be obtained through a process of successive approximation of the boundary field.

Air Force Requirements

Dr. Walter Dale Meyer
Headquarters Air Weather Service/XOXT
102 West Losey Street, Room 105
Scott AFB, IL 62225-5206
Tel: (618) 256-5631 ext 444
Fax: (618) 256-6306
meyerw@hqaws.safb.af.mil

AIR FORCE / ARMY REQUIREMENTS FOR E-M MODELS

- OVERVIEW
  - OPERATIONAL REQUIREMENTS
  - TECHNICAL NEEDS
  - SCIENCE NEEDS
  - AIR FORCE SOLUTIONS
  - SUMMARY

OPERATIONAL REQUIREMENTS

- AIR FORCE SUPPORTS A FULL-RANGE OF E-M SYSTEMS IN SEVERAL WAVELENGTHS
  - AWACS / JOINT STARS / EF-111 STAND-OFF / B-2 HARPOON / TERRAIN AVOIDANCE RADAR / HAVE-STARE RADAR / WARNING SYSTEMS / E-O PRECISION-GUIDED WEAPONS
  - MICROWAVE / INFRA-RED / VISUAL
- AIR FORCE USES SOME NAVY MICROWAVE E-M MODELS
  - IREPS / EREPS / RAYTRACE / VTRP

TECHNICAL NEEDS
Better Weather Data

- **AMOUNT AND QUANTITY OF WEATHER DATA INSUFFICIENT FOR AIR FORCE / ARMY OPERATIONS**
  - ACCURACY OF NWP SPECIFICATION / FORECAST INPUTS TO E-M MODELS SENSITIVE TO ACCURACY AND RESOLUTION OF CONVENTIONAL WEATHER OBSERVATIONS
  - NEED:
    - » HIGHER RESOLUTION UPPER AIR MEASUREMENTS
    - » MORE AUTOMATED SURFACE OBSERVATIONS
    - » IMPROVED REMOTELY-SENSED OBSERVATIONS
    - » AUTOMATED DATA QUALITY CONTROL

TECHNICAL NEEDS
Better Weather Models

- **RESOLUTION AND PHYSICS OF NWP MODELS INSUFFICIENT FOR AIR FORCE / ARMY OPERATIONS**
  - RESOLUTION OF NWP MODELS INSUFFICIENT TO RESOLVE PHYSICAL PROCESSES IMPACTING E-M SYSTEMS
  - PHYSICS OF NWP MODEL INSUFFICIENT TO DESCRIBE THESE PHYSICAL PROCESSES
  - NEED:
    - » HIGHER RESOLUTION NWP MODELS
    - » IMPROVED MODEL PHYSICS
      - HYDOLOGICAL PROCESSES
      - COMPLEX TERRAIN AND VEGETATION PROCESSES

SCIENCE NEEDS
Better Models, Data, QC

- **RESEARCH IS NEEDED**
  - TO IDENTIFY THE BEST HIGH-RESOLUTION NWP MODEL FOR AIR FORCE AND ARMY OPERATIONS
  - THE BEST SUITE OF IN-SITU AND REMOTE ATMOSPHERIC AND HYDROLOGICAL MEASUREMENTS FOR A HIGH-RESOLUTION NWP MODEL
  - TO IDENTIFY THE BEST WAY TO
    - » QUALITY CONTROL
    - » INTEGRATE, AND
    - » REPRESENT

    HIGH-RESOLUTION WEATHER DATA AND FORECASTS

AIR FORCE / ARMY SOLUTIONS
Observations

- **TROPOSPHERIC**
  - METEOROLOGICAL MEASURING SYSTEM (ARMY)
  - AUTOMATED METEOR PROFILING SYSTEM (ARMY)
  - TAC UAV W/ MET SENSORS AND DROPSONDE (ARMY)
  - ATMOS PROFILES FROM SATELLITE MEA (DMSP)
- **SURFACE**
  - AUTOMATED METEOR SENSOR SYSTEM (ARMY)
  - AUTOMATED SURFACE OBSERVING SYSTEM (NWS /AF)
  - IMPROVED REMOTELY MONITORED BATTLEFIELD SENSOR SYSTEM (ARMY)

AIR FORCE / ARMY SOLUTIONS
Observations - Continued

- **GROUND**
  - AGRICULTURE METEOROLOGY DATABASE (AIR FORCE)
  - SOIL MOISTURE AND TEMPERATURE SENSORS (TBD)
  - SATELLITE REMOTE SENSING (AIR FORCE)

AIR FORCE / ARMY SOLUTIONS
Models

- **HIGH RESOLUTION WEATHER MODELS**
  - THEATER FORECAST MODEL (TBD)
  - GLOBAL / THEATER WEATHER ANALYSIS AND PREDICTION SYSTEM (AIR FORCE)
  - ONE-DEGREE GLOBAL WEATHER MODEL (NAVY)
  - CLOUD DEPICTION AND FORECAST SYSTEM II (AIR FORCE)
  - BATTLEFIELD WEATHER MODEL (ARMY)
- **VERY HIGH RESOLUTION WEATHER MODEL**
  - TO BE DEFINED

AIR FORCE / ARMY SOLUTIONS
Data QC and Representation

- AUTOMATED QUALITY CONTROL
  - METEOROLOGICAL OPERATIONAL CAPABILITY (AWS)
  - AFGWC AND USAFETAC COMPUTER UPGRADES
- INTEGRATION AND REPRESENTATION OF BATTLEFIELD WEATHER DATA
  - TACTICAL OBSERVING AND FORECASTING SYSTEM (AF)
  - INTEGRATED METEOROLOGICAL SYSTEM (ARMY)
- INTEGRATION AND REPRESENTATION OF AFGWC WEATHER DATA
  - AFGWC MODELS AND COMPUTER UPGRADES (AIR FORCE)
  - OPERATIONAL 4D DATA ASSIMILATION (AIR FORCE)

SUMMARY

- AIR FORCE SUPPORTS A FULL-RANGE OF E-M SYSTEMS
- AFW EFFORTS TO IMPROVE SUPPORT TO AIR FORCE MICROWAVE E-M SYSTEMS FOCUSED ON IMPROVING WEATHER INPUTS TO NAVY MICROWAVE E-M MODELS
- AIR FORCE WILL CONTINUE TO LOOK TO NAVY FOR IMPROVED STATE-OF-THE-ART MICROWAVE E-M MODELS

Dr. Dale Meyer, "Air Force Requirements"

DISCUSSION

D. DOCKERY

Has the Air Force quantified the requirements for environmental data over complex terrain?

AUTHOR'S REPLY

We have searched our requirements database and did not find an entry for "complex terrain". The database does include a grid resolution requirement for 1 nm - which implies complex terrain should be considered.

SESSION III. ENVIRONMENTAL INPUTS FOR PROPAGATION MODELS

Chair: Dr S. Burk

EFFECTS OF THE VARIABILITY OF ATMOSPHERIC REFRACTIVITY

L. Ted Rogers
Ocean and Atmospheric Sciences Division
Naval Command Control and Ocean Surveillance Center
Research Development Test and Evaluation Division
San Diego, CA 92152

Atmospheric refractivity varies in time and space. Recent advances in propagation modeling allow for the rapid computation of propagation estimates using range dependent refractivity structures. The major question is thus: "How, how often, and where must refractivity be sensed to produce the most accurate propagation estimates within cost and operational constraints?" A method is presented for the determination on limitations on the accuracy of propagation estimates from time series of measured propagation loss. Using data from the Variability Of Coastal Atmospheric Refractivity (VOCAR) experiment, the RMS error of propagation estimates calculated from radiosondes where horizontal homogeneity was assumed, are compared to the limiting accuracy. The conclusion is that range dependent refractivity measurements will yield little improvement in accuracy over the use of horizontally homogeneous structures, unless the update times for the structures are on the order of, at most, an hour. The conclusion, of course, applies to the area where the VOCAR experiment was conducted with the frequencies and geometries of the VOCAR experiment. The analysis method though, can be applied to data sets where both time series of propagation measurements and precision meteorology are both available. A paper detailing the method and results using the VOCAR data data recently been found suitable for publication in *IEEE Transactions on Antennas and Propagation.*

Effects of the Variability of Atmospheric Refractivity

L. Ted Rogers

Code 543

Ocean and Atmospheric Sciences Division

Naval Command, Control and Ocean Surveillance Center

Variability Of Coastal Atmospheric Refractivity (VOCAR) Experiment: Measurement Results

The question: To what length do we need to go in measuring the refractive environment to obtain propagation estimates with a specified accuracy?

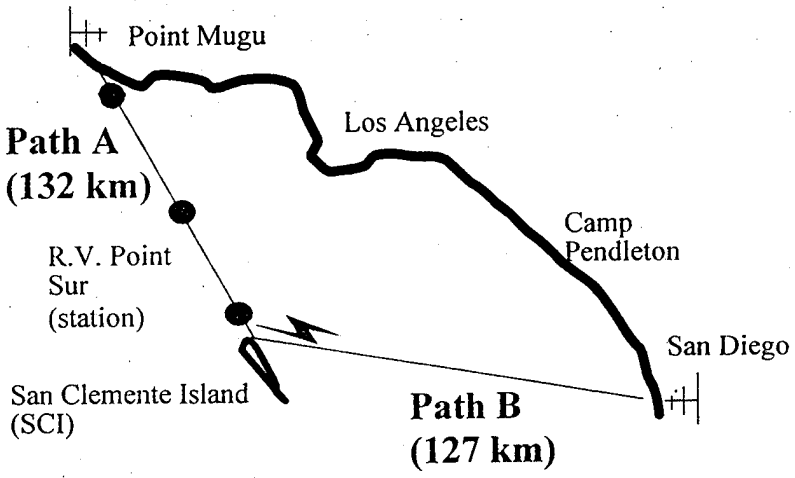

Freq: 143.09, 262.85, 374.95 MHz; xmt. / rcv. ant. ht: 17.5m / 30.5m

Accuracy

$x(t)$	-	Measured prop. factor
$\hat{x}(t)$	-	Est. prop. factor at time
$\rho_{X,\hat{X}}$	-	Correlation coefficient
σ	-	Standard deviation
μ	-	Mean

RMS error:

$$RMS_{X,\hat{X}} = \left\{\frac{1}{T}\int_0^T (x(t)-\hat{x}(t))^2 dt\right\}^{\frac{1}{2}}$$

$$= \left\{\sigma_X^2 + \sigma_{\hat{X}}^2 - 2\sigma_X\sigma_{\hat{X}}\rho_{X,\hat{X}} + (\mu_X - \mu_{\hat{X}})^2\right\}^{\frac{1}{2}}$$

Bias: $b = \mu_{\hat{X}} - \mu_X$

$$RMS_{X,\hat{X}} = 0 \Rightarrow \begin{cases} \sigma_X = \sigma_{\hat{X}} \\ \mu_X = \mu_{\hat{X}} \\ \rho_{X,\hat{X}} = 1.0 \end{cases}$$

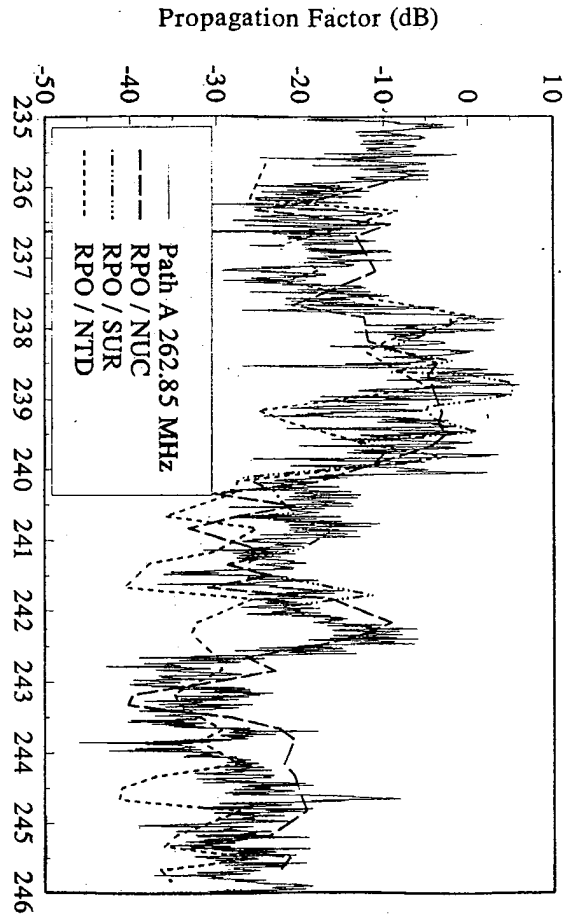

Path A 262.85 MHz

Table 11. *Zero-lag Estimation error of Path A 262.85 Mhz propagation factor[Y]* .

Estimator [X]:	#	σ_Y	σ_X	μ_Y	μ_X	RMS	STD	ρ	Bias
RPO / NUC	43	9.75	9.68	-19.30	-19.19	8.73	8.73	.60	.11
RPO / SUR	27	10.62	9.98	-13.52	-12.37	8.02	7.94	.70	1.15
RPO / NTD	43	9.76	11.17	-19.08	-25.22	10.38	8.37	.69	-6.14
B - 262.85 MHz	98	10.63	10.29	-17.27	-19.41	9.05	8.79	.65	-2.14
Free Space	98	10.63	0.00	-17.27	0.00	20.27	10.63	.00	17.27
Standard Atm.	98	10.63	0.00	-17.27	-49.10	33.56	10.63	.00	-31.83
Signal Avg.	98	10.63	0.00	-17.27	-17.27	10.63	10.63	.00	0.00

Measured and estimated propagation factor at 262.85 MHz
Path A, 27 August 1993 and 28 August 1993

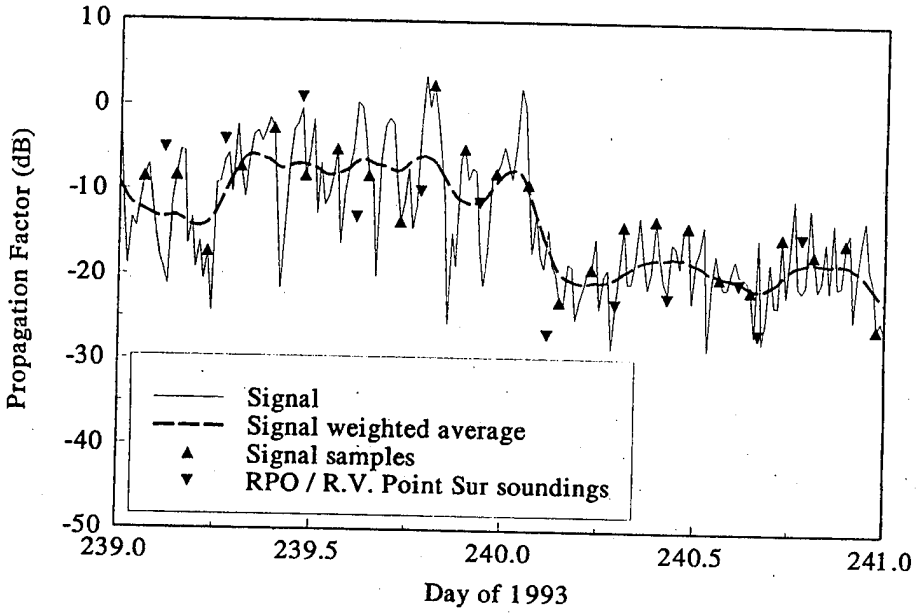

Path A 262.85 MHz

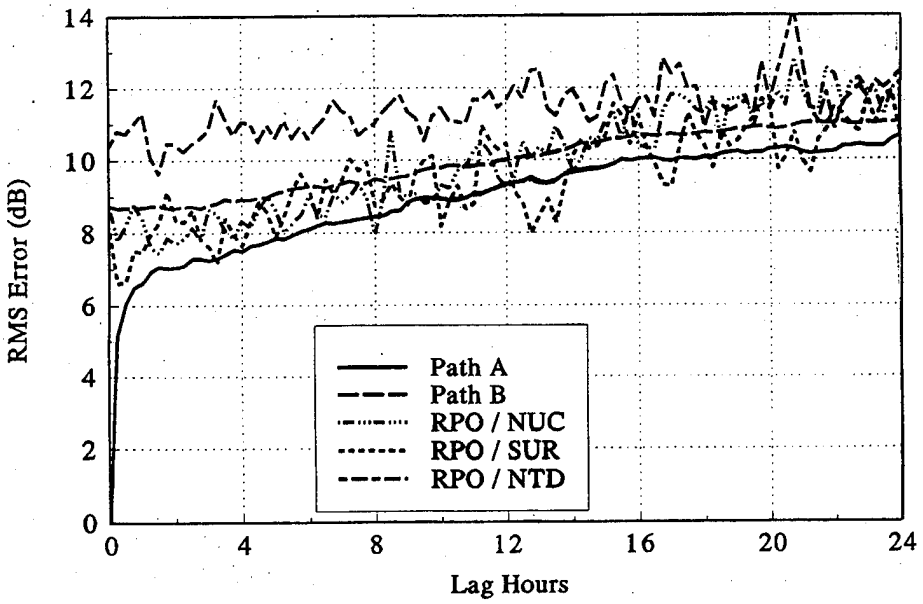

VOCAR Standard Error: Path A 262.85 MHz.

August 23, 1993 - September 2, 1993

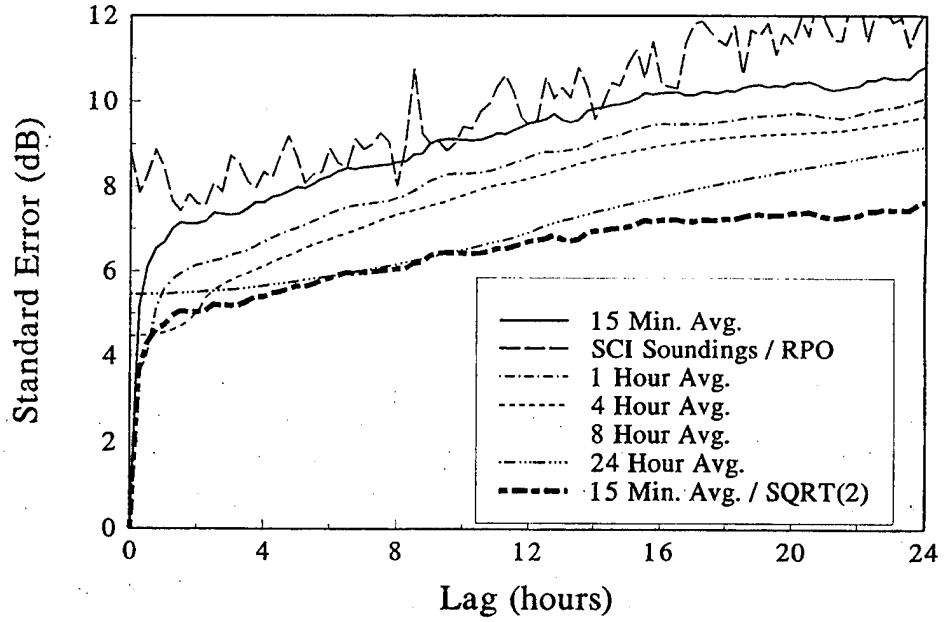

VOCAR Standard Error: Path A 262.85 MHz.

August 23, 1993 - September 2, 1993

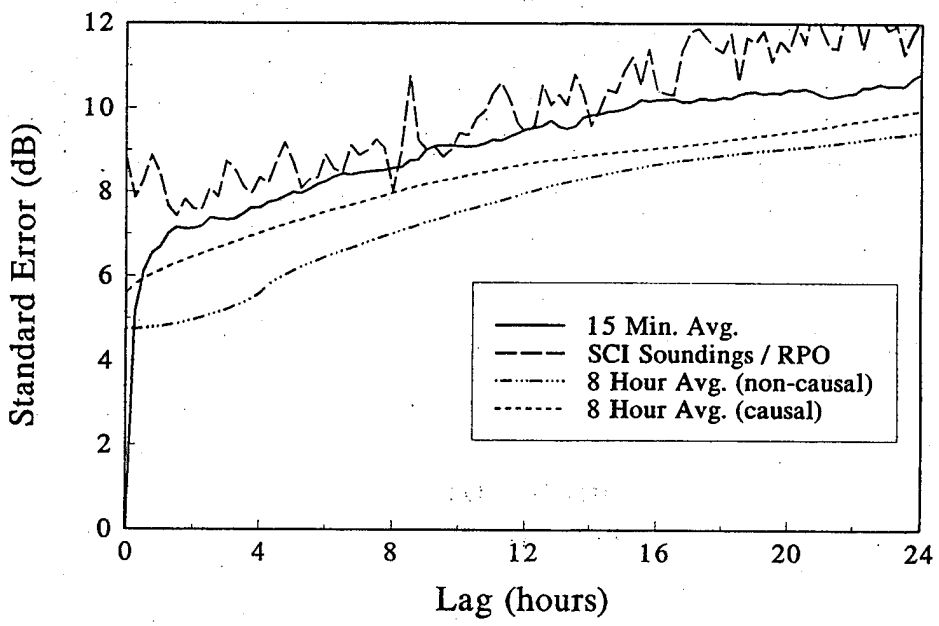

Summary

1. VOCAR Results:
   (a) SoCal area can be considered largely homogeneous.
   (b) Benefits of range dependency unlikeley for $\tau \geq 2$ hours.
   (c) Applicability:

	Duct Type		
Freq. Range	Surf.	Elev.	Evap.
UHF VHF	VOCAR	VOCAR	N/A
SHF		N/A	

2. Methods of analysis is general:
   (a) RMS error: principal statistic of estimation accuracy.
   (b) Lag time τ is a critical consideration.
   (c) Limiting errors can be calculated.

Mr. Ted Rogers, "Effects of the Variability of Atmospheric Refractivity"

DISCUSSION

R. HELVEY

Comment: the conclusion that refraction is homogeneous for "SOCAL area" should be more conservatively restricted to regions traversed by propagation paths (southeast part of SOCAL bight) - there is meteorological evidence for more significant variability (especially spatial) in the NW part of the area (downwind of Pt. Arguello).

M. VOGEL

Your showed us that when you perform radiosonde measurements on the shore in order to predict propagation over the sea, the predictions are likely to be inaccurate. Was the wind blowing from the sea or from the land during these experiments?

AUTHOR'S REPLY

It is most likely that both on-shore and off-shore flows were present during the test period.

M. PASTORE

Did you use all 3 profiles together to get an RPO propagation curve?

AUTHOR'S REPLY

No. There were only 11 instances where three profiles from the San Clemente Island to Point Mugu path were taken within 1 hour of each other, and virtually none where they were within 15 minutes of each other. Due to the timing differences and the reduction in vertical points in each profile that is performed when "feature connecting" profiles manually, *range dependent* estimates calculated using the VOCAR profiles will perform little or no better than the *homogeneous* estimates. This assertion agrees with the findings of Molly Barrios (published in AGARD CP 567, *Propagation Assessment in Coastal Environments*, Feb. 1995) that using range dependent propagation estimates for the VOCAR links resulted in little or no improvement in accuracy over that obtained using homogeneous estimates.

The problem is that if the accuracy of propagation estimates calculated using a given set of range dependent meteorological measurements with a given profile connection algorithm results in no improvement in estimation accuracy over that obtained using homogeneous estimates, it is inevitably suggested that the data collection methods or connection algorithms need improvement. The way around this problem is to determine the error minimizing performance for any (i.e. homogeneous or range dependent) *unfiltered* estimate from a high fidelity model. As shown in the slide titled "Accuracy (continued)", that minimum error is obtained if propagation estimates are exact at the time of

environmental measurements used to calculate them. To assume that range dependent estimate will have zero error at the time of the environmental measurements used for their calculation is an assumption strongly in their favor.

If environmental data are taken at a sufficiently high temporal sampling rate, then the propagation estimates can be filtered, hopefully to obtain the mean value of the signal level over some time interval. In that case the minimum RMS error is reduced by a factor of .7071.

MODELING MESOSCALE REFRACTIVITY STRUCTURE DURING THE VOCAR EXPERIMENT

Stephen D. Burk
William T. Thompson
Naval Research Laboratory
Marine Meteorology Division
7 Grace Hopper Avenue
Monterey. CA 93943-5502
tel. 408-656-4797
email: burk@nrlmry.navy.mil
fax: 408-656-4769

ABSTRACT

The Variability of Coastal Atmospheric Refractivity (VOCAR) Experiment was conducted during late August and early September, 1993 in the Southern California Bight. Throughout the 12 days of the VOCAR Intensive Observing Period (IOP) a mesoscale model (NORAPS) produced twice-daily 24h forecasts covering the VOCAR domain. This model was run at NRL in Monterey and used 20 km grid spacing in the horizontal, with 30 levels in the vertical. Fields were saved every 4h of each forecast because this coincided with four-hourly launch schedule of many special radiosondes in the region. We have analyzed this model data set and used surface observations, radiosondes, and other data sources to evaluate the mesoscale model performance.

The model forecasts the existence of a trapping layer in the Bight at the top of the marine boundary layer (MBL) during much of the period of the VOCAR IOP. This trapping layer tends to be particularly strong immediately above a model forecast stratus layer because the combined effects of cloud-top cooling and entrainment, in the presence of subsidence, enhance the strength of the vertical gradients capping the MBL. The model forecasts the trend in MBL depth in the Bight quite well throughout most of the period of the IOP. This is a very important parameter because it is often the principal factor determining if a trapping layer acts as surface-based or elevated duct. The model's vertical profiles of modified refractivity are compared with profiles from the many VOCAR soundings.

Because of the major impact stratus and stratocumulus clouds can indirectly have upon the refractivity field, we have examined the model forecasts of MBL clouds during the VOCAR IOP. We use satellite (GOES) film loops to evaluate the model's performance. By using model visualization techniques, we have been able to simulate a "satellite view" of the model's cloud behavior.

MODELING MESOSCALE REFRACTIVITY STRUCTURE DURING THE VOCAR EXPERIMENT

Stephen D. Burk and
William T. Thompson
Naval Research Laboratory
Marine Meteorology Division
Monterey, CA 93943

The Variability of Coastal Atmospheric Refractivity (VOCAR) Experiment

- 23 Aug - 3 Sep 1993
- Assess Importance of Mesoscale Refractivity Variability to EM Propagation
- SoCal Data Collection Network
  -- Soundings Every 4 Hours
  -- Ship, Aircraft, Lidar
  -- Propagation Loss Measurements
- Mesoscale Model (NORAPS) Forecasts
  -- Fields Saved Every 4 Hours

MESOSCALE MODEL DESCRIPTION

- 2160 km E-W x 1620 km N-S
- 20 km grid spacing; 30 vertical levels
- NORAPS:

  Hodur (1987)

  Burk & Thompson (1989)

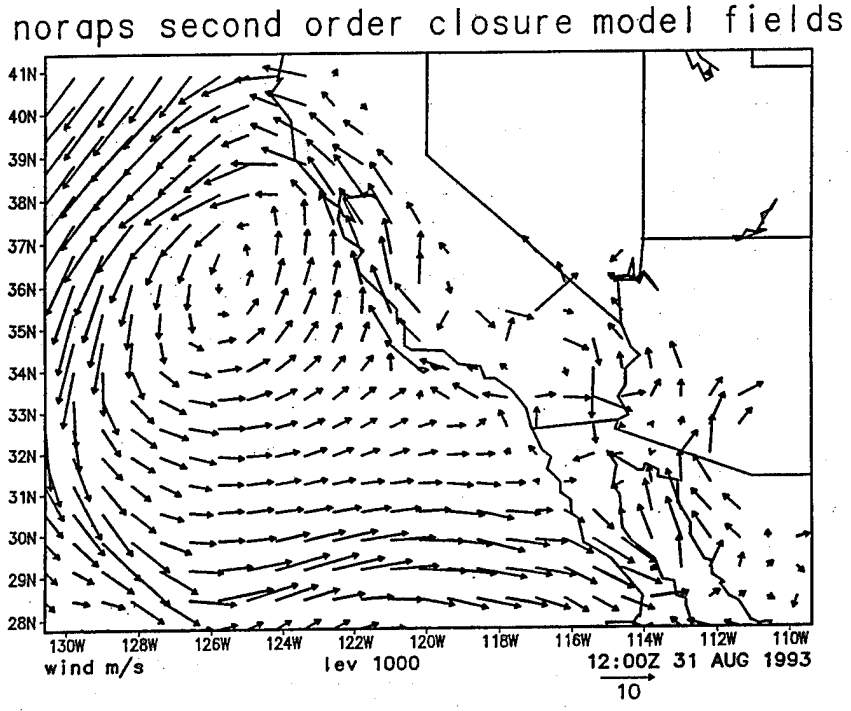

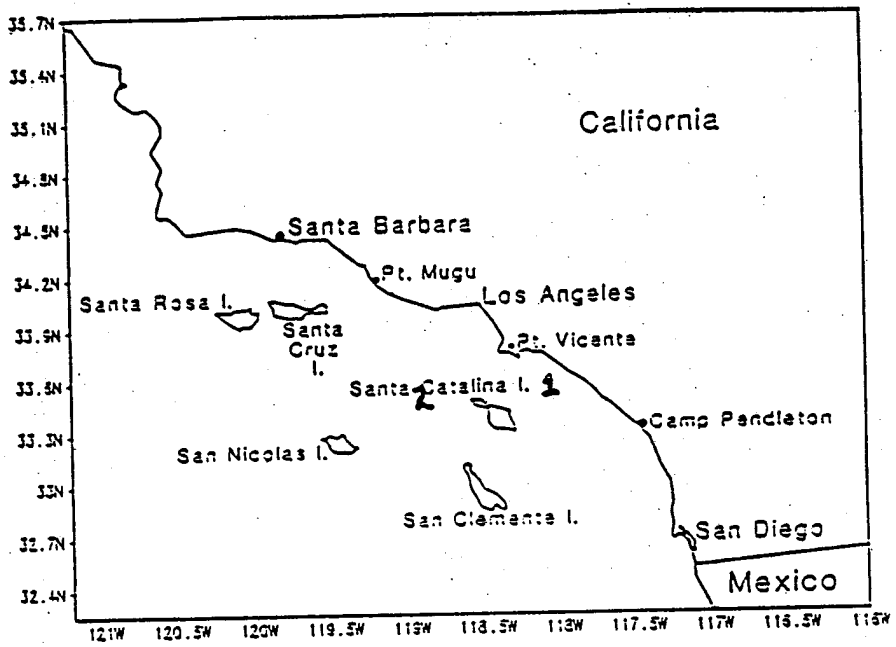

REGION OF VOCAR EXPERIMENT

(23 AUG - 3 SEP 1993)

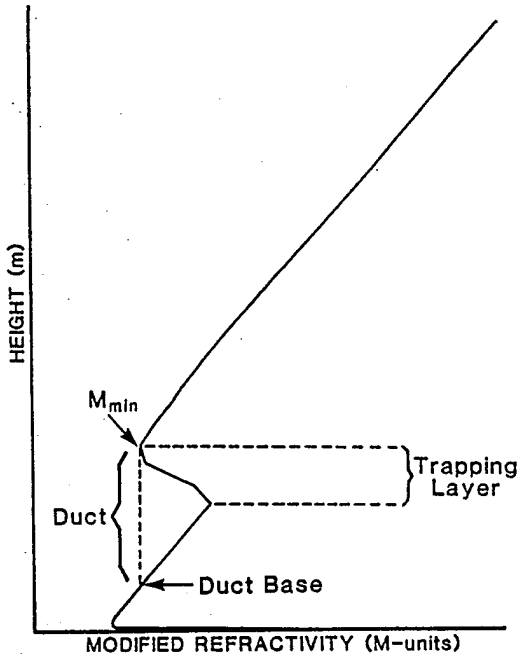

1

noraps second order closure model fields

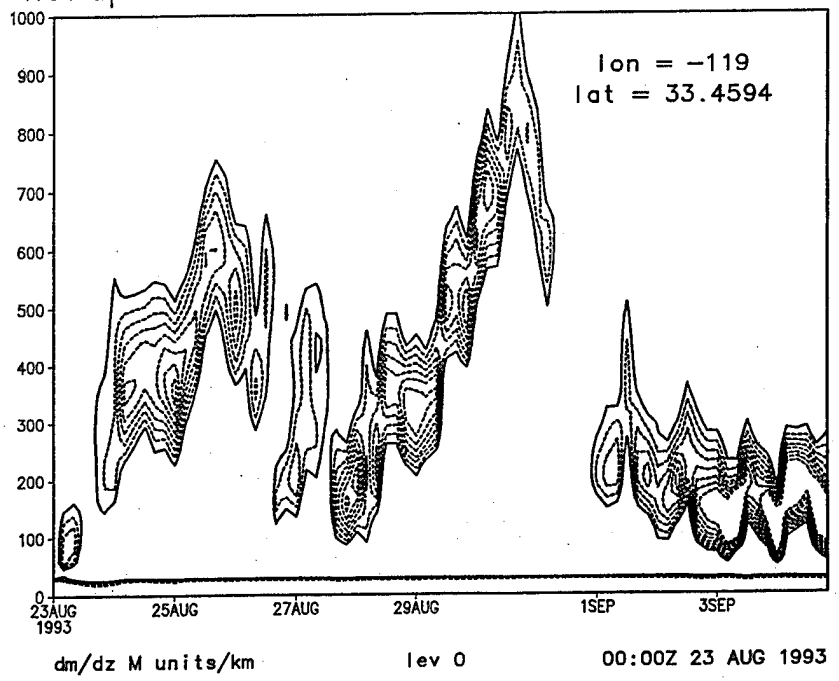

dm/dz M units/km lev 0 00:00Z 23 AUG 1993

2

noraps second order closure model fields

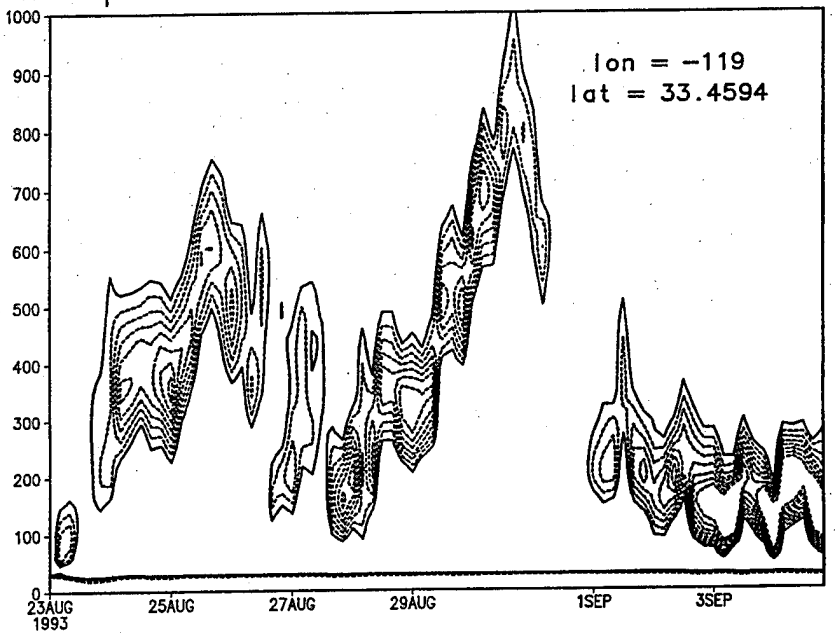

dm/dz M units/km lev 0 00:00Z 23 AUG 1993

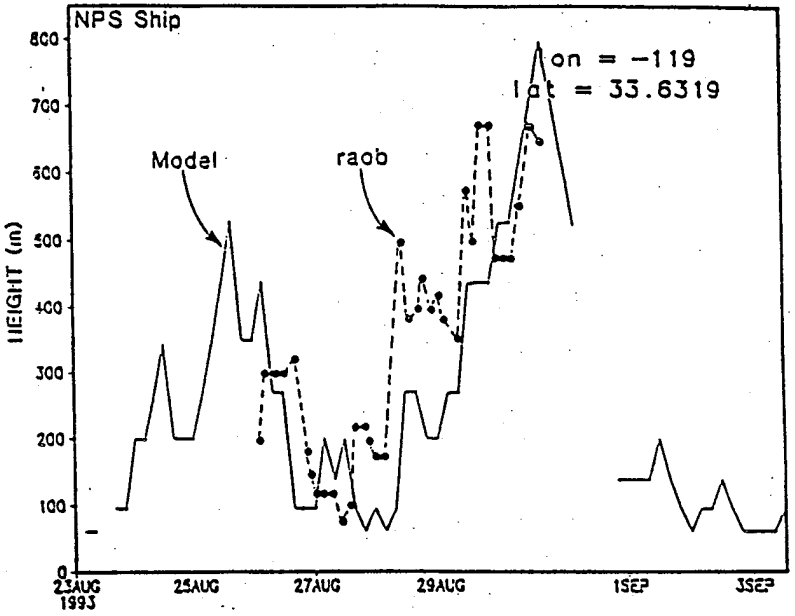

BASE OF TRAPPING LAYER FORECAST BY MODEL (SOLID LINE) AND AS FOUND FROM NAVY POSTGRADUATE SCHOO SHIP RADIOSONDES (DASHED-DOTTED LINE)

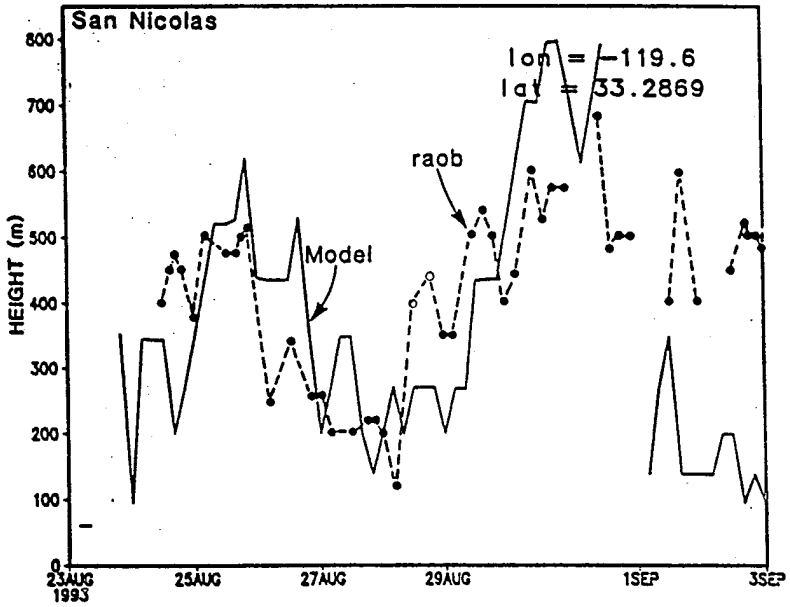

BASE OF TRAPPING LAYER FORECAST AND OBSERVED AT SAN NICOLAS ISLAND DURING VOCAR

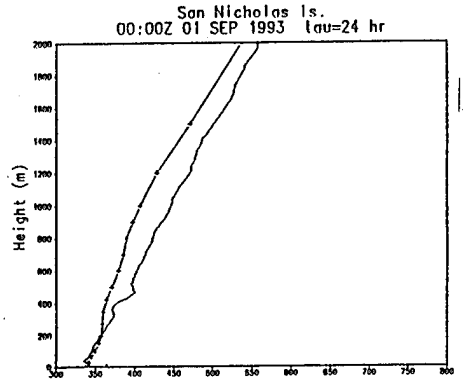
San Nicholas Is.
00:00Z 01 SEP 1993 tau=24 hr
Height (m)

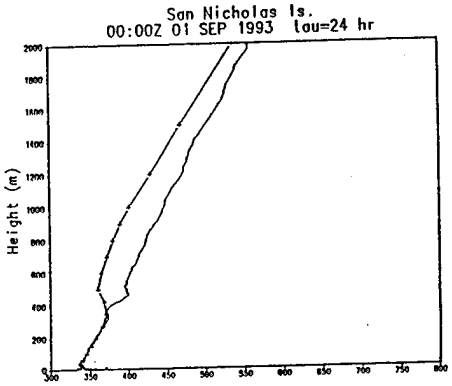
San Nicholas Is.
00:00Z 01 SEP 1993 tau=24 hr
Height (m)

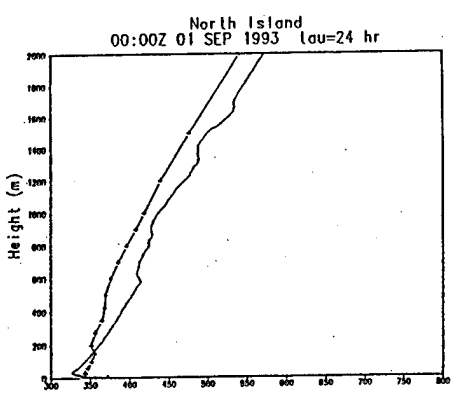
North Island
00:00Z 01 SEP 1993 tau=24 hr
Height (m)

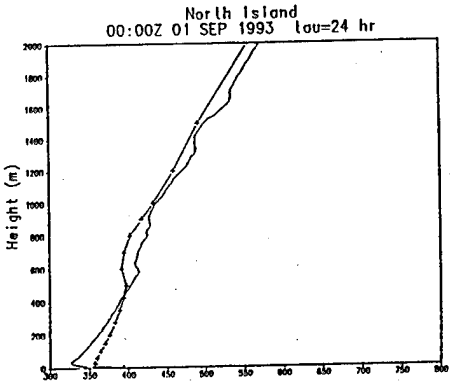
North Island
00:00Z 01 SEP 1993 tau=24 hr
Height (m)

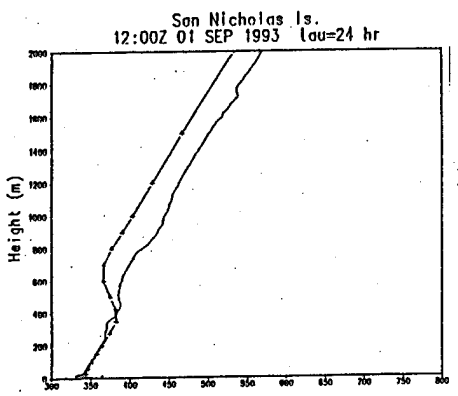
San Nicholas Is.
12:00Z 01 SEP 1993 tau=24 hr
Height (m)

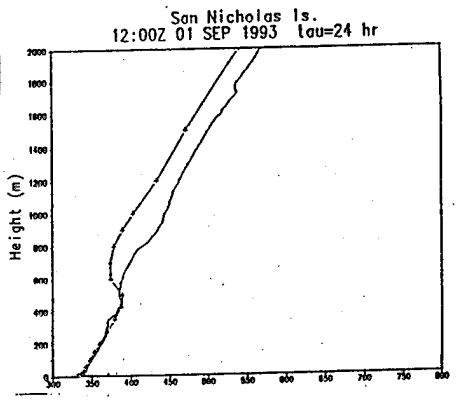
San Nicholas Is.
12:00Z 01 SEP 1993 tau=24 hr
Height (m)

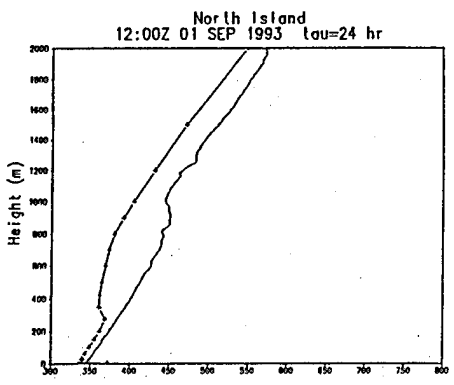
North Island
12:00Z 01 SEP 1993 tau=24 hr
Height (m)

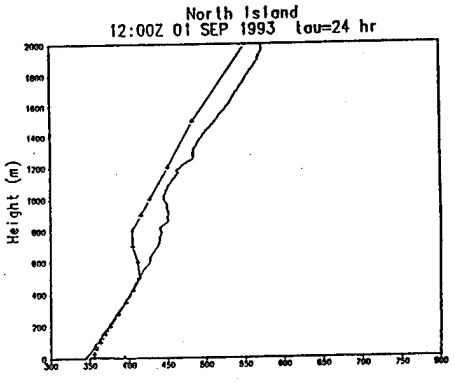
North Island
12:00Z 01 SEP 1993 tau=24 hr
Height (m)

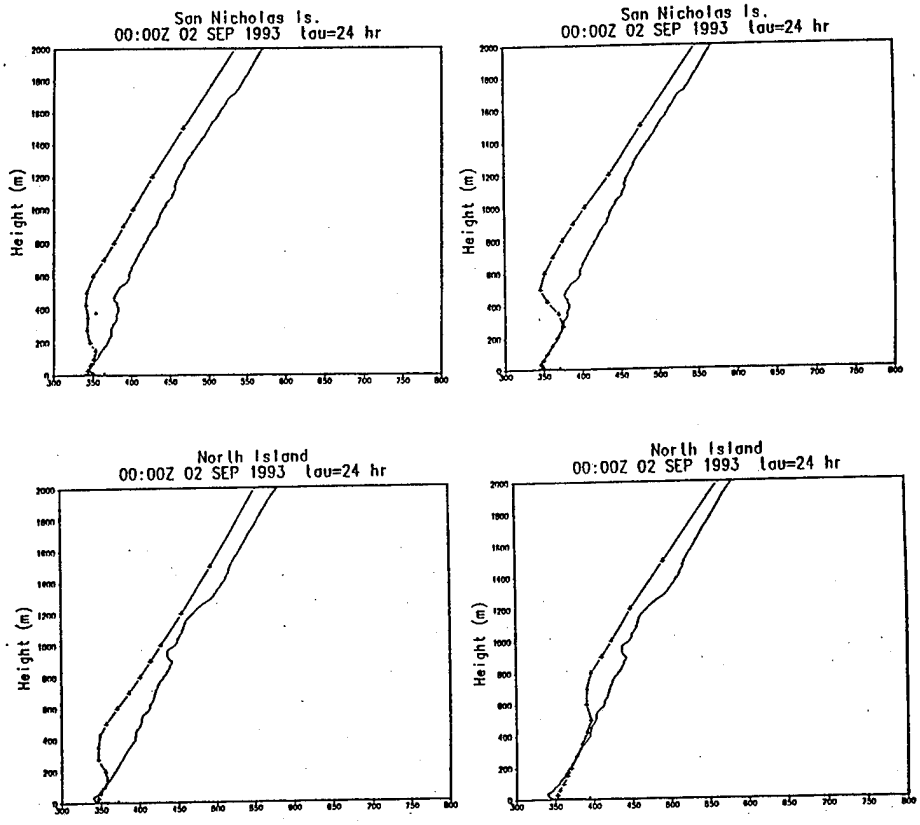

SUMMARY AND CONCLUSIONS

- Major Variations in Refractive Conditions During VOCAR Were Controlled by Synoptic Forcing
  - -- Model Forecast These Trends
- Instances of Sea-Breeze Impacts on M-Field
- Coastal Low-Level Jets & Eddies Alter M-Field
- Several Model Shortcomings:
  - -- Moisture Advection Thru Lateral Boundaries
  - -- Vertical Gradients at B.L. Top Too Weak
  - -- Bias Towards Too Shallow B.L. Depth

Dr. Steve Burk, "Modeling Mesoscale Refractivity Structure During the VOCAR Experiment"

DISCUSSION

M. VOGEL

Your have showed us how you can predict profiles of refractivity with the mesoscale model. Have you tried to use these profiles of refractivity to predict propagation loss? Were the results satisfactory? What do you think is the outlook for the near future?

AUTHOR'S REPLY

Calculation of propagation factor using RPO and M-fields from the mesoscale model were performed by John Cook of our laboratory. The initial results were disappointing - the model's tendency to under predict the M-deficit at the top of the boundary layer and bias to too shallow of boundary layer depth seemed to create problems. However, the model did do quite a good job of predicting the trend in boundary layer depth. Since the time of the VOCAR experiment, we have made several model improvements. The global model which supplies lateral boundary conditions to the mesoscale model has also been improved. Thus, in the near future we hope to have improved forecast M-fields that can be input to RPO. I am optimistic that the results will prove positive.

Variations in Atmospheric Refractivity Induced by Coastal Mesoscale Processes

William T. Thompson
Stephen D. Burk
Naval Research Laboratory
Marine Meteorology Division
7 Grace Hopper Ave.
Monterey, CA 93943-5502
(408)656-4733
fax (408)656-4769
email: thompson@nrlmry.navy.mil

ABSTRACT

Large variations in atmospheric refractivity are characteristic of the California coastal environment. While some of this variability results from changes in the synoptic weather regime and diurnal effects, mesoscale atmospheric processes can play an important role as well. For example, thinly and orographically induced coastal circulations may modify marine boundary layer structure and the extent and depth of stratus clouds. This may change the gradients 0' temperature and moisture at the top of the boundary layer and alter duct height and strength.

A mesoscale weather prediction model developed at NRL has been used extensively to make mesoscale atmospheric forecast over the California coastal region. This model features a mesoscale data assimilation system, second order closure physics. and a sophisticated cloud prediction scheme that interacts fully with the radiation parameterization.

On 21 July 1992 the model forecast a Catalina Eddy. These forecast compared very favorably to observations valid at 12:00 UTC 21 July 1992. The impact of the eddy and associated southerly flow on the microwave refractivity will be discussed.

On 29 August 1993, model forecasts indicated that a southerly surge event was in progress. Satellite imagery for this period indicated that a surge had occurred with southerly flow extending north along the coast to Pt. Arena. This event disrupted typical flaw and boundary layer stratification in a narrow zone along the coast. The dynamics of this event and its impact on microwave refractivity will be described.

VARIATIONS IN ATMOSPHERIC REFRACTIVITY INDUCED BY COASTAL MESOSCALE PROCESSES

William T. Thompson and
Stephen D. Burk
Naval Research Laboratory
Marine Meteorology Division
Monterey, CA 93943

Coastal Mesoscale Data Assimilation System

MODEL PHYSICS

- Second-Order Closure Turbulence Parameterization
- Prognostic Equations for Turbulent Variances/Covariance
- Fully Interactive Cloud-Radiation
- Implicit Time Differencing

Coastal Mesoscale Data Assimilation System

ANALYSIS/INITIALIZATION

- Optimum Interpolation Analysis
- Incremental Update
- Nonlinear Vertical Mode Initialization

Coastal Mesoscale Data Assimilation System

FORECAST MODEL FEATURES

- High Vertical and Horizontal Resolution
- Hydrostatic/Primitive Equation
- Time Dependent Lateral Boundary Conditions from NOGAPS
- Split Explicit Time Differencing

Model Literature

1. **Model Description**

   Burk and Thompson, 1989: *Mon. Wea. Rev., 117.*

   Hodur, 1987: *Mon. Wea. Rev., 115.*

2. **Numerical Investigation of Arctic Frontogenesis**

   Thompson and Burk, 1991: *Mon. Wea. Rev., 119.*

3. **Cold Frontal Passage and Air Mass Modification over the Gulf of Mexico**

   Burk and Thompson, 1992: *J. Appl. Met., 31.*

   Thompson and Burk, 1993: *J. Appl. Met., 32.*

4. **Forecast Support for LEADEX**

   Fett, Kozo, Burk, and Thompson, 1994: *Bull. Amer. Met. Soc., 75.*

   Thompson, Burk, Kozo, and Fett, 1995: *Global Atmos. and Ocean Sys.* (submitted)

5. **Forecast Support for VOCAR**

   Burk and Thompson, 1994: *AGARD Conference Proceeding 587.*

   Burk, Thompson, Cook, and Love, 1994: *IGARSS'94 Digest*

   Thompson, Burk, Cook, and Love: 1994: *IGARSS;94 Digest.*

6. **Coastal Low-Level Jets**

   Burk and Thompson, 1995: *Mon. Wea. Rev.* (submitted).

Catalina Eddy

- Forms in SOCAL Bight
- Results from enhanced NW flow over the San Rafael and Santa Ynez Mountains
- Lee troughing lowers pressure in the northern bight
- Coastally-trapped ageostrophic southerly flow to the east with NW flow to the west results in cyclonic circulation

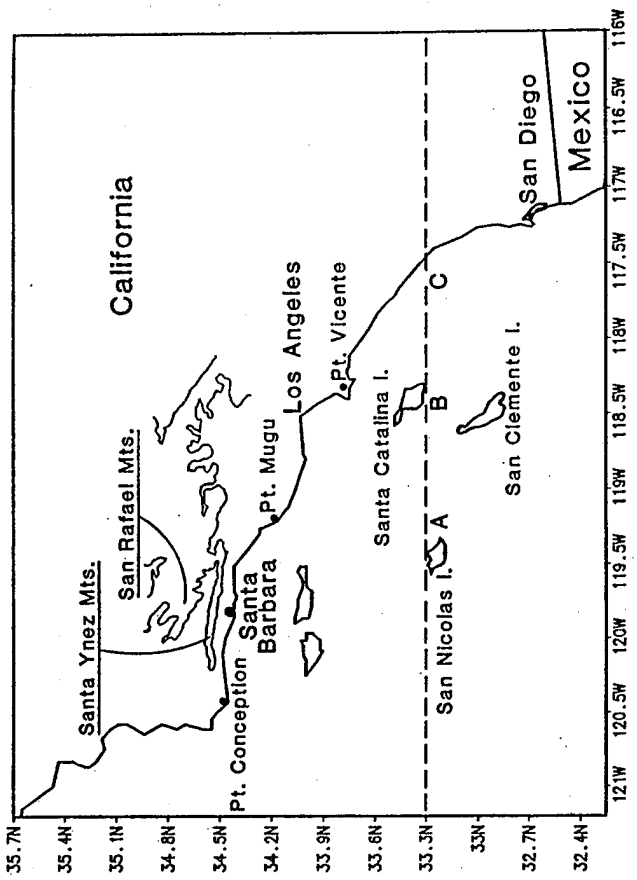

noraps second order closure model fields

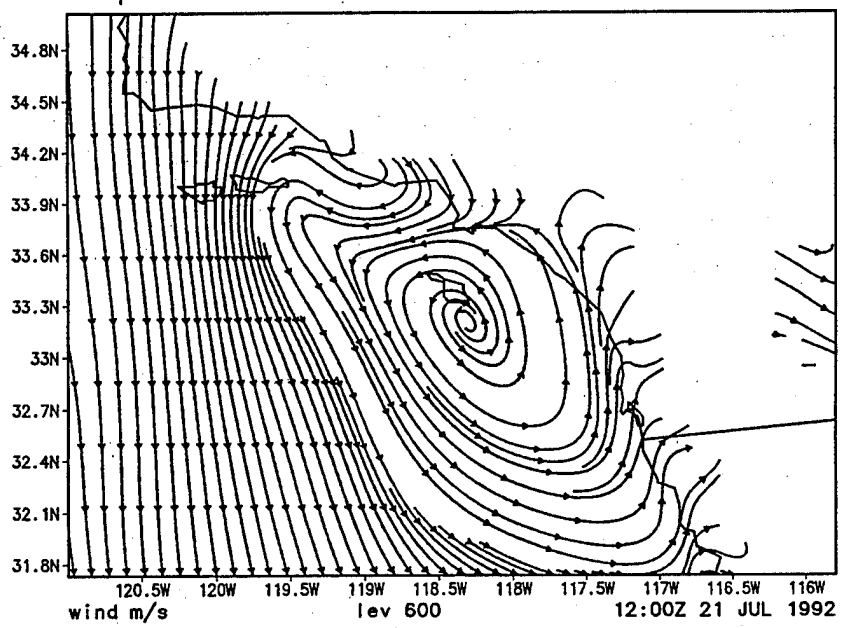

noraps second order closure model fields

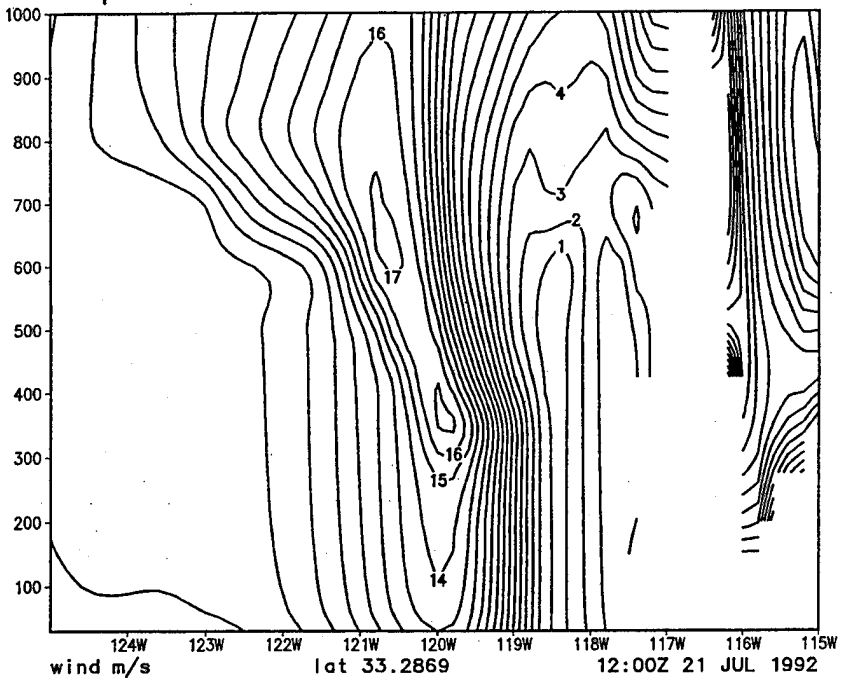

noraps second order closure model fields

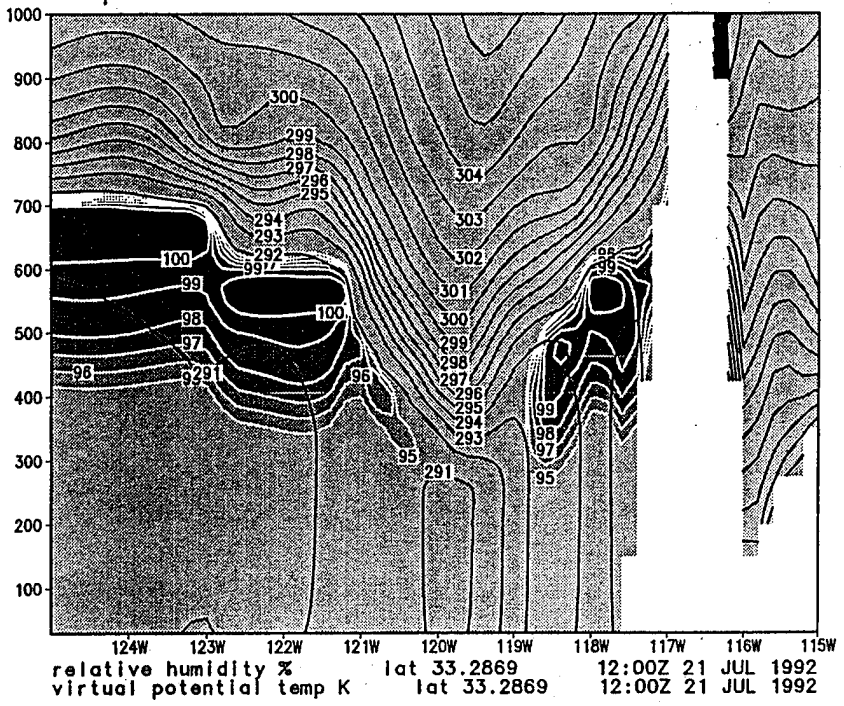

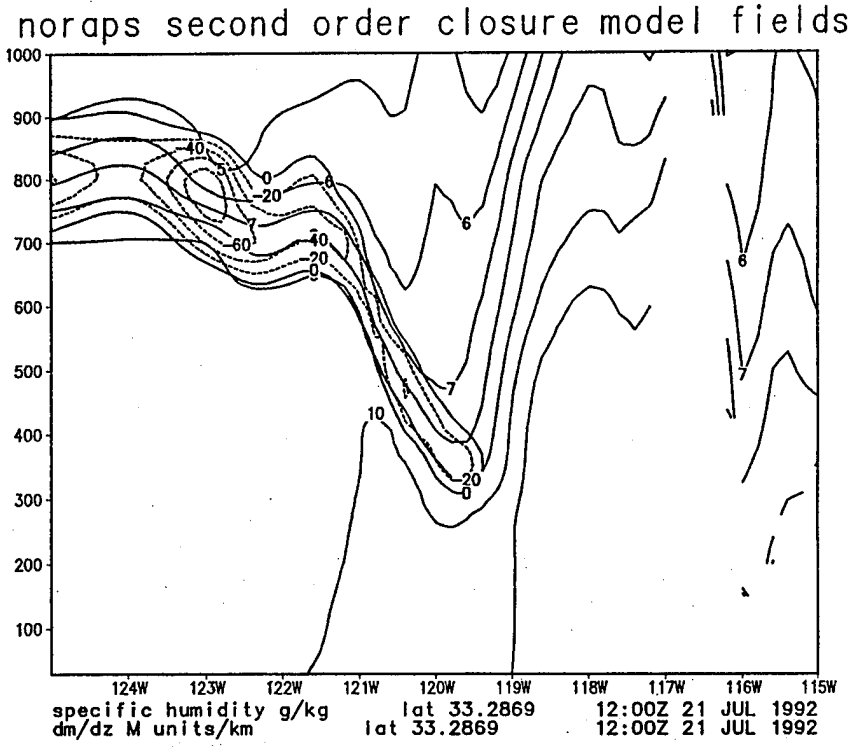

Impact on Refractivity 1

- The zone in which southerly flow occurs is characterized by strong low-level convergence and upward vertical motion
- Upward motion promotes adiabatic cooling near the inversion
- Cooling weakens the inversion, leading to further deepening

Impact on Refractivity 2

- Upward motion also reduces the vertical moisture gradient
- Deepening of the boundary layer promotes development of clouds
- Clouds cause further deepening due to cloud-top cooling instability
- Deepening of the BL and reduction in vertical gradients have a large impact on refractivity

Southerly Surge

- Also results from interactions with coastal topography
- Lee-troughing occurs downwind of the Siskiyou and Klamath Mountains in Northern California and Southern Oregon
- Coastally-trapped ageostrophic southerly flow extends north from Pt Conception
- Along with a reversal in typical flow comes disruption in normal low-level stability

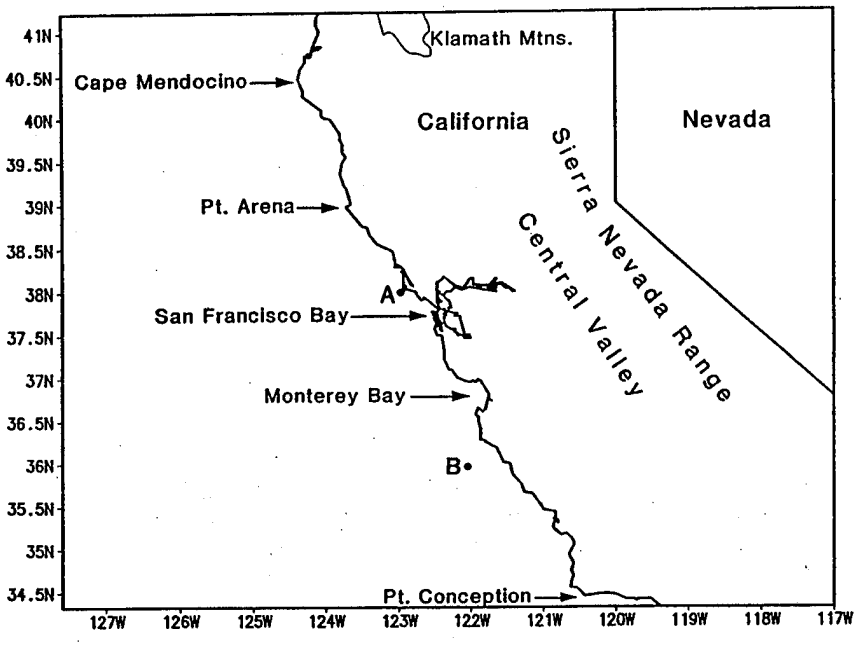

noraps second order closure model fields

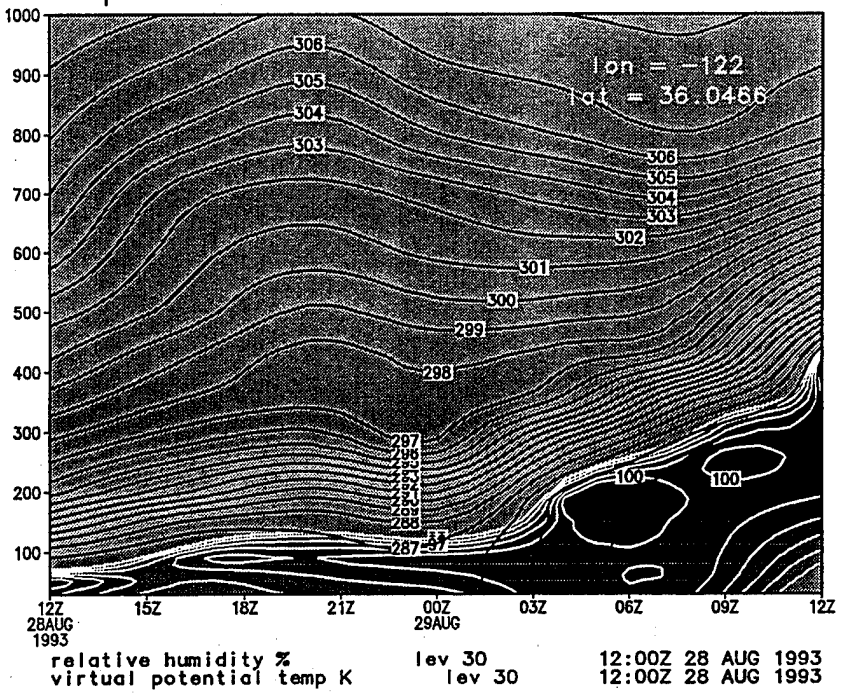

noraps second order closure model fields

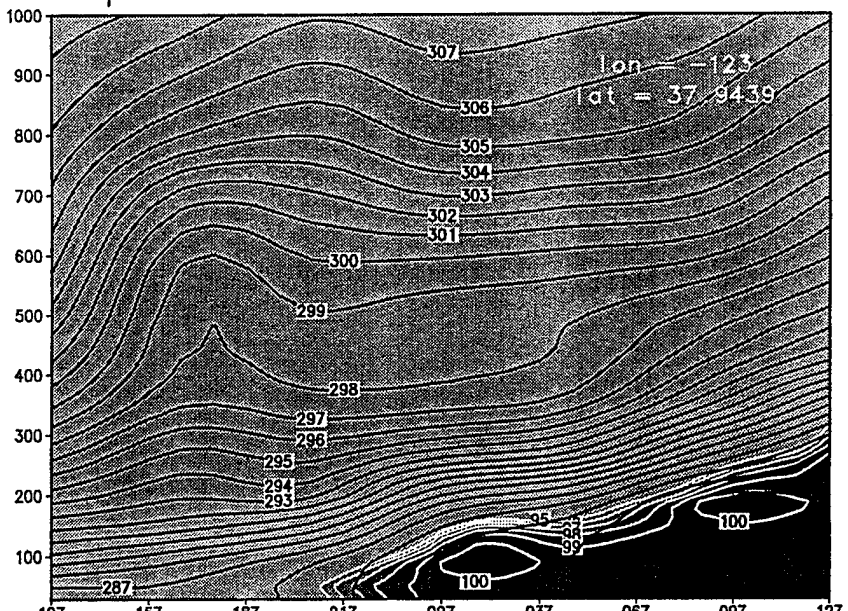

relative humidity % lev 30 12:00Z 28 AUG 1993
virtual potential temp K lev 30 12:00Z 28 AUG 1993

noraps second order closure model fields

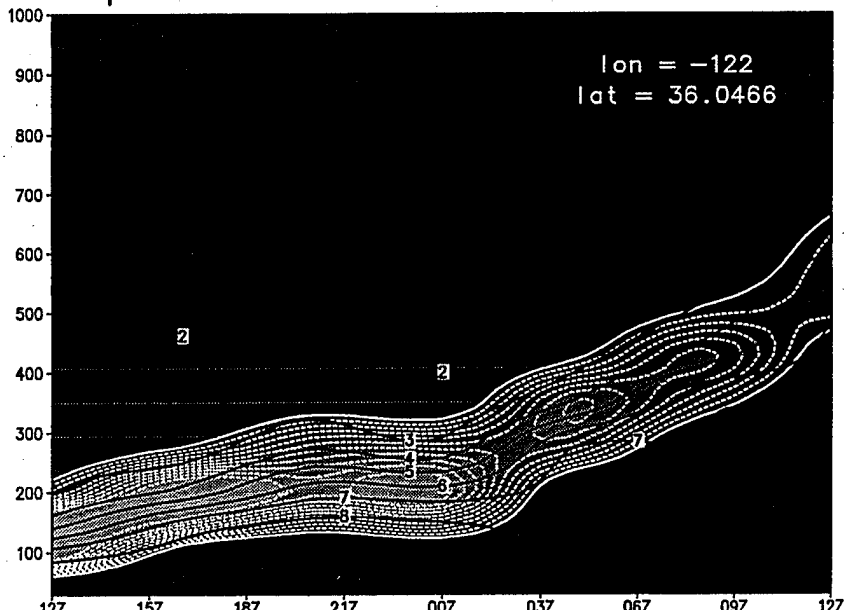

dm/dz M units/km lev 30 12:00Z 28 AUG 1993
specific humidity g/kg lev 30 12:00Z 28 AUG 1993

noraps second order closure model fields

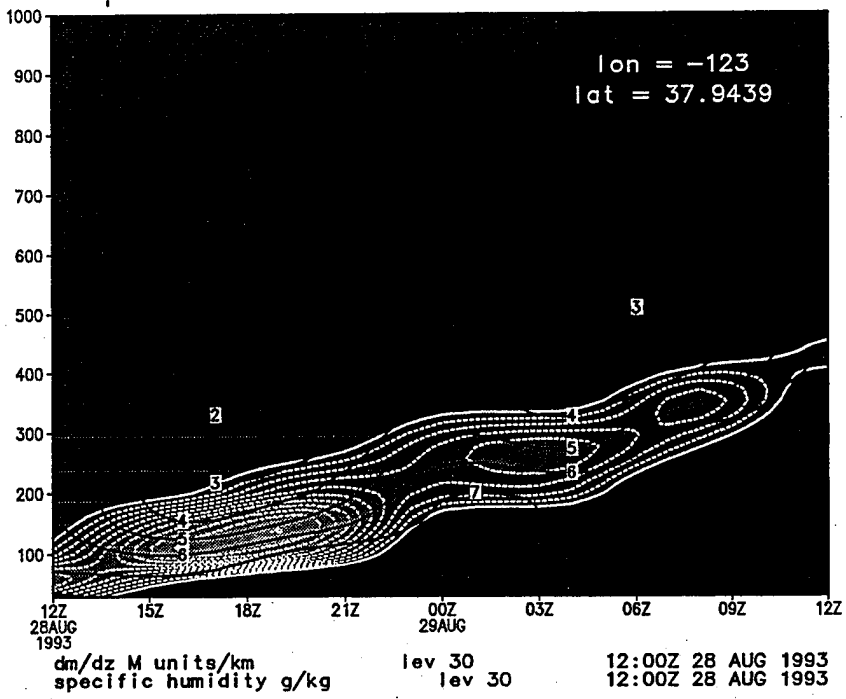

OAKLAND, CA
28 AUGUST 1993

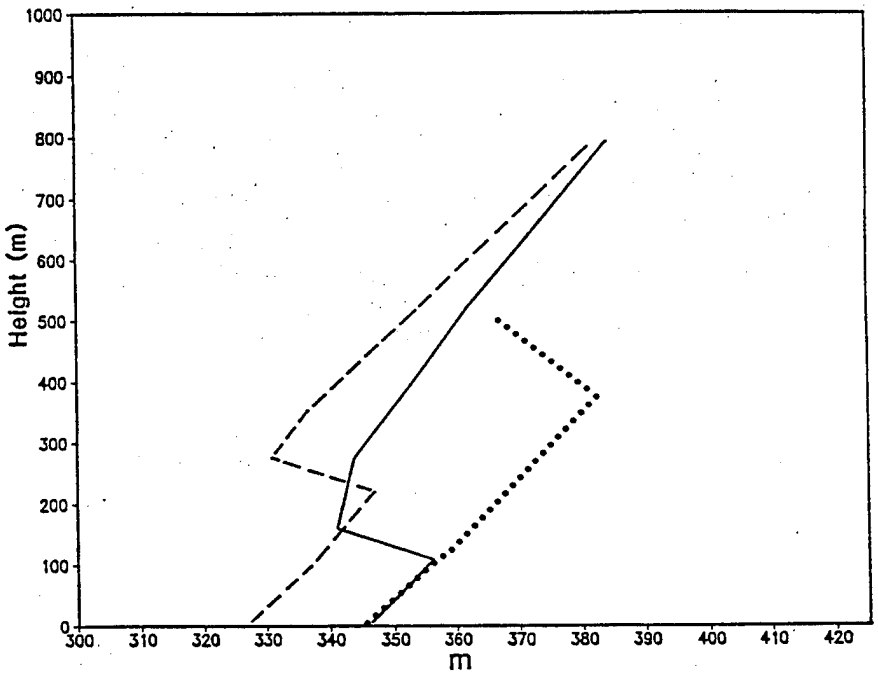

CONCLUSIONS

- Two coastal mesoscale phenomena which impact atmospheric microwave refractivity have been investigated using a mesoscale data assimilation system featuring high resolution and second-order closure physics
- The Catalina Eddy results from enhanced NW flow over the mountains east of Pt. Conception

CONCLUSIONS (cont.)

- Upward vertical motion associated with convergence along the coast in the southerly flow diminishes vertical gradients in temperature and moisture, reducing trapping
- The southerly surge results from lee troughing over northern California

CONCLUSIONS (cont.)

- The surge has similar impacts on trapping but extends over a much larger area, reducing or eliminating trapping from Pt. Conception to Pt. Arena and beyond

Mr. William Thompson, "Variations in Atmospheric Refractivity Induced by Coastal Mesoscale Processes"

DISCUSSION

J. ROSENTHAL

As shown by geostationary satellite imagery, the southerly surge you showed is often a by-product or outgrowth of coastal "Catalina Eddies" that grow and expand with time. Both features are driven by the synoptic features. Although sometimes subtle, the synoptic forcing is really the driving force which reinforces the conclusions of your previous paper as well as Ted Rogers' paper in showing synoptic variations being the source of the most prominent variations in refractive structure.

AUTHOR'S REPLY

I agree that southerly surges are often preceded by Catalina Eddy events. In many cases the southerly flow associated with the eddy is able to round Pt. Conception and move up the coast.

I agree also that the synoptic forcing is of fundamental importance. Synoptic forcing is critical in producing a large cross-terrain wind component which is largely responsible for the genesis of both the Catalina Eddy and the southerly surge.

RADIO REMOTE SENSING OF REFRACTIVITY BY COMBINATORIAL OPTIMIZATION

L. Ted Rogers
Ocean and Atmospheric Sciences Division
Naval Command Control and Ocean Surveillance Center
Research Development Test and Evaluation Division
San Diego, CA 92152

Radio remote sensing (RRS) is a method for determining the atmospheric refractivity structure from measurements of electromagnetic (EM) propagation factor. The method is developed and tested on data from the Variability Of Coastal Atmospheric Refractivity (VOCAR) experiment.

The squared error term (or residual) R(**x**) is defined by (1) where **x** is a vector estimate of the atmospheric

$$R(\mathbf{x}) = (1/2)\,(\,F(\mathbf{x}) - \mathbf{y}\,)(\,F(\mathbf{x}) - \mathbf{y}\,)^T \qquad (1)$$

refractivity structure, F(**x**) is vector of propagation factors calculated using **x** and **y** is a vector of measured propagation factors. Virtually any method for remotely sensing refractivity involves minimizing R(**x**). With sparse data, R(**x**) may have local minima and a purely *downhill* minimization may not work. For sparse data, a grid having the dimensionality of the number of refractive structure parameters to be sensed (usually 2 or 3) is pre-computed. Terms for persistence of the refractive structure are added to the objective function (1) which effectively transform the problem from being underdetermined to being over-determined. A global combinatorial optimization is performed to determine the time series of refractivity parameters that minimize the objective function. An implementation has achieved good results in determining the base height and M-deficit of surface based and elevated ducts using sparse VHF/UHF propagation data from the VOCAR experiment.

Inverse Problem Solutions

Y	-	Measured prop. factors
$\hat{X}$	-	Est. refractivity parameters
$G()$	-	Propagation model
$G(\hat{X})$	-	Estimated prop. factor

Least Squares:

$\hat{X}^*$ minimizes:

$$R(\hat{X}) = (G(\hat{X}) - Y)^T (G(\hat{X}) - Y)$$

With *priors*,(X_P)

$$R(\hat{X}) = (G(\hat{X}) - Y)^T C_1^{-1} (G(\hat{X}) - Y) + (\hat{X} - X_P)^T C_2^{-1} (\hat{X} - X_P)$$

Convexity:

Y diverse $\Rightarrow$ $R(\hat{X})$ Convex

Y non-diverse $\Rightarrow$ $R(\hat{X})$ Weakly convex or non-convex

Discrete parameter space:

X Non-Gaussian
G Non-linear
$\Rightarrow \hat{X}^* \cong \hat{X}_{ML}$

Radio Remote Sensing of Refractivity by Combinatorial Optimization

L. Ted Rogers

Code 543

Ocean and Atmospheric Sciences Division

Naval Command, Control and Ocean Surveillance Center

Ambiguity

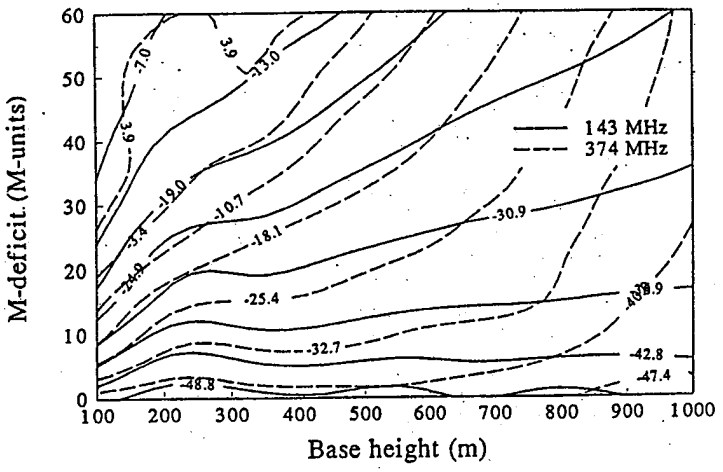

Propagation Factor Contours

1. VOCAR SCI to Point Mugu path geometry.
2. Contour lines are averaged over thicknesses of 10 to 50 meters.

Trapping Layer Parameterization

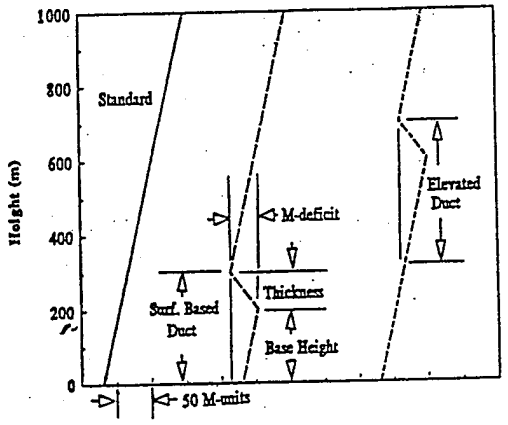

Parameter Space:

Parameter:	Symbol	Min.	Max.	Inc.
Height	h	100	1300	10
M-deficit	m	0	50	5
Thickness	d	10	50	10

Correlation of parameters with propagation factor:

Parameter:	Symbol	ρ_{143}	ρ_{262}	ρ_{374}
Height	h	-.417	-.602	-.733
M-deficit	m	.739	.635	.518
Thickness	d	-.234	-.218	-.107

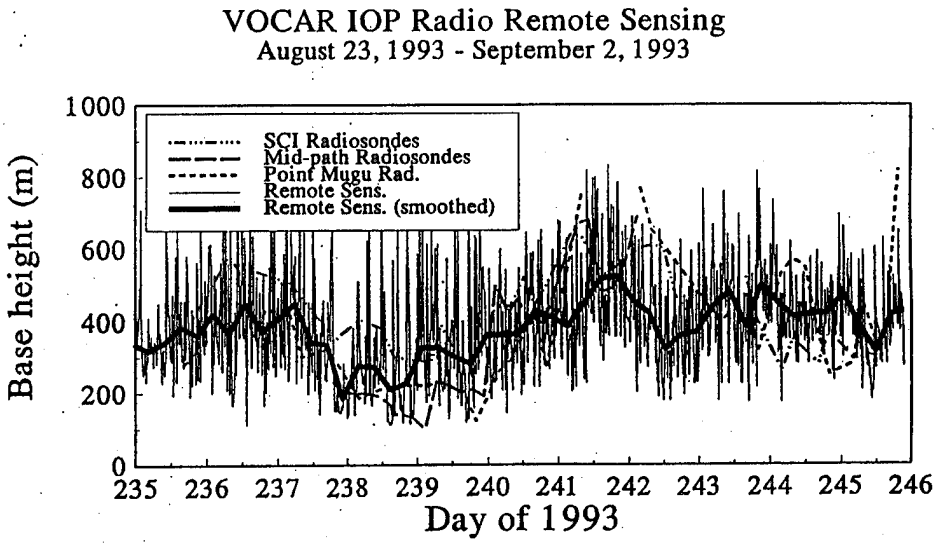
VOCAR IOP Radio Remote Sensing
August 23, 1993 - September 2, 1993
SCI Radiosondes
Mid-path Radiosondes
Point Mugu Rad.
Remote Sens.
Remote Sens. (smoothed)
Base height (m)
1000
800
600
400
200
0
235 236 237 238 239 240 241 242 243 244 245 246
Day of 1993

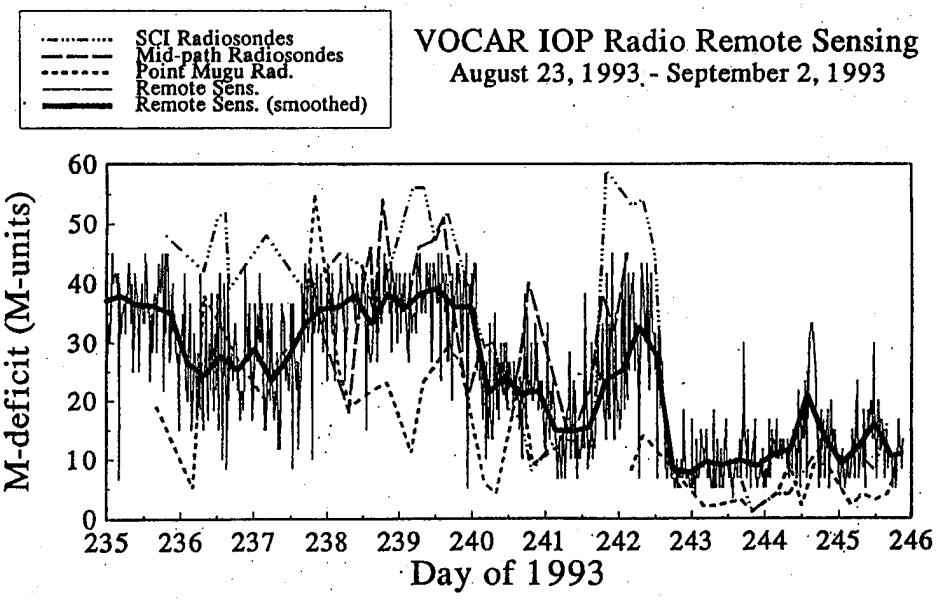
SCI Radiosondes
Mid-path Radiosondes
Point Mugu Rad.
Remote Sens.
Remote Sens. (smoothed)
VOCAR IOP Radio Remote Sensing
August 23, 1993 - September 2, 1993
M-deficit (M-units)
60
50
40
30
20
10
0
235 236 237 238 239 240 241 242 243 244 245 246
Day of 1993

Propagation Estimation using Remotely Sensed Profiles
VOCAR Experiment, August 23, 1993 - September 2, 1993

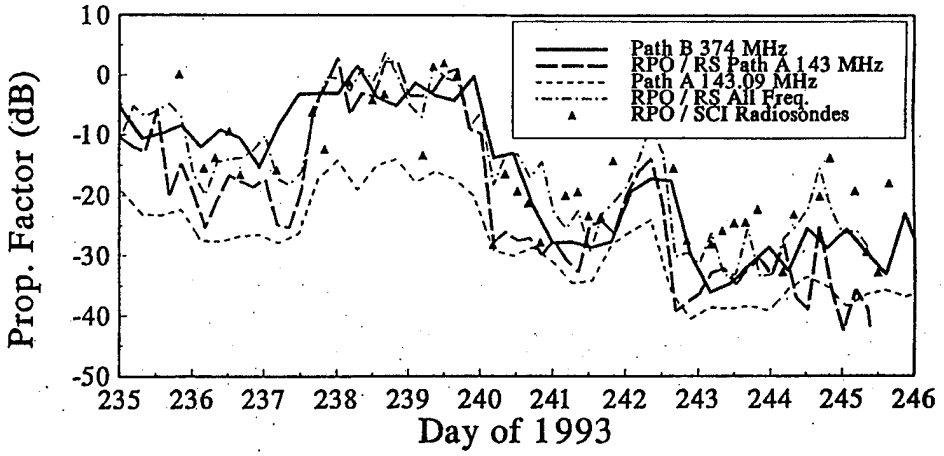

Summary

1. Radio remote sensing does work.
2. Accuracy of representation $\propto$ Diversity
3. Optimization methods ideal for sensor integration.
4. Scientific Problems:
   (a) MABL modeling
   (b) Ambiguity
5. Operational Problems:
   (a) Sparse inputs
   (b) Bias and noise in measuremnts

Mr. Ted Rogers, "Radio Remote Sensing of Refractivity by Combinatorial Optimization"

DISCUSSION

K. CRAIG

I believe you used 3 frequencies in one of your examples. Do you know how much the results are affected by the middle frequency?

AUTHOR'S REPLY

I do not think removing the middle frequency would have a large effect, but not having tested that hypothesis, I cannot give a certain answer.

Remote Environmental Sensing Techniques Based on Inverse Scattering of Electromagnetic Waves

Donald D. Boyer
Naval Surface Warfare Center
Dahlgren Division, Code N24
Dahlgren, VA 22448-5100
(703) 663-1908
Email: dboyer@relay.nswc.navy.mil

Frank J. Ryan
Naval Command, Control, and Ocean Surveillance Center
RTD&E Division, Code 712
San Diego, CA 92152-5000
(619) 553-3099
Email: ryan@nosc.mil

Greg Gentry
Naval Surface Warfare Center
Dahlgren Division, Code B32
Dahlgren, VA 22448-5100
(703) 663-6464
Email: ggentry@godsend.nswc.navy.mil

Shipboard radar and communication systems in a coastal marine environment are very sensitive to vertical and horizontal variations in the tropospheric refractivity conditions. These systems frequently experience extended or reduced detection ranges, inaccurate altitude estimates, and increased surface clutter due to the presence of nonstandard atmospheric refractivity conditions (e.g., surface or elevated ducts) and their concomitant impact on radio wave propagation. If range dependent refractivity fields were available in a timely manner aboard a ship, then a parabolic wave equation model, such as RPO, could be used to model the propagation, and optimum radar parameter choices, for the specific propagation environment could be obtained.

The proposed remote sensing algorithm uses a nonlinear Gauss-Markov estimation technique, implemented numerically with a finite difference Levenberg-Marquardt procedure. At each step of the iteration, a parabolic wave equation (PE) model is used to compute the forward solution or replica used in the matched field processor. The advantage of this proposed technique is that it offers the possibility of rapid sensing of atmospheric refractivity fields using readily available hardware assets.

This paper addresses the initial phase of the work, namely formulating the procedure and establishing the feasibility of the method. Some preliminary computational results from the numerical inversion procedure will be present using synthetic refractivity data; and, an introductory analysis of the refractivity structure from the Stapleton/Kang data set will be included.

Remote Environmental Sensing Techniques Based on Inverse Scattering of Electromagnetic Waves

Donald D. Boyer (N24) and Gregory L. Gentry (B32)
Naval Surface Warfare Center, Dahlgren Division
Dahlgren, VA 22448-5100
and
Frank J. Ryan
Naval Command Control and Ocean Surveillance Center
RDT&E Division
San Diego, CA 92152-6435

REFRACTIVITY INVERSION USING THE PE MODEL

In order to precisely define the inversion process let:

- $\left\{T_1, T_2, \cdots, T_{l_1}\right\}$ be the transmitter heights,
- $\left\{R_1, R_2, \cdots R_{l_2}\right\}$ be the receiver heights,
- $\{M_1, M_2, \cdots, M_l\}$ the refractivity profiles, the i^{th} profile parametrized with n_i parameters,
- $\{f_1, f_2, \cdots, f_k\}$ be the distinct transmission frequencies.

REFRACTIVITY INVERSION USING THE PE MODEL(continued)

- A PE model produces a path loss output at each receiver height, for each transmitter height and each frequency. Thus the model must be executed $k \cdot l_1$ times to obtain the $m = k \cdot l_1 \cdot l_2$ path loss outputs, which will be represented as $\mathbf{y} = \{y_1, y_2, \cdots y_m\}$.

- The inputs to the direct medium scattering problems will be a collection of $n = n_1 + n_2 \cdots n_l$ refractivity parameters $\mathbf{x} = \left\{x_1^1, x_2^1, \cdots, x_{n_1}^1, \cdots, x_1^l, x_2^l, \cdots, x_{n_l}^l\right\}$, for which the inversion procedure will attempt to solve.

REFRACTIVITY INVERSION USING THE PE MODEL(continued)

- The direct medium scattering equation upon which the inversion will be performed,

$$\mathbf{y} = \mathbf{F}(\mathbf{x})$$

denotes a nonlinear vector valued function, with the PE model mapping the refractivity parameter space contained in R^n into the modeled path loss space contained in R^m.

- Actually the measured path loss, $\hat{\mathbf{y}}$, does not dwell among the outputs of the PE model, so we attempt to choose an $\hat{\mathbf{x}}$ in the refractivity parameter space which minimizes the Euclidean norm of the residual between the modeled and measured path losses:

NUMERICAL INVERSION

$$R(\mathbf{x}) = \frac{1}{2}(\mathbf{F}(\mathbf{x})-\hat{\mathbf{y}})^T(\mathbf{F}(\mathbf{x})-\hat{\mathbf{y}}).$$

- The first step is to linearize the vector valued function $\mathbf{F}$ about an approximate solution $\mathbf{x}_0$

  $$\mathbf{F}(\mathbf{x}_0+\mathbf{s}) = \mathbf{F}(\mathbf{x}_0) + \mathbf{J}_0^T\mathbf{s}+o(\|\mathbf{s}\|)$$

  where

  $$\mathbf{J}_0 = \mathbf{J}(\mathbf{x}_0)$$

  and $\mathbf{J}(\mathbf{x}_0)$ is the Jacobian matrix of partial derivatives of output path losses with respect to each of the refractivity parameters. The partial derivatives are computed numerically using the PE model for the function evaluations.

NUMERICAL INVERSION(continued)

- If refractivity measurements are available, they could be used for the approximate solution $\mathbf{x}_0$, otherwise standard refractivity could be employed.

- An iterative algorithm based on the above linearization called the Finite Difference Levenberg-Marquardt procedure has proved very successful for nonlinear inversion problems

  $$\mathbf{x}_{k+1} = \mathbf{x}_k + \mathbf{s}_k$$

  where $\mathbf{s}_k$ and the scalar μ_k simultaneously solve

  $$\left(\mathbf{J}_k^T\mathbf{J}_k + \mu_k\mathbf{I}\right)\mathbf{s}_k = \mathbf{J}_k^T(\hat{\mathbf{y}} - \mathbf{F}_k)$$

NUMERICAL INVERSION(continued)

- The computation can be greatly simplified by forming a singular value decomposition on Jacobian matrix, and remove the redundant refractivity parameters.

- This reduces the dimension of the search space and assures that the Hessian approximation, $\mathbf{H}_k = \mathbf{J}_k^T \mathbf{J}_k$ is positive definite.

- With these simplifications the scalar, μ_k, usually, can be set equal to zero, and the much simpler Finite Difference Gauss-Newton method, with a positive definite Hessian results.

NUMERICAL INVERSION(continued)

- The Levenberg-Marquardt procedure selects μ_k equal to zero if the Hessian approximation $\mathbf{H}_k = \mathbf{J}_k^T \mathbf{J}_k$ is positive definite, and the direction,

$$\mathbf{d}_k = (\mathbf{H}_k)^{-1} \mathbf{J}_k^T (\hat{\mathbf{y}} - \mathbf{F}_k)$$

  is a descent direction. Otherwise it selects a step in the direction of the gradient.

NUMERICAL INVERSION(continued)

- The technique has been used very successfully in inverse scattering problems in medical imaging, and geophysical applications.

- The technique will be applied to a data set collected by Janet Stapleton and members of the Search and Track Division at The Naval Surface Warfare Center in Dahlgren, Virginia.

Status of the Software Development

- An implementation of the numerical inversion procedure, in MATLAB executes on an SGI work station, using multiple neutrally stable evaporation duct profiles.

- RPO is invoked as a MATLAB function with a set of refractivity parameters and transmitter parameters as inputs and returns to MATLAB a matrix with propagation factors, indexed by range and height.

Status of the Software Development(continued)

- All matix operations including the computation of the numerical derivatives and the singular value decompositions are performed in MATLAB; only RPO is in Fortran.

- The evaporation duct profiles are generated using the Liu, Katsaros and Businger bulk parameterization of the surface layer, implemented by John Cook and Steve Burk at NRL Monterey.

Status of Software Development(continued)

- Elevated trapping layers can be constructed in MATLAB, or measured profile data may be used and the NRL Monterey program RSMA can be invoked to match the data points in range dependent profiles, in order for RPO to model the transitions between profiles appropriately.

The Next Steps During FY-95

- Introduce more numerical sophistication in the mathematical inversion software.

- Implement an atmospheric boundary layer model provided by the Penn State Meteorology Department to generate profiles and select a finite set of parameters which are appropriate to use in the inversion procedure.

The Next Steps During FY-95

- Use MLAYER and other PE models to generate synthetic measurement data for the inversion procedure.

Plans for FY-96

- Determine how much frequency, transmitter height, receiver height and range diversity are necessary in the propagation measurements, in order to perform a meaningful inversion in any given case.

- Introduce other PE models into the inversion procedure, to be able to handle coastal environments with variable terrain heights.

Plans for FY-96(continued)

- Work closely with J. Cook and S. Burke to introduce stochastic turbulence representations into the atmospheric boundary layer models, and evaluate their effects on propagation.

- Apply the inversion technique to the VOCAR data and to the Stapleton/Kang data.

Plans for FY-96 and Beyond

- Attempt to formulate a dynamic refractivity inversion technique, based on research being performed by John Wyngaard and Nelson Seaman at Penn State University, to incorporate the dynamic effects of large eddy simulations into a marine boundary layer model.

Mr. Don Boyer, "Remote Environmental Sensing Techniques Based on Inverse Scattering of Electromagnetic Waves"

DISCUSSION

M. LEVY

Will the necessary path loss data be available in operational situations for input to the inversion algorithm?

AUTHOR'S REPLY

If a ship is situated in the middle of an ocean, then there may not be friendly transmitters available, but in a littoral environment or within a battle group there should be transmitters which can provide some frequency, range and transmitter height diversity.

THE GPS SOUNDER
A TECHNIQUE TO INFER TROPOSPHERIC REFRACTIVITY PROFILES FROM LOW ELEVATION ANGLE MEASUREMENTS OF GPS SIGNALS

KENNETH D. ANDERSON
NCCOSC RDT&E DIV 543
49170 PROPAGATION PATH
SAN DIEGO CA 92152-7385

Voice: (619)553-1420, Fax: (619)553-1417, Email: kenn@nosc.mil

In recent years, considerable effort has been put forth to create computer-based systems to assess refractive effects on signal propagation through the lower atmosphere. These assessment tools provide a near real-time capability to evaluate the performance of radar and communication systems and include tactical decision aids to mitigate or exploit atmospheric effects on propagation. However, a crucial factor for these analytical tools is a thorough knowledge of the spatial distribution of refractivity. Quantifying the refractivity structure is a difficult problem especially in the littoral zone where the sharp contrast between land and sea strongly contributes to both spatial and temporal variability.

A technique to remotely sense the vertical refractive profile of the lower atmosphere is examined. This technique infers the refractive structure from ground- or ship-based measurements of GPS satellite signals as the GPS satellite rises or sets on the horizon. There are obvious advantages to this concept. First, the inferred profiles will be representative of the integrated refractive effects along the range-height path instead of a single time and space line representation of refractivity, which is typical with current direct sensing systems. Second, with the completion of the GPS constellation, there will be at most 84 times per day when a GPS satellite will be in the proper position. A third advantage of this concept is the leveraging of a multibillion dollar system that is fully operational. The satellites are in place, the signal structure is well known, the hardware is mature, and high quality GPS receivers are commercially available.

Results from a series of satellite-to-ground signal measurements will be presented. It will be shown that these measurements can be inverted to accurately determine the height of the GPS antenna above the water surface, which is the first step in the inversion process to determine the refractivity profile.

GPS Sounder

Global Positioning System Sounder

The GPS Sounder

A Technique to Infer Tropospheric Refractivity Profiles from Low-Elevation Angle Measurements of GPS Signals

Kenneth Anderson
Ocean and Atmospheric Sciences
NCCOSC RDTE DIV
San Diego CA 92152

GPS Sounder

The Concept of the Inversion Technique

Hitney, H.V., Modelling Tropospheric Ducting Effects on Satellite-to-Ground Paths, AGARD CP-543, Oct. 1993

Anderson, K.D., Tropospheric Refractivity Profiles Inferred From Low-Elevation Angle Measurements of GPS Signals, AGARD CP-567, Sept. 1994

Received Signal

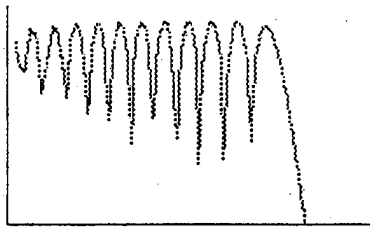

Time/Range/Angle

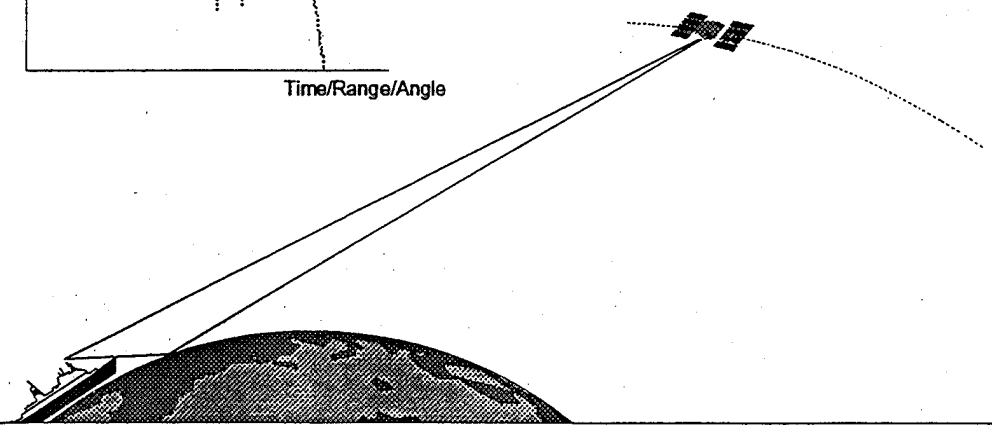

GPS Sounder

Sample Data

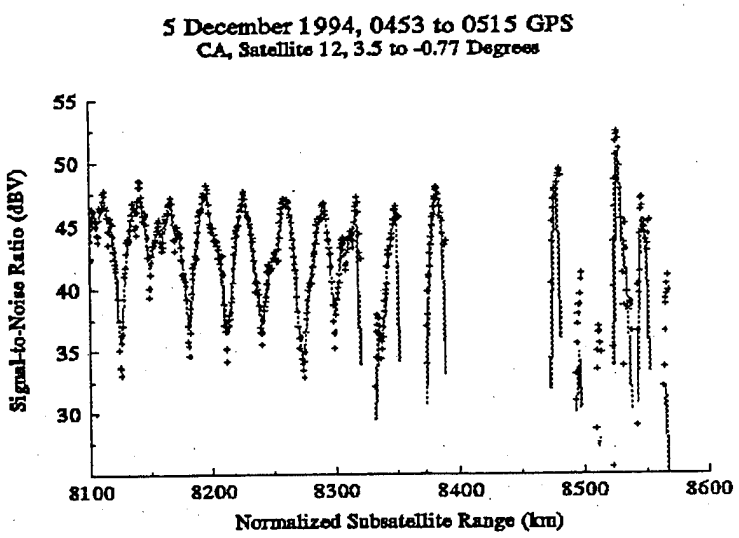

GPS Sounder

The Inversion Process

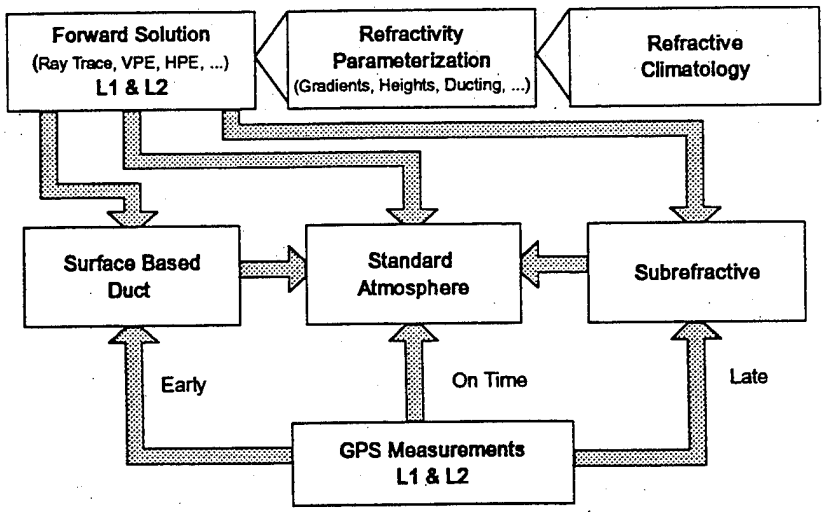

LS
MLE
SA
GA

GPS Sounder

Scientific & Technical Issues

TURBULENCE	Elevation angle RMS error of 0.6 mrad
SURFACE	Rough surface effects
KINEMATIC	Roll, Yaw, Pitch & Heave effects
BRIDGE EFFECT	Receiver control loops lose lock
POPUP	Rapid acquisition of GPS signal

GPS Sounder

Status in Mid '96

- Turbulence and surface roughness effects are either in hand or they are a show-stopper.
- Start measurements to determine RYP&H effects
- Incorporate AVLN firmware solutions
- Investigate separate channel/processor to handle popup problem

GPS Sounder

Geometric Optics Raytrace for GPS

L1, Zr=21.2 m, dM/dZ=130 M/km

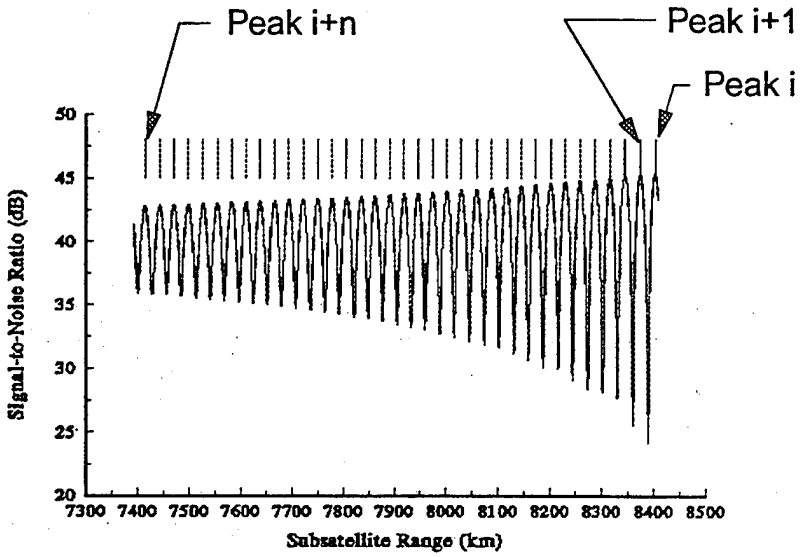

GPS Sounder

Geometric Optics Raytrace for GPS

L1, Zr=10, 12, ..., 30 m

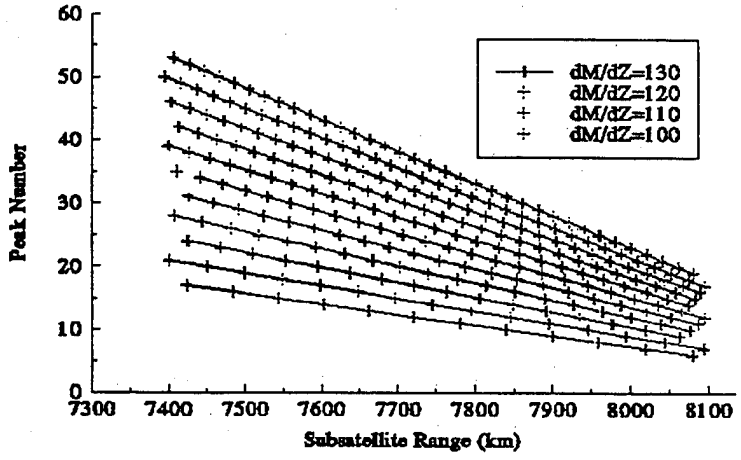

GPS Sounder

GPS Antenna Height Above Sea Surface
5-8 December 1994, NRaD BM 'B'

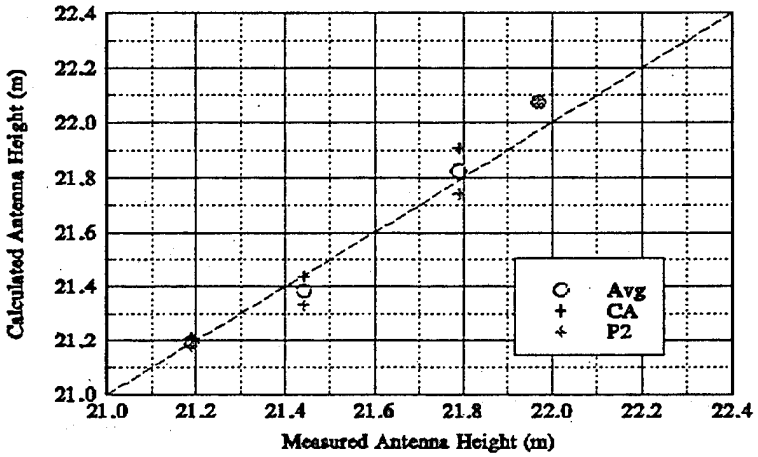

GPS Sounder

GPS Sounder Status
July 1995

- Demonstrated that the interferrence pattern can be recovered from low-elevation angle measurements
- Demonstrated that the antenna height above the water surface can be inferred from the measurements
- Investigating refractivity parameterization, forward solutions, & inversion algorithms

Mr. Kenneth Anderson, "The GPS Sounder - A Technique to Infer Tropospheric Refractivity Profiles from Low Elevation Angle Measurements of GPS Signals"

DISCUSSION

D. BLOOD

On the "early" or "late" time of arrival as an indicator of the existence of surface-based ducting, how do you identify the "early or late" time? Do you use 1st peak or null associations?

AUTHOR'S REPLY

The "late" and "early" indications are based on the receiver signal crossing the noise floor. These indications do not rely on identifying a peak or a null.

R. GIANNOLA

Can you give a rough order of magnitude time for when a GPS signal is received "early" (surface duct) and "late" (subrefractive situation)?

AUTHOR'S REPLY

In a strong surface based duct, I would expect to receive a signal 30-45 seconds earlier than anticipated. In strong subrefractive conditions, I would expect a delay of 10-15 seconds. These estimates assume that the satellite is rising and that the azimuth angle is constant.

Lidar Atmospheric Profile Sensor (LAPS): Remote Sensing of Atmospheric Properties

C. R. Philbrick and D. B. Lysak, Jr.
(crp3@psu.edu)
Penn State University
Applied Research Laboratory and
Department of Electrical Engineering
University Park, PA 16802

Abstract

A sensor capable of measuring profiles of atmospheric properties has been prepared. The Lidar Atmospheric Profile Sensor (LAPS) instrument is currently undergoing tests of its automated operation to determinate its performance under a wide range of meteorological conditions. The instrument measures the water vapor profile based on the vibrational Raman scattering and the temperature profile based on the rotational Raman scattering. These measurements provide real-time profiles of RF refractivity. Profiles are obtained each 5 minutes with a vertical resolution of 75 meters from the surface to 7 km. The prototype instrument, which includes several sub-systems to automate and monitor the operation, has been designed to provide the real-time measurements of profiles. The instrument includes an X-band radar which detects aircraft as they approach the beam and automatically protects a 6 degree cone angle around the beam. The instrument includes self calibration, performance testing and built-in-tests to check many functions.

In addition to the water vapor and temperature profiles, the true extinction and ozone profiles are also measured. By comparing the molecular profiles of the Raman and rotational Raman with the neutral atmosphere gradient, the extinction profile can be obtained. The day time measurements of water vapor are determined using the solar blind ultraviolet wavelengths. The ratio of the N_2 and O_2 vibrational Raman measurements on the slope of the Hartley band of ozone provides a DIAL measurement of the ozone profile in the lower atmosphere, up to 3 km. Initial results from the instrument are presented. The LAPS instrument will provide profiles of RF refractivity in real time from the measured temperature and water vapor profiles. LAPS is expected to become a SMOOS sensor which will provide ship and shore data inputs to the TESS3 system.

PENNSTATE

Applied Research Laboratory

Lidar Atmospheric Profile Sensor (LAPS): Remote Sensing of Atmospheric Properties

presented by

C. Russell Philbrick
Electro-Optics Department, Head
Professor of Electrical Engineering

for

EM Propagation Workshop
18 - 20 July 1995
Applied Physics Laboratory, Johns Hopkins University

Outline

Objective
Background
Scientific Basis
- Vibrational Raman - H_2O
- Rotational Raman - Temperature

System Overview
Example of LAPS Data
Status
Future Developments

Lidar Atmospheric Profile Sensor (LAPS)

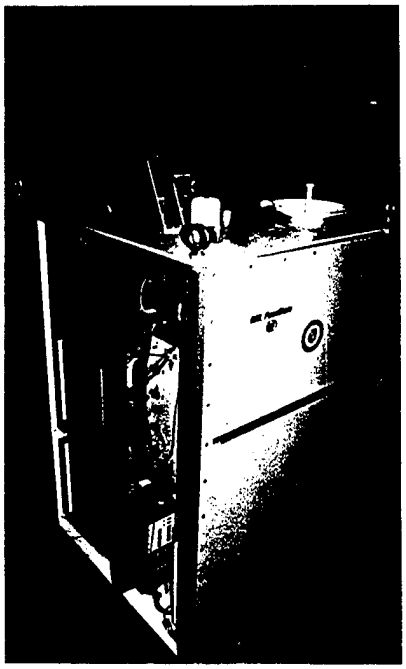

Objective...

- Develop a lidar profiler capable of providing real time measurements of atmospheric and meteorological properties, particularly the RF refractivity in an operational environment

Lidar Atmospheric Profile Sensor (LAPS)

Exploitation of other RDT&E...

- Measurements with NRaD VOCAR project
- Use of RF Propagation model developed by NRaD and APL for evaluation
- Leveraging with NSGC effort
- Development of EO capability with EOPACE

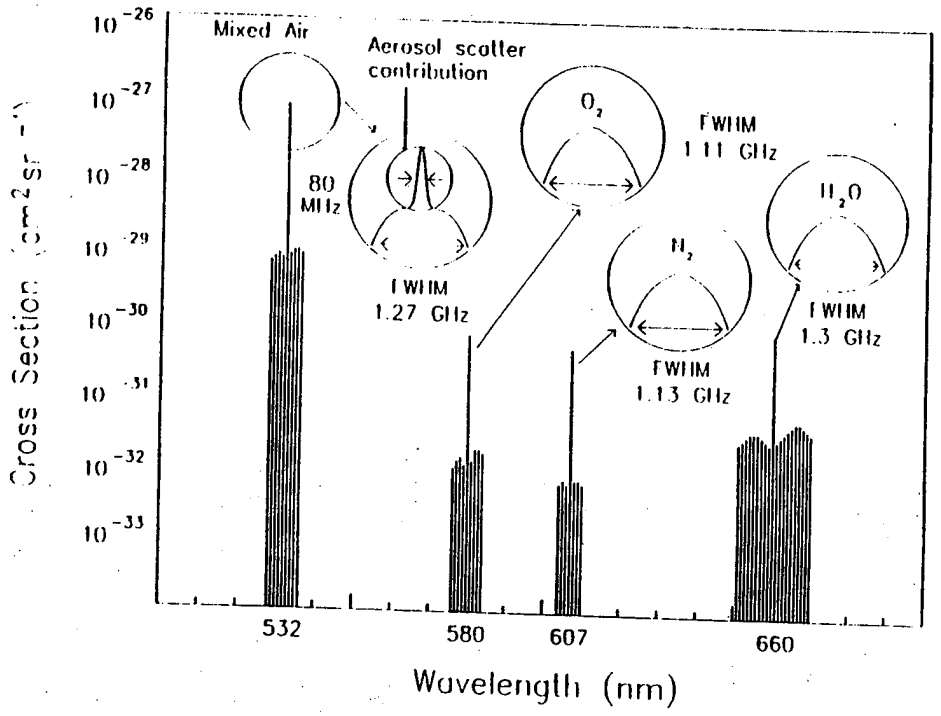
Mixed Air
Aerosol scatter contribution
80 MHz
FWHM 1.27 GHz
O_2
FWHM 1.11 GHz
N_2
FWHM 1.13 GHz
H_2O
FWHM 1.3 GHz
532
580
607
660
Wavelength (nm)

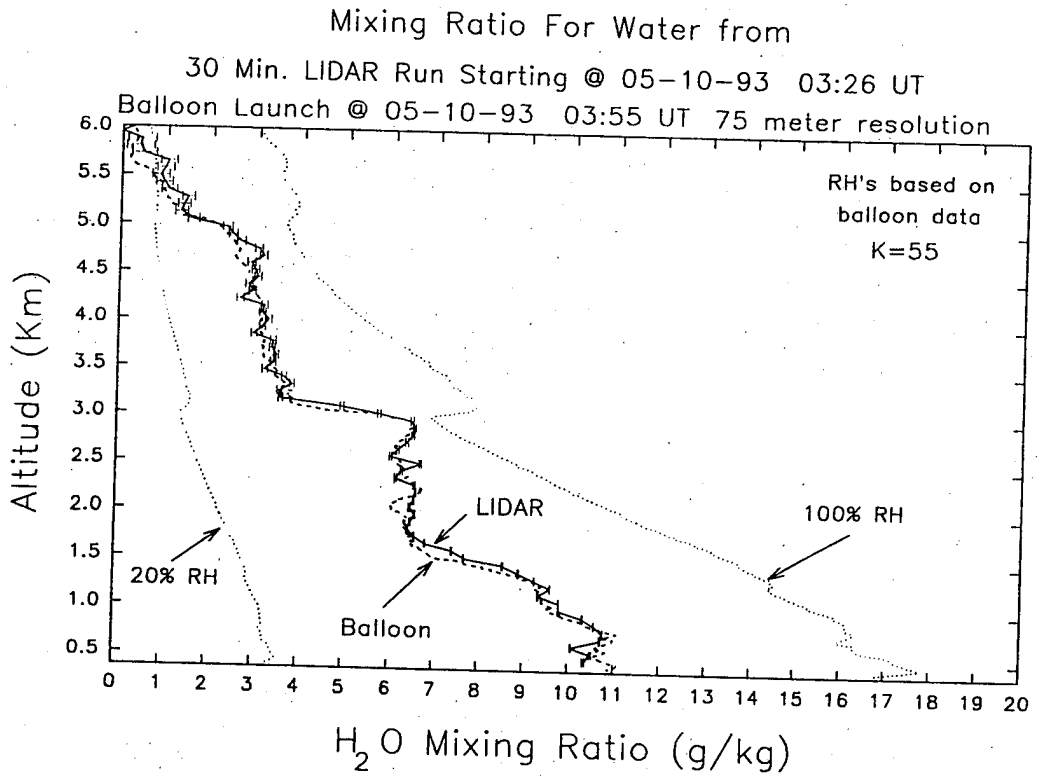
Mixing Ratio For Water from
30 Min. LIDAR Run Starting @ 05-10-93 03:26 UT
Balloon Launch @ 05-10-93 03:55 UT 75 meter resolution
RH's based on balloon data
K=55
LIDAR
100% RH
20% RH
Balloon
Altitude (Km)
H_2O Mixing Ratio (g/kg)

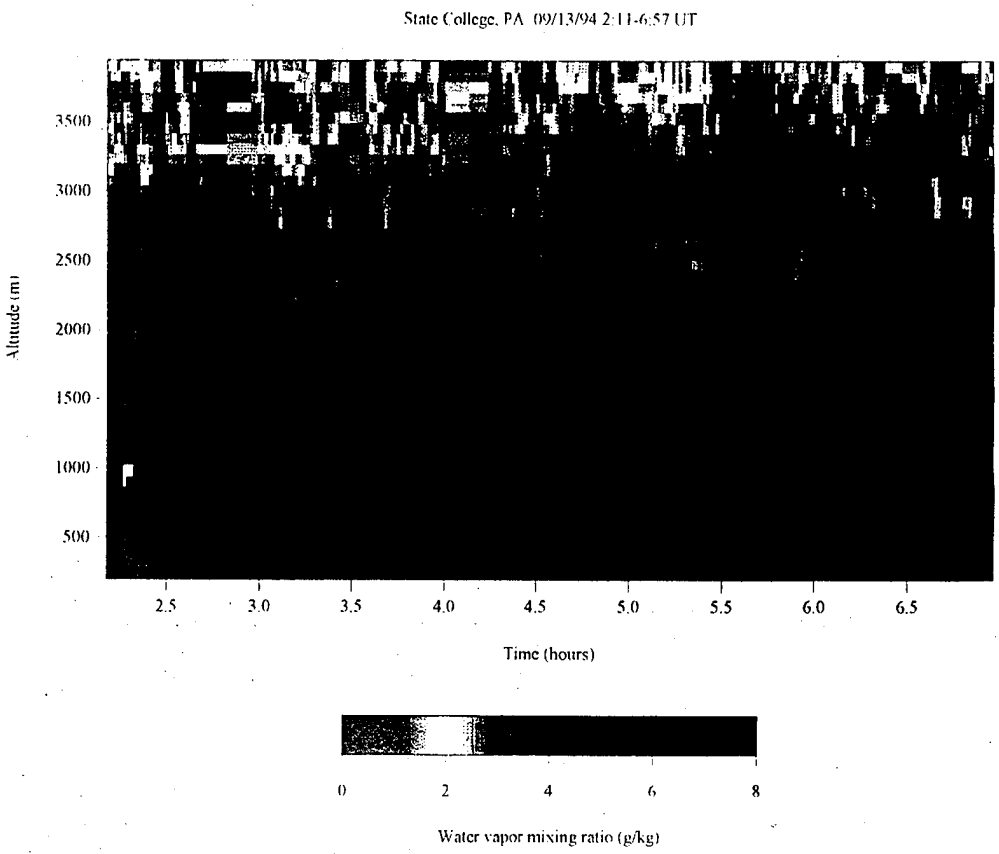
State College, PA 09/13/94 2:11-6:57 UT
Altitude (m)
3500
3000
2500
2000
1500
1000
500
2.5
3.0
3.5
4.0
4.5
5.0
5.5
6.0
6.5
Time (hours)
0
2
4
6
8
Water vapor mixing ratio (g/kg)

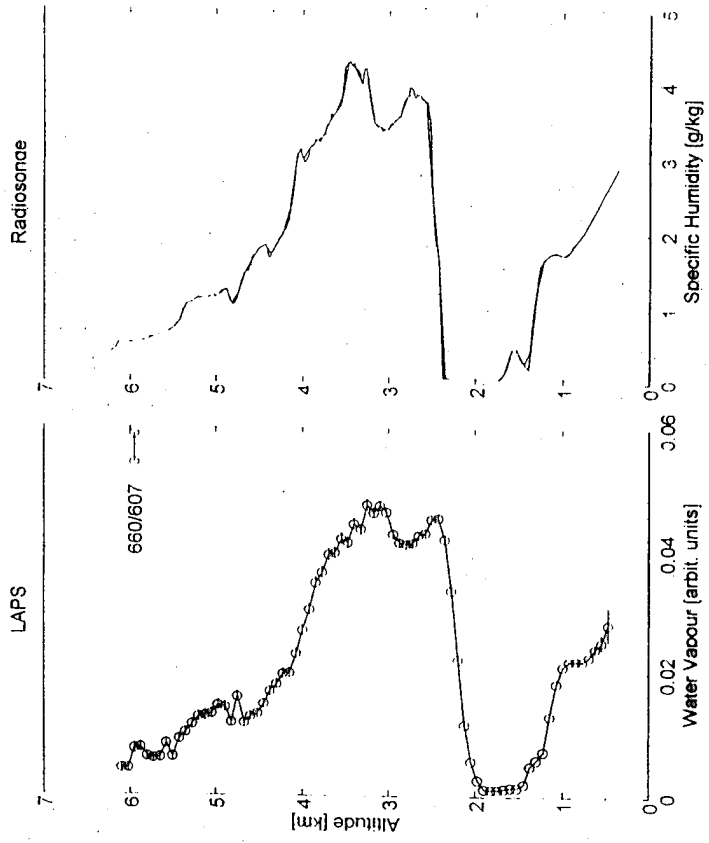
Radiosonde
LAPS
660/607
Altitude [km]
Specific Humidity [g/kg]
Water Vapour [arbit. units]

Rotational Raman Spectrum

Rotational Raman Spectrum for N2 and O2 at 310 K along with the Elastic Backscattering Cross Section of Air. Rotational Intensities include Species' Fraction of Air.

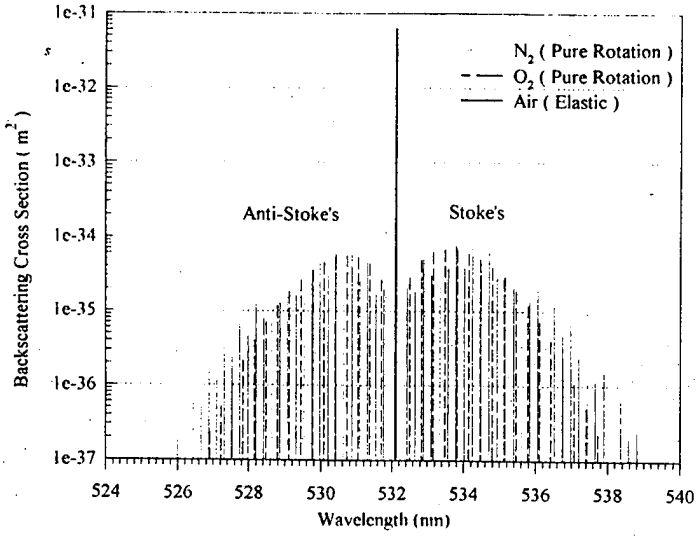

Quantum Line Strength

$$(J,T) = \sigma_s(J)\left[\frac{g_s(J)}{Q(T)}(2J+1)\exp\left[-1\frac{B_s hc}{kT}J(J+1)\right]\right.$$

S : molecular species
J : quantum number
σ(J) : backscatter cross section
g(J) : nuclear spin statistical weight factor
Q(J) : rotational partition function
B : rotational constant
T : Temperature (K)
h : Plank's constant
k : Boltzman's constant
c : Speed of sound

ROTATIONAL RAMAN TEMPERATURE

ADVANTAGES
- Ratio measurement
- Range independent
  extinction
  telescope form factor

CRITICAL FACTOR
- Laser line rejection

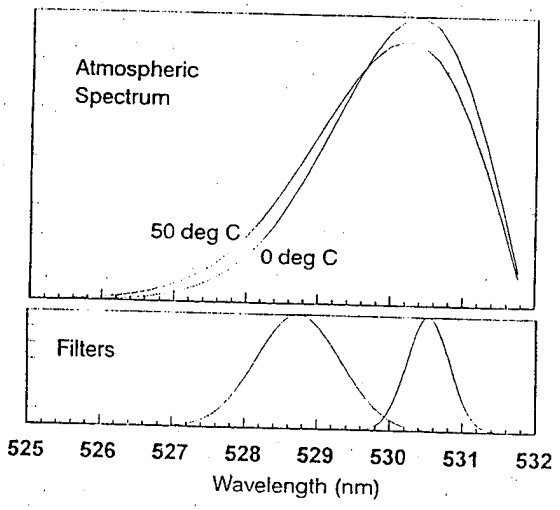

from Inaba 1976

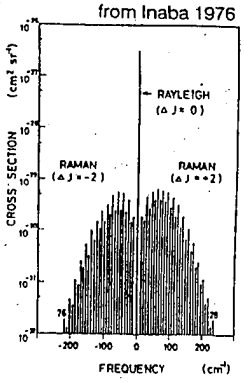

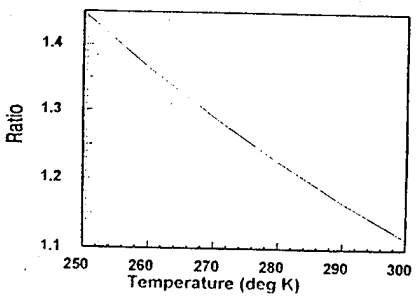

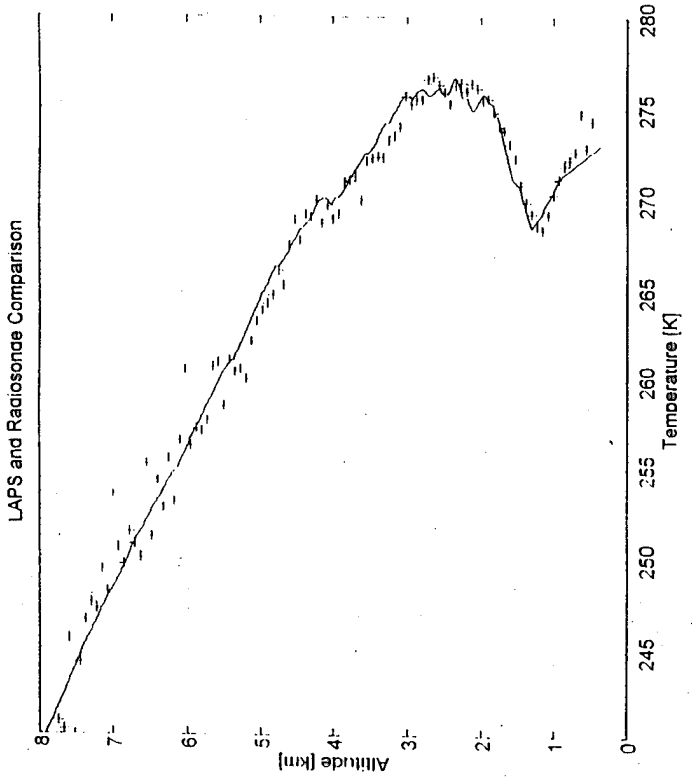

Raw Ratio of Raman Temp. Data
lidar run starting at 06/10/93 04:43 UT
balloon launch at 06/10/93 04:42 UT

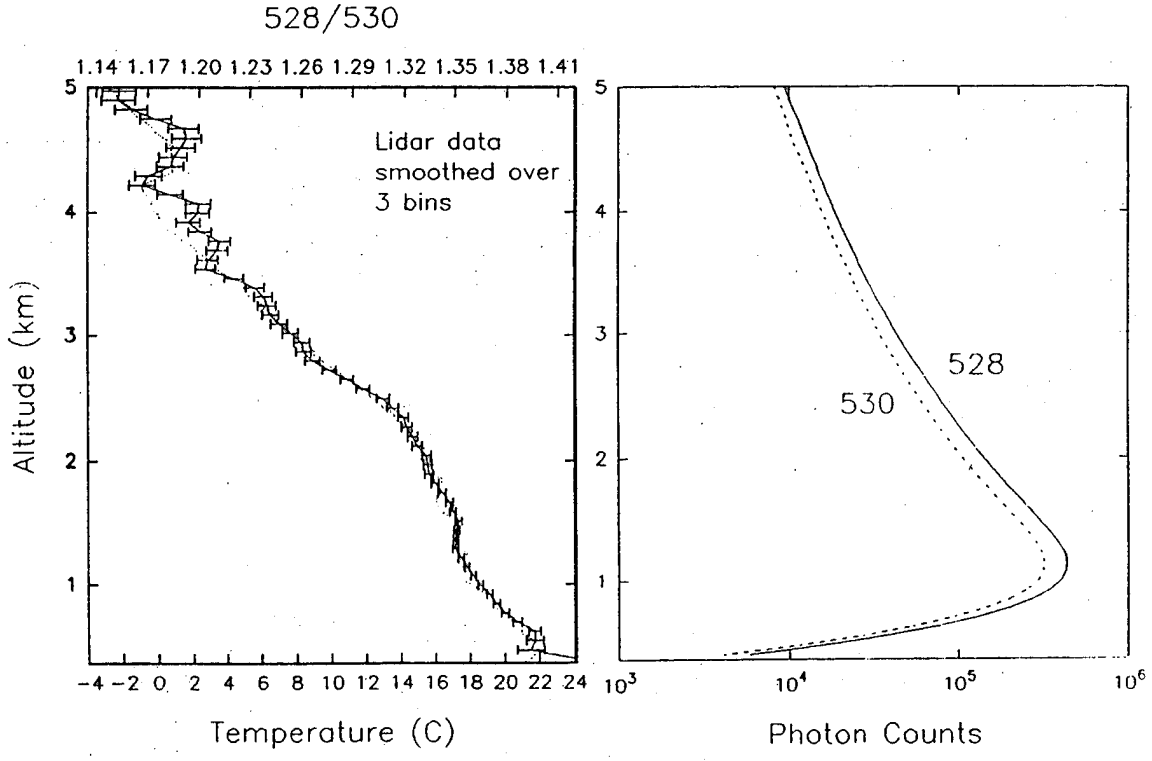

Lidar Rotational Raman Temperature Data 09/11/94 02:16 - 06:30
Plot Consists of Seven Successive 30 Minute Average Lidar Runs

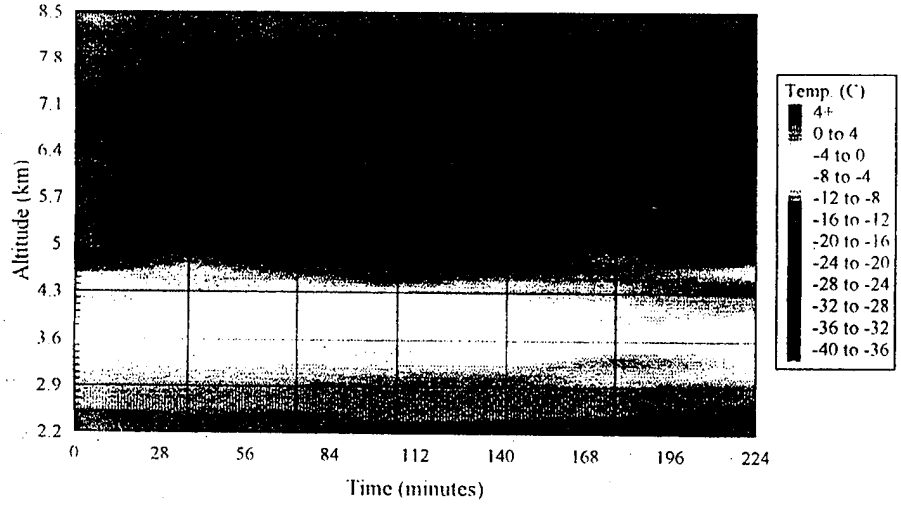

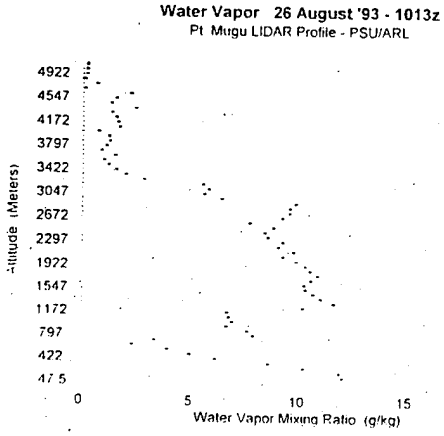

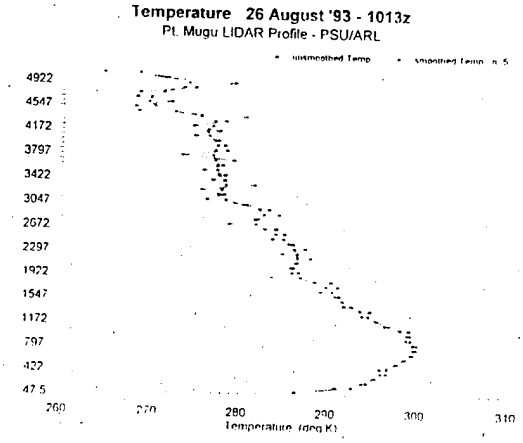

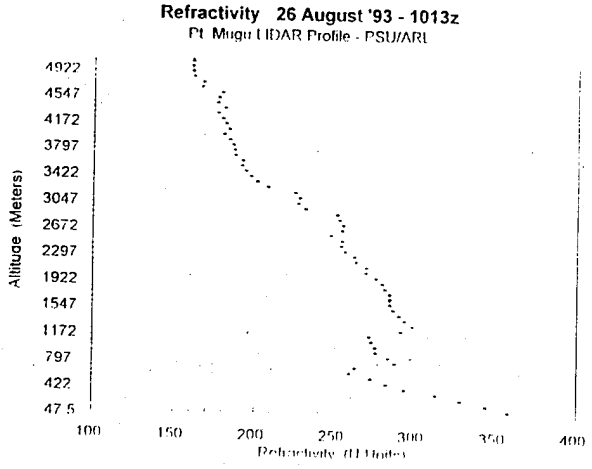

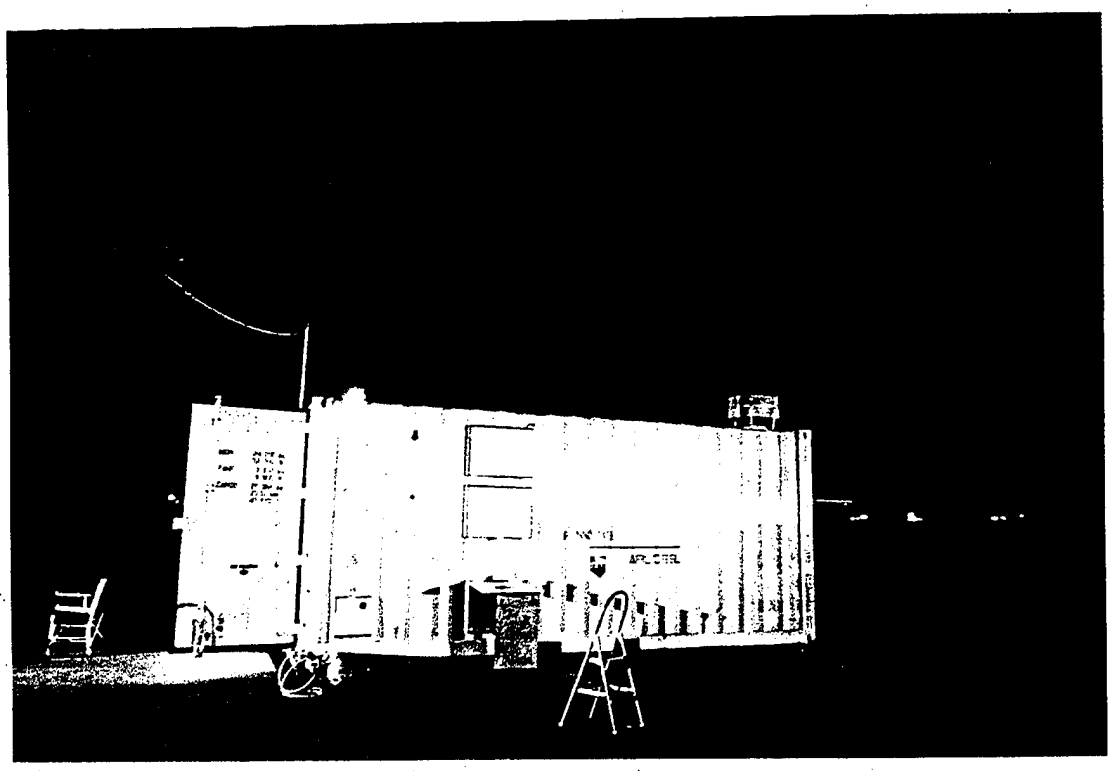

Dr. Russ Philbrick, "Lidar Atmospheric Profile Sensor (LAPS): Remote Sensing of Atmospheric Properties"

DISCUSSION

K. CRAIG

(1) What integration times were assumed in your performance estimates?
(2) What is the prospect of daytime operation at 532 nm using reduced field of view?

AUTHOR'S REPLY

(1) The integration time expected to be most useful for the LAPS instrument is 10 minutes, which is the time considered for the performance estimate.
(2) The problem with severely limiting the field of view for daytime measurements is that the sensitivity is increased to the mechanical alignment of the laser beam on the axis of the telescope. It certainly does help and we do plan to use a field stop to increase our S/N at visible wavelengths. At present I do not know how far we can push this capability. However, I expect that the better daytime measurements will be obtained from the "solar blind" region between 260 and 300 nm using the 266 nm 4th harmonic of the Nd:YAG laser.

D. WILLIAMS

How does the warning radar work on the LAPS?

AUTHOR'S REPLY

It automatically cuts off the laser, to avoid damage to eye if aircraft crew should look down into the laser. The radar protects a 6° cone angle, at the beam half power points, to altitudes above 40,000 ft.

MEASUREMENTS OF TROPOSPHERIC REFRACTIVITY PROVIDE ENVIRONMENTAL INPUT TO EM WAVE PROPAGATION ANALYSIS/PREDICTION

David W. Blood
Applied Research Laboratory/Penn State University
P.O. Box 30, State College, PA 16804
(814) 863-9916, Fax (814)863-8783

ABSTRACT

The measurements of the atmospheric refractive environment during the 1993 VOCAR Campaign at Point Mugu, CA provided input to analysis of RF propagation path data. Radiosondes and Point Mugu PSU/ARL lidar instruments measured temperature and water vapor profiles that are used to compute refractivity, N and modified refractivity, M in the lower tropospheric region. These profiles are then analyzed as input to propagation models to interpret the conditions prevailing during periods of radio signal level data collection at UHF and VHF.

This presentation will discuss two contributions to the computed refractivity that give rise to the statistical variations of the profile. An assessment of the influences of water vapor and temperature contributions to the refractive profile is given. This leads to a discussion of the impact of statistical errors in basic water vapor and temperature measurements on refractivity profiling. The RF propagation analysis characterization which proceeds from using the profile data, will be highly influenced by the environmental data collection averaging and the final processing technique used in providing the input.

PENNSTATE

Applied Research Laboratory

MEASUREMENTS OF TROPOSPHERIC REFRACTIVITY PROVIDE ENVIRONMENTAL INPUT TO EM WAVE PROPAGATION ANALYSIS/PREDICTION

David W. Blood
Ocean and Atmospheric Sciences and Technology Division
PSU/ARL

July 18-20, 1995
Electromagnetic Wave Propagation Workshop
JHU/APL, Laurel, MD

PENNSTATE

Applied Research Laboratory

TOPIC OUTLINE:

- Basic lidar measurements and refractivity
  - LAMP at Pt. Mugu during '93 VOCAR
  - Over-sea representation (no evaporative duct model)
  - Low altitude critical to VHF/UHF propagation
- Use of statistical errors in refractivity measurements
- Profile pre-conditioning at lowest altitudes
  - Altitudes from sea level to valid upper air measurements
  - Alternative methods (interpolation and extrapolation)
- Summary of lidar observations and recommendations

Equations for Atmospheric Refractivity Profiling

Refractivity:

$$N(z) = 77.6\,\frac{P(z)}{T(z)} + 3.73\times10^{5}\,\frac{e(z)}{(T(z))^{2}}$$

Modified refractivity:

$$M(z) = N(z) + (0.157)\times z$$

where:

$N=(n-1)\times10^{6}$

(parts per million of refractive index of air, n)

n = refractive index of air (nominally ~1.0003)
z = geometric height (m>m.s.l.)

e(z) = water vapor press. = r(z) x P(z)/[r(z)+621.97] (mb)

r(z) = water vapor mixing ratio (g/kg)
P(z) = absolute atmospheric pressure (mb)
T(z) = absolute atmospheric temperature (K)

LIDAR ATMOSPHERIC MEASUREMENTS

Each 5 - 30 minutes Lidar yields atmospheric profile data at a resolution of 75 meters (15 m near-term goal)

BASIC TROPOSPHERIC MEASUREMENTS:

- Water Vapor Profile,
  r(z) = specific humidity, WVMR (g/kg)
- Temperature Profile, T(z)
- Surface Parameters, P_0, T_0, & RH

DERIVED PROFILES:

- Pressure, P(z)
- Refractivity, N(z)
- Modified Refractivity, M(z)

HIGHLY REFRACTIVE DAY
(DUCTING CONDITIONS)
26 AUGUST 1993

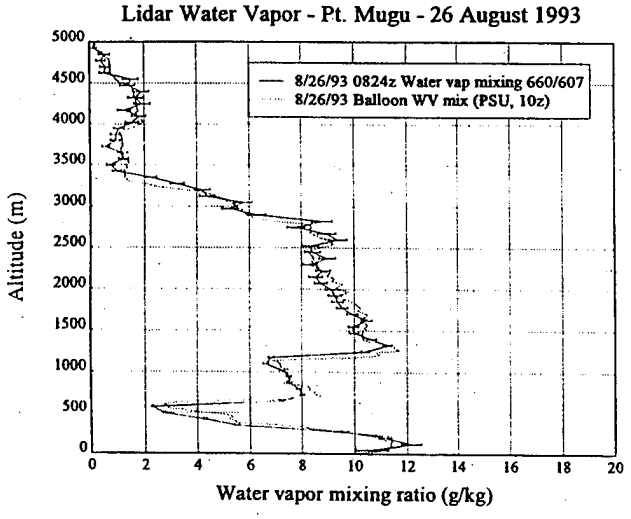

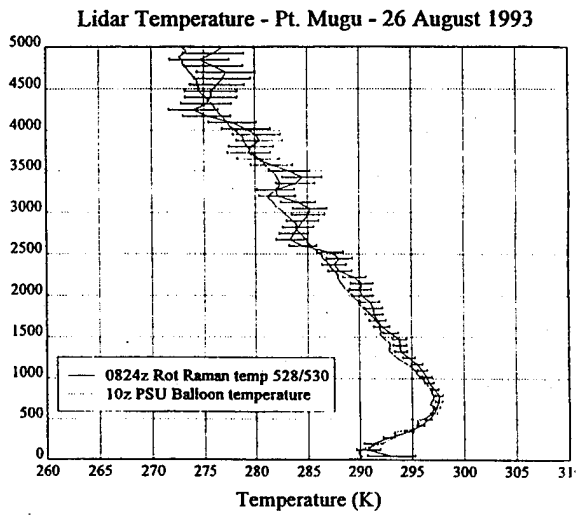

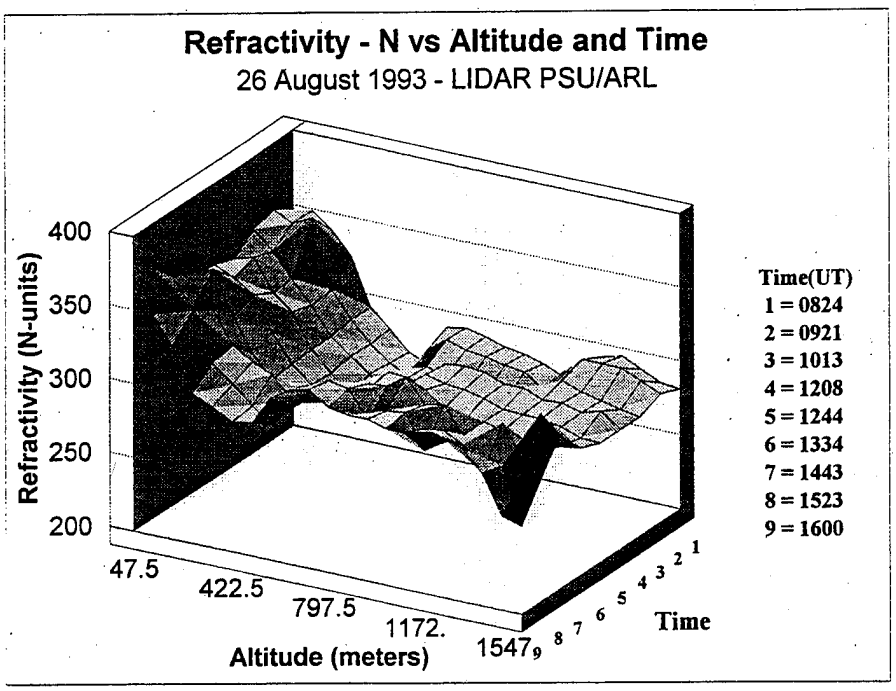

BASIC LIDAR MEASUREMENTS

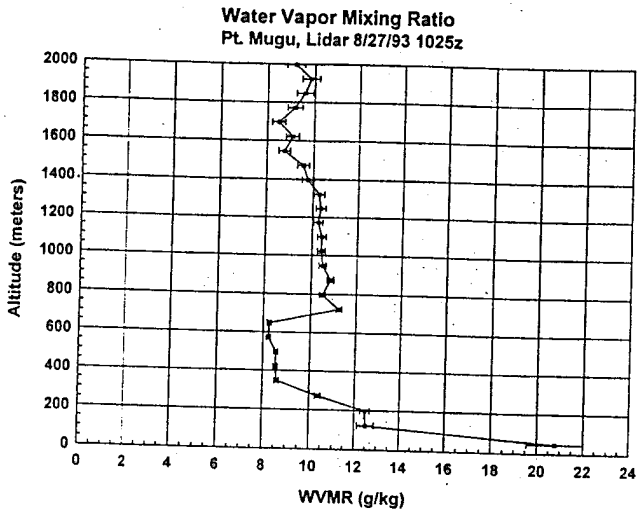

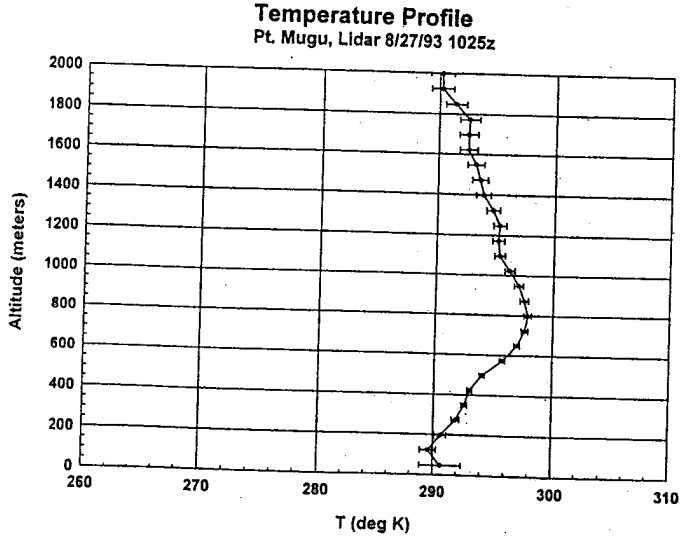

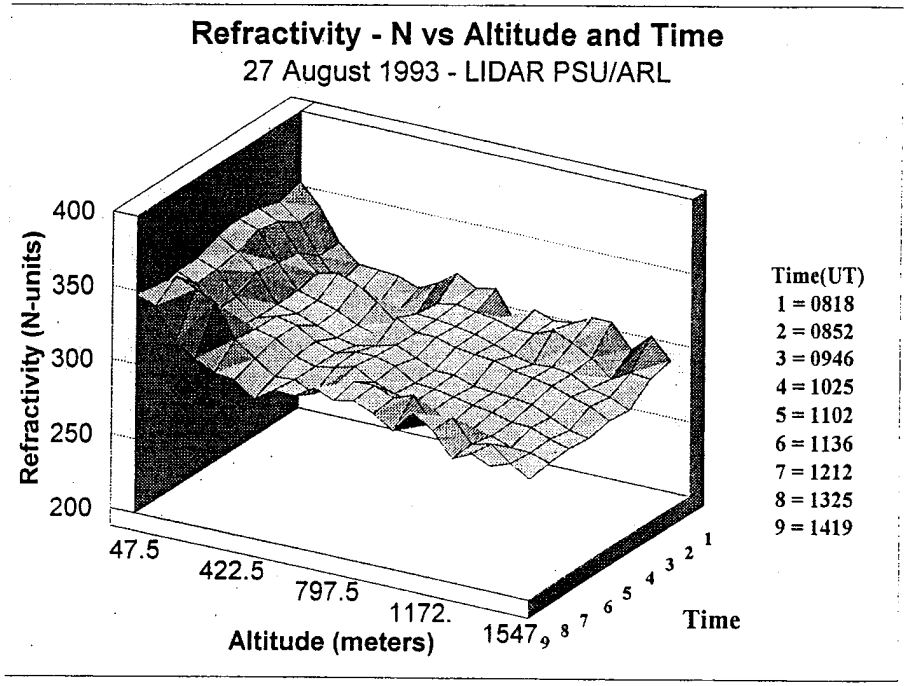

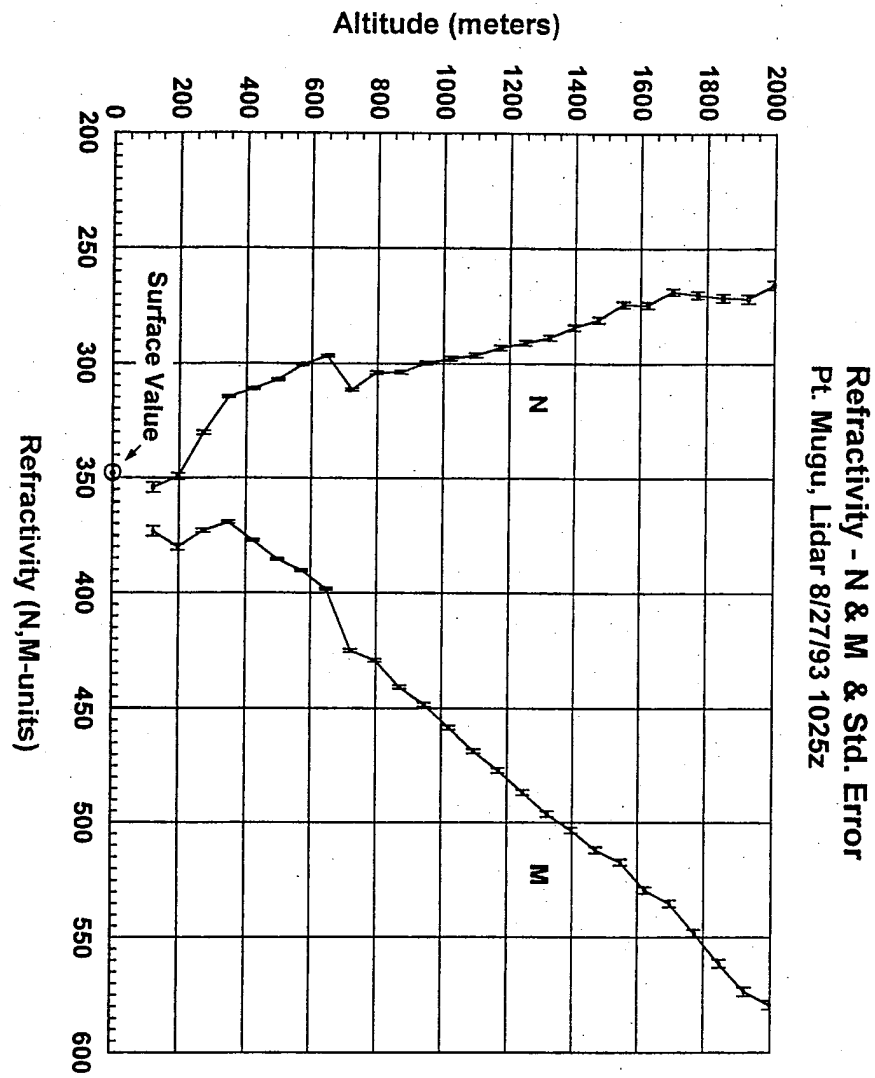

Equations for Refractivity Standard Error

$$\delta N = \frac{\partial N}{\partial P} \times \delta P + \frac{\partial N}{\partial T} \times \delta T + \frac{\partial N}{\partial P_{WV}} \times \delta P_{WV}$$

Assuming no error in estimating P,

the RMS error in Refractivity is:

$$N(1\Sigma, RMS) = \sqrt{(a_N \times \frac{P}{T^2} + 2 \times b_N \times \frac{P_{WV}}{T^3})^2 \times \Delta_T^{\,2} + (\frac{b_N}{T^2})^2 \times \Delta_{WV}^{\,2}}$$

where the Partial Pressure of Water Vapor:

$$P_{WV} = \frac{r \times P}{r + 621.97} \; (mb) \;, \quad \Delta_{WV} = \frac{C_{WV} \times P}{(r + C_{WV})^2} \times \Delta r$$

and where: $a_N = 77.6$ $b_N = 3.73 \times 10^5$ Cwv = 621.97,

Δ_T = standard error in temperature (measured),

Δ_r = standard error in water vapor (measured),

r = water vapor mixing ratio (g/kg) (measured),
T = absolute atmospheric temperature (K) (measured),
P = absolute atmospheric pressure (mb) (meas./derived).

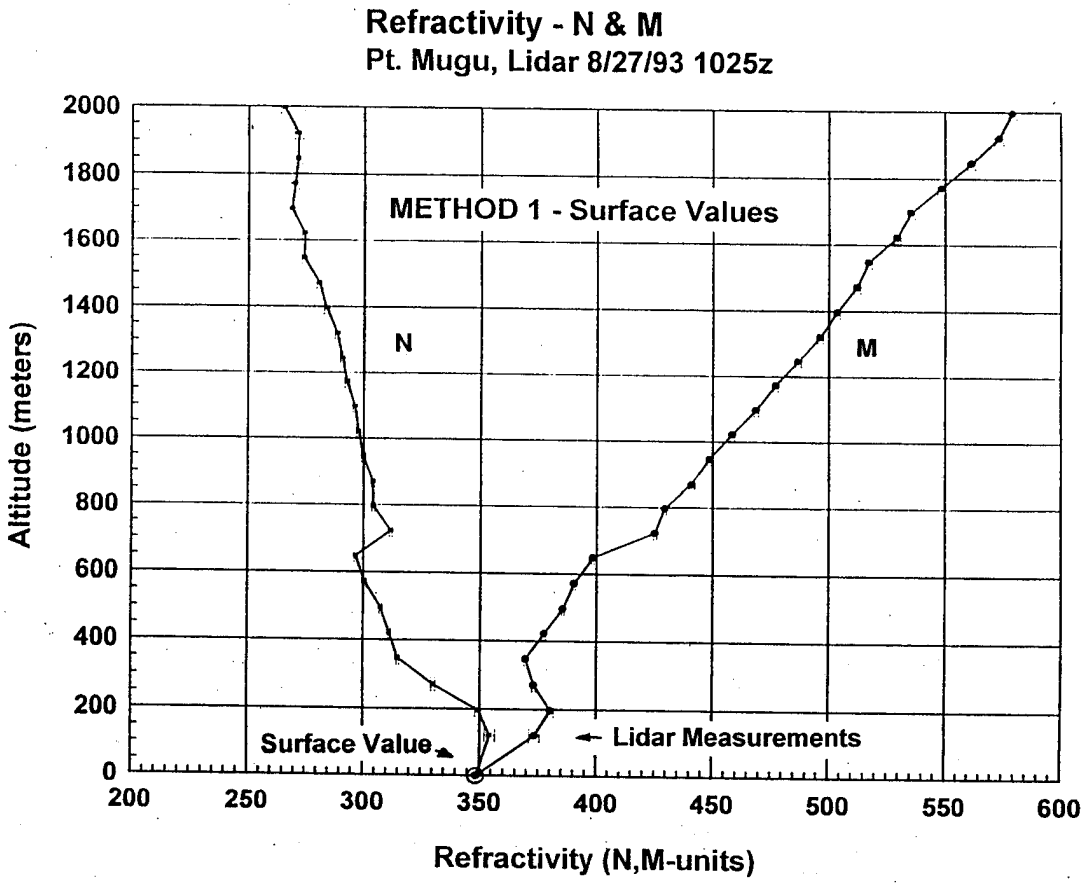
Refractivity - N & M
Pt. Mugu, Lidar 8/27/93 1025z
METHOD 1 - Surface Values
N
M
Surface Value
Lidar Measurements
Altitude (meters)
Refractivity (N,M-units)
0
200
400
600
800
1000
1200
1400
1600
1800
2000
200
250
300
350
400
450
500
550
600

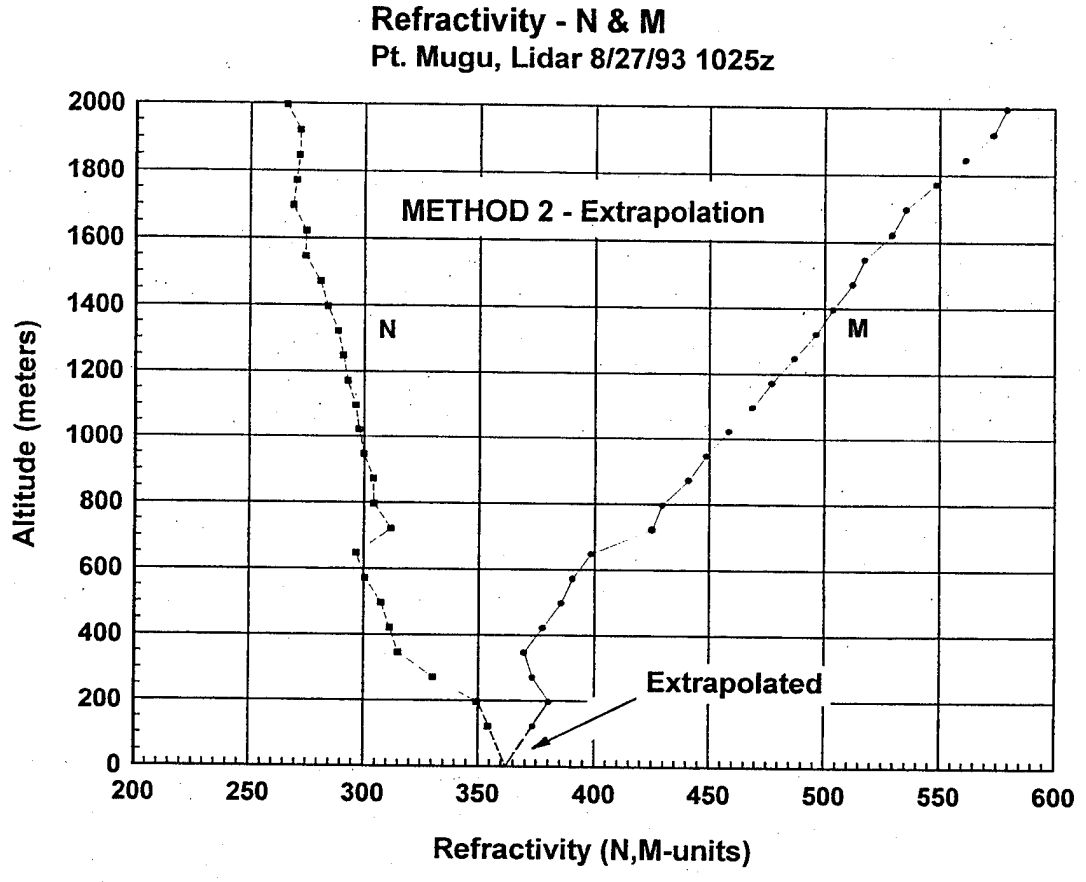
Refractivity - N & M
Pt. Mugu, Lidar 8/27/93 1025z
METHOD 2 - Extrapolation
N
M
Extrapolated
Altitude (meters)
Refractivity (N,M-units)
0
200
400
600
800
1000
1200
1400
1600
1800
2000
200
250
300
350
400
450
500
550
600

PENNSTATE

Applied Research Laboratory

SUMMARY

- Lidar & surface measurements provide the input to propagation
- Standard errors in refractivity offer additional means of validating
- Methods of pre-conditioning low altitude profile:

  1- use of near-surface and upper air measurement
  2- extrapolation of lowest measurements
  3- using standard M slope extrapolation: $M_h = M_{ho} + (0.131)x(h-h_o)$
  4- combination of 1- to 3- with an 'odd man out' approach
- At Pt. Mugu, Lidar successfully detailed refractive layering
- During VOCAR, lidar provided measurements for refractive variability
  - fixed spatial (true vertical) profiling
  - rapid-sequence (temporal) sampling
- High resolution (15m), goal to better low-altitude characterization

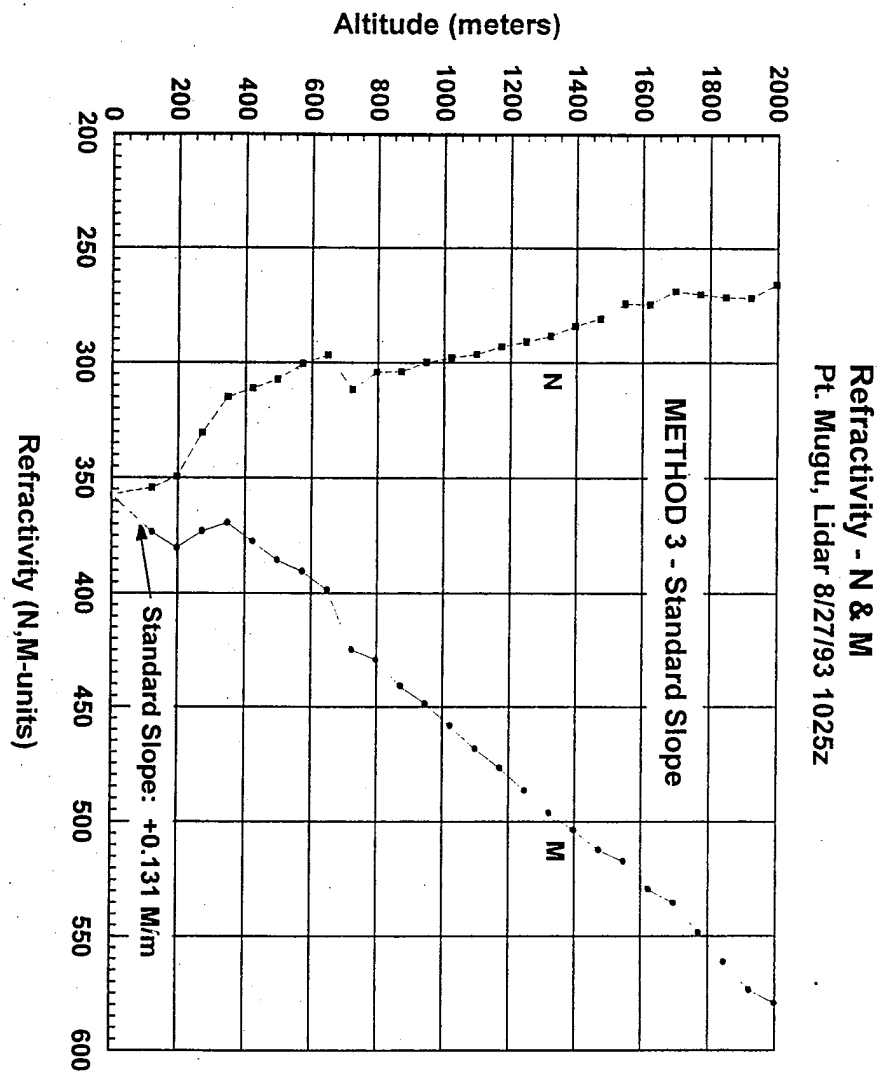

Mr. David Blood, "Measurements of Tropospheric Refractivity Remote Sensing of Atmospheric Properties"

DISCUSSION

H. HITNEY

1. Your data all appear to be collected at night. Do you have such good performance during the day?
2. Have you compared the computed propagation loss based on your profiles to measured loss versus time for the VOCAR IOP?

AUTHOR'S REPLY

1. With LAMP at Pt. Mugu we operated mostly at night with some measurements past sunrise which were of good quality when using UV (solar blind) measurement channels for water vapor. For daytime, a temperature model is required, but water vapor is the prime contributor to refractive profiling effects.
2. Propagation losses have been looked at from 5 days of VOCAR varying from highly refractive to non-refractive conditions. Many samples collectively showed agreement between RPO and measured signal levels to within 1 dB but individual cases differed high or low by 8-10 dB. These results were presented at the special AGARD symposium in 1994 in Germany (AGARD CP 567, *Propagation Assessment in Coastal Environments*, Feb. 1995).

SEAWASP AUTOMATED ENVIRONMENTAL ASSESSMENT INSTRUMENTATION

John R. Rowland
Johns Hopkins University Applied Physics Laboratory
Johns Hopkins Road
Laurel, MD 20723 (301)953-6000 x8660

The Johns Hopkins University Applied Physics Laboratory (JHU/APL) is tasked by the AEGIS Shipbuilding Program (PMS-400) to lead the development of a prototype tactical decision aid for in situ assessment of radar and weapon system capability. The system under development is called SEAWASP (Shipboard Environmental Assessment & Weapon System Performance). The instrumentation used in SEAWASP was developed and operated over a ten year period in support of numerous fleet exercises and research efforts. This equipment is being tailored to operate autonomously in an AEGIS shipboard environment with minimal impact on normal ship operations, while providing sufficient data fidelity to support tactically useful weapon system assessments. Primary meteorological sensor systems currently integrated into SEAWASP include (1) dual meteorological poles, which provide the data necessary to exercise new JHU/APL evaporation duct models, (2) a floating sensor which provides direct measurement of surface parameters for evaporation duct model validation, and (3) a rocketsonde system for obtaining refractivity profiles above the evaporation duct. Developmental versions of SEAWASP's environmental instrumentation have been field tested on AEGIS cruisers on five occasions. Other capabilities demonstrated during the at-sea tests include downlinking range-dependent refractivity profiles from an instrumented helicopter, and receiving visible and IR images from polar-orbiting satellites. Additional sensors being developed for future integration into SEAWASP include aerosol and scanning DIAL lidar sytems. A description of the instrumentation and associated algorithms, and examples of data collected during the AEGIS installations, will be presented in this paper.

SYSTEM THAT MAY BE USED BY AEGIS TO CHARACTERIZE RADAR PROPAGATION

Elevated And Surface Ducts

1. Rocketsonde
2. Instrumented LAMPS Helo

Evaporation Duct

Surface Measurement Model

1. 6 m Temperature, Relative Humidity And Wind Speed Sensors On Port And Starboard With Wind Vanes To Select Uncontaminated Measurements
2. Disposable Buoy Measurement Of Temperature And Relative Humidity At 2 cm
3. Calculations Made Only When Buoy Data Is Available

Constant Virtual Temperature Model

1. 6m Measurements Only
2. Calculations Made Continuously
3. A Rough Measurement Of Water Temperature (+/-1C) With An IR Thermometer To Prevent Incorrectly Calculating Duct Height In Very Stable Conditions
4. Surface Humidity Calculated Using APL Developed Empirical Equation

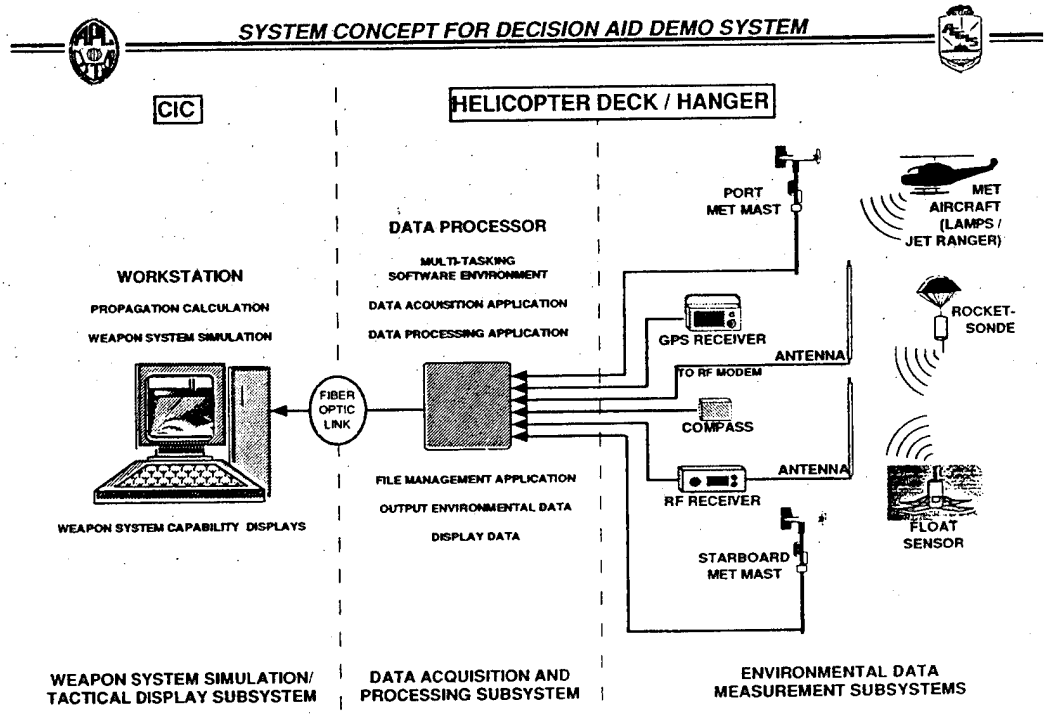

METEOROLOGICAL EQUIPMENT

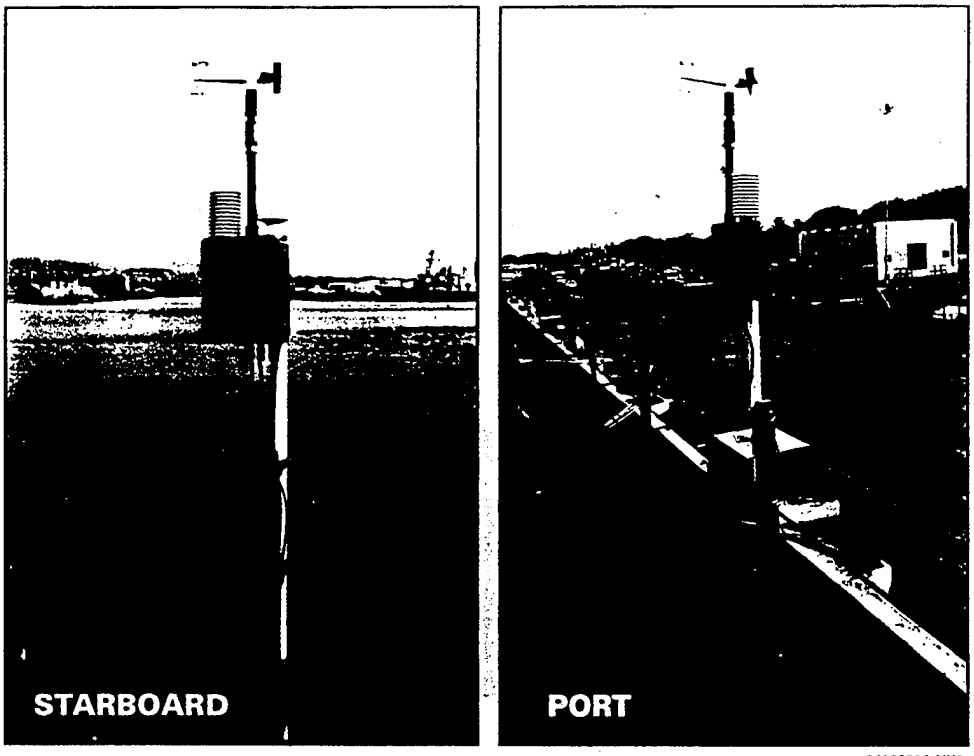

9406686A.UK2

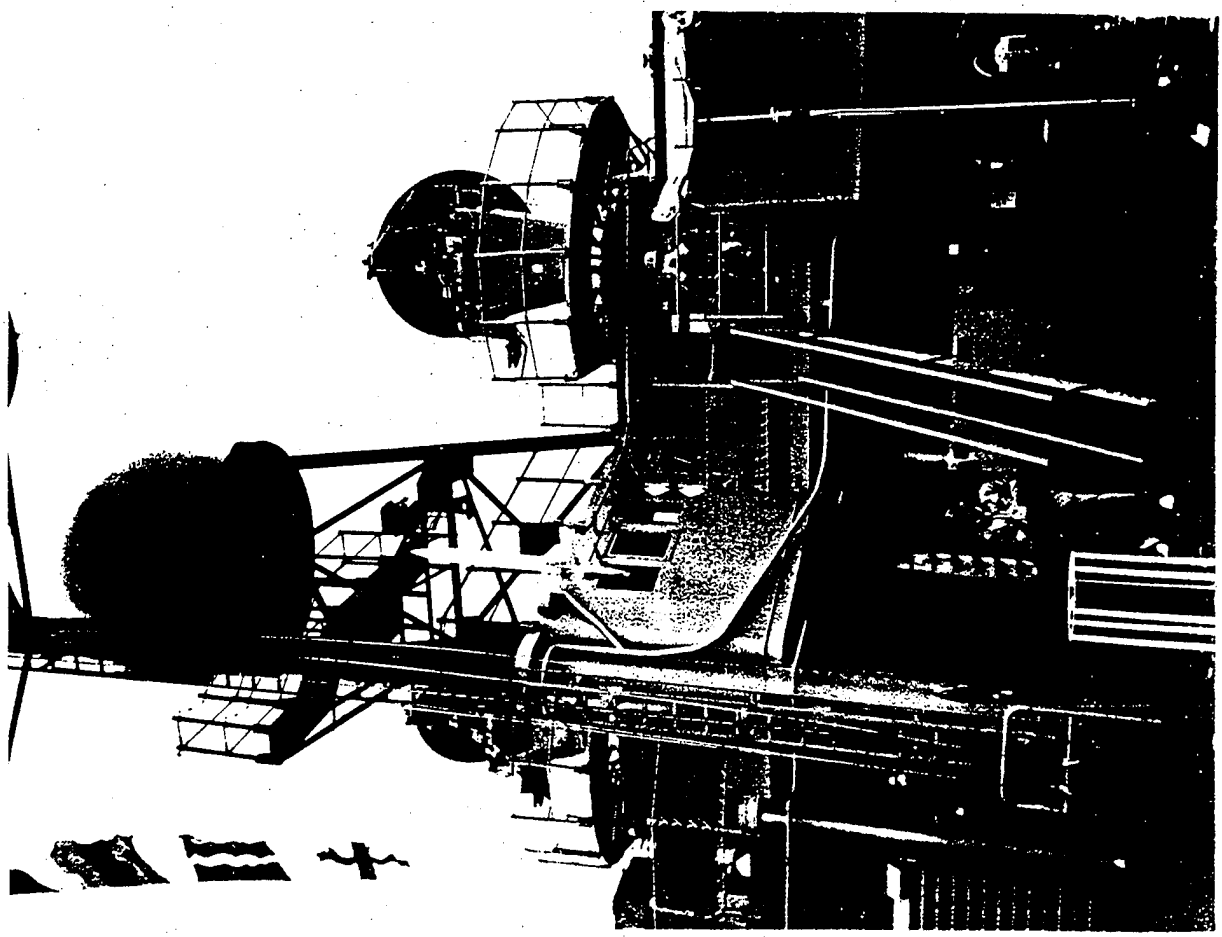

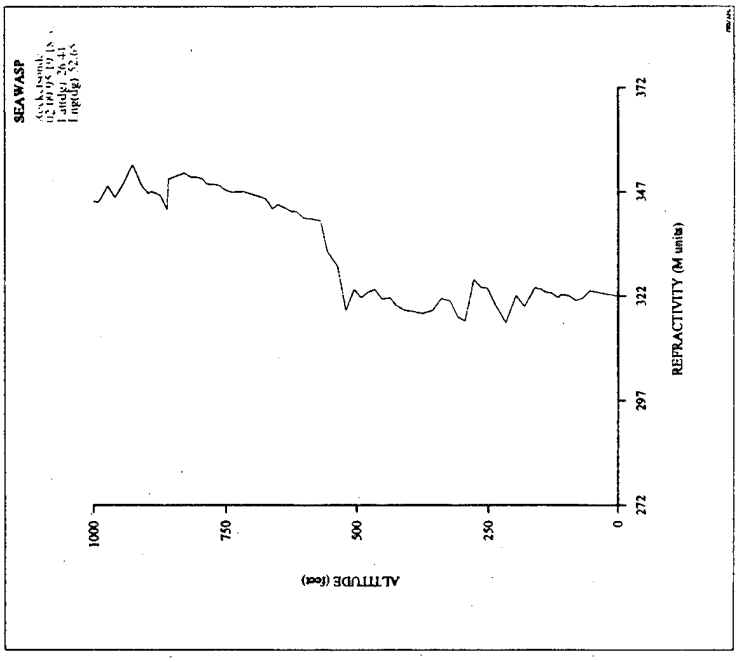
SEAWASP
ALTITUDE (feet)
1000
750
500
250
0
REFRACTIVITY (M units)
272
297
322
347
372

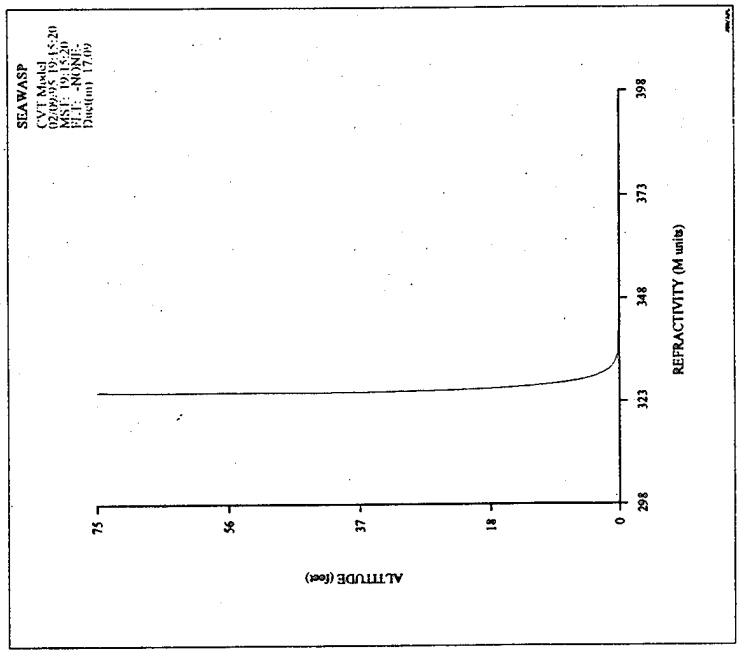
SEAWASP
CVT Model
02/09/95 19:15:20
MST: 19:15:20
FLT: -NONE-
Duct(m) 17.09
ALTITUDE (feet)
75
56
37
18
0
REFRACTIVITY (M units)
298
323
348
373
398

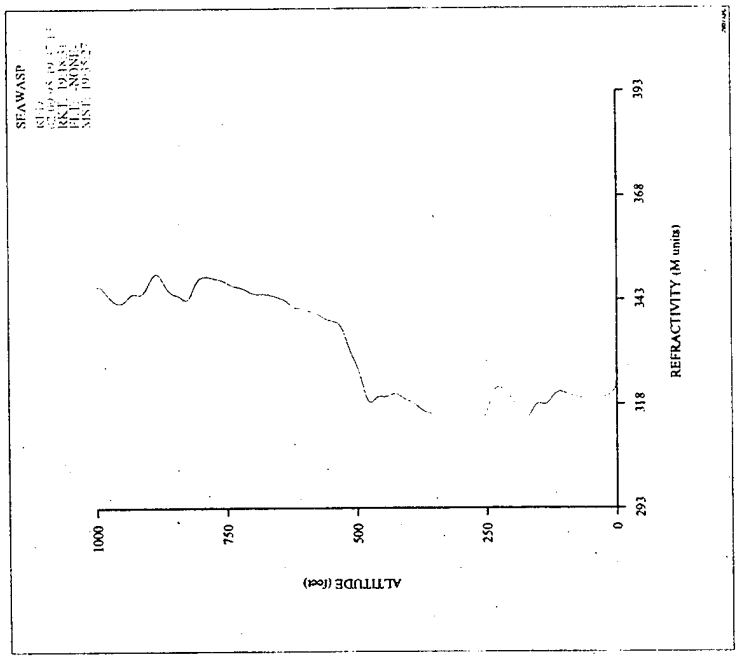
SEAWASP
ALTITUDE (feet)
1000
750
500
250
0
293
318
343
368
393
REFRACTIVITY (M units)

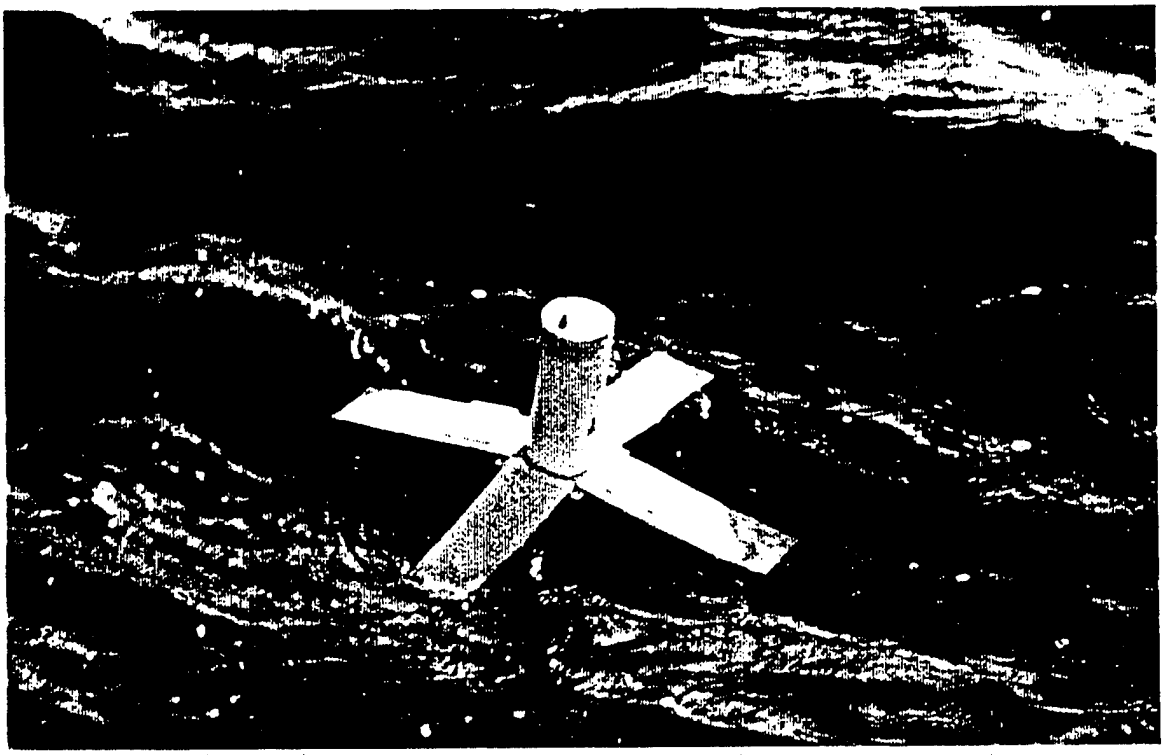

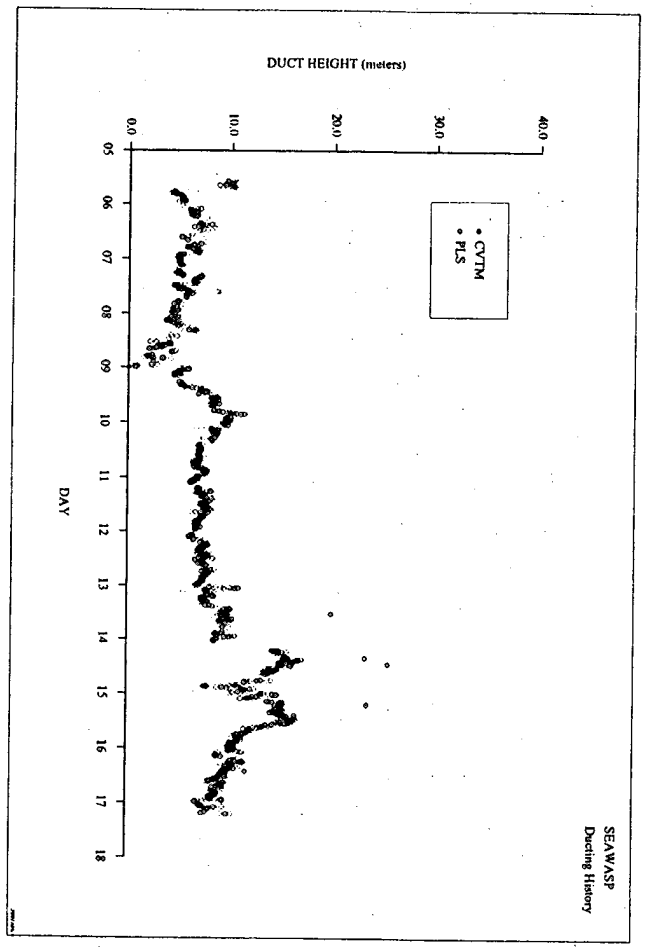

SHAREM 110
FEBRUARY 1995

FLOAT 02/14/95

Time	Press (mb)	Air T (c)	DP (c)	RH (%)	Ref (M)	Alt (m)	Elsp	Water T (c)
11:44:08.57	1012.85	22.78	11.2	47.80	324.7	16	302.95	23.7
11:44:10.39	1012.96	22.74	9.8	43.82	319.7	15	304.77	23.7
11:44:12.20	1012.91	22.76	10.7	46.56	323.1	15	306.58	23.7
11:44:14.01	1012.97	22.71	9.2	42.03	317.6	15	308.39	23.7
11:44:15.88	1012.84	22.83	12.5	52.07	329.8	16	310.26	23.7
11:44:17.69	1012.79	22.85	13.0	53.79	332.0	16	312.07	23.7
11:44:19.50	1012.85	22.85	12.4	51.73	329.5	16	313.88	23.7
11:44:21.32	1012.85	22.91	14.3	58.54	337.7	16	315.70	23.7
11:44:23.18	1012.85	22.97	15.0	60.88	340.7	16	317.56	23.7
11:44:25.00	1012.85	22.87	14.1	57.80	336.7	16	319.38	23.7
11:44:25.00	1012.85	22.95	14.8	60.31	340.0	16	319.38	23.7
11:44:28.62	1012.80	22.82	11.8	49.64	327.0	16	323.00	23.7
11:44:30.49	1012.92	22.83	11.6	49.03	326.1	15	324.87	23.7
11:44:32.30	1012.85	22.91	13.9	56.86	335.7	16	326.68	23.7
11:44:34.11	1013.09	22.88	14.1	57.84	336.5	14	328.49	23.7
11:44:35.93	1012.97	22.89	12.9	53.22	331.2	15	330.31	23.7
11:44:37.79	1012.91	22.91	13.9	56.83	335.6	15	332.17	23.7
11:44:39.61	1012.97	22.90	13.3	54.65	332.9	15	333.99	23.7
11:44:41.42	1013.03	22.90	14.1	57.62	336.4	14	335.80	23.7
11:44:43.23	1012.97	22.87	13.2	54.58	332.8	15	337.61	23.7
11:44:45.05	1013.03	22.86	12.3	51.22	328.7	14	339.43	23.7
11:44:50.54	1012.91	22.83	11.9	50.11	327.4	15	344.92	23.7
11:44:52.35	1012.91	22.80	10.7	46.33	322.9	15	346.73	23.7
11:44:54.16	1012.86	22.81	11.8	49.99	327.3	16	348.54	23.7
11:44:56.03	1013.03	22.87	13.6	55.90	334.3	14	350.41	23.7
11:44:57.84	1013.03	22.88	13.7	56.41	334.9	14	352.22	23.7
11:44:59.66	1012.91	22.81	10.8	46.65	323.3	15	354.04	23.7
11:45:01.47	1012.80	22.83	11.9	50.08	327.5	16	355.85	23.7
11:45:03.28	1012.92	22.82	11.1	47.67	324.5	15	357.66	23.7
11:45:05.15	1012.98	22.86	12.3	51.45	329.0	15	359.53	23.7
11:45:06.96	1012.86	22.78	11.2	47.94	324.8	16	361.34	23.7
11:45:08.77	1012.92	22.91	14.4	58.73	337.9	15	363.15	23.7
11:45:08.77	1012.91	22.91	13.6	55.66	334.2	15	363.15	23.7
11:45:12.40	1012.98	22.92	13.1	54.08	332.3	15	366.78	23.7
11:45:19.70	1012.69	22.92	13.1	53.86	332.4	17	374.08	23.7
11:45:21.57	1012.93	22.85	11.6	48.98	326.1	15	375.95	23.7
11:45:23.38	1012.69	22.90	12.1	50.56	328.4	17	377.76	23.7
11:45:25.20	1012.92	22.81	10.9	46.77	323.4	15	379.58	23.7
11:45:30.69	1012.88	22.82	12.6	52.37	330.1	15	385.07	23.7
11:45:34.31	1012.93	22.78	11.3	48.37	325.2	15	388.69	23.7
11:45:36.13	1012.81	22.76	11.6	49.16	326.2	16	390.51	23.7
11:45:37.94	1013.04	22.79	11.4	48.69	325.5	14	392.32	23.7
11:45:37.94	1013.04	22.79	11.4	48.69	325.5	14	392.32	23.7
11:45:39.81	1012.93	22.88	14.7	59.92	339.2	15	394.19	23.7
11:45:39.81	1012.81	22.83	11.6	49.22	326.5	16	394.19	23.7
11:45:43.43	1012.76	22.77	10.1	44.69	321.0	16	397.81	23.7
11:45:48.92	1012.99	22.94	15.0	60.91	340.5	15	403.30	23.7
11:45:59.85	1012.86	22.82	11.7	49.36	326.6	16	414.23	23.7
11:46:08.97	1012.81	22.88	12.6	52.27	330.2	16	423.35	23.7

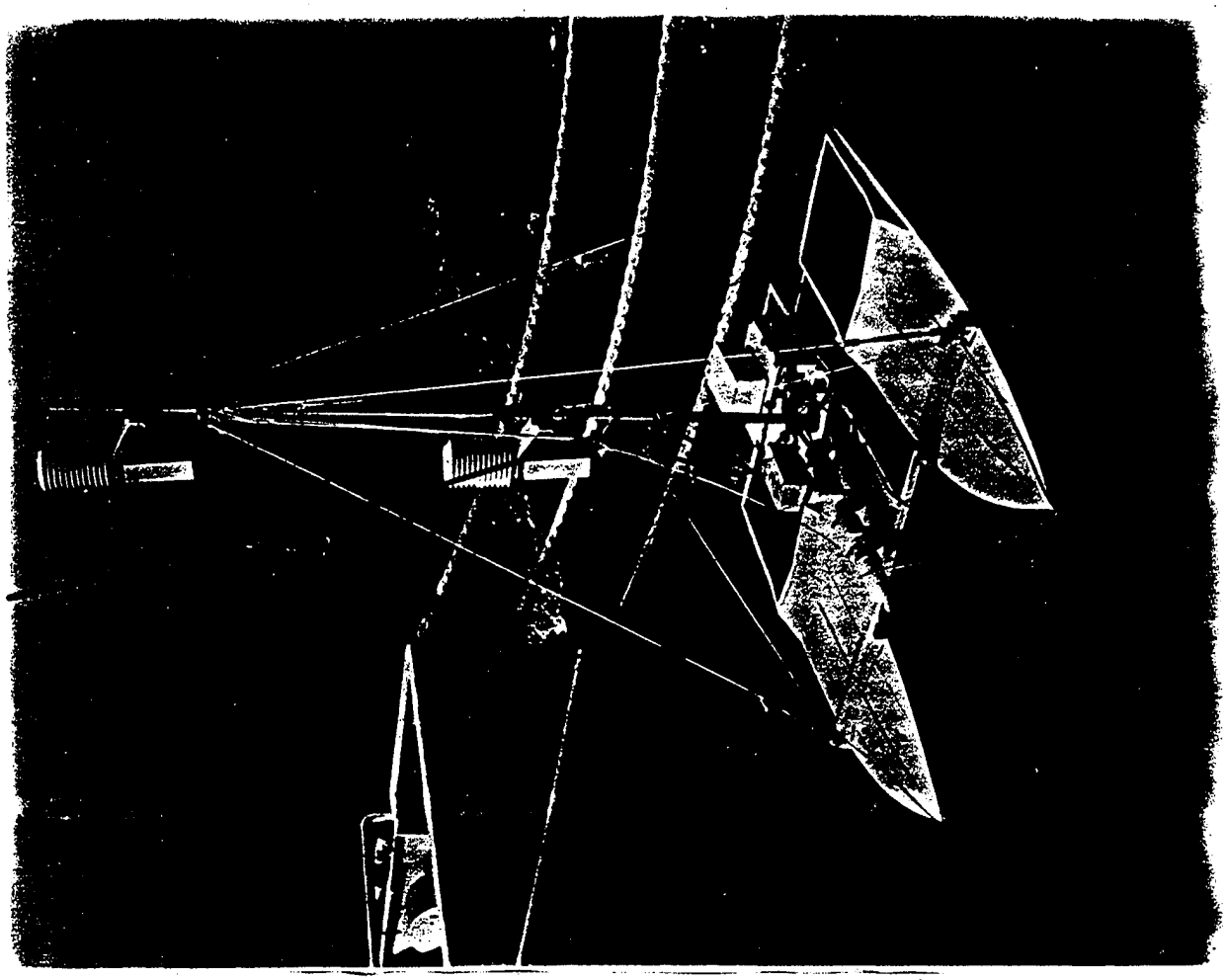

RELATIVE HUMIDITY OVER "WATER"

HUMIDITY	CONDITION
100%	DISTILLED WATER
75%	SATURATED NaCl
98%	STIRRED SEA WATER
88%	STILL SEA WATER
93%	KRUSPE 1977

ANY MODEL THAT USES 100% RH
FOR A SURFACE VALUE IS INCORRECT

SHIPBOARD AND SATELLITE SENSING OF REFRACTIVE CONDITIONS

K. L. Davidson and C. H. Wash
Department of Meteorology
Naval Postgraduate School
589 Dyer Rd., Room 254
Monterey, CA 93943-5114, USA
T/F: 408 656-2309/3061
e-mail: davidson@nps.navy.mil, wash@nps.navy.mil

Commercial off the shelf (COTS) measurement, acquisition, and display systems are being merged and evaluated for providing real-time assesments of near-surface refractive conditions. Sensor systems represent several different approaches for obtaining surface and air flow measurements. They include in situ versus radiometric obtained SST and measuring turbulent as well as mean to caluculate scaling paramters. Acquisition systems that can handle various inputs are important so their imposed contraints don't dictate the sensors. Two extended (10-12 days each) at sea evaluations have been performed since last November and two more are planned this year. Results will be from two experiments, conducted off the central California coast under quite different synoptic conditions. All measurements are evaluated on the basis of current scaling formulations for near-surface profiles. A demonstration of selected candidate systems is planned at the end of FY96.

Data from operational satellite sensors are being evaluated with regard to assesment of coastal refractiive conditions. Currently a multispectral approach using visible and IR data is being tested to indirectly estimate important variables such as the depth of the MABL, surface moisture and seasurface temperature. The method relies on previously developed techniques for estimating aerosol optical depth and total column water vapor. The approach uses the redvisible radiance measurements of the NOAA AVHRR (channel 1) and the direct relation between of this radiance to optical depth.

Satellite measurements of water vapor variations are also employed. The method relates total column water vapor to the difference between split window brightness temperatures from the NOAA AVHRR (channels 4 and 5). Since both estimates are derived from the same sensor, the boundary layer estimates can be derived from a single satellite data source. Satellite estimates of optical depth and column water vapor are both related to the MABL height and moisture. Remote data describe high resolution horizontal/temporal variations, important in the coastal, but not described by point measured in situ data.

SMALL COMBATANT METOC EM/EO SENSORS

PROGRAM OBJECTIVES :

- Determine HW/SW Specifications for " State-of-the-Art" Autonomous METOC Data Collection for SMALL COMBATANT use with NITES for:

  -- EM TACAIDS
  -- EO TACAIDS

SMALL COMBATANT METOC EM/EO SENSORS

PROGRAM APPROACH :

- EVALUATE State-of-the-Art METOC INSTRUMENTS in the LABORATORY and AT SEA
- DETERMINE FEASIBILITY of COTS HW/SW to PROVIDE IN SITU EM/EO MEASUREMENTS NEEDED as INPUTS for EM/EO TACAIDS

SMALL COMBATANT METOC EM/EO SENSORS

System evaluation/selection based on ship measurements

* Durability
* Exposure
* RF interference
* Sampling methods

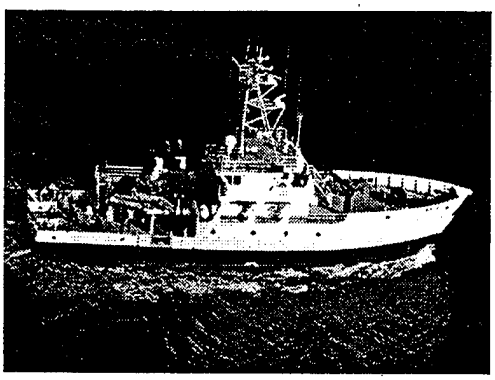

R/V Point Sur is available as platform > 30 days per year

SMALL COMBATANT METOC EM/EO SENSORS

Intercomparison platform : Multiple sensors suites

* Relative wind:
  propeller anemometer
  sonic anemometer
* Air temperature and humidity
* Aerosol spectrometers

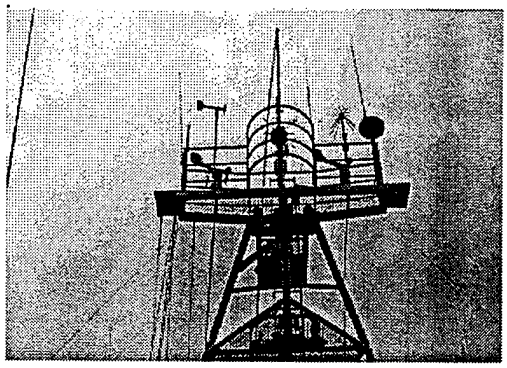

Measurement height is 63 ft.

SMALL COMBATANT METOC EM/EO SENSORS

Evaluation with ideal exposure on bow mast

Emphasized measurements :

* IR obtained SST
* Relative wind
* Air temperature

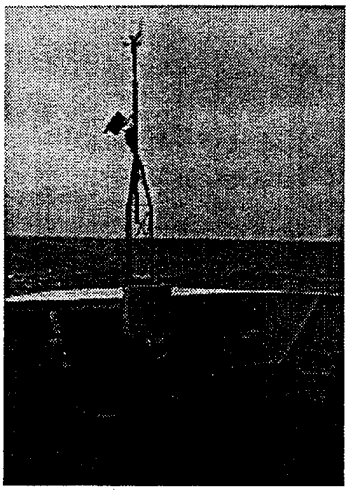

Compared with ship mast, Ship intake and Buoy Measurements

SMALL COMBATANT METOC EM/EO SENSORS

Evaporation duct dependence on measured values (Wind speed)

* Wind speed can have important effect on duct; below 10 knots
* Effect of measured value becomes more important if air is warmer than water

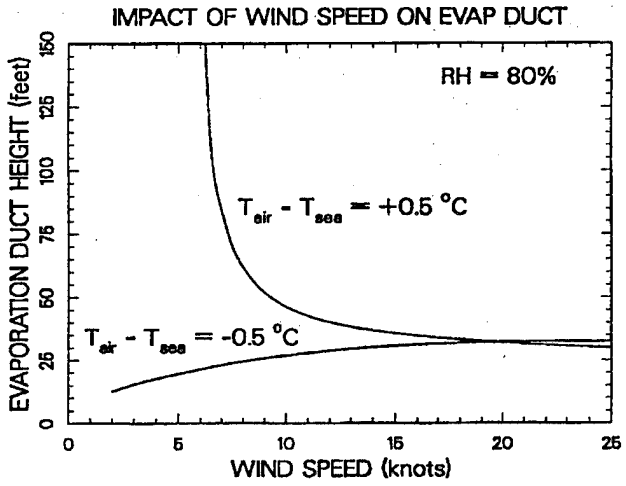

BULK MODEL PREDICTED EVAPORATION DUCT HEIGHT

SMALL COMBATANT METOC EM/EO SENSORS

Comparison of sensor systems (wind) : ship and buoy

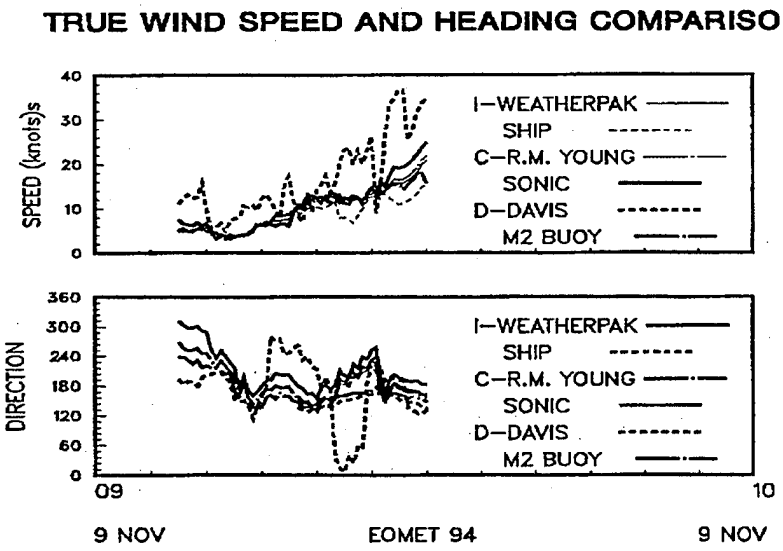

SMALL COMBATANT METOC EM/EO SENSORS

Evap duct dependence on measured values (Air humidity and SST)

* Duct height changes a lot with small changes of air-sea humidity differences

* Measured air-sea humidity differences become more important if air is warmer than water

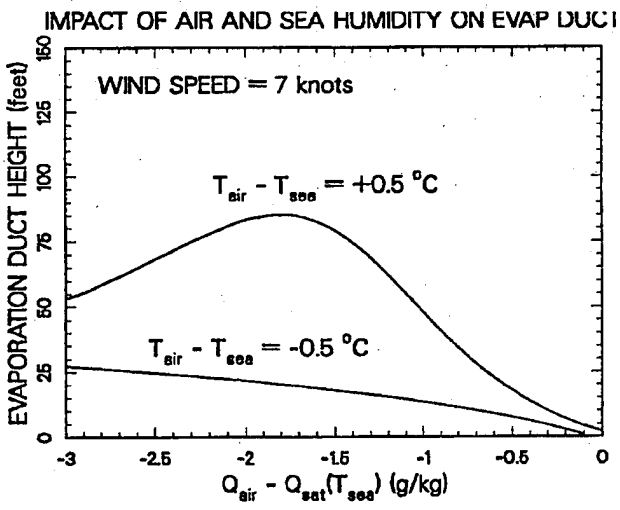

BULK MODEL PREDICTED EVAPORATION DUCT HEIGHT

SMALL COMBATANT METOC EM/EO SENSORS

Evaporation duct dependence on measured values (air-sea temperatures)

* Air-sea temperature difference values can be very important to duct height under cetain conditions

* Measured air-sea temperature difference is more important when wind is low; less than 10 knots

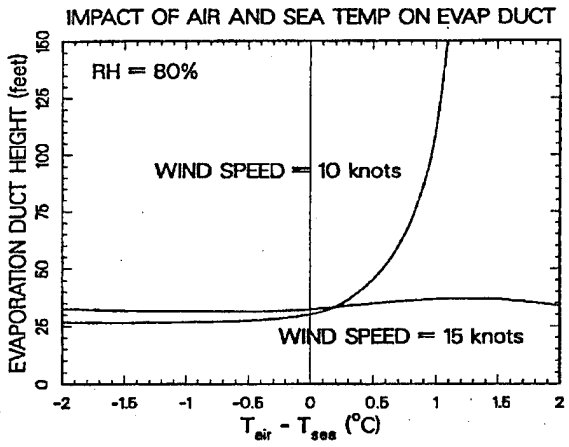

BULK MODEL PREDICTED EVAPORATION DUCT HEIGHT

SMALL COMBATANT METOC EM/EO SENSORS

Comparison of sensor systems (air temp and humidity) : ship and buoy

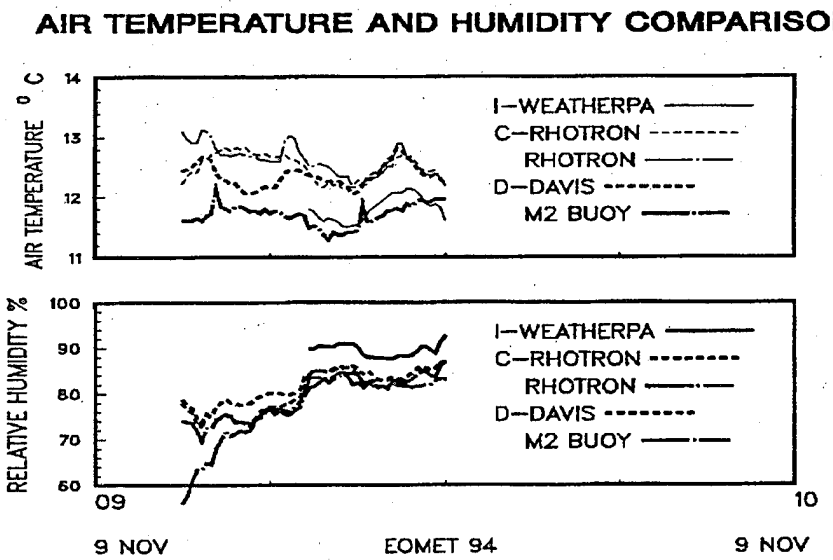

SMALL COMBATANT METOC EM/EO SENSORS

Comparison of sensor system derived evaporation ducts

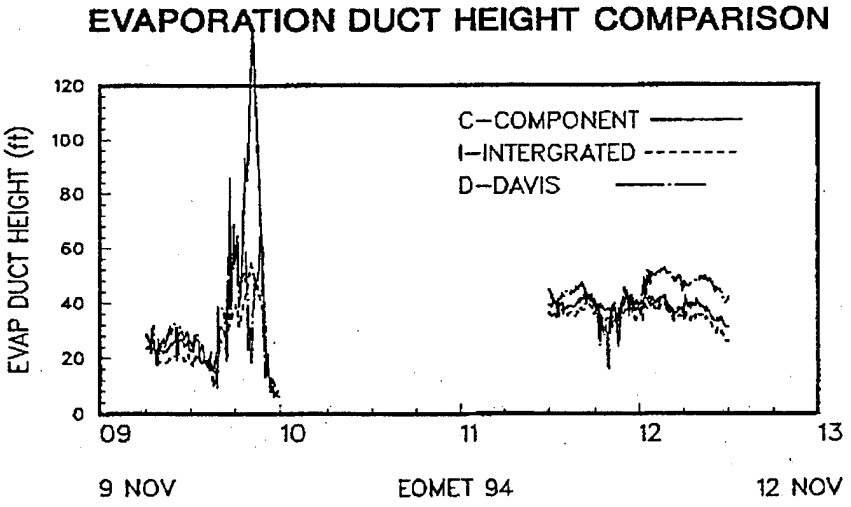

Multispectral MABL Analysis Background

- Follows the work of Kren (1987) and Smolinski (1988)
- Approach uses VIS and IR channels of NOAA AVHRR (1 km)
- Assume
  - * MABL is well-mixed
  - * All aerosols contributing to visual radiance are in MABL
  - * Apply in clear regions
  - * Avoid sun glint
- Determine % of path moisture in the MABL
- All measurements made with same satellite sensor along the same optical path

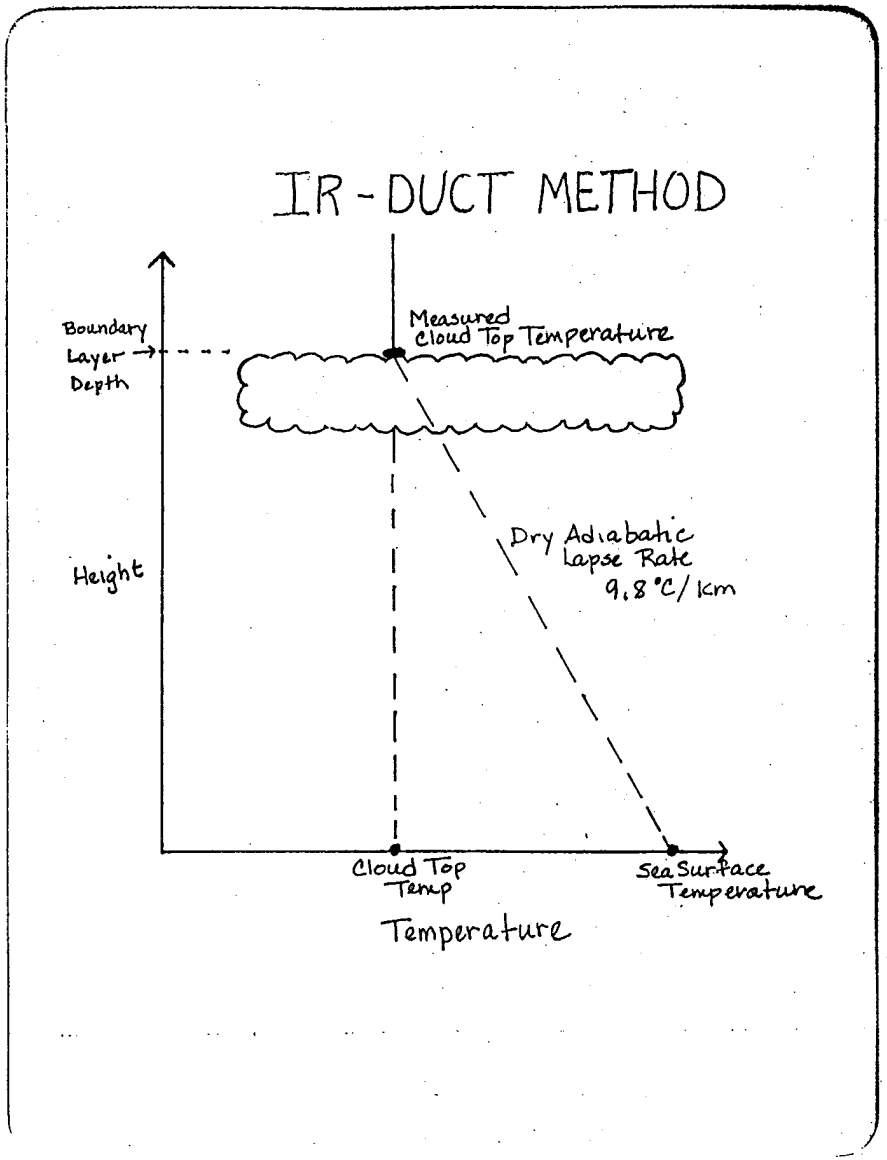

Multispectral MABL Analysis Method

- Split Window IR channels (4/5) to determine SST
- Visual Channel to determine aerosol optical depth and boundary layer relative humidity
- Split Window Difference (Channel 4-5) to determine total column water vapor
- From reference soundings, determine % of water vapor in MABL
- Asume linear variation of RH in MABL

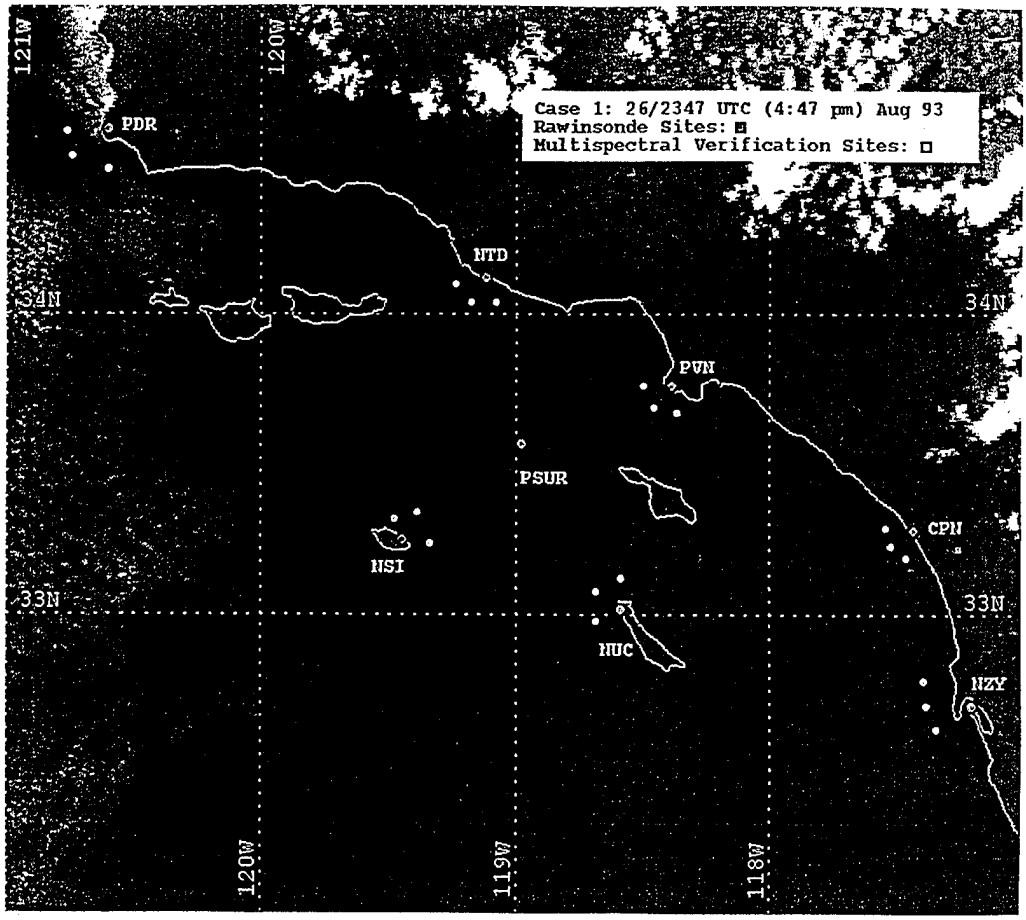
Case 1: 26/2347 UTC (4:47 pm) Aug 93
Rawinsonde Sites: ■
Multispectral Verification Sites: □
PDR
NTD
PVN
PSUR
NSI
CPN
NUC
NZY
34N
33N
121W
120W
119W
118W

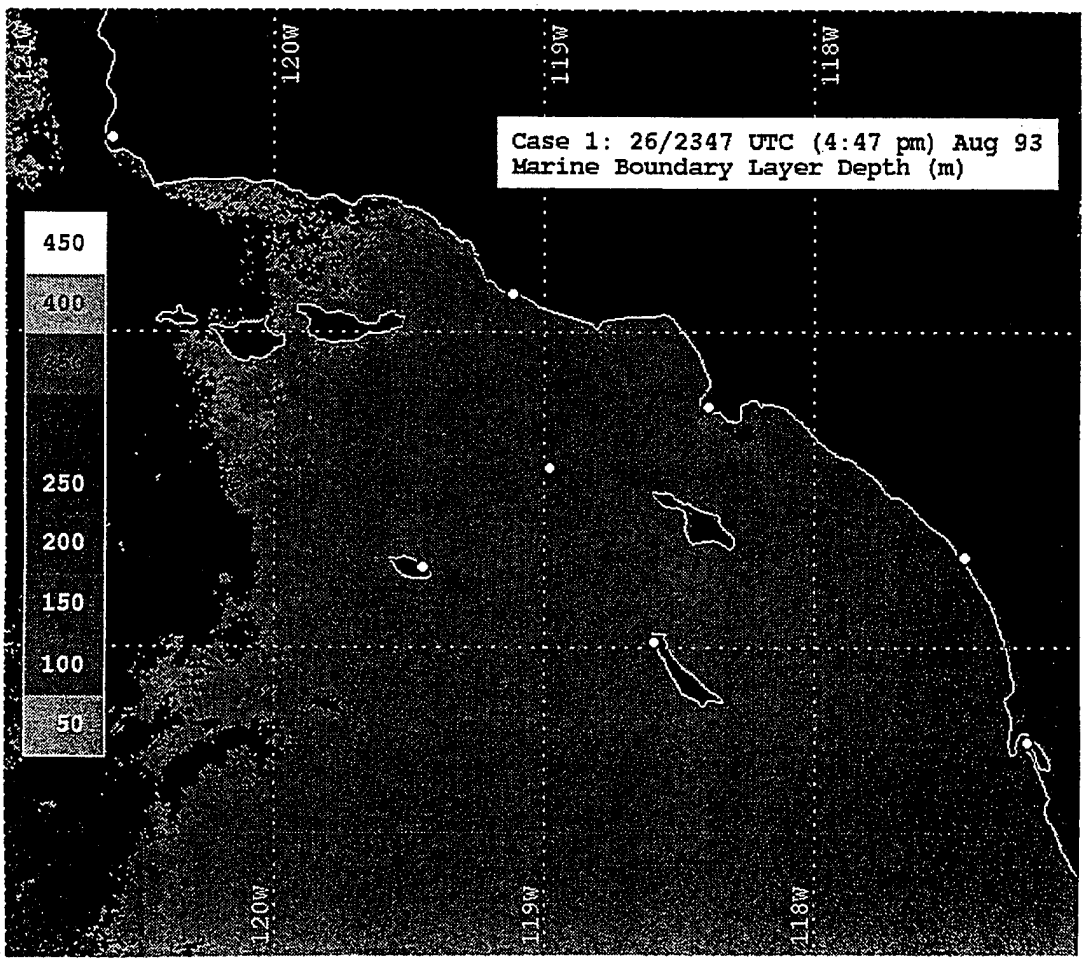
Case 1: 26/2347 UTC (4:47 pm) Aug 93
Marine Boundary Layer Depth (m)
450
400
250
200
150
100
50
124W
120W
119W
118W

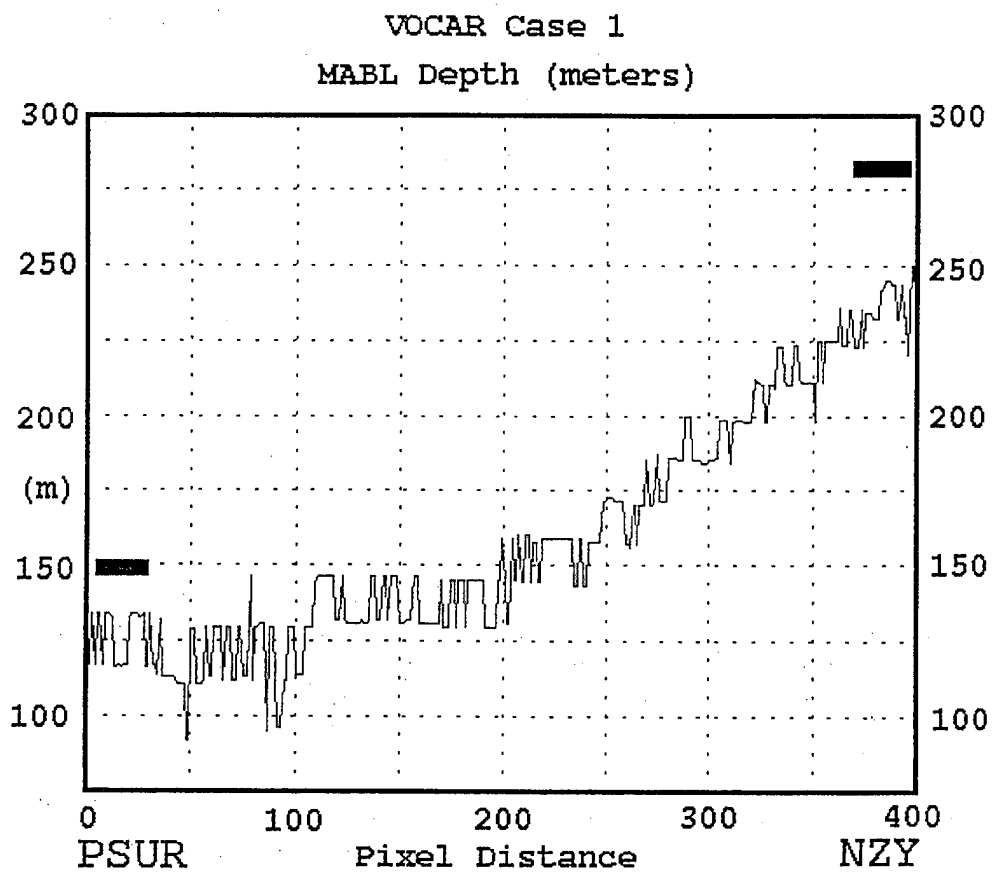
VOCAR Case 1
MABL Depth (meters)
300
250
200
(m)
150
100
0
100
200
300
400
PSUR
Pixel Distance
NZY

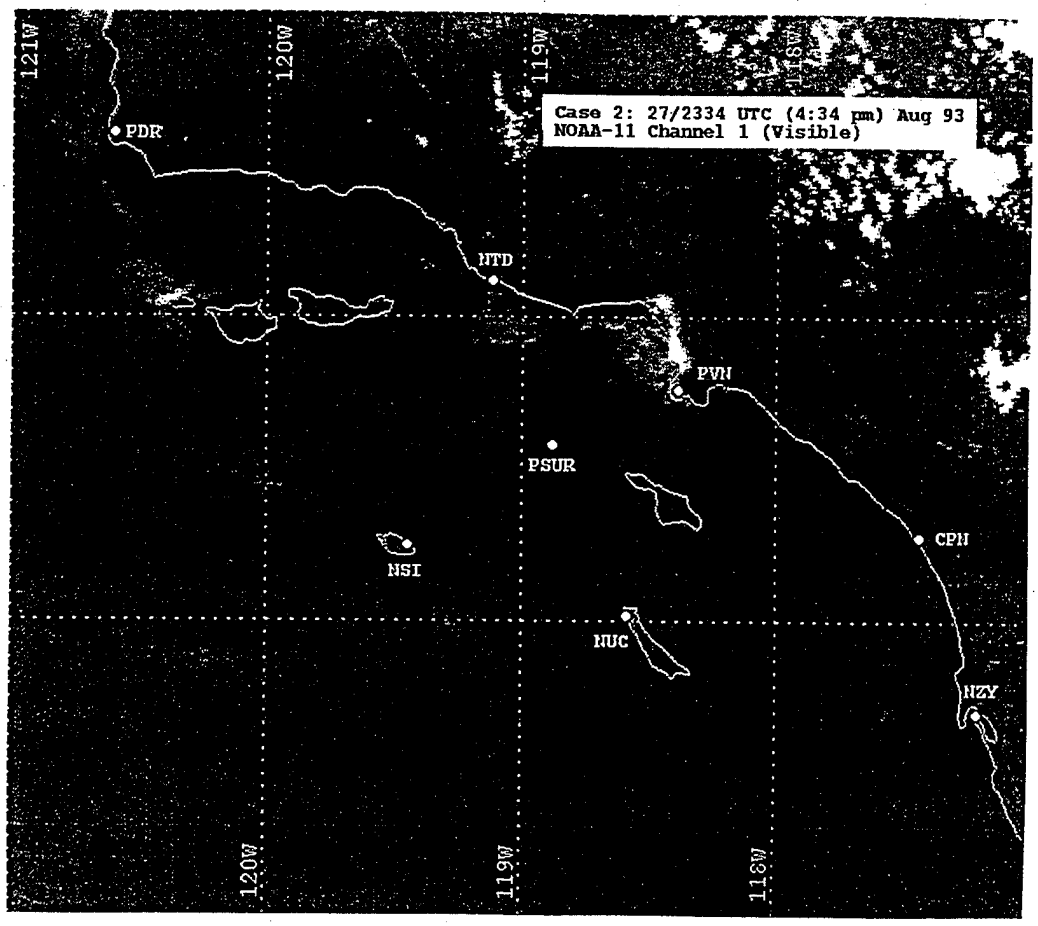
Case 2: 27/2334 UTC (4:34 pm) Aug 93
NOAA-11 Channel 1 (Visible)
121W
120W
119W
118W
PDR
NTD
PVH
PSUR
NSI
CPH
NUC
NZY

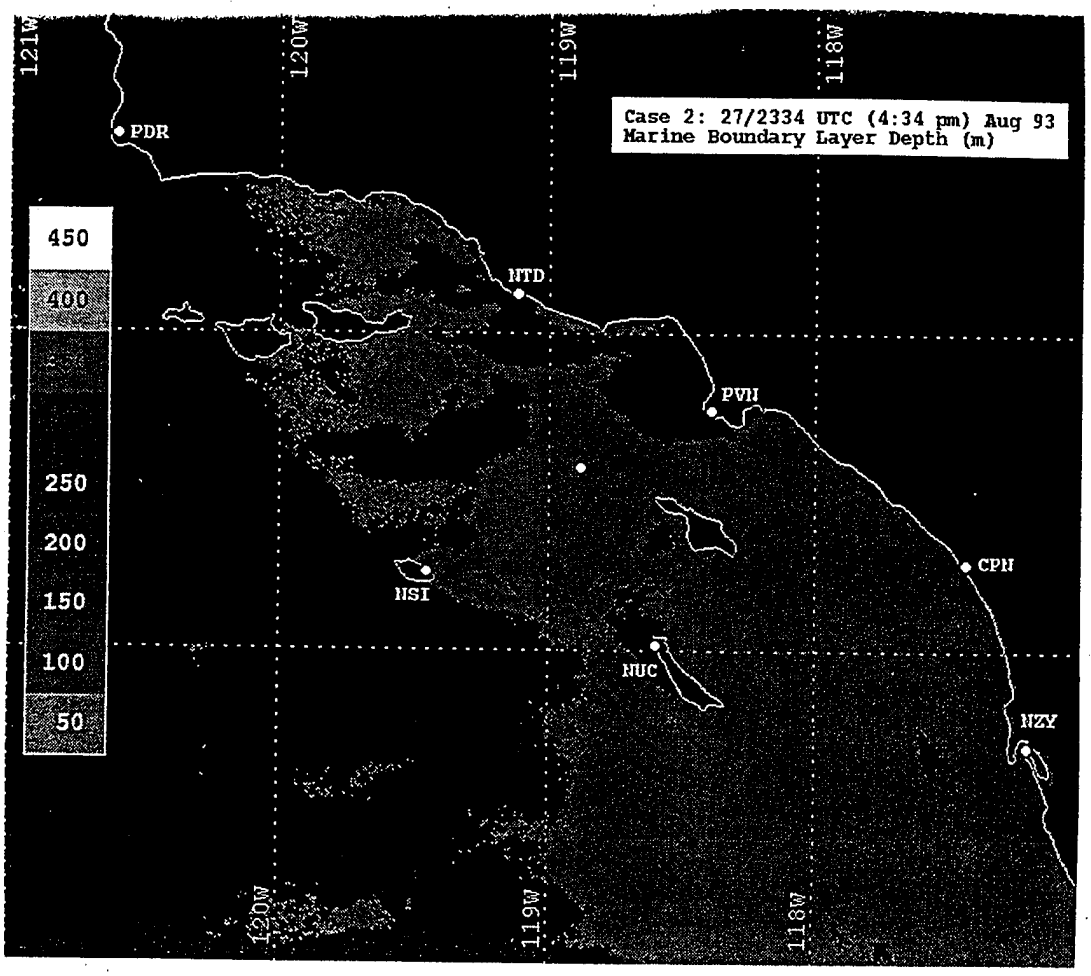
Case 2: 27/2334 UTC (4:34 pm) Aug 93
Marine Boundary Layer Depth (m)
121W
120W
119W
118W
PDR
MTD
PVH
CPH
NSI
NUC
NZY
450
400
250
200
150
100
50

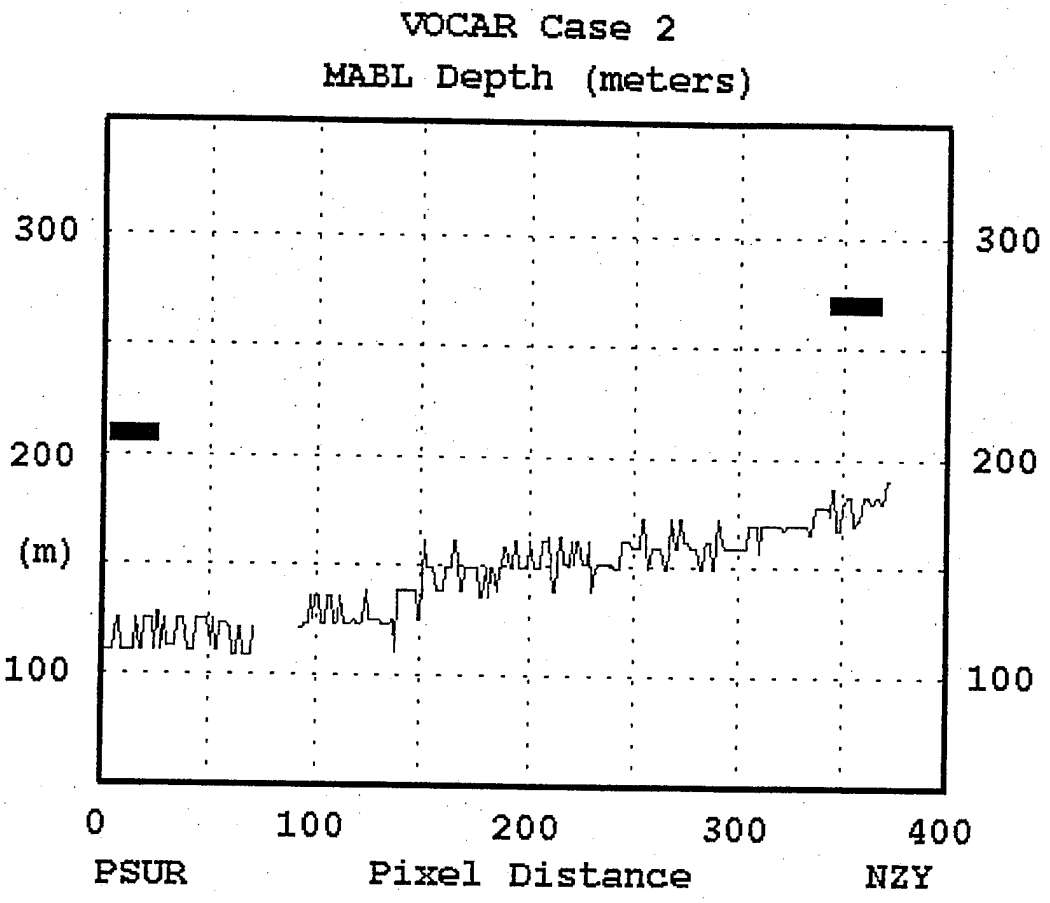
VOCAR Case 2
MABL Depth (meters)
300
200
(m)
100
0
100
200
300
400
PSUR
Pixel Distance
NZY

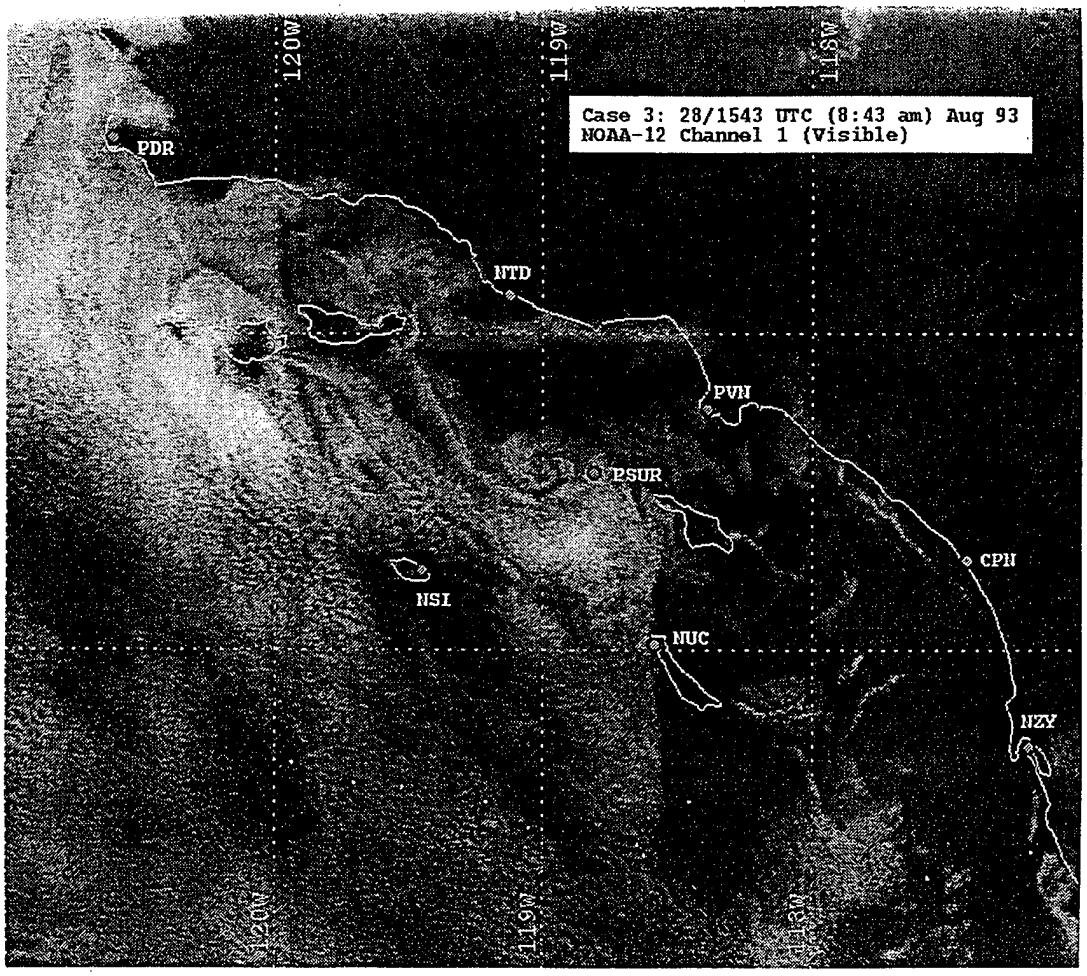
Case 3: 28/1543 UTC (8:43 am) Aug 93
NOAA-12 Channel 1 (Visible)
120W
119W
118W
PDR
NTD
PVH
PSUR
CPH
NSI
NUC
NZY

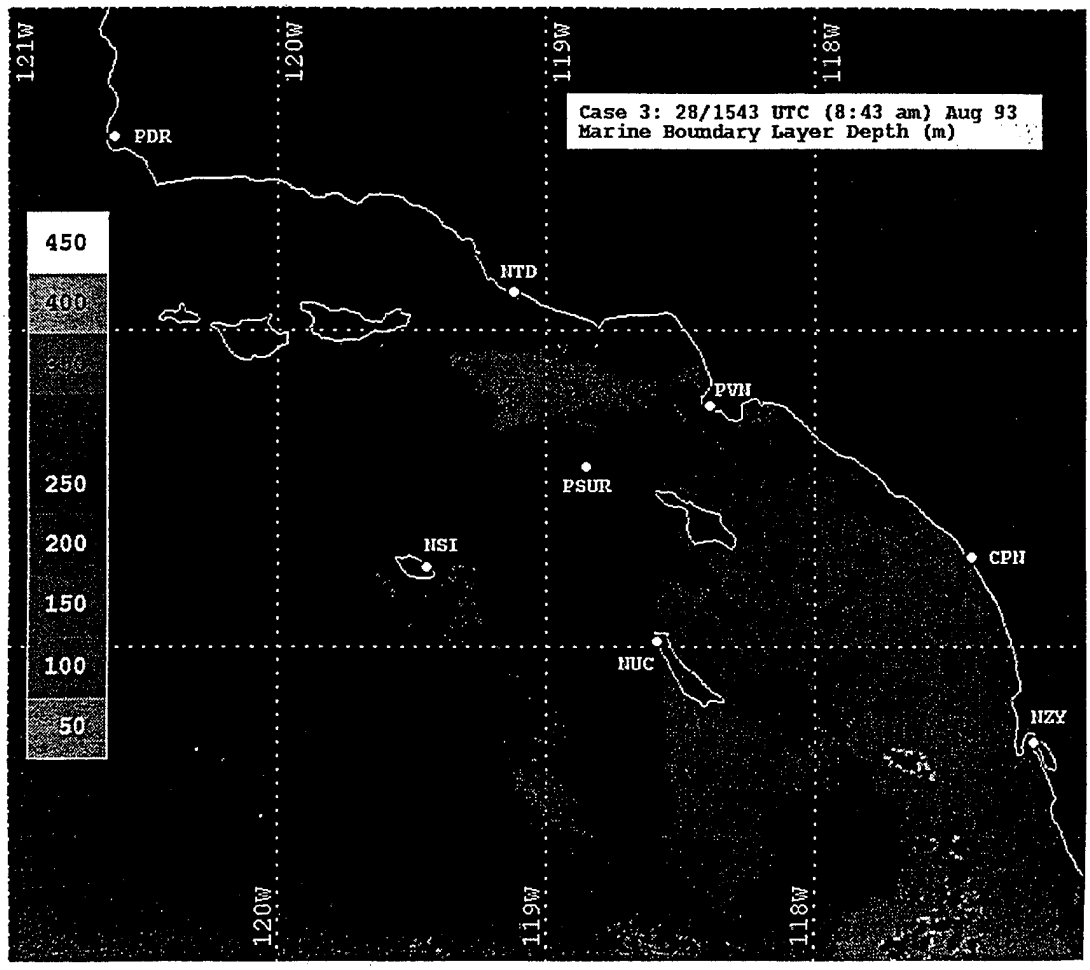
Case 3: 28/1543 UTC (8:43 am) Aug 93
Marine Boundary Layer Depth (m)
121W
120W
119W
118W
450
400
250
200
150
100
50
PDR
NTD
PVH
PSUR
NSI
CPH
NUC
NZY

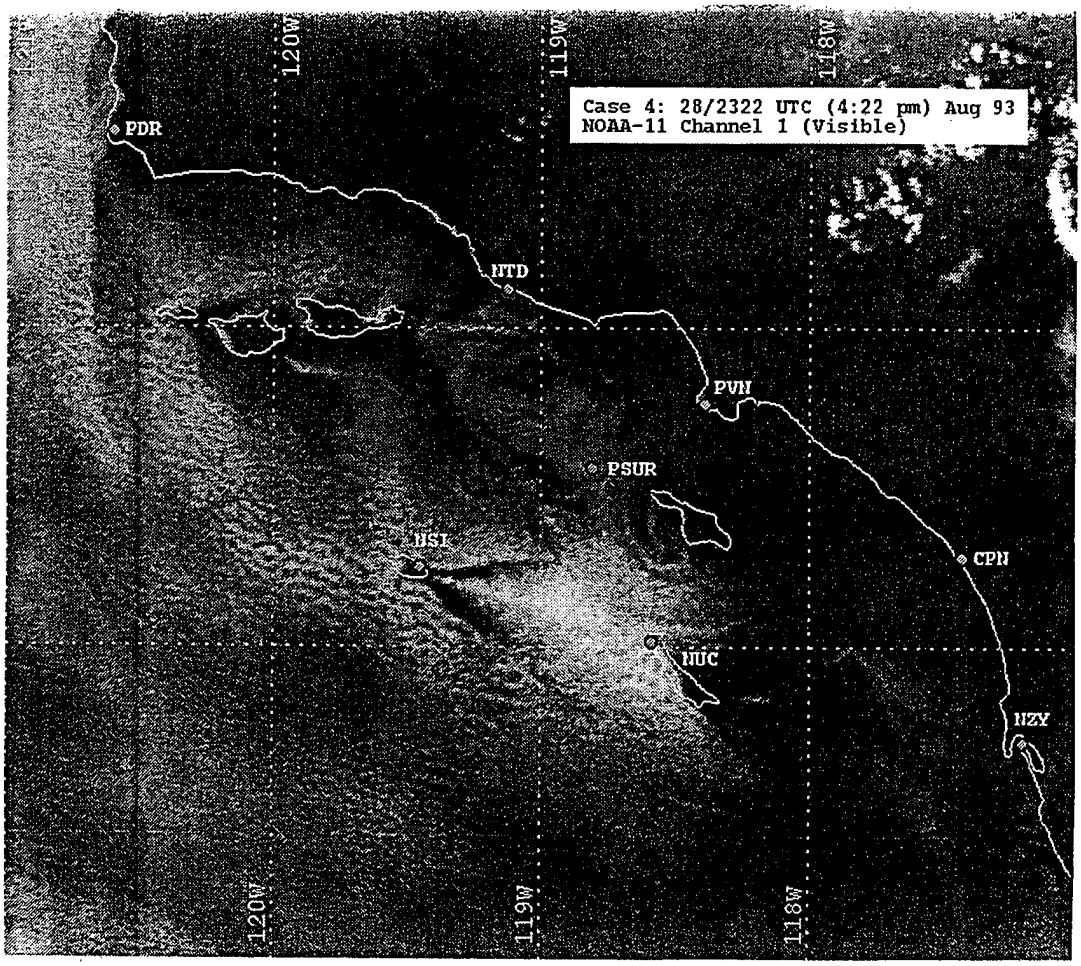
Case 4: 28/2322 UTC (4:22 pm) Aug 93
NOAA-11 Channel 1 (Visible)
120W
119W
118W
PDR
MTD
PVH
PSUR
NSI
CPH
HUC
HZY

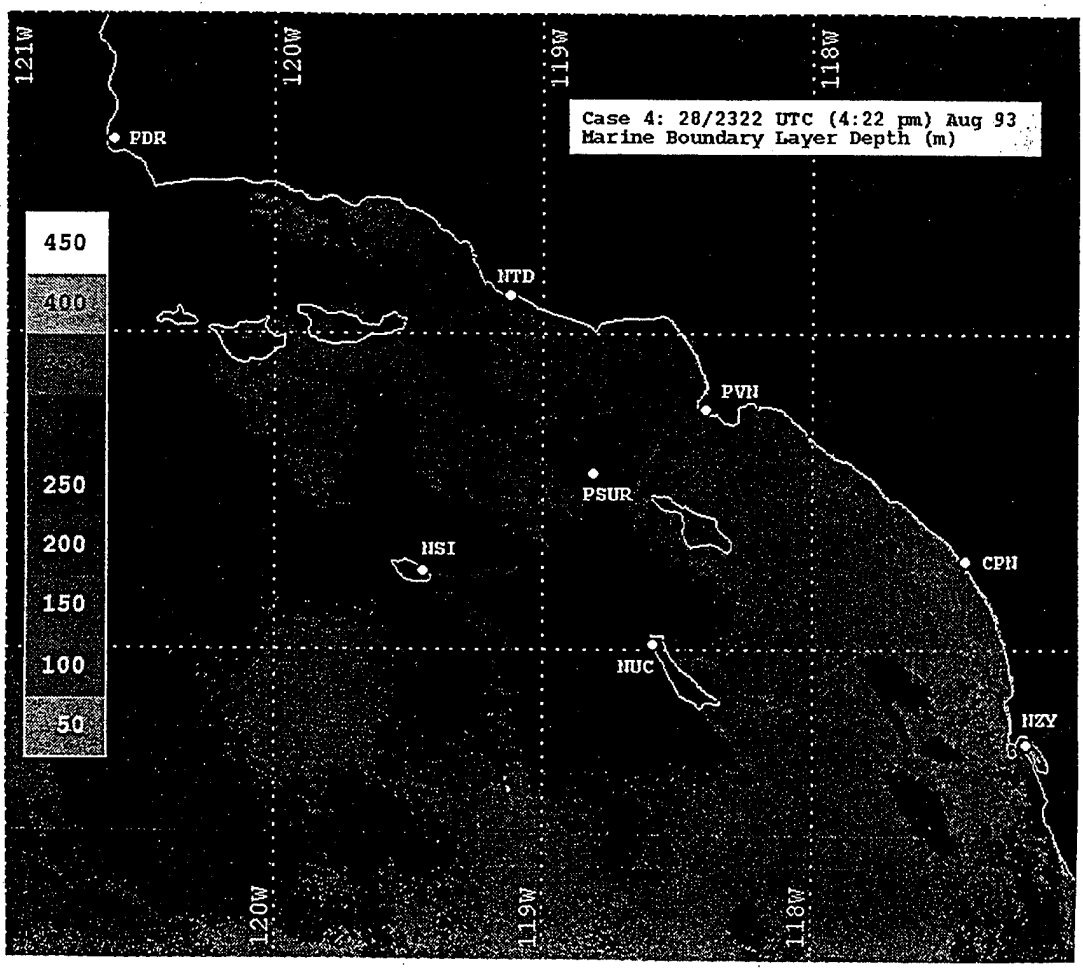
Case 4: 28/2322 UTC (4:22 pm) Aug 93
Marine Boundary Layer Depth (m)
121W
120W
119W
118W
450
400
250
200
150
100
50
PDR
MTD
PVH
PSUR
NSI
CPH
HUC
HZY

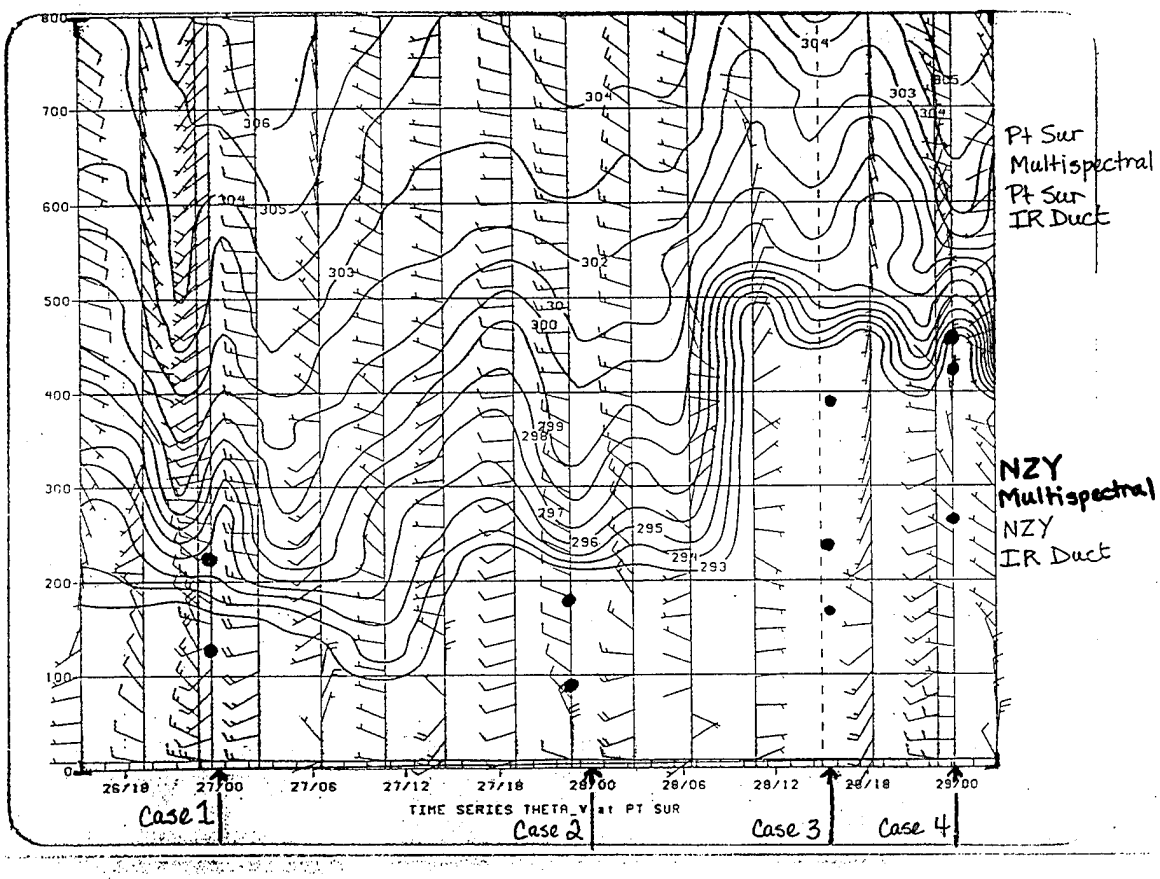

SUMMARY and CONCLUSIONS

- Multi-spectral method to estimate MABL depth was evaluated
- Convergence / Solutions affected by clouds and sun-glint
- IR-Duct technique enables MABL depth estimate in cloud areas
- Multi-spectral method MABL depth estimates in 4 coastal cases were low, approximately 20%

Dr. Ken Davidson, "Shipboard and Satellite Sensing of Refractive Conditions"

DISCUSSION

J. ROSENTHAL

We've been talking about and planning to merge your multi-spectral (clear region) duct assessment technique with our IR-duct (cloudy region) duct assessment technique. We should probably really try to do that now to get an automated approach into TESS.

AUTHOR'S REPLY

This should be started because in only a few cases, when the whole VOCAR region was clear and not sunglint, could we not have to use IR-duct to get the cross-section of MBL depths. Automation will require knowledge of when solutions cannot be obtained even though all requirements are met.

"PERSISTENCE OF REFRACTIVE LAYERING IN ISENTROPIC COORDINATES"

Roger A. Helvey
Naval Air Warfare Center Weapons Division
521 9th Street
Point Mugu, CA 93042-5001
Tel: (805) 989-8383
Fax: (805) 989-4817

Vertical profiles through the atmosphere commonly exhibit irregularities which may be interpreted as temporally or laterally persistent layering, or alternatively as transient features of limited extent associated with mixing processes. It is important to distinguish between these two type of features when establishing refractive structure for application of range-dependent propagation assessments or tracking refractive changes, since only the former should be connected between adjacent profiles. Potential temperature is a quasi-conservative parameter which constitutes a natural vertical coordinate for diagnosing such structures, as in isentropic cross-section analysis. Statistics are presented for a VOCAR data set which show the scale-dependent persistence of refractive features in a potential temperature framework. The purpose is to develop guidance for determining when to connect such features and when to remove them as nonrepresentative.

(PRELIMINARY) PERSISTENCE OF REFRACTIVE LAYERING IN ISENTROPIC COORDINATES

R. Helvey, NAWCWPNS Point Mugu

OBJECTIVE: As an aid to analysis of range-dependent refractive atmospheres, develop empirical guidance for connectivity of layering observed in refractive profiles, and elimination of laterally or temporally limited features.

APPROACH: From radiosonde profiles at various intervals in space and time, determine statistics of layer persistence in an isentropic vertical coordinate system, according to layer strength and thickness, relationship to static stability and other factors.

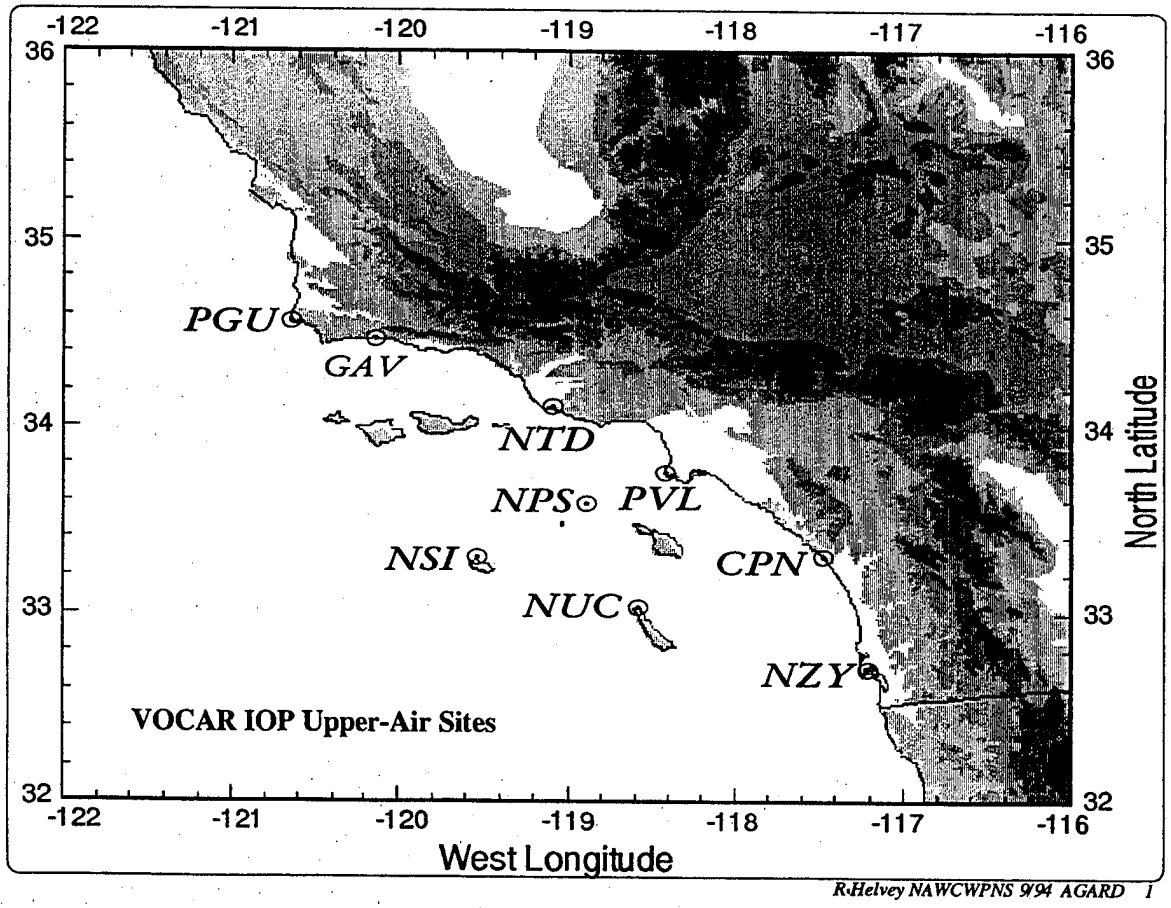

R.Helvey NAWCWPNS 9/94 AGARD 1

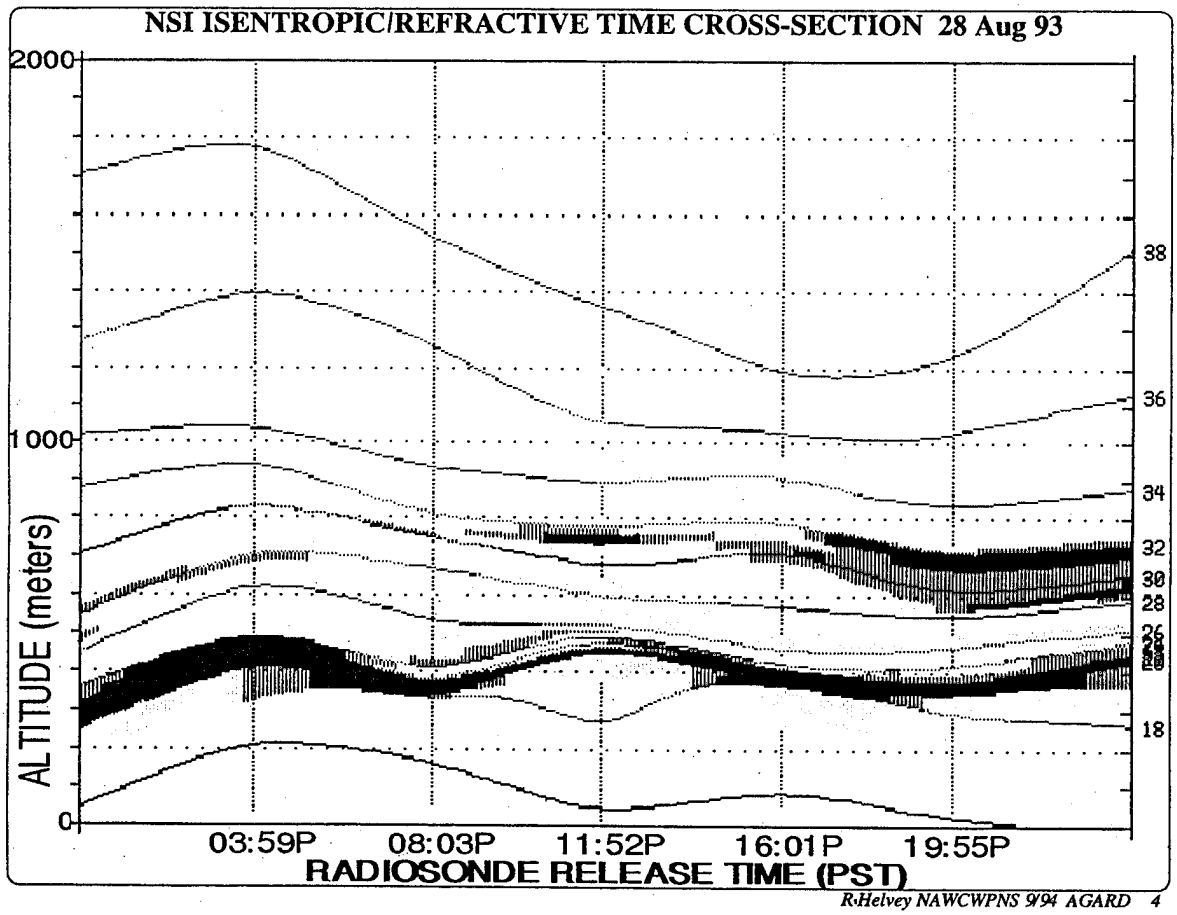

R.Helvey NAWCWPNS 9/94 AGARD 4

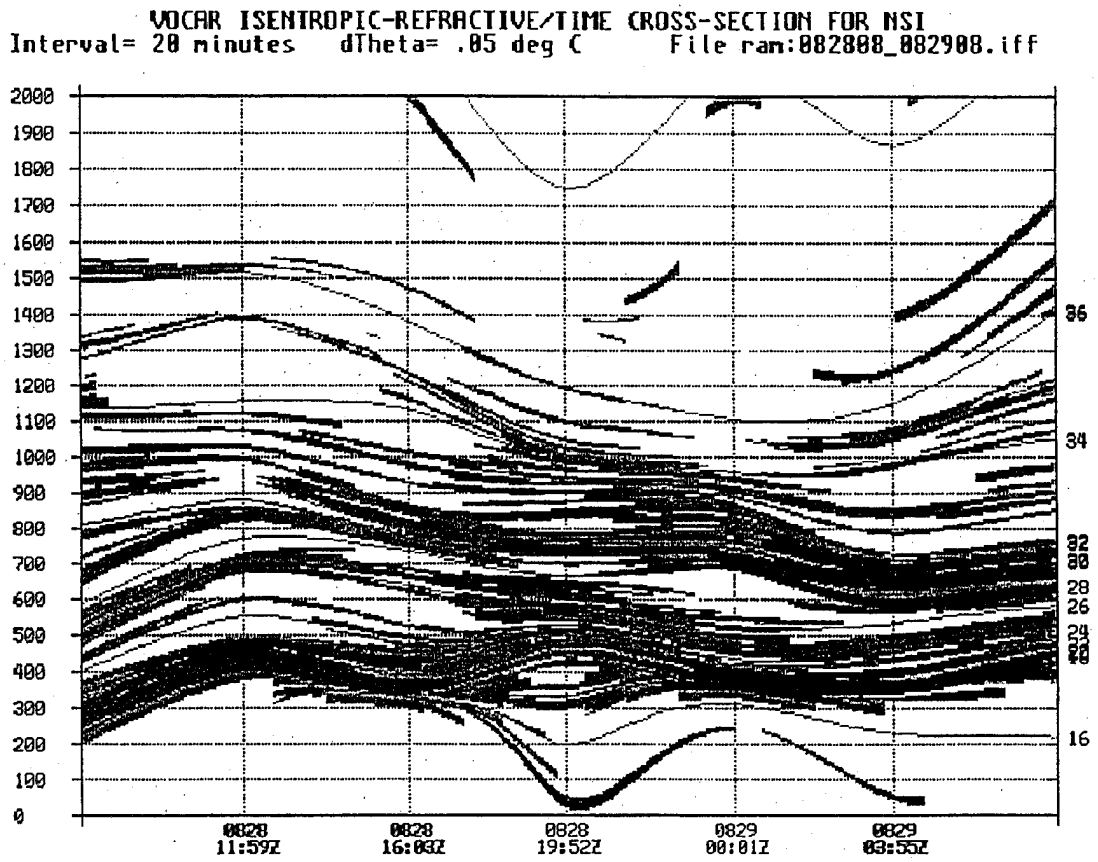

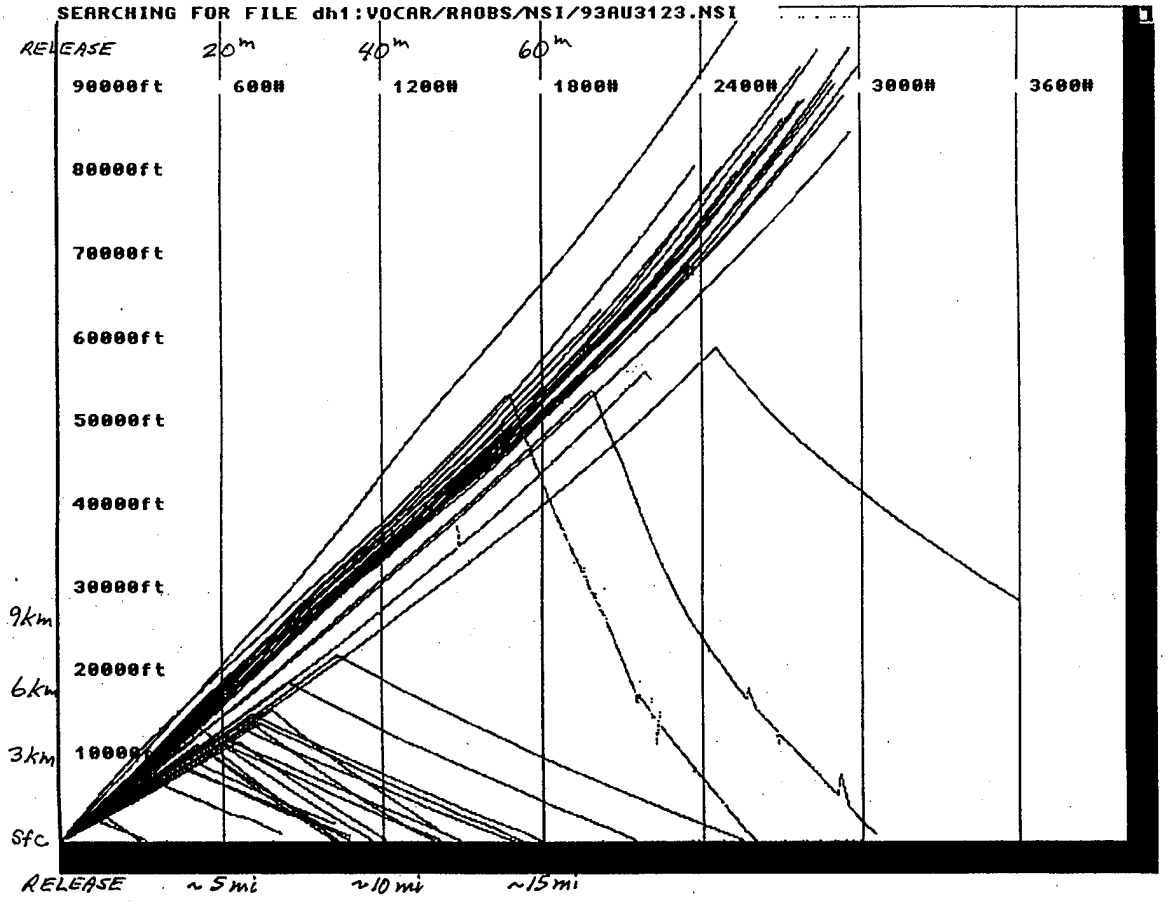
SEARCHING FOR FILE dh1:VOCAR/RAOBS/NSI/93AU3123.NSI
RELEASE
20m
40m
60m
90000ft
600M
1200M
1800M
2400M
3000M
3600M
80000ft
70000ft
60000ft
50000ft
40000ft
30000ft
9km
20000ft
6km
3km
10000
Sfc
RELEASE
~5mi
~10mi
~15mi

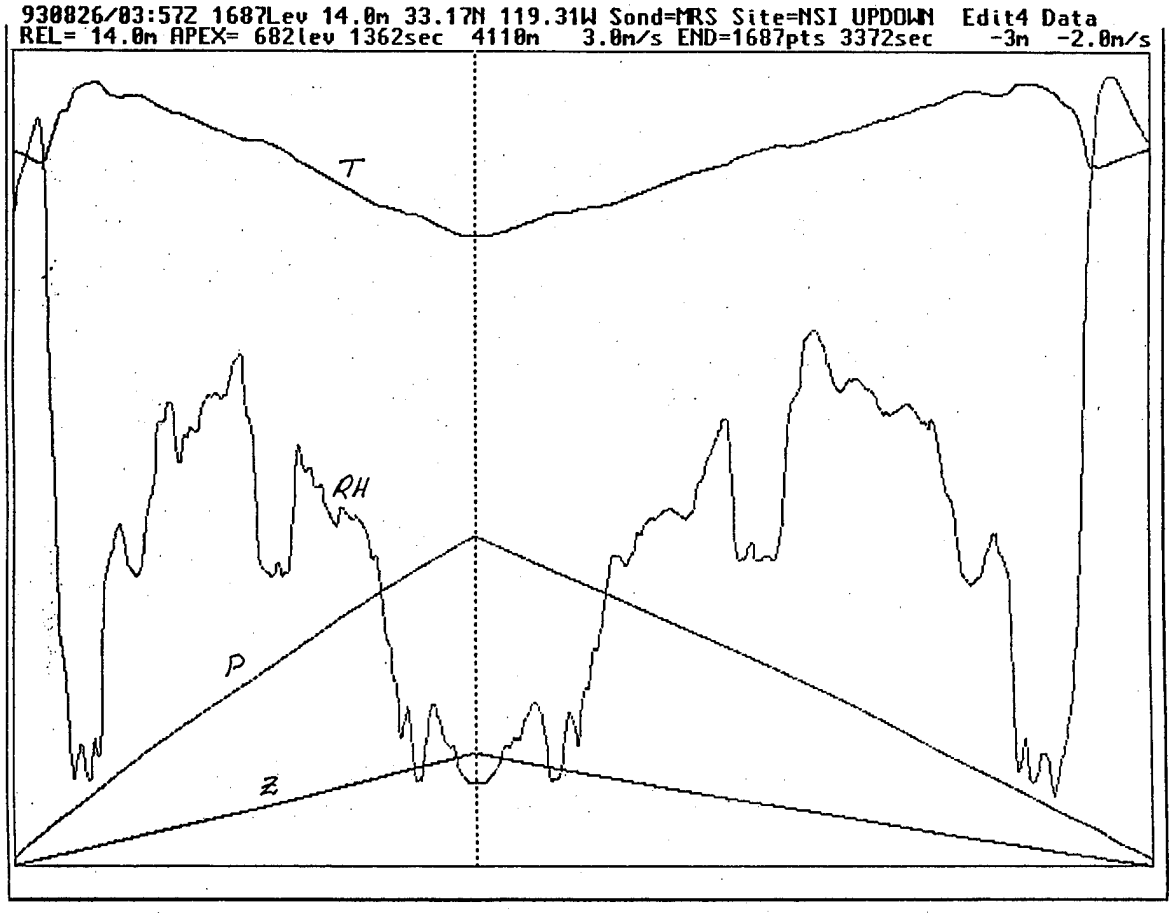
930826/03:57Z 1687Lev 14.0m 33.17N 119.31W Sond=MRS Site=NSI UPDOWN Edit4 Data
REL= 14.0m APEX= 682lev 1362sec 4110m 3.0m/s END=1687pts 3372sec -3m -2.0m/s
T
RH
P
Z

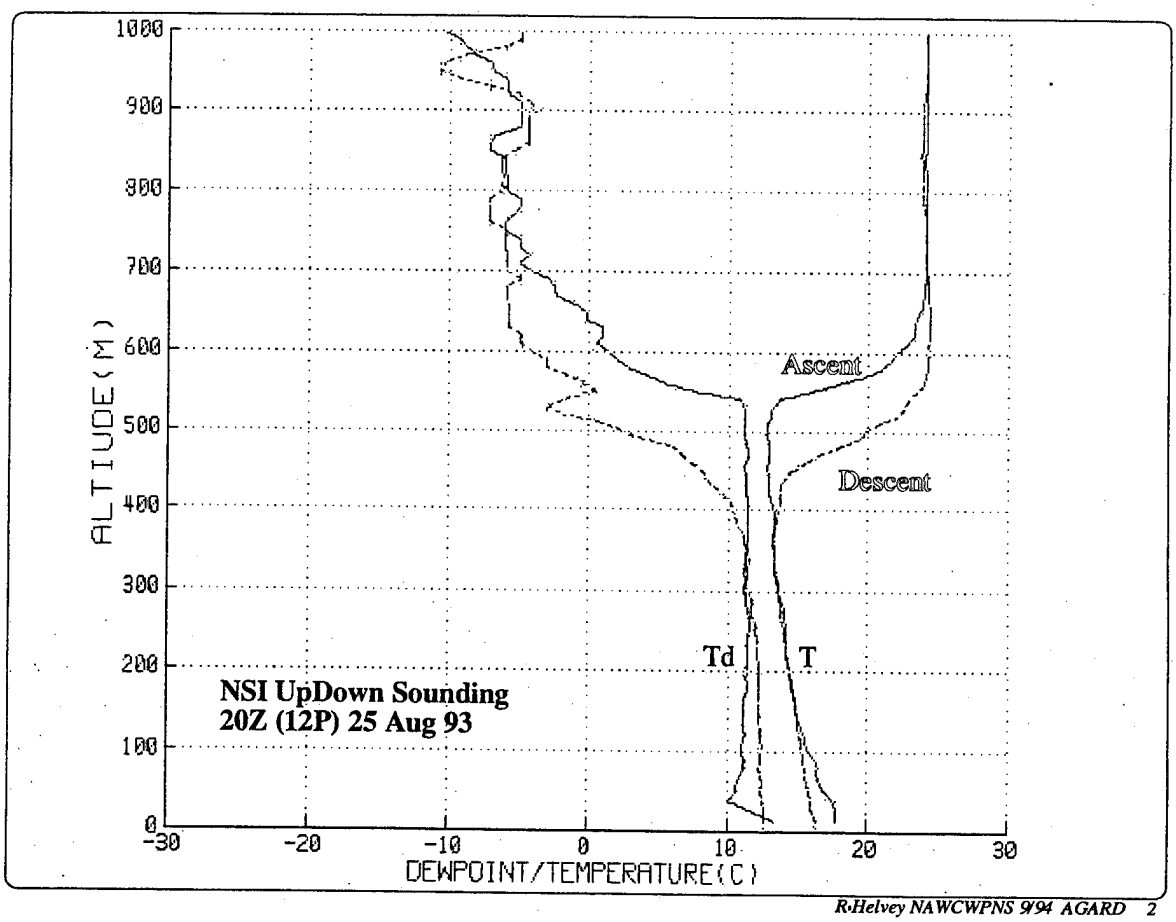

R.Helvey NAWCWPNS 9/94 AGARD 2

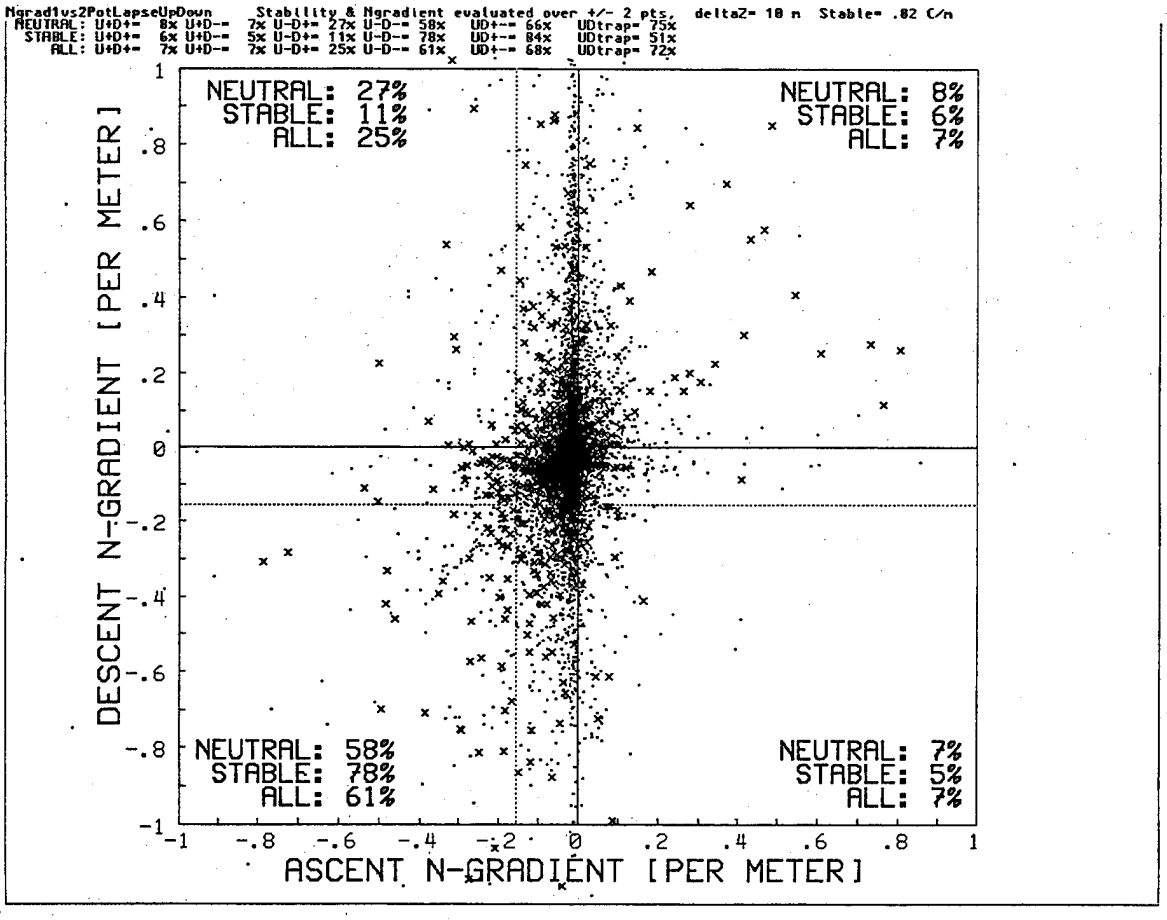

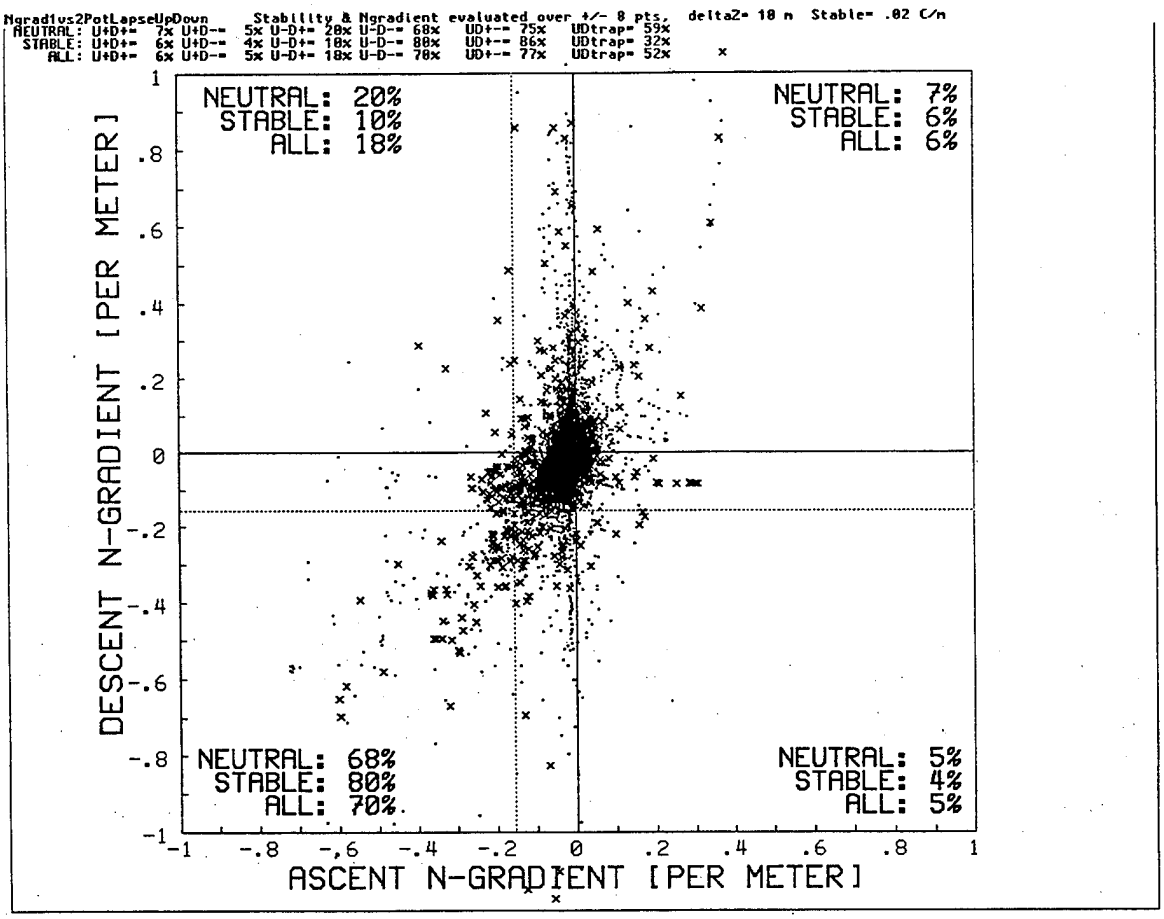
Ngradlvs2PotLapseUpDown Stability & Ngradient evaluated over +/- 8 pts, deltaZ= 10 m Stable= .02 C/m
NEUTRAL: U+D+= 7% U+D-= 5% U-D+= 20% U-D-= 68% UD+-= 75% UDtrap= 59%
STABLE: U+D+= 6% U+D-= 4% U-D+= 10% U-D-= 80% UD+-= 86% UDtrap= 32%
ALL: U+D+= 6% U+D-= 5% U-D+= 18% U-D-= 70% UD+-= 77% UDtrap= 52%
NEUTRAL: 20%
STABLE: 10%
ALL: 18%
NEUTRAL: 7%
STABLE: 6%
ALL: 6%
NEUTRAL: 68%
STABLE: 80%
ALL: 70%
NEUTRAL: 5%
STABLE: 4%
ALL: 5%
DESCENT N-GRADIENT [PER METER]
ASCENT N-GRADIENT [PER METER]

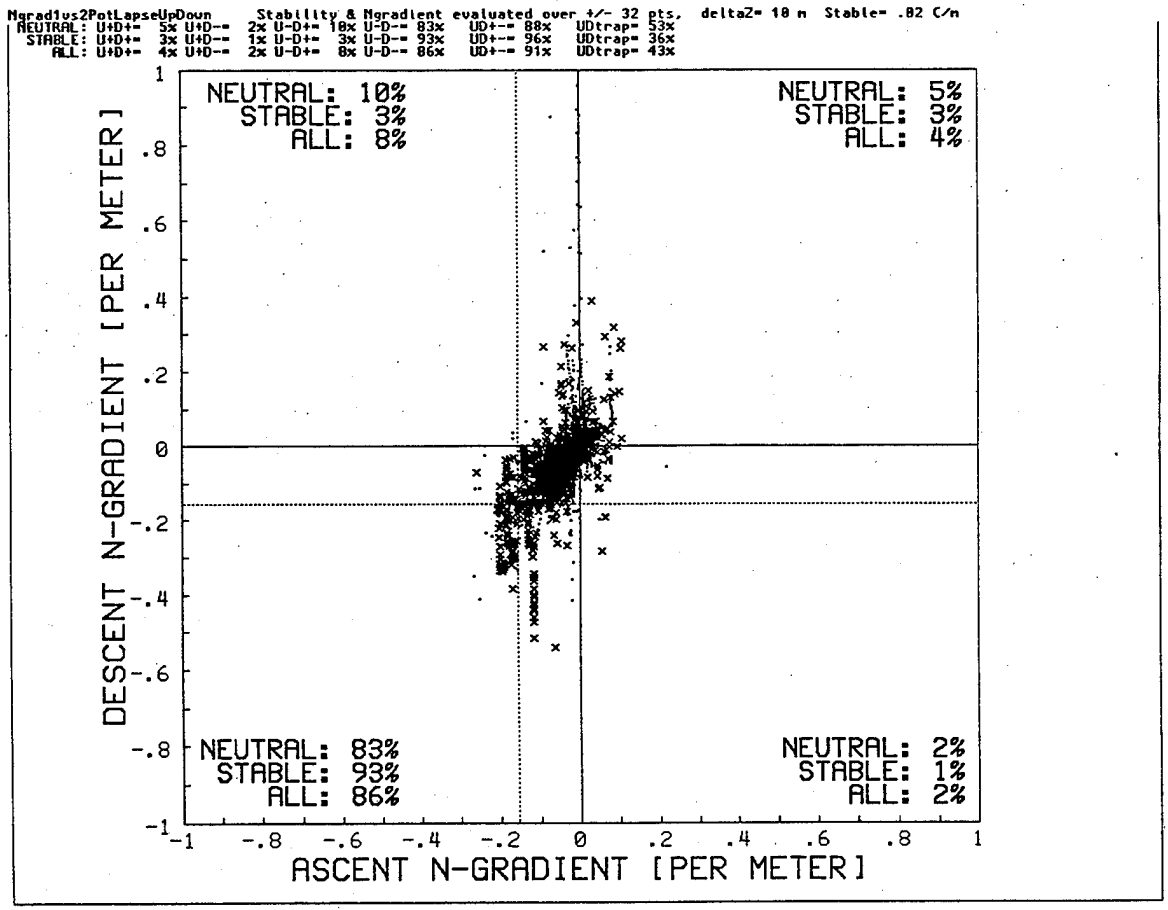
Ngradlvs2PotLapseUpDown Stability & Ngradient evaluated over +/- 32 pts, deltaZ= 10 m Stable= .02 C/m
NEUTRAL: U+D+= 5% U+D-= 2% U-D+= 10% U-D-= 83% UD+-= 88% UDtrap= 53%
STABLE: U+D+= 3% U+D-= 1% U-D+= 3% U-D-= 93% UD+-= 96% UDtrap= 36%
ALL: U+D+= 4% U+D-= 2% U-D+= 8% U-D-= 86% UD+-= 91% UDtrap= 43%
NEUTRAL: 10%
STABLE: 3%
ALL: 8%
NEUTRAL: 5%
STABLE: 3%
ALL: 4%
NEUTRAL: 83%
STABLE: 93%
ALL: 86%
NEUTRAL: 2%
STABLE: 1%
ALL: 2%
DESCENT N-GRADIENT [PER METER]
ASCENT N-GRADIENT [PER METER]

SESSION IV. EM PROPAGATION MODEL DESCRIPTIONS

Chair: Dr K. Craig

Standard EM Propagation Model

Claude P. Hattan

NCCOSC RDTE DIV. CODE 543
49170 PROPAGATION PATH
SAN DIEGO CA 92152-7385

ABSTRACT

The US Navy's standard electromagnetic (EM) propagation model was developed at the Naval Command Control and Ocean Surveillance Center Research, Development, Test and Evaluation Division (NRaD.). The model provides the user with a method of assessing EM propagation in the frequency regime from 100 MHz to 20,000 MHz in the marine environment for a variety of atmospheric conditions. The model is currently incorporated into several assessment systems which provide Naval forces with the ability to predict the effects of the environment on EM sensor performance in near real time. The standard propagation model is a part of the Navy's Oceanographic and Atmospheric Master Library (OAML.). Propagation assessment systems which use the standard model include the Tactical Environmental Support System (TESS); the Geophysical Fleet Mission Planning Library (GFMPL); the Integrated Refractive Effects Prediction System (IREPS); and the Engineers Refractive Effects Prediction System (EREPS), which includes some slight variations of the standard model. Workshop Case's 1, 2, and 3 are examined using the EREPS program to demonstrate the capability of the standard model to produce propagation assessment in non range dependent propagation environments.

US NAVY
STANDARD EM PROPAGATION MODEL
DEVELOPED BY NRaD

A PART OF THE US NAVY
OCEAN & ATMOSPHERIC MASTER LIBRARY

STANDARD EM PROPAGATION MODEL IMPLEMENTIONS:

- **TESS: Tactical Environmental Support System (1983)**
- **EREPS: Engineer's Refractive Effects Prediction System (1988)**
- **IREPS: Integrated Refractive Effects Prediction System (1978)**

US NAVY STANDARD EM PROPAGATION MODEL

- FREQUENCY REGIME: 100 MHz - 20 GHz.
- ACCOUNTS FOR TWO-PATH PROPAGATION, REFRACTION & DIFFRACTION.
- RANGE INDEPENDENT (ASSUMES HORIZONTAL HOMOGENITY - VALID IN OPEN OCEAN 85% OF THE TIME.)

DESIGN GOALS:

- Provide the fleet with a practical way of assessing the effect of the environment on EM sensor performance in near real time.
- Indicate surveillance radar coverage for exploitation by naval aviation attack squadrons in war-at-sea engagements.
- Provide relative EM system performance assessments.
- Usability.
- Minimize computer run time.

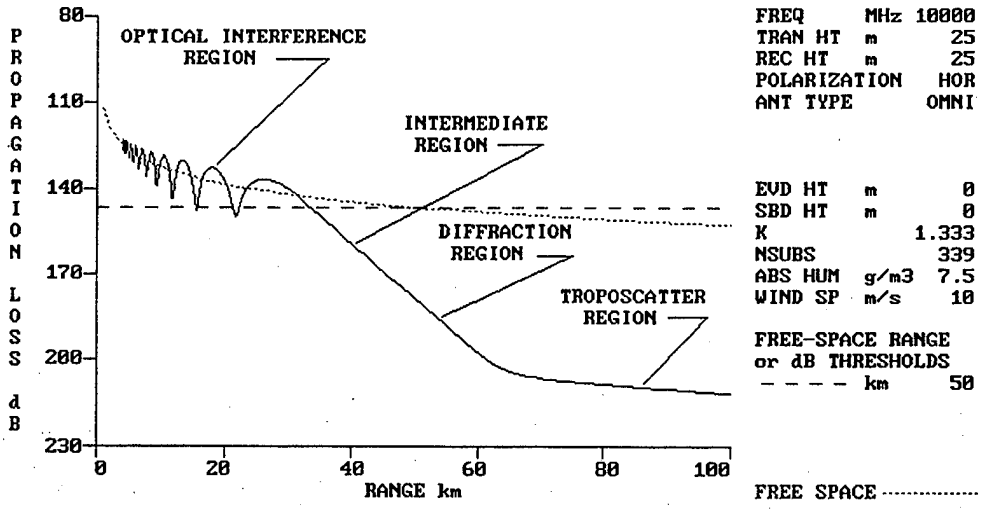

OPTICAL REGION MODELS:

- **Earth flattening - effective earth radius factor.**
- **Two-path propagation (direct and sea-reflected.)**
- **Reflection coefficient as a function of antenna polarization and surface constants.**
- **Surface roughness effects.**
- **Divergence factor.**
- **Antenna patterns: Omnidirectional; Sin(x)/x; Csc^2; Height-finder.**

OPTICAL REGION MODELS
DIFFERENCES:

STANDARD MODEL (TESS / IREPS):

- Blake's curve fits to Kerr's values of dielectric constant and conductivity for salt water.
- Ament-Beard-Barrick surface roughness model.
- Raytrace used to determine both effective earth radius factor and direct-ray position.

EREPS:

- CCIR model for sea water dielectric constants and conductivity.
- CCIR (Miller-Brown) surface roughness model.
- CCIR water vapor absorption model (important only above 10 GHz).
- Gaussian antenna pattern included.
- NRaD-modified Georgia Tech clutter model.
- Optical region shortened for higher evaporation duct heights.

DIFFRACTION REGION MODELS:
TESS / IREPS / EREPS

- NRaD evaporation duct model. A single-mode model based on a curve-fit to wave-guide program results for standard diffraction and evaporation duct propagation.

- NRaD surface-based duct model. A single-mode empirical model for surface-based duct from elevated layers.

- Troposcatter model from Yeh - modified with NBS height-gain corrections.

DIFFRACTION REGION MODEL DIFFERENCES:

EREPS:

- CCIR single-mode diffraction model for non-trapping environments. (Used only when the evaporation duct height input is 0.)

- Skip-zone model for surface-based ducts. Skip zone calculation is made assuming a tri-linear profile for the surface-based duct. The trapping layer is the upper 10% of the specified surface-based duct height with a gradient below the layer equal to the inverse of the effective earth radius factor ($dMdh = .001/a_e$).

INTERMEDIATE REGION MODEL:

TESS / IREPS / EREPS

- Kerr's method of "bold interpolation." (Interpolation on 20 $LOG_{10}(F)$), between the last valid value in the optical region and the first valid value in the diffraction region. (F is the pattern propagation factor.)

STANDARD EM PROPAGATION MODEL - EREPS IMPLEMENTATION

RESULTS FOR WORKSHOP SAMPLE CASES 1 - 3.

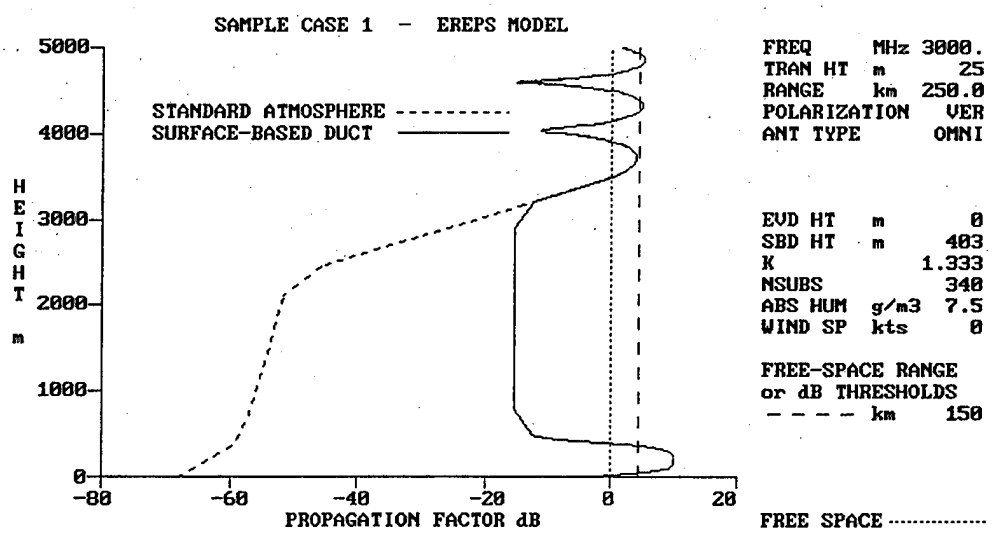

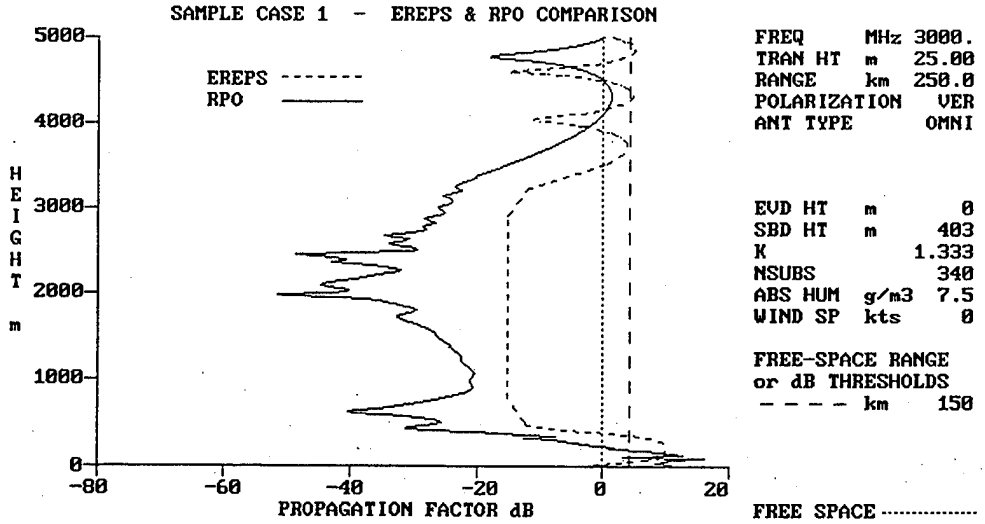
SAMPLE CASE 1 - EREPS & RPO COMPARISON
EREPS
RPO
HEIGHT m
5000
4000
3000
2000
1000
0
-80
-60
-40
-20
0
20
PROPAGATION FACTOR dB
FREQ MHz 3000.
TRAN HT m 25.00
RANGE km 250.0
POLARIZATION VER
ANT TYPE OMNI
EVD HT m 0
SBD HT m 403
K 1.333
NSUBS 340
ABS HUM g/m3 7.5
WIND SP kts 0
FREE-SPACE RANGE
or dB THRESHOLDS
km 150
FREE SPACE

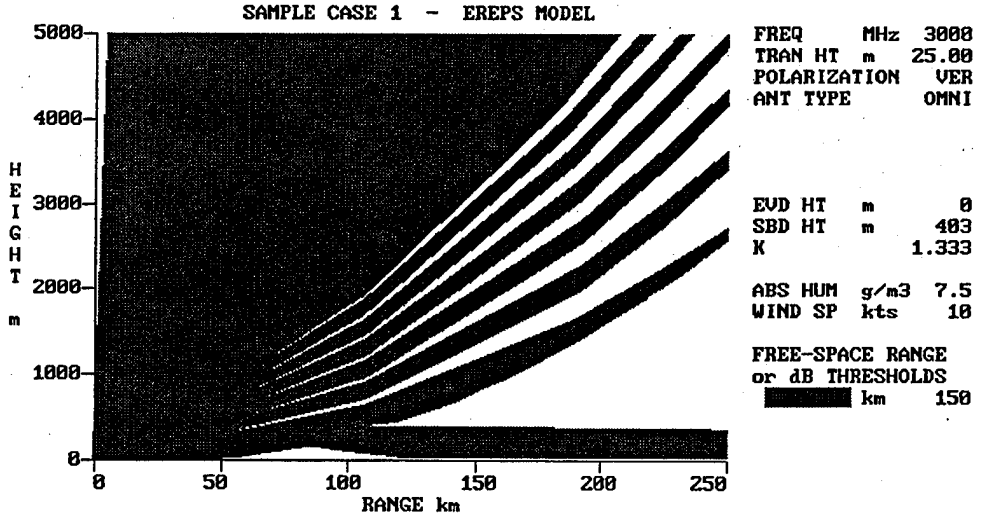
SAMPLE CASE 1 - EREPS MODEL
HEIGHT m
5000
4000
3000
2000
1000
0
0
50
100
150
200
250
RANGE km
FREQ MHz 3000
TRAN HT m 25.00
POLARIZATION VER
ANT TYPE OMNI
EVD HT m 0
SBD HT m 403
K 1.333
ABS HUM g/m3 7.5
WIND SP kts 10
FREE-SPACE RANGE
or dB THRESHOLDS
km 150

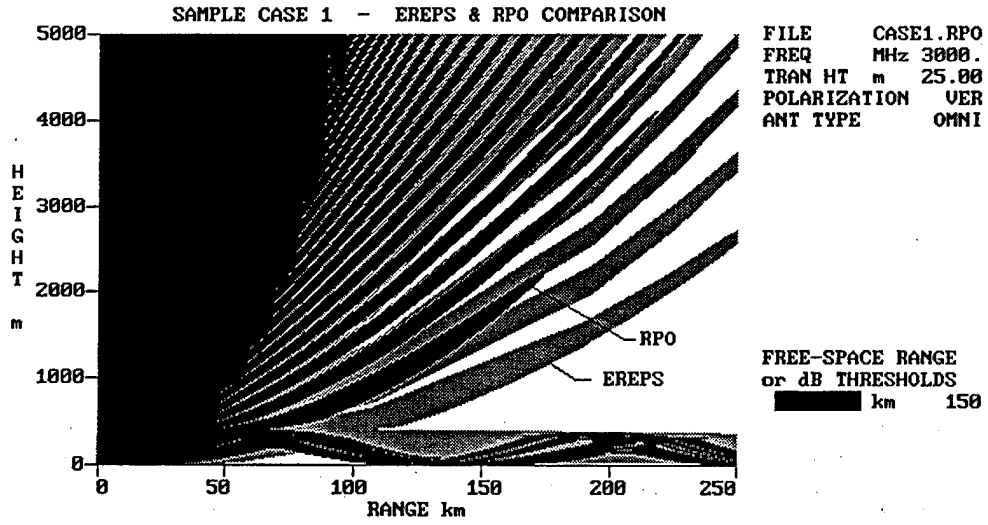
SAMPLE CASE 1 - EREPS & RPO COMPARISON
HEIGHT m
5000
4000
3000
2000
1000
0
0
50
100
150
200
250
RANGE km
RPO
EREPS
FILE CASE1.RPO
FREQ MHz 3000.
TRAN HT m 25.00
POLARIZATION VER
ANT TYPE OMNI
FREE-SPACE RANGE
or dB THRESHOLDS
km 150

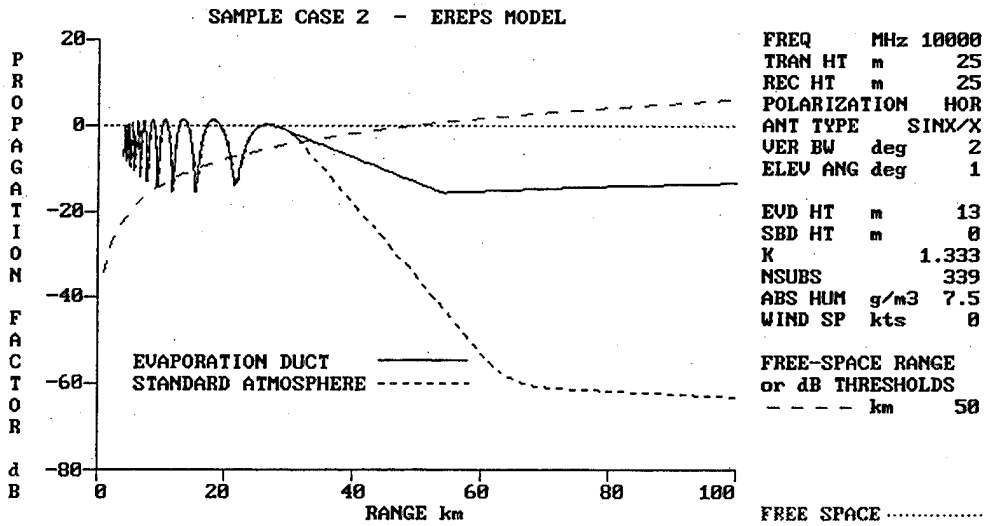
SAMPLE CASE 2 - EREPS MODEL
PROPAGATION FACTOR dB
20
0
-20
-40
-60
-80
0
20
40
60
80
100
RANGE km
EVAPORATION DUCT
STANDARD ATMOSPHERE
FREQ MHz 10000
TRAN HT m 25
REC HT m 25
POLARIZATION HOR
ANT TYPE SINX/X
VER BW deg 2
ELEV ANG deg 1
EVD HT m 13
SBD HT m 0
K 1.333
NSUBS 339
ABS HUM g/m3 7.5
WIND SP kts 0
FREE-SPACE RANGE
or dB THRESHOLDS
km 50
FREE SPACE

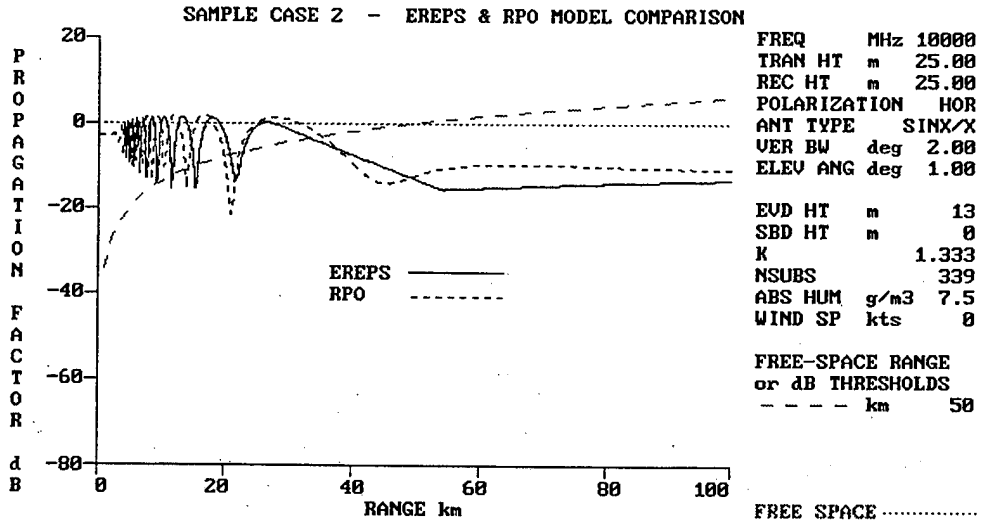
SAMPLE CASE 2 - EREPS & RPO MODEL COMPARISON
PROPAGATION FACTOR dB
20
0
-20
-40
-60
-80
0
20
40
60
80
100
RANGE km
EREPS
RPO
FREQ MHz 10000
TRAN HT m 25.00
REC HT m 25.00
POLARIZATION HOR
ANT TYPE SINX/X
VER BW deg 2.00
ELEV ANG deg 1.00
EVD HT m 13
SBD HT m 0
K 1.333
NSUBS 339
ABS HUM g/m3 7.5
WIND SP kts 0
FREE-SPACE RANGE
or dB THRESHOLDS
km 50
FREE SPACE

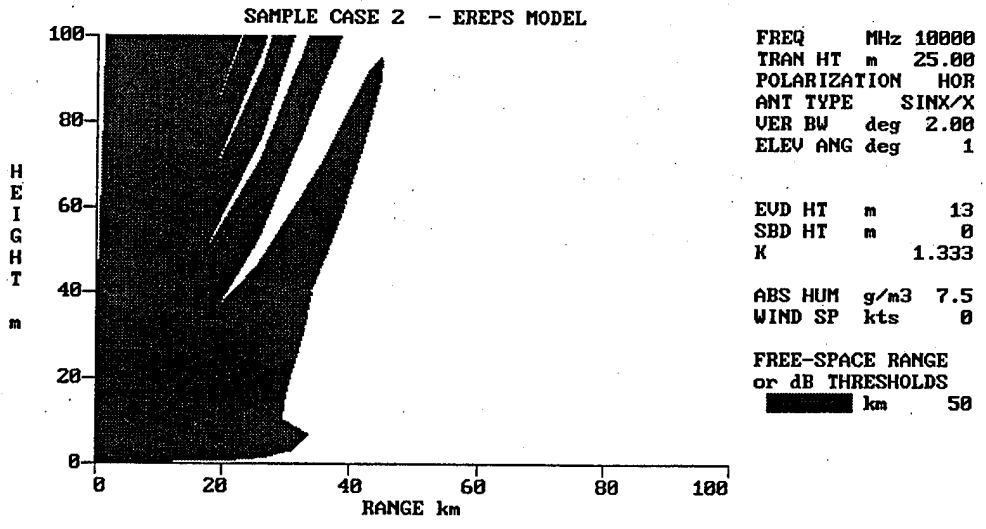
SAMPLE CASE 2 - EREPS MODEL
HEIGHT m
100
80
60
40
20
0
0
20
40
60
80
100
RANGE km
FREQ MHz 10000
TRAN HT m 25.00
POLARIZATION HOR
ANT TYPE SINX/X
VER BW deg 2.00
ELEV ANG deg 1
EVD HT m 13
SBD HT m 0
K 1.333
ABS HUM g/m3 7.5
WIND SP kts 0
FREE-SPACE RANGE
or dB THRESHOLDS
km 50

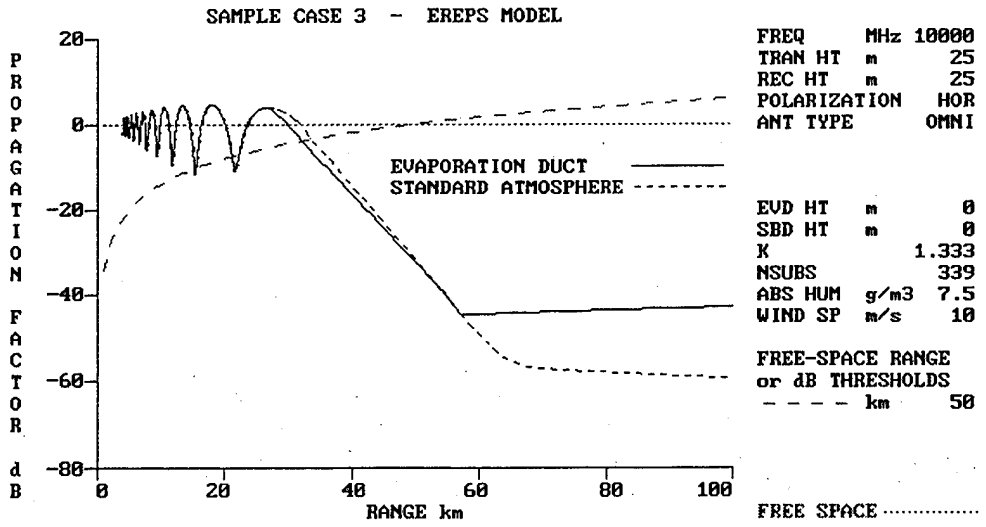
SAMPLE CASE 3 - EREPS MODEL
PROPAGATION FACTOR dB
20
0
-20
-40
-60
-80
0
20
40
60
80
100
RANGE km
EVAPORATION DUCT
STANDARD ATMOSPHERE
FREQ MHz 10000
TRAN HT m 25
REC HT m 25
POLARIZATION HOR
ANT TYPE OMNI
EVD HT m 0
SBD HT m 0
K 1.333
NSUBS 339
ABS HUM g/m3 7.5
WIND SP m/s 10
FREE-SPACE RANGE
or dB THRESHOLDS
- - - - km 50
FREE SPACE

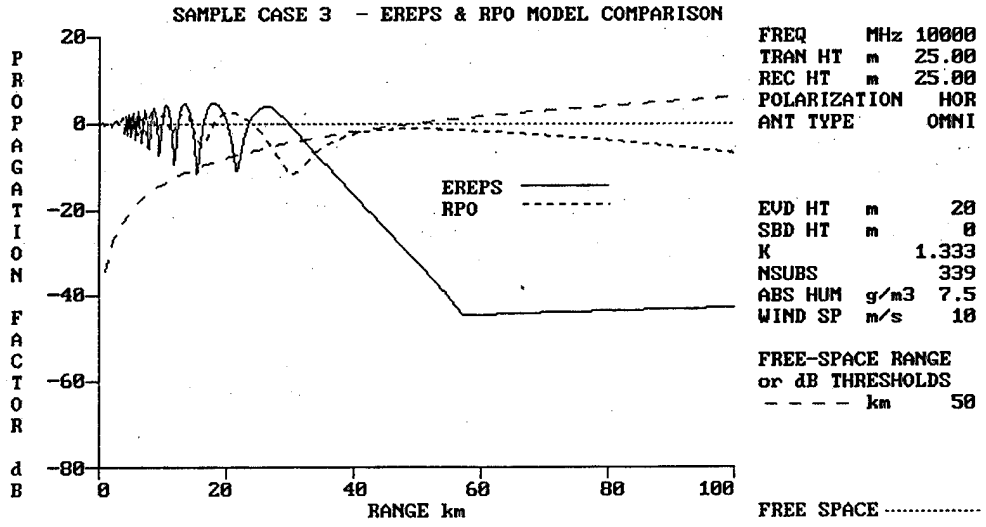
SAMPLE CASE 3 - EREPS & RPO MODEL COMPARISON
PROPAGATION FACTOR dB
20
0
-20
-40
-60
-80
0
20
40
60
80
100
RANGE km
EREPS
RPO
FREQ MHz 10000
TRAN HT m 25.00
REC HT m 25.00
POLARIZATION HOR
ANT TYPE OMNI
EVD HT m 20
SBD HT m 0
K 1.333
NSUBS 339
ABS HUM g/m3 7.5
WIND SP m/s 10
FREE-SPACE RANGE
or dB THRESHOLDS
- - - - km 50
FREE SPACE

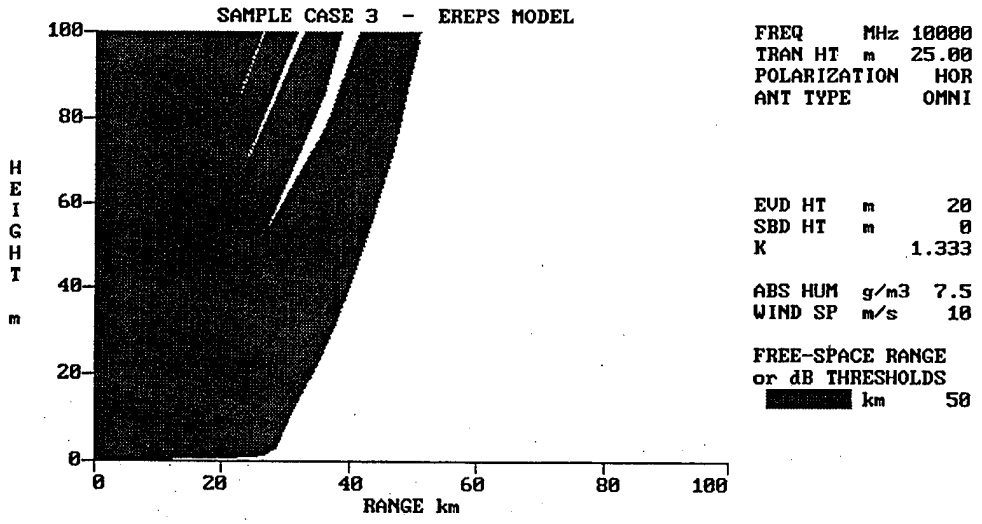

CONCLUSIONS:

- **The Standard EM Propagation Model has been used with a great deal of success for nearly 20 years.**
- **The Standard EM Propagation Model will continue to provide useful assessments for the next few years but should be replaced by a more-capable model.**

MLAYER
A MULTILAYER WAVEGUIDE COMPUTER PROGRAM FOR PROPAGATION ANALYSIS

KENNETH D. ANDERSON
NCCOSC RDT&E DIV 543
49170 PROPAGATION PATH
SAN DIEGO CA 92152-7385

Voice: (619)553-1420, Fax: (619)553-1417, Email: kenn@nosc.mil

The fundamentals of the MLAYER program can be traced back to the mid 1940s [*Booker and Walkinshaw*, 1946]. Later contributions to the numerical evaluation of the wave equation by *Budden* [1961], *Morfitt and Shellman* [1976], *Marcus* [1982], and *Baumgartner* [1983], with extensions to an arbitrary number of refractive layers, have made MLAYER a valuable laboratory tool. It treats both polarization and surface roughness effects in a rigorous manner. In practice, it is limited to range independent refractive conditions. Range dependency has been investigated (*Pappert*, [1989]), but the procedures are cumbersome and time consuming. It is also impractical to calculate the propagation factor at close in ranges because many, perhaps thousands, of modes are required to develop a stable solution. Further, antenna pattern effects are not included as MLAYER assumes an isotropic dipole. Even with all its limitations and faults, MLAYER results can provide an important cross-check for the current generation of propagation models.

References

Baumgartner, G.B., Jr., XWVG: A waveguide program for trilinear ducts, Naval Command, Control and Ocean Surveillance Center, RDT&E Division (NRaD), San Diego, CA, Tech. Doc. 610, June 1983.

Booker, H.G., and W. Walkinshaw, The mode theory of tropospheric refraction and its relation to waveguides and diffraction, in *Meteorological Factors in Radio Wave Propagation.* London: England: The Physical Society, 1946, pp. 80-127.

Budden, K.G., *The Waveguide Mode Theory of Wave Propagation.* London, England: Logos, 1961.

Morfitt, D.G., and C.H. Shellman, MODESRCH: an improved computer program for obtaining ELF/VLF/LF mode constants in an earth atmosphere waveguide, NRaD, San Diego, CA, Interim Rep. 77T, Oct. 1976.

Marcus, S.W., A model to calculate EM fields in tropospheric duct environments at frequencies through SHF, *Radio Science*, vol. 17, pp. 895-901, 1982.

Pappert, R.A., Propagation modeling for some horizontally varying tropospheric ducts, AGARD CP 453, paper 22, May 1989.

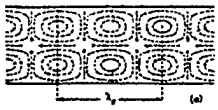

MLAYER

A Multilayer Waveguide Computer Program for Propagation Analysis

Kenneth Anderson
Ocean & Atmospheric Sciences
NCCOSC RDTE DIV 543
San Diego CA 92152

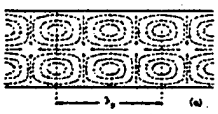

Theory

$$\Pi(r,z) = \frac{1}{4\pi}\int_C \rho\, d\rho\, H_0^{(2)}(r\rho)\,\tilde{\Pi}(\rho,z)$$

$$\left\{\frac{d^2}{dz^2} + k^2\left[m_j^2(z) - \frac{\rho^2}{k^2}\right]\right\}\tilde{\Pi}_j(\rho,z) = -p\,\delta(z - z_t)$$

$$\left\{\frac{d^2}{dz^2} + k^2\left[n_g^2 - \frac{\rho^2}{k^2}\right]\right\}\tilde{\Pi}_g(\rho,z) = 0$$

$$m_j^2(z) \cong 1 + 2\times 10^{-6} M_j(z) + i\eta$$

$$n_g^2 = \varepsilon_g - i\frac{\sigma_g}{\varepsilon_0\omega}$$

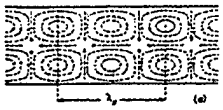

Stokes' Equation

$$q_j(z) = \left(\frac{k}{\left| 2 \times 10^{-6} \frac{dM_j}{dz} \right|} \right)^{2/3} \left[m_j^2(z) - \left(\frac{\rho}{k} \right)^2 \right]$$

$$\left\{ \frac{d^2}{dq_j^2} + q_j \right\} \tilde{\Pi}_j(\rho, q_j) = 0$$

$$\tilde{\Pi}_j(\rho, q_j) = A_j(\rho) f_j(q_j) + B_j(\rho) g_j(q_j)$$

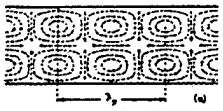

MLAYER References

- S.W. Marcus, A Model to Calculate EM Fields in Tropospheric Duct Environments at Frequencies through SHF, *Radio Sci.*, vol. 17, pp. 895-901, 1982
- G.B. Baumgartner, Jr., XWVG: A Waveguide Program for Trilinear Tropospheric Ducts, NOSC TD 610, June 1983
- R. Pappert, Field Strength and Path Loss in a Multilayer Tropospheric Waveguide Environment, NOSC TN 1366, October 1984

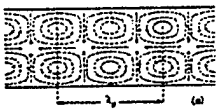

Mlayer & RPO Comparisons

Tropospheric EM Propagation Workshop
3 GHz, HH, 10 m EVD, 0 m/s, Zt=25, Zr=5

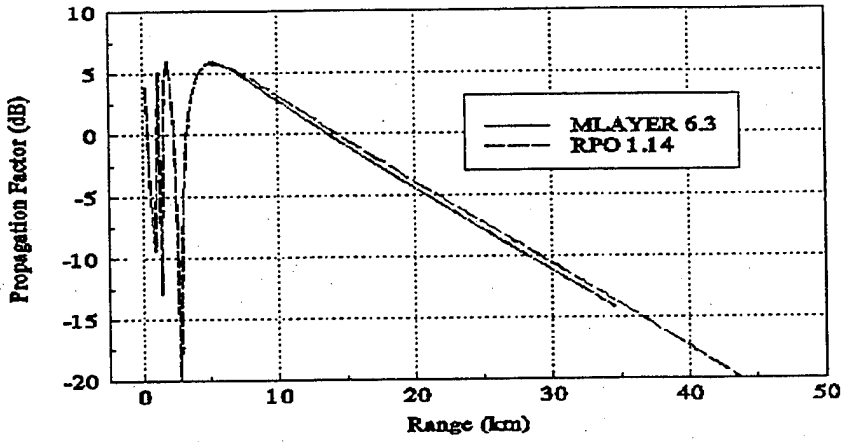

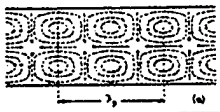

Mlayer & RPO Comparisons

Tropospheric EM Propagation Workshop
10 GHz, HH, 10 m EVD, 0 m/s, Zt=25, Zr=5

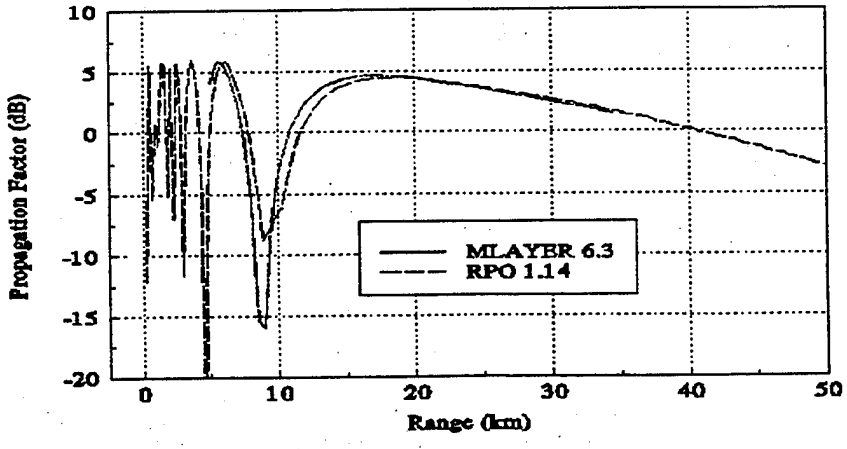

Case 1 Comparisons

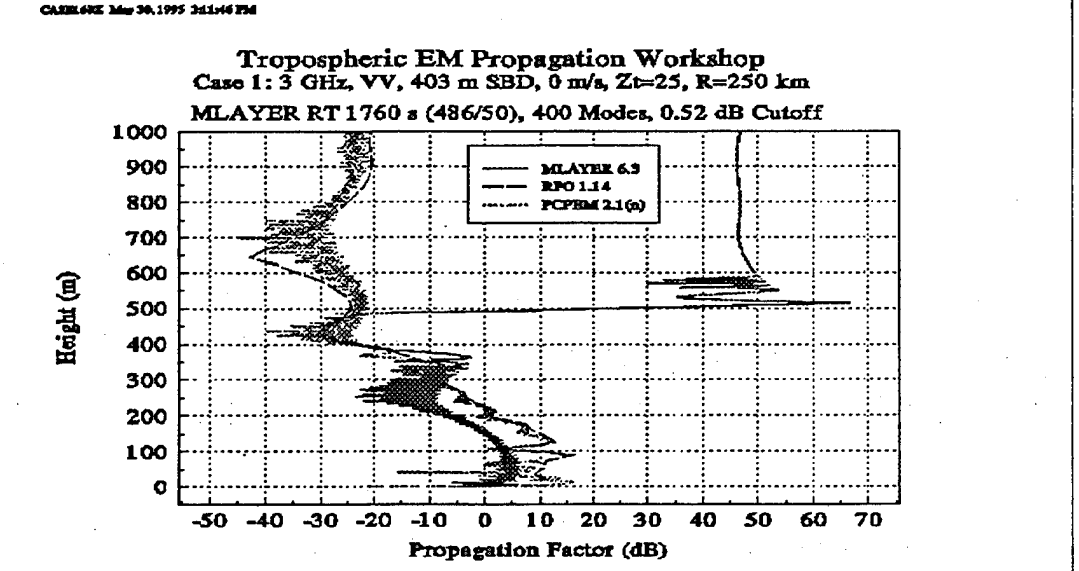

Case 3 Comparisons

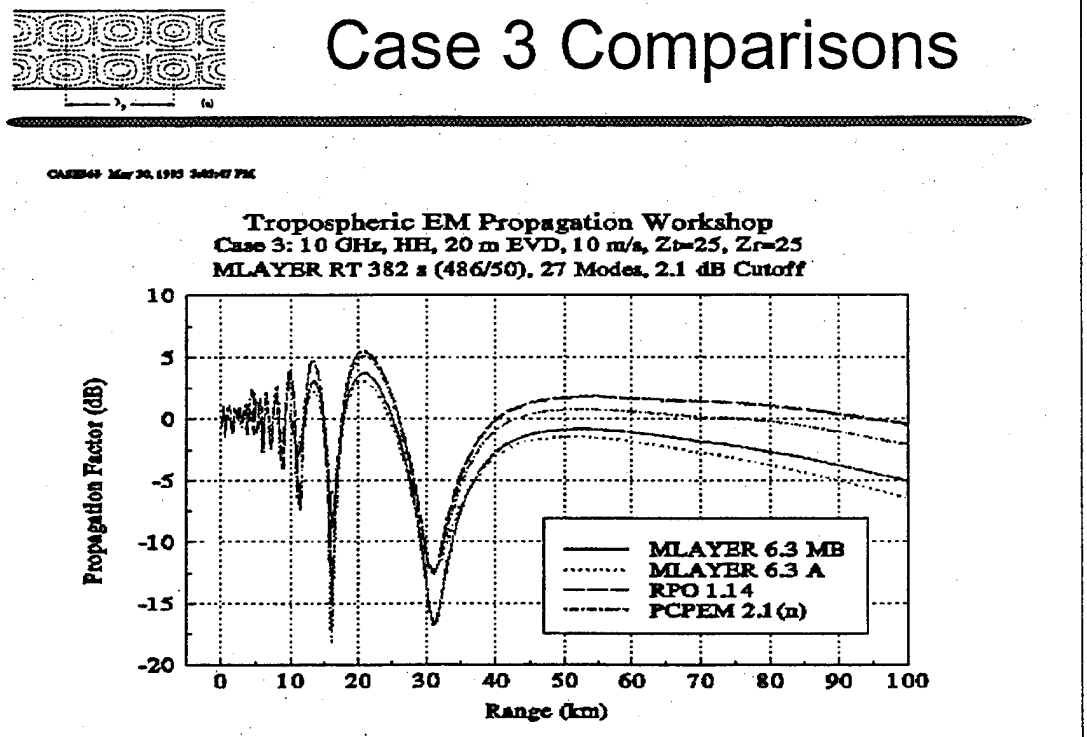

Smooth Surface Case 3

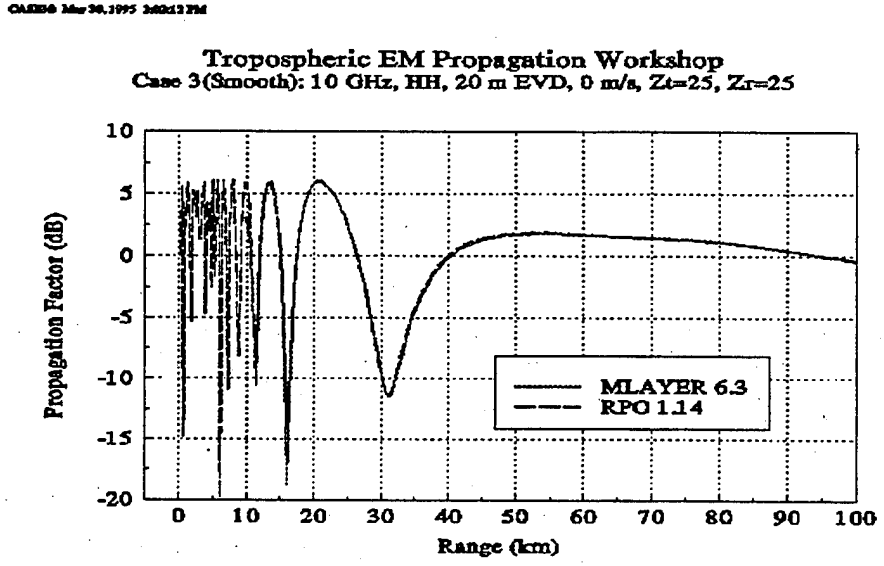

Comments

- Propagation analysis using waveguide methods needs considerable skill to interpret results
- Waveguide methods are applicable for
  - Horizontally homogeneous conditions
  - Ranges near and beyond the horizon
  - Smooth and rough sea surface

Mr. Kenn Anderson, "MLAYER, A Multilayer Waveguide Computer Program for Propagation Analysis"

DISCUSSION

S. MARCUS

Do you have reason to believe that the use of the Ament-Beard-Barrick correction to the reflection coefficient to account for rough earth scattering is valid for duct propagation? Have you used RPO to simulate roughness directly?

AUTHOR'S REPLY

The Ament-Beard-Barrick correction decreases signal intensity as the wind speed or roughness increases, which is consistent with the few measurements that are available. However, I believe that additional measurements should be taken to correctly answer your question. A PE model has been compared to MLAYER results for backscatter and the agreement is good (Pappert, Paulus, Tappert, *Radio Science, 27*(2), 1992) and I believe that if the backscatter results are good so are the forward scatter results.

DESCRIPTION OF THE TROPOSPHERIC ELECTROMAGNETIC PARABOLIC EQUATION ROUTINE (TEMPER)

G. Daniel Dockery
Johns Hopkins University Applied Physics Laboratory
Johns Hopkins Road
Laurel, MD 20723 (301)953-5461 (Dockery)
G_D_Dockery@aplmail.jhuapl.edu

The TEMPER propagation model is based on the Fourier split-step solution to the parabolic wave equation. In addition to frequency, polarization, etc., TEMPER inputs include surface electrical properties, surface roughness, terrain profiles, antenna pattern specification, and general refractivity characteristics. The features, capabilities, and limitations of TEMPER are described and illustrative examples presented in this paper.

GENERAL DESCRIPTION OF THE TROPOSPHERIC ELECTROMAGNETIC PARABOLIC EQUATION ROUTINE (TEMPER)

G. DANIEL DOCKERY

THE JOHNS HOPKINS UNIVERSITY APPLIED PHYSICS LABORATORY
LAUREL, MARYLAND

GENERAL DESCRIPTION

FOURIER SPLIT-STEP SOLUTION TO THE WIDE ANGLE PARABOLIC EQUATION (WPE)

IMPEDANCE SURFACE BOUNDARY CONDITION (GROUND ELECTRICAL PARAMETERS, SURFACE ROUGHNESS)

FEATURES/INPUTS:

- FREQUENCY, POLARIZATION
- ANTENNA HEIGHT AND POINTING DIRECTION
- ANTENNA PATTERN OPTIONS: BUILT-IN SINC, USER-SPECIFIED SYMMETRIC & ANTISYMMETRIC PATTERNS
- SURFACE ELECTRICAL PARAMETERS: CONDUCTIVITY & PERMITTIVITY (BUILT-IN OPTION FOR SEA WATER)
- SURFACE ROUGHNESS (MILLER-BROWN MODEL)
- VOLUME ABSORPTION (SINGLE COEFFICIENT OR SINGLE VERTICAL PROFILE OF COEFFICIENTS)
- TERRAIN PROFILE ("SIMPLE MASKING" METHOD)
- ARBITRARY REFRACTIVITY VARIATIONS IN RANGE & ALTITUDE

ALGORITHMS

SPLIT-STEP ALGORITHM: DISCRETE VERSION OF MIXED-FOURIER TRANSFORM USING ONLY SINE TRANSFORMS AND RECURSIVE ODE SOLUTION

SOURCE FUNCTION (INITIAL SOLUTION): USES FOURIER RELATIONSHIP BETWEEN FAR-FIELD PATTERN & APERTURE FIELD TO SYNTHESIZE INITIAL SOLUTION FROM DESIRED PATTERN. FOURIER SHIFT THEOREM USED TO IMPLEMENT ANTENNA HEIGHT AND POINTING DIRECTION.

SURFACE ROUGHNESS: IMPEDANCE MODIFICATION BASED ON MILLER-BROWN FORMULA FOR REFLECTION FROM GAUSSIAN ROUGH SURFACES. GRAZING ANGLES REQUIRED FOR THIS CALCULATION EITHER PROVIDED BY USER OR ESTIMATED WITHIN TEMPER USING SPECTRAL ESTIMATION. DON BARRICK'S ROUGH SURFACE IMPEDANCE MODEL USED FOR HF/VHF FREQUENCIES.

NUMERICAL UPPER BOUNDARY: SIMPLE FILTER FUNCTION USED TO SMOOTHLY TRUNCATE FIELD IN BOTH ALTITUDE AND FREQUENCY SPACES.

TERRAIN: CURRENTLY NULLING FIELD BELOW LAND ELEVATION AT EACH RANGE STEP (SIMPLE MASKING). EVALUATING MORE SOPHISTICATED METHODS.

PARAMETER LIMITS

[1]FREQUENCY: 1 MHz - 20 GHz (NO IONOSPHERIC EFFECTS)

[2]MAXIMUM RANGE: 1000 KM

[2]MAXIMUM ALTITUDE: 30 KM (FREQUENCY DEPENDENT)

[2]ANTENNA ALTITUDE: 0 - 15 KM (FREQUENCY DEPENDENT)

[3]REFRACTIVITY PROFILES: 500 POINTS PER VERTICAL PROFILE

NOTES

[1] NOT FUNDAMENTAL LIMIT. REPRESENTS "VALIDATED" FREQUENCIES.
[2] LIMITED BY "EARTH-FLATTENING" APPROXIMATION AND COMPUTATION TIME.
[3] ARBITRARY ARRAY SIZE LIMIT.

PARABOLIC WAVE EQUATION

THE WIDE-ANGLE PARABOLIC WAVE EQUATION THAT IS SOLVED IN TEMPER IS

$$\partial_x u - i\sqrt{k^2+\partial_z^2}\, u - ik(m-2)u = 0$$

WHERE

$$where \quad m^2 \equiv n^2 + \frac{2z}{a_e}$$

AND n IS THE USUAL REFRACTIVE INDEX. k IS THE FREESPACE WAVENUMBER.

FOR VERTICAL ELECTRIC POLARIZATION, u(x,z) IS RELATED TO THE TANGENTIAL H FIELD ACCORDING TO

$$H_y(x,z) \approx \frac{n}{\sqrt{x}}\, u(x,z)\, e^{ikz}$$

WHERE x IS THE DISTANCE ALONG THE EARTH'S SURFACE (GROUND RANGE) AND z IS THE DISTANCE ABOVE THE GROUND (ALTITUDE).

IMPEDANCE BOUNDARY CONDITION

THE BOUNDARY CONDITION AT THE SURFACE IS (VERTICAL POLARIZATION)

$$\partial_z H_y|_{z=0} + \alpha H_y(z=0) = 0$$

WHICH IN TERMS OF u BECOMES (APPROXIMATELY)

$$\partial_z u|_{z=0} + \left[\frac{1}{n}\partial_z n + \alpha\right] u(z=0) = 0$$

α IS RELATED TO THE SURFACE IMPEDANCE, η, ACCORDING TO

$$\alpha_v = -i\omega\epsilon_s\eta_v$$

$$\alpha_h = \frac{i}{\mu_0\omega}\eta_h$$

FOR VERTICAL & HORIZONTAL POLARIZATIONS, RESPECTIVELY.

TEMPER ALSO ALLOWS THE OPTION TO ASSUME PERFECT CONDUCTIVITY.

ROUGH SURFACE IMPEDANCE MODELS

- MODIFICATION OF SURFACE IMPEDANCE TO ACCOUNT FOR CERTAIN ROUGH SURFACE EFFECTS
  - ABOVE 100 MHz: MODIFICATION OF FRESNEL REFLECTION COEFFICIENT
  - BELOW 100 MHz: USE BARRICK'S IMPEDANCE FORMULA (BASED ON PERTURBATION TECHNIQUE)

REFLECTION COEFFICIENT MODIFICATION

- REDUCES MAGNITUDE OF COHERENT REFLECTION (DOES NOT ADDRESS DIFFUSE SCATTERING)
- ASSUMED MODEL (MILLER & BROWN, 1984):

$$R_r = R_s \exp(-\xi)\ J_o(i\xi)$$

WHERE R_s IS THE SMOOTH SEA FRESNEL REFLECTION COEFFICIENT, J_o IS THE ZERO-ORDER BESSEL FUNCTION, AND

$$\xi = 8\left(\frac{\pi h}{\lambda}\sin\theta\right)^2$$

h IS THE RMS SURFACE HEIGHT AND θ IS THE GRAZING ANGLE MEASURED FROM THE LOCAL SURFACE TANGENT. ALGEBRAIC APPROXIMATIONS OF THE BESSEL FUNCTION ARE OFTEN USED TO SIMPLIFY COMPUTATIONS.

ROUGH SURFACE IMPEDANCE - CONT

THE MODIFIED REFLECTION COEFFICIENT IS USED IN THE FOLLOWING FORMULA TO ADJUST α:

$$\alpha_r = ik \sin\theta \left[\frac{1-R_r}{1+R_r}\right]$$

WHEN SMOOTH SURFACE COEFFICIENTS ARE USED, α IS INDEPENDENT OF θ (LEONTOVICH BOUNDARY CONDITION) FOR MOST TYPES OF SURFACES. HOWEVER, THE ABOVE ALGORITHM RESULTS IN α BEING STRONGLY ANGLE DEPENDENT - THUS, GRAZING ANGLE ESTIMATES ARE REQUIRED.

THREE METHODS OF OBTAINING GRAZING ANGLE ESTIMATES:

- CALCULATE FROM GEOMETRY (SIMPLE REFRACTIVE CONDITIONS)
- CALCULATE USING GEOMETRIC OPTICS (USUAL RAY TRACING DRAWBACKS)
- ESTIMATE USING SPECTRAL ESTIMATOR IN PE PROGRAM (ALSO HAS DRAWBACKS)

OFTEN PRACTICAL TO USE COMBINATION OF ABOVE METHODS

PERFORMANCE OF MFT SOLUTION

- YIELDS EXCELLENT PERFORMANCE FOR MOST VALUES OF α
- GOOD AGREEMENT WITH HF SURFACE WAVE MODELS
- USED SUCCESSFULLY FOR ROUGH SEA CALCULATIONS FOR WINDSPEEDS OF 10 M/S & SMALLER
- NUMERICAL PROBLEMS ENCOUNTERED WHEN $|\mathrm{Re}(\alpha)| \approx 0$ AND $\mathrm{Im}(\alpha) < p_{max}$.
- ADDITIONAL PROBLEMS FOR SMALL α AND VERY SMALL RANGE STEPS
- FACTOR OF 2 INCREASE IN COMPUTATION TIME OVER PERFECT-CONDUCTING HALF-SPACE CALCULATIONS
- DISCRETE VERSION OF MFT PURSUED TO SOLVE NUMERICAL PROBLEMS & DECREASE COMPUTATION TIME

COMPARISON OF USER-SPECIFIED DEFOCUSED PATTERN AND TEMPER-GENERATED PATTERN

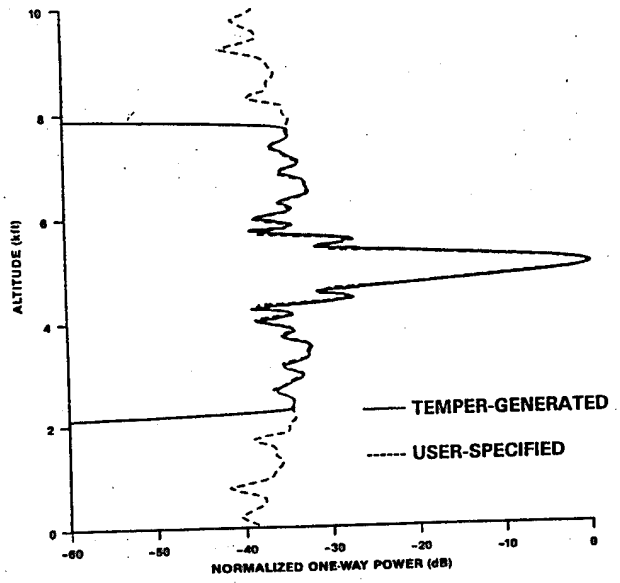

GRAZING ANGLE ESTIMATION

45 m SURFACE DUCT, 10 GHz, 23 m ANTENNA

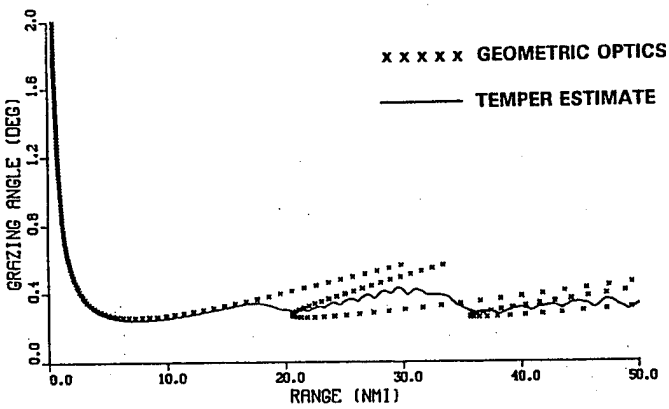

COMPARISON WITH NRaD WAVEGUIDE MODEL (MLAYER)

10 GHz, 23 m ANTENNA, 23 m ALTITUDE

0.76 m RMS WAVEHEIGHT, 45 m BILINEAR SURFACE DUCT

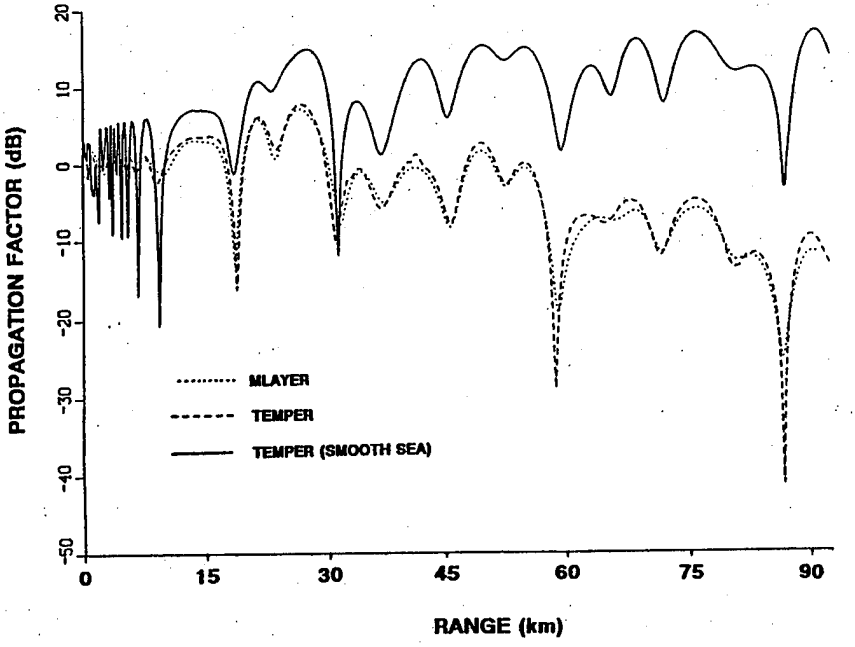

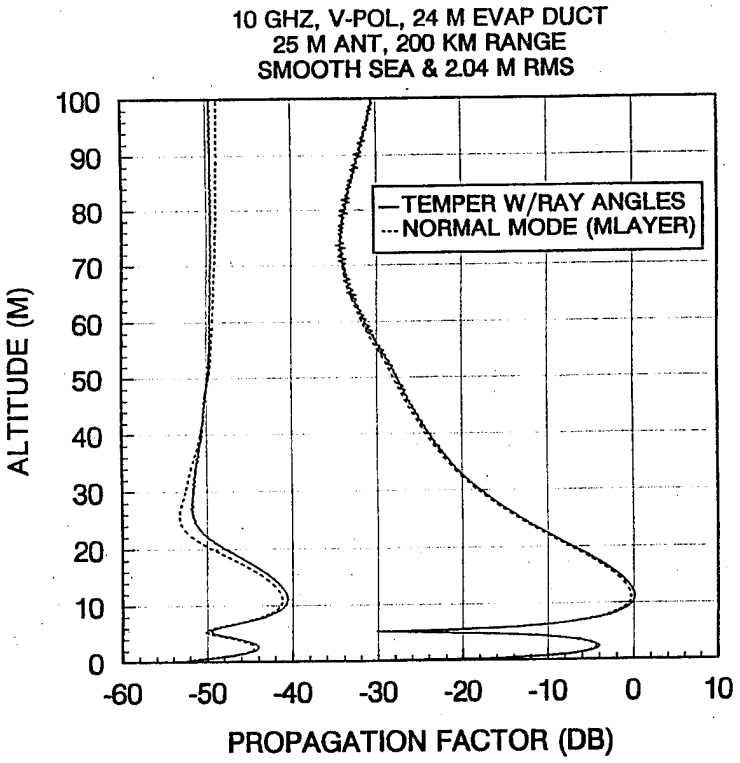
10 GHZ, V-POL, 24 M EVAP DUCT
25 M ANT, 200 KM RANGE
SMOOTH SEA & 2.04 M RMS
—TEMPER W/RAY ANGLES
---NORMAL MODE (MLAYER)
ALTITUDE (M)
100
90
80
70
60
50
40
30
20
10
0
-60
-50
-40
-30
-20
-10
0
10
PROPAGATION FACTOR (DB)

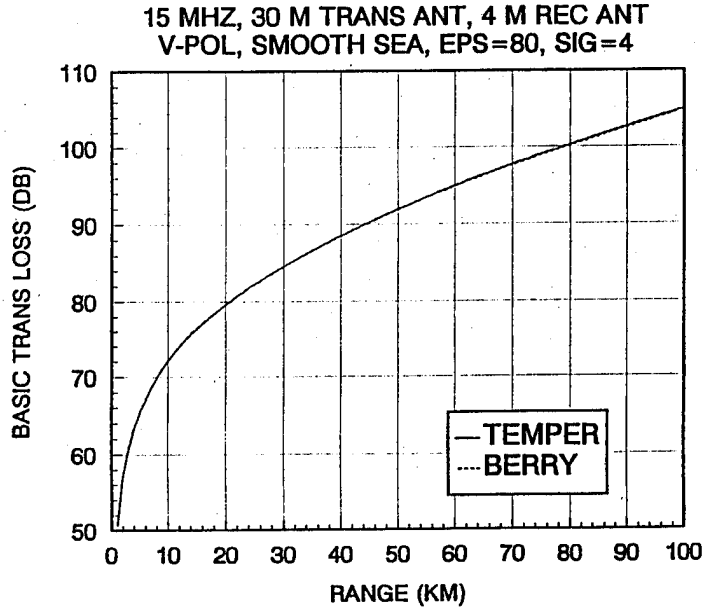
15 MHZ, 30 M TRANS ANT, 4 M REC ANT
V-POL, SMOOTH SEA, EPS=80, SIG=4
—TEMPER
----BERRY
BASIC TRANS LOSS (DB)
110
100
90
80
70
60
50
0
10
20
30
40
50
60
70
80
90
100
RANGE (KM)

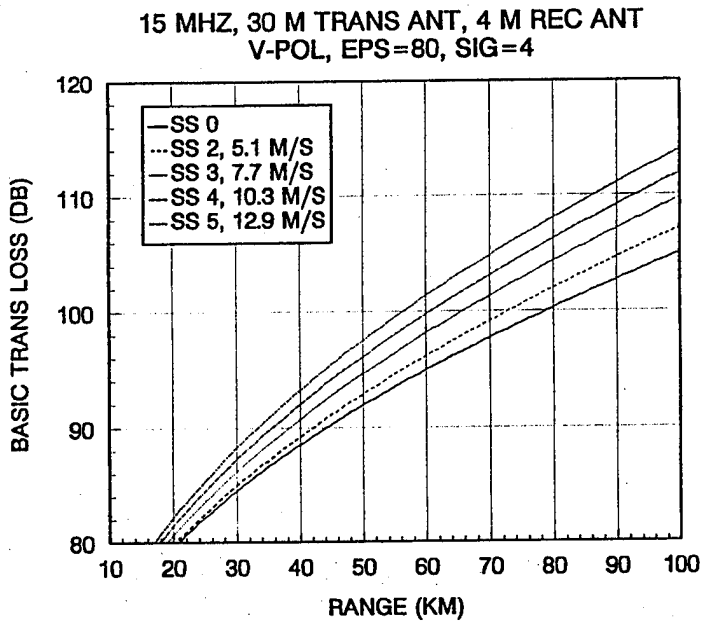
15 MHZ, 30 M TRANS ANT, 4 M REC ANT
V-POL, EPS=80, SIG=4
BASIC TRANS LOSS (DB)
120
110
100
90
80
10
20
30
40
50
60
70
80
90
100
RANGE (KM)
—SS 0
---SS 2, 5.1 M/S
—SS 3, 7.7 M/S
—SS 4, 10.3 M/S
—SS 5, 12.9 M/S

DESCRIPTION AND PERFORMANCE OF A NEW IMPEDANCE BOUNDARY ALGORITHM IN TEMPER

James R. Kuttler
G. Daniel Dockery
Johns Hopkins University Applied Physics Laboratory
Johns Hopkins Road
Laurel, MD 20723
(301)953-6222 (Kuttler)
(301)953-5461 (Dockery)
J_R_Kuttler@aplmail.jhuapl.edu
G_D_Dockery@aplmail.jhuapl.edu

This presentation discusses an improved method for implementing impedance boundary conditions in parabolic equation (PE) models using Fourier split-step techniques. Prior to discussing the new algorithm, a basic introduction to the PE wave equation and split-step solution is given. The new algorithm is based on the "Mixed Fourier Split-Step" published in 1991, but has been re-derived in the discrete domain, thereby avoiding some numerical problems and resulting in a significant increase in computational speed. Calculations using the new algorithm have produced excellent agreement with other models for HF calculations, for which surface wave effects are important, and for rough surface cases which tend to stress impedance boundary algorithms. Following a complete description of the discrete algorithm, examples of both HF and rough surface calculations will be presented.

Maxwell's equations can be reduced to a single scalar Helmholtz equation in one component of a vertically or horizontally polarized field over the exterior of a slice through the earth. See, e.g.,

> G. D. Dockery and J. R. Kuttler, "Theoretical Description of the Parabolic Approximation/Fourier Split-Step Method of Representing Electromagnetic Propagation in the Troposphere," Radio Science, Vol. 26, pp. 381-393, 1991.

After a conformal mapping, this becomes a Helmholtz equation

$$\frac{\partial^2 U}{\partial x^2} + \frac{\partial^2 U}{\partial z^2} + k^2 n^2 U = 0 ,$$

on a rectangular coordinate system $x \geq 0$, $z \geq 0$, where all geometrical effects (in particular, curved earth), accounted for by the mapping, are contained in the modified index of refraction term

$$n = n(x,z) .$$

There is an impedance boundary condition

$$\frac{\partial u}{\partial z} + \alpha u = 0$$

on $z = 0$, and in some applications α may vary with range.

A formal solution of (1) is

$$u(x,z) = \exp\left(i \int_0^x \left[\sqrt{\frac{\partial^2}{\partial z^2} + k^2 n^2} - k \right] dx \right) u(0,z) . \qquad (2)$$

where the exponential of an operator is the series expansion

$$e^A = I + A + \tfrac{1}{2} A^2 + \tfrac{1}{3!} A^3 + \cdots$$

To put (2) in a form suitable for computation, first the approximation

$$\sqrt{1 + \epsilon + \eta} \approx \sqrt{1 + \epsilon} + \sqrt{1 + \eta} - 1$$

is used to write

$$u(x,z) = \exp\left(i \left[x \sqrt{k^2 + \frac{\partial^2}{\partial z^2}} + k \int_0^x (n - 2)\, dx \right] \right) u(0,z) .$$

Now the exponent is split up. But

$$e^{A+B} \neq e^A e^B ,$$

if the operators A and B do not commute (which is the case here, since n is a function of z). So the approximation

$$e^{A+B} \approx e^{\frac{1}{2}B} e^A e^{\frac{1}{2}B}$$

is used, which is accurate up to terms of $O(x^2)$, as may be seen by multiplying out the series. (This is apparently the origin of the term "split-step.")

The solution is now in the form

$$u(x,z) = \exp(\tfrac{ik}{2}\int_0^x (n-1)dx)\ \exp\left(ix\left[\sqrt{k^2 + \frac{\partial^2}{\partial z^2}} - k\right]\right) \exp(\tfrac{ik}{2}\int_0^x (n-1)dx)\, u(0,z)\ . \tag{3}$$

This differs only slightly from the derivation in

D. J. Thompson and N. R. Chapman, "A Wide-Angle Split-Step Algorithm for the Parabolic Equation," J. Acoust. Soc. Am., Vol. 74, pp. 1848-1854, 1983,

in that a -k has been retained in the center term. The reason is that often $n \approx 1$, so the phase terms containing n-1 should be small, making the split-step approximation very accurate.

Next, the center operator is diagonalized by Fourier methods. The range step is assumed to be sufficiently small that α can be assumed to be constant over it. The operator $\partial^2 u/\partial z^2$ is diagonalized on $0 < z < \infty$, subject to the boundary conditions $\partial u/\partial z + \alpha u = 0$ on $z = 0$, $u \to 0$ as $z \to \infty$. When $\mathrm{Re}(\alpha) > 0$, there is a continuous spectrum $-p^2$ for $0 < p < \infty$ with eigenfunctions

$$\alpha \sin pz - p \cos pz\ ,$$

and a single point α^2 in the discrete spectum with eigenfunction

$$e^{-\alpha z}\ .$$

It is worth noting that these functions are orthogonal in $L_2(0,\infty)$. Let

$$U(p) = \mathcal{F}_M u \equiv \int_0^\infty u(z)[\alpha \sin pz - p \cos pz]\, dz\ , \tag{4}$$

be the *mixed Fourier transform* (MFT) of u, with inverse

$$u(z) = \mathcal{F}_M^{-1} \equiv \frac{2}{\pi}\int_0^\infty U(p)\frac{\alpha \sin zp - p\cos zp}{\alpha^2 + p^2}\, dp + Ce^{-\alpha z}\ , \tag{5}$$

where

$$C = 2\alpha\int_0^\infty u(z)e^{-\alpha z}\, dz\ . \tag{6}$$

The foregoing was essentially preamble. The main thing we want to present today is how to numerically compute the MFT accurately. The field u(x,z) is necessarily represented on a finite grid of points

$$mdz\ , \quad m = 0,1,2,\cdots,N,$$

and the Fourier transforms are done by discrete sine transforms (DST) and discrete cosine transforms (DCT) based on FFTs. The trick is to do these correctly. The most obvious discretization of (4), (5), (6) leads to some subtle numerical problems which can occasionally cause numerical instabilities. The correct discretization of (4) is

$$U(jdp) = \sum_{m=0}^{N\ \prime} u(mdz)\left[\alpha \sin\left(\frac{\pi jm}{N}\right) - \frac{\sin\left(\frac{\pi j}{N}\right)}{dz}\cos\left(\frac{\pi jm}{N}\right)\right], \tag{7}$$

where

$$dz \cdot dp = \frac{\pi}{N}\ ,$$

and the prime on the summations means that the 0 and N terms are to be weighted with a factor of ½. Note that as dz → 0,

$$\frac{\sin\left(\frac{\pi j}{N}\right)}{dz} = \frac{\sin(jdpdz)}{dz} \to jdp = p\ ,$$

so this is a discrete form of the transform variable p.

The inverse of (7) is

$$u(mdz) = \frac{2}{N}\sum_{j=0}^{N\ \prime} U(jdp)\frac{\alpha \sin\left(\frac{\pi jm}{N}\right) - \frac{\sin\left(\frac{\pi j}{N}\right)}{dz}\cos\left(\frac{\pi jm}{N}\right)}{\alpha^2 + \left(\frac{\sin\left(\frac{\pi j}{N}\right)}{dz}\right)^2} \tag{8}$$

$$+ C_1 r^m + C_2(-r)^{N-m}\ ,$$

$$C_1 = K\sum_{m=0}^{N\ \prime} u(mdz)r^m\ , \tag{9}$$

$$C_2 = K\sum_{m=0}^{N\ \prime} u((N-m)dz)(-r)^m\ ,$$

$$K = \frac{2(1-r^2)}{(1+r^2)(1-r^{2N})}\ , \tag{10}$$

and r, -1/r are the roots of the quadratic equation

$$r^2 + 2r\alpha dz - 1 = 0\ . \tag{11}$$

When α has positive real part, the root of smaller magnitude is

$$r = \sqrt{1 + (\alpha\, dz)^2} - \alpha\, dz \ , \tag{12}$$

and if $|\alpha dz| \ll 1$,

$$r^m \approx e^{-\alpha z}$$

Note that that the functions r^m, $(-r)^{N-m}$ and

$$\alpha \sin(\tfrac{\pi j m}{N}) - \frac{\sin(\frac{\pi j}{N})}{dz} \cos(\tfrac{\pi j m}{N})$$

are mutually orthogonal with respect to summation from 0 to N (and they are essentially the only linear combination of sines and cosines which are).

As a bonus for correctly discretizing the MFT, we can use a device to do the calculation which eliminates the need for the cosine transform. Define

$$w(m\,dz) \equiv \frac{u((m+1)dz) - u((m-1)dz)}{2\,dz} + \alpha\, u(m\,dz) \ , \tag{13}$$

for m = 1, ..., N-1, a difference equation in u. Then, the MFT of u is exactly the discrete sine transform of w,

$$U(j\,dp) = \sum_{m=1}^{N-1} w(m\,dz) \sin(\tfrac{\pi j m}{N}) \ ,$$

as is easily verified. Then w is recovered from U by an inverse DST

$$w(m\,dz) = \frac{2}{N} \sum_{j=1}^{N-1} U(j\,dp) \sin(\tfrac{\pi j m}{N}) \ ,$$

and we get back to u by solving the difference equation (13).

This linear difference equation is solved in exactly the same manner as an analogous differential equation. That is, to a particular solution u_P of the inhomogeneous equation, add an appropriate linear combination of the general solutions to the homogeneous equation,

$$u_p(m) + Ar^m + B(-r)^{(N-m)} ,$$

where r is the previously encountered root of the quadratic equation (11).

Finally, the particular solution u_P is found by factoring the difference equation (13) into upper and lower triangular terms, and solving by the recursions

$$y(m) - ry(m-1) = 2dzw(mdz) ,$$

for m = 1, ..., N-1, where y(0) is arbitrary, and (backsolving)

$$u_p(m+1) + \frac{1}{r} u_p(m) = y(m) ,$$

for m = 0, ..., N-1, where $u_P(N)$ is arbitrary. Direct substitution verifies that these are equivalent to (13).

Let us then summarize one complete step of the discrete split-step parabolic routine:

1. Initially f(0,mdz) is given, m = 0, 1, 2,..., N.

2. It is multiplied by half of the z-space phase term

$$u(0,mdz) = f(0,mdz) \exp\left(\frac{ik}{2}\int_0^x (n-1)dx\right) .$$

3. The coefficients

$$C_1(0) = K \sum_{m=0}^{N}{}' u(0,mdz) r^m ,$$

$$C_2(0) = K \sum_{m=0}^{N}{}' u(0,(N-m)dz)(-r)^m ,$$

are computed.

4. w is defined by the difference equation

$$w(0,mdz) = \frac{u(0,(m+1)dz) - u(0,(m-1)dz)}{2dz} + \alpha u(0,mdz) ,$$

for m = 1, ..., N-1.

5. The DST of w is computed

$$U(0,jdp) = \sum_{m=1}^{N-1} w(0,mdz)\sin\left(\frac{\pi jm}{N}\right) .$$

6. U is propagated to the new range by

$$U(x,jdp) = U(0,jdp)\exp\left(ix\left[\sqrt{k^2-(jdp)^2}-k\right]\right) ,$$

7. The coefficients are propagated to the new range by

$$C_1(x) = C_1(0)\exp\left(\frac{ix}{2k}\left(\frac{\log r}{dz}\right)^2\right) ,$$

$$C_2(x) = C_2(0)\exp\left(\frac{ix}{2k}\left(\frac{\log(-r)}{dz}\right)^2\right) .$$

[Note: log(-r) = log r - $i\pi$.]

8. Inverse sine transform

$$w(x,mdz) = \frac{2}{N}\sum_{j=1}^{N-1} U(x,jdp)\sin\left(\frac{\pi jm}{N}\right) .$$

9. Get the particular solution of the difference equation by y(0) = 0,

$$y(m) = 2dzw(mdz) + ry(m-1) ,$$

for m = 1, ..., N-1, and $v_P(N) = 0$, and then

$$u_P(N-m) = r[y(N-m) - u_P(N-m+1)] ,$$

for m = 1, ..., N.

10. $$A = C_1(x) - K\sum_{m=0}^{N}{}' u_P(m)r^m ,$$

$$B = C_2(x) - K\sum_{m=0}^{N}{}' u_P(N-m)(-r)^m .$$

11. $$u(x,mdz) = u_P(m) + Ar^m + B(-r)^{(N-m)} .$$

12. Multiply by the other half of the z-space phase term

$$f(x,mdz) = u(x,mdz)\exp\left(\frac{ik}{2}\int_0^x (n-1)dx\right) .$$

TIMING COMPARISONS

- PARAMETERS: 10 GHz, VERTICAL POLARIZATION, SMOOTH SEA, 100 KM IN 0.2 KM STEPS, 2^{12} TRANSFORM SIZE

- COMPUTER: COMPAQ 486/50L

- LANGUAGE: MICROWAY NDP FORTRAN

ALGORITHM	COMPUTATION TIME (SEC)
STANDARD SPLIT-STEP - SINE TRANSFORM - PERF. COND.	185
FULL MIXED FOURIER TRANS. SPLIT-STEP	410
DISCRETE MFT USING SINE TRANSFORM VARIATION	275

Dr. Jim Kuttler, "Description and Performance of a New Impedance Boundary Algorithm in TEMPER"

DISCUSSION

H. HITNEY

You used the wide-angle propagator in your development. Would the use of the standard PE propagator simplify your method?

AUTHOR'S REPLY

No - they give the same results when both work - the wide angle can handle a few more cases.

S. MARCUS

Is it possible to prove the numerical stability of the iterations scheme?

AUTHOR'S REPLY

Probably - but art is long & life is short.

Radio Physical Optics Model

Herbert V. Hitney

NCCOSC RDTE DIV. CODE 543
49170 PROPAGATION PATH
SAN DIEGO CA 92152-7385

The Radio Physical Optics (RPO) model computes propagation loss for over-water paths and accounts for range-dependent vertical refractive index profiles. RPO is a hybrid combination of four submodels, namely the flat earth (FE), ray-optics (RO), split-step parabolic equation (PE), and extended optics (XO) submodels. This hybrid model was developed to overcome the high computational burden of pure split-step PE methods while still preserving the range-dependent capability of the PE method for use in near-real-time operational assessments, such as the Tactical Environmental Support System (TESS). RPO uses the PE submodel only for low elevation angles and low terminal heights, where it is reasonably efficient, and relatively fast ray-optics methods everywhere else. The result is a range-dependent model that can run 25 to 100 times faster than a pure split-step PE model for stressful cases that are typical of TESS applications.

The FE submodel is used whenever ranges are less than 2500 m or elevation angles exceed 5 degrees. Since the effects from refraction and earth curvature in this region are very slight, the model uses straight-line ray-optics techniques to compute the coherent interference of the direct and sea-reflected rays. For the region beyond the FE region where the grazing angles of reflected rays from the transmitter are above a small limiting value, the RO submodel is used that does account for the full effects of refraction and earth curvature. However, the RO submodel uses only the vertical refractivity profile at the transmitter, and hence cannot take range dependent refractive effects into account. This limitation is normally not important since this region is confined to relatively short ranges over which refractive conditions are not expected to vary significantly. For ranges beyond the RO region and heights below a maximum PE altitude determined by a 1024-point fast-Fourier transform (FFT), the PE submodel is used which does allow for variation of the vertical refractive index profile with range. Finally, for ranges beyond the RO region and above the PE region, the XO submodel is used that is initialized by the PE submodel at the maximum PE altitude and uses ray-optics methods to extend the solutions up to higher heights.

The effects of polarization and surface roughness are modeled in the FE and RO regions by the Fresnel reflection coefficient for sea water, adjusted as necessary for surface roughness using the Miller-Brown roughness model. The PE submodel also includes these effects in the starting solution, but propagates the signal down range assuming perfect reflection from the sea using a sine FFT PE model. For many applications this simplification is adequate, but there are a few cases where substantial errors may arise. In particular, the model may underestimate propagation loss at long ranges in and near a strong surface duct, due to multiple interactions between the trapping and sea-reflection mechanisms. An approximate semiempirical method to correct the PE submodel for these cases has been developed and will be briefly described.

An important capability of the PE submodel is its ability to account for tropospheric scatter effects. These effects are quite important in communication and electronic-warfare support measure applications, where the propagation loss values must be accurate at high values to establish an accurate estimate of maximum range. The RPO PE submodel simulates normal troposcatter effects by adding a small random variation to the refractive index profile at all heights based on an effective median refractive-index structure parameter that varies with altitude. This semiempirical model checks well with other engineering models and measured data.

The capabilities of RPO include: frequencies from 100 MHz to 20 GHz; transmitter antenna heights from 1 to 100 m; horizontal, vertical, and circular polarization; and omnidirectional, sine(x)/x, Gaussian, cosecant-squared, and height-finder antenna patterns. There are no limits to maximum receiver height or range. The RPO method can accommodate any number of vertical levels of refractivity and any number of

profiles, provided that all profiles have the same number of vertical levels and like-numbered levels refer to the same feature. Currently, there is no provision in RPO to account for gaseous absorption, although this capability will probably be added in the near future..

Several examples of RPO applications will be presented to illustrate the model's capabilities and limitations. Examples to illustrate the limit on range dependency imposed by the RO submodel and limits on the height of surface ducts imposed by the PE submodel at high frequencies will be presented. Also examples illustrating the limits on polarization and rough surface effects under ducting conditions will be included. Plans for improvements to RPO will also be discussed.

References

1. Barrios, A.E., "Parabolic Equation Modeling in Horizontally Inhomogeneous Environments," *IEEE Trans. Antennas Propagat.*, vol. 40, no. 7, pp. 791-797, July 1992.
2. H.V. Hitney, "Hybrid Ray Optics and Parabolic Equation Methods for Radar Propagation Modeling," *IEE Int. Conf. Radar 92*, IEE Conf. Pub. 365, Brighton, England, 12-13 Oct 1992.
3. H.V. Hitney, "A Practical Tropospheric Scatter Model Using the Parabolic Equation," *IEEE Trans. Antennas Propagat.*, vol. 41, no. 7, pp. 905-909, Jul. 1993.
4. H.V. Hitney, "Modelling Surface Effects with the Parabolic Equation Method," in *IGARSS 94*, IEEE Symposium Digest, 8-12 Aug. 1994.
5. H.V. Hitney, "Modeling Nonperfect Reflection from the Sea for Range-Dependent Ducting Conditions," AGARD-SPP Symposium on Propagation Assessment in Coastal Environments, 19-22 Sep 1994, AGARD-CP-567.

Radio Physical Optics Model

Herb Hitney
NCCOSC RDTE DIV 543

Radio Physical Optics (RPO) Regions

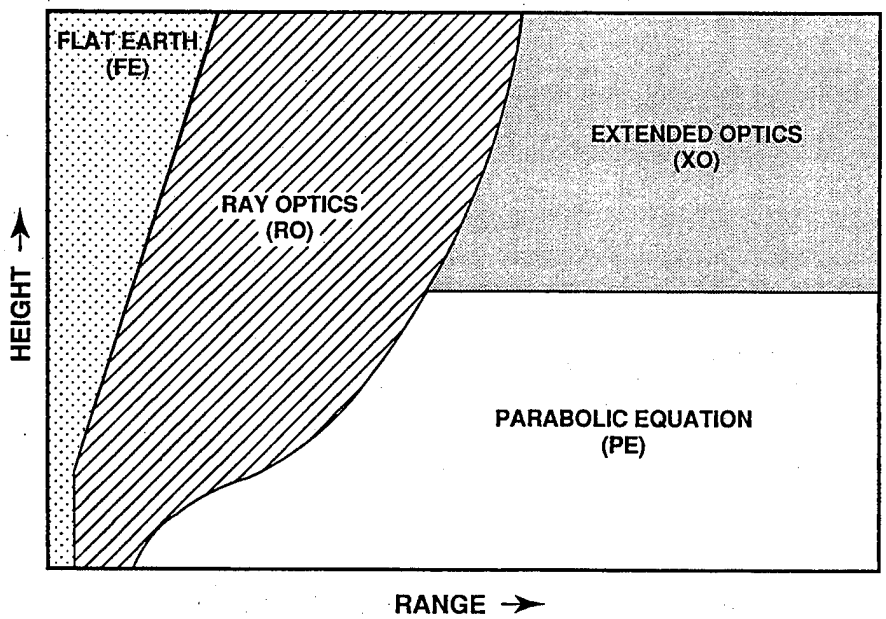

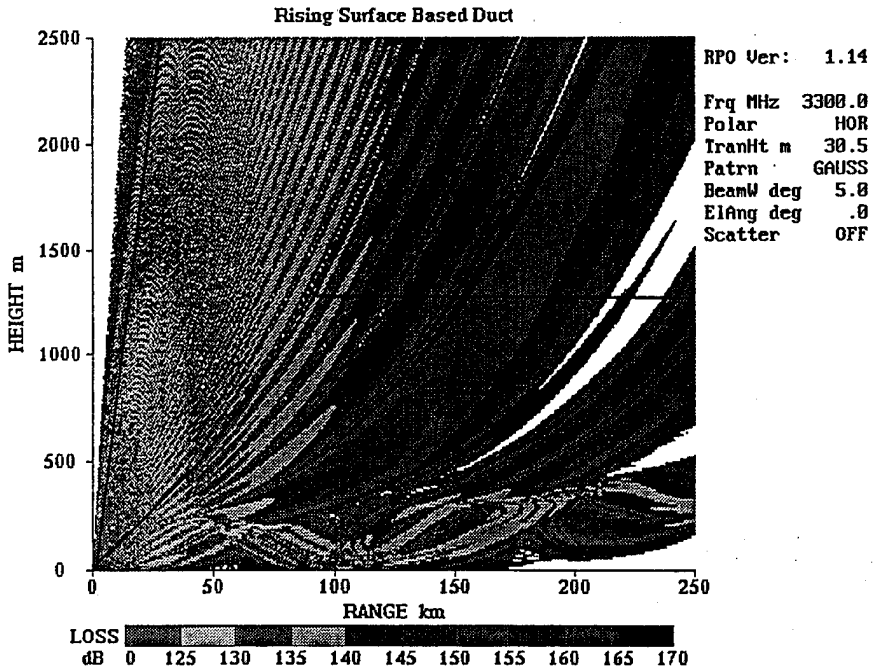

RPO Capabilities

- Range-dependent refractive structure.
- Unlimited maximum range and height.
- Includes troposcatter submodel.
- Fast compared to full PE models.
- Meets all TESS requirements.
  - 100 MHz to 20 GHz
  - Transmitter heights to 100 m
  - Horizontal, vertical, or circular polarization
  - Various antenna patterns and beamwidths

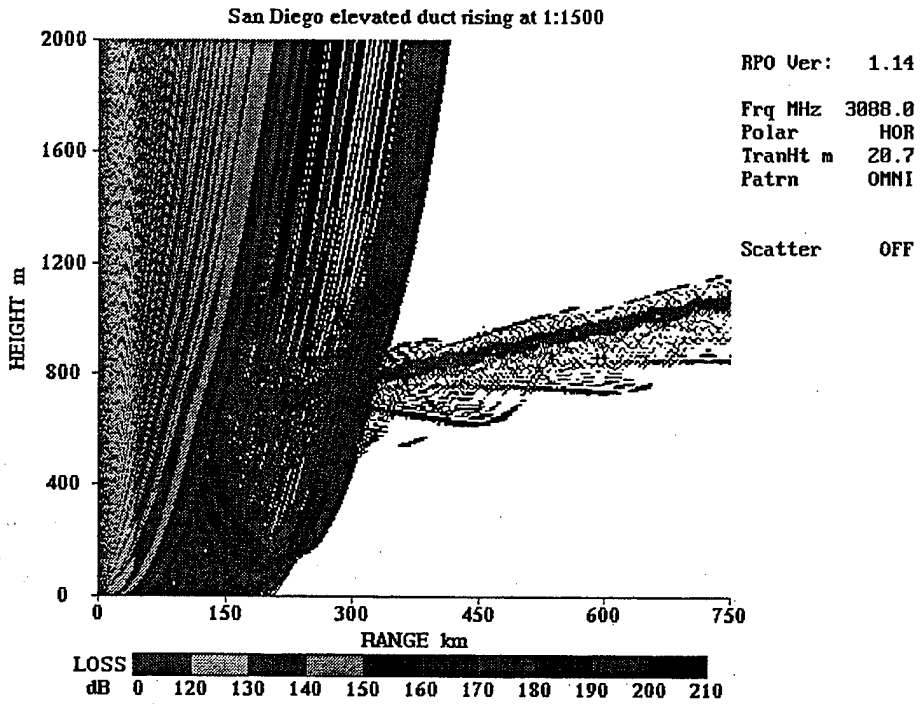
San Diego elevated duct rising at 1:1500
RPO Ver: 1.14
Frq MHz 3088.0
Polar HOR
TranHt m 20.7
Patrn OMNI
Scatter OFF
HEIGHT m
2000
1600
1200
800
400
0
0
150
300
450
600
750
RANGE km
LOSS
dB 0 120 130 140 150 160 170 180 190 200 210

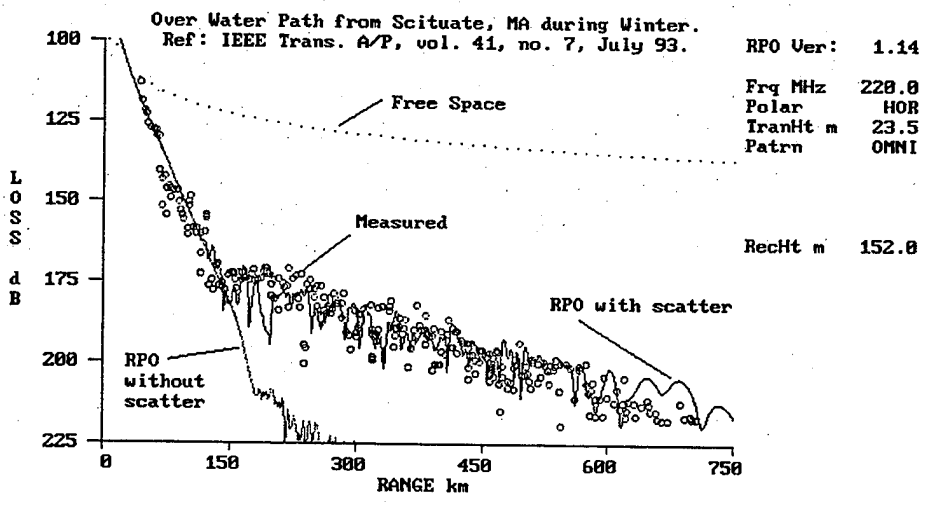
Over Water Path from Scituate, MA during Winter.
Ref: IEEE Trans. A/P, vol. 41, no. 7, July 93.
RPO Ver: 1.14
Frq MHz 220.0
Polar HOR
TranHt m 23.5
Patrn OMNI
RecHt m 152.0
Free Space
Measured
RPO with scatter
RPO without scatter
LOSS dB
100
125
150
175
200
225
0
150
300
450
600
750
RANGE km

RPO Limitations

- RO/PE mismatch for strong range-dependent refractive structures.
- Surface roughness effects in surface ducts.
- Polarization effects in surface ducts.
- Gaseous absorption.
- Height limit in PE region.

RO/PE Mismatch

- RO model assumes no change in refractive structure with range.
- PE model does allow for refractive structure change with range.
- A mismatch may exist along the RO/PE border for range dependent cases with slopes greater than 1:50.

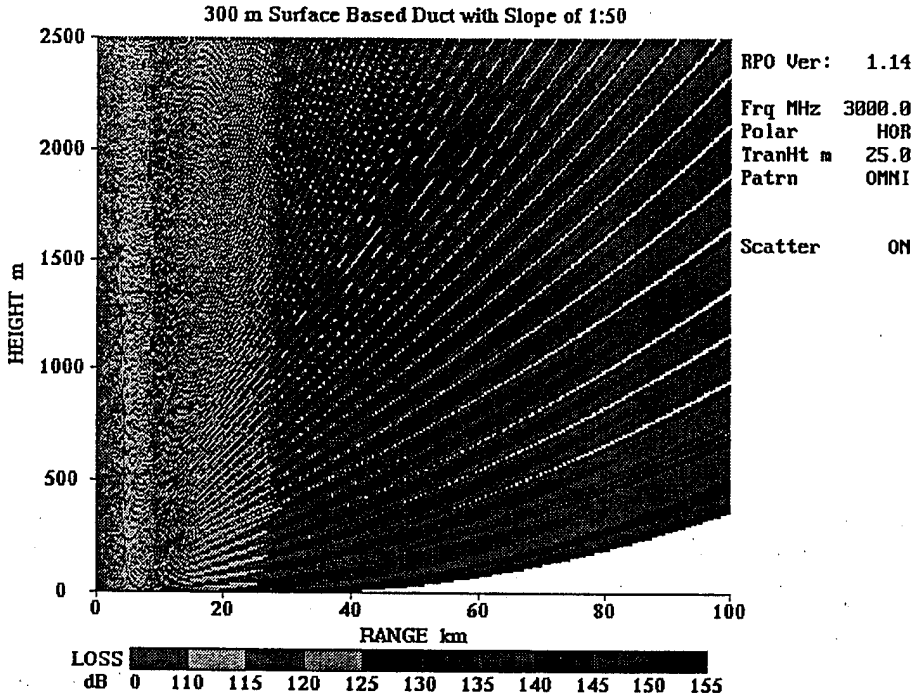

Polarization Limitation

- PE model may be in error for vertical and circular polarization applications under surface ducting conditions.
- This effect is normally minor and decreases in severity with increasing frequency.

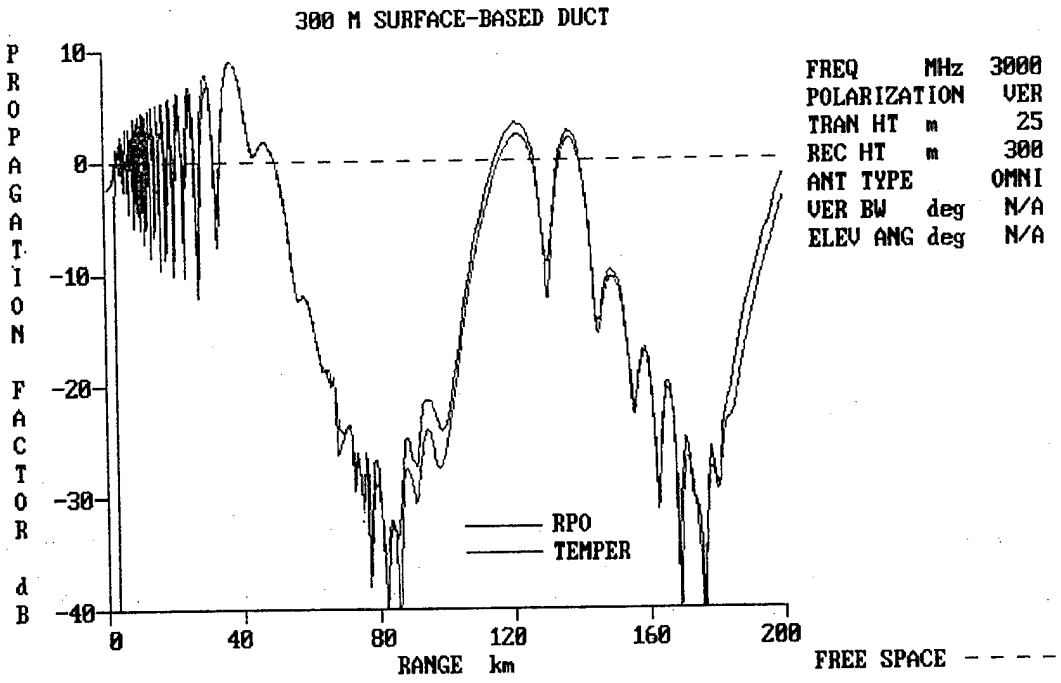

Surface Roughness Limitation

- Surface roughness effects increase with wind speed.
- For high wind speeds and surface duct conditions, PE model will underestimate propagation loss.
- This effect ranges from minor to severe and increases with frequency.

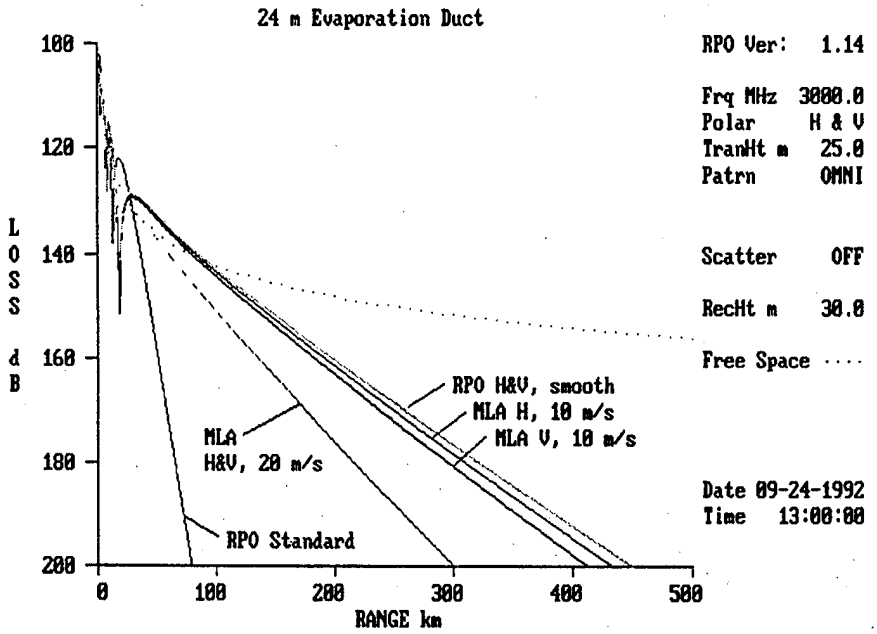
24 m Evaporation Duct
RPO Ver: 1.14
Frq MHz 3000.0
Polar H & V
TranHt m 25.0
Patrn OMNI
Scatter OFF
RecHt m 30.0
Free Space
Date 09-24-1992
Time 13:00:00
LOSS dB
100
120
140
160
180
200
0
100
200
300
400
500
RANGE km
RPO H&V, smooth
MLA H, 10 m/s
MLA V, 10 m/s
MLA H&V, 20 m/s
RPO Standard

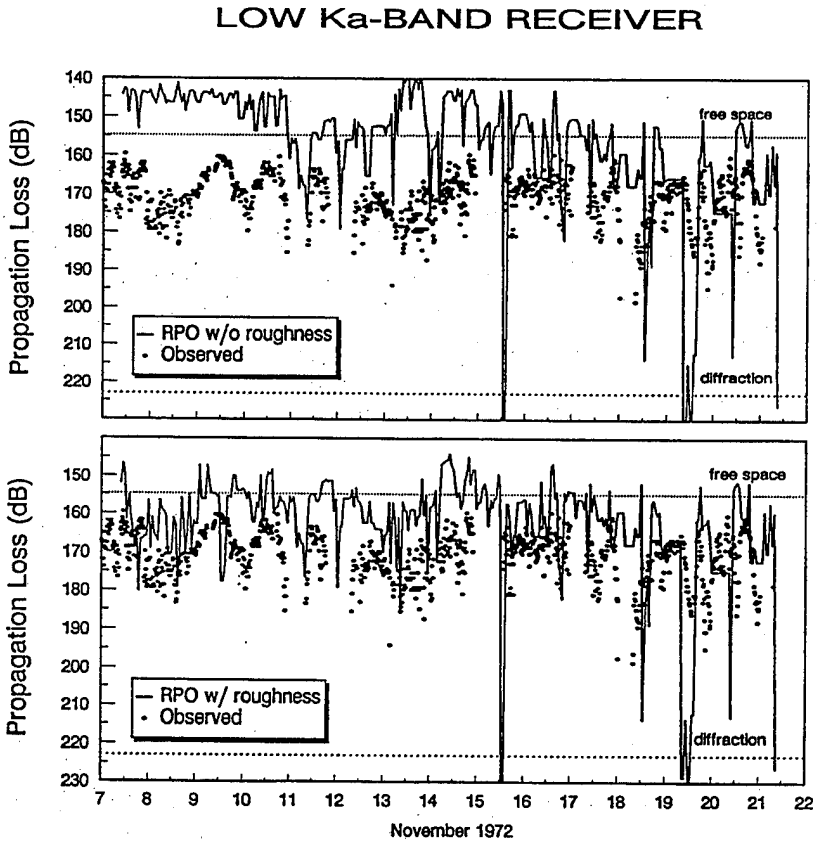
LOW Ka-BAND RECEIVER
Propagation Loss (dB)
free space
RPO w/o roughness
Observed
diffraction
RPO w/ roughness
Observed
7
8
9
10
11
12
13
14
15
16
17
18
19
20
21
22
November 1972

PE Region Height Limit

- The maximum height in the PE region is determined by a 1024-point FFT.
- For high frequencies this maximum height could be below the top of a surface based duct, thus causing severe errors in results.
- In most applications, this problem is unlikely to occur.

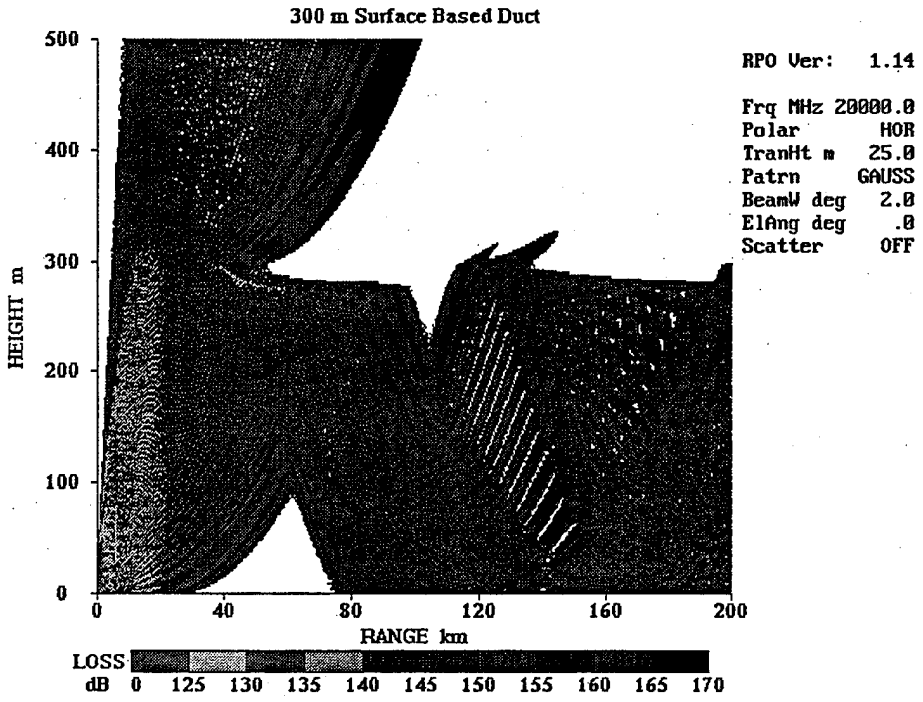

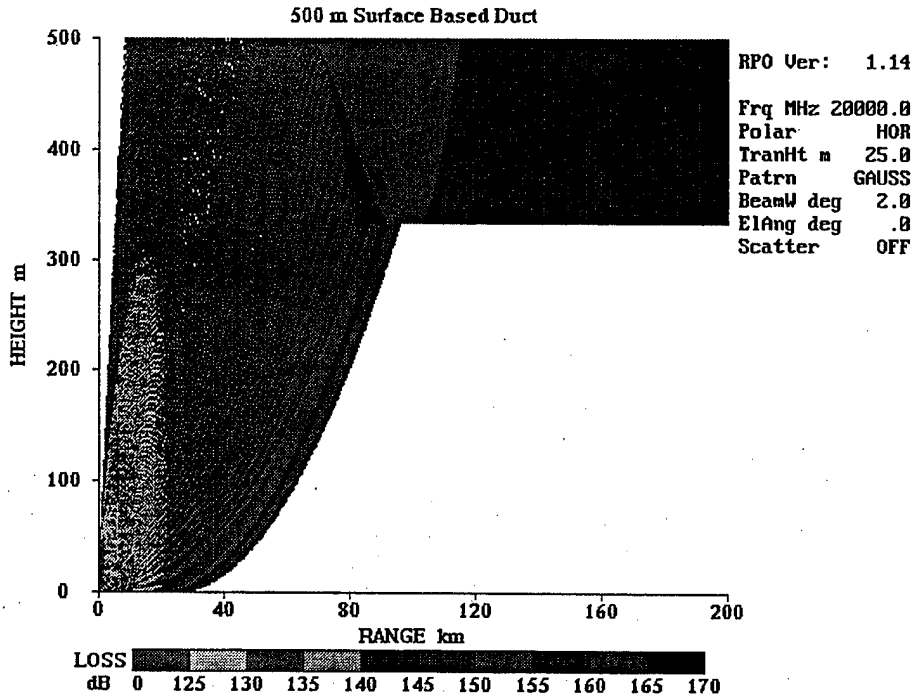

Absorption

- RPO version 1.14 does not contain a gaseous absorption submodel.
- Below 10 GHz gaseous absorption is usually not important.
- RPO CIMREP (March 95) recommended absorption be added prior to RPO inclusion in OAML.

Planned Improvements

- Gaseous absorption (version 1.15).
- RO/PE mismatch.
- Surface roughness in PE model.
- Polarization in PE model.

RPO Summary

- Accounts for range dependent structures.
- Meets all TESS requirements.
- Much better than the Standard Propagation Model currently in OAML.
- Efficient compared to pure PE models.
- RPO has a few limitations that will be corrected in the future.

Mr. Herb Hitney, "Radio Physical Optics Model"

DISCUSSION

D. DOCKERY

You presented comparisons with the 1972 measurements which show improved agreement with RPO when empirical surface roughness model is used. Are the RPO results identical to waveguide results for the same case? If so, the good agreement is a partial validation of the Miller-Brown roughness model which is used in MLAYER.

AUTHOR'S REPLY

The RPO results are not identical to the MLAYER results, but they should be pretty close. I agree that these data partially validate the use of the Miller-Brown model in conjunction with ducting conditions.

Title: Propagation Analysis Using TIREM

Authors: David Eppink and Homer Riggins
Address: JSC/IITRI
185 Admiral Cochrane Drive
Annapolis, Md., 21401

Telephone: 410-573-7555
email:rigginsh@jsc.mil

ABSTRACT

The Joint Spectrum Center (JSC) is responsible for analysis and development of capabilities that are used to ensure the efficient utilization of the electromagnetic spectrum. This responsibility includes the development of propagation models for a wide range of applications throughout the entire electromagnetic spectrum. For groundwave propagation in the troposphere at frequencies from HF through SHF, the Terrain-Integrated Rough-Earth Model (TIREM) is used. TIREM computes the path loss, accounting for the effects of the terrain, using simple solutions to estimate complex interactions. The model is applicable for any arbitrary terrain profile. The model provides for the effects of spherical earth diffraction, multiple knife-edge diffraction, and troposcatter losses. Based upon examination of the terrain profile along the great circle path between the transmitter and the receiver, the model automatically selects the appropriate propagation loss algorithm. The relatively fast TIREM module is suitable for many-on-many analysis or for contouring performance parameters over large geographic regions. The TIREM model has been used in analysis and simulations throughout the Department of Defense (DoD) for a variety of purposes including communications coverage, weapons systems evaluations, intelligence evaluations, and EW assessments. An overview of the TIREM model is provided and includes a comparison of the results of TIREM with Sample Case 8.

Propagation Analysis Using TIREM

David W. Eppink

PROPAGATION CAPABILITIES

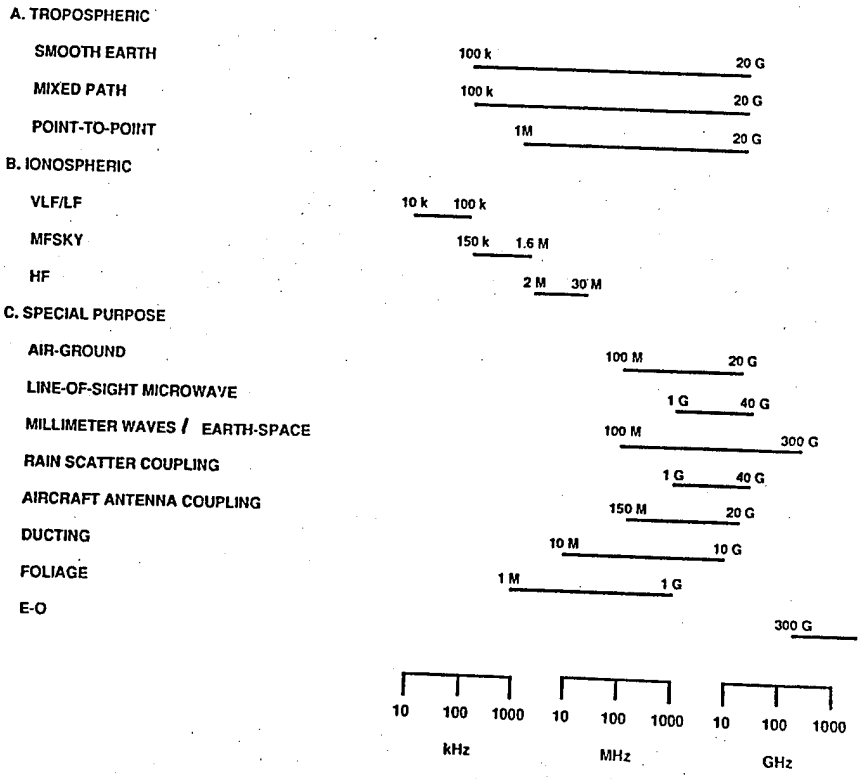

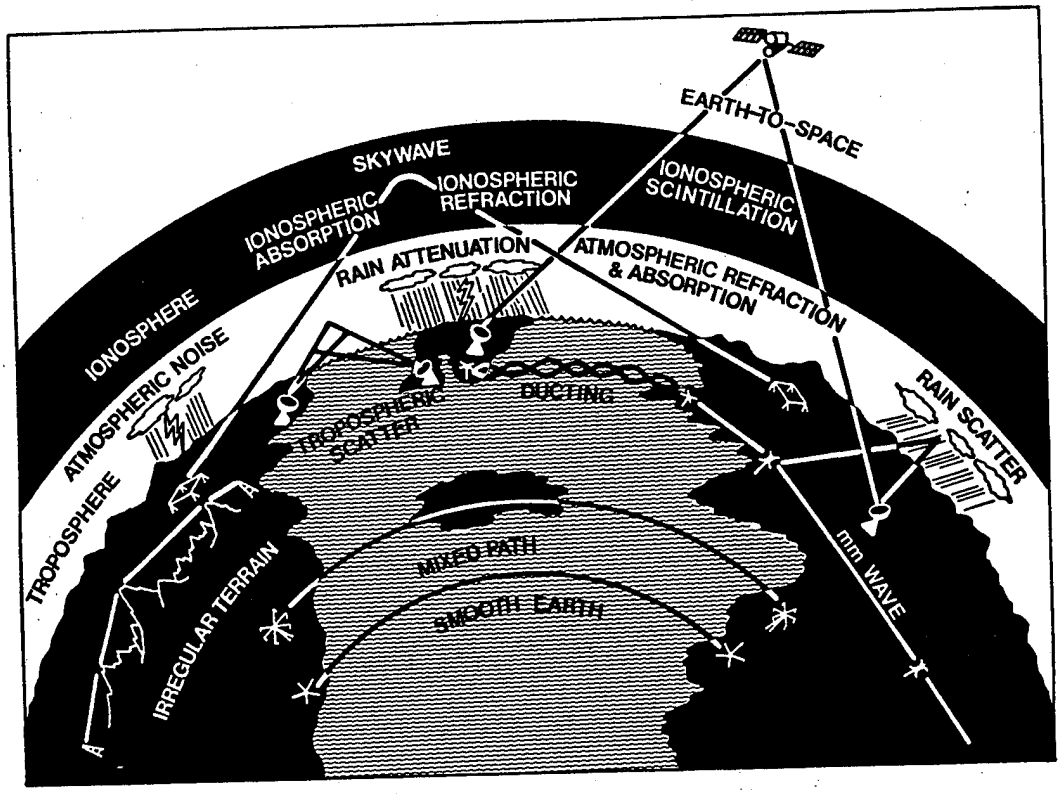

Terrain Integrated Rough Earth Model (TIREM)

- Predicts Median Propagation Loss Over Irregular Terrain
- 1 MHz to 20 GHz
- Free-Space Spreading, Reflection, Surface-Wave Propagation, Diffraction, Tropospheric-Scatter Propagation, and Atmospheric Absorption INCLUDED
- Ducting, Ionosphere, Rain, Foliage, Man-Made Obstacles NOT INCLUDED

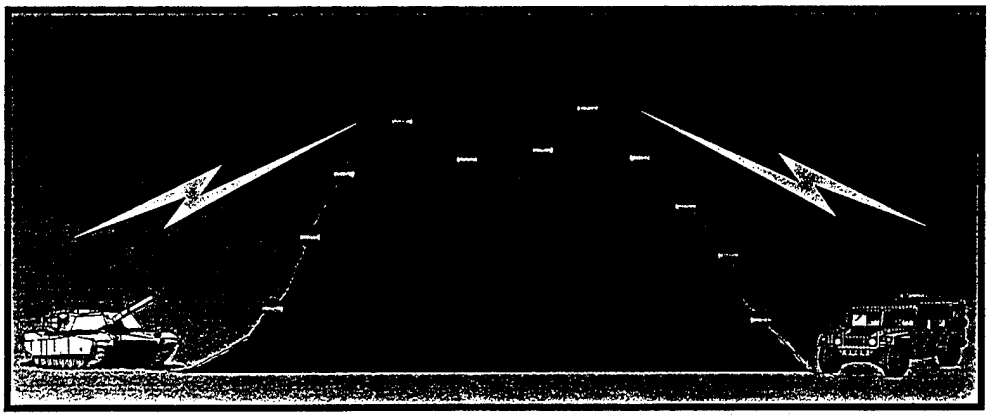

```
      SUBROUTINE TIREM 3      (TANTHT,
     ★                         RANTHT,
     ★                         PROPFQ,
     ★                         NPRFL,
     ★                         HPRFL,
     ★                         XPRFL,
     ★                         EXTNSN,
     ★                         REFRAC,
     ★                         CONDUC,
     ★                         PERMIT,
     ★                         HUMID,
     ★                         POLARZ,
     ★                         VRSION,
     ★                         MODE,
     ★                         LOSS,
     ★                         FSPLSS)
```

TIREM PATH LOSS GUIDELINES

<table>
<tr><th rowspan="2">FREQ.</th><th colspan="3">LINE-OF-SIGHT</th><th colspan="3">BEYOND LINE-OF-SIGHT</th></tr>
<tr><th>SEA</th><th>SEA/ LAND</th><th>LAND</th><th>SEA</th><th>SEA/ LAND</th><th>LAND</th></tr>
<tr><td>1 TO 16 MHz</td><td rowspan="3">SMOOTH-EARTH LOSS</td><td rowspan="3">WEIGHTING BY SEA/LAND DISTANCES</td><td>SMOOTH-EARTH OR REFLECTION LOSS</td><td rowspan="3">SMOOTH-EARTH DIFFRACTION OR TROPOSCATTER LOSS</td><td rowspan="3">WEIGHTING BY SEA/LAND DISTANCES</td><td>SMOOTH-EARTH OR TROPOSCATTER LOSS</td></tr>
<tr><td>16 TO 20 MHz</td><td>INTERPOLATION FROM 16 TO 20 MHz</td><td>INTERPOLATION FROM 16 TO 20 MHz</td></tr>
<tr><td>20 MHz TO 10 GHz</td><td>REFLECTION LOSS</td><td>SMOOTH-EARTH DIFFRACTION, ROUGH-EARTH DIFFRACTION, OR TROPOSCATTER LOSS</td></tr>
<tr><td>10 TO 20 GHz</td><td colspan="6">LOSS AS CALCULATED ABOVE PLUS ATMOSPHERIC ABSORPTION</td></tr>
</table>

LOS PATH

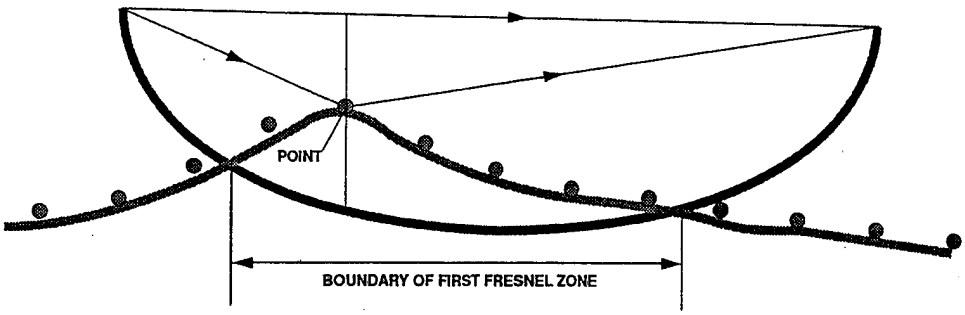

MULTIPLE KNIFE-EDGE DIFFRACTION

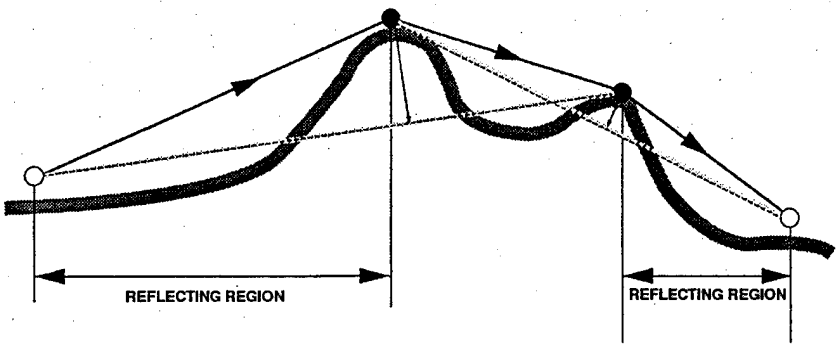

LAND/SEA PATH

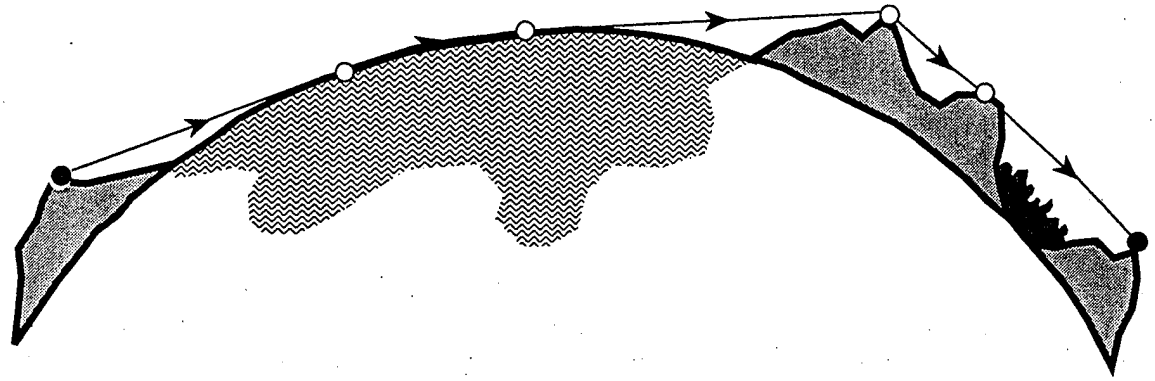

TROPOSCATTER

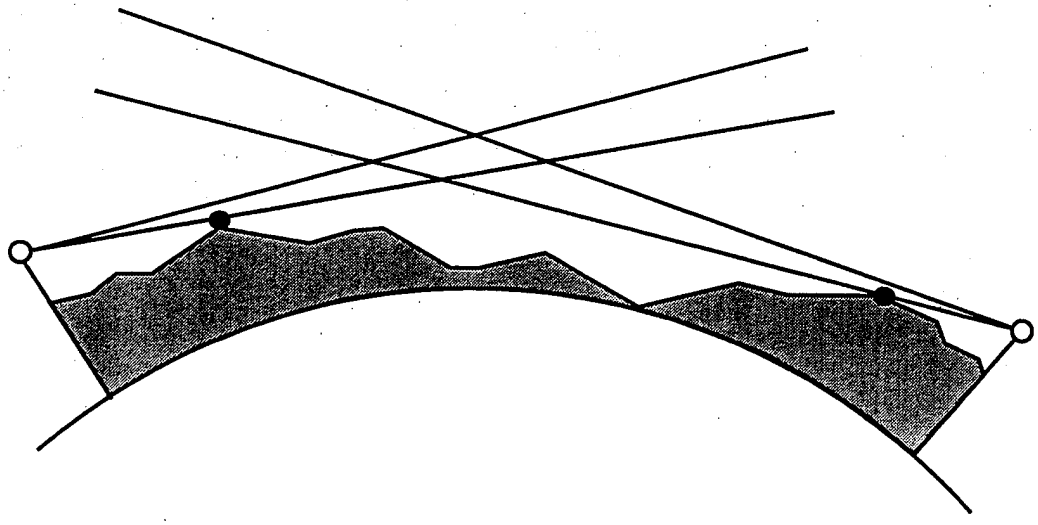

Propagation Measurement Retrieval System

Measurement Van

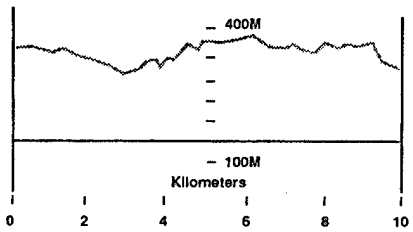

Measured Terrain Profile

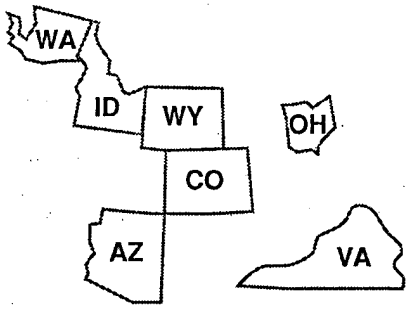

Data in PMRS

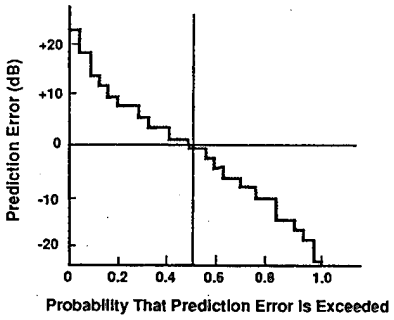

Model Error Statistics

TIREM STATISTICAL SUMMARY

Propagation Mode	Frequency MHz	Number of Measurements	Loss Difference	
			Mean dB	Standard Deviation dB
Spherical Earth	2, 4, 8, 16	102	-2.2	6.9
Line-of-sight	20, 32, 50, 64, 100, 239, 400, 800, 1800 4600, 9200	1217	-2.8	8.9
Diffraction		2798	0.2	11.4
Troposcatter	60 - 4000	358	1.5	8.8
Total	2 - 9200	4475	-0.6	10.5

Capabilities and Limitations of the Terrain Parabolic Equation Model (TPEM)

Amalia E. Barrios

Ocean and Atmospheric Sciences Division
NCCOSC RDTE DIV 543
49170 Propagation Path
San Diego, CA 92152-5001
Ph: (619) 553-1429 e-mail:barrios@nosc.mil

A parabolic equation model based on the split-step Fourier transform method has been developed at NRaD to model tropospheric propagation over variable terrain. The model is called TPEM (Terrain Parabolic Equation Model) and will be presented here with a brief discussion of how the model works, its capabilities, and its limitations. Comparisons will be made with measured data and with other existing terrain models.

The presentation will also include discussions on military operational applications and what is critical and perhaps not so critical [in regards to environmental effects on radiowave propagation over terrain] for radar assessment purposes.

Capabilities and Limitations of the Terrain Parabolic Equation Model (TPEM)

Amalia E. Barrios

Ocean and Atmospheric Sciences Division
NCCOSC RDT&E DIV 543
San Diego, CA 92152-5001

TPEM

- Split-step Fourier transform method.
- Computes field based on smooth surface assumptions.
- Shifts field by number of bins corresponding to height of terrain.

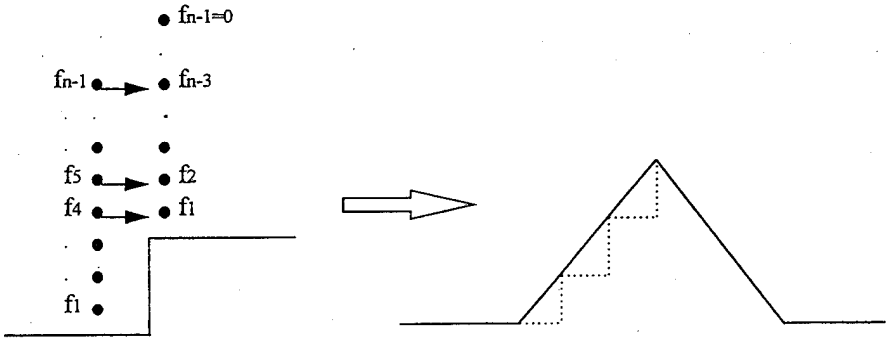

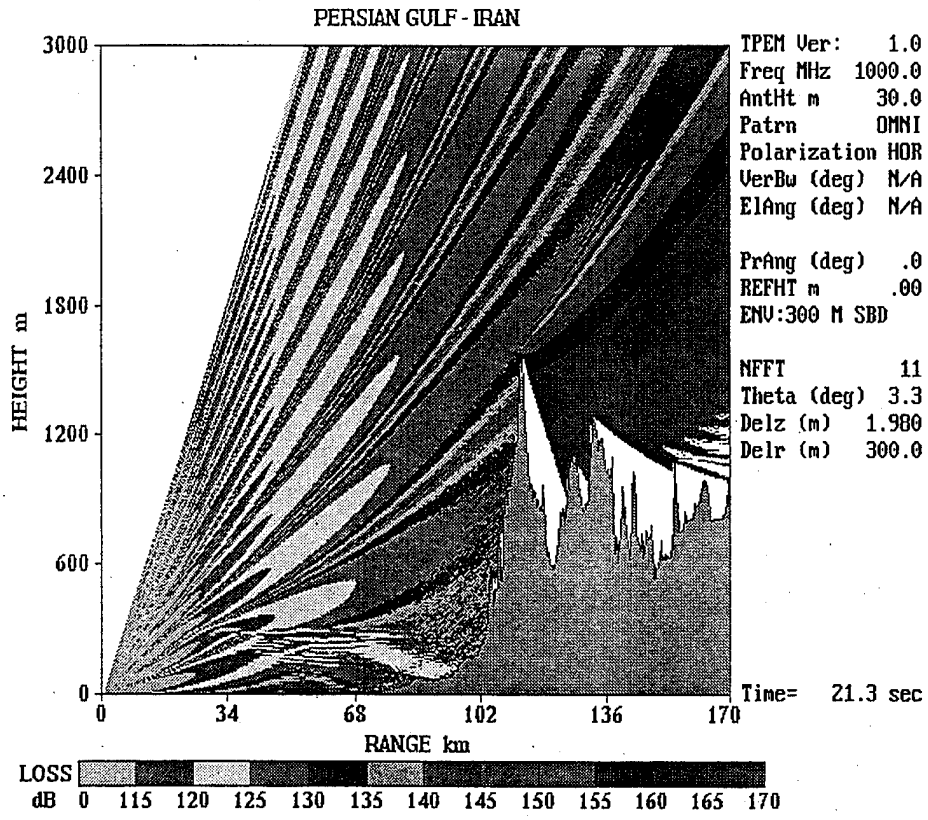
PERSIAN GULF - IRAN
HEIGHT m
3000
2400
1800
1200
600
0
0
34
68
102
136
170
RANGE km
TPEM Ver: 1.0
Freq MHz 1000.0
AntHt m 30.0
Patrn OMNI
Polarization HOR
VerBw (deg) N/A
ElAng (deg) N/A
PrAng (deg) .0
REFHT m .00
ENV:300 M SBD
NFFT 11
Theta (deg) 3.3
Delz (m) 1.980
Delr (m) 300.0
Time= 21.3 sec
LOSS
dB 0 115 120 125 130 135 140 145 150 155 160 165 170

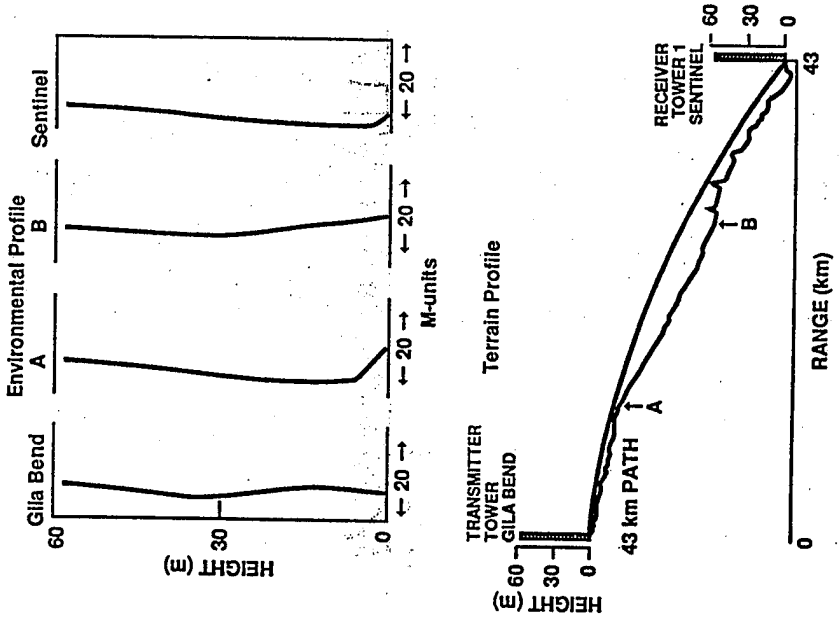
Sentinel
B
A
Gila Bend
Environmental Profile
M-units
20
60
30
0
HEIGHT (m)
Terrain Profile
TRANSMITTER TOWER GILA BEND
RECEIVER TOWER 1 SENTINEL
43 km PATH
RANGE (km)
43
0

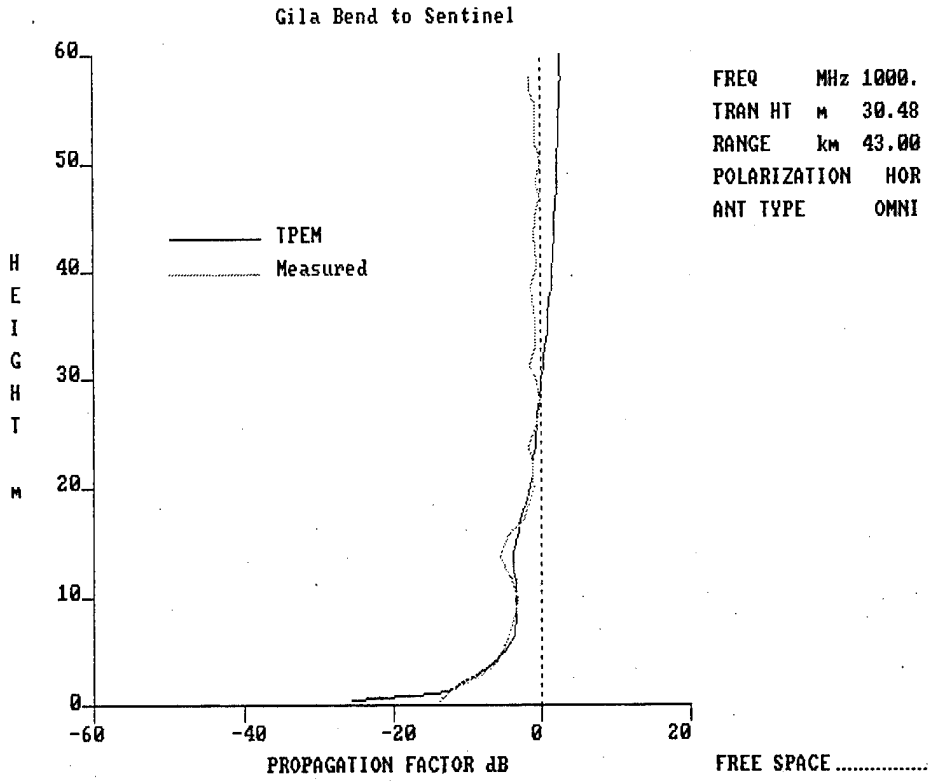
Gila Bend to Sentinel
FREQ MHz 1000.
TRAN HT m 30.48
RANGE km 43.00
POLARIZATION HOR
ANT TYPE OMNI
TPEM
Measured
HEIGHT m
60
50
40
30
20
10
0
-60
-40
-20
0
20
PROPAGATION FACTOR dB
FREE SPACE

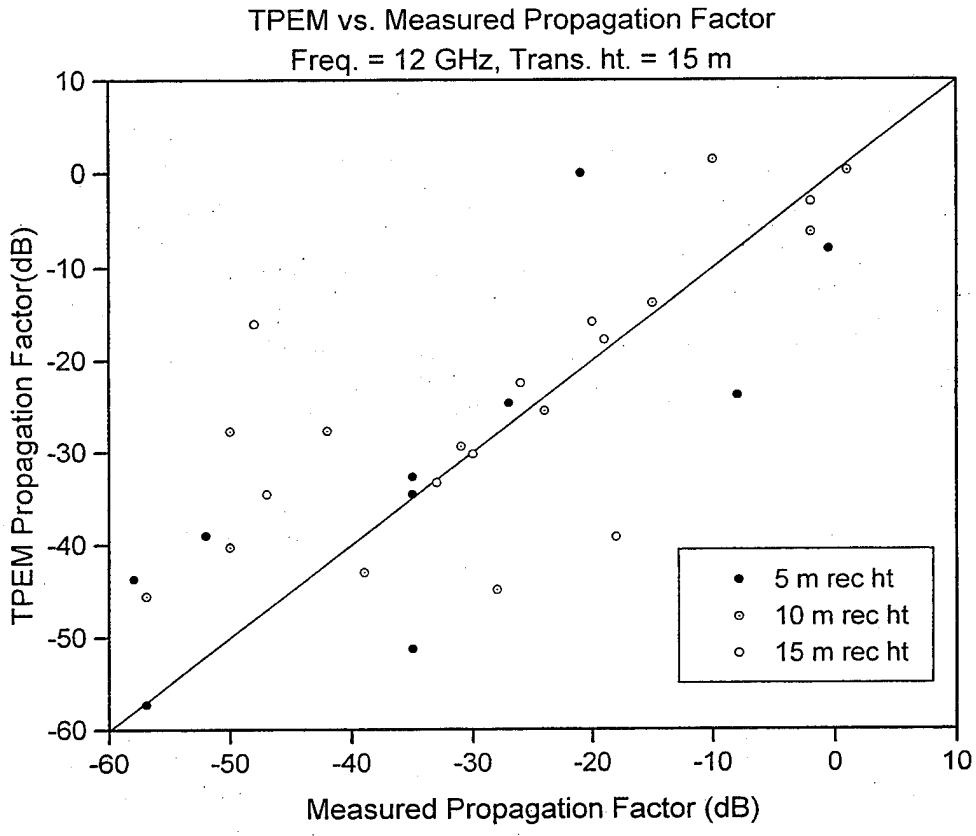
TPEM vs. Measured Propagation Factor
Freq. = 12 GHz, Trans. ht. = 15 m
TPEM Propagation Factor(dB)
10
0
-10
-20
-30
-40
-50
-60
-60
-50
-40
-30
-20
-10
0
10
Measured Propagation Factor (dB)
5 m rec ht
10 m rec ht
15 m rec ht

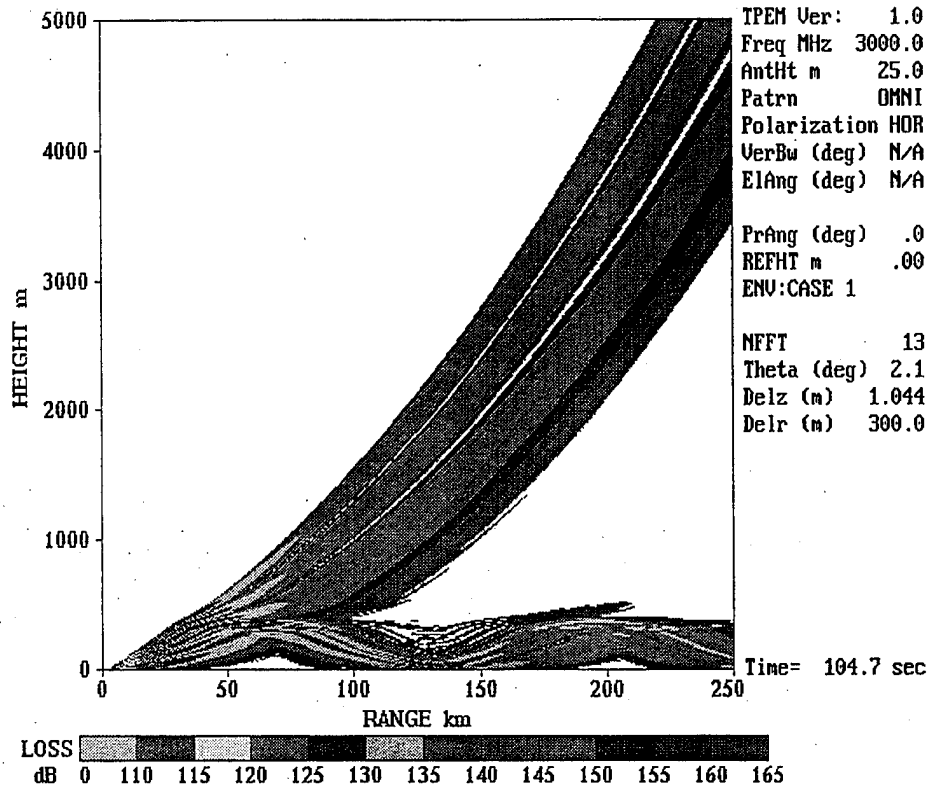
5000
4000
3000
2000
1000
0
HEIGHT m
0
50
100
150
200
250
RANGE km
TPEM Ver: 1.0
Freq MHz 3000.0
AntHt m 25.0
Patrn OMNI
Polarization HOR
VerBw (deg) N/A
ElAng (deg) N/A
PrAng (deg) .0
REFHT m .00
ENV:CASE 1
NFFT 13
Theta (deg) 2.1
Delz (m) 1.044
Delr (m) 300.0
Time= 104.7 sec
LOSS
dB 0 110 115 120 125 130 135 140 145 150 155 160 165

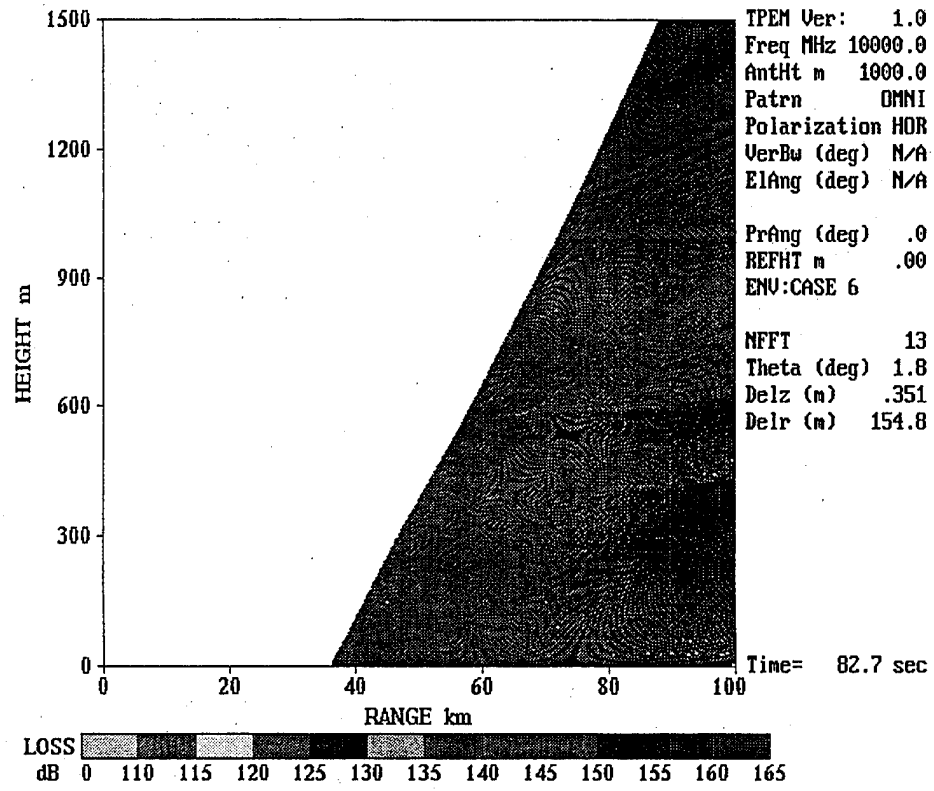
1500
1200
900
600
300
0
HEIGHT m
0
20
40
60
80
100
RANGE km
TPEM Ver: 1.0
Freq MHz 10000.0
AntHt m 1000.0
Patrn OMNI
Polarization HOR
VerBw (deg) N/A
ElAng (deg) N/A
PrAng (deg) .0
REFHT m .00
ENV:CASE 6
NFFT 13
Theta (deg) 1.8
Delz (m) .351
Delr (m) 154.8
Time= 82.7 sec
LOSS
dB 0 110 115 120 125 130 135 140 145 150 155 160 165

Capabilities

- 100 MHz - 20 GHz.
- Range - dependent environments.
- Variable terrain.
- Transmitter antenna heights limited by available transform size.
- Allows various antenna patterns and beamwidths.
- Runs on IBM PC (386 and higher).

Limitations

- Coverage limited in height.
- Does not include vegetation effects.
- Troposcatter.
- Gaseous absorption.
- Vertical polarization and finite conductivity effects.
- Rough surface effects.

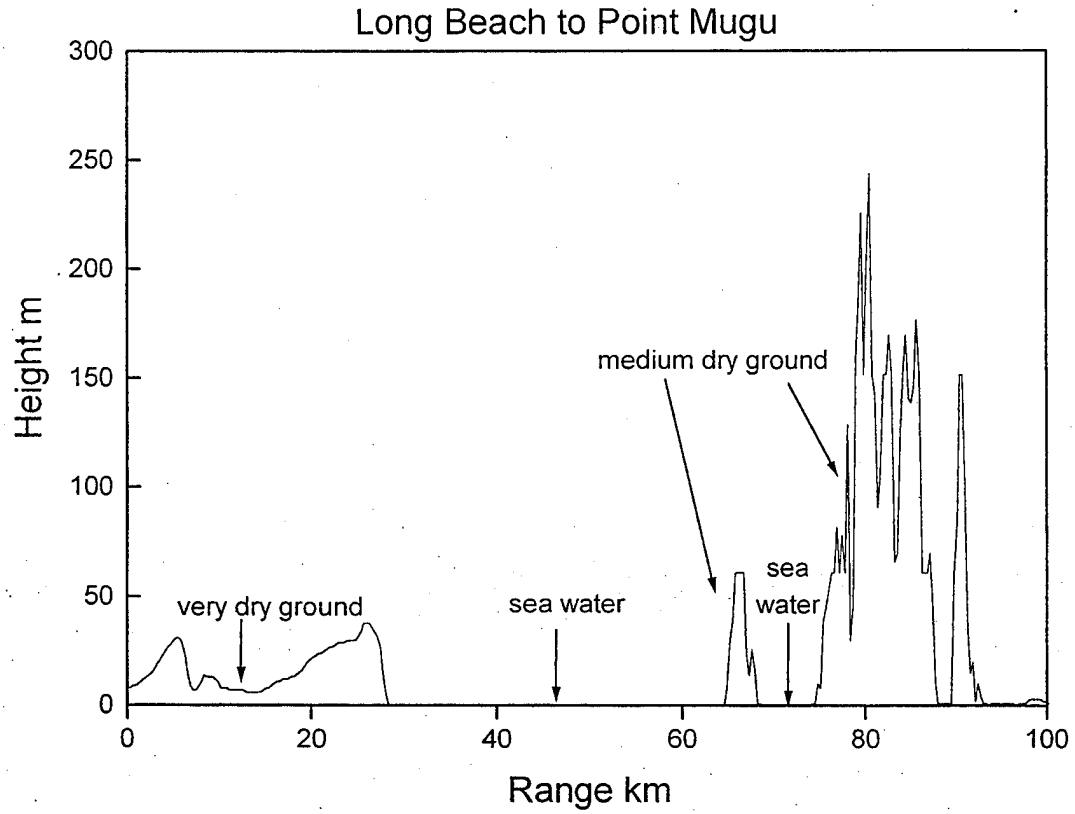
Long Beach to Point Mugu
Height m
300
250
200
150
100
50
0
0
20
40
60
80
100
Range km
very dry ground
sea water
medium dry ground
sea
water

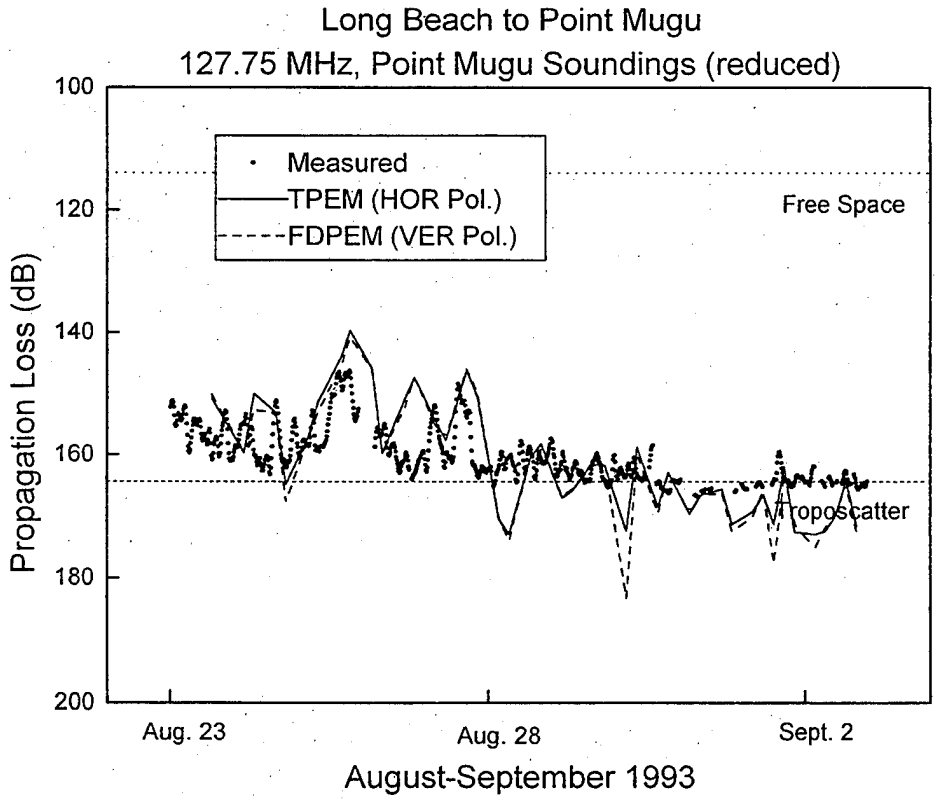
Long Beach to Point Mugu
127.75 MHz, Point Mugu Soundings (reduced)
Propagation Loss (dB)
100
120
140
160
180
200
Measured
TPEM (HOR Pol.)
FDPEM (VER Pol.)
Free Space
Troposcatter
Aug. 23
Aug. 28
Sept. 2
August-September 1993

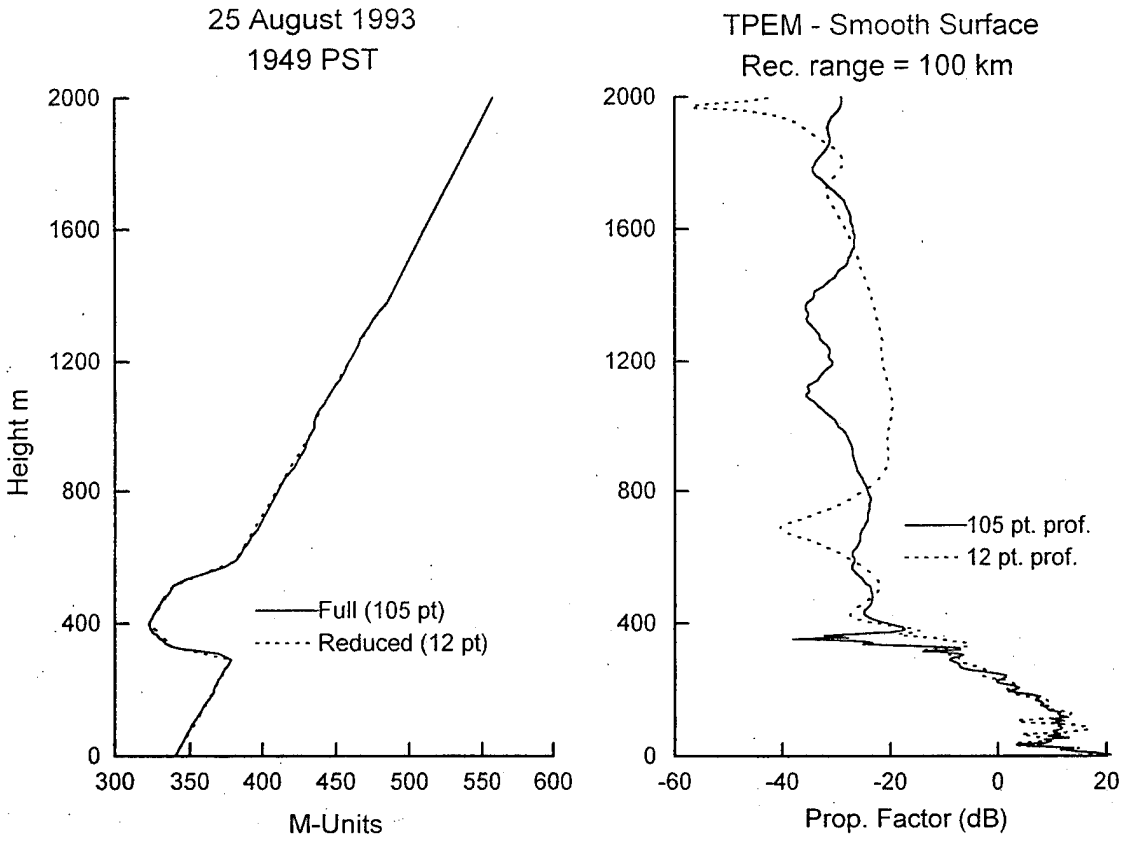
25 August 1993
1949 PST
Height m
2000
1600
1200
800
400
0
300
350
400
450
500
550
600
M-Units
Full (105 pt)
Reduced (12 pt)
TPEM - Smooth Surface
Rec. range = 100 km
-60
-40
-20
0
20
Prop. Factor (dB)
105 pt. prof.
12 pt. prof.

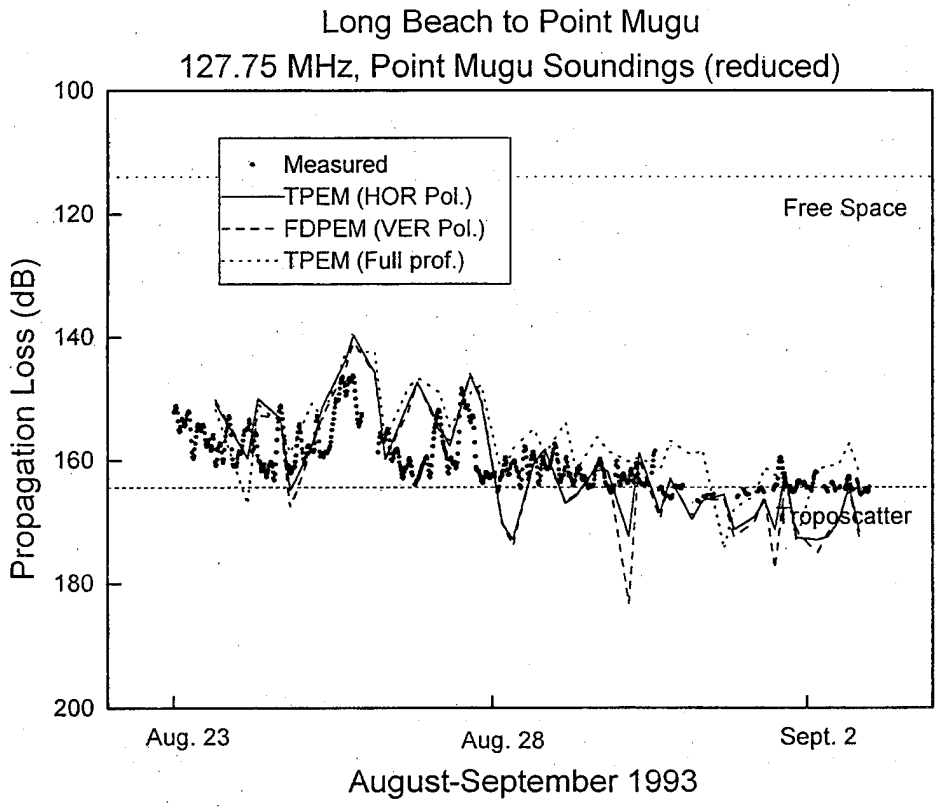
Long Beach to Point Mugu
127.75 MHz, Point Mugu Soundings (reduced)
Propagation Loss (dB)
100
120
140
160
180
200
Measured
TPEM (HOR Pol.)
FDPEM (VER Pol.)
TPEM (Full prof.)
Free Space
Troposcatter
Aug. 23
Aug. 28
Sept. 2
August-September 1993

Summary

- TPEM is an efficient radiowave propagation model.
- Agrees with measured data for homogeneous and inhomogeneous refractivity environments over varying terrain.

Ms. Molly Barrios, "Capabilities and Limitations of the Terrain Parabolic Equation Model (TPEM)"

DISCUSSION

S. MARCUS
Is the dependence of predictions on number of points characterizing the refractivity profile due to idiosyncrasies of the programs or based on the physics of the problem?

AUTHOR'S REPLY
I do not think it is due to the models since several different PE models and a waveguide model (MLAYER) gave the same result. The difference in predictions is due to the fact that you're losing information about the small scale structure of the profile when the number of points (height/refractivity pairs) is reduced.

S. Fast
(1) Would you show the locations of the transmitter and receiver on the terrain profile for the measurement vs. prediction case?
(2) Could you explain the "white" space in shadow regions in the first coverage diagram?

AUTHOR'S REPLY
(2) The white space in the diffraction regions indicates areas where the propagation loss exceeds the maximum loss threshold defined by the legend - in this case, 170 dB.

VTRPE: A Variable Terrain Electromagnetic Propagation Model for Littoral Environments

F.J. Ryan
Naval Command, Control and Ocean Surveillance Center
RDT&E Division CODE 712
San Diego, CA 92152-5000
e-mail: ryan@nosc.mil

This paper describes a novel variable terrain electromagnetic propagation model, VTRPE, that is based upon the parabolic wave equation (PE) method and designed for anomalous propagation predictions in range varying environments. The VTRPE code is a full-wave (i.e. amplitude and phase) numerical solution for the propagating electric and magnetic fields in heterogeneous media. Unlike methods based upon ray or physical optics solutions, it is a rigorous numerical solution which implicitly includes diffractive and caustic phenomena. The VTRPE code solves the parabolic wave equation using a very efficient split-step Fourier marching algorithm. Both Leontovich impedance type and two-sided type surface boundary conditions can be modeled. The code handles either vertically or horizontally polarized radiation from arbitrary source apertures including antenna side lobes. The VTRPE model allows for spatially varying atmospheric refractivity, variable terrain elevation profiles, and varying surface dielectric properties. Frequency dependent medium absorption, both in the atmosphere and earth, are also modeled. The nominal frequency range of the model is HF-MMW (1MHz-100GHz) with execution times increasing with frequency.

The VTRPE model is configured to operate on computers ranging from PCs to super-computers. Sample outputs from the VTRPE model will be shown that illustrate various types of anomalous propagation effects including: 1) knife-edge diffraction over ridges, 2) beyond-line-of-sight propagation, 3) atmospheric ducting, 4) surface wave propagation, and 5) rough surfaces. Comparison of VTRPE outputs with selected analytical test cases including Norton's solution for Sommerfeld problems, normal mode methods, and wave number integration methods will be made.

[*Editor's note: no presentation graphics were provided by the author for inclusion in this proceedings.*]

The EEMS Hybrid PE Models for Fast Propagation Assessment

M.F. Levy and K.H. Craig
Signal Science Ltd and Rutherford Appleton Laboratory
U.K.

For EM propagation forecasting in mixed land/sea environments, traditional PE techniques are too slow for operational requirements. One way forward is provided by hybrid PE techniques, which satisfy speed constraints without loss of accuracy. The horizontal PE technique (HPE) is used to extend low altitude results obtained with the usual vertical PE method (VPE). In many instances further speed-ups are possible with the use of non-local boundary conditions to truncate the VPE integration domain. We apply these hybrid PE techniques to the fast calculation of coverage diagrams for airborne or shipborne antennas, in environments including terrain and anomalous atmospheric refraction.

The EEMS hybrid PE models for fast propagation assessments

M.F. Levy and K.H. Craig
Signal Science Ltd
Rutherford Appleton Laboratory
U.K.

EEMS propagation models

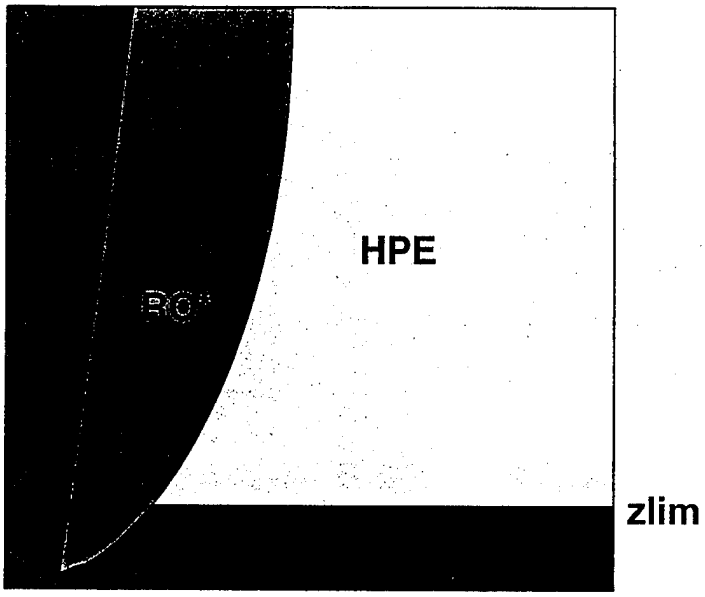

FE: Flat Earth *adapted from RPO
RO: Ray Optics *adapted from RPO
VPE: Vertical Parabolic Equation
HPE: Horizontal Parabolic Equation

Horizontal PE Method

- The propagation medium is usually "standard" above a certain height
- HPE is a novel method which permits rigorous integration of the outgoing wave equation above that height
- HPE allows considerable speed-up of PE coverage calculations
- HPE also provides substantial economies of memory
- HPE is valid for any antenna height
- Terrain and atmosphere can be arbitrary below the threshold height

Improved HPE method

- Can cope with negative M-gradients above antenna
- OK if no energy propagates back down, i.e. layers are not trapping
- Allows lower zlim threshold between VPE and HPE regions, as high layers can be modelled with HPE.

Choice of regions

- VPE/HPE limit determined by zlim
  - include in VPE region all ducting layers starting less than 500 m above antenna
  - zlim must be larger than maximum terrain height
- RO/PE limit determined by psilim
  - psilim large enough to avoid trapping
  - psilim large enough to avoid terrain

FFT sizes

- FFT size in VPE depends on psilim and zlim. VPE must cope with propagation angles reached below VPE by rays reflected from the ground at an angle less than psilim.
- FFT size in HPE depends on maximum propagation angle in HPE region at height zlim.

EEMS integration times

- Not very sensitive to antenna pattern
- Dependence on domain size:
  - approximately linear on maximum range
  - approximately logarithmic on maximum height
- Dependence on frequency is approximately linear
- Main constraints are antenna height, maximum terrain height and height of ducting layers.

Typical EEMS integration times on 100 MHz Pentium

Freq (GHz)	Antht (m)	Xmax (km)	Zmax (m)	Tmax (m)	Dmax (m)	Timing
3	25	200	5000	0	100	6s
10	25	200	5000	0	100	15s
3	25	300	5000	300	300	40s
10	1000	300	5000	300	300	8min

EEMS: 3 GHz example

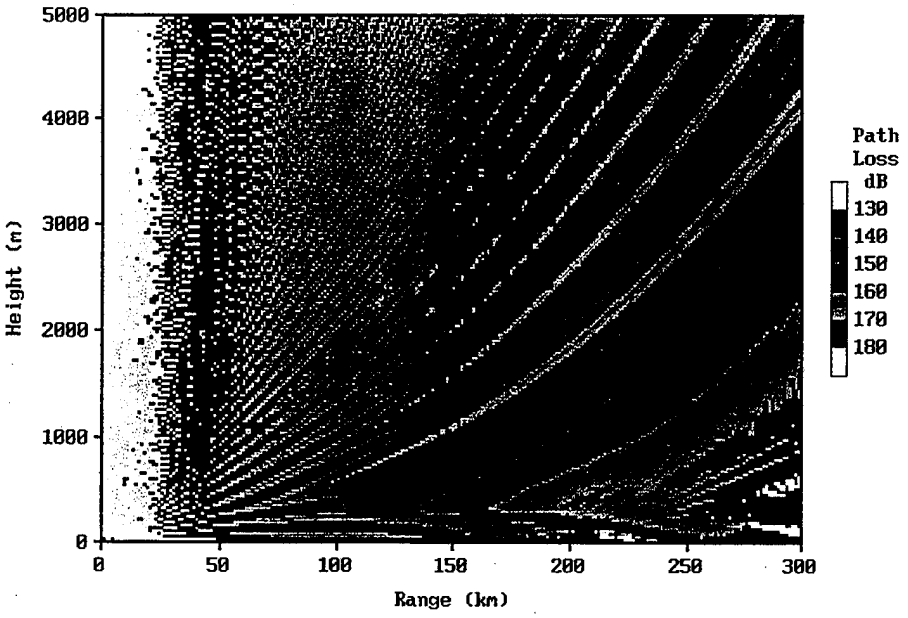

Work for EEMS phases 2 and 3

- Speed-up for high antennas
- Optimisation of hybrid model for land-to-sea and land-to-land applications
- Range-dependent models
- Mixed transform VPE for better treatment of terrain effects
- Models for HF comms

Speed-up for high antennas

- Standard VPE domain must include source
  - Large VPE domain for high antennas
  - Longer integration times
- Idea: use non-local boundary conditions (NLBCs) to truncate PE domain
  - Truncated VPE domain need not include source
  - Truncated VPE domain related to environment
  - Extend to high altitudes with generalized HPE
- Applications
  - Helicopters
  - E-3

PE methods for high altitude source

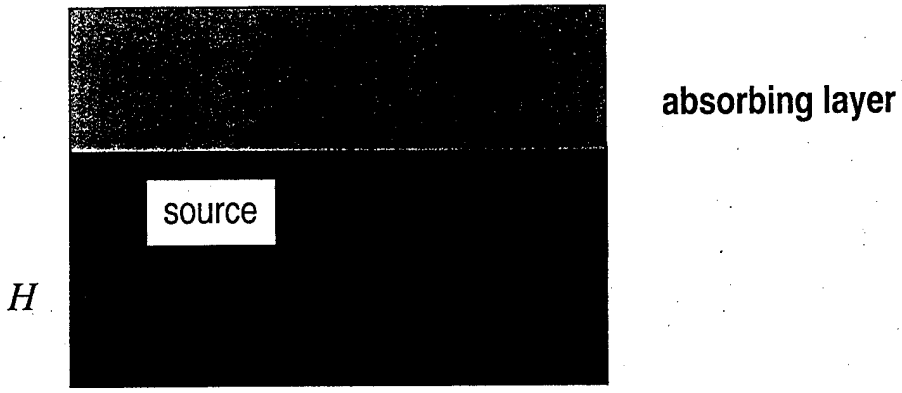

Traditional PE method: domain must include source and absorbing layer

PE with NLBC: no need to include source for low altitude coverage

Current EEMS for high antennas

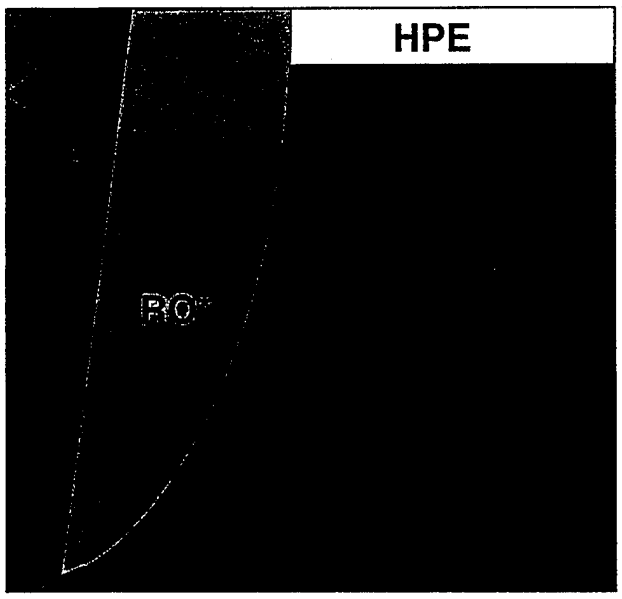

zlim

* FE and RO models are adapted from RPO

Future EEMS for high antennas

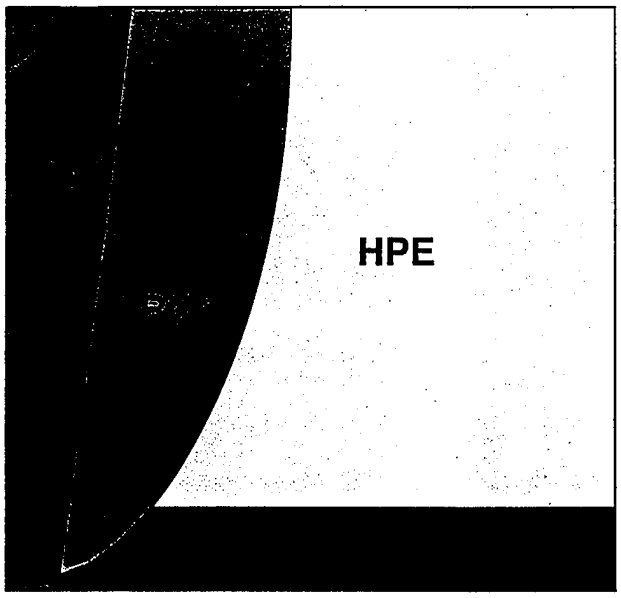

zlim

* FE and RO models are adapted from RPO

Local and non-local boundary conditions

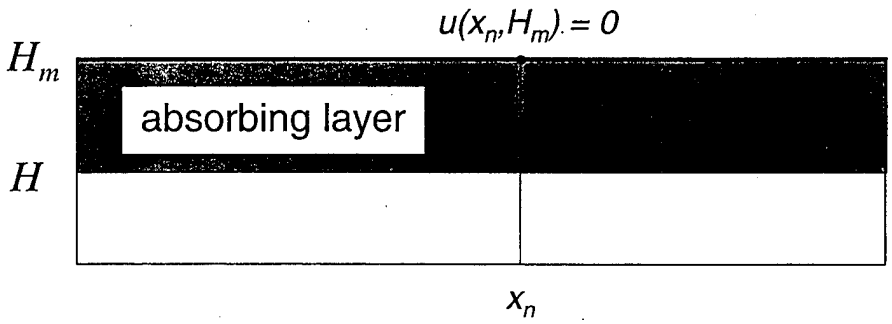

local BC at range x_n : only local range is involved

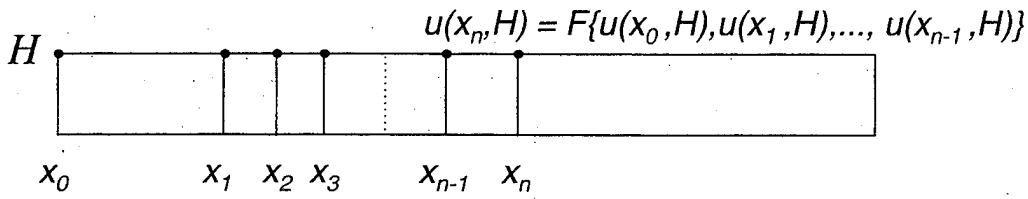

NLBC at range x_n : all previous ranges are involved

Derivation of NLBCs

- Obtained by matching the field above *H* (closed-form solution of a partial differential equation) with the field below *H*.
- In the form of a convolution integral + a term representing incoming energy from sources above the domain
  - Convolution kernel involves Airy functions for the linear case
  - Incoming energy term expressed with Fresnel-like integrals

Truncated PE methods

- Finite difference:
  - models ground reflections
  - needs small range step (typically 25 m)
- FFT:
  - will treat ground as non-reflecting (could be an advantage for high antennas)
  - allows large range step (typically 250 m)

Truncated PE work

- Implemented:
  - source can be below or above VPE domain
  - beam pattern is Gaussian
  - finite-difference implementation
  - generalized HPE
- Future:
  - arbitrary beam pattern
  - FFT implementation
  - optimization of generalize HPE
  - Merge with FE/RO models

Truncated PE + HPE example

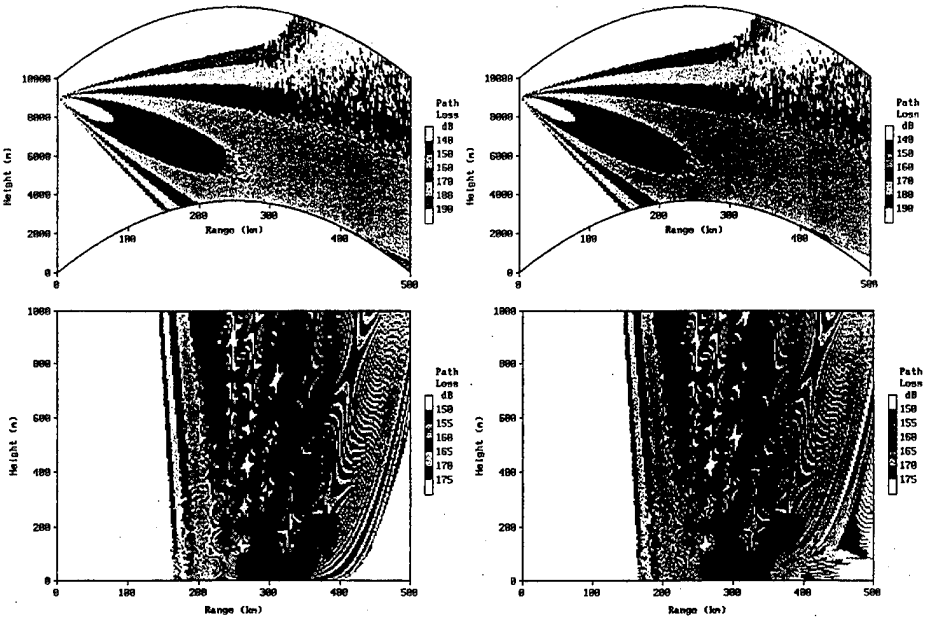

Standard atmosphere Ducting layer 0-100m

3 GHz source VPE/HPE boundary at 100 m

Conclusions

- EEMS engine based on hybrid VPE, HPE, ray-trace
- EEMS models both terrain and atmospheric effects
- EEMS allows arbitrary antenna beam pattern
- EEMS engine is very fast for low antennas
- Speed-up for high antennas in next phase

Ms. Mireille Levy, "The EEMS Hybrid PE Models for Fast Propagation Assessment"

DISCUSSION

S. MARCUS

1) Is the sequence of calculations: (1) VPE and then (2) HPE?
2) What is the upper boundary condition for the VPE?

AUTHOR'S REPLY

1) First the VPE is used to obtain the solution on the initial HPE horizontal (this initial solution could also be obtained with any other method calculating both amplitude and phase of the field, like mode theory). Then HPE can be run.
2) The upper boundary condition for the VPE can be an exact NLBC if one wished to stop the VPE region exactly at the VPE/HPE boundary. It can also use an absorbing layer above the VPE/HPE boundary. The only requirement is that the VPE solution must be accurate on the VPE/HPE boundary.

D. Dockery

In your model, have you been able to implement a NLBC at the top of the "VPE" region and simultaneously a good surface boundary condition while using a split-step solution?

AUTHOR'S REPLY

No, I have not been able to apply "good" conditions simultaneously on the top and bottom of the domain with a Fourier split-step solution. I suspect that if a solution exists, it involves very complex transforms.

H. HITNEY

For a high-altitude source near an elevated duct, wouldn't the VPE region need to exceed the top of the elevated duct?

AUTHOR'S REPLY

Yes, the VPE region would have to include all the ducts below the source, at least for the simplest implementation of the model. At a later stage it should be possible to limit the VPE region to a strip including trapping layers and to extend the solution on either side with HPE methods.

S. Burk

In meteorological models, terrain-following* coordinates are frequently used rather than a fixed, Cartesian grid. Are such coordinate systems also used in PE models such as the one you describe?

* that is, a coordinate transformation is made such that the lower surface everywhere becomes a coordinate surface

AUTHOR'S REPLY

The split-step PE model in EEMS does indeed use such a coordinate system, as it makes implementation of the boundary condition at the ground easier.

R. JANASWAMY

When you have an elevated antenna above Z_{lim}, how do you couple energy into the VPE through the NLBC? Will the NLBC that permits energy propagation downward into the VPE region be compatible with the terminating condition at Z_{lim} for NLBC?

AUTHOR'S REPLY

The NLBC couples energy into the VPE region via an integral term which matches the source. There is no difficulty adding this term to the homogenous NLBC expressed with a convolution kernel.

The IFDG Package for Propagation Predictions in an Inhomogeneous Troposphere over Irregular Terrain

Sherman Marcus
RAFAEL
Haifa, Israel

Until recently, computational investigations of electromagnetic duct propagation in the troposphere were limited to horizontally uniform media. The advent of numerical grid methods based on parabolic equations led to the capability for considering horizontal variations, but until recently the split step methods on which most of these were based only permitted such variations in the atmospheric medium and not in the ground boundary. This limitation and others were overcome by a finite difference implementation which, in addition to fully accounting for terrain and atmospheric variations, does not utilize an artificial absorbing layer to truncate the computational domain. This method is called IFDG (Implicit Finite Difference - Green's function) [1].

Although the capability to consider irregular terrain has since been incorporated into models based on split step algorithms, the fact that IFDG does not require an artificial absorbing layer as its upper boundary makes it unique. Instead of such an absorbing layer, IFDG places an imaginary bounding plane above the highest point of the terrain and above all inhomogeneities of the propagation medium. Since the region above this plane is homogenous, an analytical solution may be found there based on the fields along the plane. This solution is based on a Green's function formalism. For each successive horizontal range, this field in the homogeneous region is matched to the field in the lower inhomogeneous region along the plane interface [2]. Because of this "localization" of the computational grid, IFDG could be expected to be particularly advantageous for problems in which the height difference between highest and lowest points is small. The Green's function boundary condition has also been used successfully in underwater acoustic propagation [2,3] and in propagation of gravity waves [4].

The "initial" condition for the finite difference procedure is obtained from standard solutions in horizontally homogeneous environments. Thus, if the atmosphere is standard, the Norton expressions are used for small initial distances [5], and a Bremmer series is used for large initial distances [6]. For large initial distances in a duct environment, a modal series is used to compute the initial condition [7].

IFDG has been included in several impartial comparison studies. One such study compared it and other models to measured data [8]. In this evaluation, IFDG produced the best

results based on standard deviations from the measurements, but all the models produced poorer results at higher frequencies.

REFERENCES

[1] Marcus, S.W., "A hybrid (finite difference - surface Green's function) method for computing transmission losses in an inhomogeneous atmosphere over irregular terrain", IEEE Trans. Antennas Propagat., Vol. 40, No. 12, Dec. 1992.

[2] Marcus, S., "A generalized impedance method for application of the parabolic approximation to underwater acoustics", J. Acoust. Soc. Am., Vol. 90, No. 1, July 1991.

[3] Marcus, S., "A generalized impedance method for application of the parabolic approximation to propagation in an ocean overlying an elastic bottom", in Structural Acoustics, Scattering and Propagation, J.E. Flowcs Williams, D. Lee, A.D. Pierce, Eds.,World Scientific Publishing, 1994.

[4] Dalrymple, R.A., Martin, P.A., "Perfect boundary conditions for parabolic water-wave models", Proc. R. Soc. Lond. A, Vol. 437, pp. 41-54, 1992.

[5] Norton, K.A., "The propagation of radio waves over the surface of the earth and in the upper atmosphere, Part II", Proc. IRE, vol. 25, no. 9, pp. 1203-1236, Sept. 1937.

[6] Bremmer, H., Terrestrial Radio Waves, Elsevier Publishing Co., New York, 1949.

[7] S. Marcus, "A model to calculate em fields in tropospheric duct environments at frequencies through shf", Radio Science, vol. 17, no. 5, pp. 895-901, Sept.-Oct. 1982.

[8] Andersen, J.B., Hviid, J.T., Toftgard, J., "Comparison between different path loss prediction models", COST 231-TD(93)-06, Jan. 1993, Barcelona.

THE *IFDG* PACKAGE

FOR PROPAGATION PREDICTIONS

IN AN INHOMOGENEOUS ATMOSPHERE

OVER IRREGULAR TERRAIN

- TECHNICAL BACKGROUND, UNIQUENESS
- SAMPLE COMPUTATIONS
- VERIFICATION, OTHER APPLICATIONS
- ADVANTAGES / DISADVANTAGES

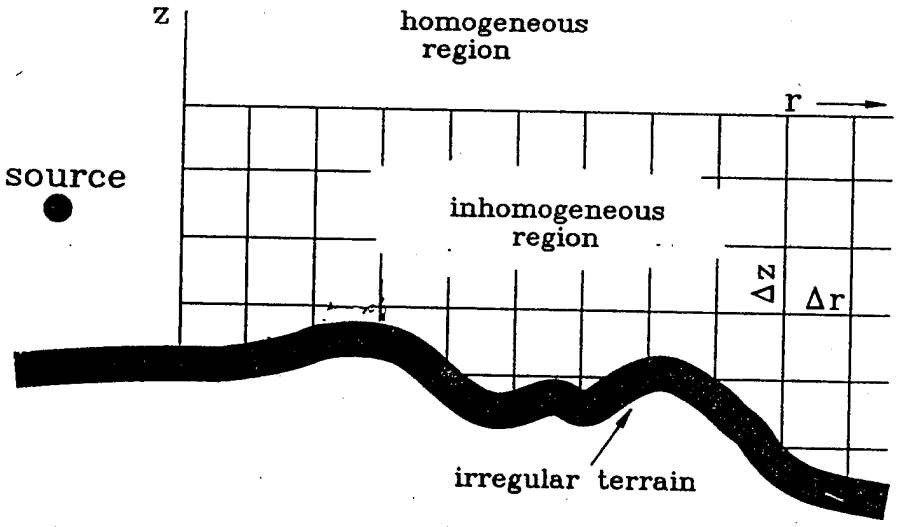

Numerical mesh configuration for IFDG method.

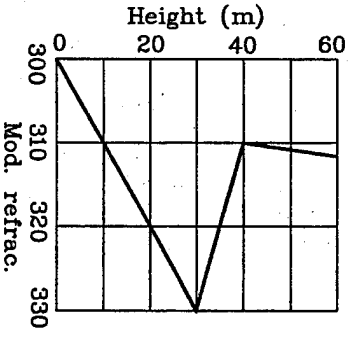

Fig. 2 Modified refractivity profile producing a 30 m thick duct.

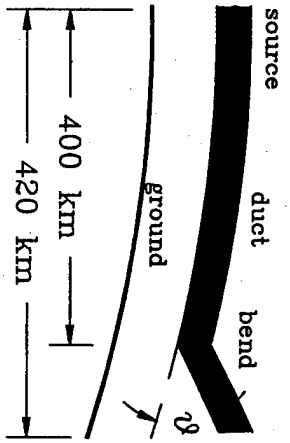

Fig. 1 Duct with bend.

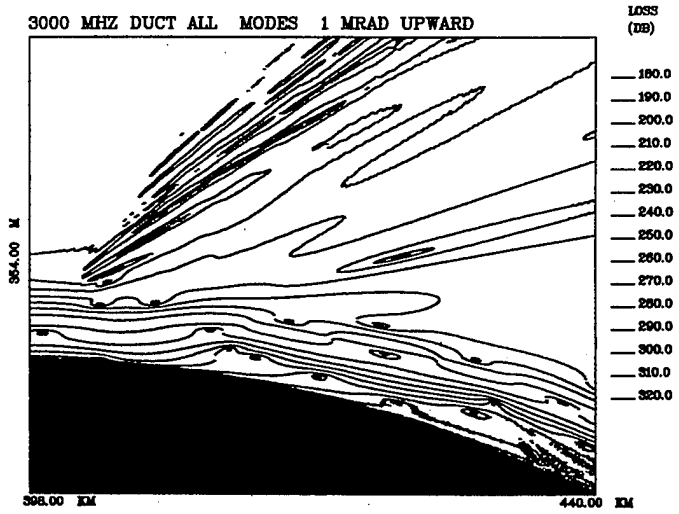

Path losses in duct with mrad bend at r=400 km, f=3 GHz.

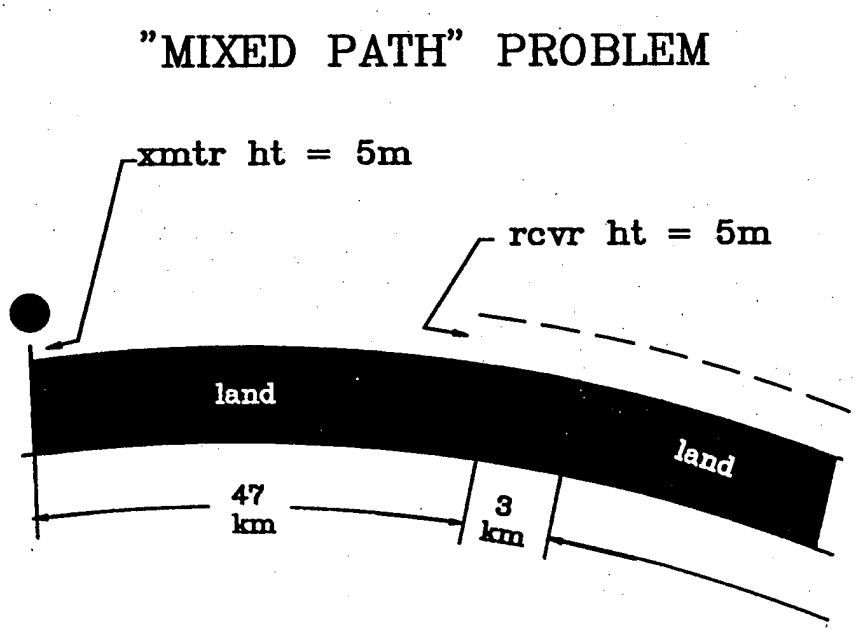

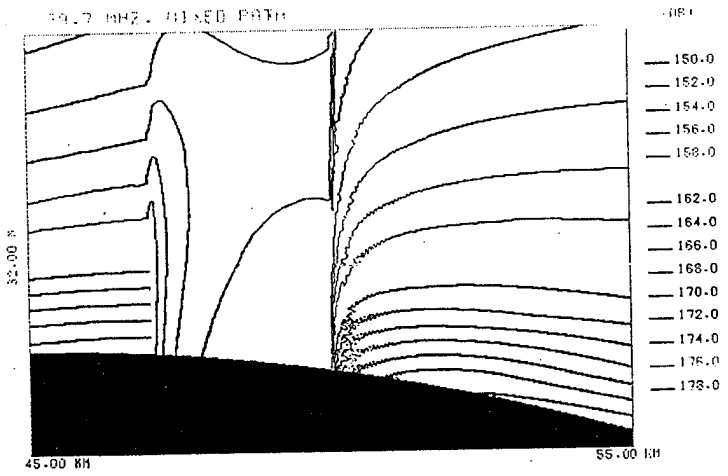
150.0
152.0
154.0
156.0
158.0
162.0
164.0
166.0
168.0
170.0
172.0
174.0
176.0
178.0
45.00 KM
55.00 KM

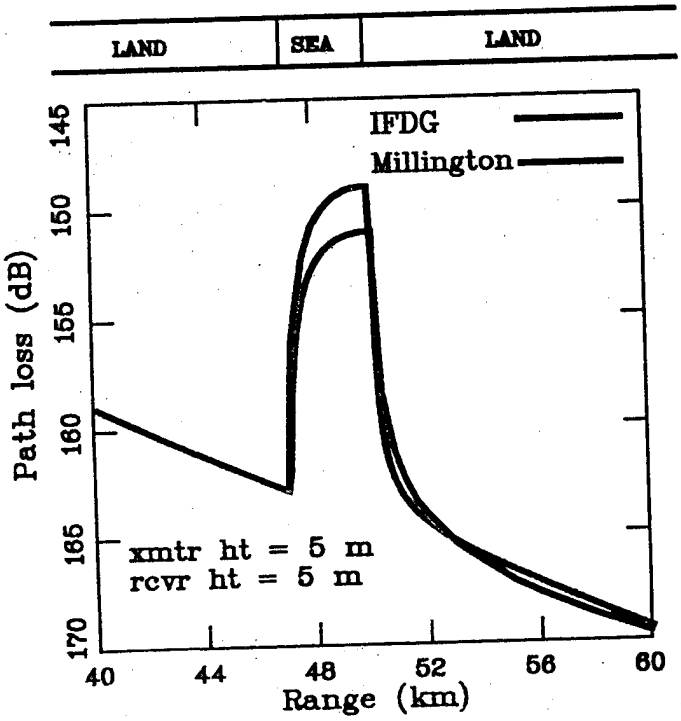
LAND
SEA
LAND
IFDG
Millington
xmtr ht = 5 m
rcvr ht = 5 m
Path loss (dB)
145
150
155
160
165
170
40
44
48
52
56
60
Range (km)

ADVANTAGES

- no artificial absorbing layer
- efficient for small height differentials
- can start iterations far from source

DISADVANTAGES

- impractical for large height differentials

OTHER AREAS OF APPLICATION

underwater acoustic propagation
(with and w/o bottom shear)
S. Marcus

atmospheric acoustic propagation
non-reflecting b.c.'s
R. Jardine, W. Siegmann,J. Robertson

gravity (water) waves
perfect b.c.'s
R. Dalrymple, P. Martin

PROPAGATION MODELS USED FOR SAMPLE CASES

IFDG

implicit finite differences
general atmosphere
irregular terrain

HAP

mode expansions
ray expansions
horizontally homogeneous atmosphere
smooth earth

RADAR PROPAGATION IN A TURBULENT ATMOSPHERE: A RANDOM PROFILES GENERATOR

E.MANDINE [1][2], M.C.PELISSIER [2], and C.GIANNILEVIGNE [1]

[1]: CTSN/LSA - B.P. 28 - 83800 Toulon Naval (France)
Tel: (33) 94 11 41 67 - Fax: (33) 94 06 88 69
[2]: Universite de Toulon - Laboratoire Modelisation et Signal/ETMA/MNC -
B.P. 132 - 83957 La Garde (France)
Tel: (33) 94 14 24 80 - Fax: (33) 94 14 24 48 - Email: mcpel@isitv.univ-tln.fr

Abstract:

In the frequency range of 100 MHz-20 GHz, and more precisely in the case of grazing angles of emission, the effects of atmospheric turbulence on radar propagation cannot be neglected any longer.

We now come to model these effects as random fluctuations of the refractive index. Two problems have then to be solved:

1 - numerical generation of realistic random fluctuations,
2 - resolution of the propagation equation with random coefficients.

In a first step, we mainly concentrated our efforts on problem 1.

Problem 2 has been solved in a simple way : our propagation model is a (deterministic) usual 2D parabolic code, with a finite differences - Crank Nicolson solver. We use a standard Monte Carlo method to obtain the mean electromagnetic field from a distribution of random refractive index.

We now come to problem 1 : turbulent processes are usually characterized through their spectrum; it describes, in the spatial frequencies domain, the spectral distribution of index fluctuations induced by the turbulent motion of the fluid. We check the inadequacy of some well known turbulence model for the radar configuration and the frequency range concerned, and propose a new model, which we call the K.G. spectrum. We then test the influence of anisotropic turbulence, at grazing angles, in a frequency range of 100 MHz to 20 GHz.

References:

(1) E.Mandine : *Rapport d'avancement°2*, document CTSN/LSA, Oct 1994

(2) E.Mandine, M.C.Pelissier : *Construction d'un generateur de profils aleatoires - Application a la propagation radar en milieu turbulent*, 15eme Colloque GRETSI, 18-22 sept. 1995, Juan les Pins (France)

ELECTROMAGNETIC PROPAGATION WORKSHOP
July 18-20, 1995

RADAR PROPAGATION IN A TURBULENT ATMOSPHERE : A RANDOM PROFILES GENERATOR

E.MANDINE (1)(2), M.C.PELISSIER (2), and C.GIANNILEVIGNE (1)

(1) : CTSN/LSA - B.P. 28 - 83800 Toulon Naval (France)
Tel : (33) 94 11 41 67 - Fax : (33) 94 06 88 69

(2) : Universite de Toulon - Laboratoire Modelisation et Signal /ETMA/MNC - B.P. 132 - 83957 La Garde (France)
Tel : (33) 94 14 24 80 - Fax : (33) 94 14 24 48 - Email : mcpel@isitv.univ-tln.fr

Abstract :

The influence of atmospheric turbulence on electromagnetic propagation is well known over the 10 GHz frequencies. We attempt to show that, in the case of grazing angle of propagation, strong anisotropic components of atmospheric turbulence can also have significant effects at lower frequencies. We choose to model this effects as random fluctuations of the refractive index and propose a new realistic turbulence model : the K.G. spectrum. We then use it as an input in a parabolic propagation model to test the influence of anisotropic turbulence, at grazing angles, for a 3 GHz frequency.

Introduction :

In order to deduce the radar coverage, a propagation model has to incorporate the effects of the atmospheric flow over the concerned area. Of course large-scale phenomena dominate. But they are not the only cause of the deterioration in radar performances : small scale, highly chaotic perturbations lead to random fluctuations of the refractive index. Their influence increases with the frequency, the order of magnitude of the radar wave approaching that of the medium heterogeneousness.

It is thus interesting to parametrize, in a propagation model, the effects of atmospheric turbulence. These effects are well known over the 10 GHz frequencies. But in the case of grazing angles of transmission it seems that much lower frequencies can be concerned.

In a first part we briefly present the parabolic propagation model. Part two focuses on the representation of the turbulent process : we propose a random profiles generator based on a spectral characterisation of the turbulence. We discuss the relevance of the usual Kolmogorov spectrum and propose a new model, which we call the K.G. spectrum.

In the last part, some numerical results are presented.

I) The parabolic propagation model Corafin

Corafin (for COuverture RAdar FINe in french) is a usual 2D parabolic code, with a finite differences - Crank Nicolson solver, developped by M. Fournier ([1]). The initial field is calculated by a geometrical optics method ; we assume that the distance beetween the transmitter and the 0-range is sufficiently small to keep the refractive index constant over the path. It is to be noted that the evaluation of this starting field does not take into account the roughness of the sea in the Fresnel reflexion coefficient.

The lower boundary condition is, at present, the simplest : the sea surface is supposed to be perfectly plane, the dielectric permittivity being sufficiently high to allow Leontovich approximation and characterization of the sea effect by a surface impedance.

On the upper bound, a Sommerfeld condition on the field is simulated by adding an artificial absorbing layer to the physical domain.

II) - Radar propagation in a turbulent atmosphere

2.1 - Random profiles generator

Propagation modelling in a turbulent atmosphere is a well studied subject, particulary since the parabolic equation method has appeared, because of the tractable aspect of this model for numerical simulations.

In this study, we model the turbulent effects as random fluctuations of the refractive index, and add them to the mean deterministic refractive profile. The propagation equation with random coefficients is then solved in a simple way : using the (deterministic) model Corafin, we develop a standard Monte Carlo method to obtain the mean electromagnetic field from a distribution of random refractive index.

The main problem is the generation of this random refractive index term. Turbulent processes are usualy

characterized through their spectrum ; it describes, in the spatial frequencies domain, the spectral distribution of index fluctuations induced by the turbulent motion of the fluid. Our random profiles generator is thus based on inverse Fourier transform from a given turbulent spectrum ϕ. We construct an intermediate spectrum ψ in order to obtain by FT^{-1} the spatial fluctuations of the refractive index, with the expected spectral distribution ϕ. (An inverse transform applied on the spectrum ϕ would have given the correlation function).

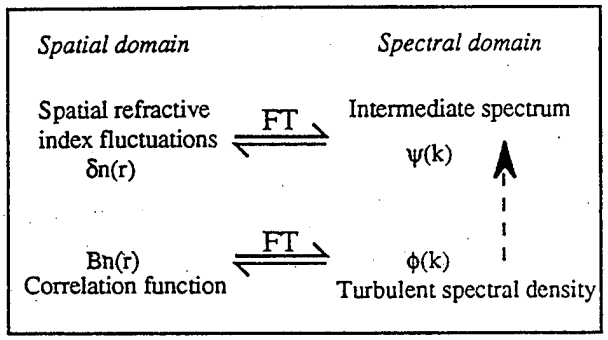

More precisely, ψ is the complex spectrum, $\psi = \psi_r + j\psi_i$, where ψ_r and ψ_i are, respectively, even and odd spectral processes obtained by the filtering of independant gaussian noises B and B' by $\sqrt{\phi}$.:

$$\begin{cases} \psi_r(\vec{k}) = B\sqrt{\phi(\vec{k})} \\ \psi_i(\vec{k}) = Bsign(\vec{k})\sqrt{\phi(\vec{k})} \end{cases}$$

where k is the spatial wave vector of the turbulence, and the two white noises B and B' both have a zero mean value, and variance : $\langle B^2 \rangle = \langle B'^2 \rangle = \frac{1}{2}$

We can then prove that the result of the inverse Fourier transform has the required spectral distribution ϕ :

$$E\{|\delta n^2(r)|\} = E\{|\psi^2(k)|\} =$$
$$\phi_n(k)E\{B^2 + B'^2\} = \phi_n(k)$$

In the case of an inhomogeneous atmosphere, ϕ_n can depend on the height z : $\phi_n = \phi_n(k,z)$. An additional operation has then to be made : the atmosphere is discretised into horizontal homogeneous layers, inside which ϕ_n is kept constant in z. We then compute the FT^{-1} in each layer and apodize in z the different realizations obtained. It will be so with the second spectrum studied.

The main problem is now the choice of the turbulent spectrum.

2.2 - Kolmogorov spectrum.

Most of the works dealing with this subject turbulence choose the Kolmogorov spectrum [2],[3],[4]. It decreases like $k^{-11/3}$, for vertical wave numbers between the inner and the outer scales of turbulence, in the inertial subrange.

Furthermore, during the propagation, the assumption is usually made that two successive range steps are totally decorrelated, and new random refractive fluctuations are generated at each step during the computation.

A main characteristic of this spectrum is that the turbulent motions are assumed to be locally homogeneous and locally isotropic, i.e. the correlation function has to be replaced with the structure function. This enables the inhomogeneous behavior of the turbulent motion, particulary with respect to height, to be taken into account .

Doing this, one studies the effects of isotropic turbulence on radar propagation, and the results show that this effects become important and cannot be neglected in the frequency range over 10 GHz. Below this frequence, the isotropic turbulence is less influent and could be ignored.

But the theory of propagation in a turbulent medium shows that anisotropic components of turbulent motion can also have significant effects, particulary in the case of grazing angles of propagation and low observation angles of the scattered field, which represents a common radar detection configuration [5], [6]. For instance, at 3 GHz, and for low angles of elevation paths, the spatial turbulent wave number "selected" by the incident radar wave is approximatively of the order of 100 meters, which is strongly anisotropic turbulence scaleand cannot be represented by the Kolmogorov spectrum.

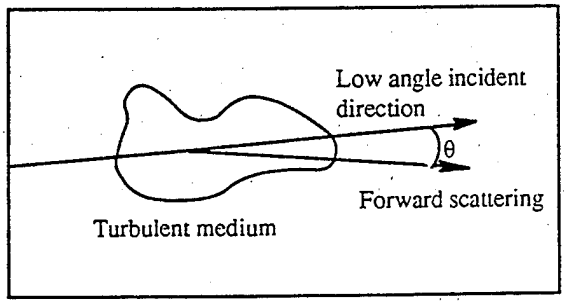

2.3 - K.G. Spectrum

To realistically assess tropospheric turbulence, we propose a new model, called the K.G. spectrum. This model enables us to generate stochastic index fluctuations with different correlation lengths L_h and L_v in horizontal and vertical directions. L_h is much greater than L_v, and simulate large eddies of turbulent motion, much more expanded in the horizontal direction due to the weightlessness.

In the vertical direction the spectrum keeps the Kolmogorov behaviour, in $k_z^{-11/3}$ where k_z is the vertical spatial wave number of the turbulence.

In the horizontal one, a problem appears when seaking for a theorical anisotropic spectrum : no fully satisfying expression is available, because this physical domain, where energy is introduced in the turbulent motion (input range), is not well known. We choose to assume a gaussian variation for the correlation function, $B_n(r)$, that is:

$$B_n(r) \propto \exp\left(-x^2/L_h^2\right)$$

where x is the horizontal coordinate.
The spectrum ϕ_n is then given by :

$$\phi_n(k_x) \propto \exp\left[-(k_x L_h)^2/4\right]$$

where k_x is the horizontal spatial wave number of the turbulence.

Furthermore, we add some inhomogenity by making L_h vary with respect to z ($L_h(z)$). This allows us to take into account the change of the horizontal eddy size with height, when weightlessness decreases, $\phi_n\left(\overset{\perp}{k}, z\right)$.

To keep the coherence of the model, L_h had to be larger than the range step size used to compute the parabolic equation solution.

III) Numerical results.

An exemple of the preliminary results obtained with Kolmogorov and K.G. spectrum is presented below ; we apply this method to the case of a 3 GHz antenna, located at 20 m above the sea, in the presence of a strong 100m surface duct. The " deterministic" loss propagation coverage is shown in fig.1, while fig. 2 and 3 present the mean loss diagram at 100m height and the field structure at 80km range, for the Kolmogorov spectrum and the K.G. spectrum. As expected, the isotropic turbulence appears to have no influence upon the propagation wave (fig 2). On the contrary, with the K.G. spectrum, scattered energy appears, particulary in the propagation hole just above the duct top.

Conclusion.

We propose a random profiles generator based on a spectral characterization of the turbulence. In some important cases, the usual Kolmogorov turbulent spectrum appears to be non relevant, because of the non-isotropy of the turbulent flow. It is for example the case at frequencies below 10 GHz , when grazing angles of propagation and low angles of observation of the scattered field are involved.

We construct a new model, which we call the K.G. spectrum, keeping the Kolmogorov isotropic characteristics in the vertical direction z, but allowing anisotropy in range by the mean of a Gaussian z-dependant component.
The preliminary numerical results are encouraging.

References :

(1) M. Fournier : *Etude de la propagation dans une atmosphere inhomogene par la methode de l'equation parabolique* ,
AGARD Conference Proceeding n° 453

(2) D. Roussef, *Simulated microwave propagation through tropospheric turbulence*,
IEEE Transactions on antennas and propagation, vol 40, n° 9, sept. 92.

(3) M.F. Levy, K.H. Graig, *millimetre-wave propagation in the evaporation duct*,
AGARD Conference Proceeding n° 454

(4) H.V. Hitney, *A practical tropospheric scatter model using the parabolic equation*,
IEEE Transactions on antennas and propagation, vol 41, n° 7, july 93.

(5)E. Mandine : *Rapport d'avancement n°2*, document CTSN/LSA, Oct. 1994

(6) E.Mandine, M.C.Pelissier : *Construction d'un generateur de profils aleatoires - Application a la propagation radar en milieu turbulent*, 15eme Colloque GRETSI, 18-22 sept. 1995, Juan les Pins (France)

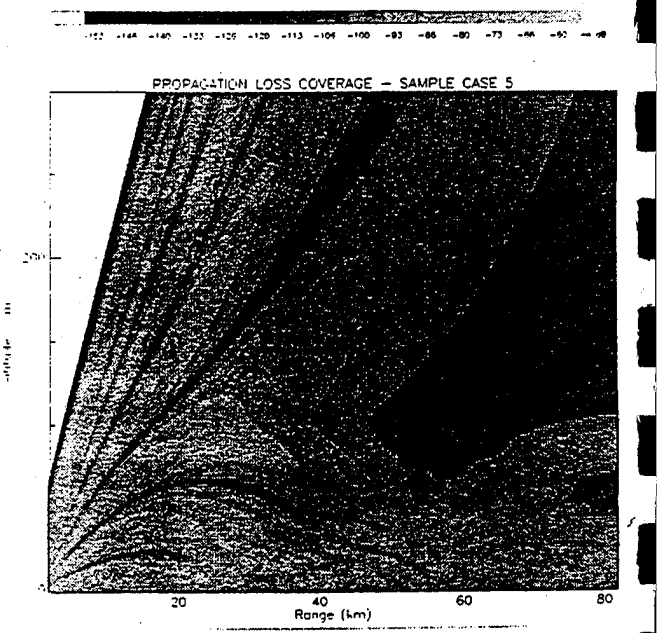

Fig 1 : Propagation loss coverage, 3 GHz transmission, transmitter height m, 100m duct

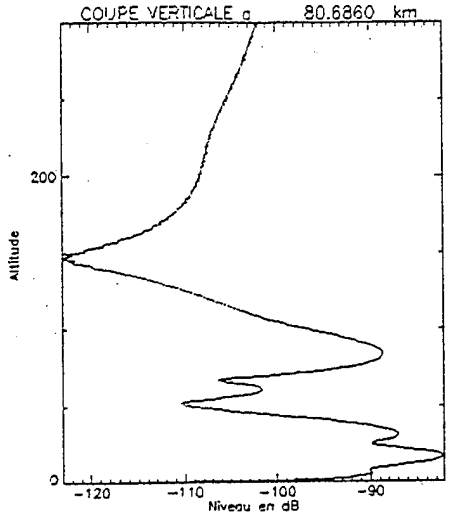

Fig 2: result with Kolmogorov spectrum: a-loss diagram b-field z-structure

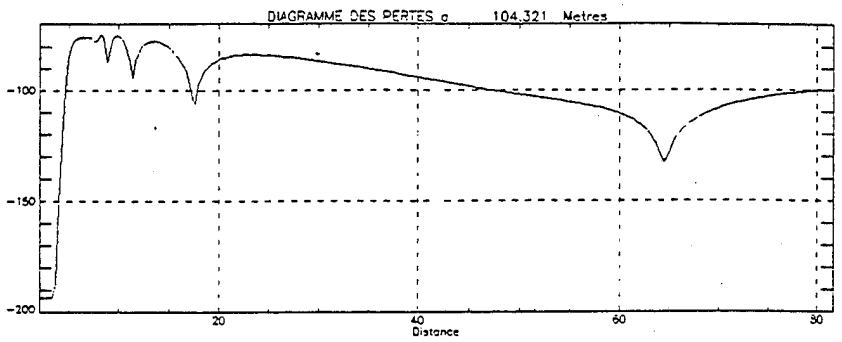

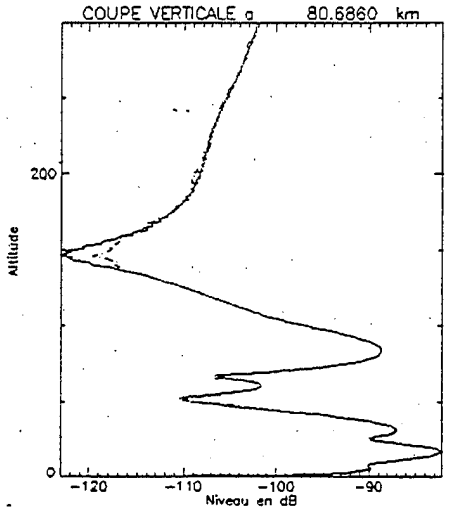

Fig 3: result with K-G spectrum: a-loss diagram b-field z-structure

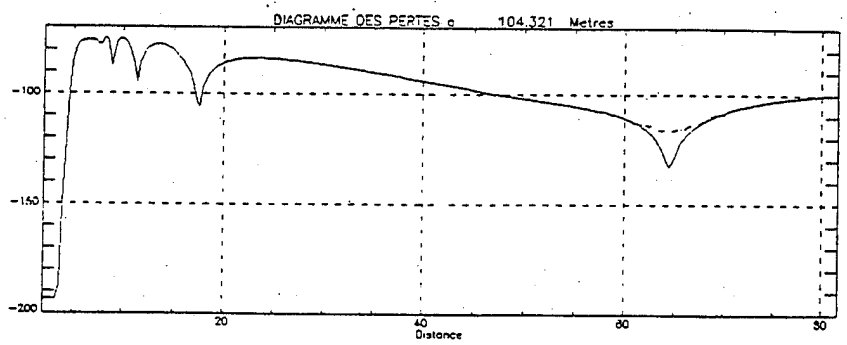

Example of realizations using :

- K.G. spectrum

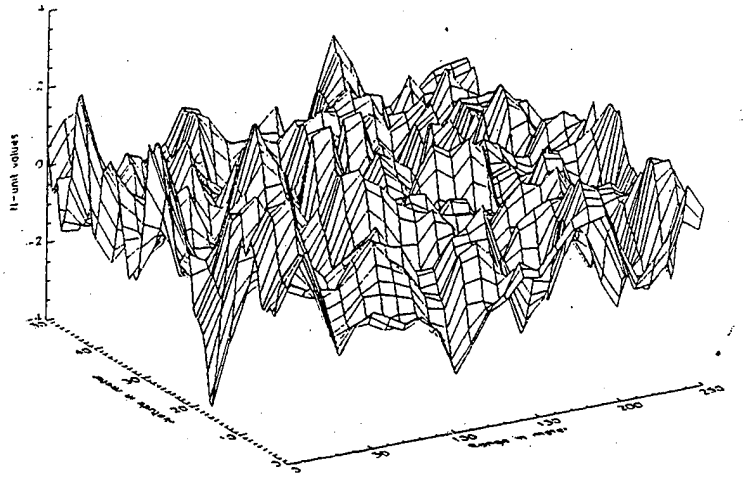

- Kolmogorov spectrum

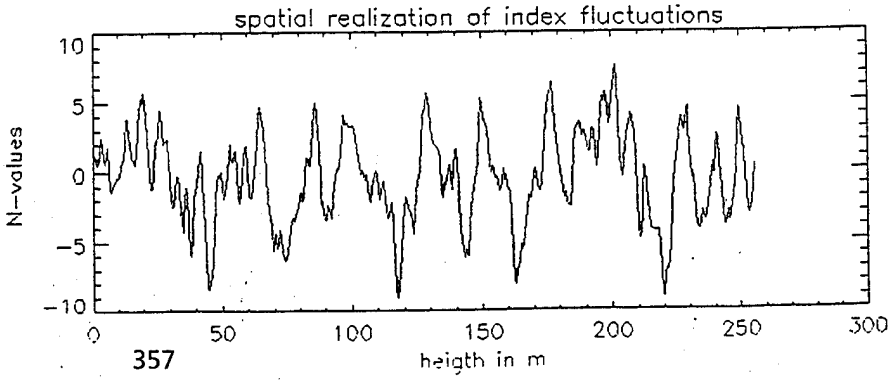

Mr. Eric Mandine, "Radar Propagation in a Turbulent Atmosphere: A Random Profile Generator Approach"

DISCUSSION

M. LEVITAS

Did the authors have a temporal correlation model for the turbulent atmosphere to complement their spatial correlation model?

AUTHOR'S REPLY

No, I didn't. PE model requires spatial refractive index fluctuations and gives coverage result for one-way propagation. So, it's assumed that the turbulence is "frozen" during all the propagation time, and we don't need to characterize the time variations of the turbulent motion.

ACCELERATED-INTERMEDIATE-REGION PROPAGATION MODEL

David G. Kenney*

The Accelerated Intermediate Region (AIR) propagation model is a collection of subroutines or modules whose primary output is the calculated reference basic median propagation loss (i.e., path loss) and mode of propagation based on spherical-earth propagation theory. Since AIR is a collection of subroutines, it can be integrated into a larger system to be used as an analysis tool.

When AIR is used, path loss is determined by using one of seven propagation modes. Six of the modes can be derived as ray-theory or wave-theory solutions from a single integral equation known as the diffraction equation. The seventh mode is based on an empirical troposcatter model. (The latest CCIR water-vapor and oxygen absorption models are incorporated to include absorption loss in all propagation modes). Only three of the seven propagation modes are required to develop a spherical-earth propagation model. The other four propagation modes were included to accelerate convergence of the solution in the intermediate region. The large number of propagation modes used to evaluate path loss is one of the features that distinguish AIR from existing spherical-earth propagation models.

Propagation mode selection is determined by empirical delimiters or curve-fits to empirical data. The mathematical expressions used in the mode-selection process are difficult to construct because of the complex dependence of propagation-mode applicability on several input parameters such as link geometry, ground constants, and frequency.

AIR is used to render the average deviation from exact theory negligible over a set of input parameters. The AIR mode-selection process yields the propagation mode with the fastest execution time that maintains a negligible deviation for a given set of input parameters. The AIR propagation model is valid over the following ranges of the input parameters:

frequency:	1 to 20000 MHz
antenna heights:	0 to 20000 meters
path distance:	0.01 to 2000 kilometers
atmospheric refractivity:	200 to 450 N-units
relative permittivity:	1 to 100
ground conductivity:	0.0001 to 100 S/m
water-vapor density:	0 to 110 g/m^3

The model has been coded in MICROSOFT FORTRAN for verification and has been tested extensively, using a 486 PC with 8 MB RAM and a clock speed of 33 MHz. Execution time depends on the specific set of input parameters and ranges from several microseconds to tens of milliseconds. Worst-case errors with magnitudes on the order of 2 dB occur at the boundaries of propagation-mode applicability. Within the boundaries of propagation-mode applicability, the deviation from the exact solution is negligible. A MICROSOFT WINDOWS version of the model has recently been developed in BORLAND C^{++} with a FORTRAN DLL.

Documentation addresses the engineering theory as well as the programming aspects of the algorithms used in the model.

*The author is with IIT Research Institute (JSC Division), under contract to the U.S. government. Presentations of papers and/or demonstrations are subject to government approval. D. Kenney (410) 573-7371.

ACCELERATED INTERMEDIATE REGION PROPAGATION MODEL

David Kenney
IIT Research Institute

ELECTROMAGNETIC PROPAGATION WORKSHOP
18 - 20 JULY 1995
JOHN HOPKINS UNIVERSITY APPLIED PHYSICS LAB

ACCELERATED INTERMEDIATE REGION PROPAGATION MODEL

- **ASSUMPTIONS**
  - homogeneous earth
  - standard atmosphere
  - Hertzian dipole source
  - primarily specular reflection (smooth earth)

ACCELERATED INTERMEDIATE REGION PROPAGATION MODEL

INPUT PARAMETER	RANGE
frequency	1 to 20000 MHz
antenna heights	0 to 20000 meters
path distance	0.01 to 2000 kilometers
atmospheric refractivity	200 to 450 N-units
relative permittivity	1 to 100
ground conductivity	0.0001 to 100 S/m
water vapor density	0 to 110 g/m^3

ACCELERATED INTERMEDIATE REGION PROPAGATION MODEL

INPUT PARAMETER	RANGE
frequency	1 to 20000 MHz
antenna heights	0 to 20000 meters
path distance	0.01 to 2000 kilometers
atmospheric refractivity	200 to 450 N-units
relative permittivity	1 to 100
ground conductivity	0.0001 to 100 S/m
water vapor density	0 to 110 g/m^3

ACCELERATED INTERMEDIATE REGION PROPAGATION MODEL

- AIR is an integrated collection of algorithms whose primary output is median propagation loss.
- propagation loss is determined by selecting one of seven propagation modes.
- only three modes are required to construct a non-interpolating spherical earth propagation model.
- other four propagation modes were included to *accelerate* convergence of the solution in the *intermediate region*.

ACCELERATED INTERMEDIATE REGION PROPAGATION MODEL

PROPAGATION MODES

- SPACE
  - » ray theory. direct + reflected
- GROUND
  - » ray theory. direct + reflected + surface
- RAYWAVE
  - » surface wave correction terms to extend ray theory solution to the common radio horizon.
- WAVEG
  - » wave theory. general Bremmer series solution.
- WAVEP
  - » wave theory. particular Bremmer series solution.
- WAVE-TROPO
  - » wave theory/troposcatter splice
- TROPO
  - » troposcatter solution

PROPAGATION MODE: WAVEG

For vertical polarization with $F_{MHz} < F_c$ or $h_1 < h_c$ or $h_2 < h_c$:

$$\frac{E}{E_o} = 2\sqrt{j\pi x}\sum_{s=1}^{\infty} \frac{1}{1+\tau^2 a_s} \frac{\overline{Ai}\left[(a_s + y_1)e^{j\frac{\pi}{3}}\right]}{e^{j\frac{\pi}{3}}Ai'\left(a_s e^{j\frac{\pi}{3}}\right)} \frac{\overline{Ai}\left[(a_s + y_2)e^{j\frac{\pi}{3}}\right]}{e^{j\frac{\pi}{3}}Ai'\left(a_s e^{j\frac{\pi}{3}}\right)}$$

$$\cdot \exp\left\{j a_s x - \frac{2}{3}\left[(a_s + y_1)e^{j\frac{\pi}{3}}\right]^{\frac{3}{2}} - \frac{2}{3}\left[(a_s + y_2)e^{j\frac{\pi}{3}}\right]^{\frac{3}{2}}\right\}$$

where

$$F_c = 65\sqrt{\sigma} \qquad h_c = \frac{5\lambda}{\pi}\sqrt{|\epsilon_c|}$$

$$\tau = -j\left(\frac{\lambda}{\pi a_e}\right)^{\frac{1}{3}} \frac{\epsilon_c}{\sqrt{\epsilon_c - 1}}$$

$\overline{Ai}(w) = Ai(w)\exp\left(\frac{2}{3}w^{\frac{3}{2}}\right)$ and $Ai'(w)$ from AIRYBAR

$$x = \frac{d}{d_o} \qquad y_1 = \frac{h_1}{h_o} \qquad y_2 = \frac{h_2}{h_o}$$

$$h_o = \frac{1}{2}\left(\frac{a_o\lambda^2}{\pi^2}\right)^{\frac{1}{3}} \qquad d_o = \left(\frac{a_o^2\lambda}{\pi}\right)^{\frac{1}{3}}$$

ϵ_c	=	complex dielectric constant
a_s	=	eigenvalues from AIT
λ	=	wavelength
a_e	=	effective earth radius
d	=	great-circle separation distance
$h_{1,2}$	=	link endpoint elevations

RAY-THEORY SOLUTIONS

For horizontal polarization in general,
or vertical polarization with $\delta_o > \lambda/4$ or $F_{MHz} > 100$:

SPACE

$$F = \left| 1 + \rho_{ss} D \Gamma e^{-jk\delta_o} \right|$$

$$= \left[1 + (\rho_{ss}\rho D)^2 + 2\rho_{ss}\rho D\cos(k\delta_o + \phi)\right]^{\frac{1}{2}}$$

otherwise,

GROUND

$$F = \left|1 + \rho_{ss} D \Gamma e^{-jk\delta_o} + (1-\Gamma) F(w) e^{-jk\delta_o}\right|$$

where

D	=	divergence factor
F_{MHz}	=	frequency
k	=	$2\pi/\lambda$
λ	=	wavelength
δ_o	=	path length difference
Γ	=	Fresnel reflection coefficient
ρ_{ss}	=	specular scattering coefficient
F(w)	=	Sommerfeld attenuation function

PROPAGATION MODE: WAVEP

For horizontal polarization or vertical polarization with $F_{MHz} > F_c$ and $h_1 > h_c$ and $h_2 > h_c$:

$$\frac{E}{E_o} = 2\sqrt{j\pi x}\sum_{s=1}^{\infty} \frac{\overline{Ai}\left(\alpha_s + y_1 e^{j\frac{\pi}{3}}\right)}{e^{j\frac{\pi}{3}}Ai'(\alpha_s)} \frac{\overline{Ai}\left(\alpha_s + y_2 e^{j\frac{\pi}{3}}\right)}{e^{j\frac{\pi}{3}}Ai'(\alpha_s)} \cdot \exp\left\{e^{j\frac{\pi}{6}}\alpha_s x - \frac{2}{3}\left(\alpha_s + y_1 e^{j\frac{\pi}{3}}\right)^{\frac{3}{2}} - \frac{2}{3}\left(\alpha_s + y_2 e^{j\frac{\pi}{3}}\right)^{\frac{3}{2}}\right\}$$

where

$$F_c = 65\sqrt{\sigma} \qquad h_c = \frac{5\lambda}{\pi}\sqrt{|\epsilon_c|}$$

$$\overline{Ai}(w) = Ai(w)\exp\left(\frac{2}{3}w^{\frac{3}{2}}\right) \text{ is from AIRYBAR}$$

$$x = \frac{d}{d_o} \qquad y_1 = \frac{h_1}{h_o} \qquad y_2 = \frac{h_2}{h_o}$$

$$h_o = \frac{1}{2}\left(\frac{a_e\lambda^2}{\pi^2}\right)^{\frac{1}{3}} \qquad d_o = \left(\frac{a_e^2\lambda}{\pi}\right)^{\frac{1}{3}}$$

ϵ_c = complex dielectric constant

α_s = s^{th} zero of the Airy function

$Ai'(\alpha_s)$ = derivative of the Airy function evaluated at the s^{th} zero of the Airy function

a_e = effective earth radius
d = great-circle separation distance
$h_{1,2}$ = link endpoint elevations

EIGENVALUES FOR WAVEG

EIGENVALUES are solutions to the characteristic equation:

$$Ai\left(e^{j\frac{\pi}{3}}z\right) - \tau e^{j\frac{\pi}{3}}Ai'\left(e^{j\frac{\pi}{3}}z\right) = 0 \qquad \tau = -j\left(\frac{\lambda}{\pi a_e}\right)^{\frac{1}{3}}\frac{\epsilon_c}{\sqrt{\epsilon_c - 1}}$$

ALGORITHM for the s^{th} eigenvalue

$$a_{s,c} = \left\{\frac{3}{4}\left[\left(2s - \frac{3}{2}\right)\pi + \frac{\pi}{2}\right]\right\}^{\frac{2}{3}} e^{j\frac{2\pi}{3}} \qquad \tau_c = \frac{1}{\sqrt{a_{s,c}}}$$

$$a_{st} = \begin{cases} a_{s,o} = \left\{\frac{3}{4}\left[(2s-1)\pi + \frac{\pi}{2}\right]\right\}^{\frac{2}{3}} e^{j\frac{2\pi}{3}} & \tau \le \tau_c \\ a_{s,\infty} = \left\{\frac{3}{4}\left[(2s-2)\pi + \frac{\pi}{2}\right]\right\}^{\frac{2}{3}} e^{j\frac{2\pi}{3}} & \tau > \tau_c \end{cases}$$

Initial Condition:

$$Re^{-j\phi} = \frac{\sqrt{a_{st}} - j/\tau}{\sqrt{a_{st}} + j/\tau} \qquad a_s(0) = \left\{\frac{3}{4}\left[(2s-2)\pi + \frac{\pi}{2} + \phi + j\ln R\right]\right\}^{\frac{2}{3}} e$$

Iteration: $k = 0, 1, \ldots$

$$\tau_s(k) = \frac{Ai\left(a_s(k)\, e^{j\frac{\pi}{3}}\right)}{e^{j\frac{\pi}{3}}Ai'\left(a_s(k)\, e^{j\frac{\pi}{3}}\right)} \qquad T(k) = \frac{\tau - \tau_s(k)}{1 + a_s(k)\,\tau_s(k)\,\tau} \qquad a_s(k+1) = a_s$$

Exit Condition: If $|T(k)| < 10^{-4}$ then $a_s = a_s(k)$

PROPAGATION MODE: RAYWAVE

RAY-THEORY CORRECTION FACTORS

If $h_1 + h_2 < h_L$ and $d_{ray} < d < d_H$:

$$\frac{E}{E_o} = 2G\left\{F(p) - \frac{\delta^3}{2}\left[1 - j(\pi p)^{\frac{1}{2}} - (1+2p)F(p)\right] + \delta^6\left[1 - j(\pi p)^{\frac{1}{2}}(1-p) - 2p + \frac{5}{6}p^2 + \left(\frac{p^2}{2} - 1\right)F(p)\right]\right\}$$

where

$$F(p) = 1 - j(\pi p)^{\frac{1}{2}} e^{-p}\,\mathrm{erfc}\left(jp^{\frac{1}{2}}\right)$$

$$\delta^3 = \frac{j}{k a_e \Delta^3} \qquad p = -j\frac{kd}{2}\Delta^2$$

$$\Delta = \begin{cases} -j\left(\frac{\lambda}{\pi a_e}\right)\frac{\epsilon_c}{\sqrt{\epsilon_c - \cos^2\psi}} & \text{vertical polarization} \\ -j\left(\frac{\lambda}{\pi a_e}\right)\frac{1}{\sqrt{\epsilon_c - \cos^2\psi}} & \text{horizontal polarization} \end{cases}$$

$$G \approx (1 + jkh_1\Delta)(1 + jkh_2\Delta)$$

and

- a_e = effective earth radius
- ϵ_c = complex dielectric constant of the ground
- ψ = grazing angle
- k = $2\pi/\lambda$
- λ = wavelength
- d = great-circle distance of field point
- h_1 = transmit antenna height
- h_2 = receive antenna height
- h_L = limit of $h_1 + h_2$ from HLIM

ZEROS OF THE AIRY FUNCTION

α_s is the s^{th} zero of the Airy function evaluated as:

$$\alpha_s = -f_1\left[\frac{3\pi(4s-1)}{8}\right]$$

where

$$f_1(z) \sim z^{\frac{2}{3}}\left(1 + \frac{5}{48}z^{-2} - \frac{5}{36}z^{-4} + \frac{77125}{82944}z^{-6} - \frac{108056875}{6967296}z^{-8} + \frac{162375596875}{334430208}z^{-10}\right)$$

DERIVATIVE OF THE AIRY FUNCTION EVALUATED AT THE ZEROS OF THE AIRY FUNCTION

α_s is the s^{th} zero of the Airy function. $Ai'(\alpha_s)$ is the Airy function derivative evaluated at the s^{th} zero of the Airy function as:

$$Ai'(\alpha_s) = (-1)^{s-1} f_2\left[\frac{3\pi(4s-1)}{8}\right]$$

where

$$f_2(z) \sim \pi^{-\frac{1}{2}} z^{\frac{1}{6}}\left(1 + \frac{5}{48}z^{-2} - \frac{1525}{4608}z^{-4} + \frac{2397875}{663552}z^{-6}\right)$$

PROPAGATION MODE: TROPO

TROPOSCATTER MODEL CORRECTION FACTORS

SCATTERING EFFICIENCY CORRECTION FACTOR:

$$F_o = 1.086\,\eta_s\left(2 - \frac{d_H}{d}\right)$$

where η_s is defined for the troposcatter frequency gain function H_o and

d = great-circle distance between link endpoints

d_H = great-circle distance equal to the sum of the radio horizons of the transmit and receive antennas

SURFACE REFRACTIVITY CORRECTION FACTOR:

$$A_{N_s} = \begin{cases} -5.0 & N_s < 250 \\ 0.09041455\,N_s - 27.452260 & 250 \le N_s < 350 \\ 0.13703534\,N_s - 43.769536 & 350 \le N_s < 400 \\ 0.03335600\,N_s - 2.289640 & N_s \ge 400 \end{cases}$$

where

N_s = surface refractivity

SOMMERFELD ATTENUATION FUNCTION

If $|w| \le 50$ then:

$$F(w) = 1 - j(\pi w)^{\frac{1}{2}} e^{-w} \operatorname{erfc}\left(j w^{\frac{1}{2}}\right)$$

$$w = p\left[1 + \frac{h_1 + h_2}{\Delta(M_1 + M_2)}\right)$$

$$p = -\frac{j k (M_1 + M_2)}{2}\,\Delta^2$$

$$\Delta = \frac{\sqrt{\epsilon_c - \cos^2\psi}}{\epsilon_c}$$

$$\operatorname{erfc}\left(j w^{\frac{1}{2}}\right) = 1 - \frac{4}{\pi}\sum_{\substack{n=1 \\ n\ \text{odd}}}^{\infty} \frac{e^{-\left(\frac{n^2\Omega_s^2}{2}\right)} \sin\left(j n \Omega_s \sqrt{2w}\right)}{n}$$

otherwise:

$$F(w) = \frac{1}{2|w| - 3.7}\, e^{j[\pi - \arg(w)]}$$

where

k = $2\pi/\lambda$

Ω_s = $2\pi/28$ if $|w| < 30$ = $2\pi/56$ otherwise

λ = wavelength

h_1 = transmit antenna height

h_2 = receive antenna height

$M_{1,2}$ = reflected ray line segment lengths

ϵ_c = complex dielectric constant

ψ = grazing angle

PROPAGATION MODE: TROPO

$$F = A_{N_s} - H_o - F_o + 10\log_{10}\left[\frac{\mu_T \sigma_n^2 d}{L_o k \theta_o^2}\right]$$

where

μ_T = 22000

σ_n^2 = variance of refractive index fluctuations
= $6.7 \times 10^{-14} e^{-h_T/3.2}$

L_o = correlation distance of refractive index = $2\sqrt{h_T/1000}$

h_T = elevation from TROPO geometry

θ_o = scatter angle from TROPO geometry

k = $2\pi/\lambda$

λ = transmission wavelength

A_{N_s} = surface refractivity correction factor in dB

H_o = frequency gain function in dB

F_o = scattering efficiency correction factor in dB

PROPAGATION MODE: TROPO

FREQUENCY GAIN FUNCTION:

$$H_o = \begin{cases} H_1 + \Delta H_o & \text{if } \Delta H_o \le H_1 \\ 2H_1 & \text{otherwise} \end{cases} \quad \text{and} \quad H_o \ge 1$$

$$H_1 = \frac{H_o(x_1) + H_o(x_2)}{2}$$

$$H_o(x_k) = c_1(x_k + c_2)^{-\frac{4}{3}} \qquad k = 1,2$$

$$x_k = \frac{4\pi\theta_o h_k}{\lambda} \qquad k = 1,2 \qquad x_k \ge 0.1$$

$$c_1 = 16.3 + 13.3\eta_s$$

$$c_2 = 0.40 + 0.16\eta_s$$

$$\eta_s = 0.5696 h_z\left[1 + \left(0.031 - 0.00232N_s + 5.67\times10^{-6}N_s^2\right)e^{-3.8\times10^{-4}h_z^4}\right]$$

$$0.01 \le \eta_s \le 5.0$$

$$q = \frac{x_2}{s x_1} \qquad 0.1 \le q \le 10$$

$$\Delta H_o = 6(\log_{10}s)(\log_{10}q)(0.6 - \log_{10}\eta_s)$$

where

h_z = elevation from TROPO geometry

θ_o = scatter angle from TROPO geometry

s = path asymmetry factor from TROPO geometry

$h_{1,2}$ = link endpoint elevations

λ = transmission wavelength

N_s = surface refractivity

ACCELERATED INTERMEDIATE REGION PROPAGATION MODEL

PROPAGATION MODE SELECTION PROCESS

FOR A GIVEN SET OF INPUT PARAMETERS:

- each propagation mode will yield a solution that differs from the exact solution by an amount that can be described as *negligible* or *significant*.
- significant deviation can result from
  - numerical instability
  - violation of assumptions used in derivation.
- negligible deviation is defined as the maximum permissible deviation from the exact solution.
- more conservative definitions of negligible deviation result in slower execution times by limiting the applicability of faster propagation modes.

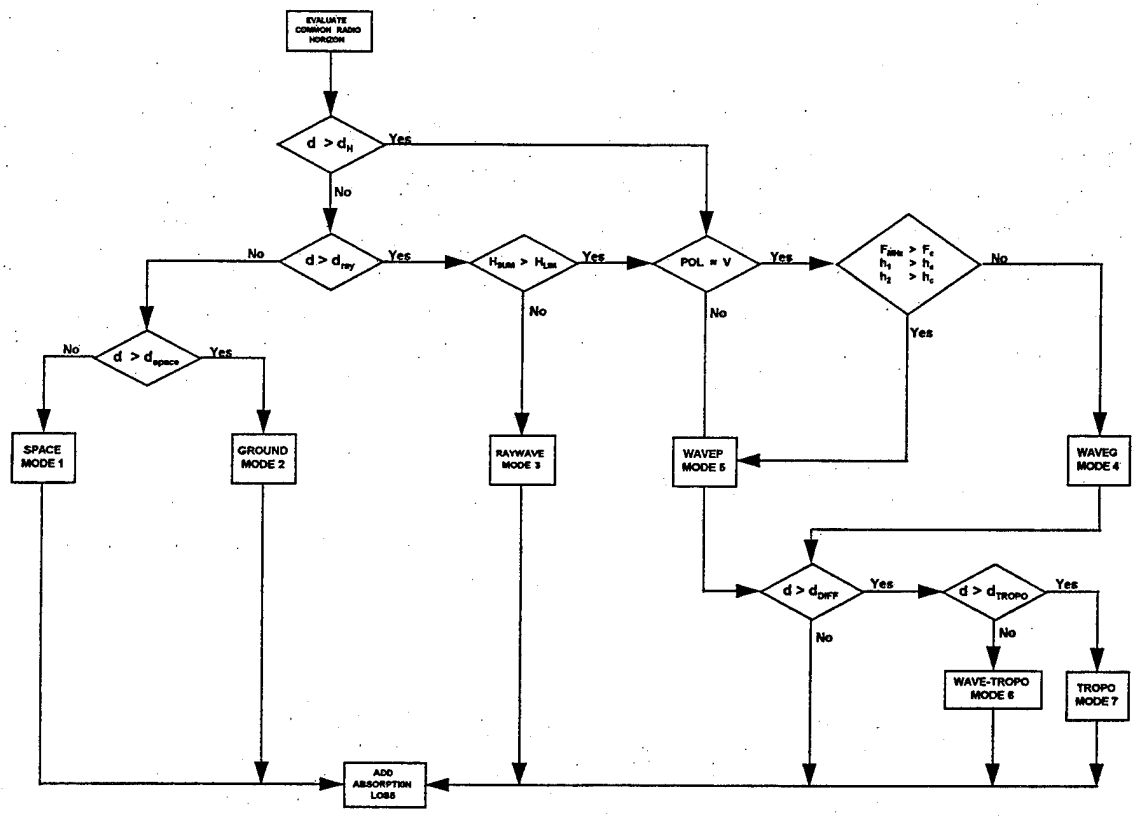

ACCELERATED INTERMEDIATE REGION PROPAGATION MODEL

PROPAGATION MODE SELECTION PROCESS

- FOR HORIZONTAL POLARIZATION IN GENERAL, OR VERTICAL POLARIZATION WITH $\delta_o > \lambda/4$ or $F_{MHz} > 100$

  » SPACE (direct + reflected)

- OTHERWISE

  » GROUND (direct + reflected + surface)

ACCELERATED INTERMEDIATE REGION PROPAGATION MODEL

PROPAGATION MODE SELECTION PROCESS

- FOR HORIZONTAL POLARIZATION IN GENERAL, OR VERTICAL POLARIZATION WITH

  $F_{MHz} > F_C$ and $h_1 > H_C$ and $h_2 > H_C$

  » WAVEP (particular Bremmer series solution)

- OTHERWISE

  » WAVEG (general Bremmer series solution)

$$F_C = 65\sqrt{\sigma} \qquad H_C = \frac{5\lambda}{\pi}\sqrt{|\varepsilon_c|}$$

ACCELERATED INTERMEDIATE REGION PROPAGATION MODEL

- **DOCUMENTATION**
  - **Report No: ECAC-CR-94-011**
  - **Source: Joint Spectrum Center Annapolis, MD**

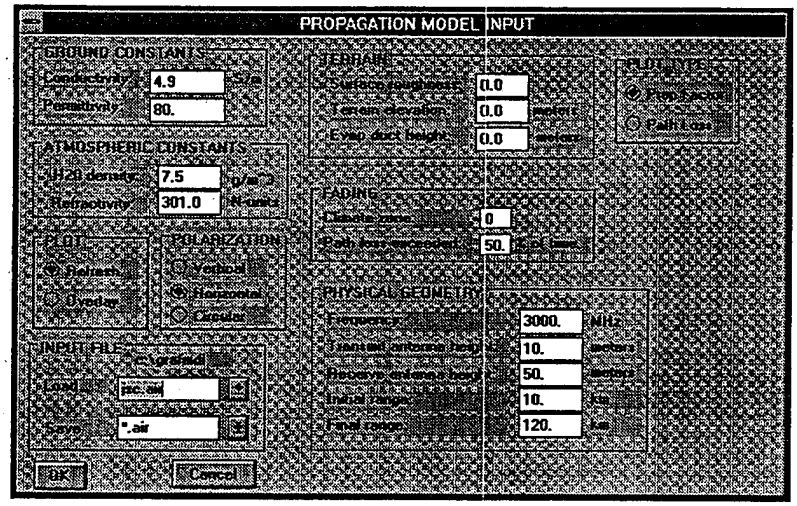

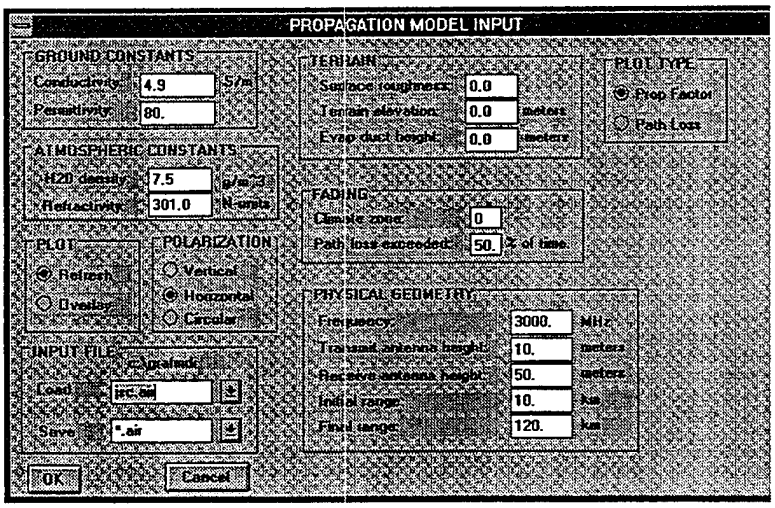
PROPAGATION MODEL INPUT
GROUND CONSTANTS
Conductivity 4.9 S/m
Permittivity 80.
ATMOSPHERIC CONSTANTS
H20 density 7.5 g/m^3
Refractivity 301.0 N-units
PLOT
Refresh
Overlay
POLARIZATION
Vertical
Horizontal
Circular
INPUT FILE
Coverage pre.cvg
Terrain *.ter
OK
Cancel
TERRAIN
Surface roughness 0.0
Terrain elevation 0.0 meters
Evap duct height 0.0 meters
FADING
Climate zone 0
Path loss exceeded 50. % of time
PHYSICAL GEOMETRY
Frequency 3000. MHz
Transmit antenna height 10. meters
Receive antenna height 50. meters
Initial range 10. nm
Final range 120. nm
PLOT TYPE
Prop Factor
Path Loss

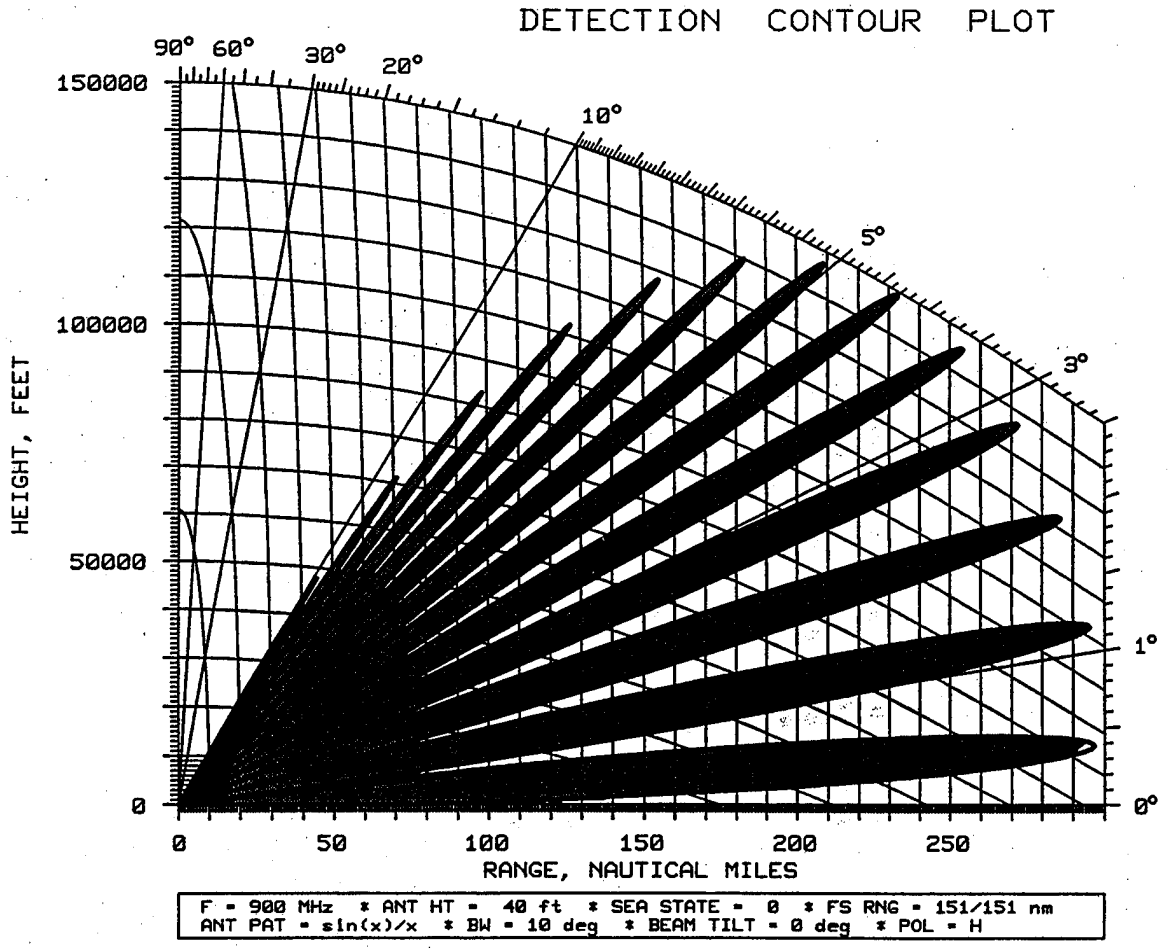
DETECTION CONTOUR PLOT
90° 60° 30° 20° 10° 5° 3° 1° 0°
150000
100000
50000
0
HEIGHT, FEET
0 50 100 150 200 250
RANGE, NAUTICAL MILES
F = 900 MHz * ANT HT = 40 ft * SEA STATE = 0 * FS RNG = 151/151 nm
ANT PAT = sin(x)/x * BW = 10 deg * BEAM TILT = 0 deg * POL = H

MODELING ELECTROMAGNETIC WAVE PROPAGATION OVER THE ROUGH SEA SURFACE OR OVER THE TERRAIN USING THE PARABOLIC EQUATION METHOD

N.DOUCHIN

CERT-ONERA/DERMO
2, avenue Edouard Belin - B.P. 4025
31055 TOULOUSE Cedex (FRANCE)
Tel : (33) 62 25 27 17
Fax: (33) 62 25 25 77
E.mail : douchin@reseau.onecert.fr

The radiation pattern of the antenna of a radar situated above the sea surface or the terrain exhibits nulls and constructive interference lobes due to reflection from the surface. But the latter is nearly always rough, and so, scattering effects can perceptibly modify the radar coverage, which prediction becomes difficult, especially at low altitudes because of shadowing and multiple scattering effects. In addition refraction effects like ducting due to the evaporation duct can also perceptibly modify the above mentioned interference pattern. So it is of great importance to be able to include all these effects in a prediction model ; that's the reason why the Parabolic Equation method is used because thanks to it scattering from the rough sea surface or the terrain, and refraction effects can be taken into account simultaneously.

Two main numerical techniques are available to solve the Parabolic Equation:

- there is the split-step FOURIER algorithm, which uses FOURIER transforms and is the most efficient method for implementing the PE method on a computer. But this approach does not allow one to take account of diffuse reflection. Then only the reflection coefficient in the specular direction can be modified, according to the Miller, Brown & Vegh's model for example ; the impedance at the sea surface is also modified according to the new value of the reflection coefficient and then propagation is calculated over a less reflective surface using the split-step FOURIER algorithm.

But this approach is not satisfactory because the modification of the antenna heights due to sea roughness is not taken into account and shadowing effects are not modelised.

- The second numerical approach is based on a finite-differences formulation of the PE and of the associated boundary condition at the surface. The latter includes the local slope of the surface so that scattering effects are taken into account (and also shadowing effects at very low grazing angle), along with refraction effects. The finite-differences scheme is the CRANK-NICHOLSON one which is unconditionally stable and as precise as the explicit scheme.

Two softwares have been developed at CERT [[1]:

PE-CERT, which is based on the split-step Fourier algorithm and is used only in the "smooth surface" cases,

DIF-CERT, which is based on finite differences and is used in the "rough surface" cases or over the terrain.

In both models, the dielectric properties of the terrain can be taken into account.

For the workshop, sample cases 3, 8 and 9 have been calculated using DIF-CERT, because either the sea surface is rough or the terrain is present.

The sea surface is considered as a random process, realizations of which are obtained by filtering realizations of a gaussian white noise. The appropriate filter is obtained using an appropriate wave spectrum related to the gravity waves at the sea surface which are responsible for forward scattering ; in our model the Phillips spectrum, suitable for the description of the gravity waves, is used and the wind speed is the single parameter. Once a realization of the random process is obtained, the propagation is calculated over a deterministic surface as for the case of an actual terrain profile.

REFERENCE

N. DOUCHIN, S. BOLIOLI, F. CHRISTOPHE, P. COMBES
Theoretical study of the evaporation duct effects on satellite-to-ship radio links near the horizon IEE proceedings-H, Microw. Antennas Propag., Vol. 141, No. 4, August 1994.

[*Editor's note: No presention was made at the workshop. However, it was the author's desire to have DIF-CERT included in the Sample Case Comparisons of Session V .*]

SESSION V. PROPAGATION SAMPLE CASES

Chair: Dr G. Brooke

Towards Benchmark Solutions for EM Tropospheric Propagation Problems

by
Gary H. Brooke and Eleanor S. Holmes
Numerical Decisions Group, Inc.
947 Fort St., Suite 8A
Victoria, BC V8V 3K3

Abstract

Tropospheric EM propagation problems are extremely demanding both in terms of complicated physics and shear volume of numerical calculations required. The spherical nature of the earth-atmosphere waveguide in conjunction with ducted environments and variable terrain constrain applicable propagation models to have a high degree of sophistication. Not surprisingly, there is a proliferation of models used in the community each of which has distinct features designed to handle one or more aspects of a complicated problem. Ultimately, operational requirements of speed and accuracy will determine which models are most useful. Benchmark solutions to well-designed test cases are necessary to establish the underlying validity of each particular model.

In this paper, an attempt is made to visit the issues involved in obtaining benchmark solutions for EM tropospheric problems with the hope that further discussion will be stimulated. An analogy is drawn to similar problems in underwater acoustics where benchmarking exercises have lead to significant advances in model development and have impacted on operational models as well. Preliminary investigations indicate that the tools exist and that the community should be optimistic about obtaining benchmark solutions.

TEST CASE 6 – Underwater Acoustic Model Predictions vs. Measured Field Data

This case tested the ability of the various PE models to match acoustic data taken in a region where the environmental and geoacoustic parameters are believed to be well-known. The data track starts in shallow water (200 m) and traverses 100 km to deep water (~4 km). The ocean bottom along the track is sediment overlying a rough shear-supporting subbottom. None of the model predictions agreed with the data but were so consistent in their predictions that the PE Workshop II participants concluded

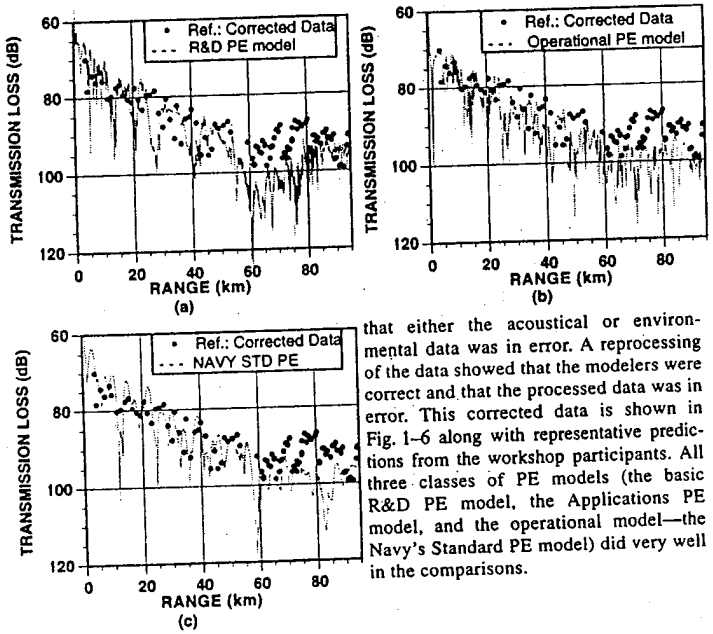

Fig. 1–6. Test Case 6 results from three classes of PE models.

that either the acoustical or environmental data was in error. A reprocessing of the data showed that the modelers were correct and that the processed data was in error. This corrected data is shown in Fig. 1–6 along with representative predictions from the workshop participants. All three classes of PE models (the basic R&D PE model, the Applications PE model, and the operational model—the Navy's Standard PE model) did very well in the comparisons.

TOWARDS BENCHMARK SOLUTIONS FOR EM TROPOSPHERIC PROPAGATION PROBLEMS

by

Gary H. Brooke
Numerical Decisions Group
Victoria, BC Canada

and

Eleanor S. Holmes
Integrated Performance Decisions
Arlington, VA USA

SPAWAR

SPHERICAL EARTH

Earth' Radius

$a \sim 6370 km$

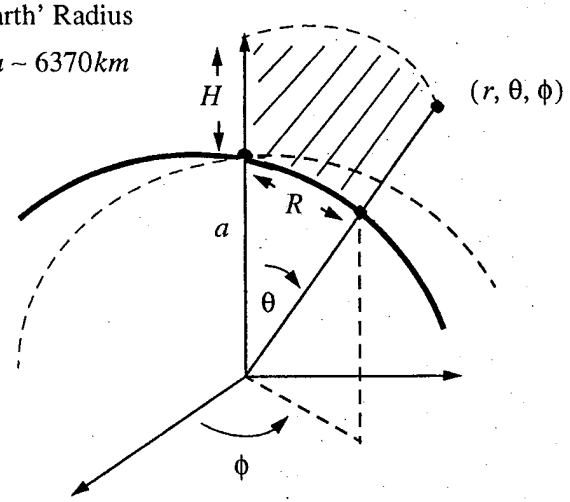

Typically, H < 10 km and 0< R < 500 km

Then $0 < \theta < 4.5°$

$\sin(\theta) \sim \theta$, $r \sim a$

$z = r - a$ and $x = a\theta$

BENCHMARK SOLUTIONS

- Include all of the spectral components

"PHYSICS"

1. Range-independent problems

" SAFARI "

2. Range-dependent problems ??????

" COUPLED MODES "

" FINITE-DIFFERENC PE "

"NOT" against real data

FIELD EQUATIONS (con't)

1. Vertical Polarization :

Vertical Electric Dipole

H_ϕ, E_θ, E_r

Propagation :

$$\nabla\times\nabla\times H_\phi - \left(\frac{\nabla\varepsilon_r}{\varepsilon_r}\right)\times\nabla\times H_\phi - k^2 H_\phi = 0$$

Substitute :

$$H_\phi = \frac{\sqrt{\varepsilon_r}}{\sqrt{r\sin\theta}}\psi$$

Use Earth-Flattening approximations, then :

$$\frac{\partial^2}{\partial x^2}\psi + \frac{\partial^2}{\partial z^2}\psi + k_o^2 n^2\left(1 + 2\frac{z}{a}\right)\psi = 0$$

FIELD EQUATIONS

1. Horizontal Polarization :

Vertical Magnetic Dipole

E_ϕ, H_θ, H_r

Propagation:

$$\nabla\times\nabla\times E_\phi - k^2 E_\phi = 0$$

$$k^2 = k_o^2\varepsilon_r = k_o^2 n^2$$

Substitute :

$$E_\phi = \frac{1}{\sqrt{r\sin\theta}}\psi$$

Use Earth-Flattening approximations, then :

$$\frac{\partial^2}{\partial x^2}\psi + \frac{\partial^2}{\partial z^2}\psi + k_o^2 n^2\left(1 + 2\frac{z}{a}\right)\psi = 0$$

BOUNDARY CONDITIONS

- *Horizontal Polarization :* E_ϕ, H_θ continuous

  implies → ψ , $\frac{\partial \psi}{\partial z}$ continuous

- *Vertical Polarization :* H_ϕ, E_θ continuous

  implies → $m(z)\,\psi$, $\frac{1}{m(z)}\frac{\partial \psi}{\partial z}$ continuous

Earth's Surface : $z = 0$ → $m(0) = n(0)$

$$n_e(0) = (\varepsilon_r - i\sigma / \omega \varepsilon_o)^{1/2}$$

LAYERED MEDIUM

- ***Spherical Earth***

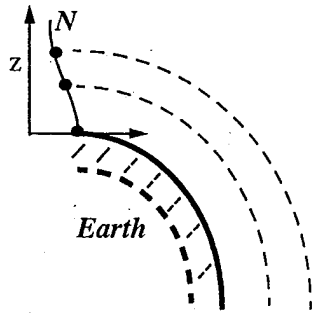

Refractivity N(z) :

$$N(z) = (n(z) - 1)10^6$$

$$n(z) = c_o/c(z)$$

- ***Flat Earth Approximation***

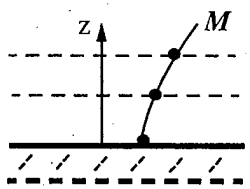

Modified Refractivity M(z) :

$$M(z) = N(z) + (z/a)10^6$$
$$\sim N(z) + 0.157z$$
$$M(z) = (m(z) - 1)10^6$$

$$m(z) = c_o/c_{eff}(z)$$

THE SAFARI MODEL (Range-Independent)

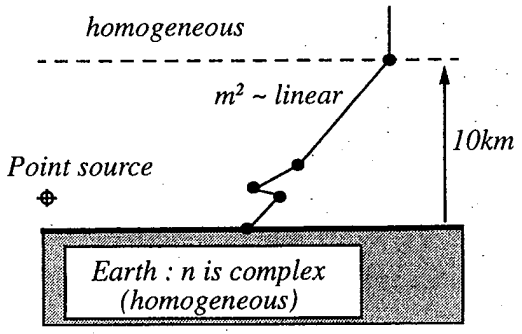

Solve:

$$\frac{\partial^2}{\partial x^2}\psi + \frac{\partial^2}{\partial z^2}\psi + k_o^2 m^2(z)\,\psi = -\delta\left(z - z_s\right)\delta(x)$$

Integral Transform:

$$\Psi(k,z) = \int_{-\infty}^{\infty} x\ x\ e^{ikx}\ \psi(x,z)\,dx$$

$$\psi(x,z) = \int_{-\infty}^{\infty} e^{-ikx}\ \Psi(k,z)\,dk$$

EARTH PROPERTIES

Sea Water

f (Ghz)	*n*	*c (10^7 m/s)*	σ *(s/m)*	α *(dB/λ)*
0.128	*70*	*3.58569*	*5*	*273.80*
0.450	*70*	*3.58569*	*5*	*77.89*
3.000	*69.1*	*3.60896*	*7.2*	*17.04*
3.300	*68.7*	*3.61945*	*7.5*	*16.23*
10.00	*53.5*	*4.10152*	*17.0*	*15.59*

Medium Dry Ground

f (Ghz)	*n*	*c (10^7 m/s)*	σ *(s/m)*	α *(dB/λ)*
0.128	*15*	*7.75*	*0.002*	*0.51*
3.000	*15*	*7.75*	*0.23*	*2.51*
10.00	*11.9*	*8.69*	*1.64*	*6.76*

Spectral Content

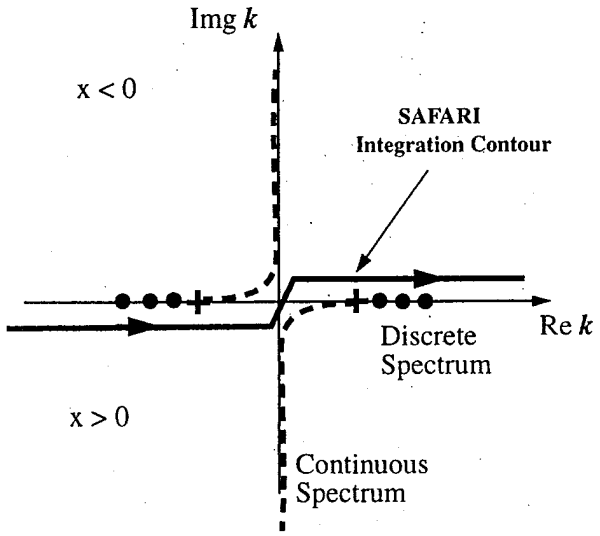

- Discrete Spectrum (Modes) due to ducting.
- Continuous Spectrum represents energy which is not trapped in ducting layers. If we chose the branch cut appropriately, we uncover Leaky modes.
  - in a standard atmosphere, only have continuous spectrum

SAFARI

Helmholtz eqn:

$$\frac{\partial^2}{\partial z^2}\Psi - \left[k^2 - k_o^2 m^2(z)\right]\Psi = -\delta\left(z - z_s\right)$$

Solution:

- *horizontal layering*
- *m^2 is linear or constant*
- *multiple point sources*
- *surface roughness (Kirchoff scattering)*
- *homogeneous half-space above and below*

Inverse Transform:

$$\psi(x,z) = \int_{-\infty}^{\infty} dk\hat{\Psi}\left(k_m, z\right)e^{-ikx}$$

$$\psi\left(x_j, z\right) \approx \Delta k e^{-ik_{min}x_j}\sum_{m=0}^{M}\hat{\Psi}\left(k_m, z\right)e^{-i2\pi m\frac{j}{M}}$$

$$\Delta x \Delta k = 2\pi/M$$

$$k_m = k_{min} + m\Delta k \qquad x_j = j\Delta x$$

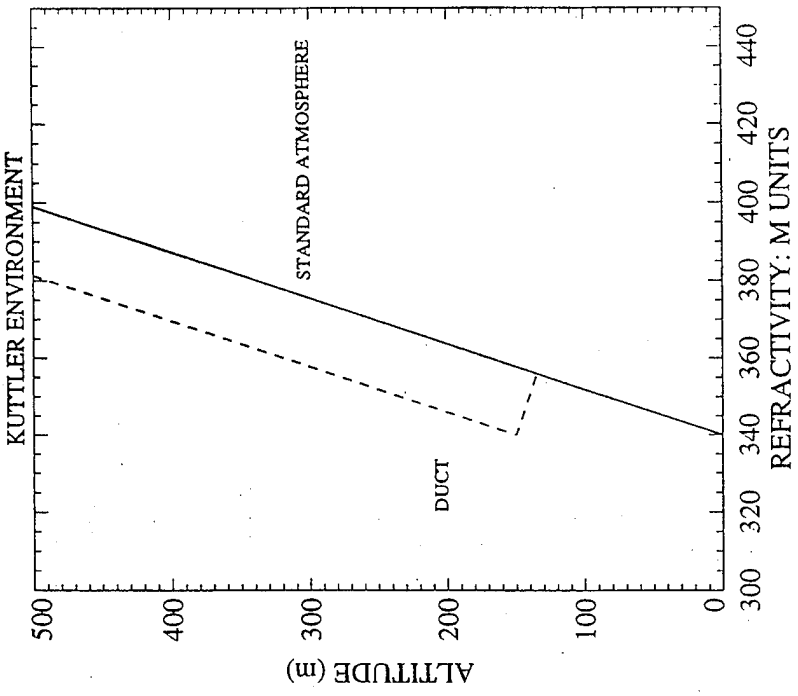
KUTTLER ENVIRONMENT
STANDARD ATMOSPHERE
DUCT
ALTITUDE (m)
500
400
300
200
100
0
300
320
340
360
380
400
420
440
REFRACTIVITY: M UNITS

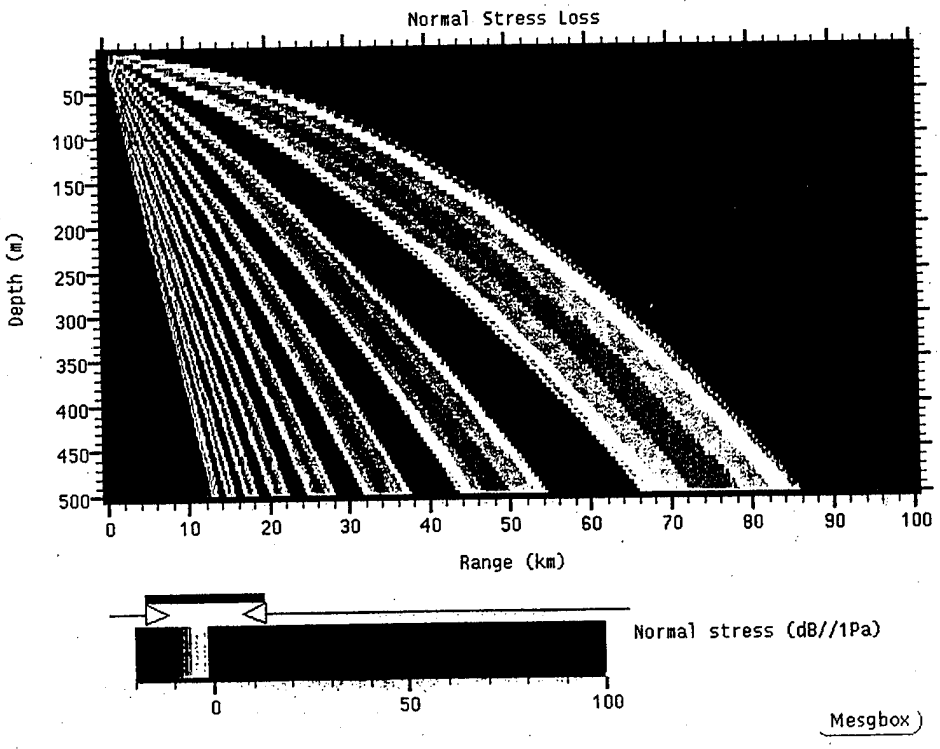
Normal Stress Loss
Depth (m)
50
100
150
200
250
300
350
400
450
500
0
10
20
30
40
50
60
70
80
90
100
Range (km)
Normal stress (dB//1Pa)
0
50
100
Mesgbox

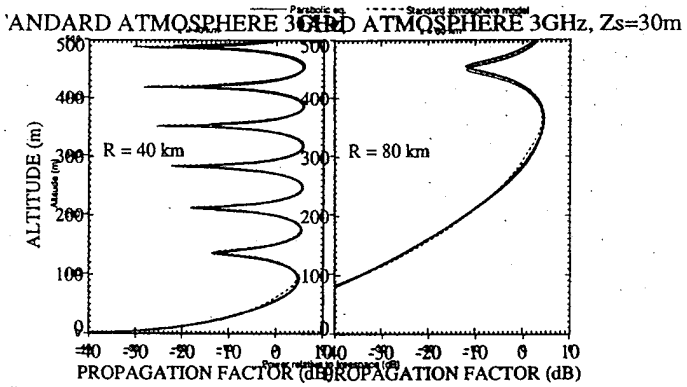

Fig. 2. Normalized power for 3-GHz horizontal polarization propagation in a standard atmosphere.

requires that Im (α) > 0; this is always the case as can be shown using (35)–(37).

It remains to determine an appropriate initial solution to begin calculations using the split-step algorithm. The initial solution should include the characteristics of the specified source such as antenna height, radiation pattern, and pointing direction. A method for generating initial solutions corresponding to specified sources using the Fourier transform relationship between the aperture distribution and the radiation pattern of an antenna is described by *Dockery* [1988]; the pointing direction and antenna altitude are incorporated by means of two applications of the Fourier shift theorem.

NUMERICAL EXAMPLES

Comparisons between parabolic equation/split-step results and those of other models have been presented previously by *Dockery* [1988] and *Ko et al.* [1988]; the examples given in the later reference include comparisons with the calculations performed by *Cho and Wait* [1978] for a horizontally inhomogeneous atmosphere. The parabolic equation method is found to agree with the other propagation models in all cases where the other models are valid. Two such comparisons are included in

A quantity frequently used to describe atmospheric refractive conditions is the modified refractivity, which is related to the usual index of refraction as follows:

$$M = (n - 1 + z/a_e) \times 10^6. \tag{46}$$

Negative vertical gradients of M are associated with atmospheric ducts or trapping layers. Whether energy is strongly trapped by a given ducting layer depends on the angle the incident wave fronts make with the layer boundaries and on the size of the layer relative to a wavelength.

In the following examples, propagation over a smooth finitely conducting sea is assumed; values for the relative permittivity of the sea are taken from *Saxon and Lane* [1952], assuming a water temperature of 20°C and a salinity of 3.6%. For "standard atmosphere" calculations a linear refractivity gradient of 0.118 m^{-1} is a good approximation of the usual exponential profile for altitudes below a few kilometers; the linear profile is used in the parabolic equation calculations at all ranges.

Propagation in a standard atmosphere may also be modeled adequately using an "effective Earth radius" method described by *Kerr* [1951]. This method uses geometric optics inside the optical

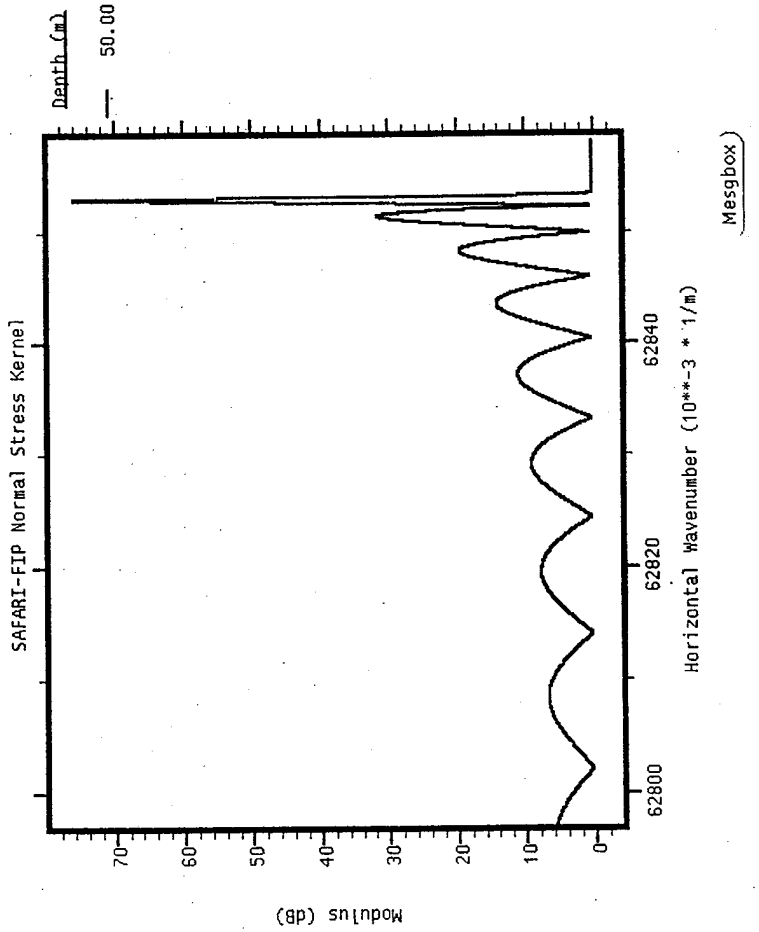

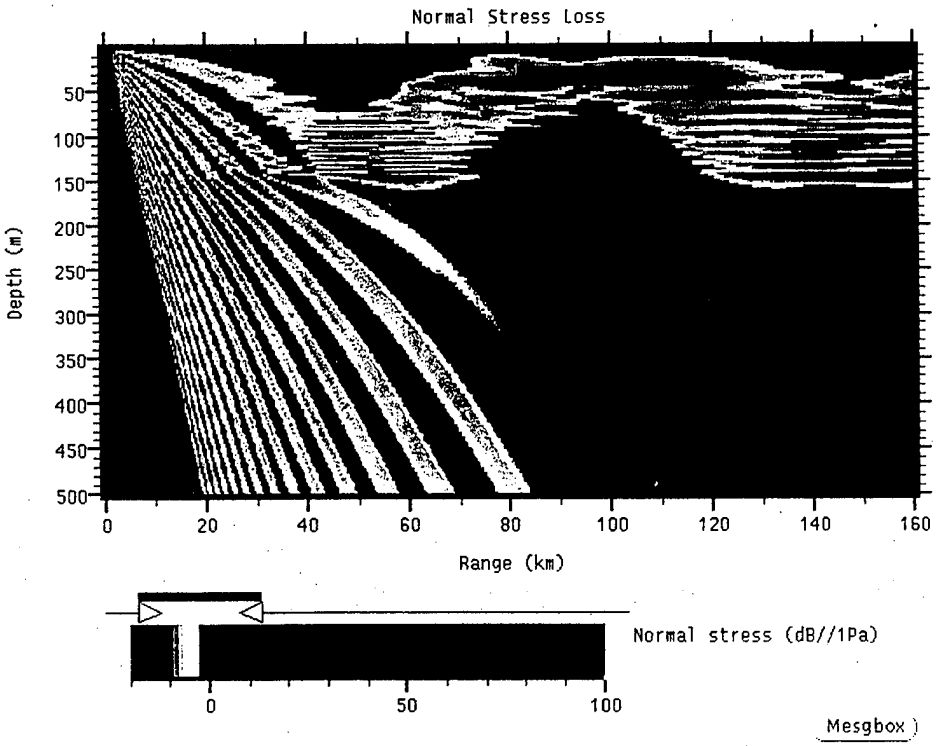
Normal Stress Loss
Depth (m)
50
100
150
200
250
300
350
400
450
500
0
20
40
60
80
100
120
140
160
Range (km)
Normal stress (dB//1Pa)
0
50
100
Mesgbox

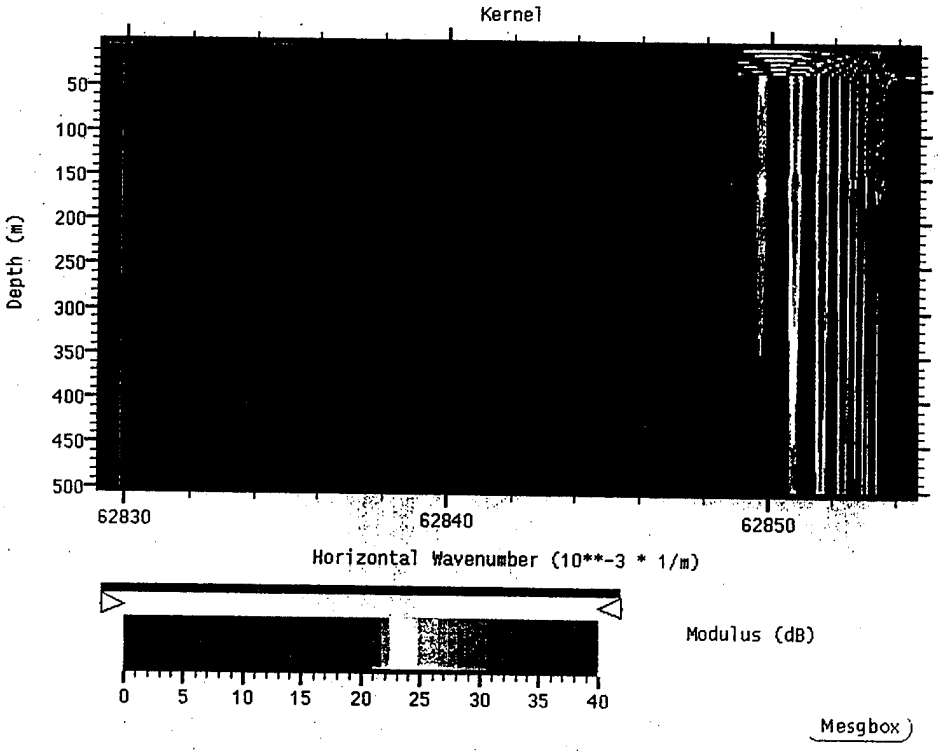
Kernel
Depth (m)
50
100
150
200
250
300
350
400
450
500
62830
62840
62850
Horizontal Wavenumber (10**-3 * 1/m)
Modulus (dB)
0
5
10
15
20
25
30
35
40
Mesgbox

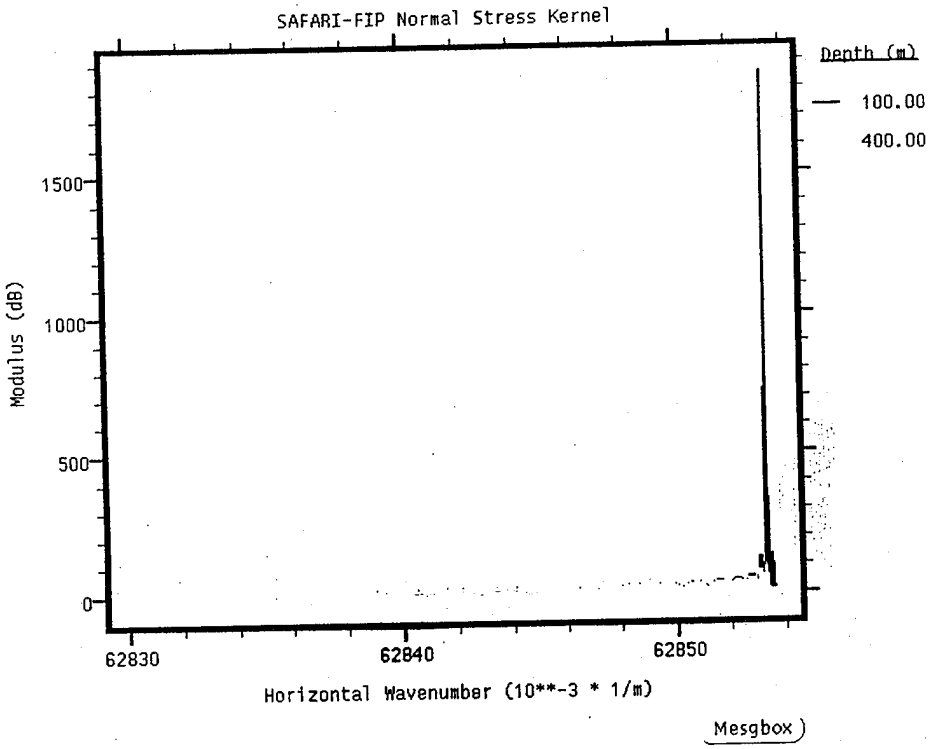
SAFARI-FIP Normal Stress Kernel
Depth (m)
100.00
400.00
1500
1000
500
0
Modulus (dB)
62830
62840
62850
Horizontal Wavenumber (10**-3 * 1/m)
Mesgbox

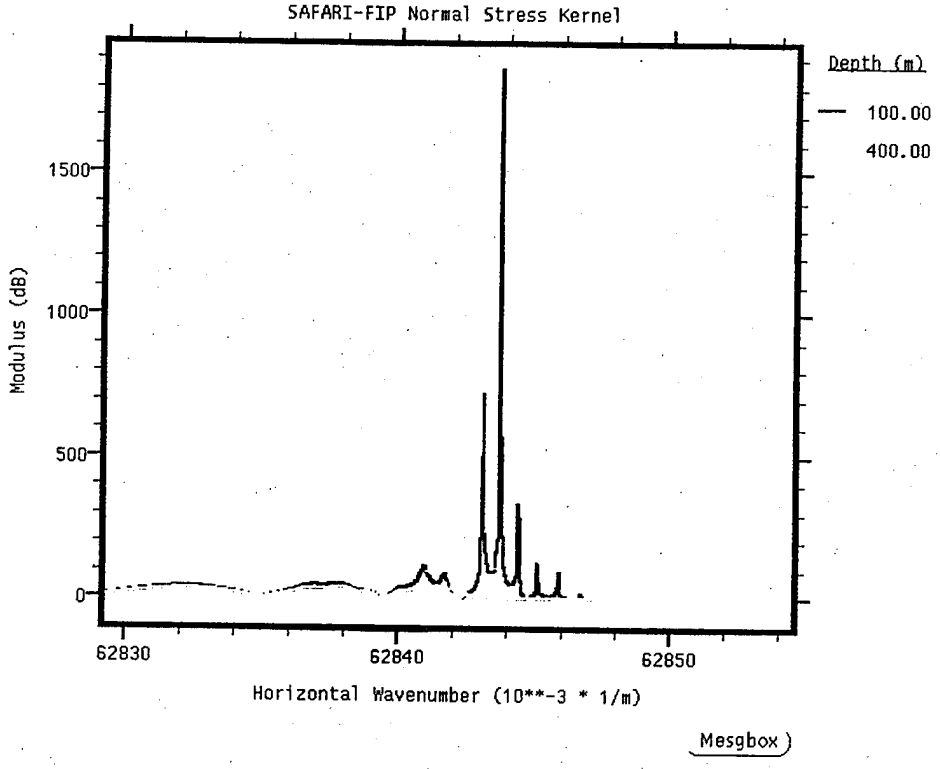
SAFARI-FIP Normal Stress Kernel
Depth (m)
100.00
400.00
1500
1000
500
0
Modulus (dB)
62830
62840
62850
Horizontal Wavenumber (10**-3 * 1/m)
Mesgbox

?? Range-Dependent Benchmark Models ??

1. Modes

a) **step-wise coupled modes (severe range-dependence)**

- cumbersome, large numbers of modes.

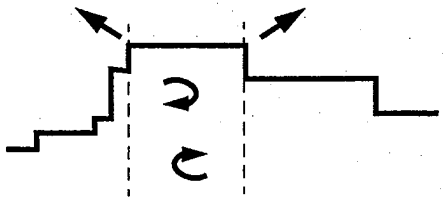

b) adiabatic modes (weak range-dependence)

-fewer Adiabatic Leaky Modes (limited applicability)

2. Parabolic Equation (Finite Difference)

- ***two-way PE or energy conserving PE*** **- satisfy appropriate boundary conditions**

- ***nonlocal boundary conditions*** **- limits domain of calculation**

- ***split-step PADE algorithm*** **- improves grid size problem**

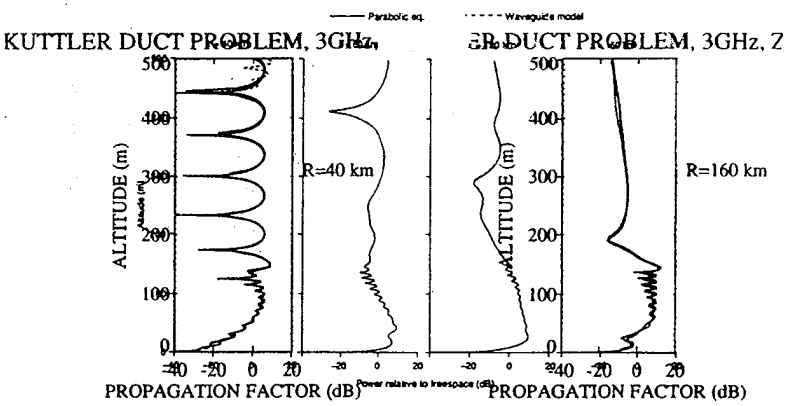

Fig. 4. Normalized power for 3-GHz horizontal polarization propagation in the presence of the surface-based duct.

that the conditions mentioned are not restrictive in realistic environments, and this claim has thus far been supported by comparisons with other propagation models and, more importantly, with measured signal levels.

In the past the Fourier split-step solution has been considered to be computationally intensive, but for problems involving a large number of significant modes it can be much faster than waveguide techniques, and it is capable of handling refractive conditions that are beyond the capabilities of the other currently available propagation models. Although the required execution time for the split-step technique is directly related to the distances of interest from the source (i.e., one must "march" out to a given location rather than simply make a calculation at that point), advances in computer technology have extended the useful application of this method to regions that encompass most microwave tropospheric propagation problems.

APPENDIX

In this appendix, some of the approximations and resulting errors that are encountered in the text are cation of the conformal mapping described in section 3.

Using (11)–(13), one can easily show that

$$x = \frac{4a_e^2 r \sin\theta}{D} \tag{A1}$$

$$z = \frac{2a_e(r^2 - a_e^2)}{D} \tag{A2}$$

with

$$D = r^2 + a_e^2 - 2ra_e\cos\theta. \tag{A3}$$

If the problem is constrained to small values of θ, then the approximations $\sin\theta \approx \theta$ and $\cos\theta \approx 1$ can be used to give

$$x \approx \frac{4a_e^2 r\theta}{(r - a_e)^2} \tag{A4}$$

$$z \approx \frac{2a_e(r - a_e)}{r - a_e} \tag{A5}$$

Also, for the altitude region where $r \approx a_e$,

Dr. Gary Brooke, "Towards Benchmark Solutions for EM Tropospheric Propagation Problems"

DISCUSSION

K. ANDERSON

Two questions. Are you aware of the work that Dick Pappert has done in RF coupled modes? Are you proposing a new FD PE model?

AUTHOR'S REPLY

(1) I am aware of Pappert's work but unfortunately have not been able to review it completely. Coupled mode solutions are computationally intensive but for benchmark problems that may be acceptable.
(2) I think with minimal effort we can adapt the acoustic PE models (finite difference or FFT) to radar problems. Finite-difference PE would seem to be most appropriate for range-dependent benchmarking.

D. MARKHAM

How will operational EM propagation models benefit from the establishment of a "benchmark" model(s)?

AUTHOR'S REPLY

1) Benchmarks provide a baseline for evaluating modifications to operational models. Unlike comparisons with measured data, you are sure whether the change you just made will improve your answer or otherwise.
2) Benchmarks provide an "innovation pull". Difficult underwater test cases have stimulated innovative solutions (which, by the way, add little or no run time) in areas of:

- high angle propagation
- high angle sources
- rough surface loss (N.S. PE uses a very clever solution developed in response to a benchmark test case)
- discontinuous boundary interfaces,

all of which have analogies in EM.

A Comparison of Electromagnetic Wave Propagation Software Using Standard Terrain Cases

Stephen A. Fast

Abstract

Many models and computer programs have been created to predict electromagnetic propagation over ground. Each has been developed to apply to specific problems. Some apply rigorous techniques to solve Maxwell's equations and others combine classical results with empirical data collected in the past. We have developed test cases to answer various questions about various models' behavior. Each question is posed in the context of our applications. The test cases answer some simple questions, e.g., are the results continuous? Other test cases help quantify the differences between diffraction and reflection algorithms, e.g., the existence and position of diffraction/reflection lobes or the intensity of the shadow region. By using a standard set of test cases, one can understand the differences between the programs and choose the program best suited to an application. Results of the standard test cases, however, do not validate a program, but do answer many questions about its behavior. This paper describes a process used to develop test cases to assist the decision making process and examples of the model comparisons. The emphasis is on studying diffraction and reflection effects predicted by the models/programs.

A Comparison of Electromagnetic Wave Propagation Software Over a Single Diffracting Wedge

Stephen A. Fast, Ph.D.

Applied Research Laboratories

University of Texas at Austin

Motivation

To be able to quantify differences between propagation methods and models for users of RF planning systems.

Questions to be Answered by this Study

What are the differences between three popular methods of modelling diffraction, i.e. knife edge diffraction, uniform theory of diffraction, and parabolic equation methods?

Which parameters most effect the differences?

Programs Used in the Comparison

Knife Edge Techniques:

SEKE, Smooth Earth Knife Edge, S. Ayasli, MIT Lincoln Laboratory.
TIREM, Terrain Integrated Rough Earth Model, D. Eppink, Electromagnetic Compatibility and Analysis Center.

Geometrical Theory of Diffraction:

GELTI, Geometrical Theory of Diffraction Estimated Loss due to Terrain Interaction, R. Luebbers and K. Chamberlin, PSU and NHU.

Parabolic Equation Technique:

VTRPE, Variable Terrain and Refractivity Parabolic Equation, F. Ryan, NOSC

Inclusion Planned

Huygen Sources:

CRC VHF/UHF Propagation Prediction Program, J. Whitteker, Communications Research Center.

Parameter Selection

The parameters effecting the diffraction coefficient are receiver and transmitter position, wedge angle, polarization, frequency, and dielectric constants of the wedge.

Parameter Values Chosen for the Comparison

Three frequencies: 30 MHz, 300 MHz, and 3000 MHz.
Three transmit heights: even with the wedge top, 500 meters below the wedge top, and 500 meters above the wedge top.
Three wedge angles: 12, 90, 172 degrees.
Horizontal and vertical polarization.
Perfectly conducting and finite conducting with relative permittivity = 7.5 and conductivity = 0.01 S/m.

Determine the difference beyond the wedge between propagation loss methods with the above parameters sets.

Results:

Results presented focus on 300MHz, the lowest transmitter height, all wedge angles, both polarizations, and both sets of dielectric constants for all models.

Polarization and Dielectric Constant Effects:

Exact Knife Edge Solution: Does not depend on polarization or dielectric constants.

SEKE, TIREM: Polarization had no effect on the results. (These models do not provide a facility for a perfectly conducting surface nor does the knife edge solution depend on the dielectric constants.)

GELTI: Vertical polarization results over a perfectly conducting 177 degree wedge were significantly different than over a finite conducting wedge. Vertical polarization with a finite conducting wedge, horizontal polarization with a finite conducting wedge, and horizontal polarization with a finite conducting wedge showed minimal differences (μ, $\sigma < 1$ dB).

VTRPE: Polarization and conductivity did not effect the results significantly (μ, $\sigma < 1$ dB).

Results cont':

Wedge Shape Effects:

SEKE: The only difference was in the region containing the direct, reflected, and diffracted contributions. As with knife edge diffraction no difference found in the shadow or direct/diffracted regions. Questionable results were generated for the 12 degree wedge.

TIREM: The only differences were near the ground of the 172 degree wedge. No difference was found elsewhere.

VTRPE: The only differences were near the ground of the 172 degree wedge and at the shadow boundary. No other differences were found. Questionable results were generated for the 12 degree wedge.

GELTI: Differences were noted in the shadow region and the reflected, diffracted, and direct ray region for all cases. More loss was noted in the shadow behind the 172 degree wedge. The loss in the shadow region had means between 3.5 and 4.5 and standard deviation between 1 and 4.

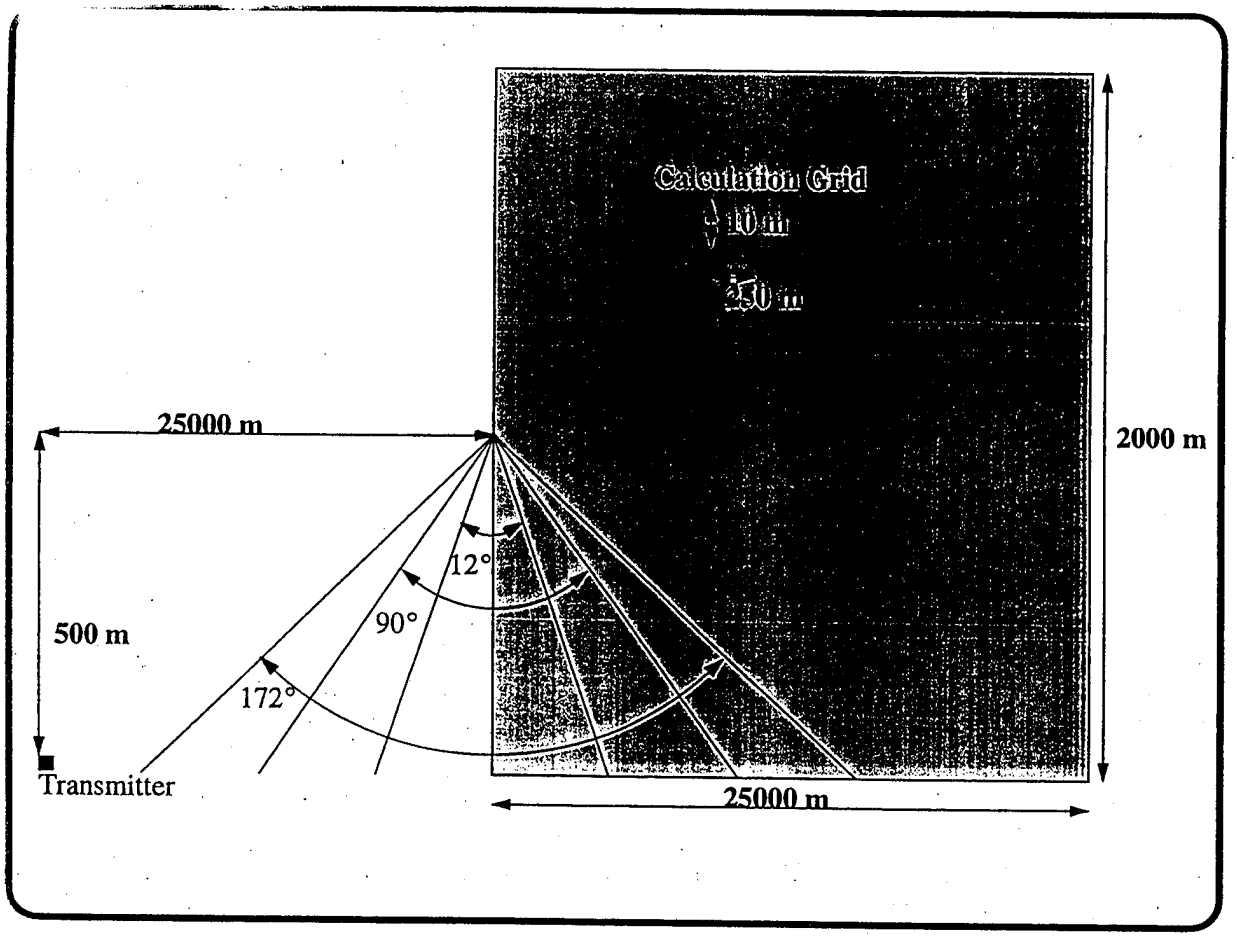
Calculation Grid
10 m
250 m
25000 m
2000 m
500 m
12°
90°
172°
Transmitter
25000 m

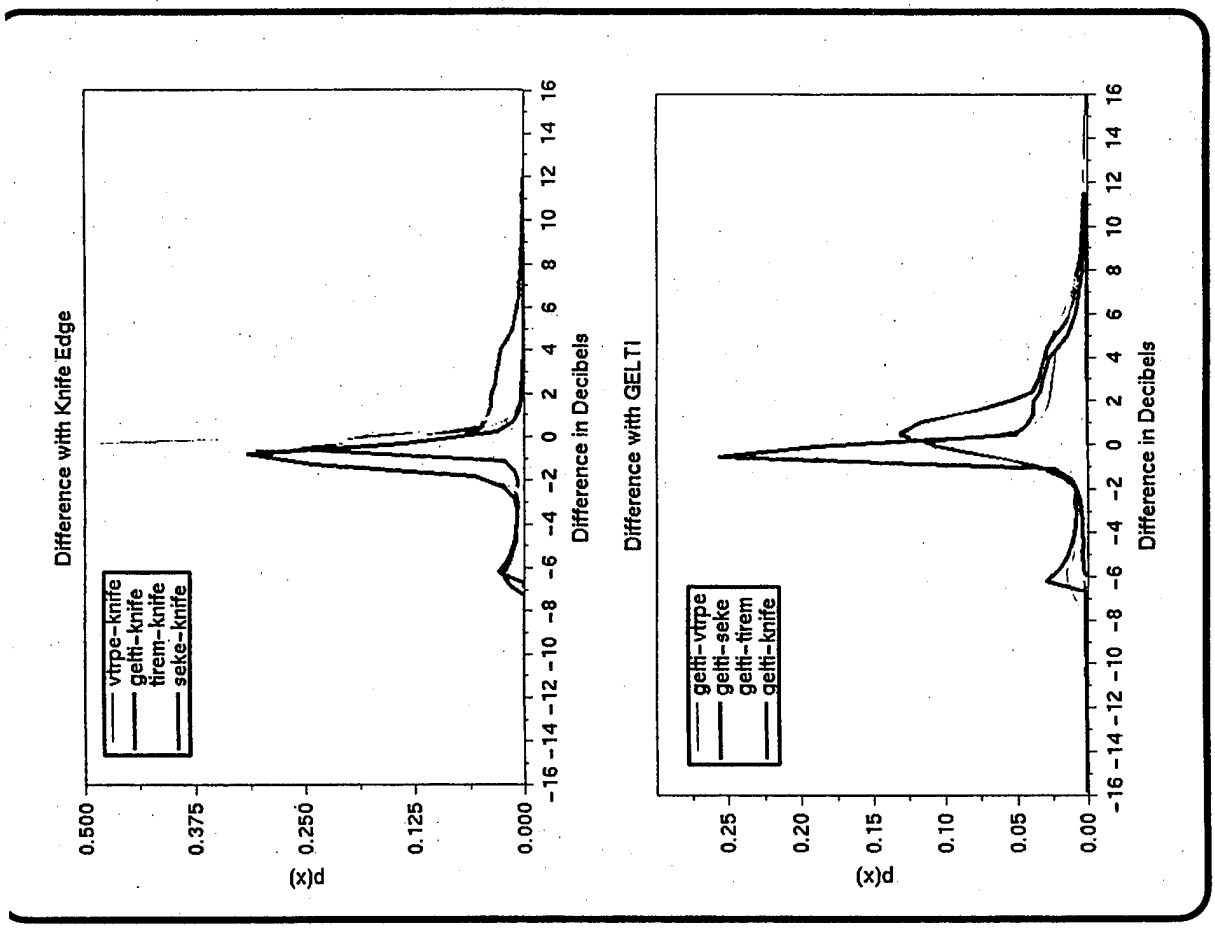
Difference with Knife Edge
vtrpe-knife
gelti-knife
tirem-knife
seke-knife
p(x)d
Difference in Decibels
Difference with GELTI
gelti-vtrpe
gelti-seke
gelti-tirem
gelti-knife
p(x)d
Difference in Decibels

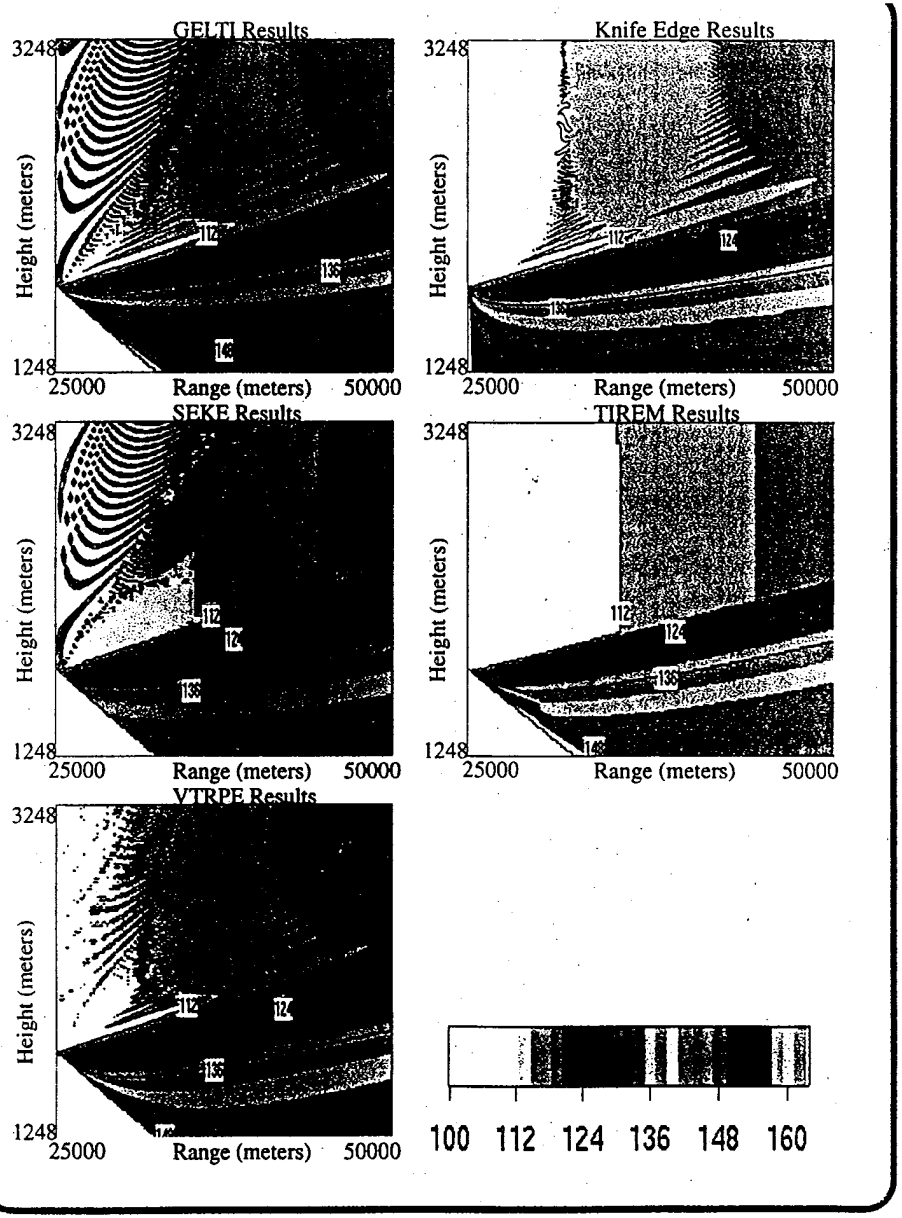
GELTI Results
Knife Edge Results
SEKE Results
TIREM Results
VTRPE Results
Height (meters)
3248
1248
25000
Range (meters)
50000
112
124
136
148
100 112 124 136 148 160

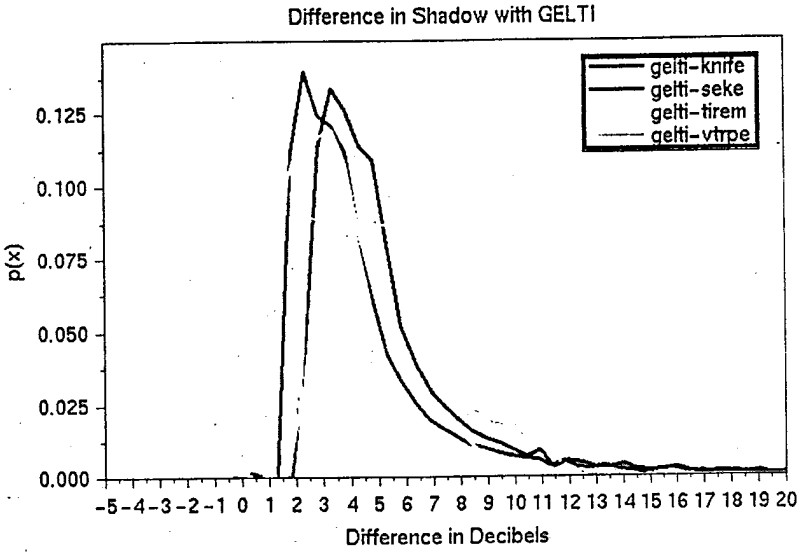
Difference in Shadow with GELTI
gelti-knife
gelti-seke
gelti-tirem
gelti-vtrpe
p(x)
0.125
0.100
0.075
0.050
0.025
0.000
-5 -4 -3 -2 -1 0 1 2 3 4 5 6 7 8 9 10 11 12 13 14 15 16 17 18 19 20
Difference in Decibels

Conclusions:

For finite conductivity results do not depend on polarization.

For horizontal polarization results are not effected by dielectric constants.

For various wedge shapes the only regions with significant differences are the direct, reflected, and diffracted region and the shadow region.

When the wedge angle is large and the receive point is in the deep shadow region, knife edge approximations are poor.

For single diffraction paths TIREM produces adequate results except in a small region near the ground in the deep shadow.

SAMPLE CASES
TROPOSPHERIC EM PROPAGATION WORKSHOP

Ten sample cases were selected by a committee composed of Ken Craig, RAL; Dan Dockery, APL; and Herb Hitney, NRaD to compare the various electromagnetic propagation models presented at the workshop. These cases consider several propagation mechanisms and effects that are considered important for military tactical applications. However, these cases should not be thought of as benchmarks or standards against which the various models will be compared for the purpose of evaluating, ranking, or grading the models, but rather as sample cases to provide a common basis for discussions of each model's capabilities. The consensus of the committee members was that the establishment of true benchmarks would require a detailed technical exchange between the various model developers and careful establishment of selection or grading criteria if the various models were to be fairly graded. Such an effort was judged beyond the scope and schedule of this workshop. Beyond that, some committee members expressed concern that clear requirements for radio propagation models have not been established by the assessment system developers, so it would be nearly impossible to select a set of meaningful benchmarks for their applications. This workshop will help in articulating these system-level requirements.

The frequency range of the sample cases is 128 MHz to 10 GHz. Refractive effects were selected to represent realistic conditions and consist of surface-based ducts, evaporation ducts, elevated ducts, range-dependent ducting conditions, and a standard atmosphere refractivity profile. Propagation over a terrain path is also included for four cases. Many of the cases were derived from measurements made during the Variability of Coastal Atmospheric Refractivity (VOCAR) [1-2] experiment Intensive Observation Period (IOP).

All direct comparisons of model outputs are performed using one-way propagation factor in dB plotted versus height or range of the receiver terminal or time of the assessment. Coverage diagrams are also shown, when practical, for most of the sample cases, but it is not the intent to directly compare or overlay these coverage diagrams. Each coverage diagram should show only one free-space range threshold as defined in each applicable sample case; however, any color or gray-shade scale based on one or more thresholds (e.g. propagation loss, propagation factor, free space range, etc.) could also be used. Hence, coverage diagrams vary in scale and depiction. The primary intent of the coverage diagrams is to demonstrate a model's capability to generate them and to provide a basis for model timing.

In the following sample case descriptions, it is assumed that all modified refractivity profiles are extrapolated in height above the highest height listed at the rate defined by the highest two levels. For all cases of propagation over terrain, the heights in the refractivity profiles and the receiver heights are referenced to sea level (not to the local terrain height). Two of the cases include measured radio data.

All cases except Case 2 assume an omnidirectional antenna for widest applicability to existing models. A smooth sea and horizontal polarization are assumed unless otherwise stated.

The last 4 cases include a real terrain path from Long Beach to Point Mugu, California, which consists of terrain heights up to 38 m, then sea, then heights up to 244 m, then sea again, and then onto the beach at Point Mugu.

For models that require electrical characteristics of the lower boundaries, the values described in the Recommendations and Reports of the CCIR [3] were used. The appropriate values for the relative permittivity ε_r and the conductivity σ (S/m) are listed in Table 1 for each frequency needed in the sample cases. The values for the terrain case are based on the values described for "medium dry ground."

Frequency	Sea Water		Medium Dry Ground	
MHz	ε_r	σ (S/m)	ε_r	σ (S/m)
128	70.0	5.0	15.0	0.002
450	70.0	5.0	---	---
3000	69.1	7.2	15.0	0.23
3300	68.7	7.5	---	---
10000	53.5	17.0	11.9	1.64

Table 1. Electrical characteristics of the lower boundaries.

Modelers were requested to submit a brief report listing the type of computer used, the run time required, and any comments deemed appropriate for each sample case performed. These comments, provided by the modelers follow:

Kenneth D. Anderson, MLAYER

For case 1, I have only the height gain curve (MLAYER is a mode model and generating a coverage diagram is not practical). For case 3, I have only the range gain curve. Both cases were run on a 486 DX/50 MHz PC. The specifics of runtimes are:

Case 1: RunTime 1760 Seconds (400 Modes, 0.52 dB Attenuation cutoff)
Case 3: RunTime 382 Seconds (27 Modes, 2.1 dB Attenuation cutoff)
I would estimate an order of magnitude increase in runtimes to do a "coverage" diagram.

Also, when you plot case 1 results, MLAYER "blows up" at heights in excess of 480 m. This kind of behavior happens with MLAYER when there are very strong, very thick surface ducts. My estimate is that several orders of magnitude increase in runtime is needed to get all of the significant modes (We may also need to specifically tune the Airy function integrations). It may not be practical.

For case 3, the closest range that I provide is 10 km. At reduced ranges more modes are required. My estimate is an order of magnitude increase in runtime is needed to get to 5 km, two

to three orders increase is needed to get to 1 km, and I doubt that we could get accurate results for ranges less than 1 km.

Amalia E. Barrios, TPEM

Comments regarding results for sample cases 1-10 that were produced by TPEM.

All cases were run on a Pentium 90 MHz PC.

Case 1: Although the case called for vertical polarization, I assumed horizontal polarization, since currently TPEM does not have the capability to model finite conductivity. Runtime: 104.7 secs.

Case 2: No comments. Runtime: 3.0 secs.

Case 3: No results produced for this case.

Case 4: No comments. Runtime: 7.3 secs.

Case 5: No comments. Runtime: 76.4 secs.

Case 6: No comments. Runtime: 82.7 secs

Case 7: The antenna height displayed on the coverage diagram refers to the antenna height above the local ground at range 0. The sample case required the antenna be located 1000 m above mean sea level, however, the height of the ground at range 0 is 8 m. Therefore I've placed the antenna height at 992 m above the ground to simulate a 1000 m above-mean-sea-level antenna height. The results are given in terms of height above mean sea level (m) vs. propagation factor in dB. Runtime: 116.4 secs.

Case 8: Results are given in terms of height above mean sea level (m) vs. propagation factor in dB. Runtime: 7.9 secs.

Case 9: Results are given in terms of height above mean sea level (m) vs. propagation factor in dB. Runtime: 8.2 secs.

Case 10: Horizontal polarization was assumed for this case (see comments for Case 1).

Gary Brooke, SAFARI

Case 1. I consider the results for this test case to be very accurate!!

Case 2 These results are also pretty good, however, there is a discrepancy at longer range which I have not sorted out!!

Case 3: Results for rough surface - Kirchoff approximation with correlated surface spectrum. Interpret results with caution because roughness spectrum is not Miller Brown!!

Case 5: This result is undersampled - a challenging problem for SAFARI!!

Case 6: I thought I would get better agreement with others in this test case - SAFARI likely not sampled enough in wavenumber space !!

Case 8: Note that these results are for a range-independent environment defined at range zero (i.e. at source). They should show the difference between terrain and no terrain!!

Case 9: These are results for a range-independent environment defined at the source - again intended to show difference between terrain and no terrain!!

G. Daniel Dockery, TEMPER Version 2.01

General Notes:

- All computations performed on Compaq 486/50L (50 MHz) using Microway NDP Fortran

- Transform sizes and range steps chosen to be "safe" with respect to accuracy. Smaller transform sizes and/or larger ranges steps, resulting in shorter execution times, may have provided adequate performance in some cases.

Case 1

- All parameters exactly as stated in case description.
- Half-space transform size: 2^{13}; range step: 0.2 km.
- Execution time: 1438 seconds.

Case 2

- All parameters exactly as stated in case description.
- Half-space transform size: 2^{11}; range step: 0.1 km.
- Execution time: 272 seconds.

Case 3

Case 3a:

- Uses grazing angles calculated by geometric optics to modify surface impedance to account for roughness.
- All parameters exactly as stated in case description.
- Half-space transform size: 2^{10}; range step: 0.1 km.
- Execution time: 141 seconds.

Case 3b:

- Uses grazing angles estimated by MUSIC spectral estimator within TEMPER V2.01 to modify surface impedance (less accurate for evaporation duct refractivity profiles).
- All parameters as in Case 3a.
- Execution time: 257 seconds.

Case 4

- All parameters exactly as stated in case description.
- Half-space transform size: 2^{11}; range step: 0.2 km.
- Execution time: 304 seconds.

Case 5

- All parameters exactly as stated in case description.
- Half-space transform size: 2^{14}; range step: 0.5 km.
- Execution time: 2007 seconds.

Case 6

- All parameters exactly as stated in case description.
- Half-space transform size: 2^{13}; range step: 0.1 km.
- Execution time: 1210 seconds.

Case 7

- All parameters exactly as stated in case description.
- Half-space transform size: 2^{14}; range step: 0.1 km.
- Execution time: 2451 seconds.

Case 8

- All parameters exactly as stated in case description except that surface electrical parameters of terrain are not modeled.
- Half-space transform size: 2^{10}; range step: 0.1 km.
- Execution time: 141 seconds.
- Output data provided from mean sea level.

Case 9

- All parameters exactly as stated in case description except that surface electrical parameters of terrain are not modeled.
- Half-space transform size: 2^{10}; range step: 0.1 km.

- Execution time: 141 seconds.
- Output data provided from mean sea level.

Case 10

- All parameters exactly as stated in case description except that surface electrical parameters of terrain are not modeled.
- Half-space transform size: 2^{10}; range step: 0.1 km.
- Execution time for each time sample: 141 seconds.

Nicolas Douchin, DIF-CERT

I have only tried sample cases 3, 8 and 9 because the other cases would have taken too much time for the adaptation of my model.

The simulations have been done using our PE-model, at CERT, called "DIF-CERT".
In this propagation model, the Parabolic Equation method is used, and this equation is solved using finite differences (CRANK-NICHOLSON algorithm). The electrical characteristics of the lower boundary are taken into account, and also the roughness of the sea surface which is simulated using realisations of a stochastic process and the PHILLIPS wave spectrum (cf. sample case 3).

I can not use a "sin(x)/x" antenna pattern in DIF-CERT, but I only consider the main lobe of this pattern and a gaussian model for it. Also, can not consider the case of an omnidirectionnal pattern.

Sample case 3.

In my simulation:
theta 3dB = 3 deg.
vertical sampling step = 0.05 m
horizontal sampling step = 2 m
total height of the calculation domain = 300 m
The calculation took 29 mn on a HP/730 workstation.

Sample cases 8 and 9.

In my simulation:
theta 3dB = 3 deg.
vertical sampling step = 0.2 m
horizontal sampling step = 5 m
total height of the calculation domain = 1200 m

The calculation took: 12 mn on the same workstation.

In the ascii file, the heights are above sea level and not above local terrain. That is why the values at 0m and 1m are missing.

Claude P. Hattan, EREPS

Case 1

File generated by EREPS ffactr.bas subroutine; Pentium 90MHz - 13.1 secs.

Case 2

File generated by EREPS ffactr.bas subroutine; Pentium 90MHz - 2.85 secs.

Case3

File generated by EREPS ffactr.bas subroutine; Pentium 90MHz - 2.85 secs.

Herbert V. Hitney, RPO

Results are for the first four sample cases using the Radio Physical Optics (RPO) propagation model. Results for all four cases were run using RPO Version 1.14. Sample Case 3 was also run using RPO Version 1.14x, which includes a correction to take surface roughness into account. Specific comments for each case follow.

Sample Case 1.
This case calls for vertical polarization for a strong surface-based duct. This case is dominated by the PE and XO regions of RPO 1.14, which do not rigorously model vertical polarization for this condition.

Sample Case 2.
This case is exclusively in the PE region of RPO 1.14.

Sample Case 3.
This case is exclusively in the PE region of RPO. Version 1.14 does not account for surface roughness effects. An additional result is submitted for RPO version 1.14x, which does have a correction for surface roughness.

Sample Case 4.
This case is exclusively in the PE region of RPO 1.14.

RUN TIMES:

All computations were performed on a 90 MHz Pentium PC. The following run times refer to the complete generation of the coverage diagram for each case. For Sample Case 3, the run times are the same for both RPO 1.14 and 1.14x.

Sample Case 1: 10.7 seconds.
Sample Case 2: 5.5 seconds.

Sample Case 3: 5.2 seconds.
Sample Case 4: 10.8 seconds.

Mireille Levy, EEMS & PCPEM

Brief report on our results:

Computers used:
- for EEMS, 100 MHz Pentium PC
- for PCPEM, T800 transputer PC-plug-in board

Run times:
- Sample case 1: 4 minutes
- Sample case 2: 7 seconds
- Sample case 3: 7 seconds
- Sample case 4: 20 minutes
- Sample case 5: 3 minutes 10 seconds
- Sample case 6: 2 minutes
- Sample case 7: 3 minutes 10 seconds
- Sample case 8: 20 seconds
- Sample case 9: 42 seconds
- Sample case 10: 40 minutes

Additional comments:
- Sample case 1: the run-time is relatively long because the current version of EEMS uses the vertical PE in a height domain including all ducts.

I have just implemented a new version of HPEM which can deal with ducting layers provided they are not strong enough to send energy back downwards. Our EEMS model can be greatly speeded up by this, since the region in which we have to use the vertical PE method can be substantially reduced in some cases.

This is in particular applicable to sample case 1, where a high weak duct is present. Sample case 1 timings for EEMS 1.5 on 100 MHz Pentium: 28 seconds

- Sample case 3: roughness is not modelled by the current version of EEMS.

- Sample case 4: PCPEM does not include an omni-directional antenna model. The run was done for a Gaussian beam pattern, with beamwidth 3 degrees.

- Sample cases 5,6,7:

1) With high antennas results are very dependent on the modelling of ground reflections. We have used a perfectly conducting ground.

2) Since the output grid is likely to undersample the interference lobing, the output, in particular the coverage diagram, depends on whether or not smoothing is applied. Currently

EEMS does no smoothing or interpolation in the vertical PE part of the domain, and uses an interpolation procedure in the rest of the domain.

E.MANDINE, Corafin

I - P.E. model Corafin.

Our electromagnetic propagation model Corafin is a usual 2D parabolic code, with a finite differences - Crank Nicolson solver. This prototype was first developed by M. Fournier at LCTAR([1]). It is still under development, and we cannot yet simulate complex electromagnetic features such as realistic radiation patterns or elevation angle. It cannot either take into account propagation over an irregular terrain or a rough sea.

2 - Selected sample cases.

For the reasons set above, we can only submit results for cases 2 and 5, and partial results for cases 3 and 6; cases 1 and 4, and cases 3 and 6 with beamwidth larger than 6 degrees all require prohibiting computational times, due to the very large integration domains considered ; the last ones (7 to 10) include irregular terrain consideration, which is not allowed by Corafin. Taking into account wind-roughened sea-surface in case 3 is not possible either.

Another problem was to provide a propagation factor, the standard output of Corafin being either an electromagnetic field or a propagation loss. Due to the lack of time, it has not been possible to modify our code in order to recover the free space coverage. The result of the simple method used (direct evaluation from the distance between transmitter antenna and free space position) are clearly incorrect : all the computed propagation factors are enhanced of 10 to 12 dB.

3 - Model results

All the computations have been made using a HP 735 computer.

Sample case 2 :

- Vertical antenna pattern : sinx/x pattern, with a beamwidth of 2 degrees.
- No elevation angle.
- Run time required: 4 minutes.

Sample case 3 :

- Vertical antenna pattern : "isotropic" pattern, □with a beamwidth of 6 degrees.
- The wind-roughened sea-surface is not taken into account.
- Run time required: 6h30.

Sample case 5:

- Vertical antenna pattern : "isotropic" pattern, with a beamwidth of 10 degrees.
- Run time required : 2h00.

Sample case 6 :

- Vertical antenna pattern : "isotropic" pattern, with a beamwidth of 4 degrees.
- Run time required: 2h20.

Reference :

(1) M. Fournier, methode d'Ävaluation de la propagation dans les conduits atmospheriques, AGARD conference proceeding 567, 1986

Sample Case 1.

This case considers propagation in a strong surface-based duct over sea water. The frequency is 3 GHz, the transmitter antenna is 25 m above the sea, and vertical polarization is assumed. The refractivity profile is derived from a radiosonde measurement at Point Mugu on 25 August 1993 during VOCAR IOP, consisting of a strong surface-based duct about 400 m thick plus a weak elevated duct at about 1000 m, as described in Table 2 and plotted in Figure 1. A coverage diagram is desired for receiver heights from 0 to 5000 m and ranges from 0 to 250 km using a free-space range of 125 km. Propagation factor is required at a range of 250 km for receiver heights of 0 to 5000 m.

Height (m)	Refractivity (M units)
0	339.8
292	378.1
332	337.9
403	322.7
514	338.6
590	381.1
998	435.4
1016	435.2
1083	443.7
1328	474.5
1379	484.3
2000	557.5

Table 2. Modified refractivity profile for Point Mugu, 25 August 1993.

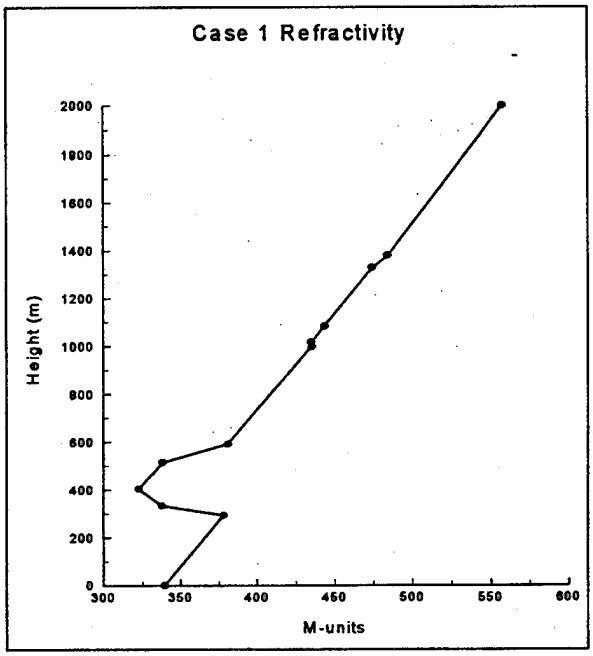

Figure 1. Plot of data in Table 2.

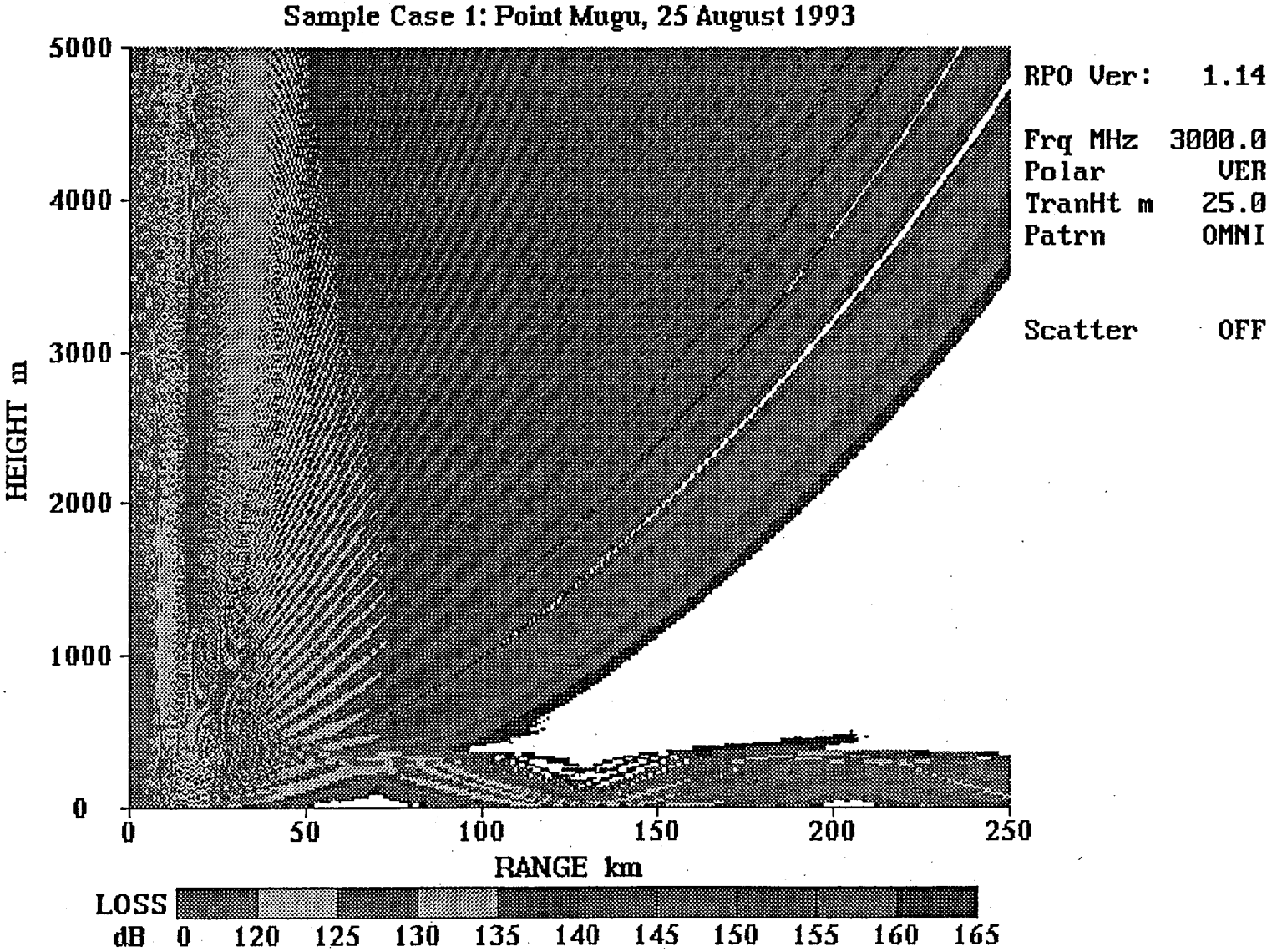
Sample Case 1: Point Mugu, 25 August 1993
HEIGHT m
5000
4000
3000
2000
1000
0
0
50
100
150
200
250
RANGE km
RPO Ver: 1.14
Frq MHz 3000.0
Polar VER
TranHt m 25.0
Patrn OMNI
Scatter OFF
LOSS
dB 0 120 125 130 135 140 145 150 155 160 165

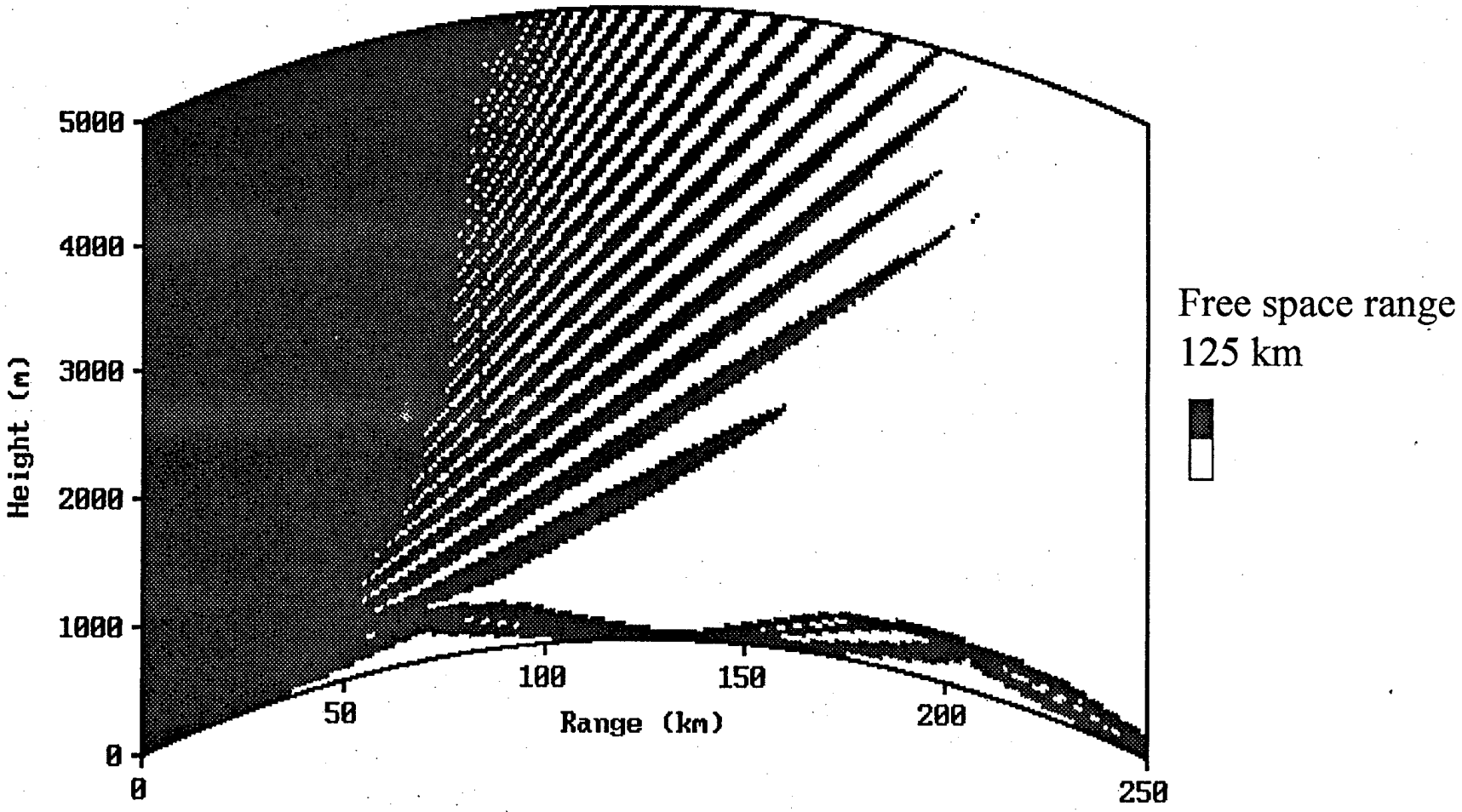

EEMS 1.0 Sample case 1

HAP

SAMPLE CASE 1

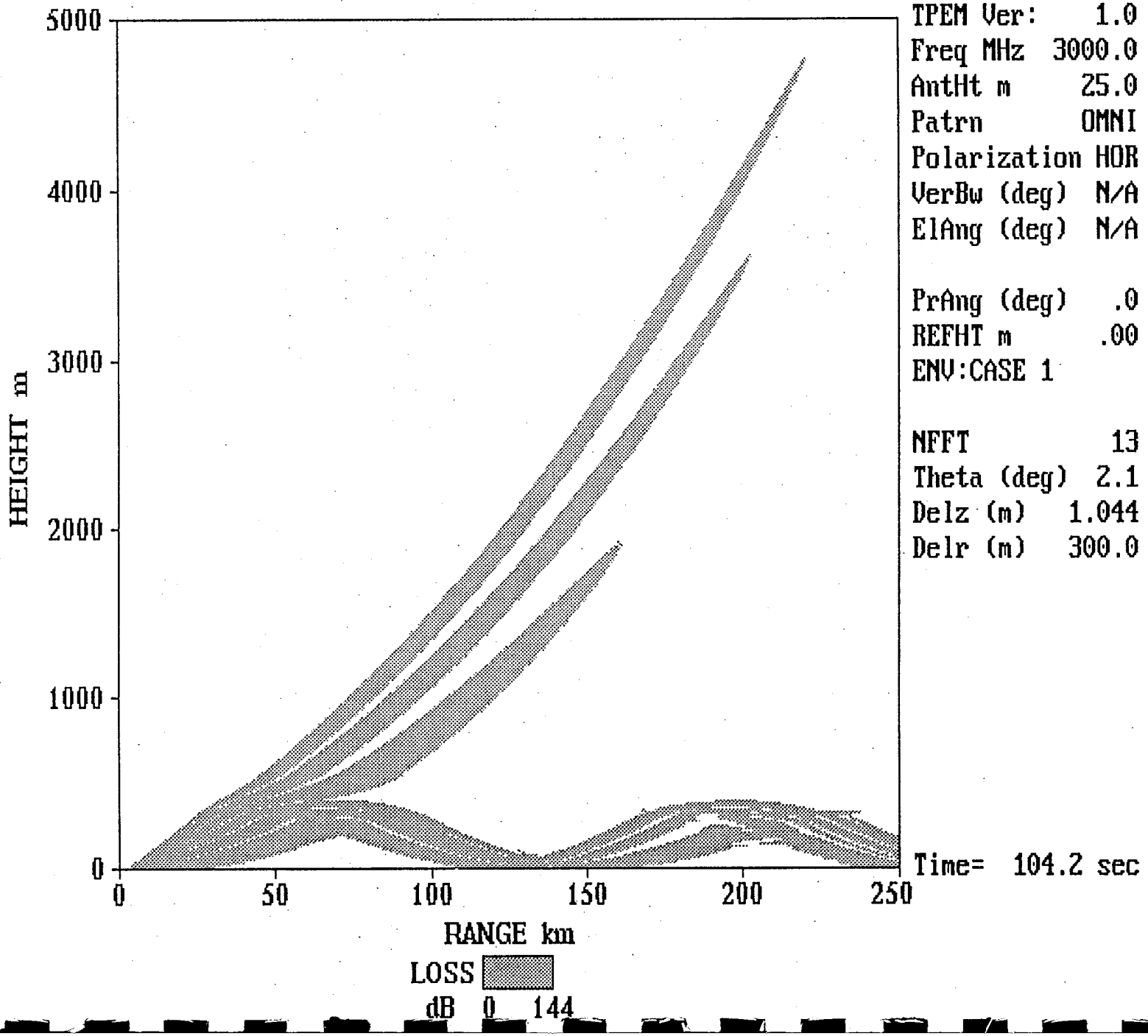
5000
4000
3000
2000
1000
0
HEIGHT m
0
50
100
150
200
250
RANGE km
LOSS
dB 0 144
TPEM Ver: 1.0
Freq MHz 3000.0
AntHt m 25.0
Patrn OMNI
Polarization HOR
VerBw (deg) N/A
ElAng (deg) N/A
PrAng (deg) .0
REFHT m .00
ENV:CASE 1
NFFT 13
Theta (deg) 2.1
Delz (m) 1.044
Delr (m) 300.0
Time= 104.2 sec

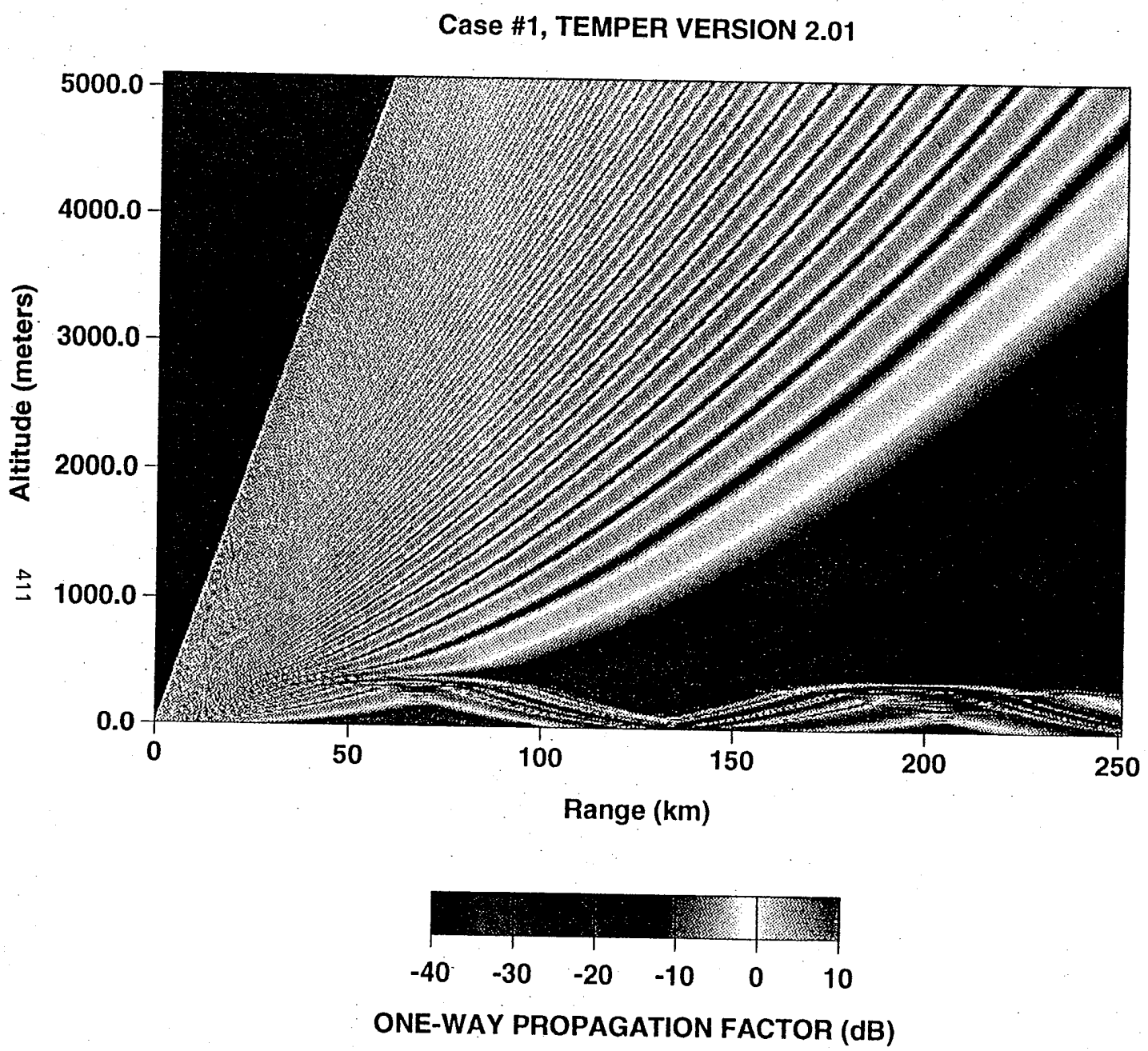
Case #1, TEMPER VERSION 2.01
5000.0
4000.0
3000.0
2000.0
1000.0
0.0
Altitude (meters)
0
50
100
150
200
250
Range (km)
-40
-30
-20
-10
0
10
ONE-WAY PROPAGATION FACTOR (dB)

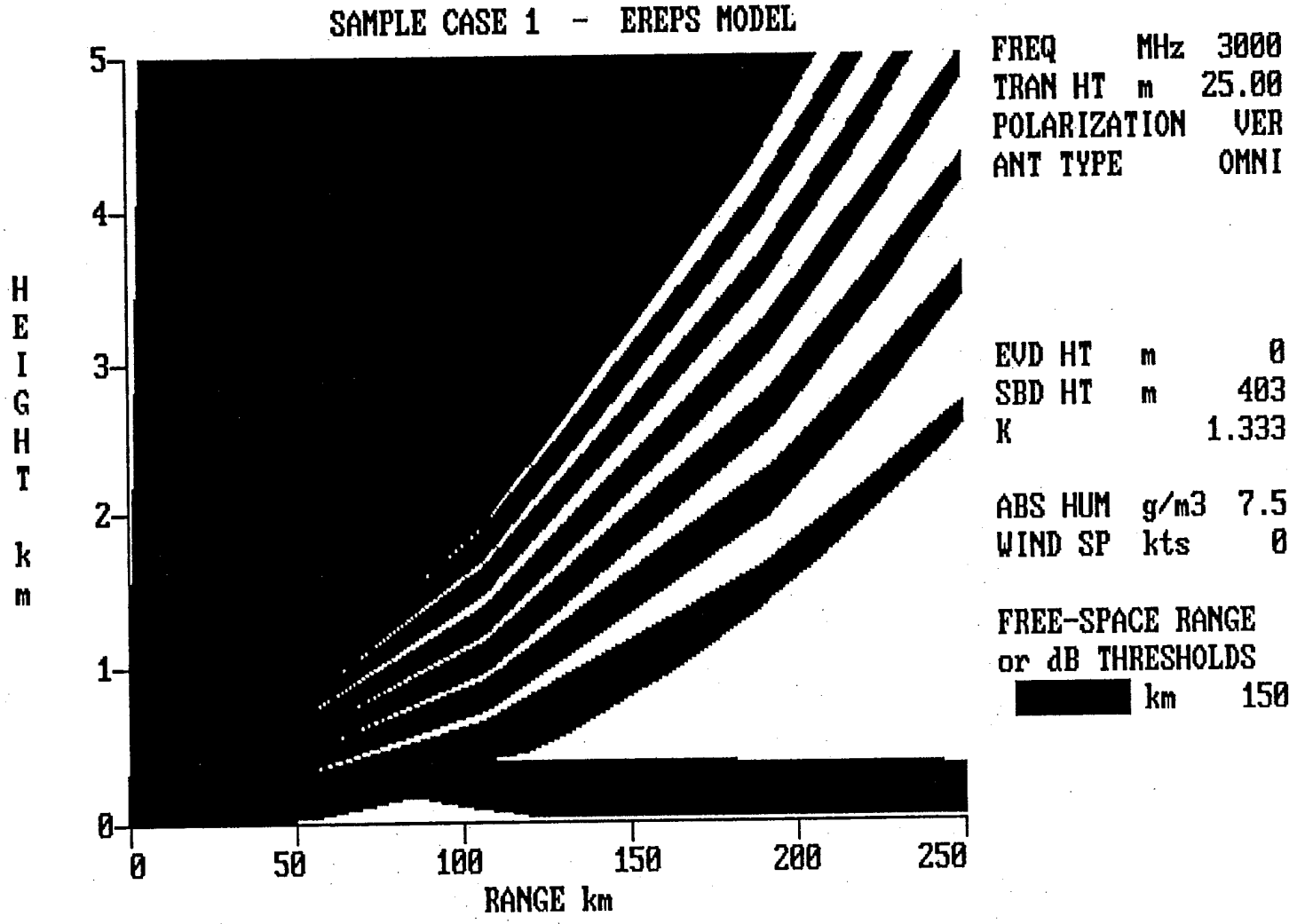
SAMPLE CASE 1 - EREPS MODEL
HEIGHT km
5
4
3
2
1
0
0
50
100
150
200
250
RANGE km
FREQ MHz 3000
TRAN HT m 25.00
POLARIZATION VER
ANT TYPE OMNI
EVD HT m 0
SBD HT m 403
K 1.333
ABS HUM g/m3 7.5
WIND SP kts 0
FREE-SPACE RANGE
or dB THRESHOLDS
km 150

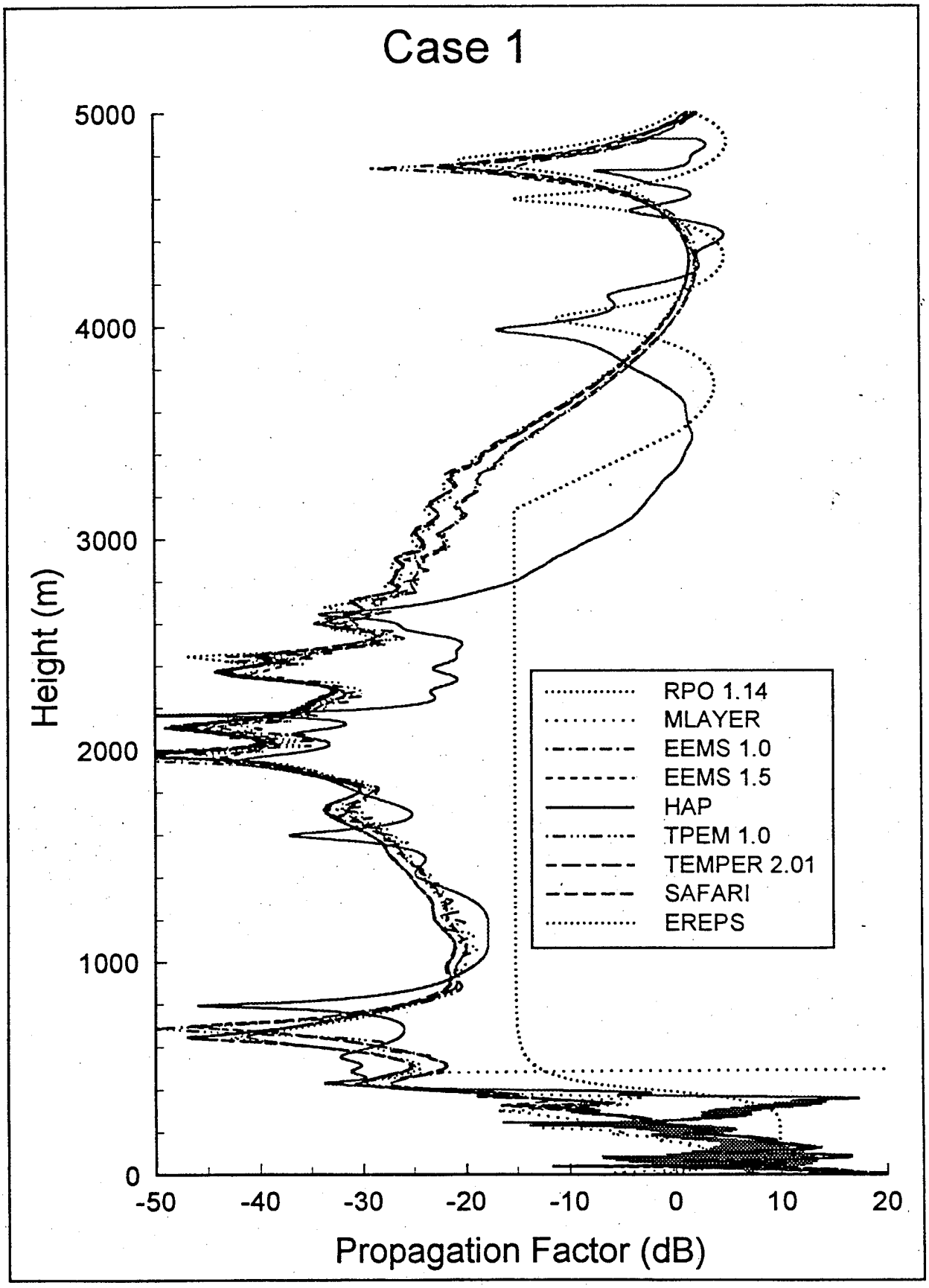
Case 1
5000
4000
3000
2000
1000
0
Height (m)
-50
-40
-30
-20
-10
0
10
20
Propagation Factor (dB)
RPO 1.14
MLAYER
EEMS 1.0
EEMS 1.5
HAP
TPEM 1.0
TEMPER 2.01
SAFARI
EREPS

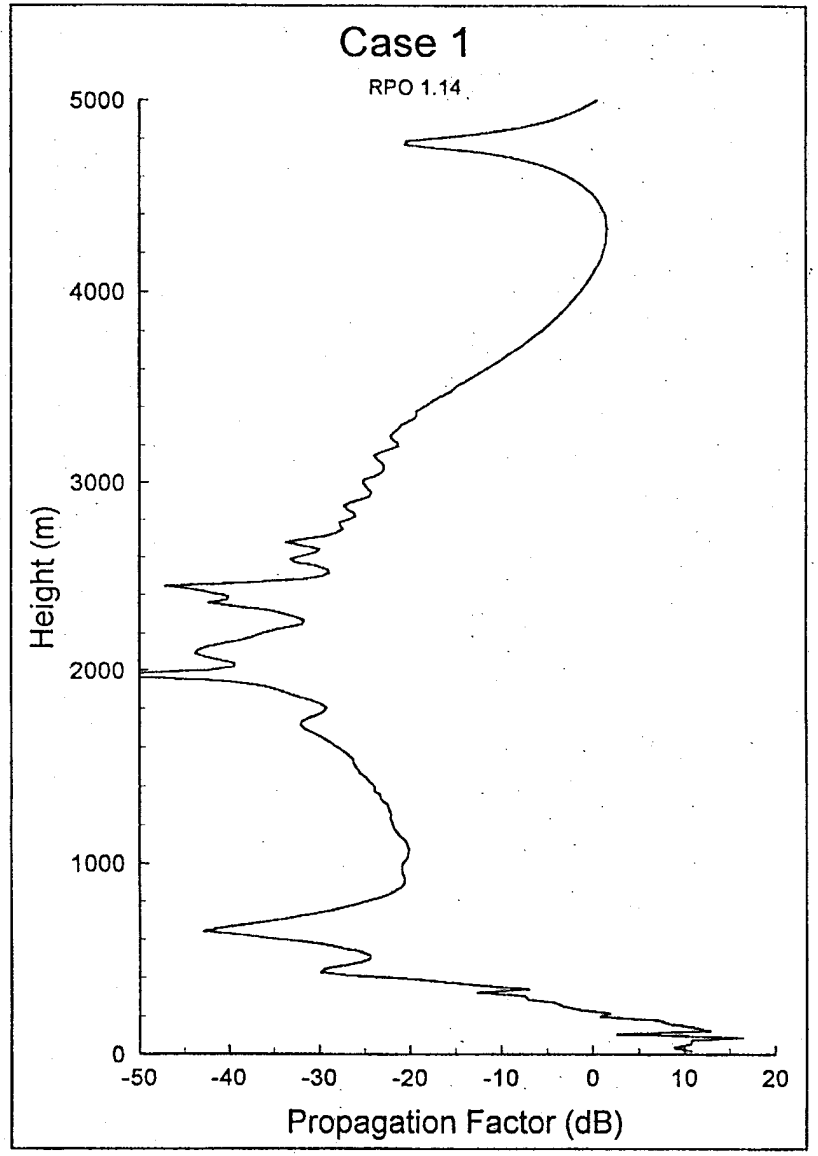
Case 1
RPO 1.14
5000
4000
3000
2000
1000
0
Height (m)
-50
-40
-30
-20
-10
0
10
20
Propagation Factor (dB)

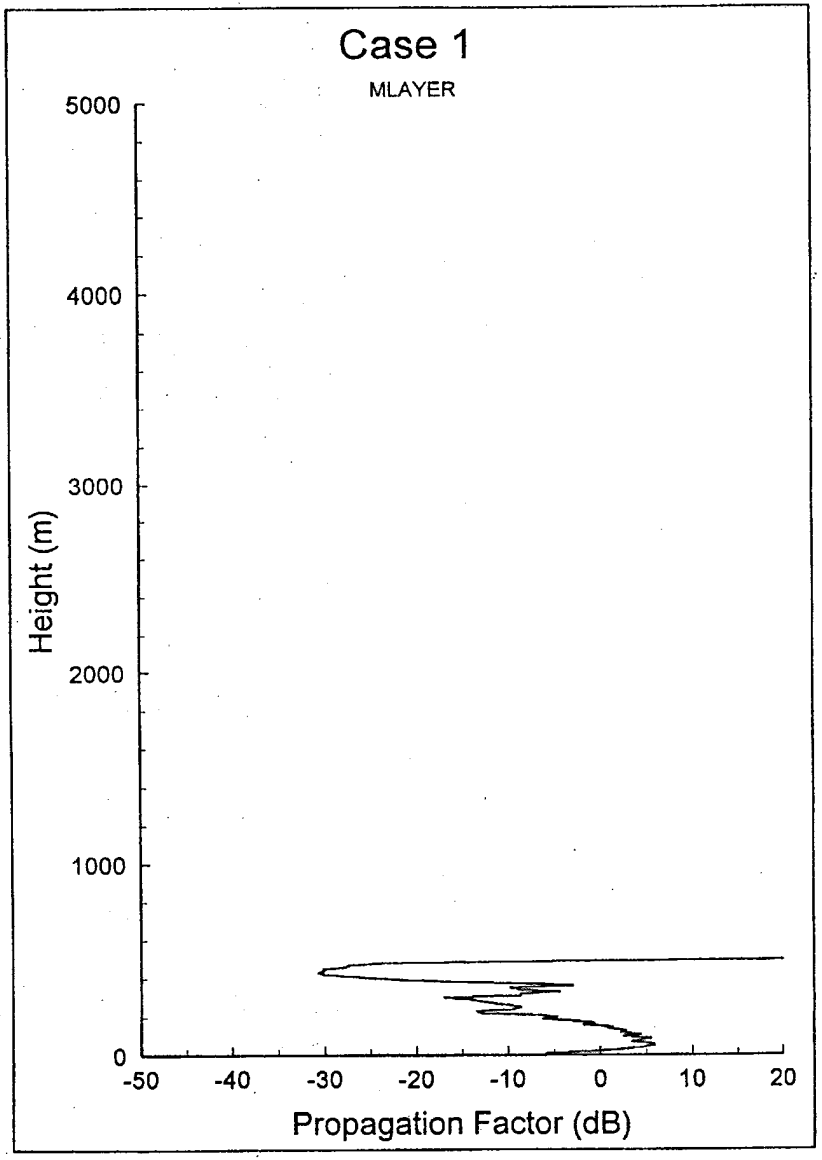
Case 1
MLAYER
5000
4000
3000
2000
1000
0
Height (m)
-50
-40
-30
-20
-10
0
10
20
Propagation Factor (dB)

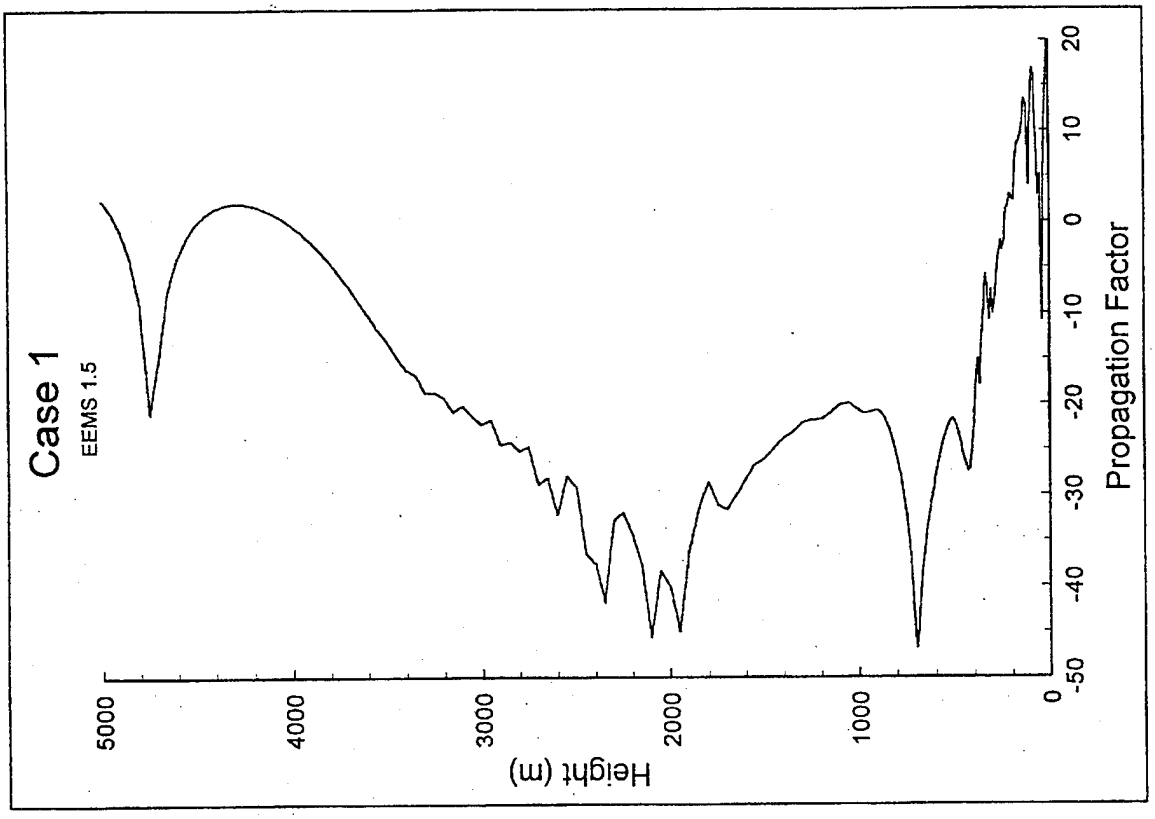
Case 1
EEMS 1.5
Height (m)
5000
4000
3000
2000
1000
0
-50
-40
-30
-20
-10
0
10
20
Propagation Factor

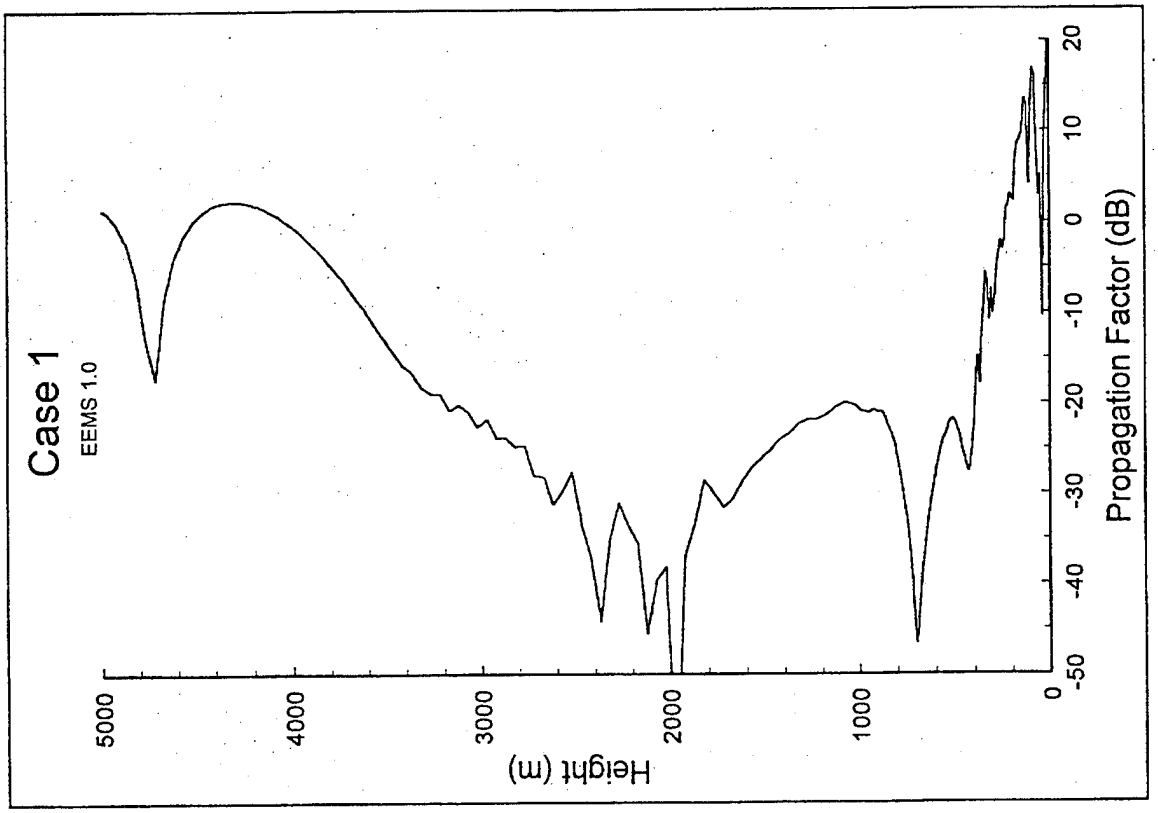
Case 1
EEMS 1.0
Height (m)
5000
4000
3000
2000
1000
0
-50
-40
-30
-20
-10
0
10
20
Propagation Factor (dB)

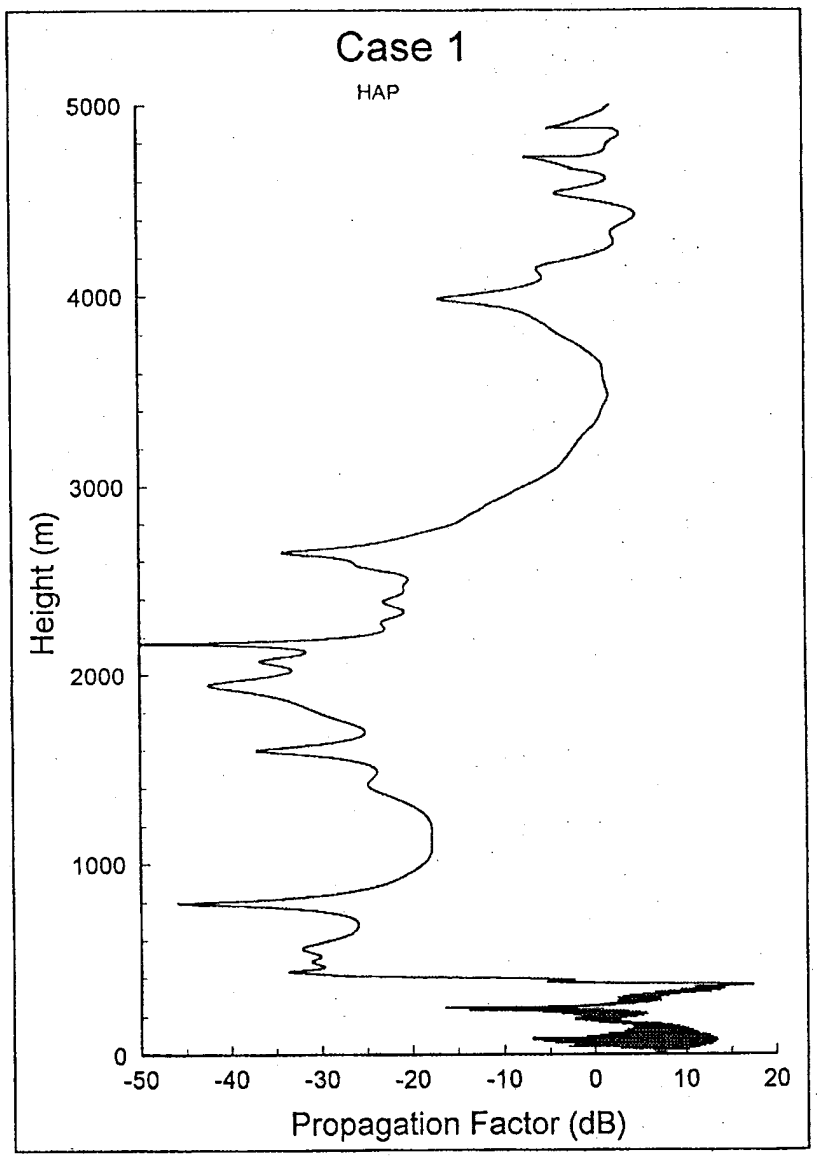
Case 1
HAP
Height (m)
5000
4000
3000
2000
1000
0
-50
-40
-30
-20
-10
0
10
20
Propagation Factor (dB)

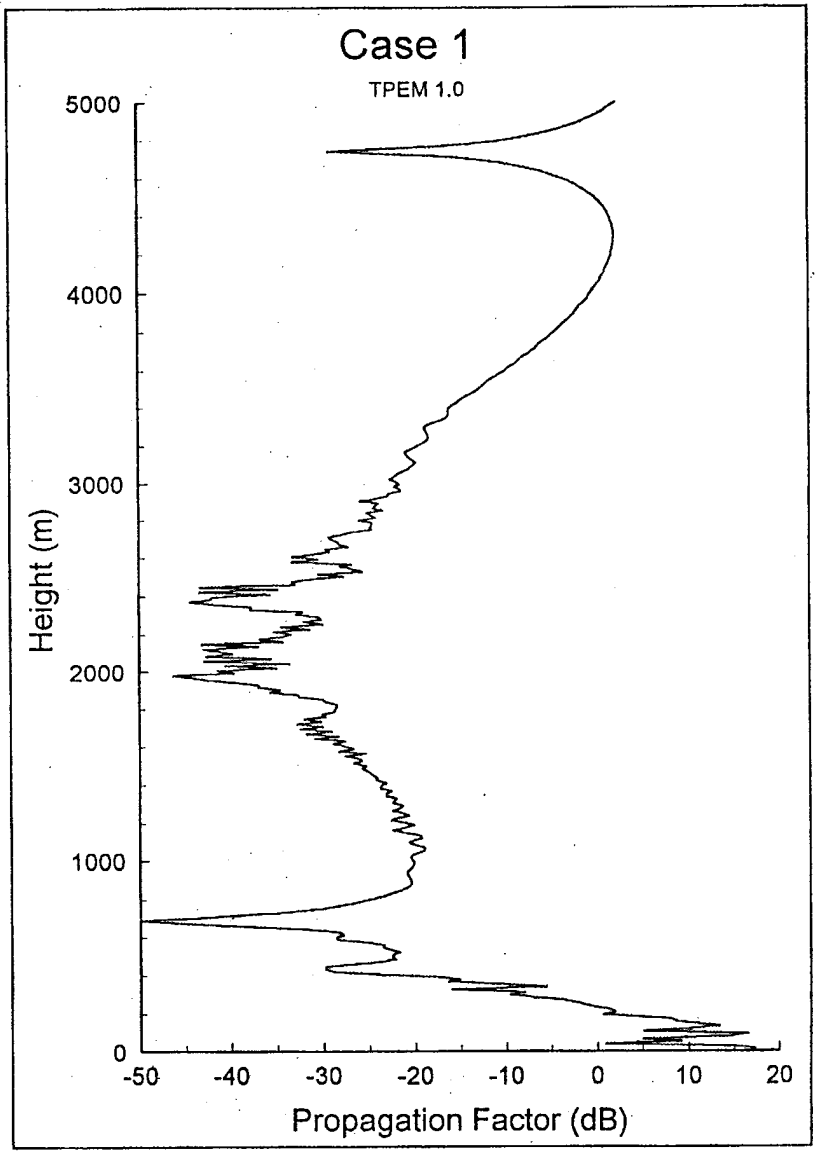
Case 1
TPEM 1.0
Height (m)
5000
4000
3000
2000
1000
0
-50
-40
-30
-20
-10
0
10
20
Propagation Factor (dB)

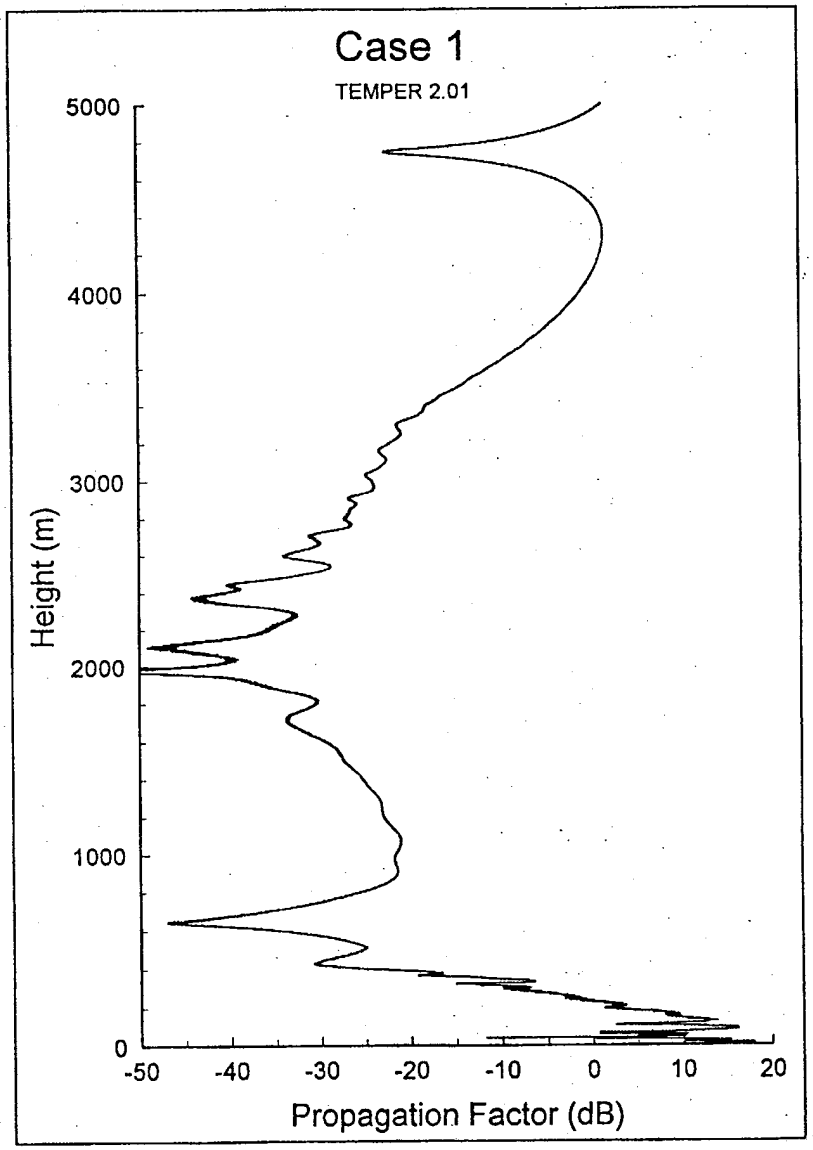
Case 1
TEMPER 2.01
Height (m)
5000
4000
3000
2000
1000
0
-50
-40
-30
-20
-10
0
10
20
Propagation Factor (dB)

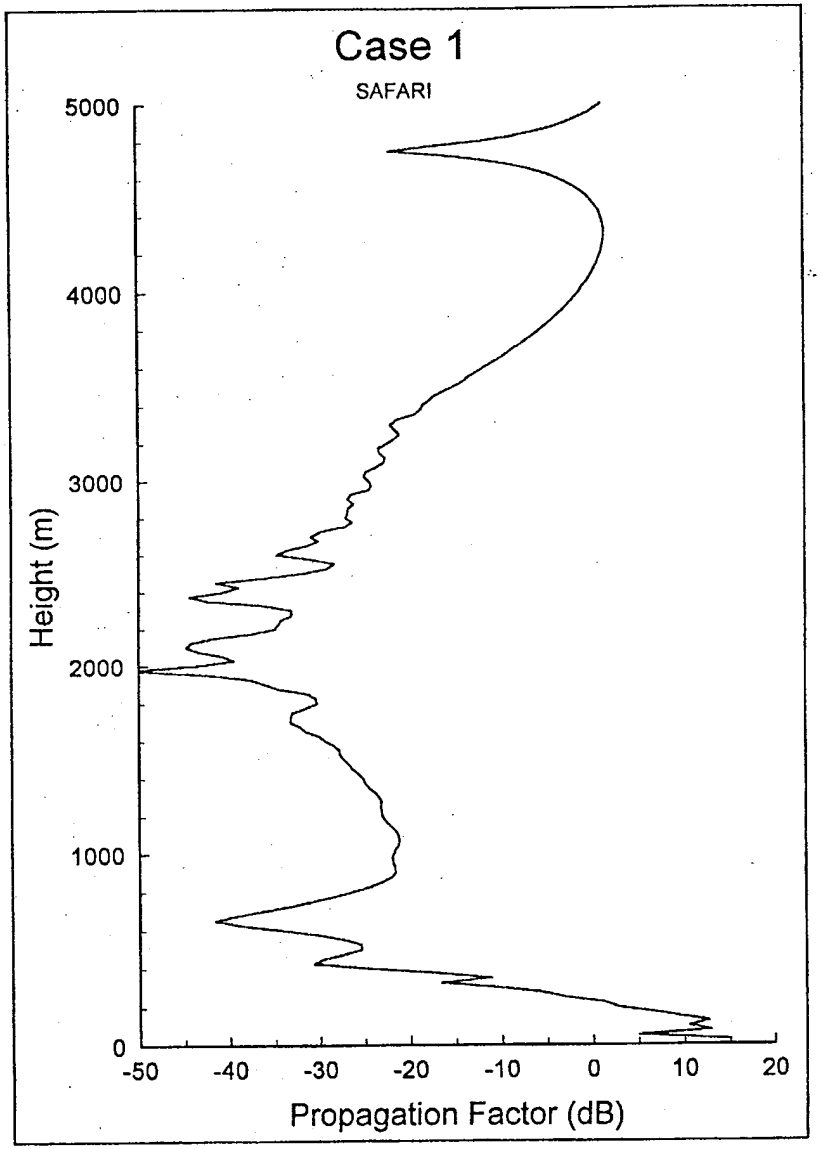
Case 1
SAFARI
Height (m)
5000
4000
3000
2000
1000
0
-50
-40
-30
-20
-10
0
10
20
Propagation Factor (dB)

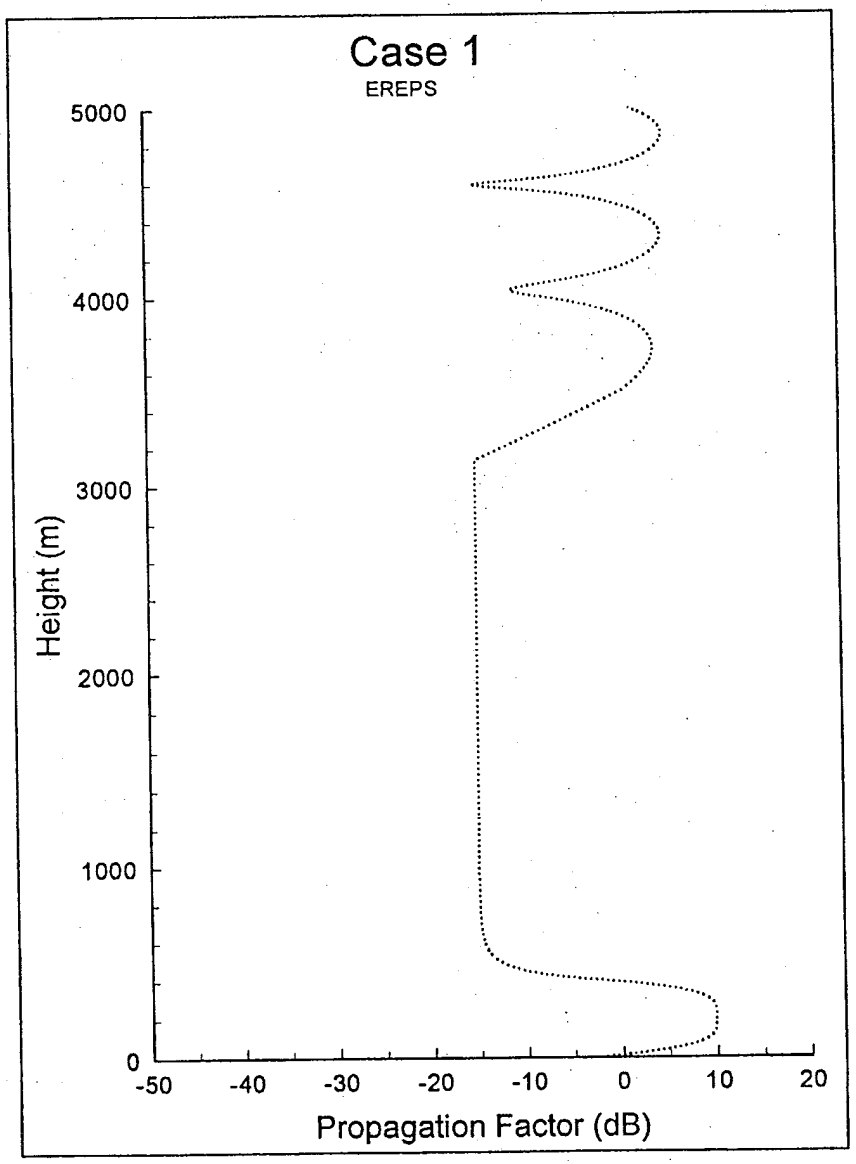
Case 1
EREPS
5000
4000
3000
2000
1000
0
Height (m)
-50
-40
-30
-20
-10
0
10
20
Propagation Factor (dB)

Sample Case 2.

This case concerns propagation in a typical evaporation duct. The frequency is 10 GHz and the transmitter antenna is 25 m above the sea. The vertical antenna pattern is a "sin(x)/x" pattern with a (full 3 dB to 3 dB) beamwidth of 2 degrees and an elevation angle of 1 degree. The refractivity profile is specified in Table 3 and plotted in Figure 2. This corresponds to the world-average evaporation duct height of 13 m, and is based on neutral stability conditions. A coverage diagram is desired for receiver heights from 0 to 100 m and ranges from 0 to 100 km, based on a free space range of 50 km. Propagation factor is required at a 25 m receiver height from 0 to 100 km range.

Height (m)	Refractivity (M units)
0.000	340.00
0.135	328.96
0.223	328.16
0.368	327.36
0.607	326.58
1.000	325.82
1.649	325.09
2.718	324.41
4.482	323.81
7.389	323.37
12.182	323.15
13.000	323.14
20.086	323.33
33.115	324.14
54.598	326.02
90.017	329.63
148.413	336.12

Table 3. Modified refractivity profile for the 13 m evaporation duct.

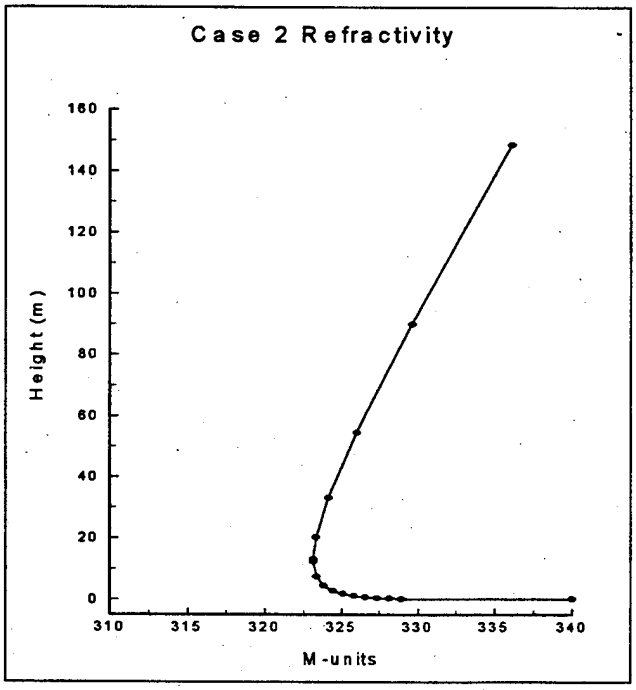

Figure 2. Plot of data in Table 3.

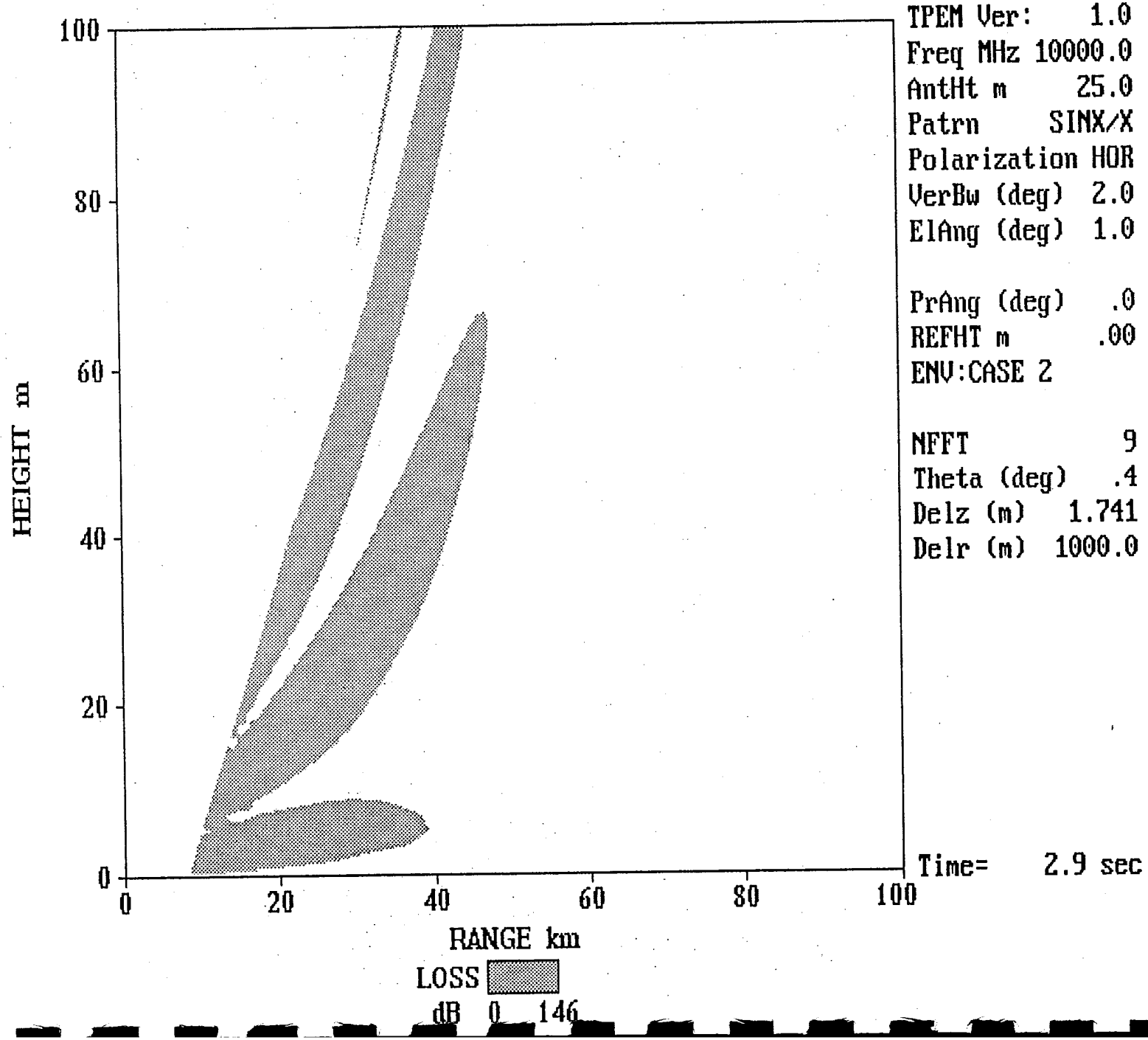
100
80
60
40
20
0
HEIGHT m
0
20
40
60
80
100
RANGE km
LOSS
dB 0 146
TPEM Ver: 1.0
Freq MHz 10000.0
AntHt m 25.0
Patrn SINX/X
Polarization HOR
VerBw (deg) 2.0
ElAng (deg) 1.0
PrAng (deg) .0
REFHT m .00
ENV:CASE 2
NFFT 9
Theta (deg) .4
Delz (m) 1.741
Delr (m) 1000.0
Time= 2.9 sec

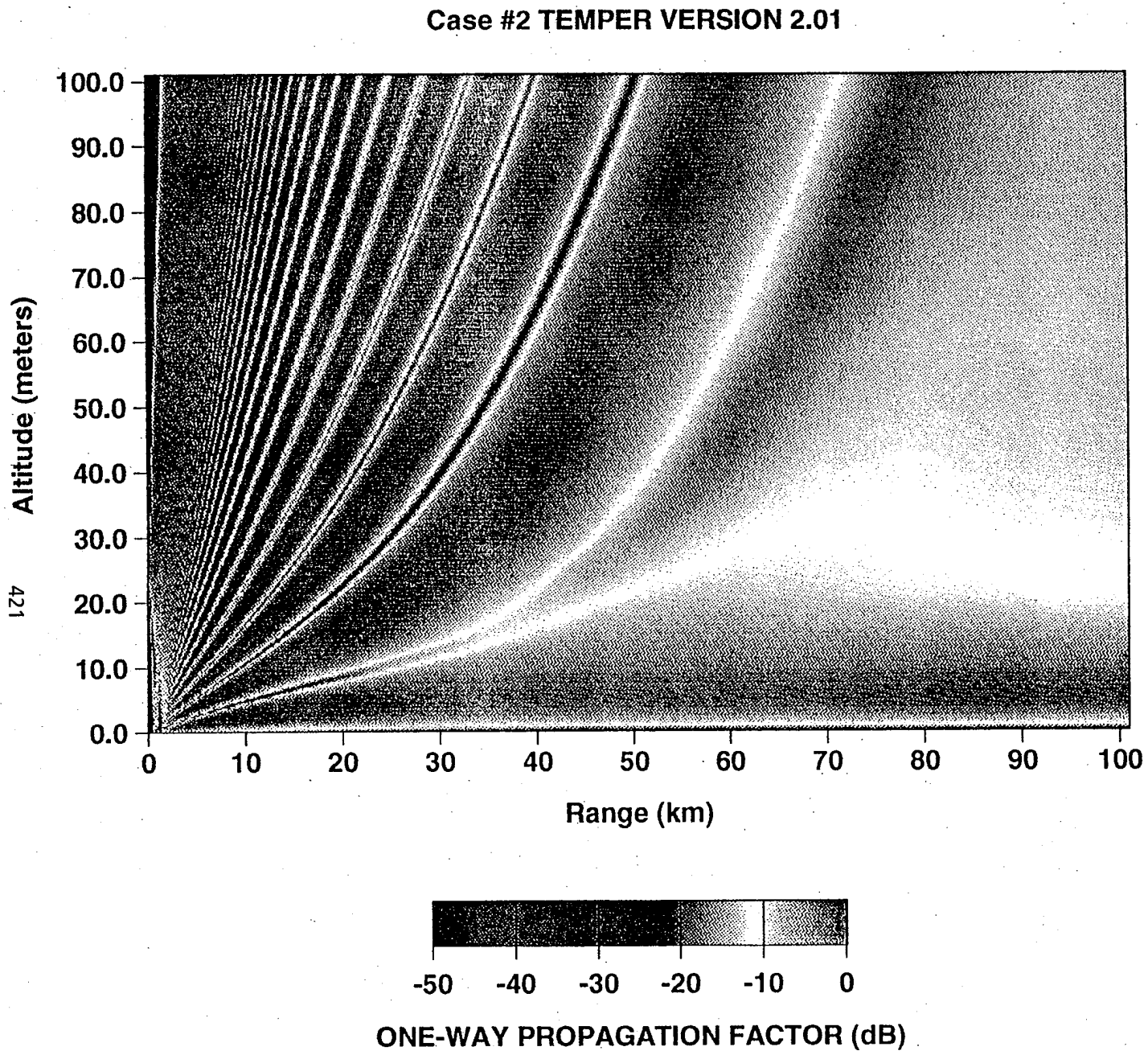
Case #2 TEMPER VERSION 2.01
Altitude (meters)
100.0
90.0
80.0
70.0
60.0
50.0
40.0
30.0
20.0
10.0
0.0
0
10
20
30
40
50
60
70
80
90
100
Range (km)
-50
-40
-30
-20
-10
0
ONE-WAY PROPAGATION FACTOR (dB)

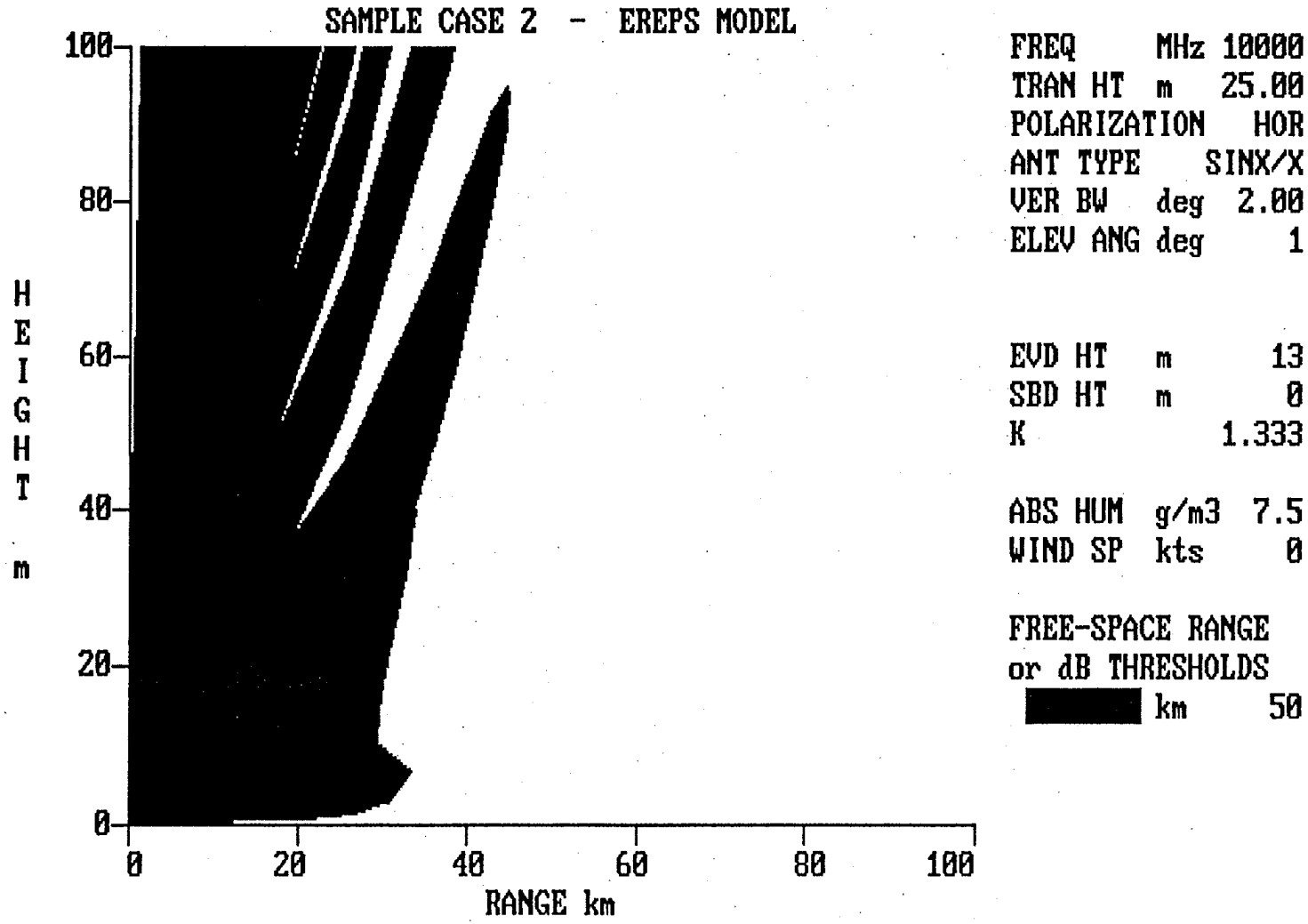
SAMPLE CASE 2 - EREPS MODEL
HEIGHT m
100
80
60
40
20
0
0
20
40
60
80
100
RANGE km
FREQ MHz 10000
TRAN HT m 25.00
POLARIZATION HOR
ANT TYPE SINX/X
VER BW deg 2.00
ELEV ANG deg 1
EVD HT m 13
SBD HT m 0
K 1.333
ABS HUM g/m3 7.5
WIND SP kts 0
FREE-SPACE RANGE
or dB THRESHOLDS
km 50

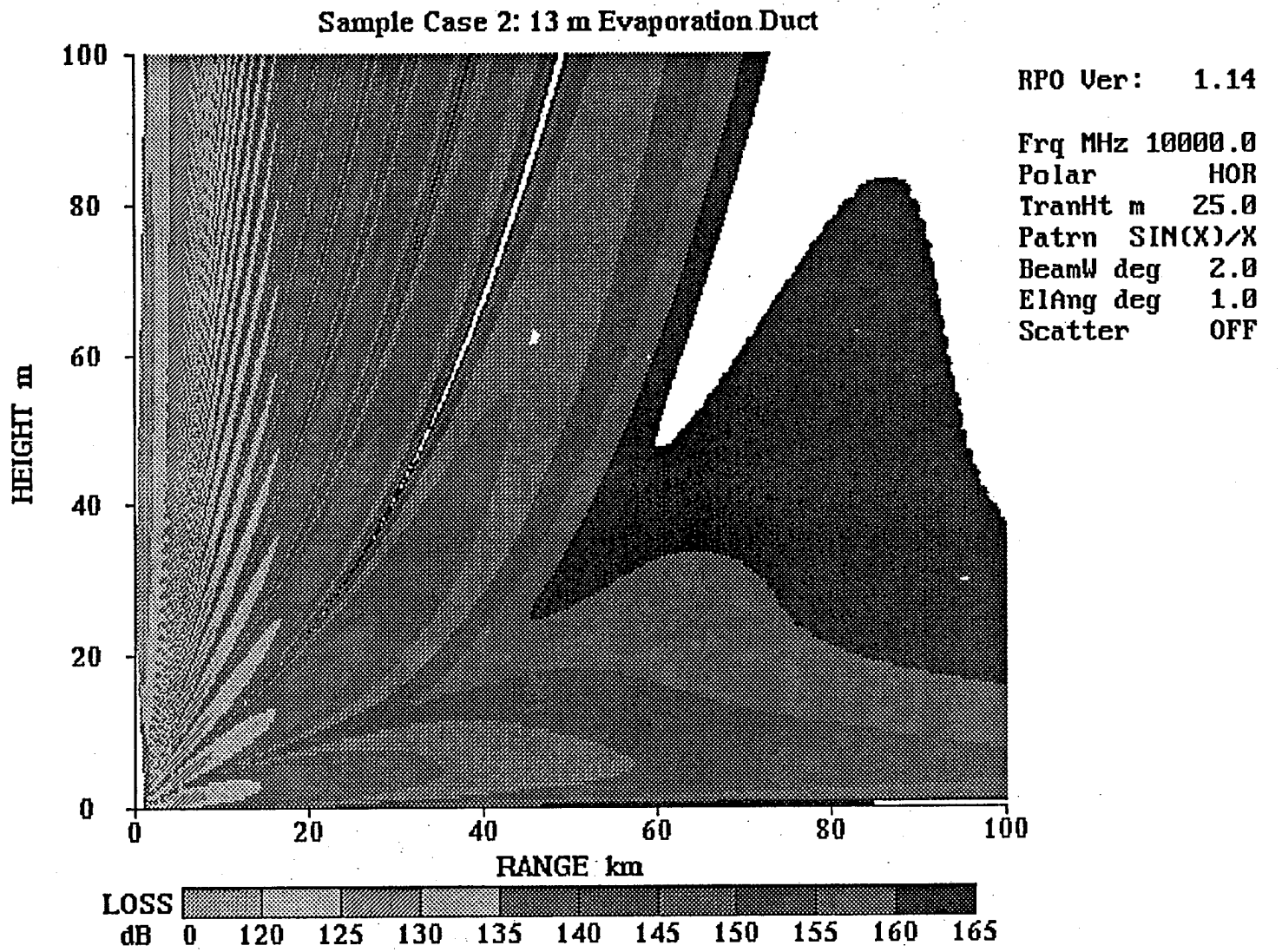
Sample Case 2: 13 m Evaporation Duct
HEIGHT m
100
80
60
40
20
0
0
20
40
60
80
100
RANGE km
LOSS
dB 0 120 125 130 135 140 145 150 155 160 165
RPO Ver: 1.14
Frq MHz 10000.0
Polar HOR
TranHt m 25.0
Patrn SIN(X)/X
BeamW deg 2.0
ElAng deg 1.0
Scatter OFF

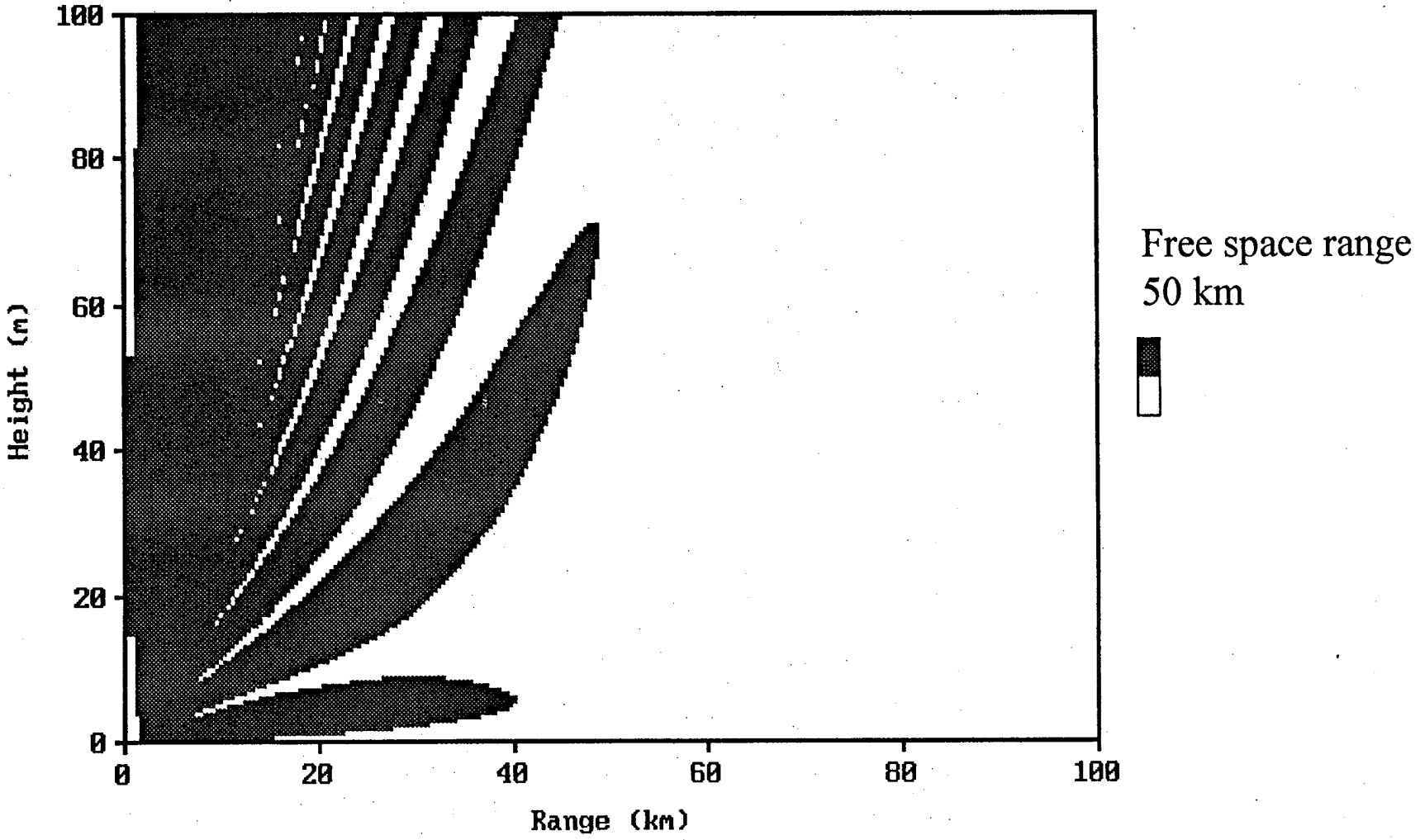

EEMS 1.0 Sample case 2

IFDG

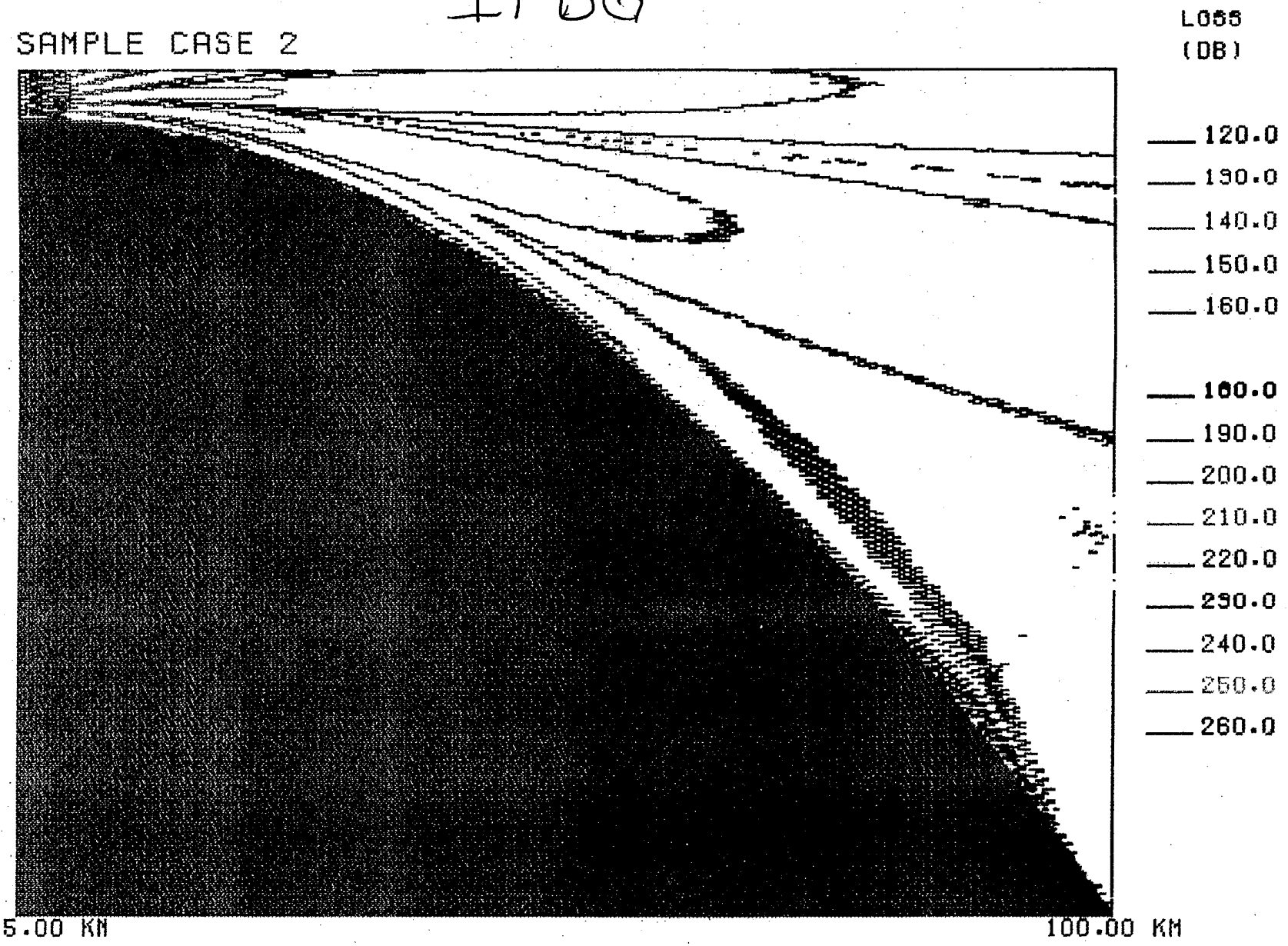
SAMPLE CASE 2
LOSS
(DB)
120.0
130.0
140.0
150.0
160.0
180.0
190.0
200.0
210.0
220.0
230.0
240.0
250.0
260.0
564.20 M
5.00 KM
100.00 KM

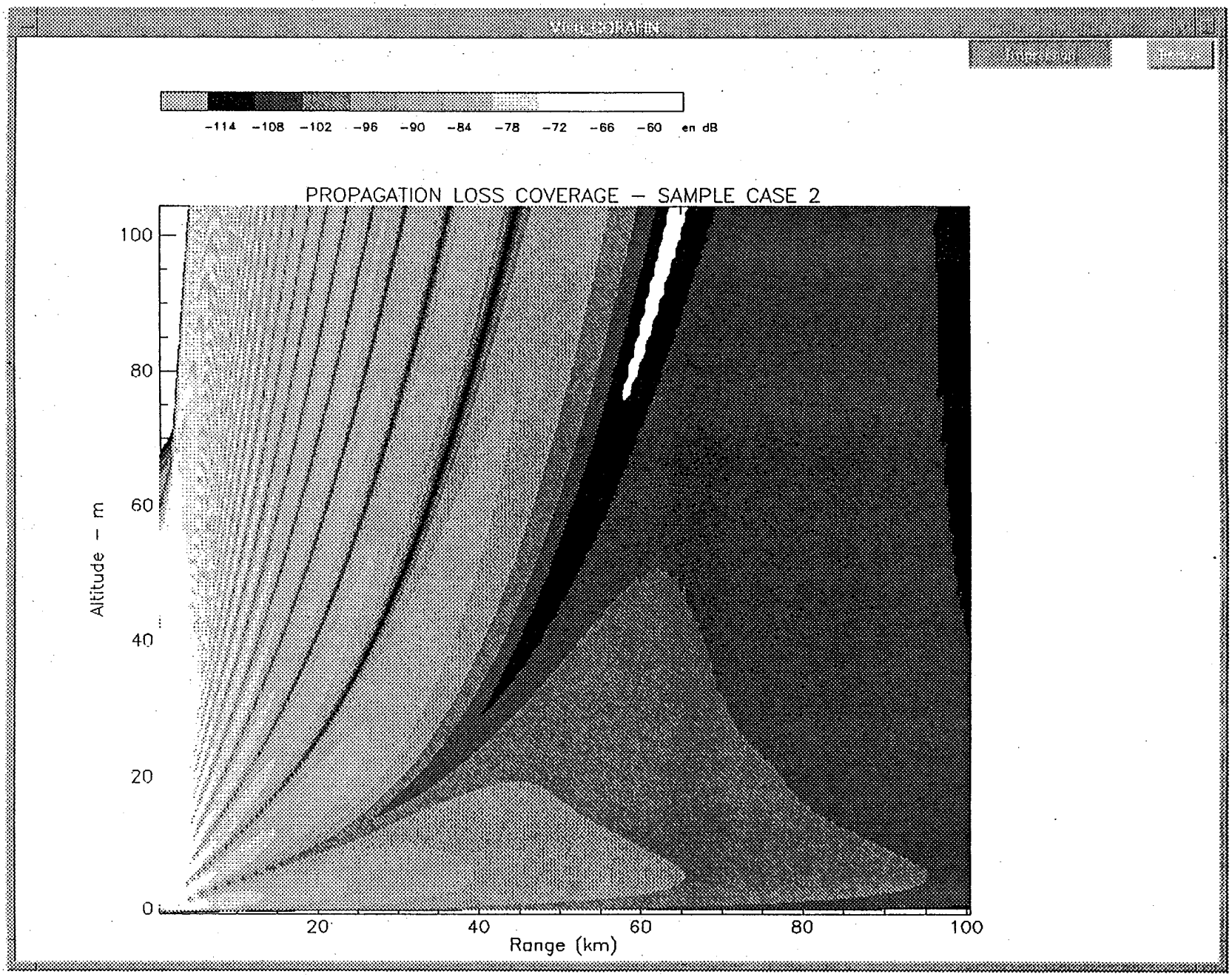
−114 −108 −102 −96 −90 −84 −78 −72 −66 −60 en dB
PROPAGATION LOSS COVERAGE – SAMPLE CASE 2
Altitude – m
0
20
40
60
80
100
20
40
60
80
100
Range (km)

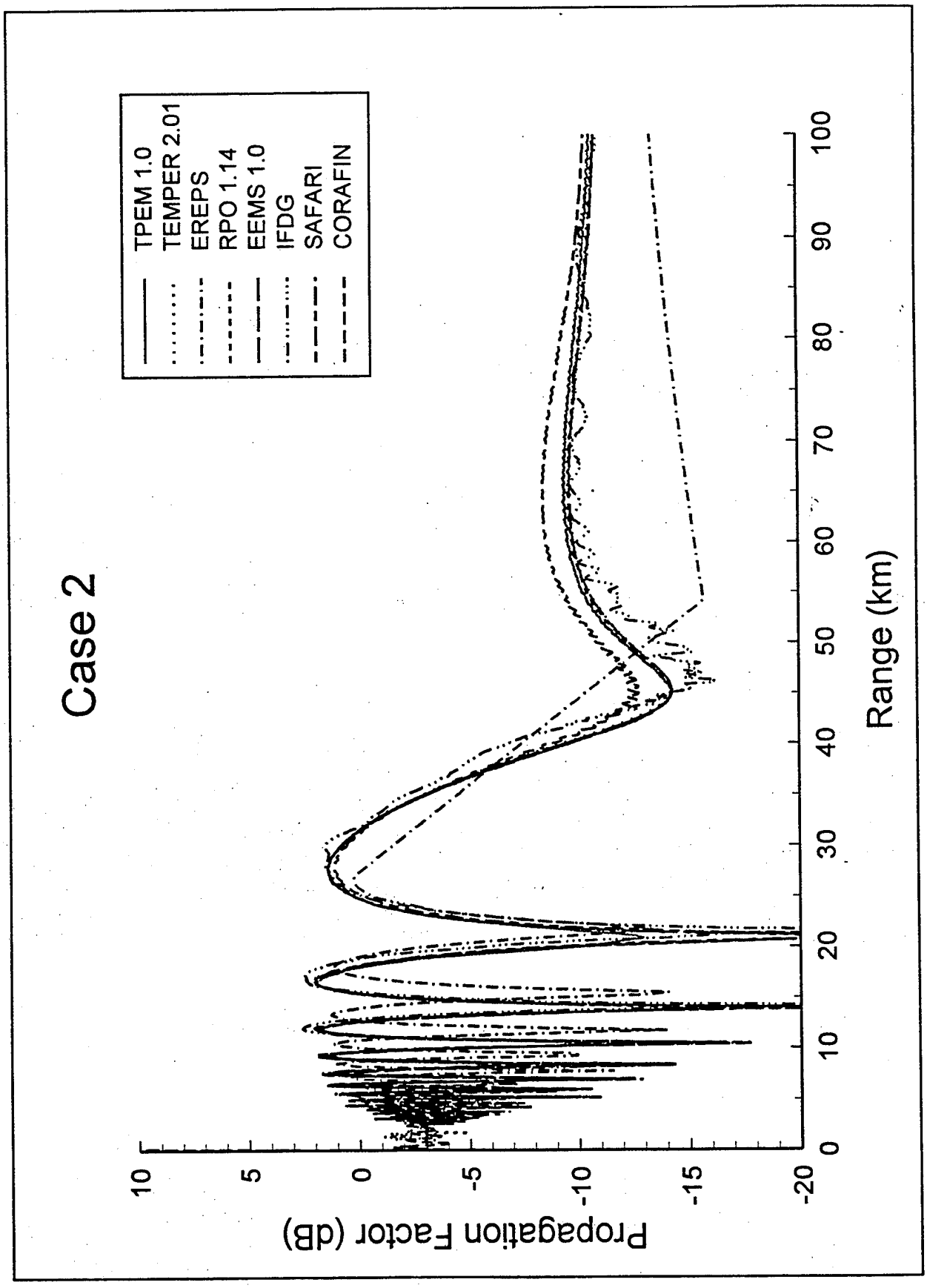
Case 2
TPEM 1.0
TEMPER 2.01
EREPS
RPO 1.14
EEMS 1.0
IFDG
SAFARI
CORAFIN
Propagation Factor (dB)
10
5
0
-5
-10
-15
-20
0
10
20
30
40
50
60
70
80
90
100
Range (km)

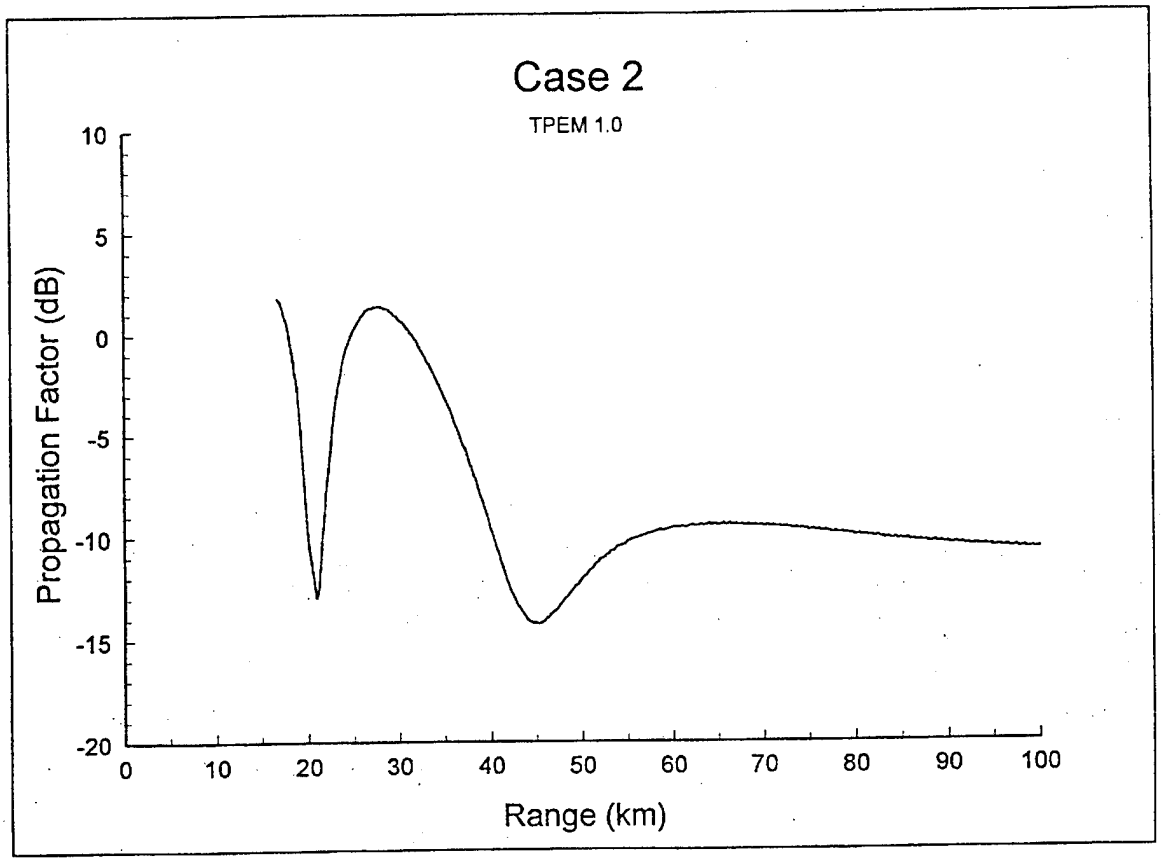
Case 2
TPEM 1.0
Propagation Factor (dB)
10
5
0
-5
-10
-15
-20
0
10
20
30
40
50
60
70
80
90
100
Range (km)

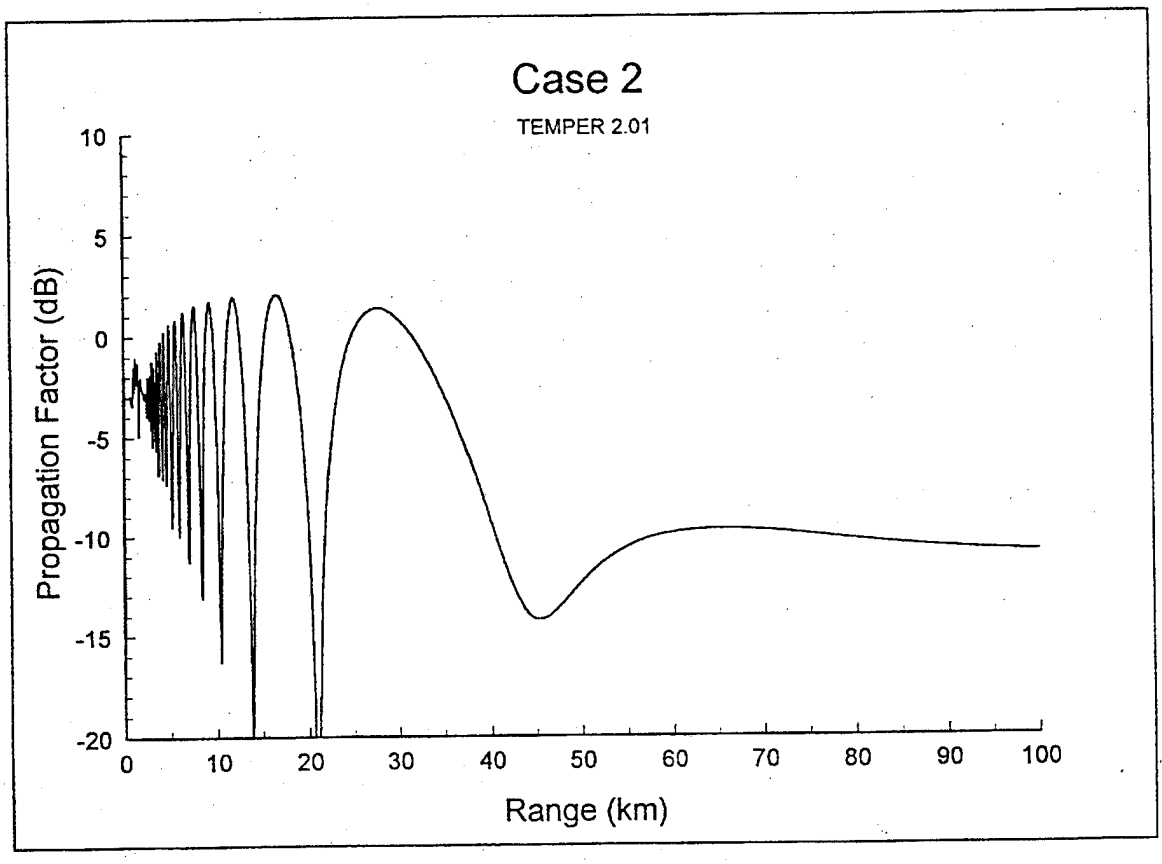
Case 2
TEMPER 2.01
Propagation Factor (dB)
10
5
0
-5
-10
-15
-20
0
10
20
30
40
50
60
70
80
90
100
Range (km)

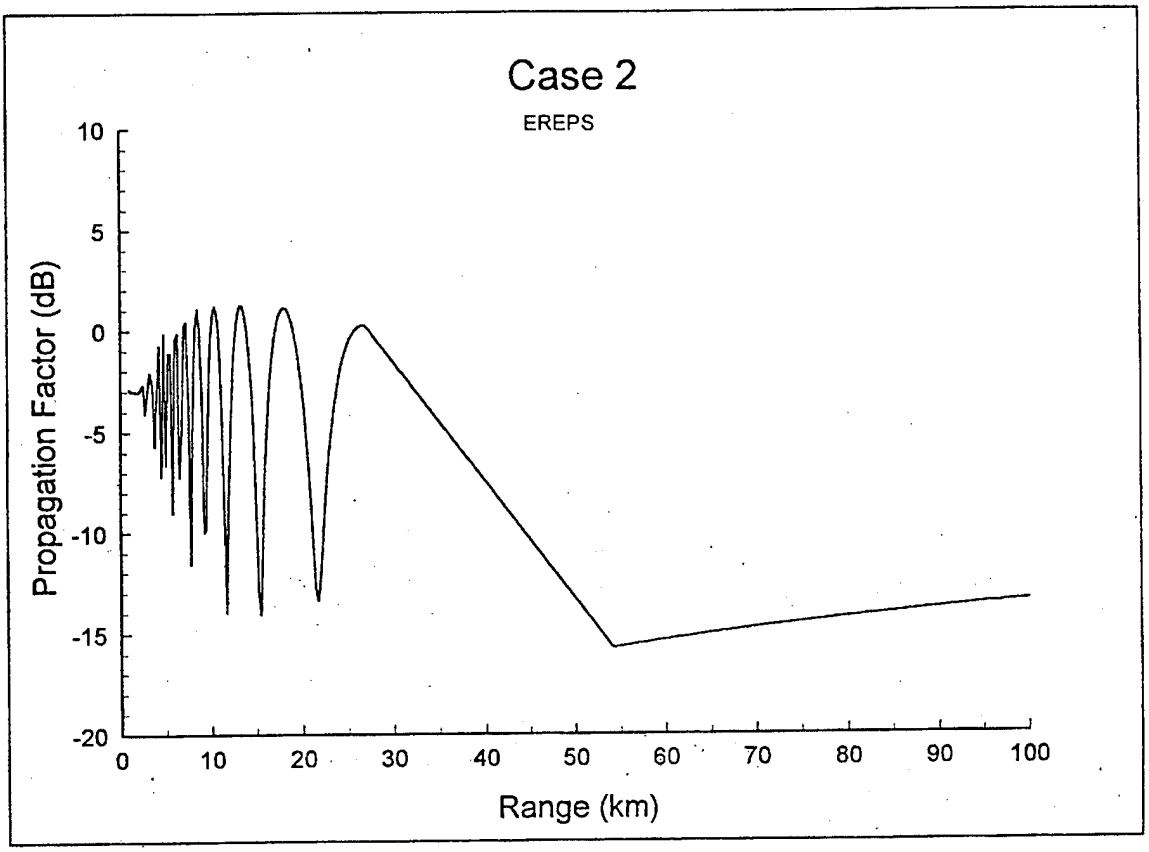
Case 2
EREPS
Propagation Factor (dB)
10
5
0
-5
-10
-15
-20
0
10
20
30
40
50
60
70
80
90
100
Range (km)

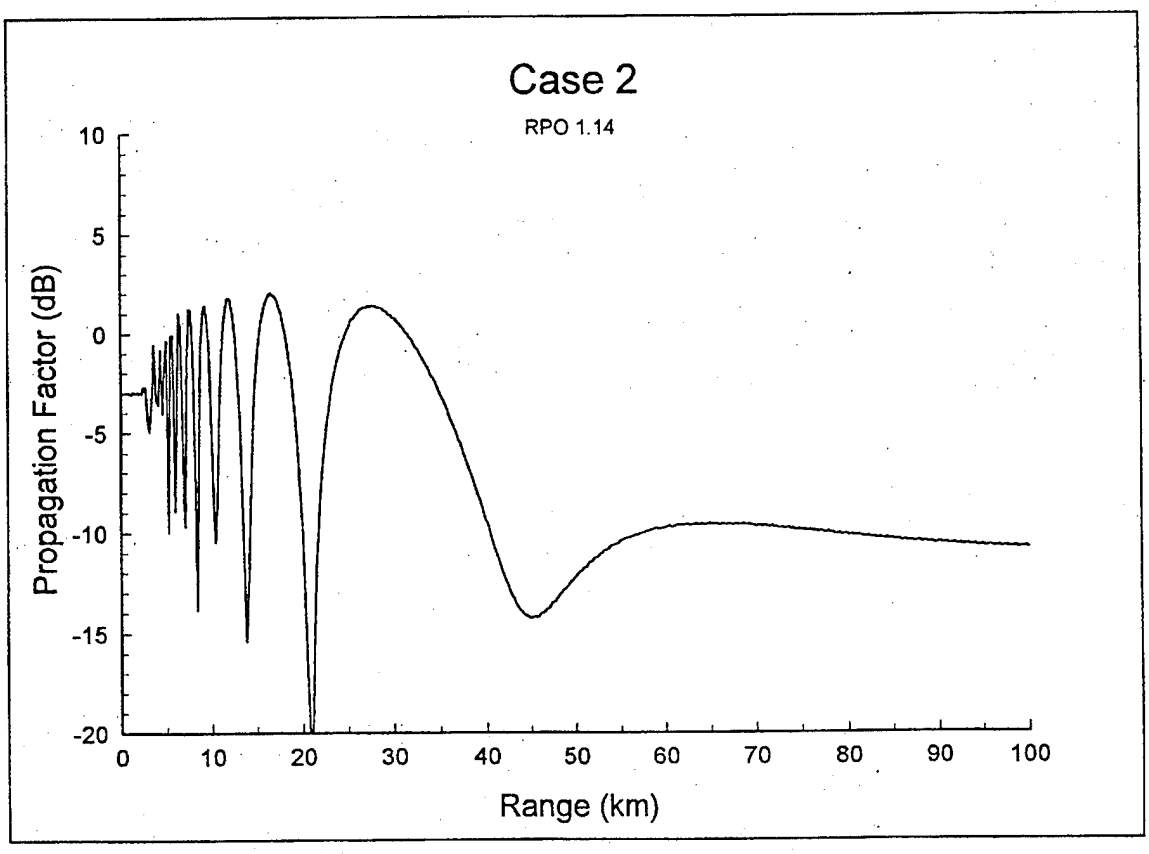
Case 2
RPO 1.14
Propagation Factor (dB)
10
5
0
-5
-10
-15
-20
0
10
20
30
40
50
60
70
80
90
100
Range (km)

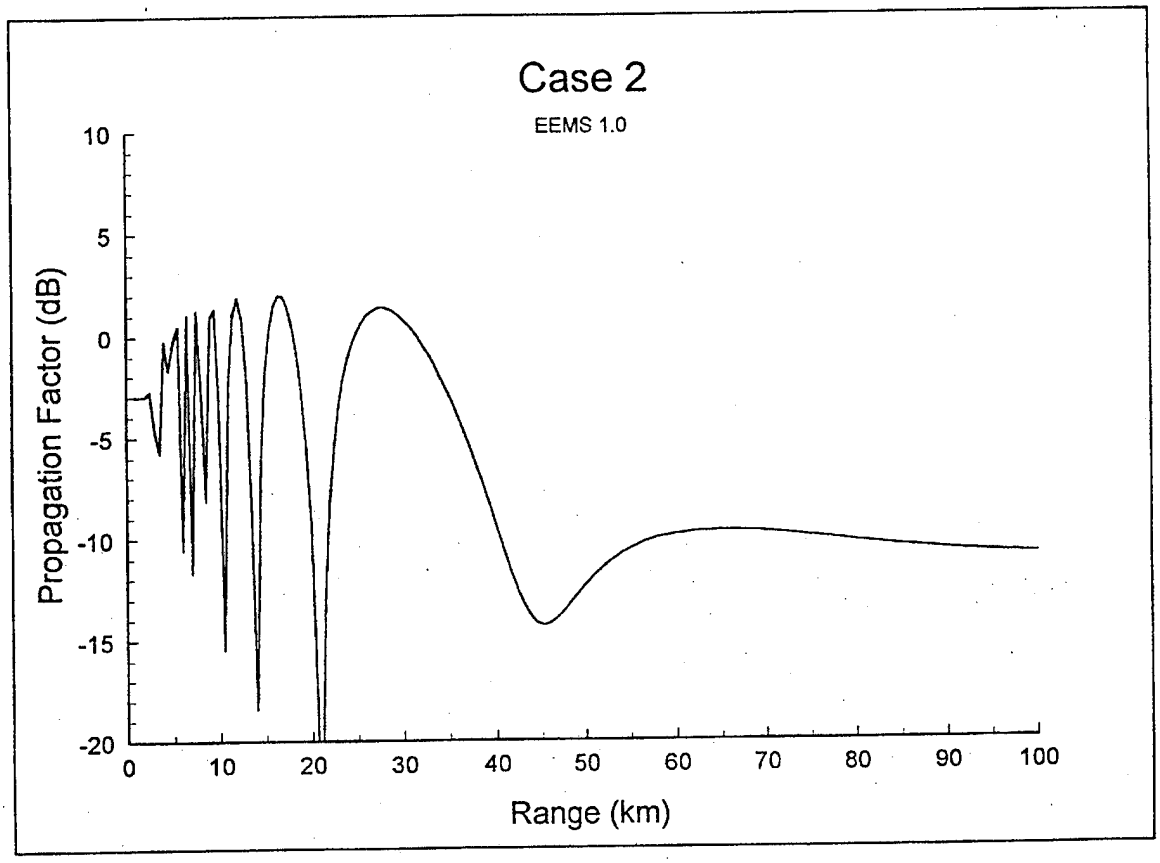
Case 2
EEMS 1.0
Propagation Factor (dB)
10
5
0
-5
-10
-15
-20
0
10
20
30
40
50
60
70
80
90
100
Range (km)

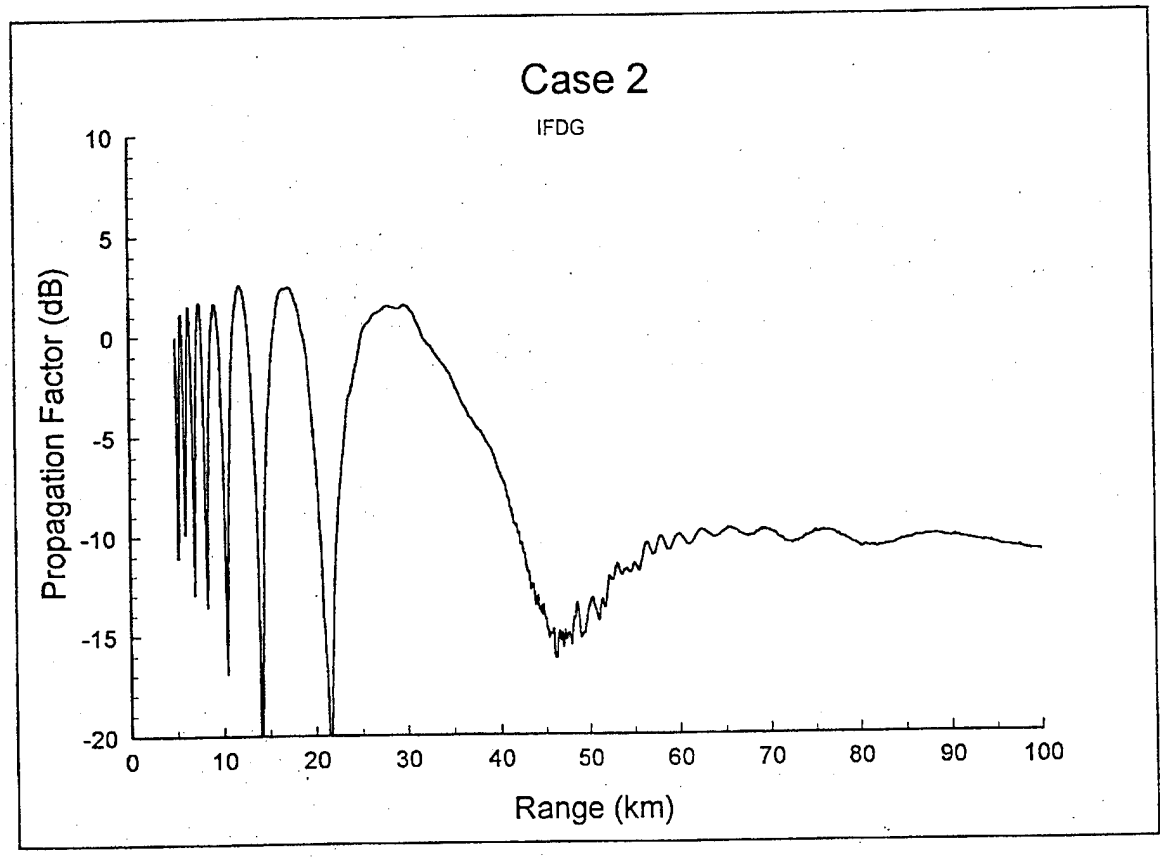
Case 2
IFDG
Propagation Factor (dB)
10
5
0
-5
-10
-15
-20
0
10
20
30
40
50
60
70
80
90
100
Range (km)

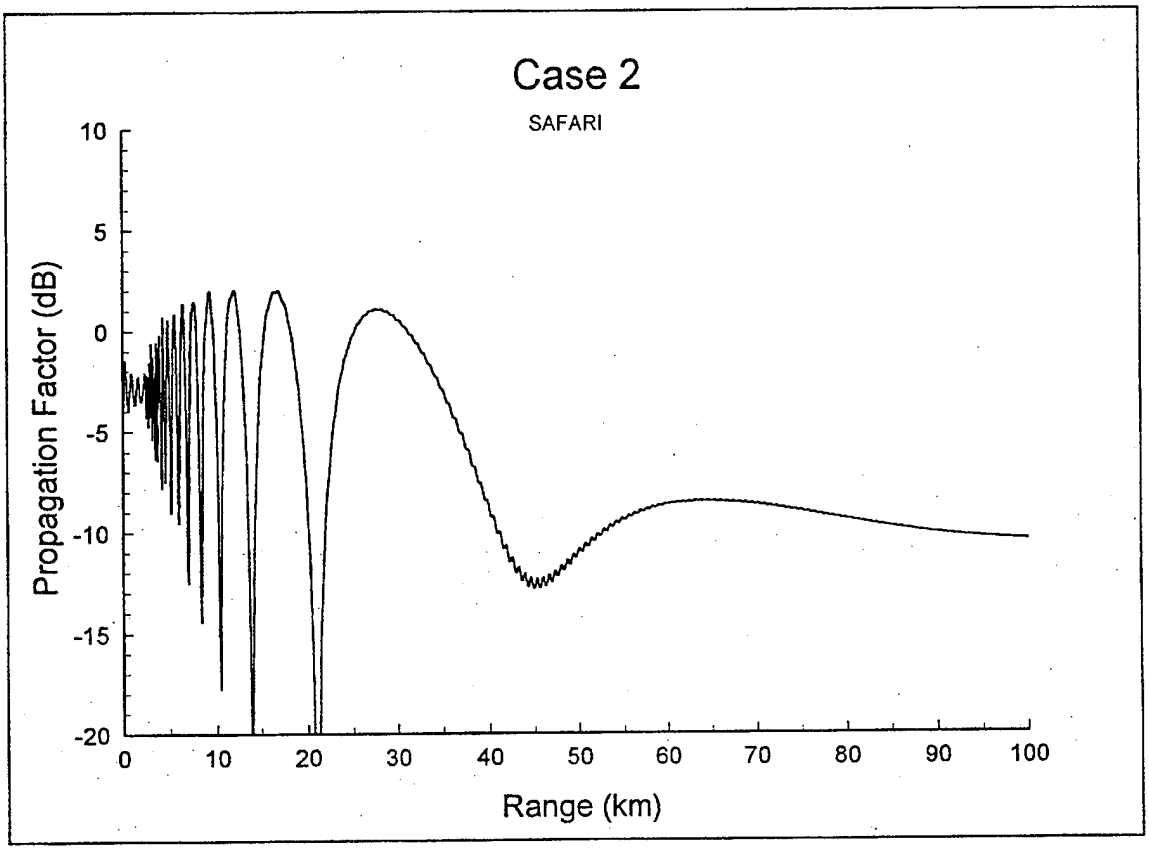
Case 2
SAFARI
Propagation Factor (dB)
10
5
0
-5
-10
-15
-20
0
10
20
30
40
50
60
70
80
90
100
Range (km)

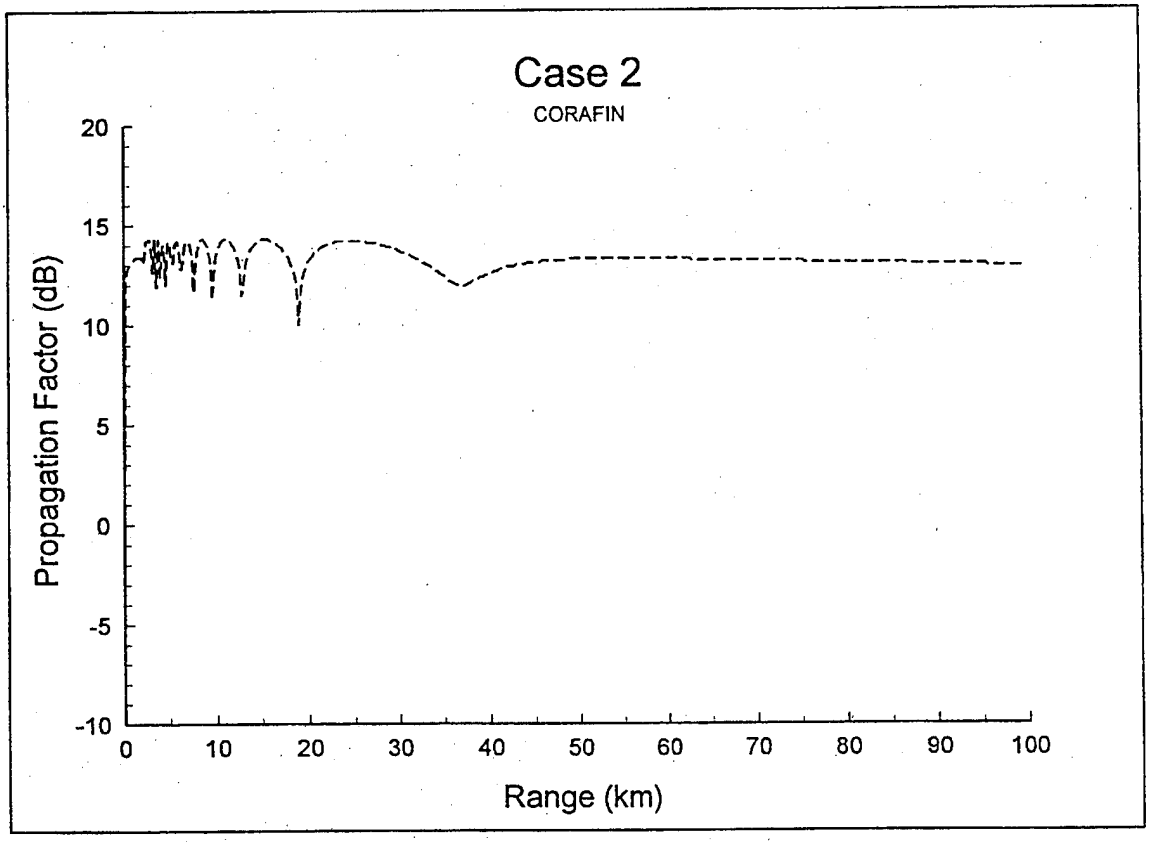
Case 2
CORAFIN
Propagation Factor (dB)
20
15
10
5
0
-5
-10
0
10
20
30
40
50
60
70
80
90
100
Range (km)

Sample Case 3.

This case concerns propagation in a strong evaporation duct over a wind-roughened sea surface. The frequency is 10 GHz and the transmitter height is 25 m above the sea. The wind speed is 10 m/s, which equates to a standard deviation of the sea surface of 0.51 m. The refractivity profile is specified in Table 4 and plotted in Figure 3. This corresponds to a very strong evaporation duct with a duct height of 20 m based on neutral stability conditions. A coverage diagram is desired for receiver heights from 0 to 100 m and ranges from 0 to 100 km for a free space range of 50 km. Propagation factor is required at a 25 m receiver height from 0 to 100 km range.

Height (m)	Refractivity (M units)
0.000	340.00
0.135	323.00
0.223	321.76
0.368	320.53
0.607	319.31
1.000	318.11
1.649	316.94
2.718	315.83
4.482	314.80
7.389	313.91
12.182	313.26
20.000	312.99
20.086	313.00
33.115	313.38
54.598	314.81
90.017	317.99
148.413	324.04

Table 4. Modified refractivity profile for the 20 m evaporation duct.

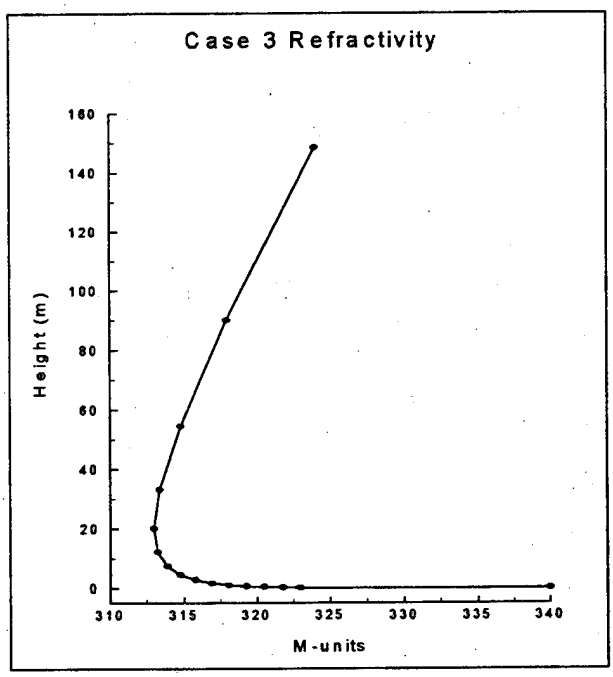

Figure 3. Plot of data in Table 4.

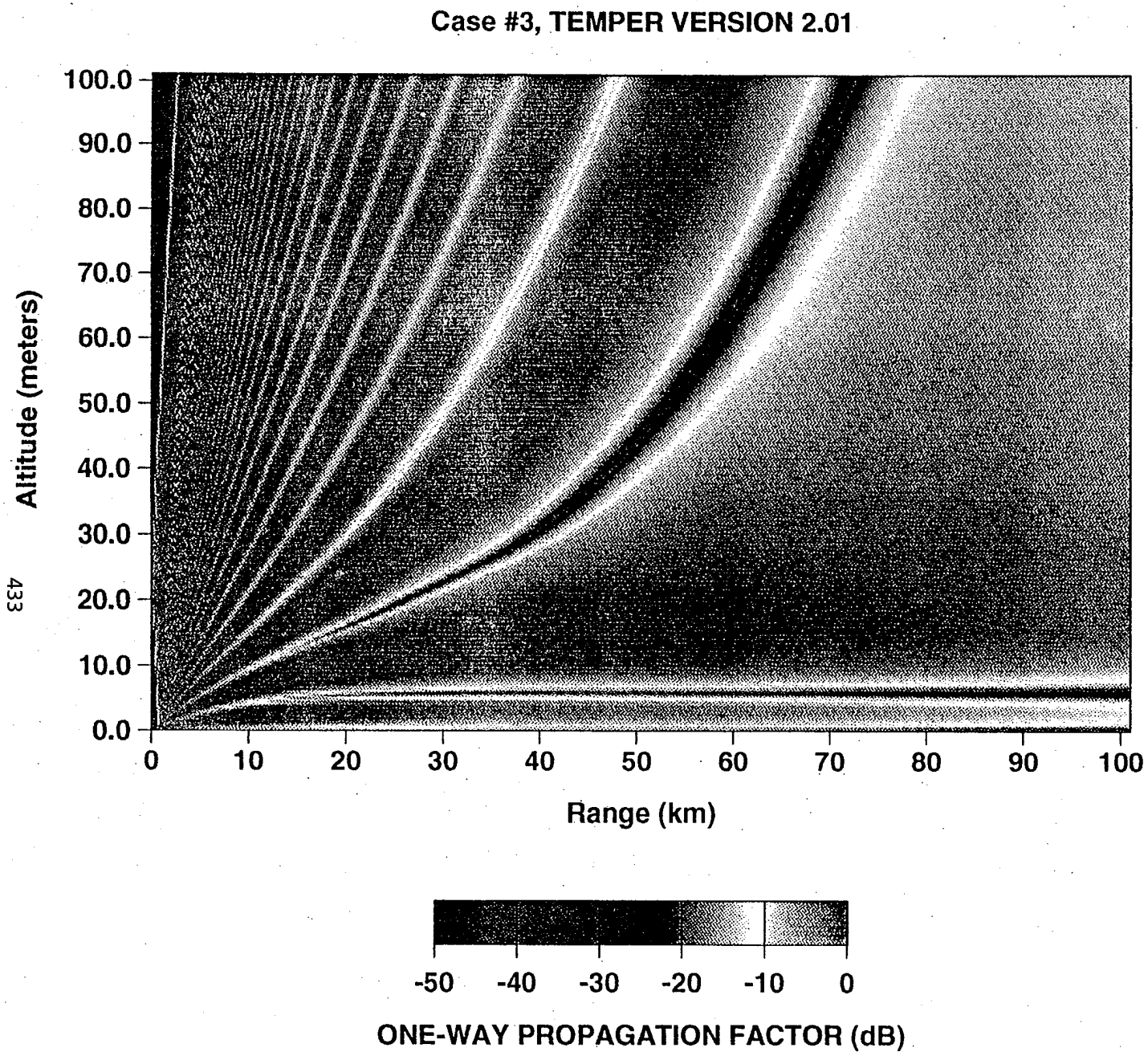
Case #3, TEMPER VERSION 2.01
Altitude (meters)
100.0
90.0
80.0
70.0
60.0
50.0
40.0
30.0
20.0
10.0
0.0
0
10
20
30
40
50
60
70
80
90
100
Range (km)
-50
-40
-30
-20
-10
0
ONE-WAY PROPAGATION FACTOR (dB)

SAMPLE CASE 3 – model : DIF–CERT

freq=10 GHz, ht=25m, hd=20m, rough sea surface (10m/s)

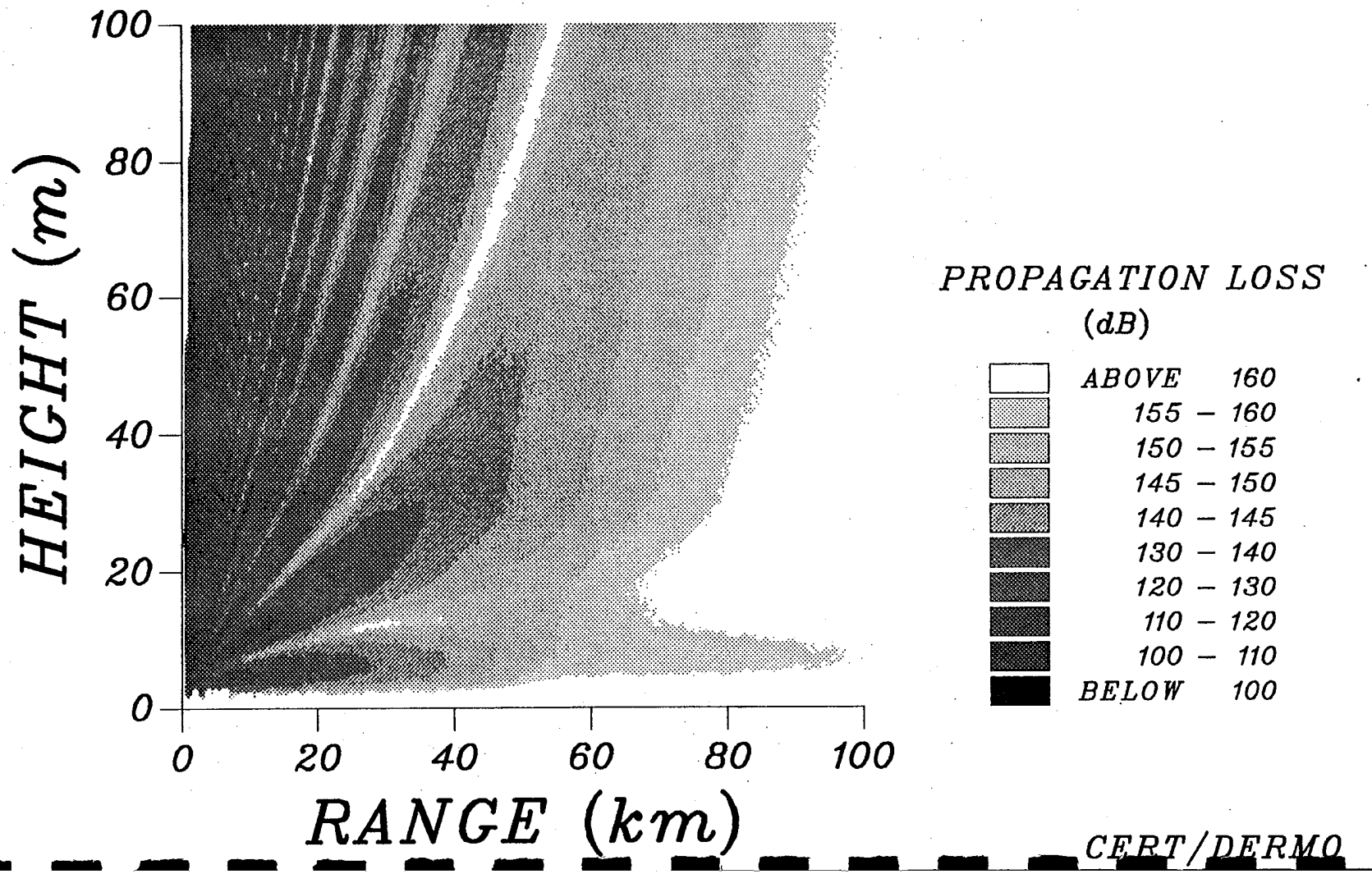

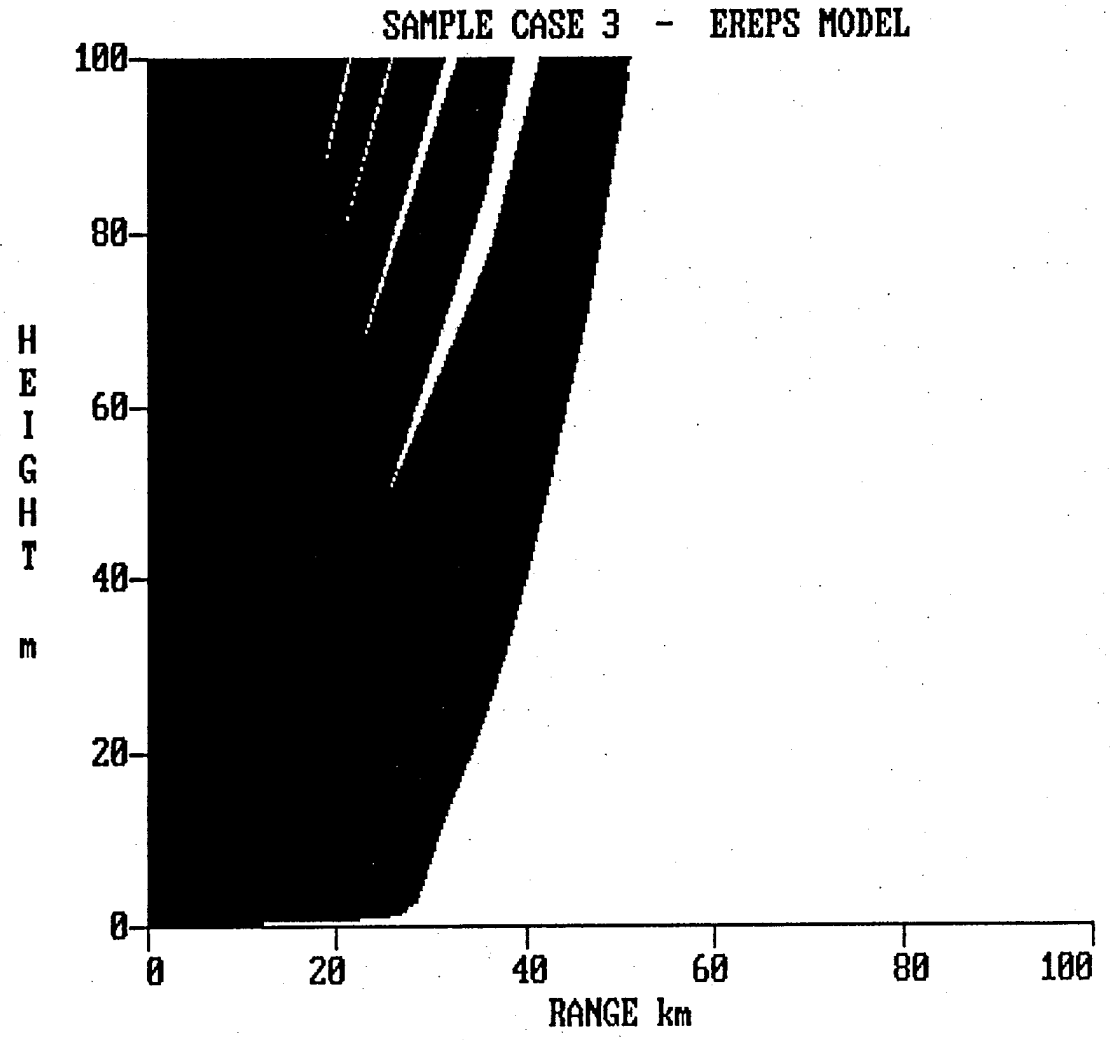

FREQ MHz 10000
TRAN HT m 25.00
POLARIZATION HOR
ANT TYPE OMNI

EVD HT m 20
SBD HT m 0
K 1.333

ABS HUM g/m3 7.5
WIND SP kts 10

FREE-SPACE RANGE
or dB THRESHOLDS
km 50

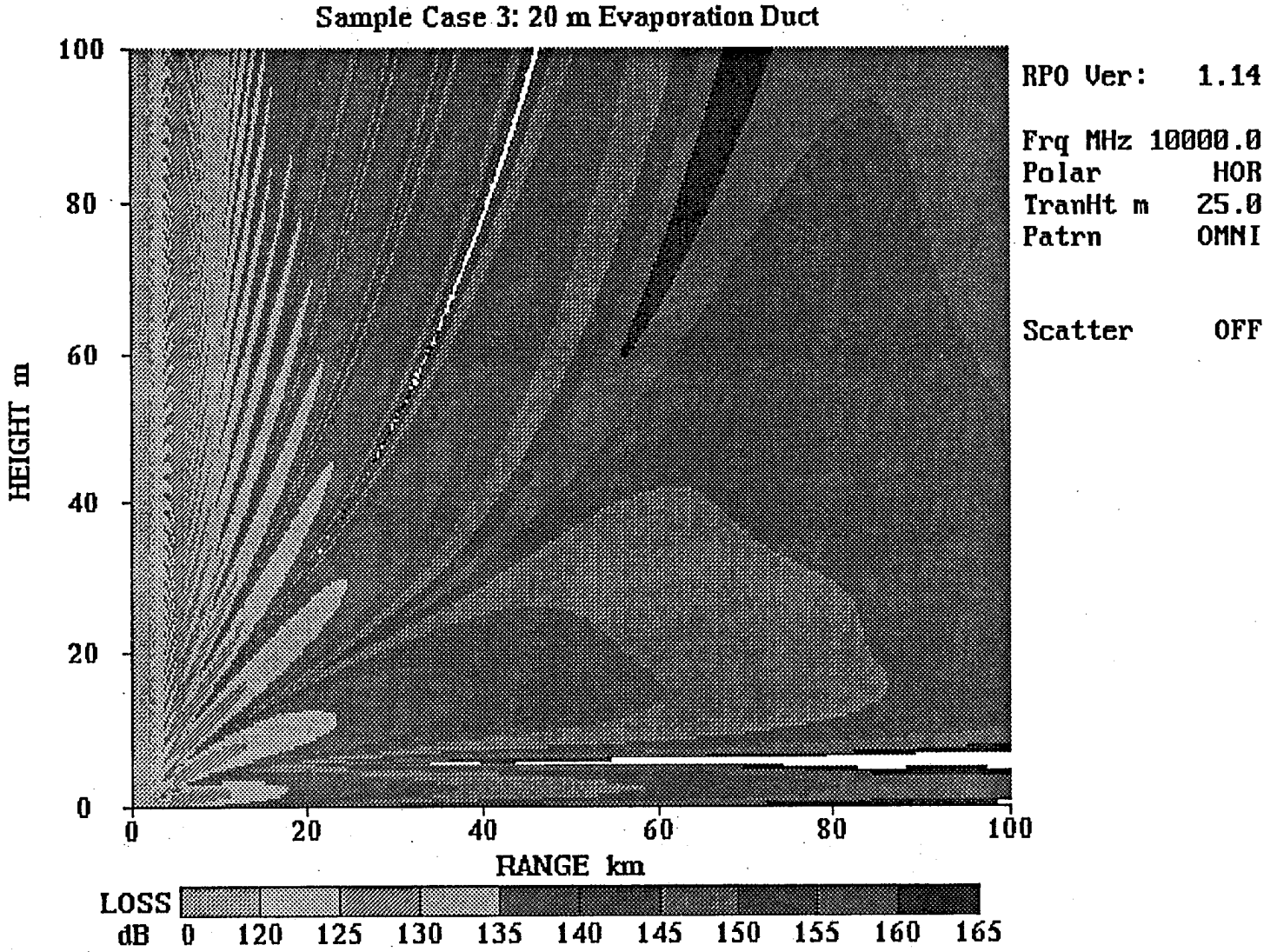
Sample Case 3: 20 m Evaporation Duct
HEIGHT m
100
80
60
40
20
0
0
20
40
60
80
100
RANGE km
RPO Ver: 1.14
Frq MHz 10000.0
Polar HOR
TranHt m 25.0
Patrn OMNI
Scatter OFF
LOSS
dB 0 120 125 130 135 140 145 150 155 160 165

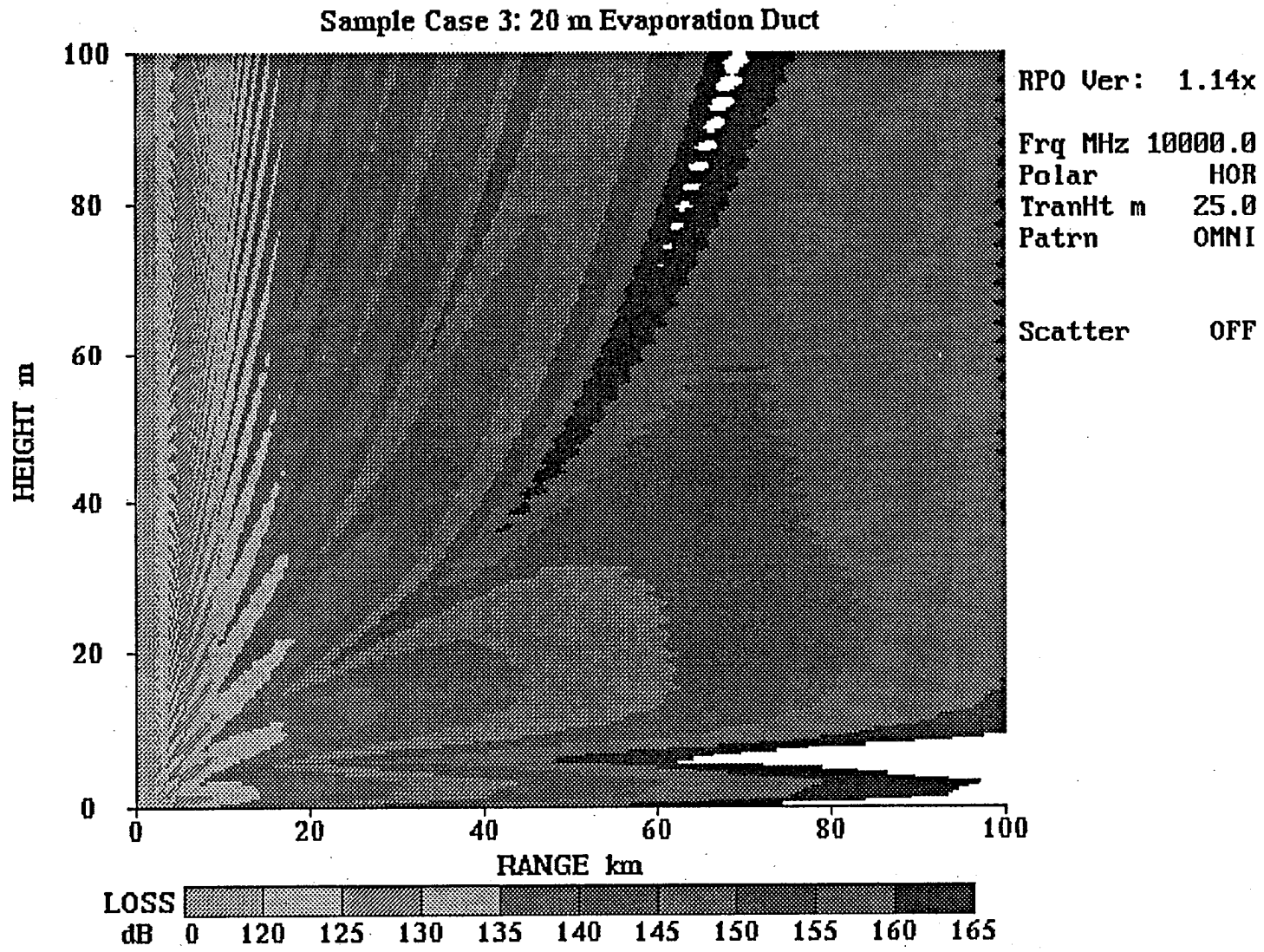
Sample Case 3: 20 m Evaporation Duct
HEIGHT m
100
80
60
40
20
0
0
20
40
60
80
100
RANGE km
LOSS
dB 0 120 125 130 135 140 145 150 155 160 165
RPO Ver: 1.14x
Frq MHz 10000.0
Polar HOR
TranHt m 25.0
Patrn OMNI
Scatter OFF

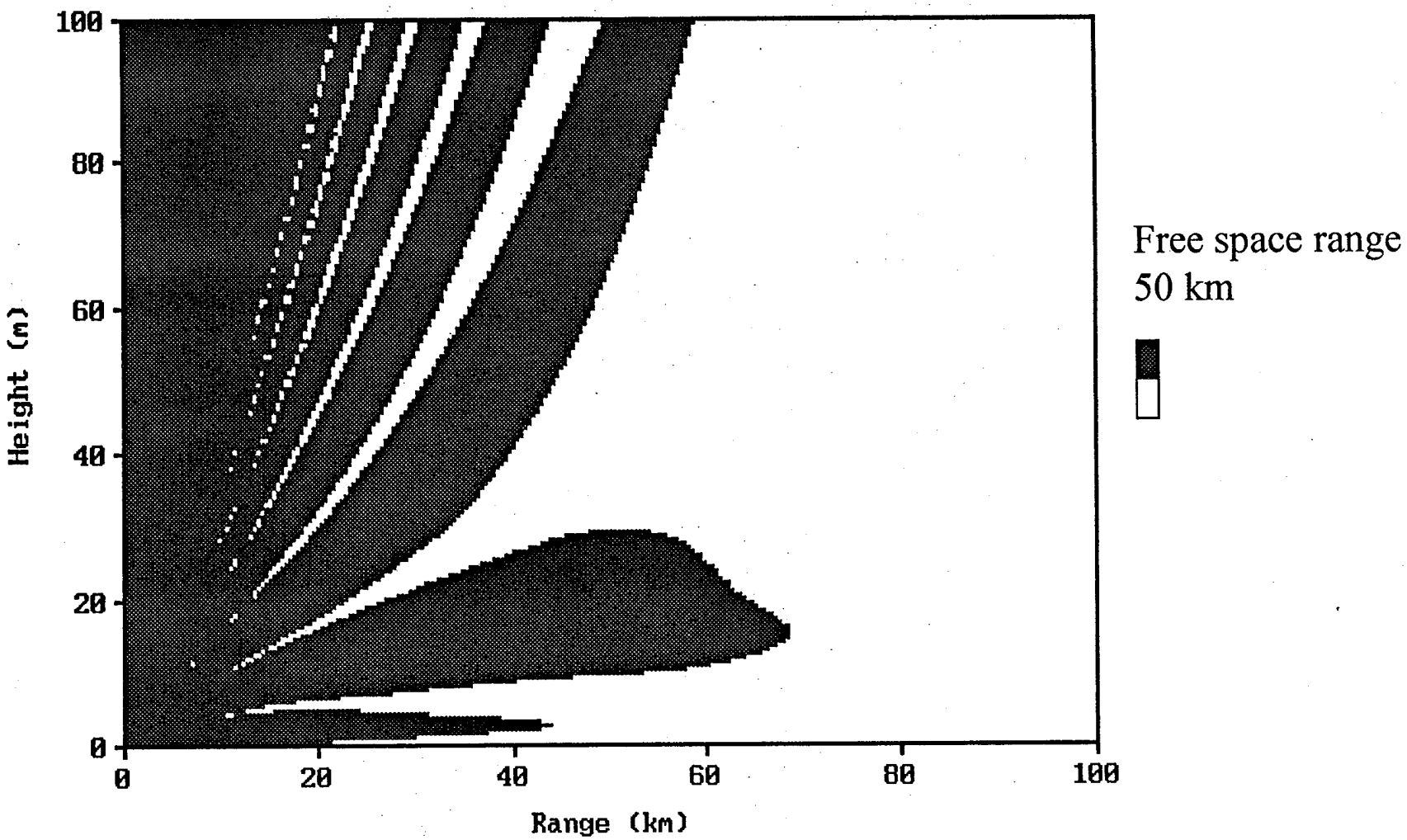

EEMS 1.0 Sample case 3

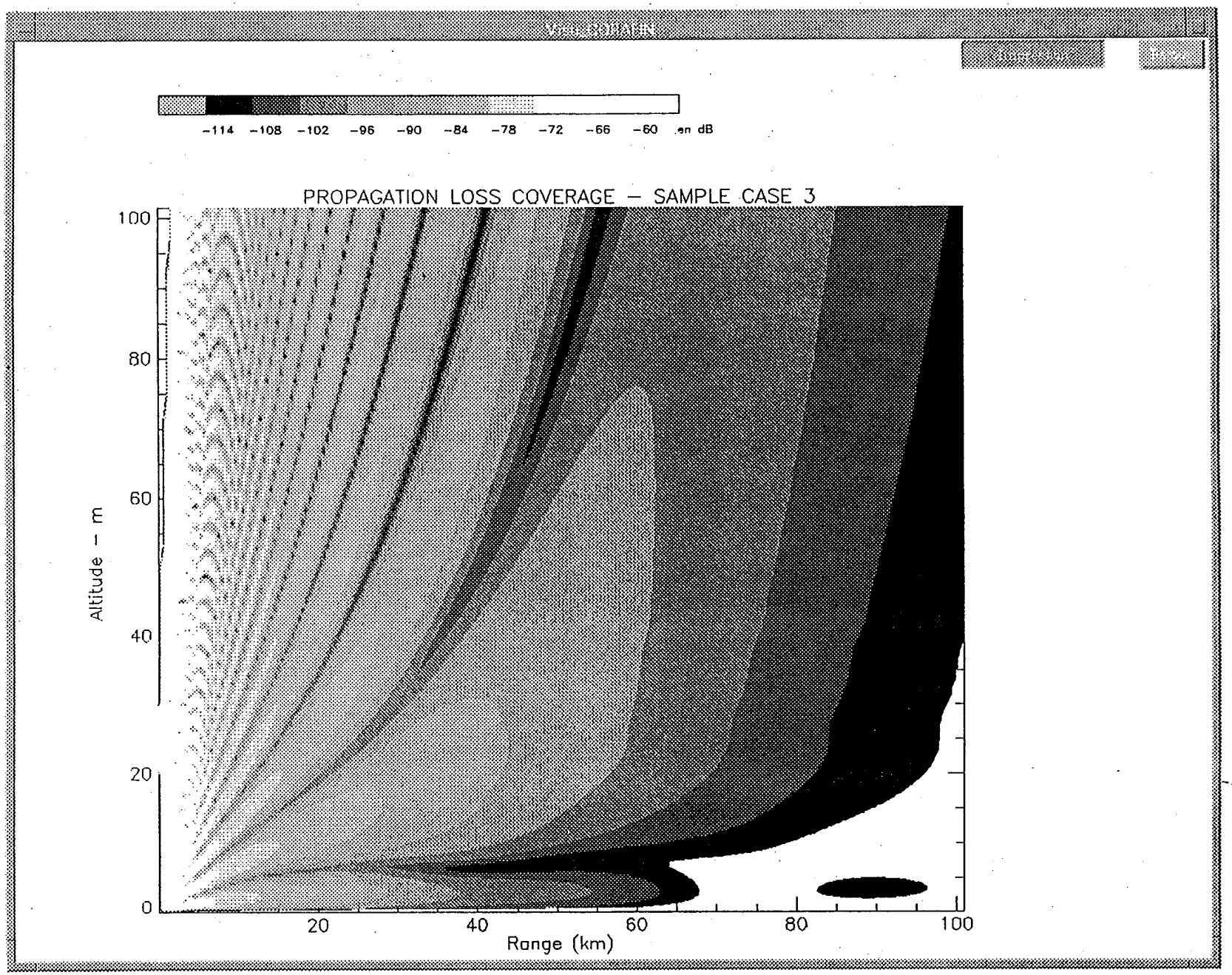
−114 −108 −102 −96 −90 −84 −78 −72 −66 −60 dB
PROPAGATION LOSS COVERAGE – SAMPLE CASE 3
Altitude – m
100
80
60
40
20
0
20
40
60
80
100
Range (km)

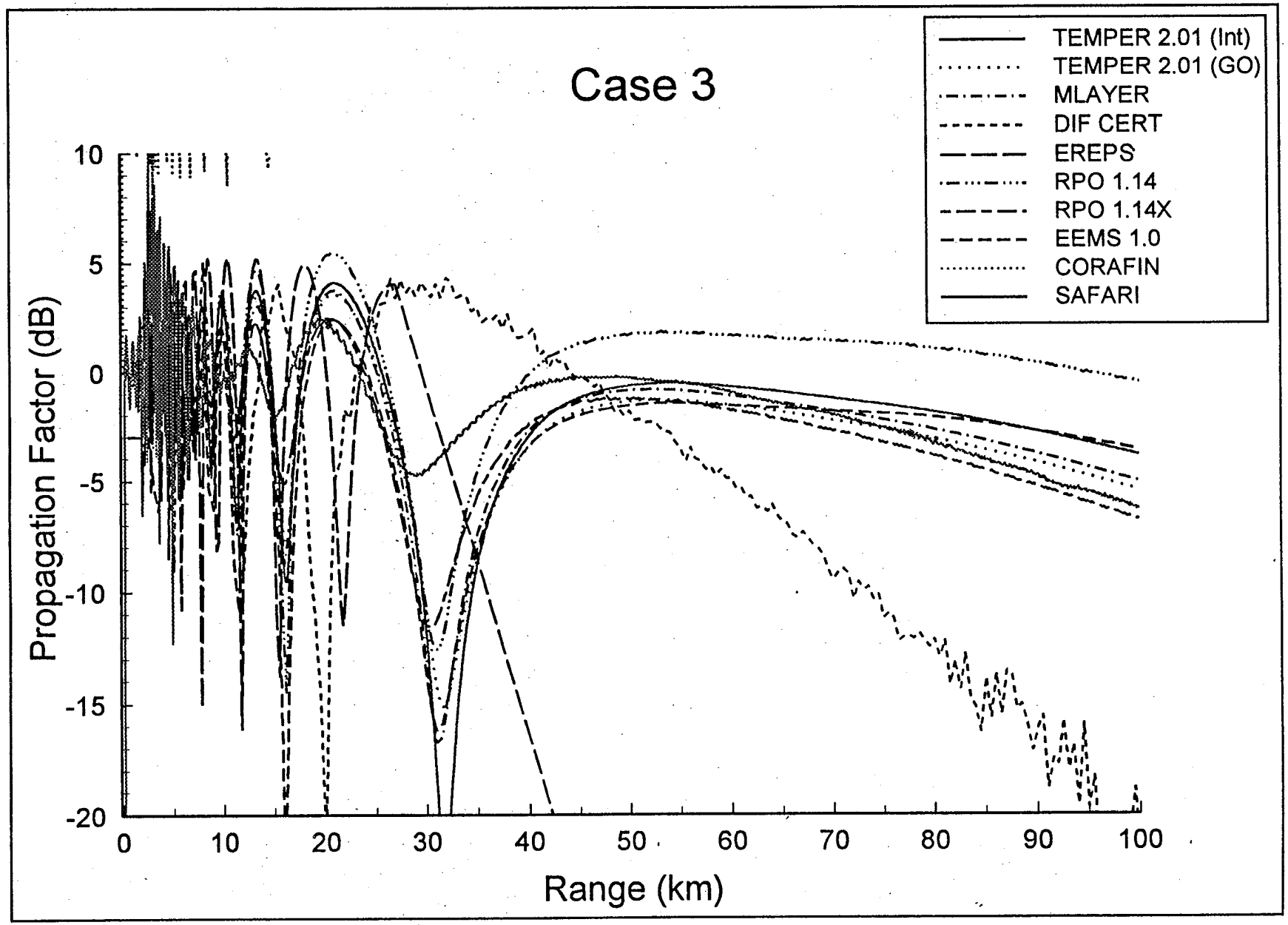
Case 3
TEMPER 2.01 (Int)
TEMPER 2.01 (GO)
MLAYER
DIF CERT
EREPS
RPO 1.14
RPO 1.14X
EEMS 1.0
CORAFIN
SAFARI
Propagation Factor (dB)
10
5
0
-5
-10
-15
-20
0
10
20
30
40
50
60
70
80
90
100
Range (km)

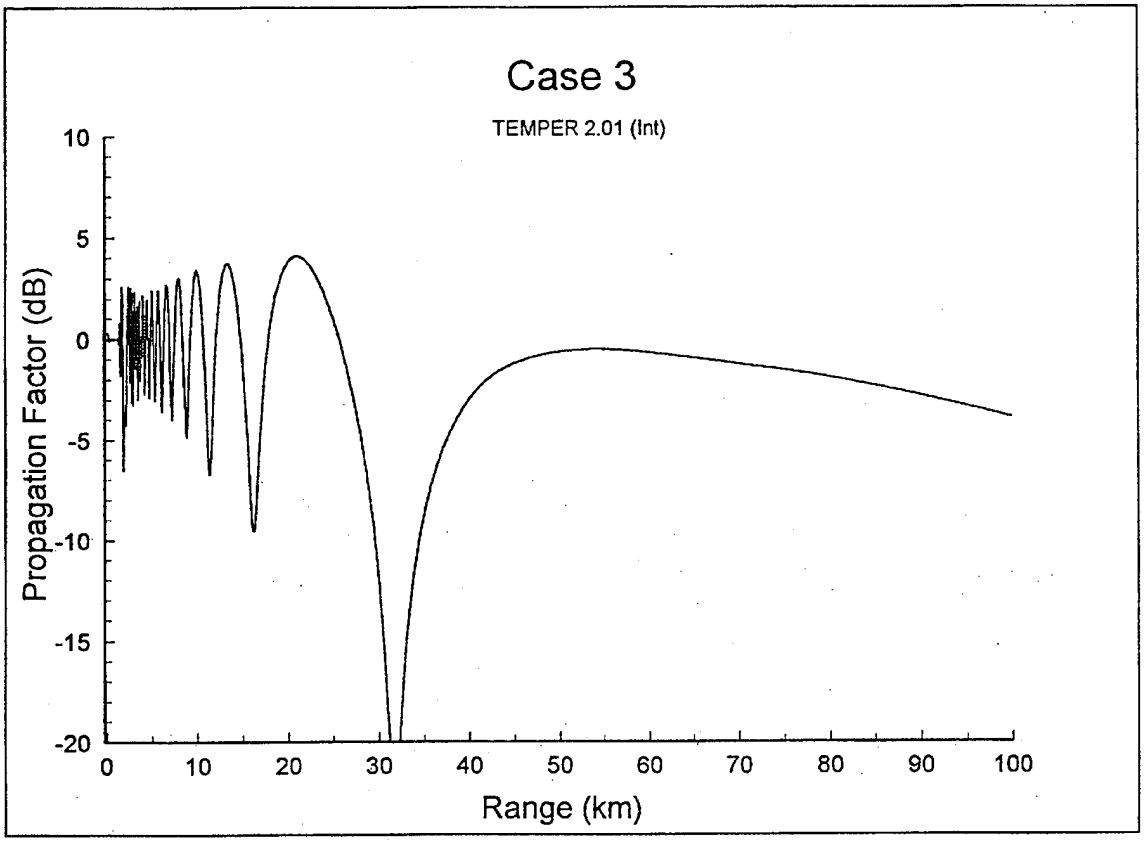
Case 3
TEMPER 2.01 (Int)
Propagation Factor (dB)
10
5
0
-5
-10
-15
-20
0
10
20
30
40
50
60
70
80
90
100
Range (km)

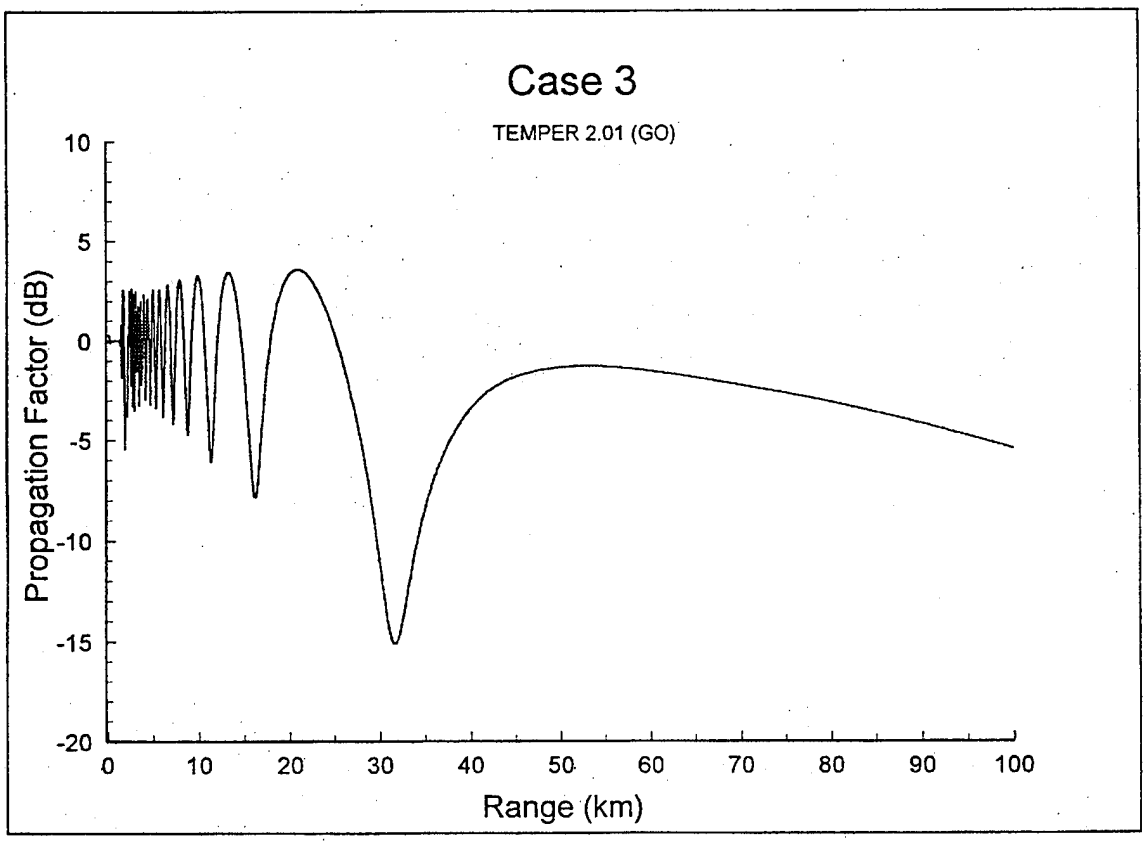
Case 3
TEMPER 2.01 (GO)
Propagation Factor (dB)
10
5
0
-5
-10
-15
-20
0
10
20
30
40
50
60
70
80
90
100
Range (km)

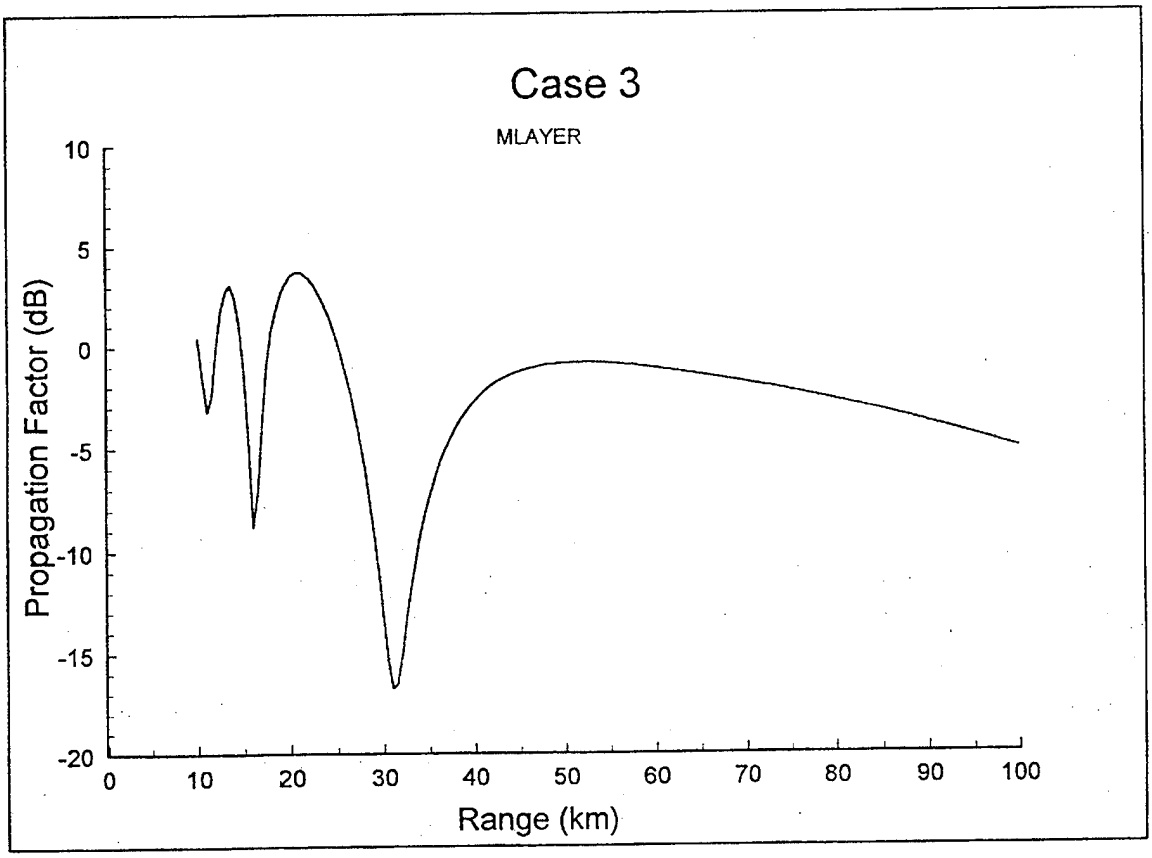
Case 3
MLAYER
Propagation Factor (dB)
10
5
0
-5
-10
-15
-20
0
10
20
30
40
50
60
70
80
90
100
Range (km)

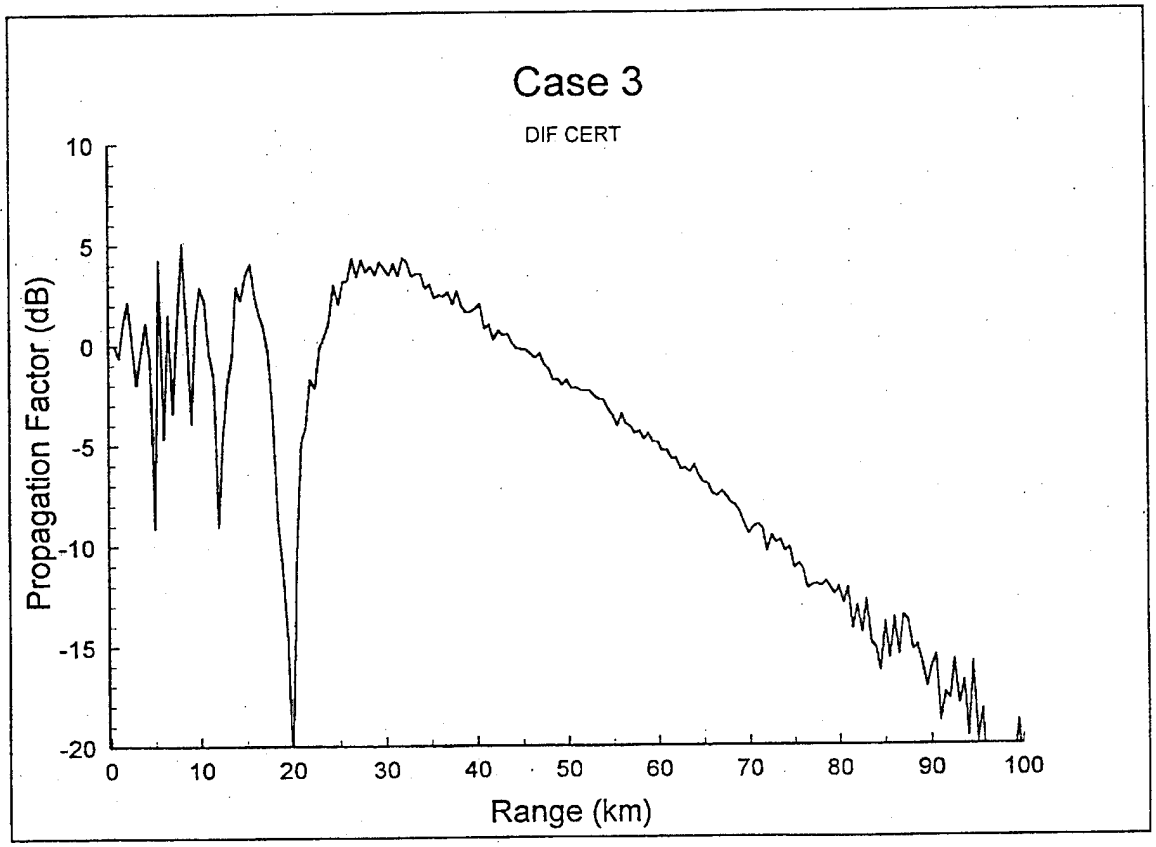
Case 3
DIF CERT
Propagation Factor (dB)
10
5
0
-5
-10
-15
-20
0
10
20
30
40
50
60
70
80
90
100
Range (km)

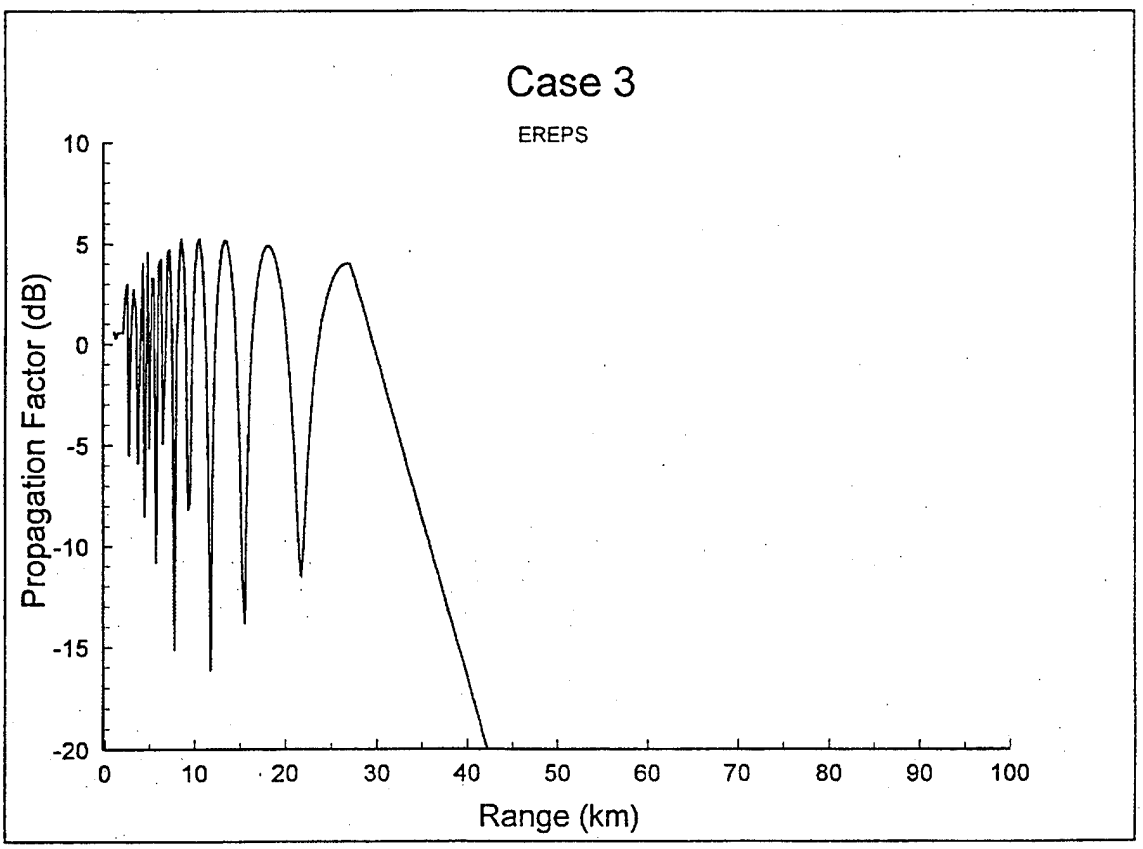
Case 3
EREPS
Propagation Factor (dB)
10
5
0
-5
-10
-15
-20
0
10
20
30
40
50
60
70
80
90
100
Range (km)

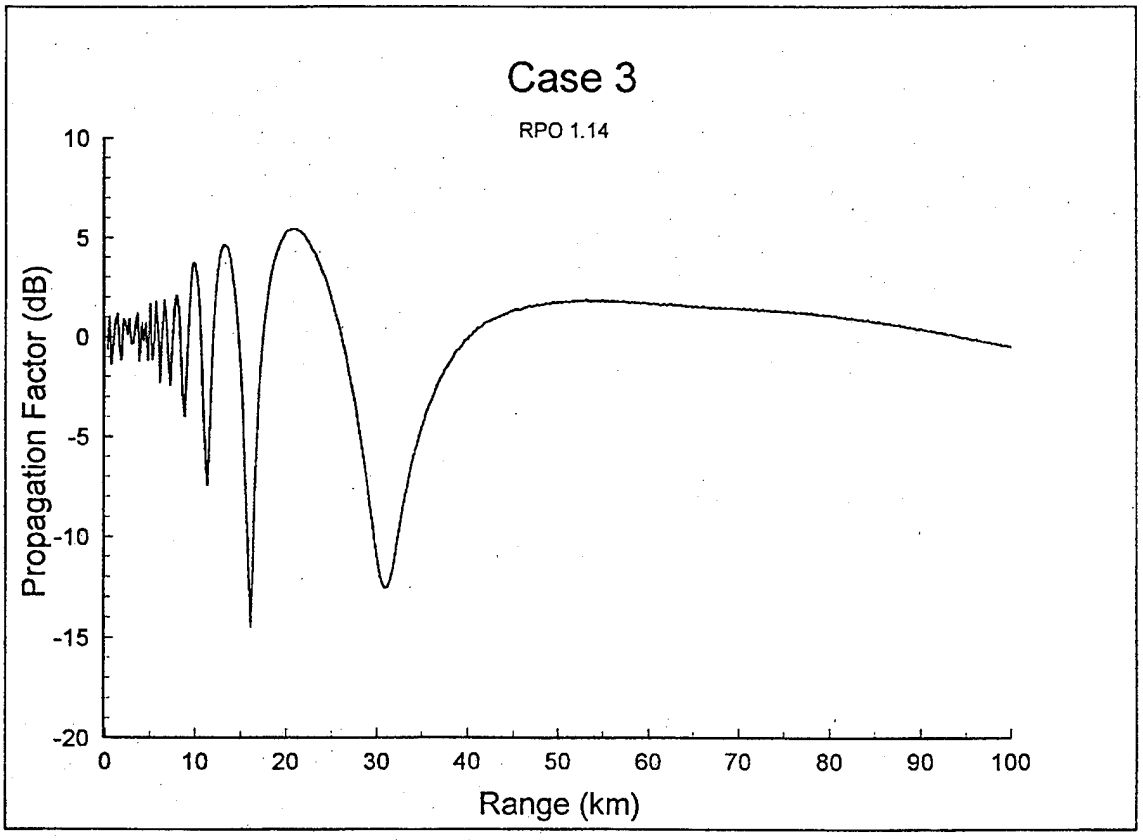
Case 3
RPO 1.14
Propagation Factor (dB)
10
5
0
-5
-10
-15
-20
0
10
20
30
40
50
60
70
80
90
100
Range (km)

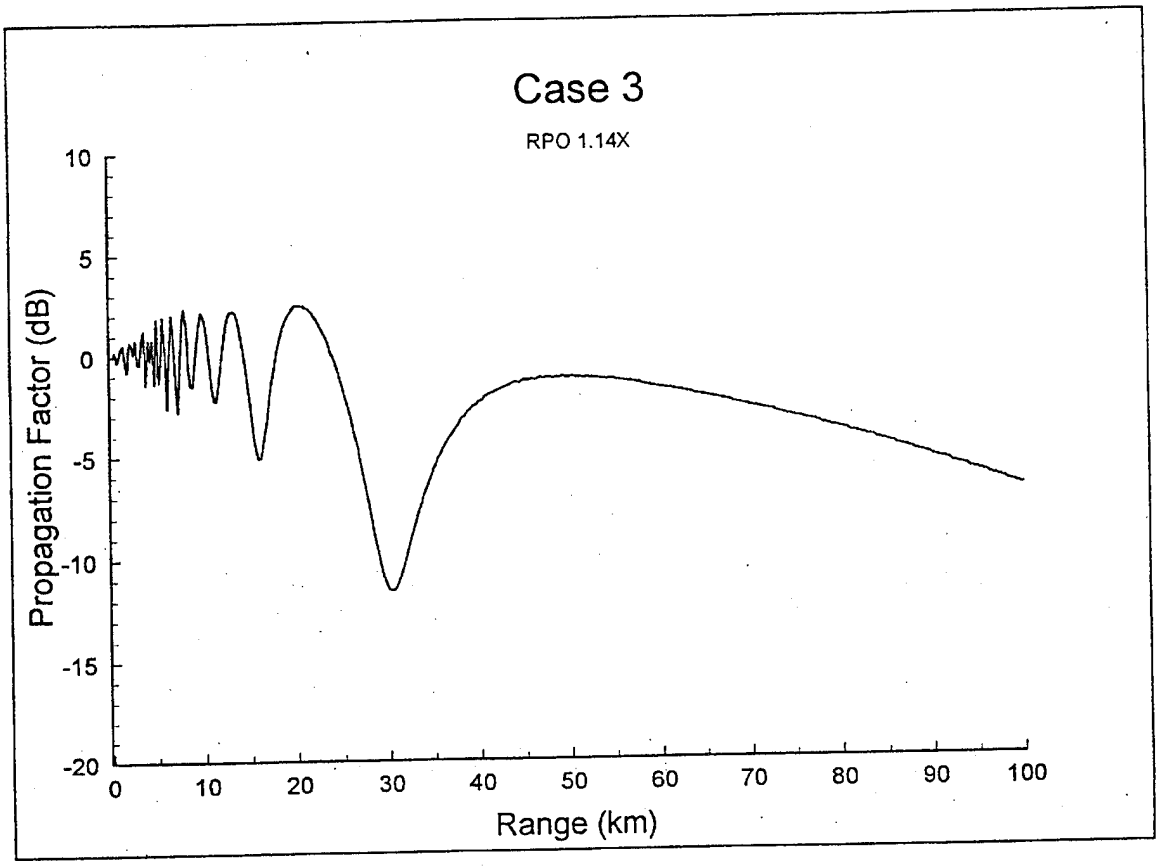
Case 3
RPO 1.14X
Propagation Factor (dB)
10
5
0
-5
-10
-15
-20
0
10
20
30
40
50
60
70
80
90
100
Range (km)

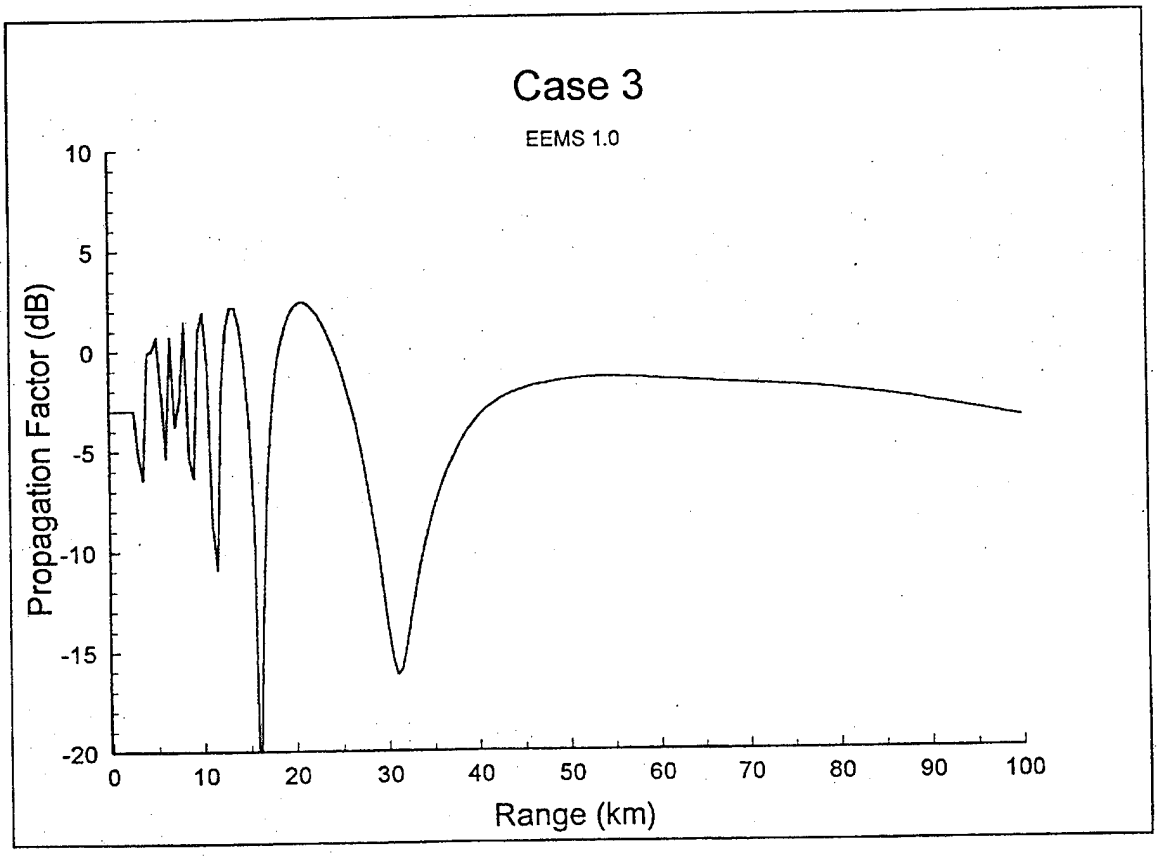
Case 3
EEMS 1.0
Propagation Factor (dB)
10
5
0
-5
-10
-15
-20
0
10
20
30
40
50
60
70
80
90
100
Range (km)

Sample Case 4.

This case considers range-dependent ducting conditions over the sea. The modified refractivity profiles for this case are given in Table 5 and plotted in Figure 4, and describe a surface-based duct at close ranges that rises to a low elevated duct at longer ranges. The first vertical profile applies to ranges 0 and 72 km, while the next two profiles apply to 158 and 231 km, respectively. Each profile has six levels. At ranges in between the specified profiles, the modified refractivity and height of each level should be linearly interpolated in range. The frequency is 3300 MHz and the transmitter antenna height is 30 m above sea level. A coverage diagram is desired for receiver heights from 0 to 1000 m and ranges from 0 to 200 km, for a free space range of 100 km. Propagation factor is required for receiver heights between 0 and 1000 m at 173 km range. Measured radio data are provided for this sample case. This case is described by Barrios [4].

Range km 0 and 72		**Range km** 158		**Range km** 231	
ht., m	***M***	**ht., m**	***M***	**ht., m**	***M***
0	337	0	337	0	336
165	358	226	365	363	383
245	325	329	344	480	358
371	335	454	356	576	371
375	334	504	352	639	371
1067	447	1067	431	1067	431

Table 5. Modified refractivity profiles for the range-dependent duct.

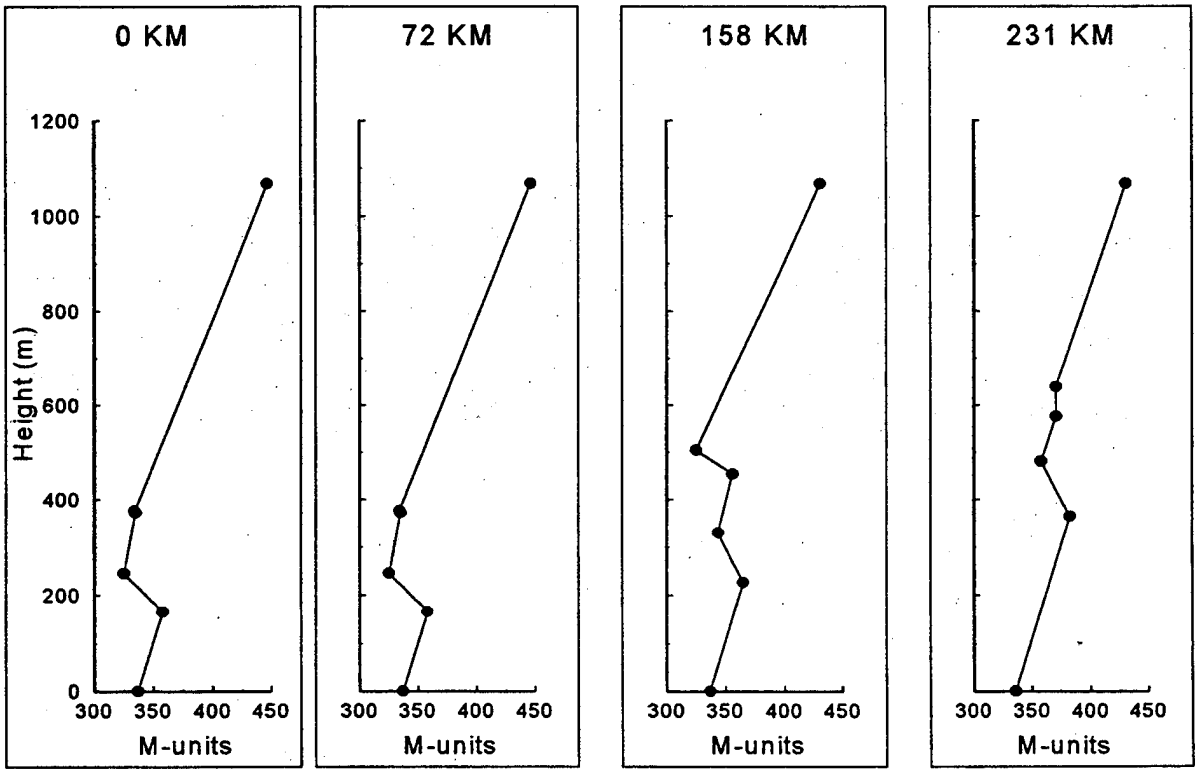

Figure 4. Plot of data in Table 5.

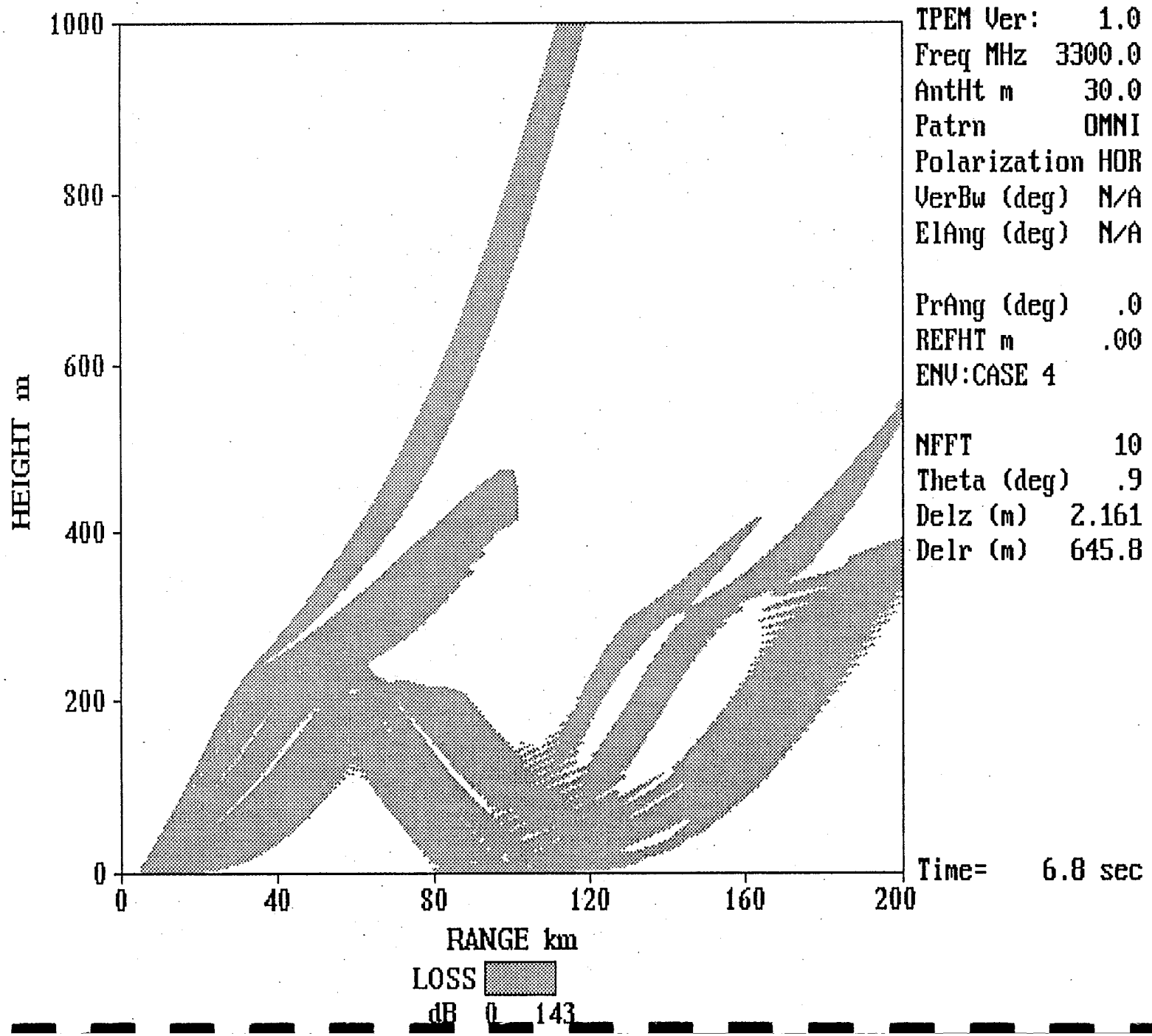
1000
800
600
400
200
0
HEIGHT m
0
40
80
120
160
200
RANGE km
LOSS
dB 0 143
TPEM Ver: 1.0
Freq MHz 3300.0
AntHt m 30.0
Patrn OMNI
Polarization HOR
VerBw (deg) N/A
ElAng (deg) N/A
PrAng (deg) .0
REFHT m .00
ENV:CASE 4
NFFT 10
Theta (deg) .9
Delz (m) 2.161
Delr (m) 645.8
Time= 6.8 sec

Case #4, TEMPER VERSION 2.01

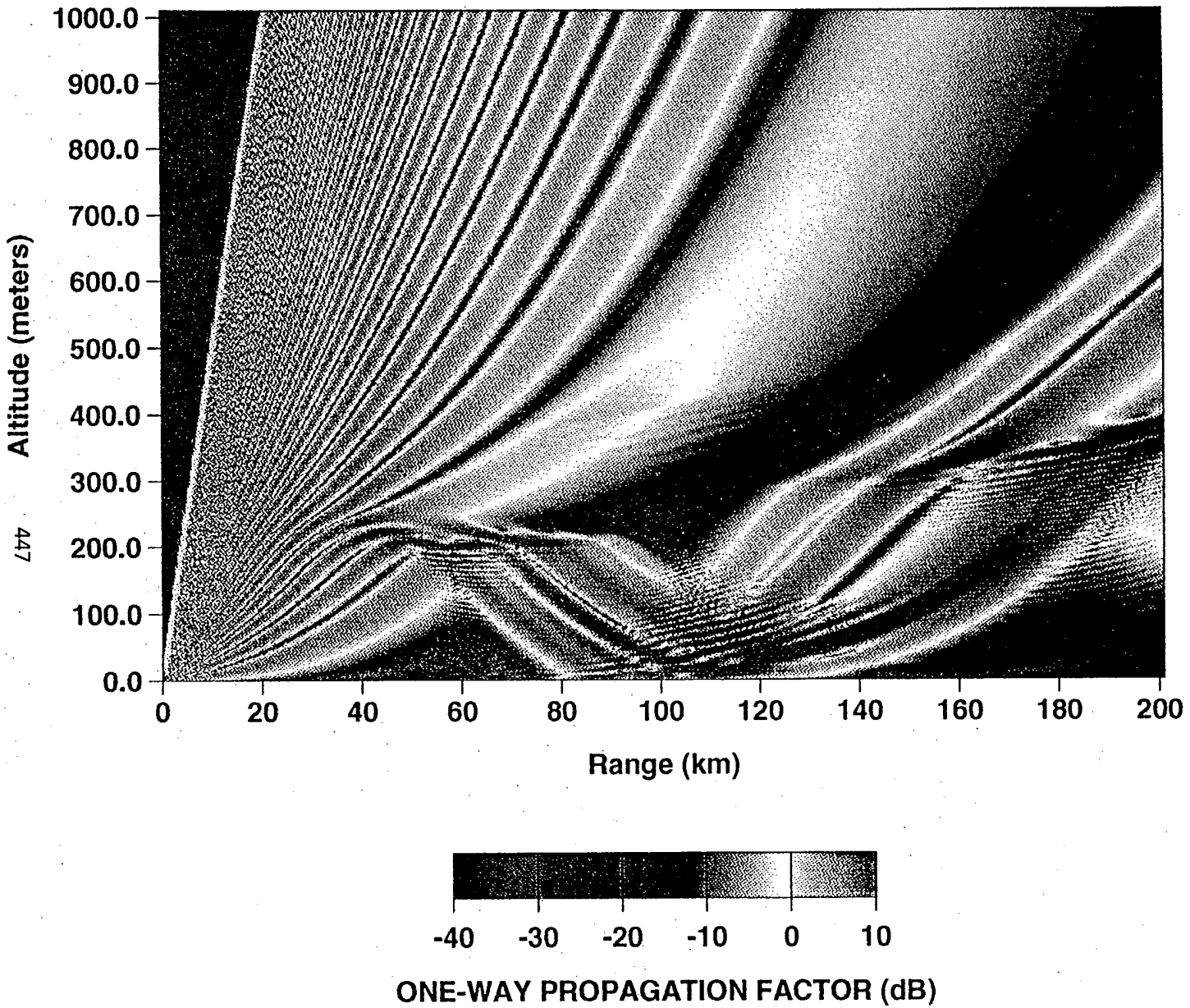

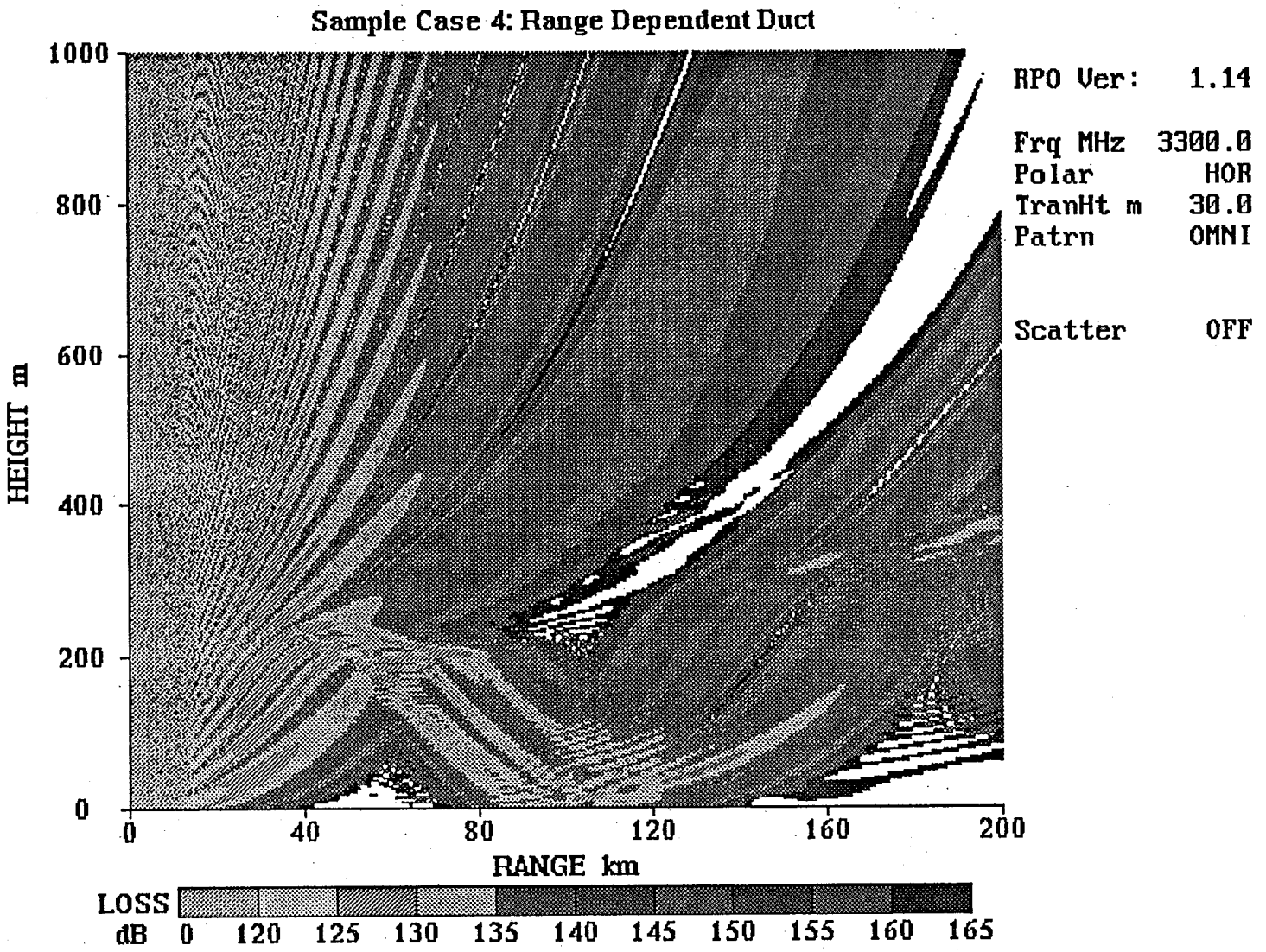
Sample Case 4: Range Dependent Duct
1000
800
600
400
200
0
HEIGHT m
0
40
80
120
160
200
RANGE km
LOSS
dB
0
120
125
130
135
140
145
150
155
160
165
RPO Ver: 1.14
Frq MHz 3300.0
Polar HOR
TranHt m 30.0
Patrn OMNI
Scatter OFF

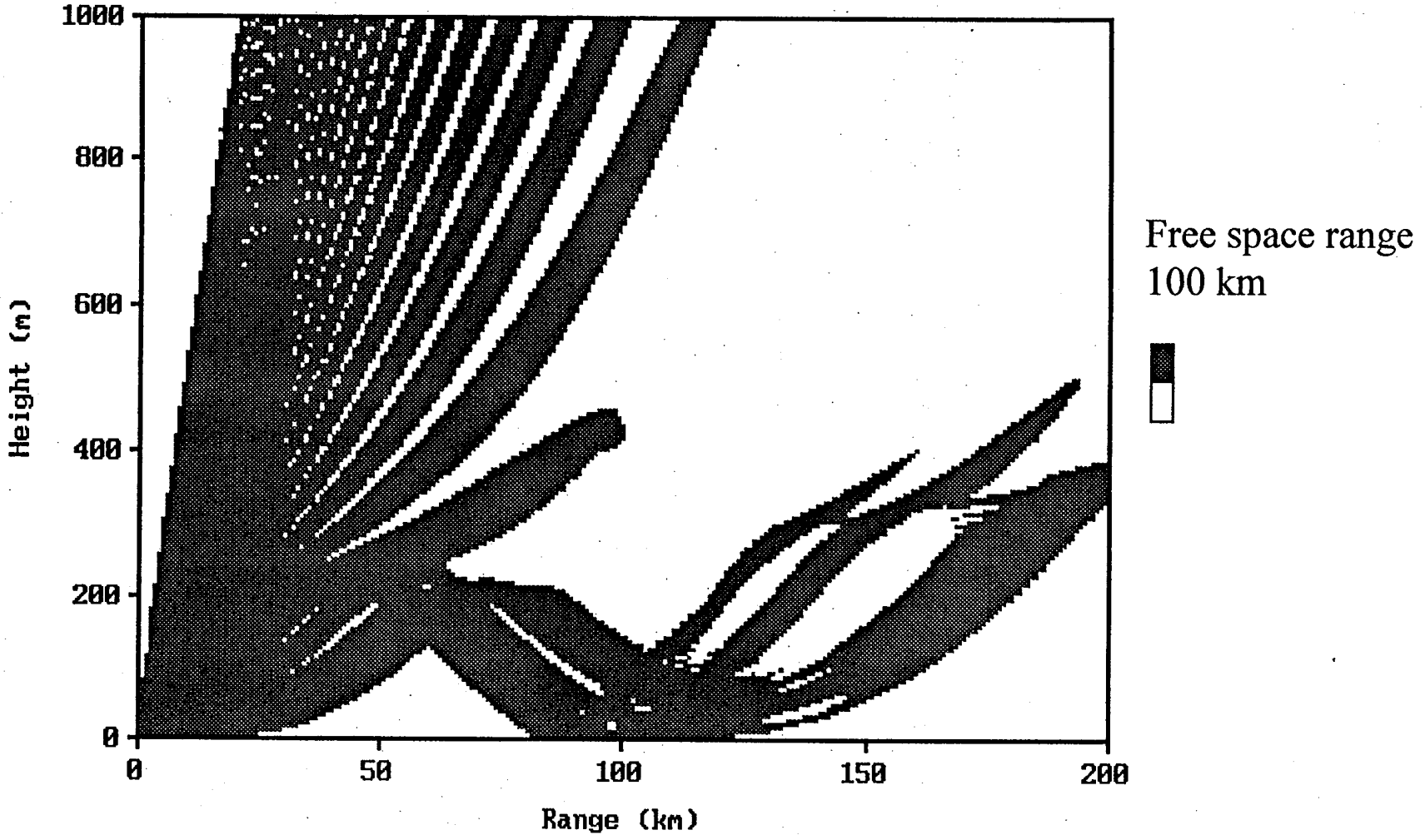

PCPEM Sample case 4

IFDG

SAMPLE CASE 4

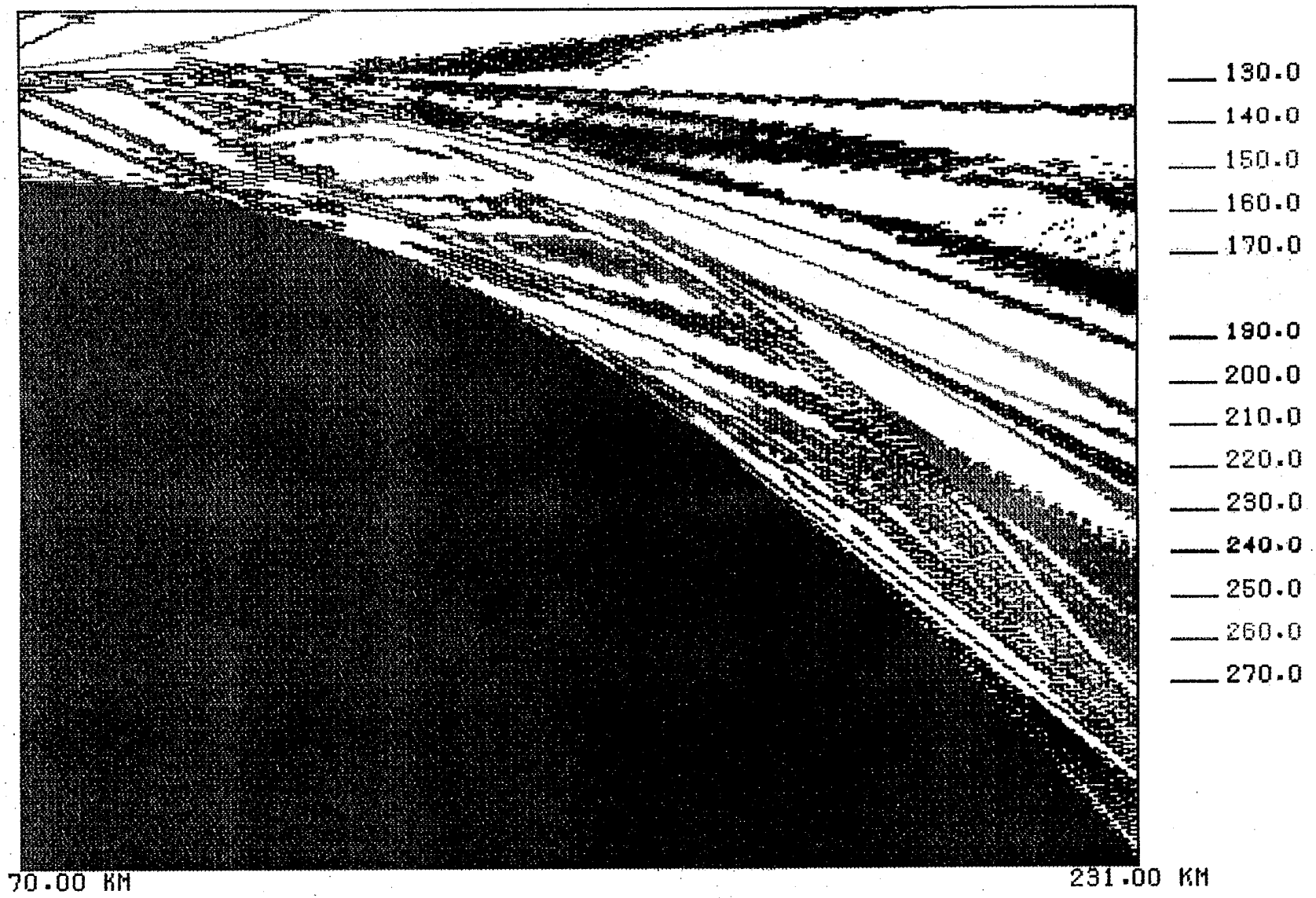

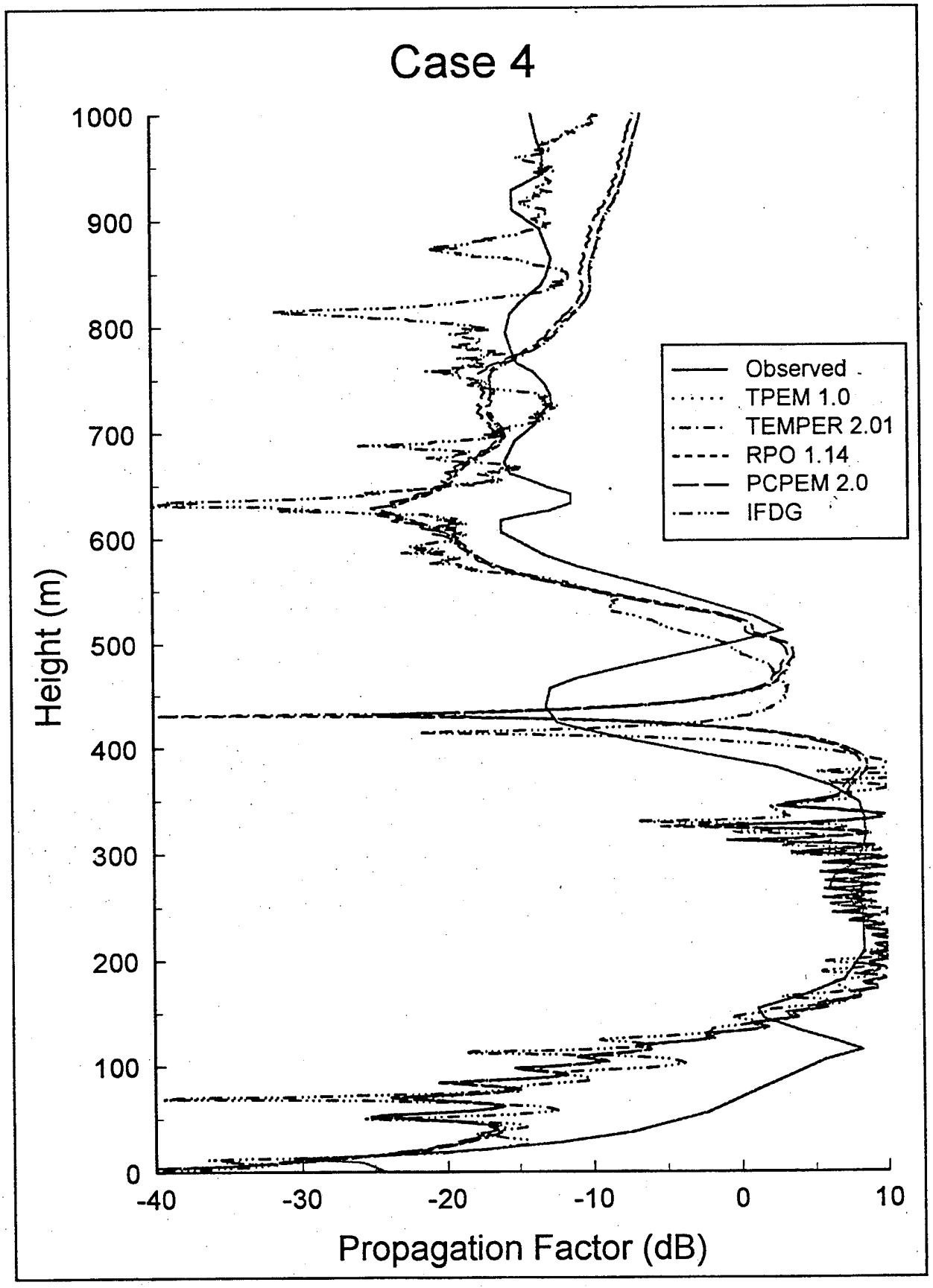
Case 4
1000
900
800
700
600
500
400
300
200
100
0
Height (m)
-40
-30
-20
-10
0
10
Propagation Factor (dB)
Observed
TPEM 1.0
TEMPER 2.01
RPO 1.14
PCPEM 2.0
IFDG

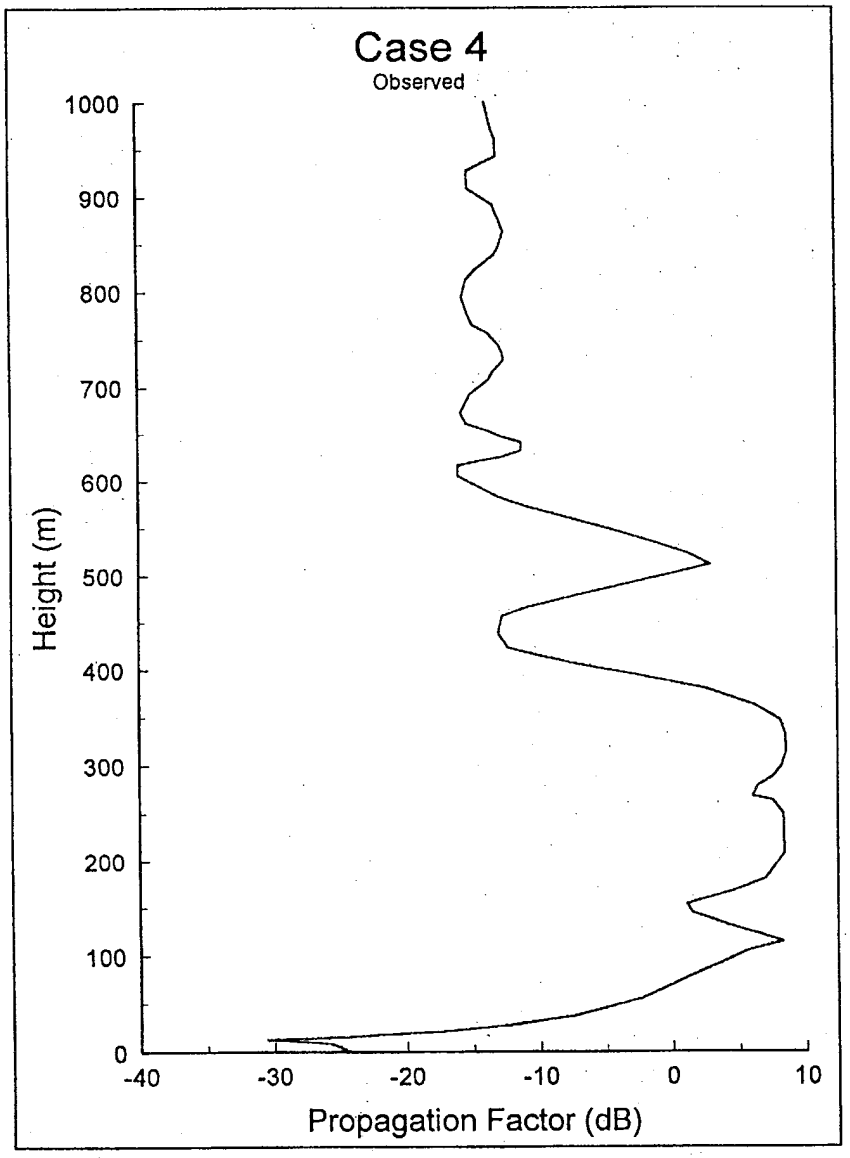
Case 4
Observed
Height (m)
1000
900
800
700
600
500
400
300
200
100
0
-40
-30
-20
-10
0
10
Propagation Factor (dB)

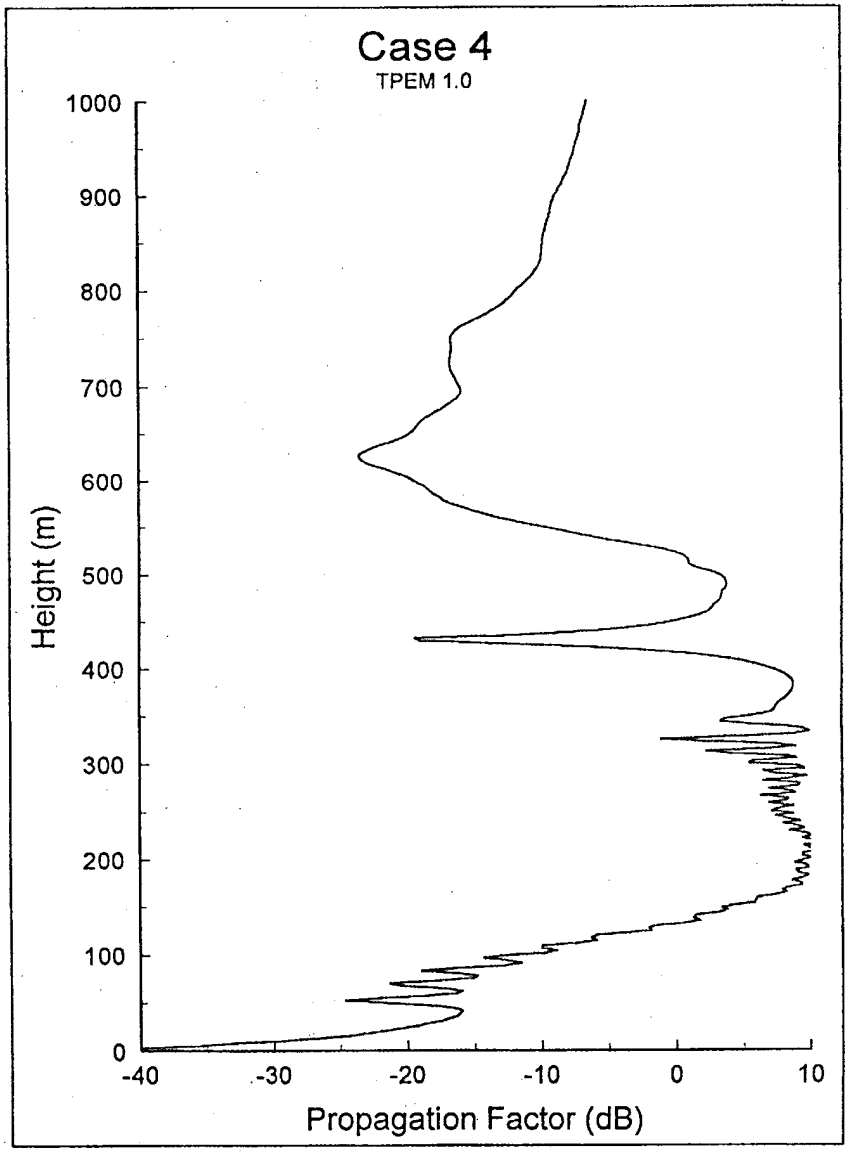
Case 4
TPEM 1.0
Height (m)
1000
900
800
700
600
500
400
300
200
100
0
-40
-30
-20
-10
0
10
Propagation Factor (dB)

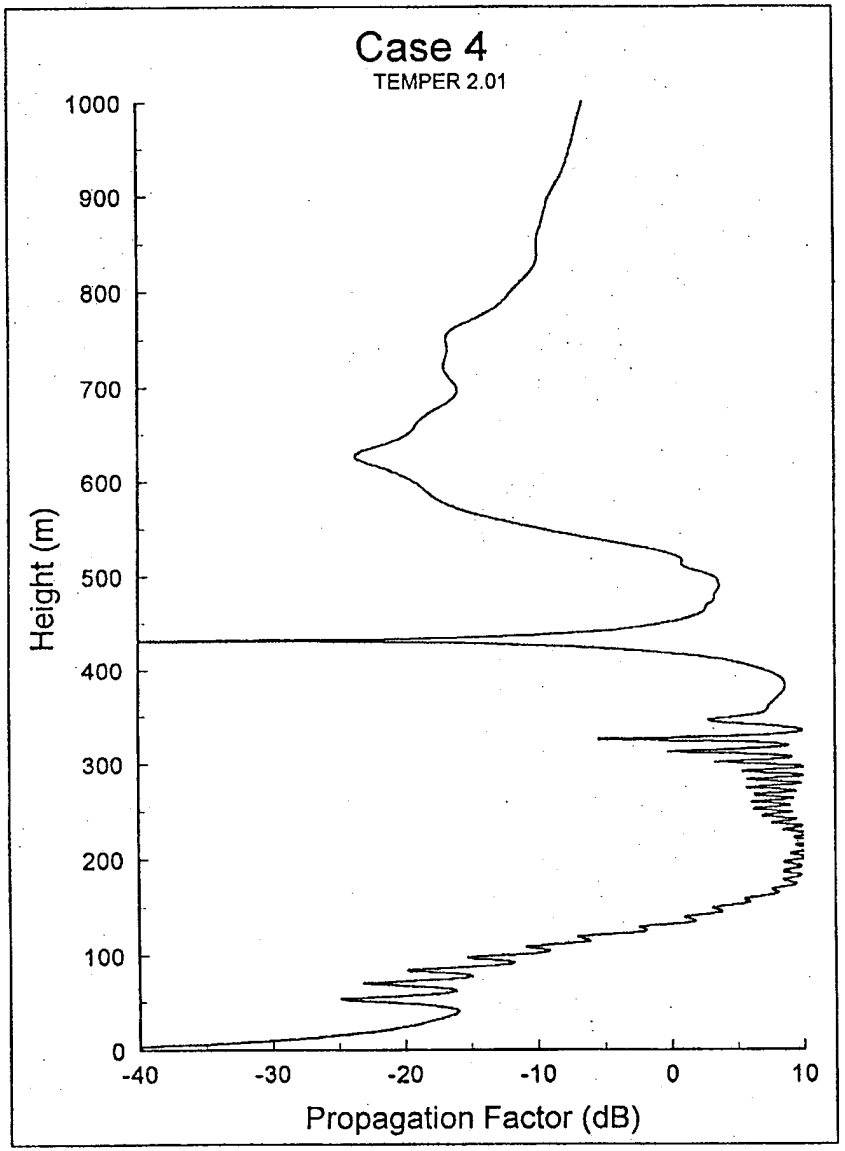
Case 4
TEMPER 2.01
Height (m)
1000
900
800
700
600
500
400
300
200
100
0
-40
-30
-20
-10
0
10
Propagation Factor (dB)

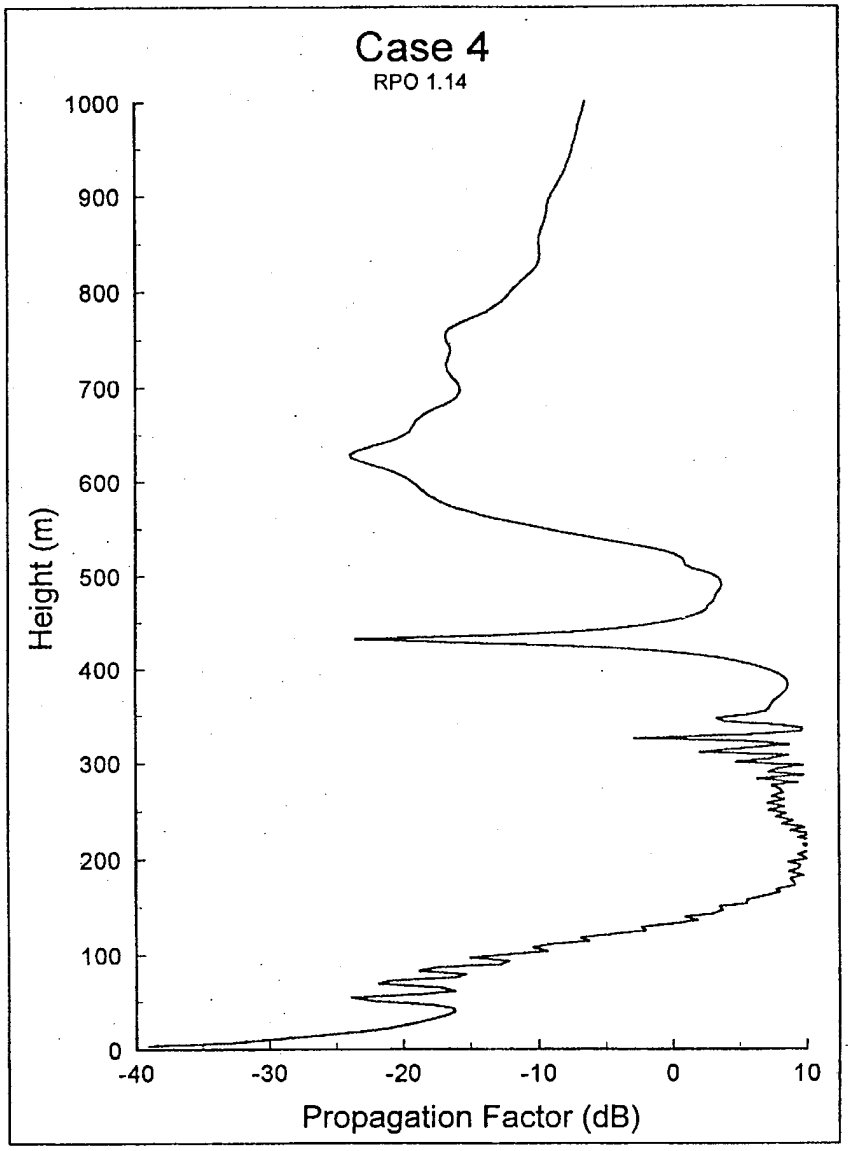
Case 4
RPO 1.14
Height (m)
1000
900
800
700
600
500
400
300
200
100
0
-40
-30
-20
-10
0
10
Propagation Factor (dB)

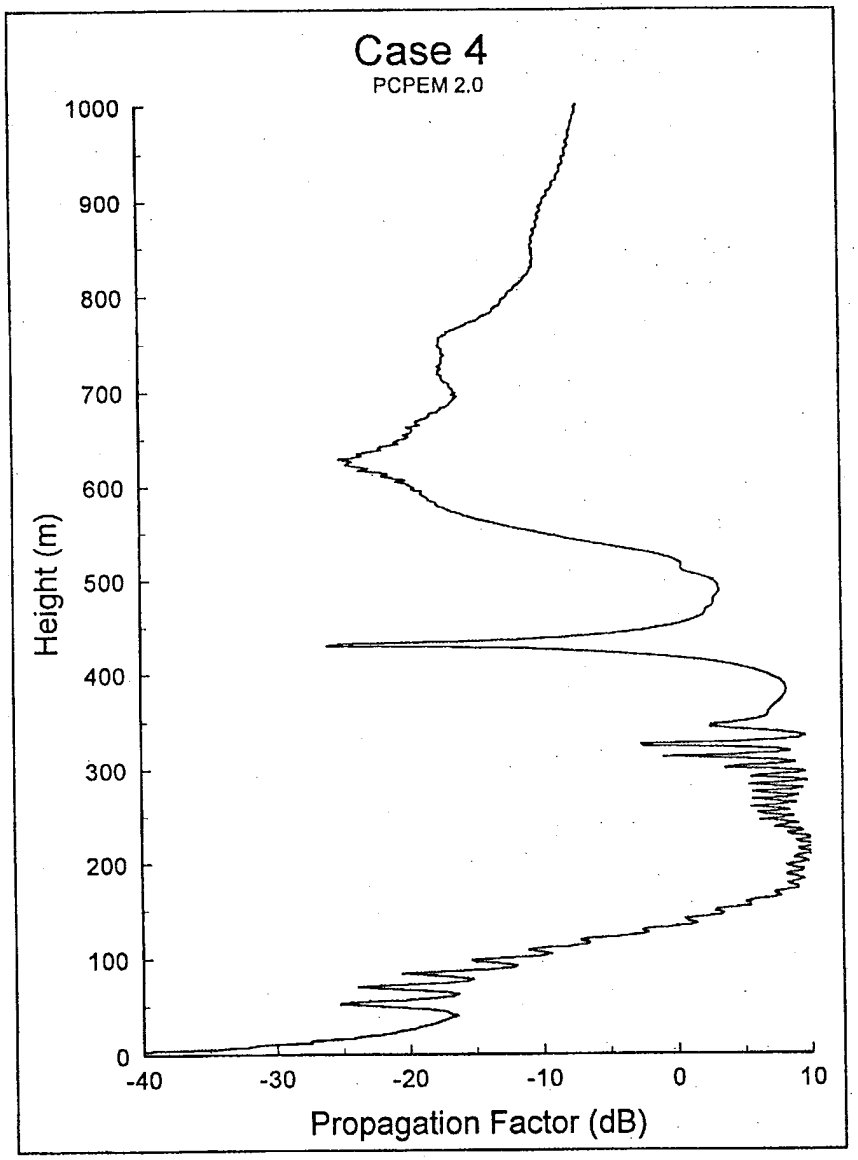
Case 4
PCPEM 2.0
Height (m)
1000
900
800
700
600
500
400
300
200
100
0
-40
-30
-20
-10
0
10
Propagation Factor (dB)

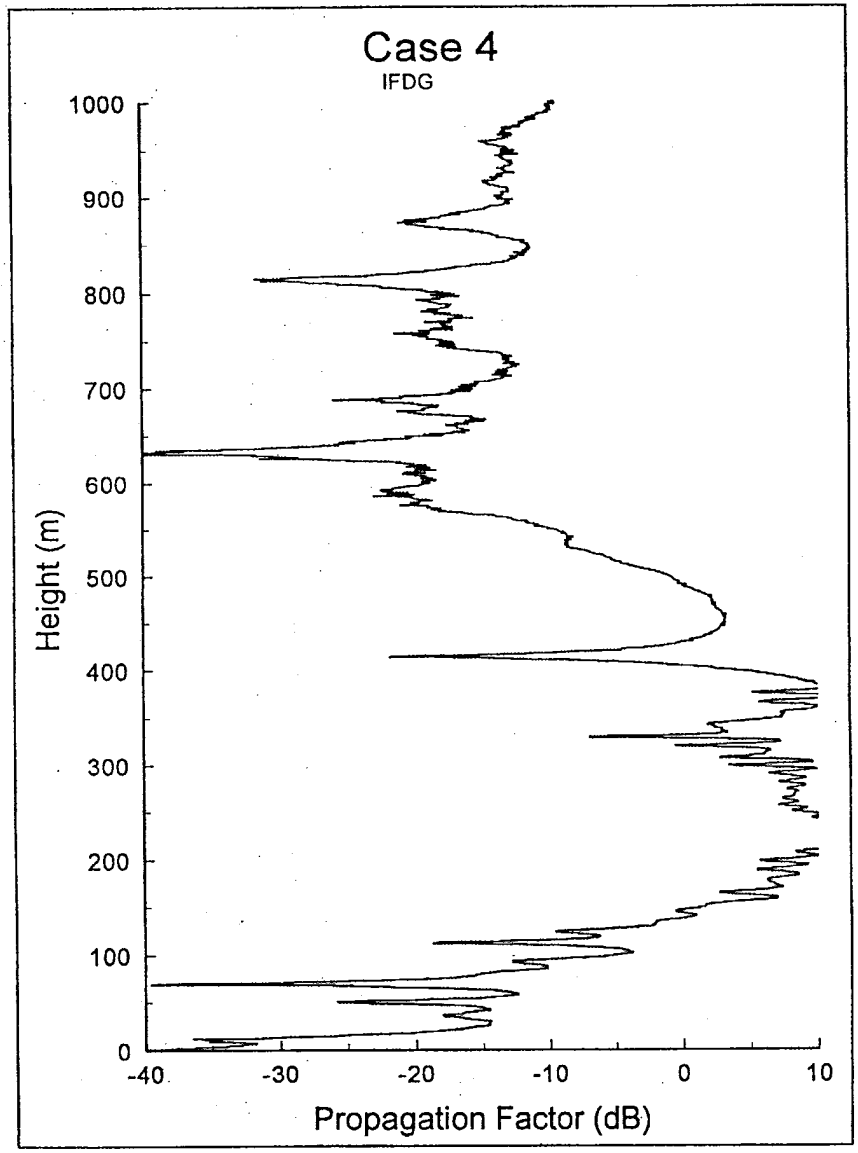
Case 4
IFDG
Height (m)
1000
900
800
700
600
500
400
300
200
100
0
-40
-30
-20
-10
0
10
Propagation Factor (dB)

Sample Case 5.

This case considers model applicability to high source heights in a complicated ducting environment over the sea. The modified refractivity profile is given in Table 6 and plotted in Figure 5 and describes a surface-based duct 300 m thick and an elevated duct located at a height of 3000 m. The frequency is 450 MHz and the transmitter height is 9000 m. A coverage diagram is desired for this case for altitudes from the surface to 10 km and ranges from 0 to 400 km, using a free space range of 400 km. Propagation factor is required for receiver heights from 0 to 10 km at a range of 400 km.

Height (m)	Refractivity (M units)
0	340
250	370
300	320
3000	690
3100	680
10000	1662

Table 6. Modified refractivity profile for a combination surface-based and elevated duct.

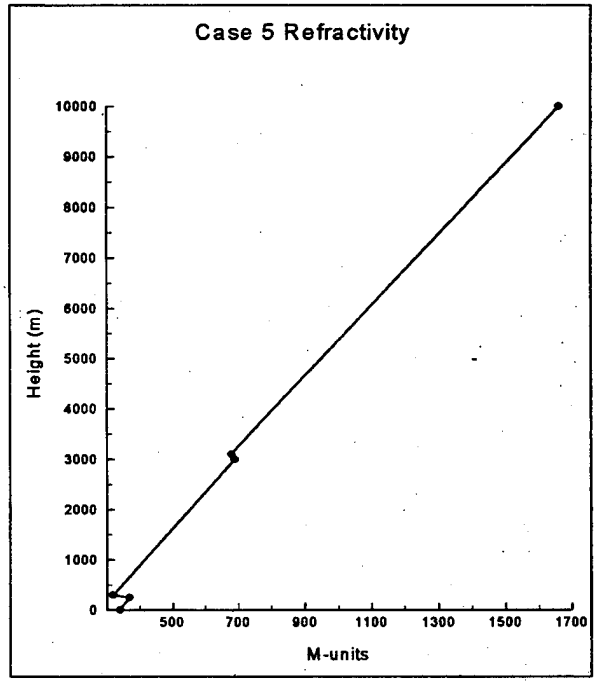

Figure 5. Plot of data of Table 6.

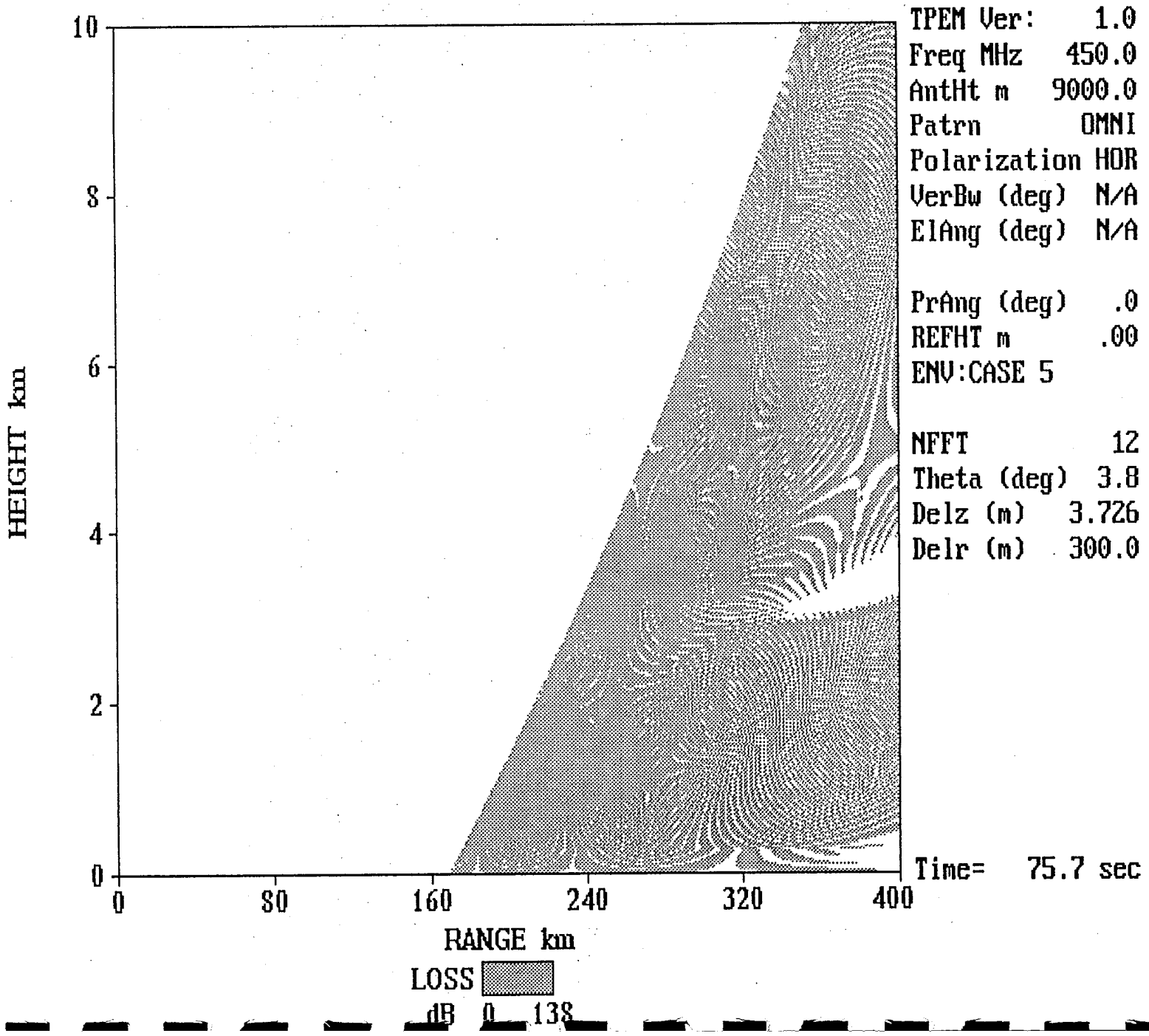
10
8
6
4
2
0
HEIGHT km
0
80
160
240
320
400
RANGE km
LOSS
dB 0 138
TPEM Ver: 1.0
Freq MHz 450.0
AntHt m 9000.0
Patrn OMNI
Polarization HOR
VerBw (deg) N/A
ElAng (deg) N/A
PrAng (deg) .0
REFHT m .00
ENV:CASE 5
NFFT 12
Theta (deg) 3.8
Delz (m) 3.726
Delr (m) 300.0
Time= 75.7 sec

CASE #5, TEMPER VERSION 2.01

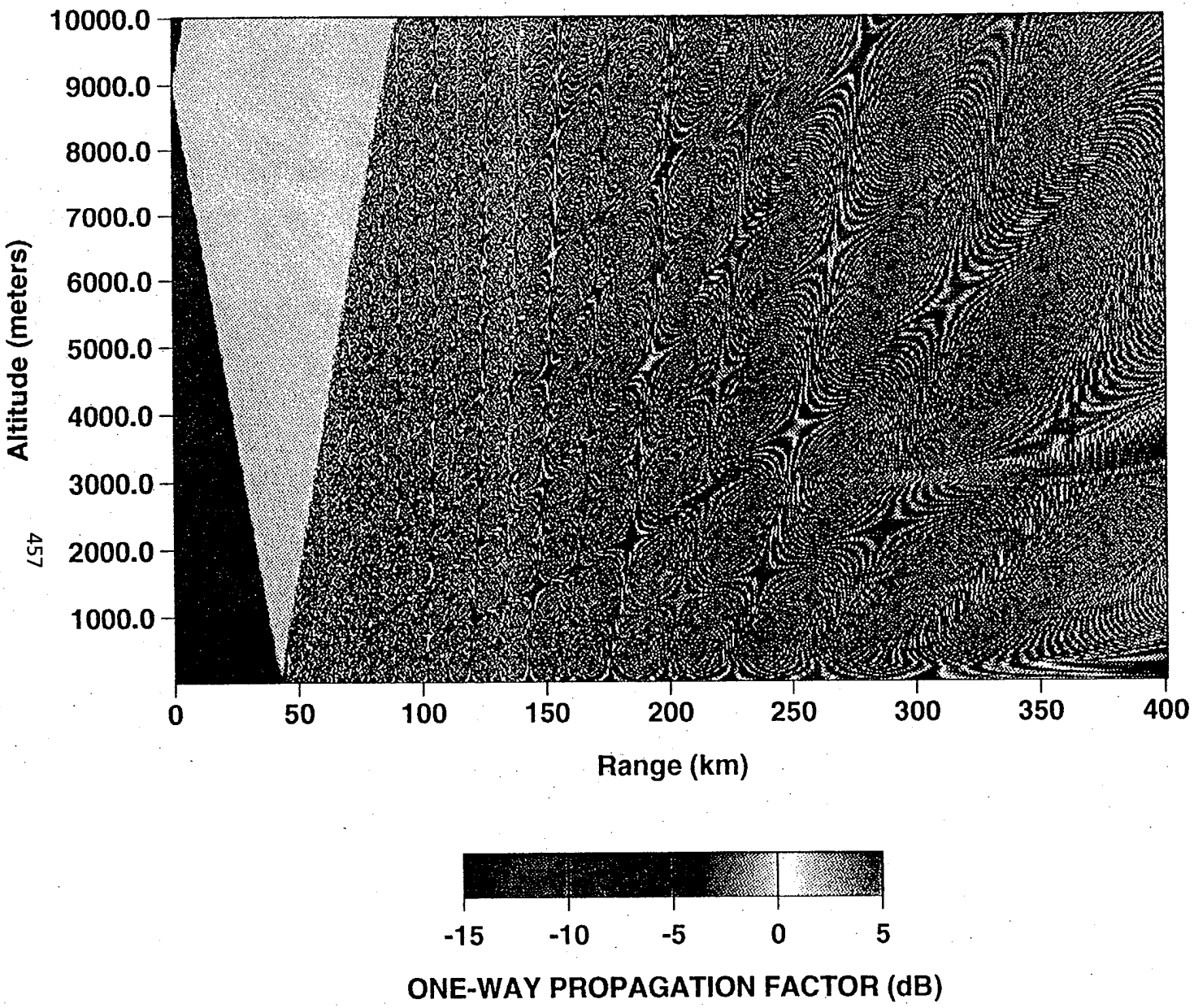

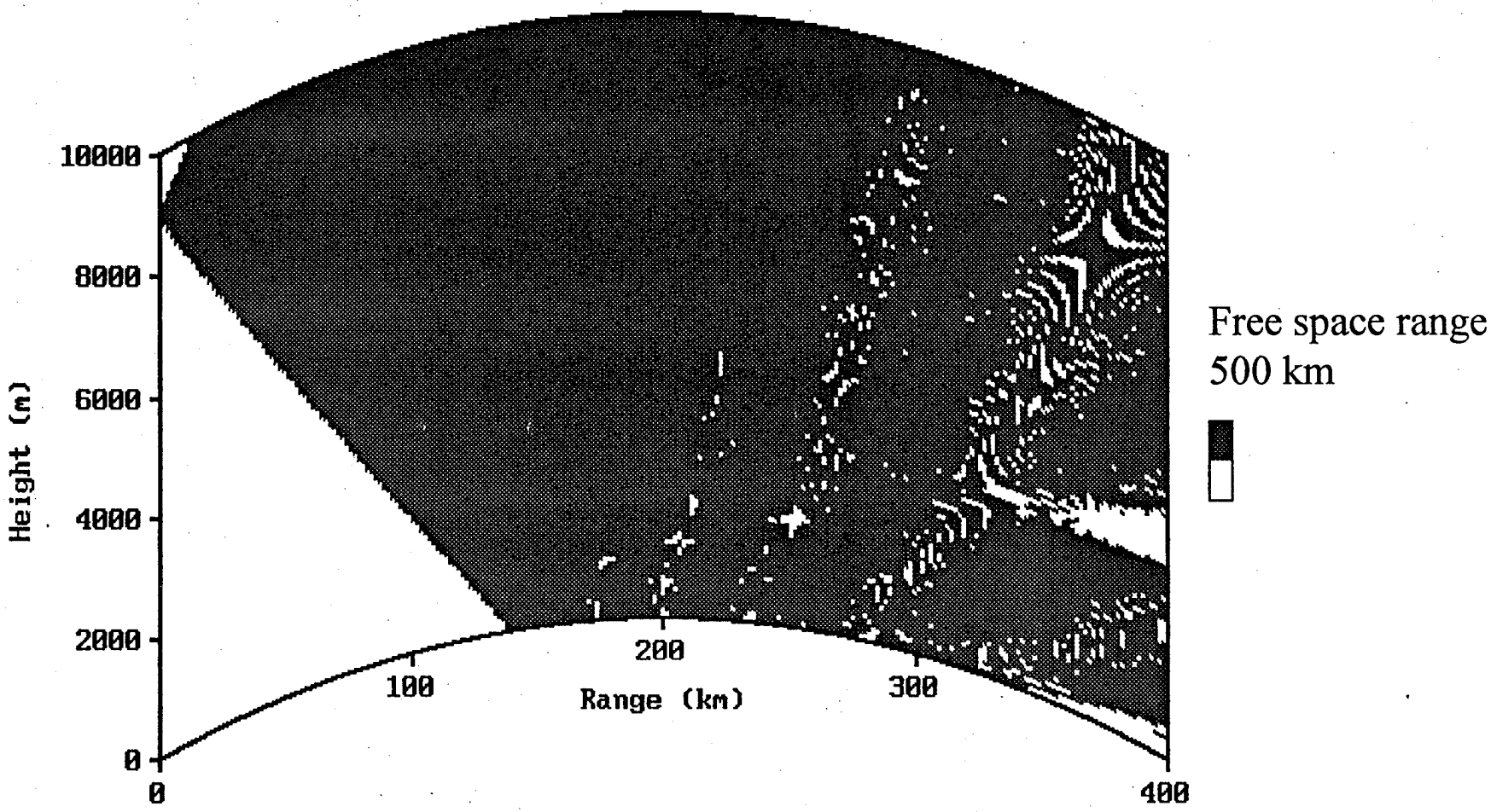

EEMS 1.5 Sample case 5

HAP

SAMPLE CASE 5

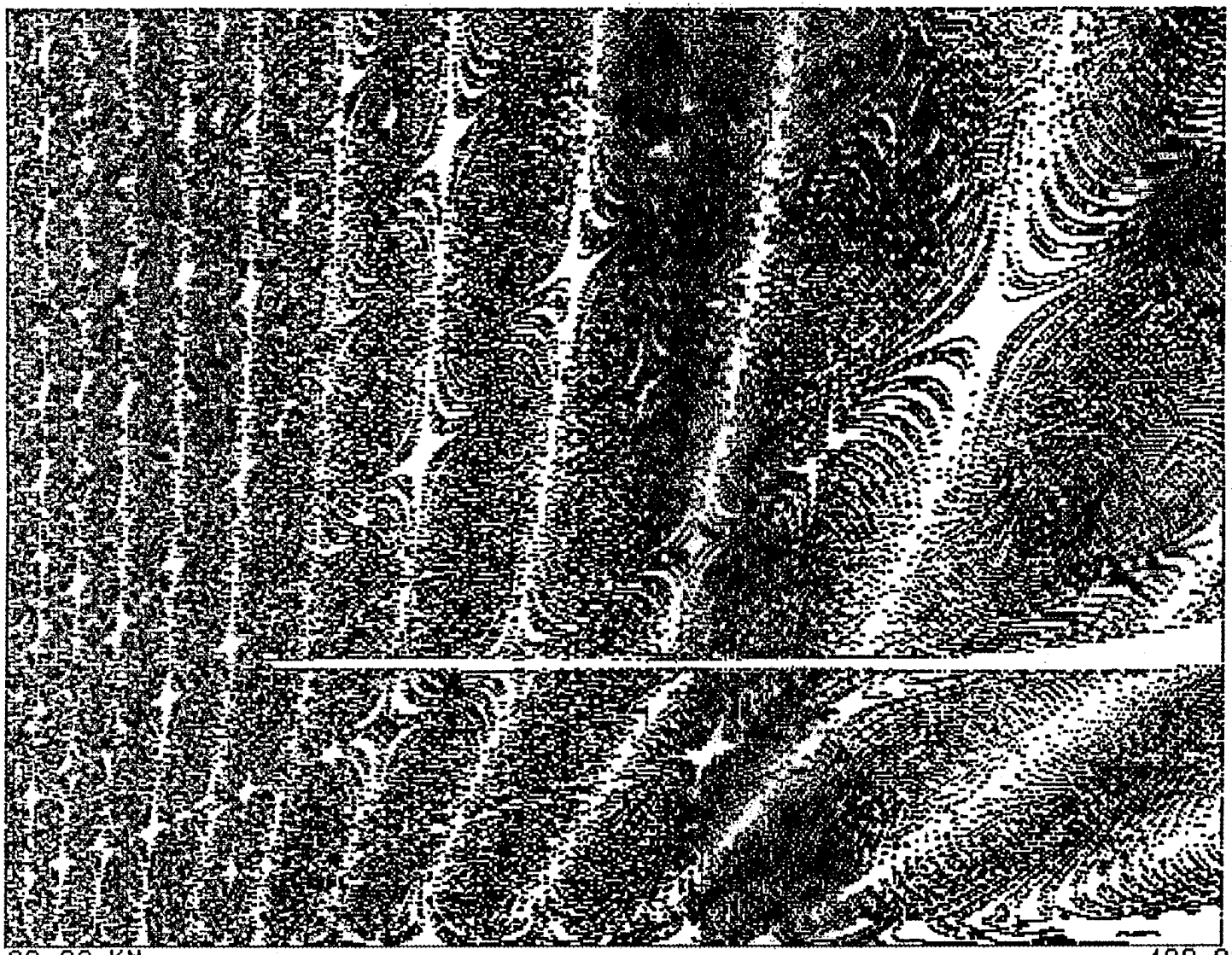

459

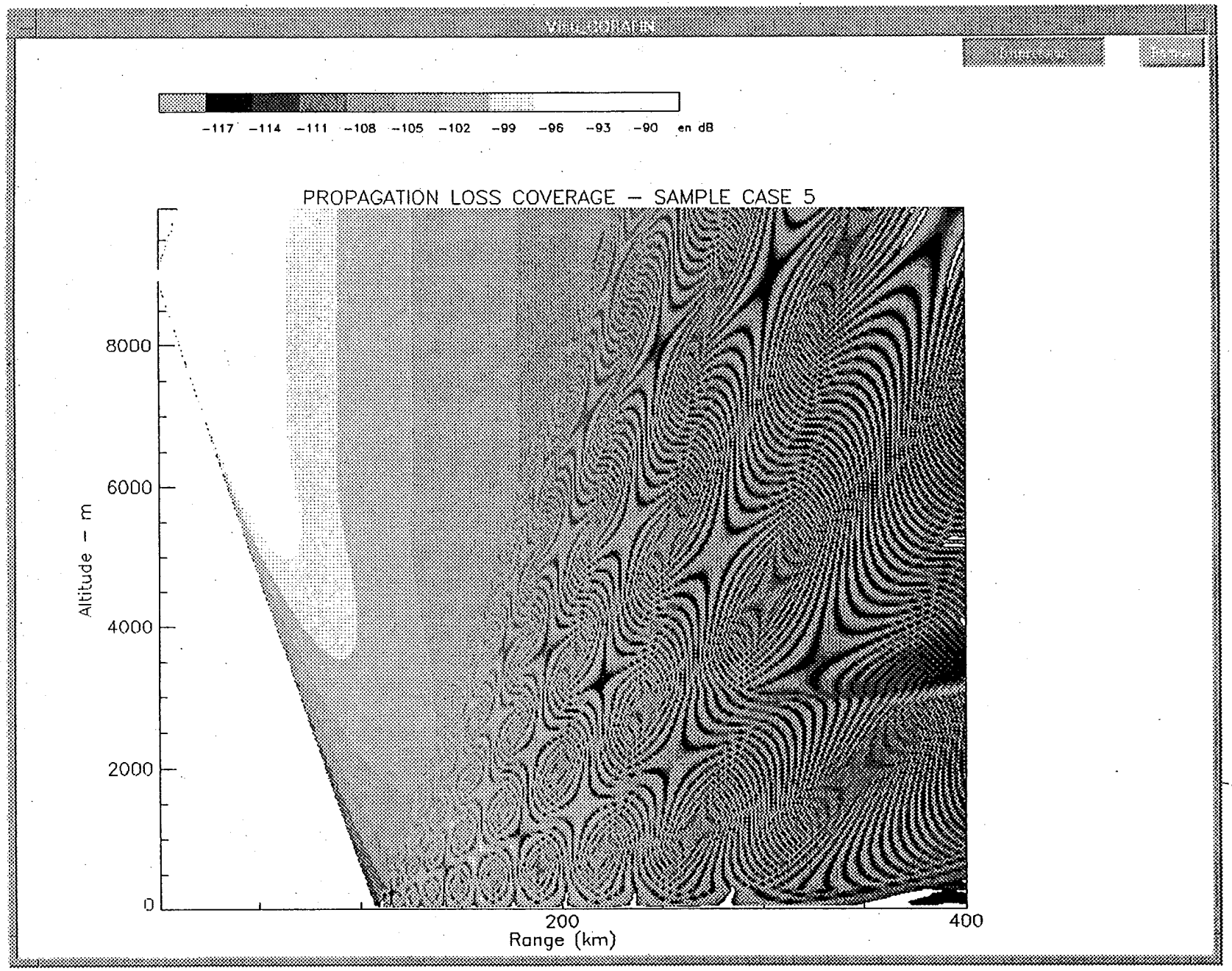
−117 −114 −111 −108 −105 −102 −99 −96 −93 −90 en dB
PROPAGATION LOSS COVERAGE — SAMPLE CASE 5
8000
6000
4000
2000
0
Altitude − m
200
400
Range (km)

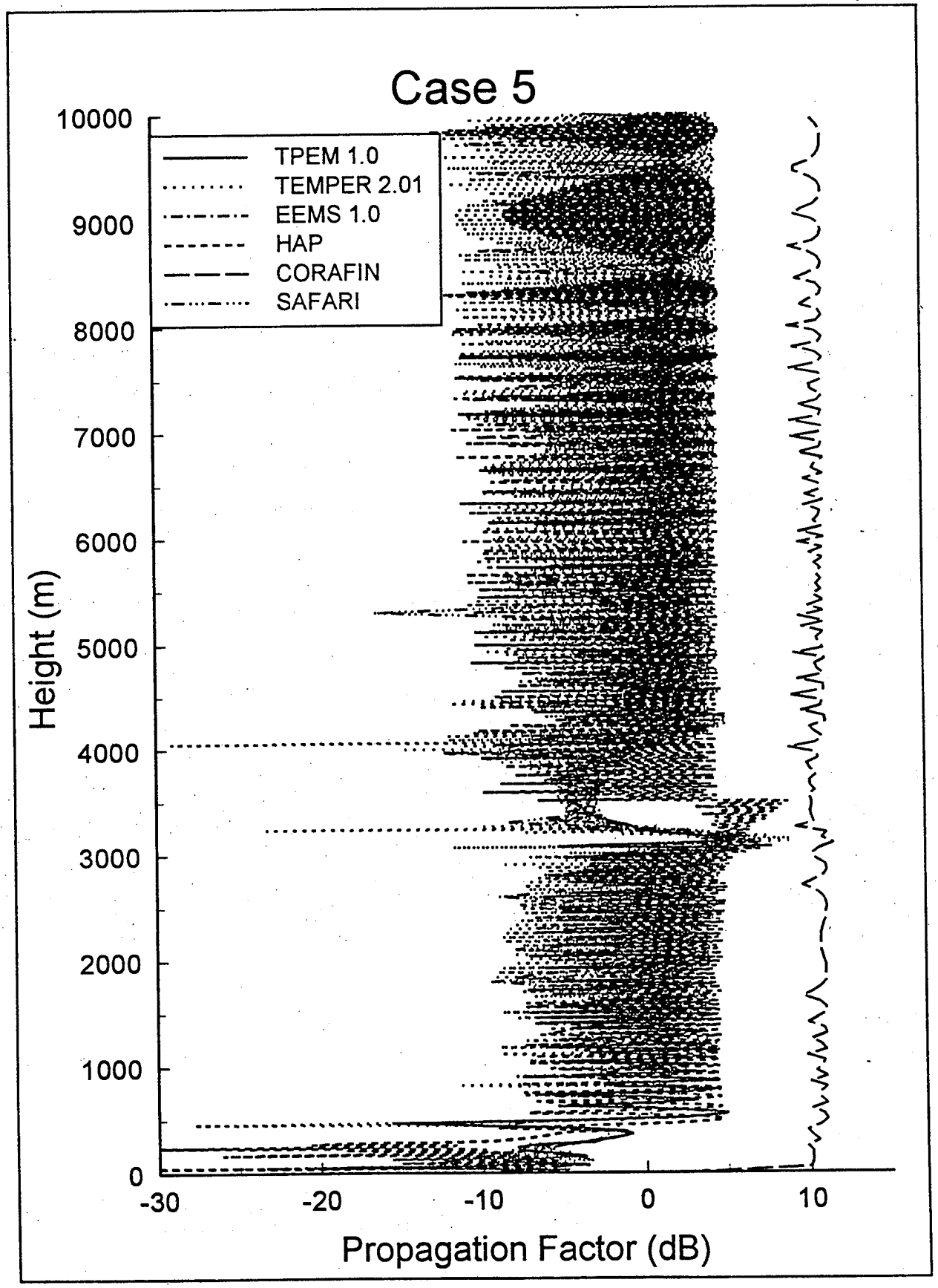
Case 5
TPEM 1.0
TEMPER 2.01
EEMS 1.0
HAP
CORAFIN
SAFARI
Height (m)
10000
9000
8000
7000
6000
5000
4000
3000
2000
1000
0
-30
-20
-10
0
10
Propagation Factor (dB)

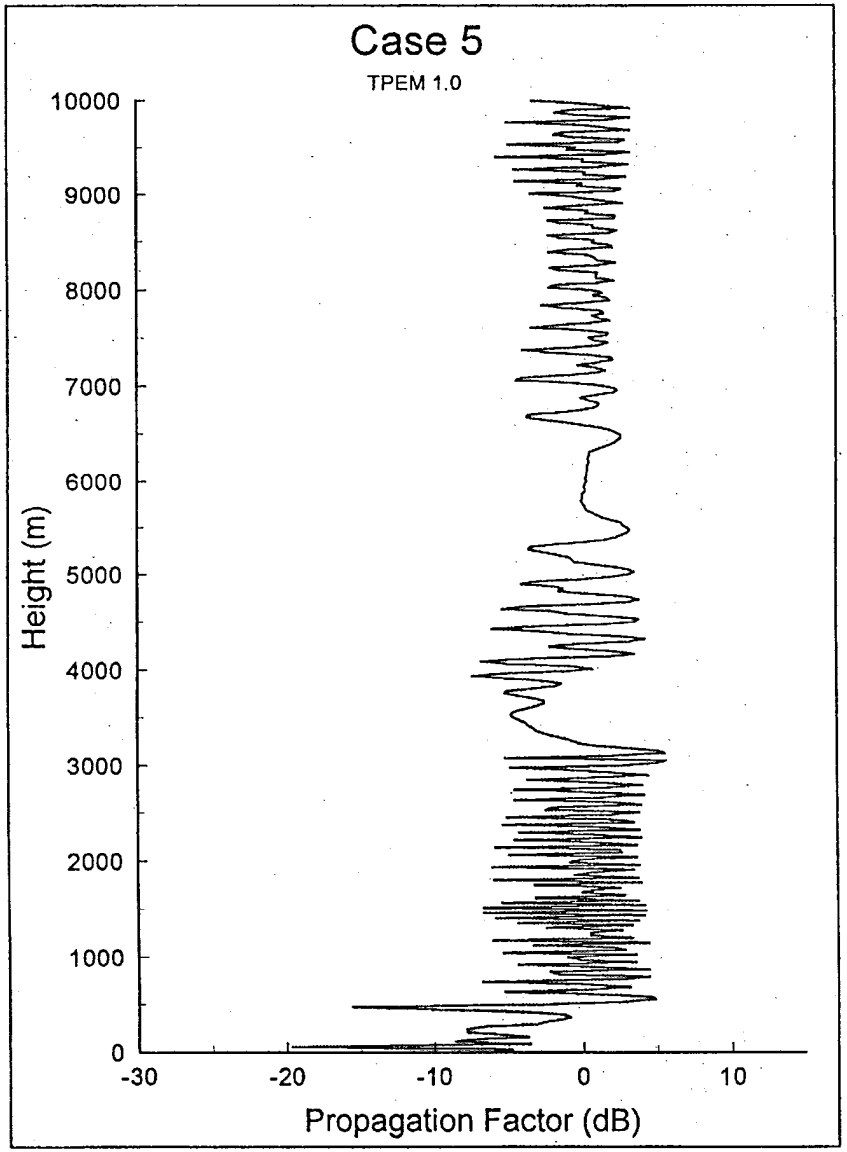
Case 5
TPEM 1.0
Height (m)
10000
9000
8000
7000
6000
5000
4000
3000
2000
1000
0
-30
-20
-10
0
10
Propagation Factor (dB)

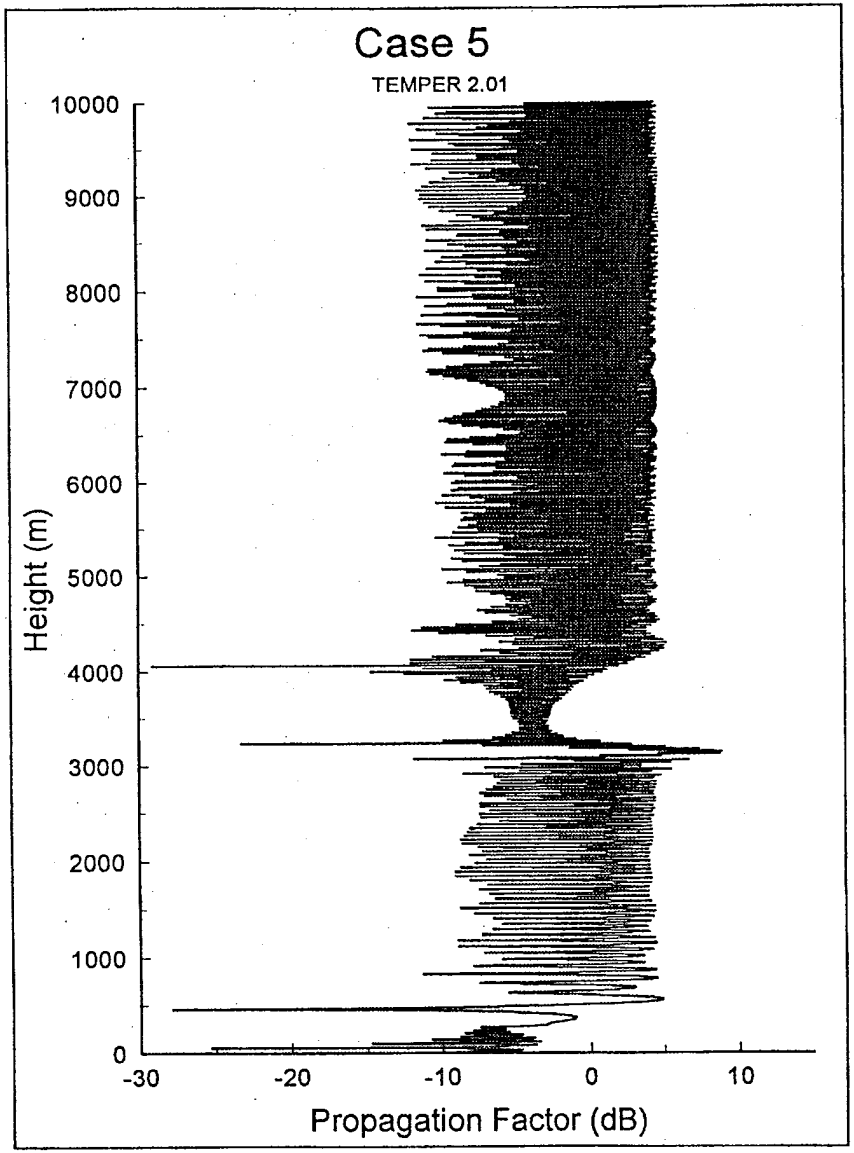
Case 5
TEMPER 2.01
Height (m)
10000
9000
8000
7000
6000
5000
4000
3000
2000
1000
0
-30
-20
-10
0
10
Propagation Factor (dB)

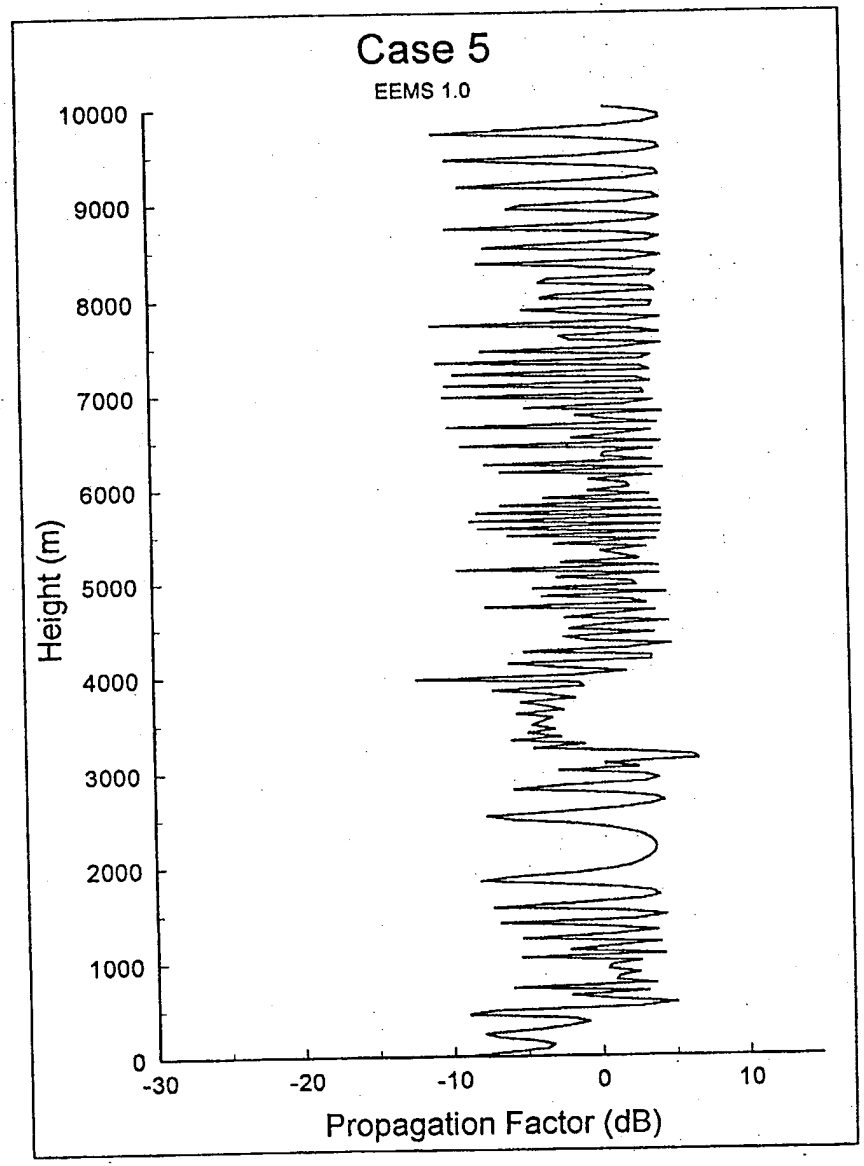
Case 5
EEMS 1.0
Height (m)
10000
9000
8000
7000
6000
5000
4000
3000
2000
1000
0
-30
-20
-10
0
10
Propagation Factor (dB)

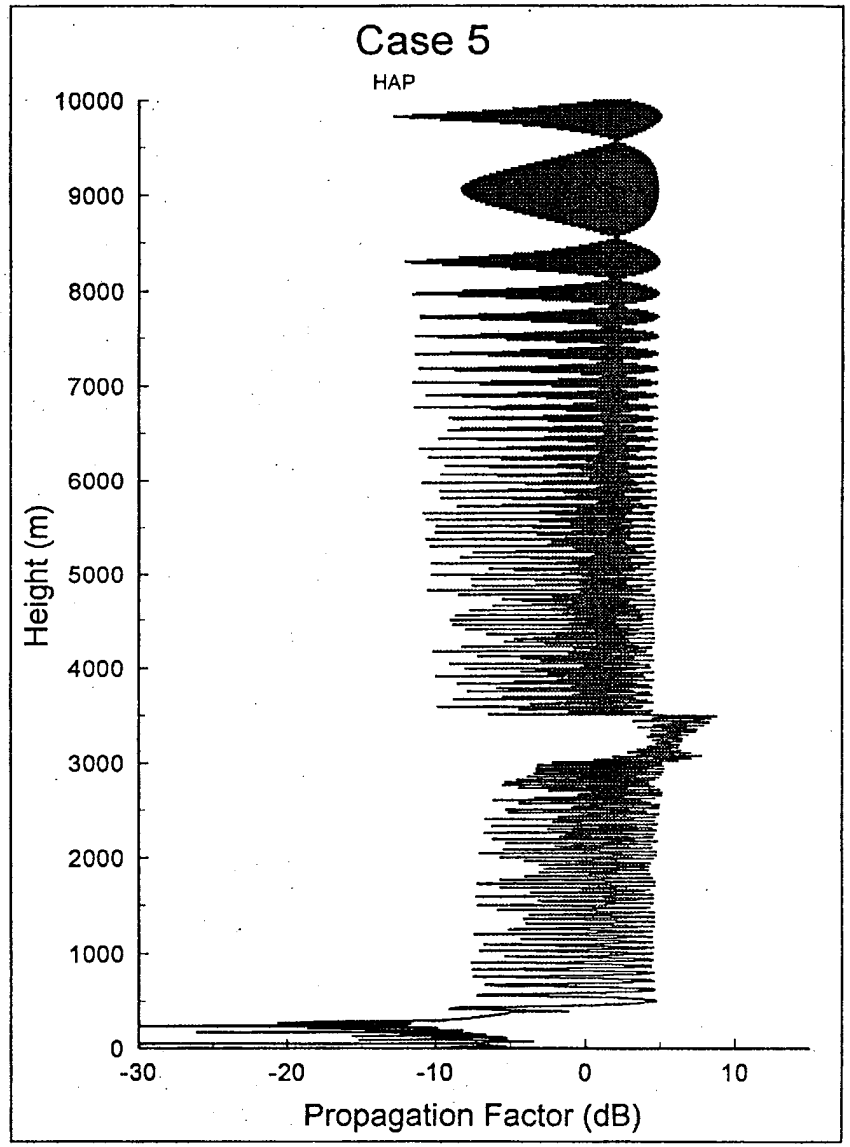
Case 5
HAP
Height (m)
10000
9000
8000
7000
6000
5000
4000
3000
2000
1000
0
-30
-20
-10
0
10
Propagation Factor (dB)

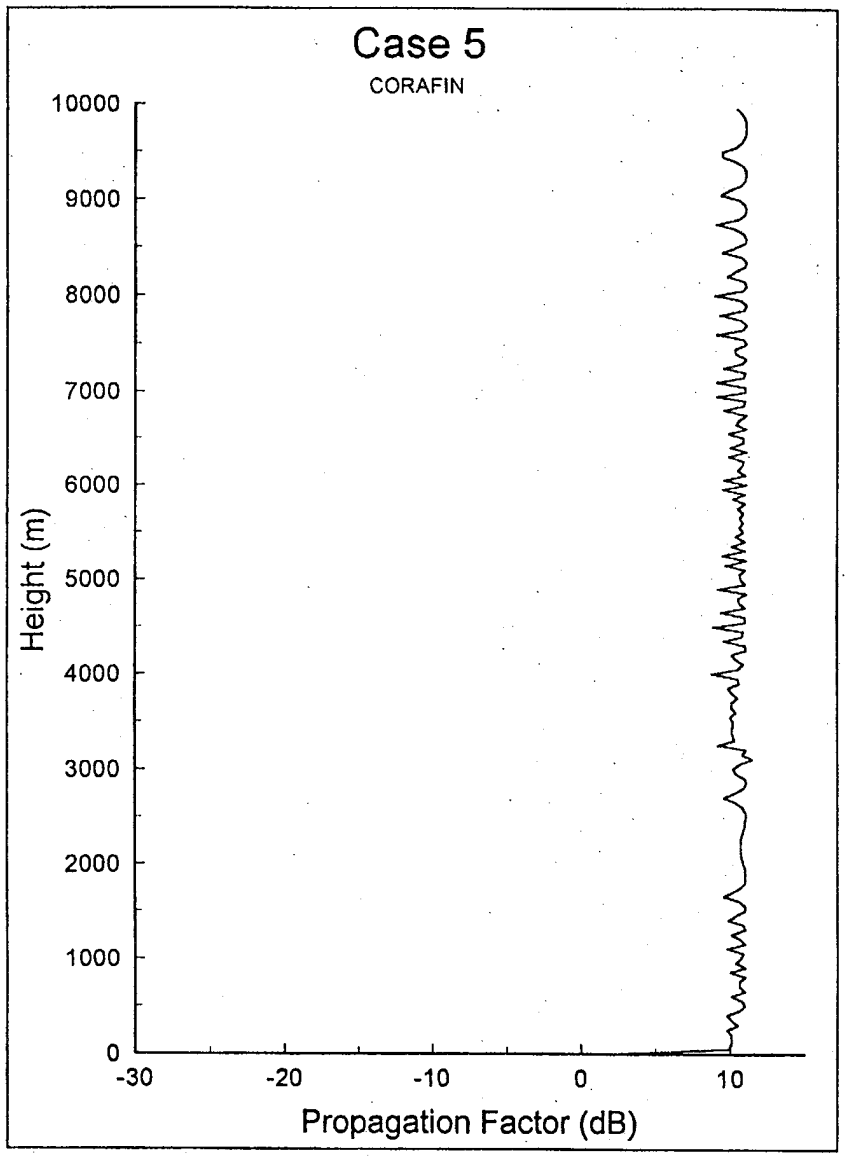
Case 5
CORAFIN
Height (m)
10000
9000
8000
7000
6000
5000
4000
3000
2000
1000
0
-30
-20
-10
0
10
Propagation Factor (dB)

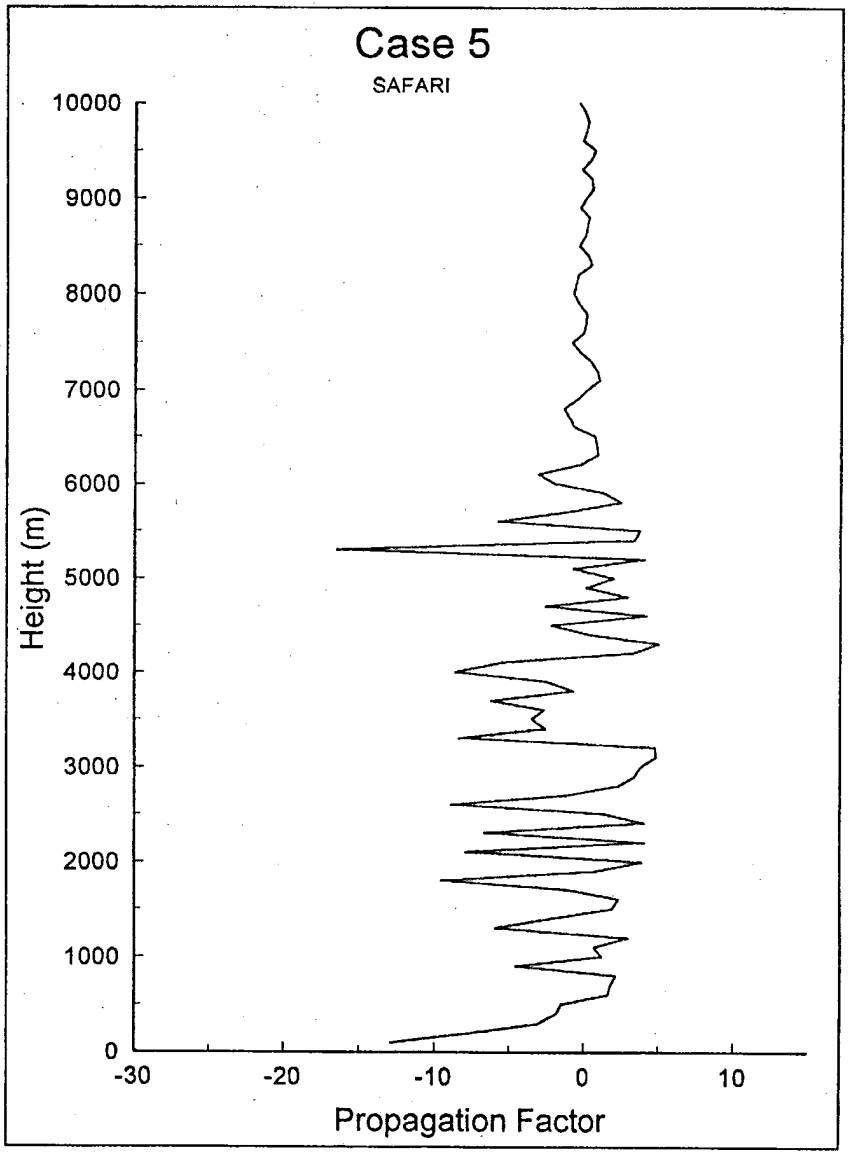
Case 5
SAFARI
Height (m)
10000
9000
8000
7000
6000
5000
4000
3000
2000
1000
0
-30
-20
-10
0
10
Propagation Factor

Sample Case 6.

This case concerns propagation from a moderately elevated source over the sea. The refractivity profile is specified in Table 2. The frequency is 10 GHz and the transmitter antenna is 1000 m above the sea. A coverage diagram is desired for receiver heights from 0 to 1500 m and for ranges from 0 to 100 km, based on a free space range of 50 km. Propagation factor is required at a range of 100 km for receiver heights of 0 to 1500 m.

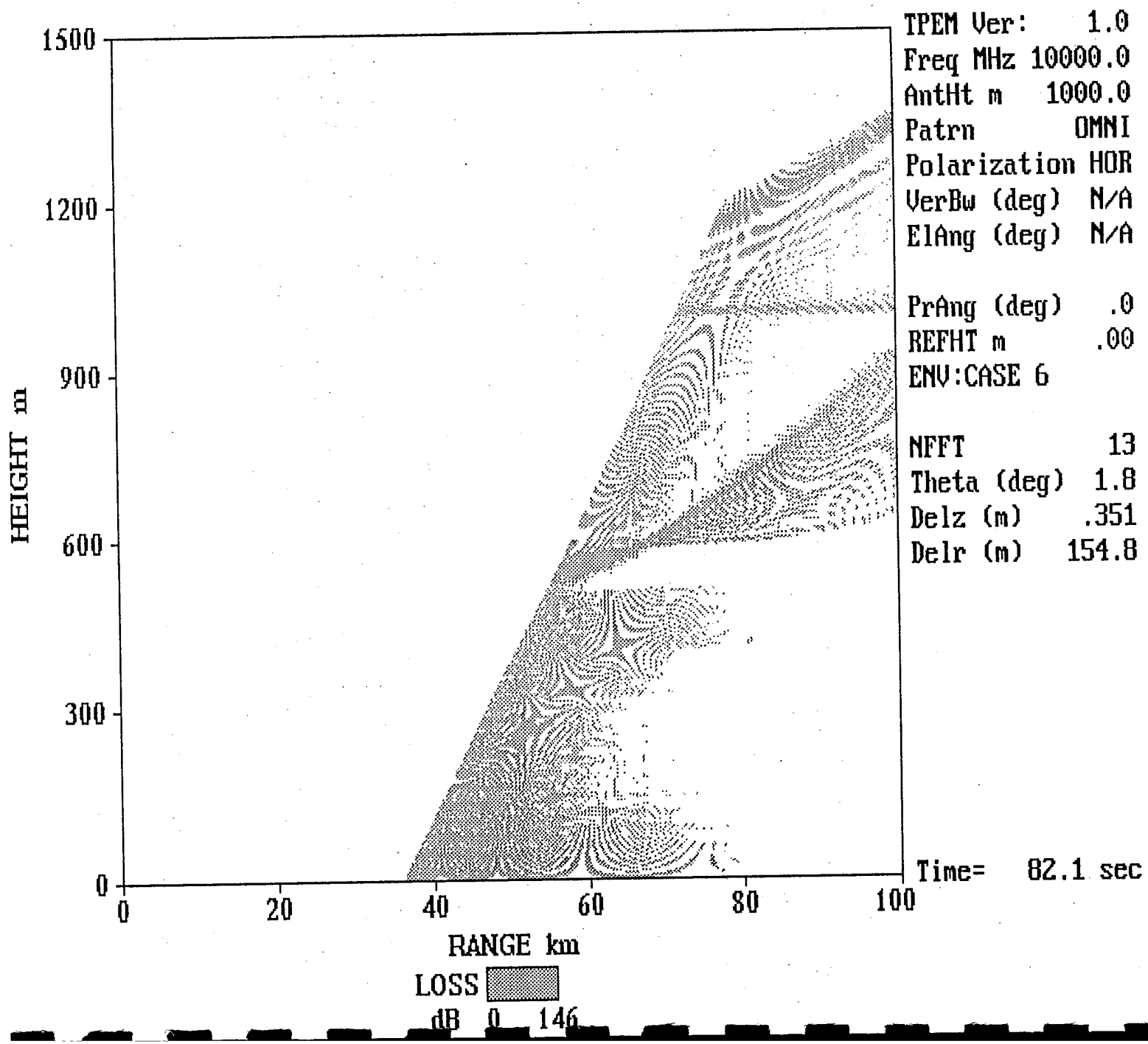
1500
1200
900
600
300
0
HEIGHT m
0
20
40
60
80
100
RANGE km
LOSS
dB 0 146
TPEM Ver: 1.0
Freq MHz 10000.0
AntHt m 1000.0
Patrn OMNI
Polarization HOR
VerBw (deg) N/A
ElAng (deg) N/A
PrAng (deg) .0
REFHT m .00
ENV:CASE 6
NFFT 13
Theta (deg) 1.8
Delz (m) .351
Delr (m) 154.8
Time= 82.1 sec

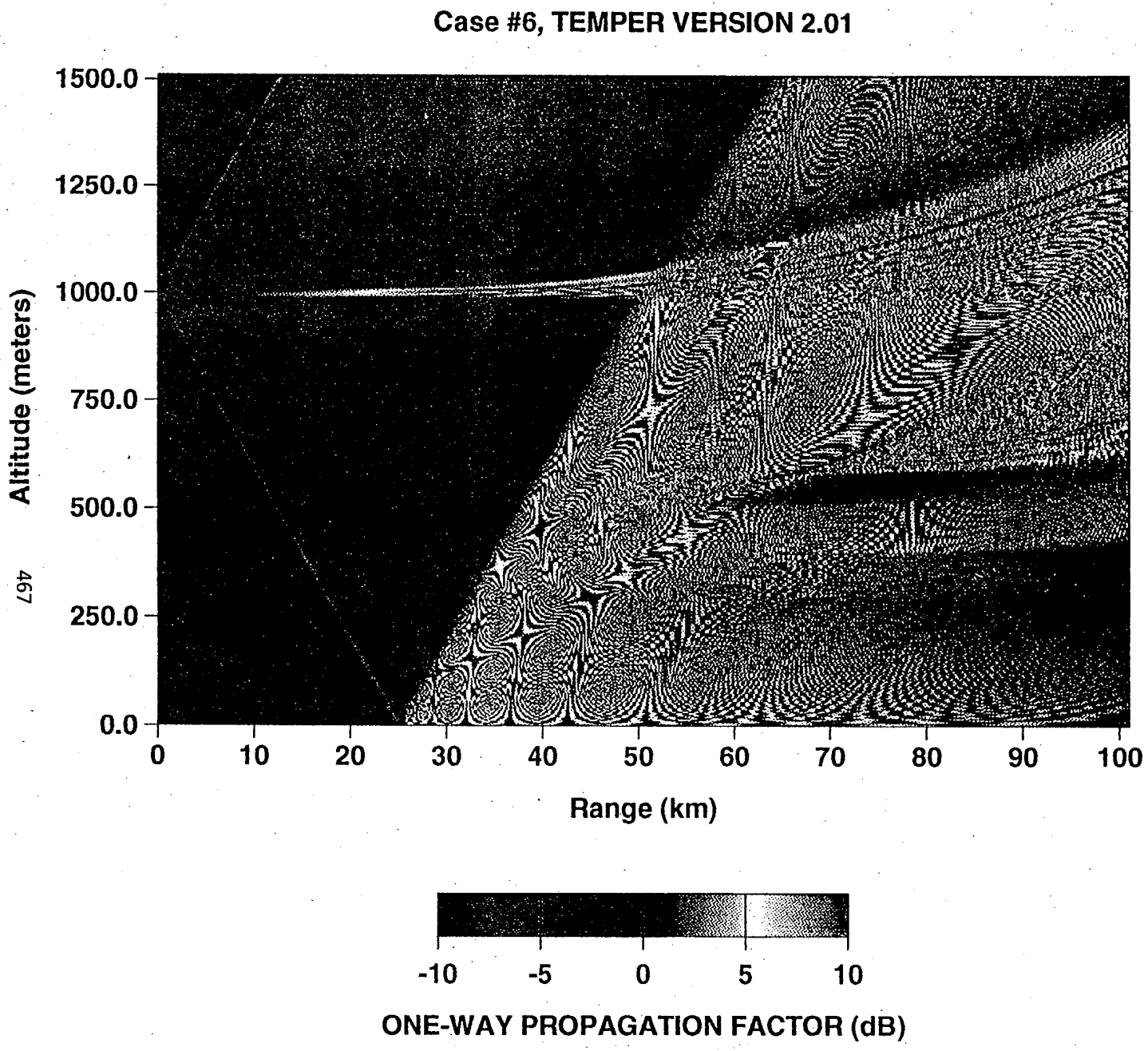
Case #6, TEMPER VERSION 2.01
1500.0
1250.0
1000.0
750.0
500.0
250.0
0.0
Altitude (meters)
0
10
20
30
40
50
60
70
80
90
100
Range (km)
-10
-5
0
5
10
ONE-WAY PROPAGATION FACTOR (dB)

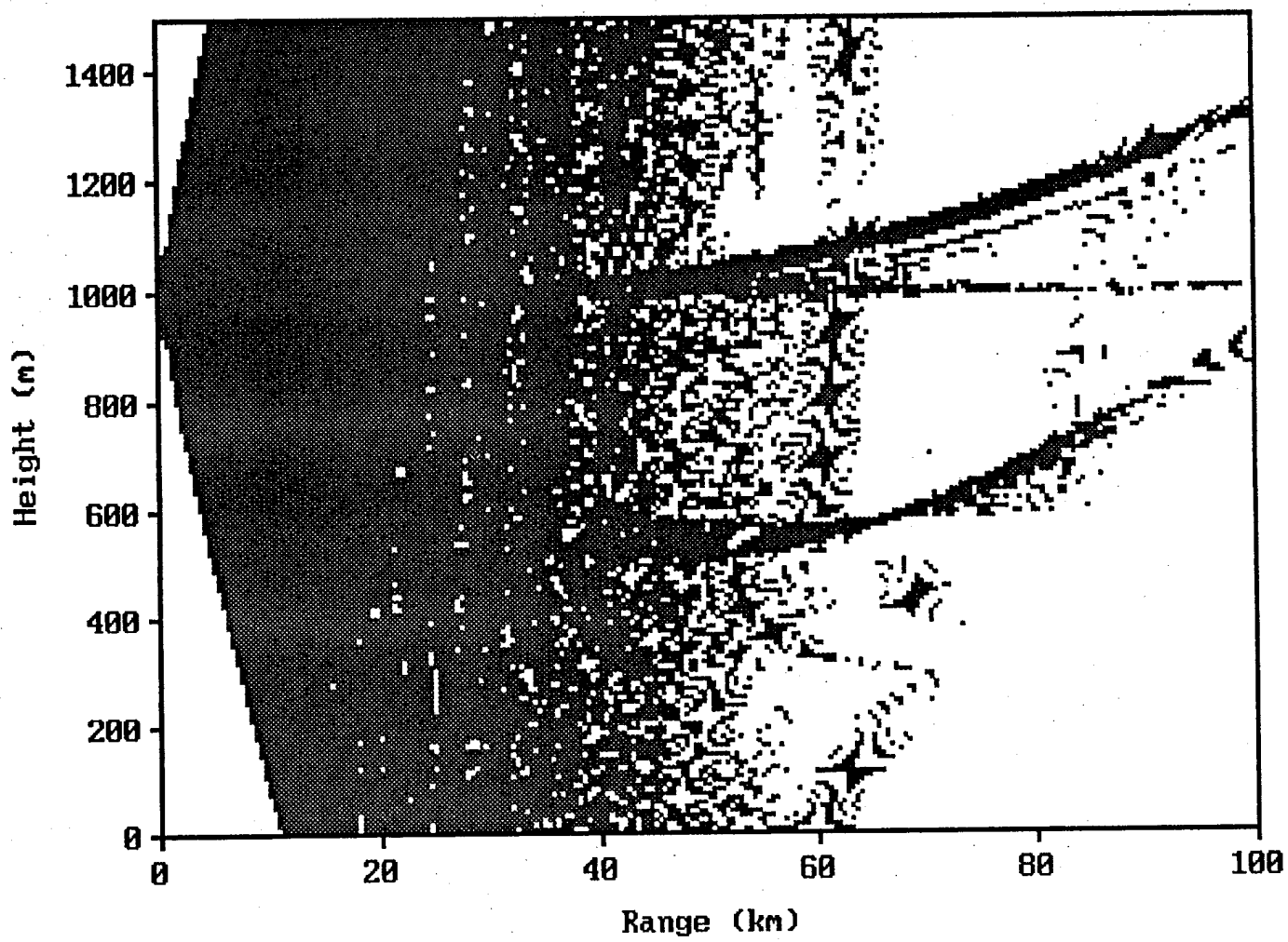

Free space range
50 km

EEMS 1.0 Sample case 6

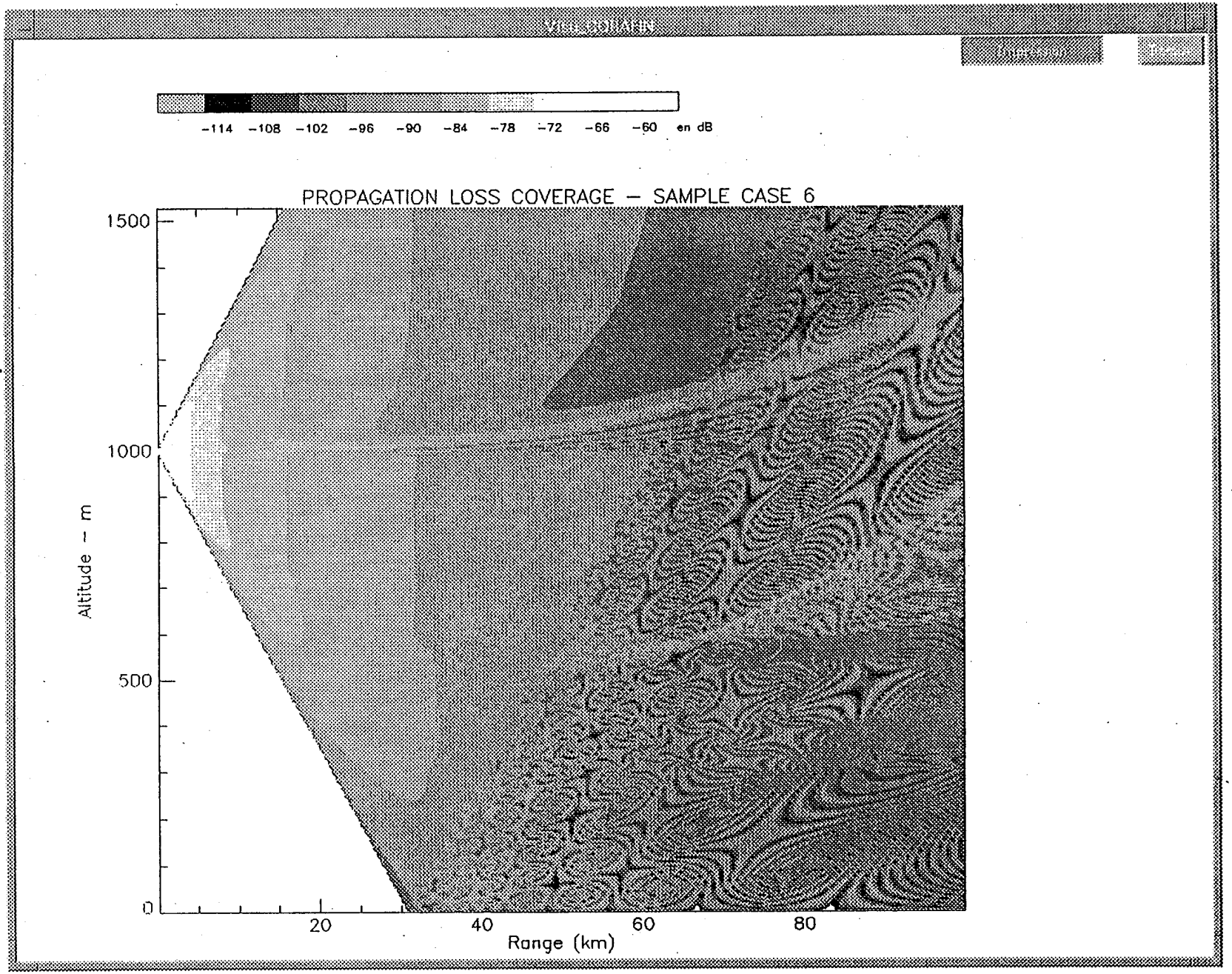
-114 -108 -102 -96 -90 -84 -78 -72 -66 -60 en dB
PROPAGATION LOSS COVERAGE – SAMPLE CASE 6
1500
1000
500
0
Altitude – m
20
40
60
80
Range (km)

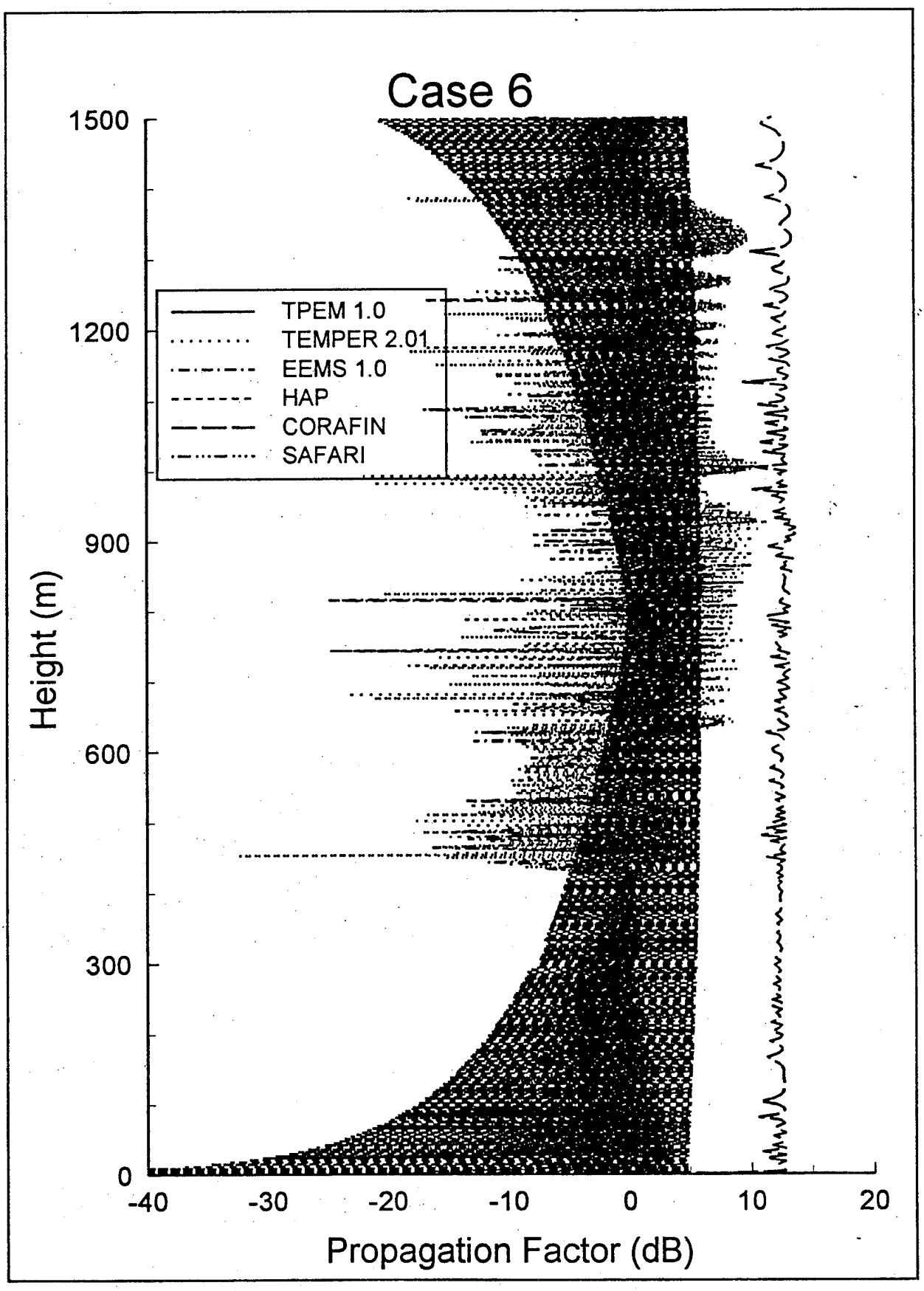
Case 6
1500
1200
900
600
300
0
Height (m)
TPEM 1.0
TEMPER 2.01
EEMS 1.0
HAP
CORAFIN
SAFARI
-40
-30
-20
-10
0
10
20
Propagation Factor (dB)

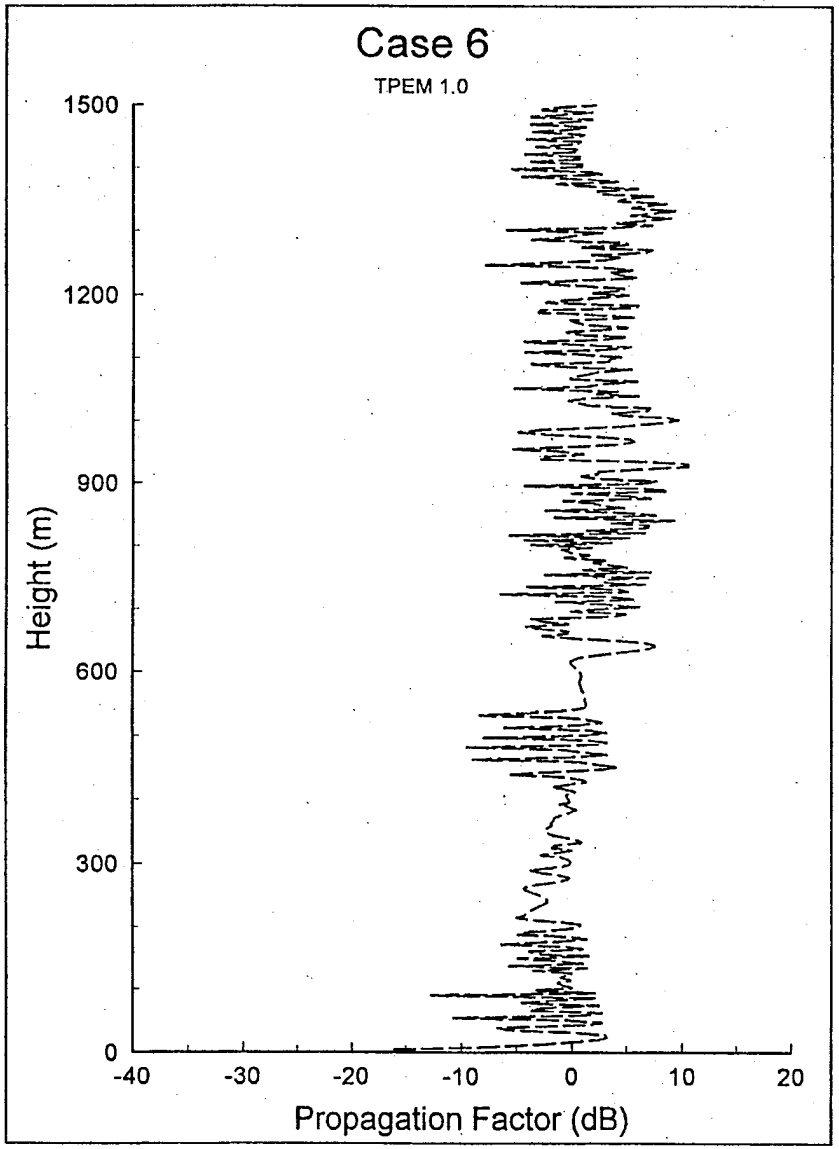
Case 6
TPEM 1.0
1500
1200
900
600
300
0
Height (m)
-40
-30
-20
-10
0
10
20
Propagation Factor (dB)

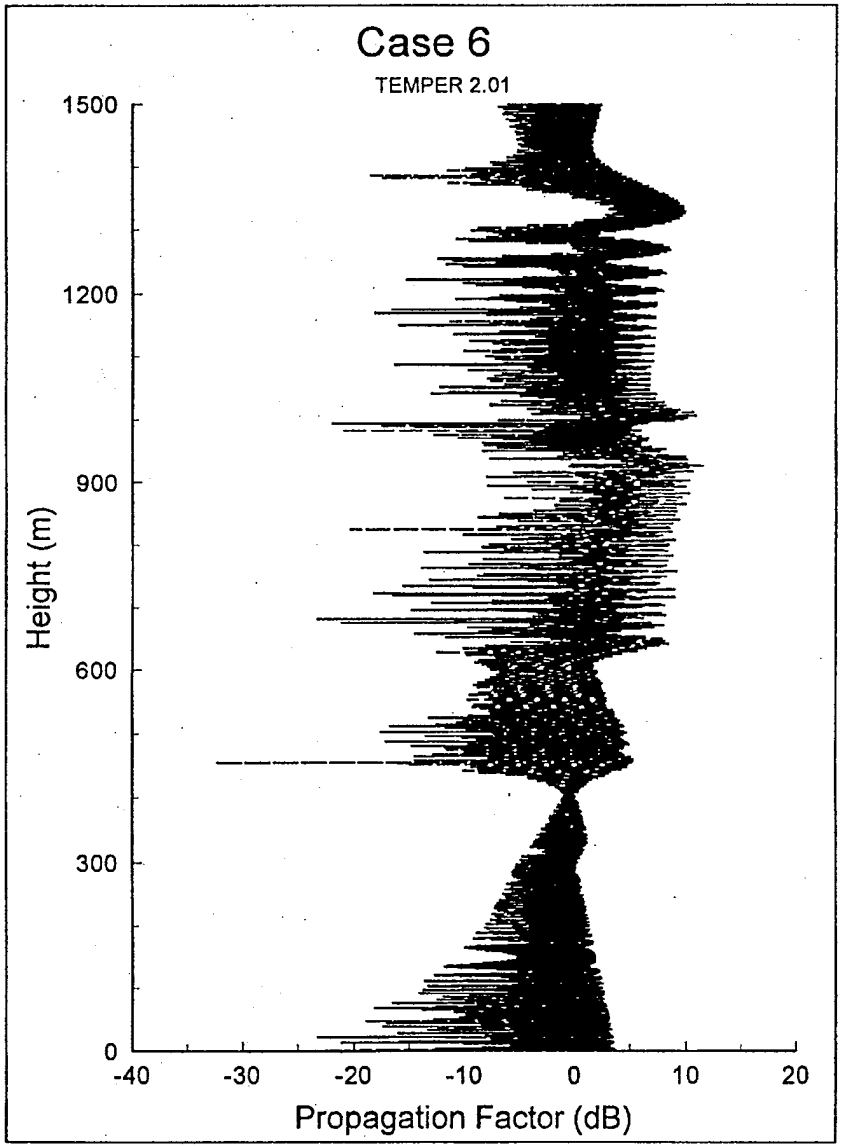
Case 6
TEMPER 2.01
1500
1200
900
600
300
0
Height (m)
-40
-30
-20
-10
0
10
20
Propagation Factor (dB)

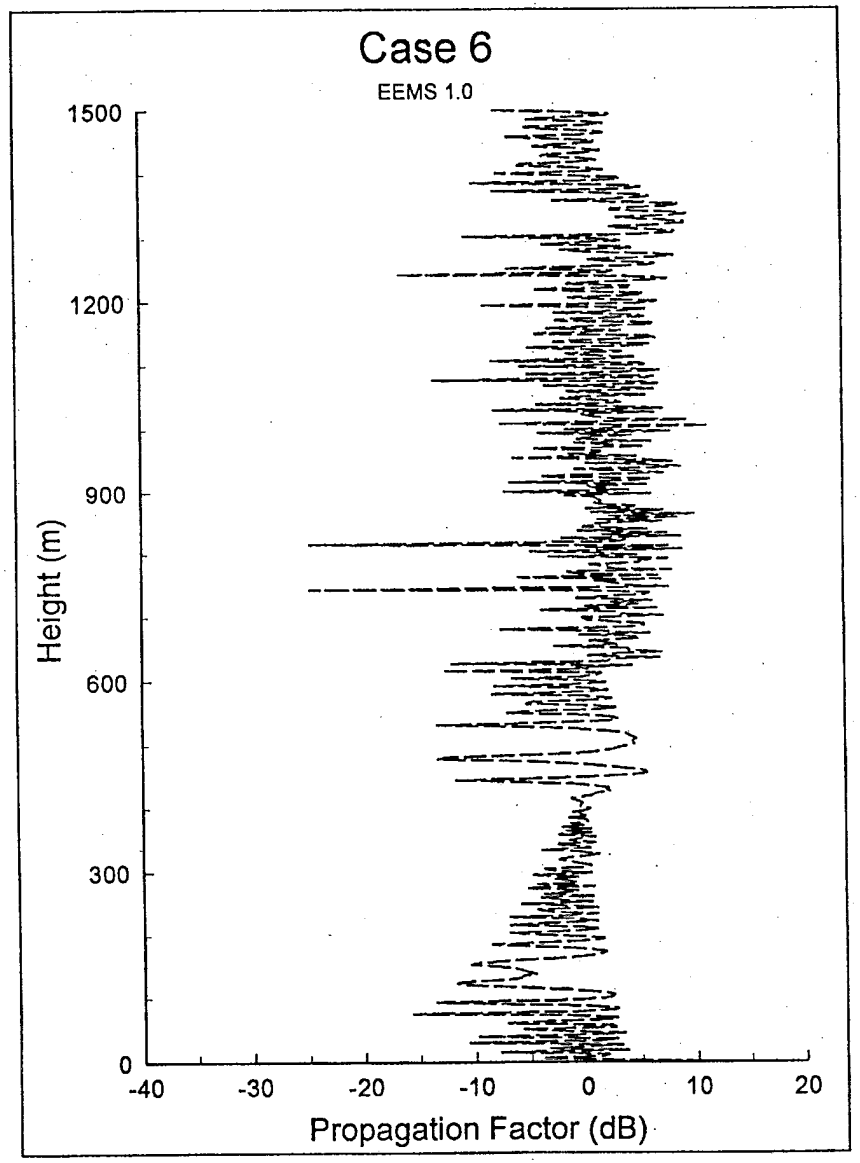
Case 6
EEMS 1.0
1500
1200
900
600
300
0
Height (m)
-40
-30
-20
-10
0
10
20
Propagation Factor (dB)

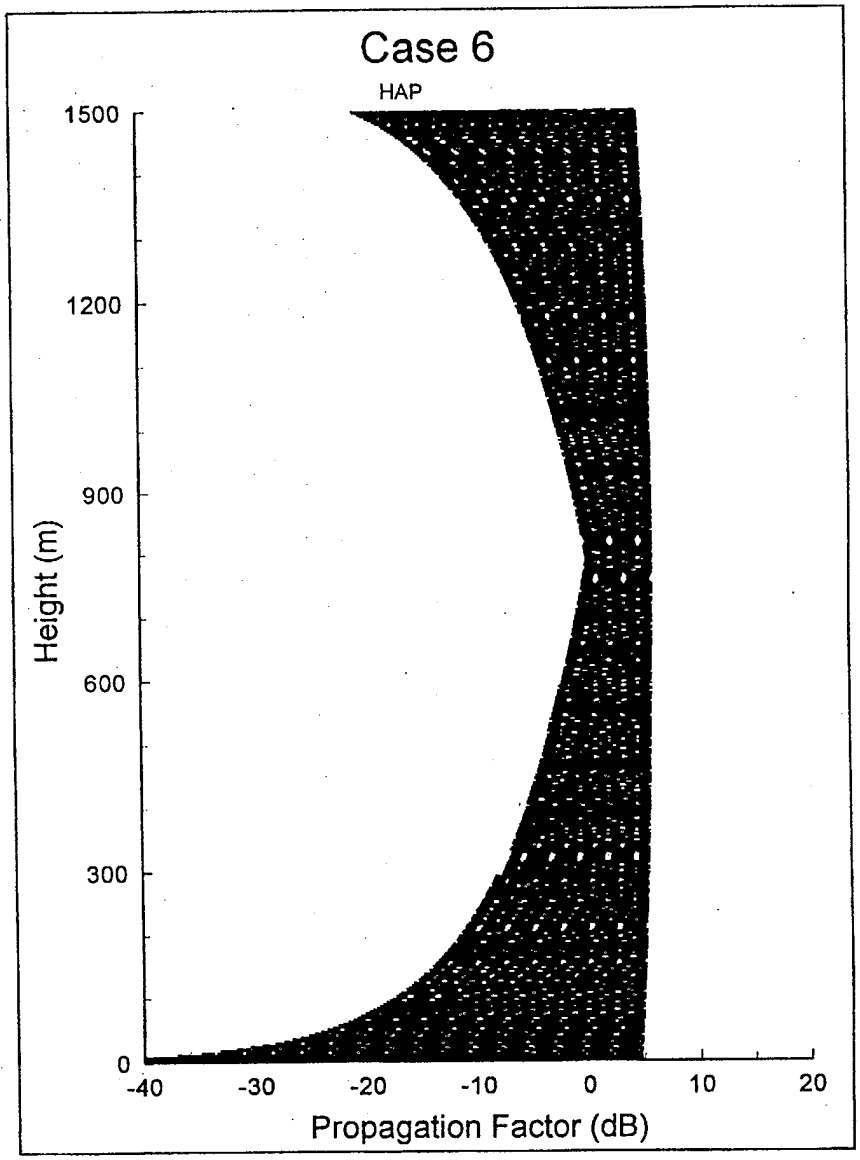
Case 6
HAP
1500
1200
900
600
300
0
Height (m)
-40
-30
-20
-10
0
10
20
Propagation Factor (dB)

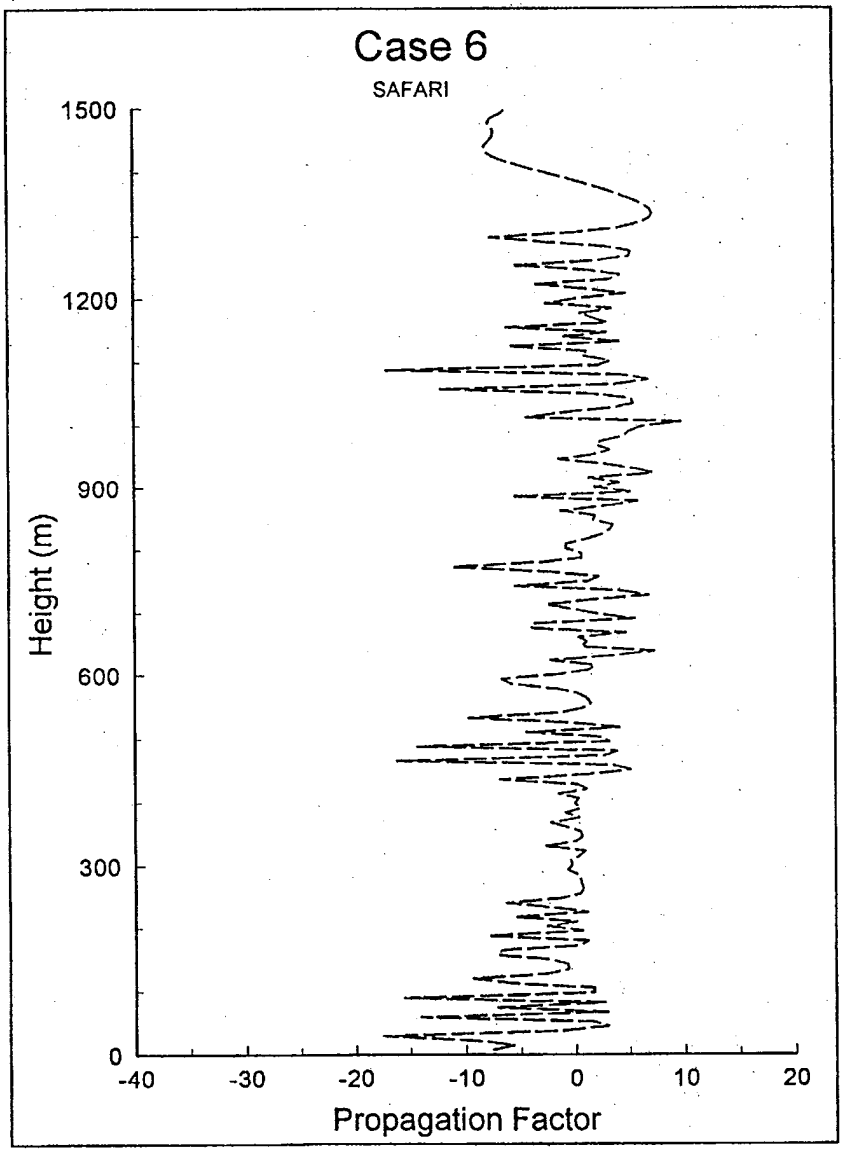
Case 6
SAFARI
Height (m)
1500
1200
900
600
300
0
-40
-30
-20
-10
0
10
20
Propagation Factor

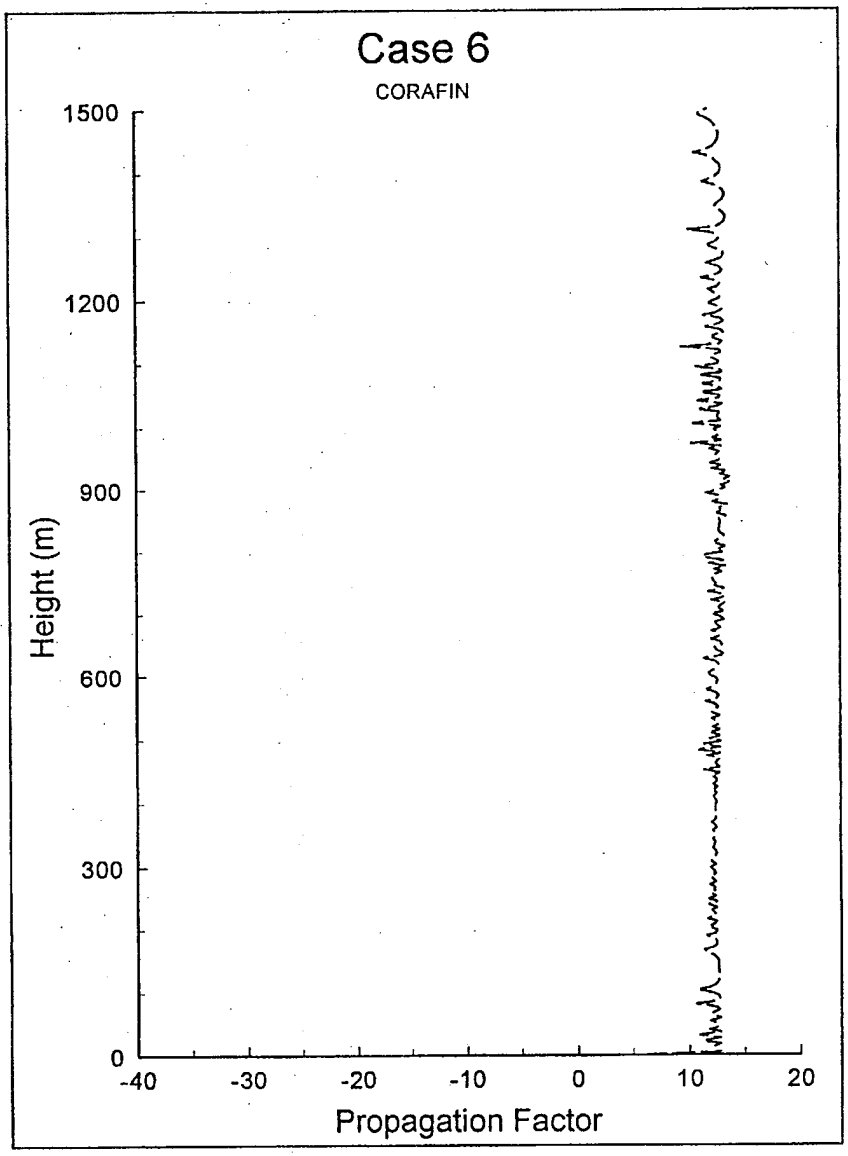
Case 6
CORAFIN
Height (m)
1500
1200
900
600
300
0
-40
-30
-20
-10
0
10
20
Propagation Factor

Sample Case 7.

This case concerns propagation from a moderately elevated source over the terrain path plotted in Figure 6. The terrain elevation data were provided in digital form for the modelers. The refractivity profile is specified in Table 2. The frequency is 10 GHz and the transmitter antenna is 1000 m above sea level. A coverage diagram is desired for receiver heights from the local ground height to 1500 m above sea level for ranges from 0 to 100 km, based on a free space range of 50 km. Propagation factor is required at a range of 100 km for receiver heights from the local ground height to 1500 m above sea level.

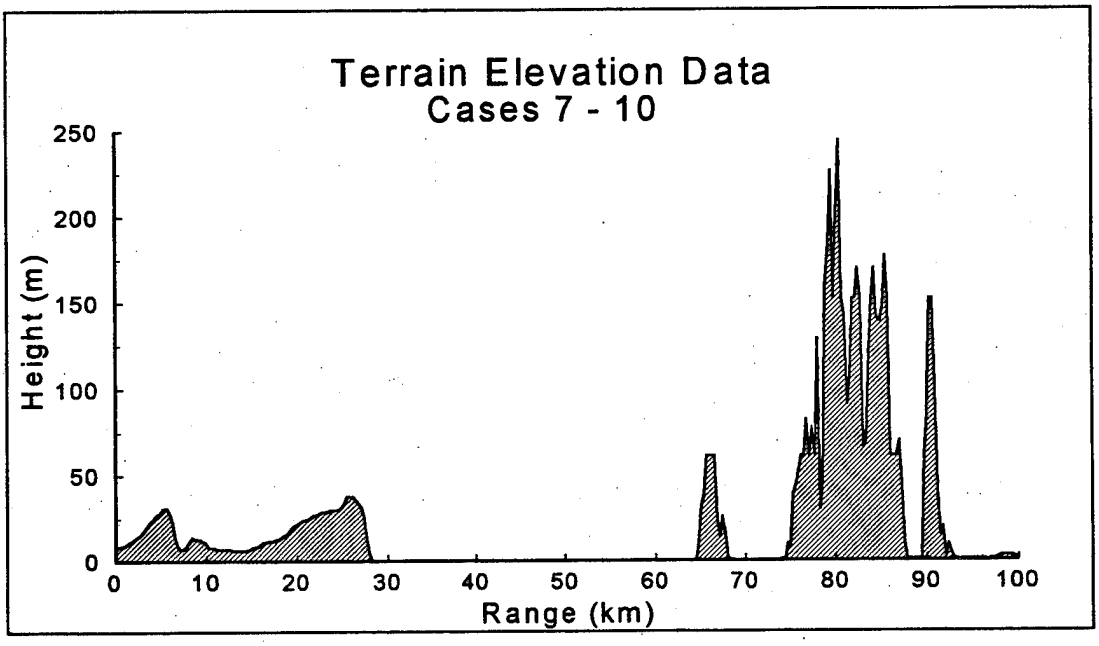

Figure 6. Plot of terrain elevation data for Sample Cases 7 through 10.

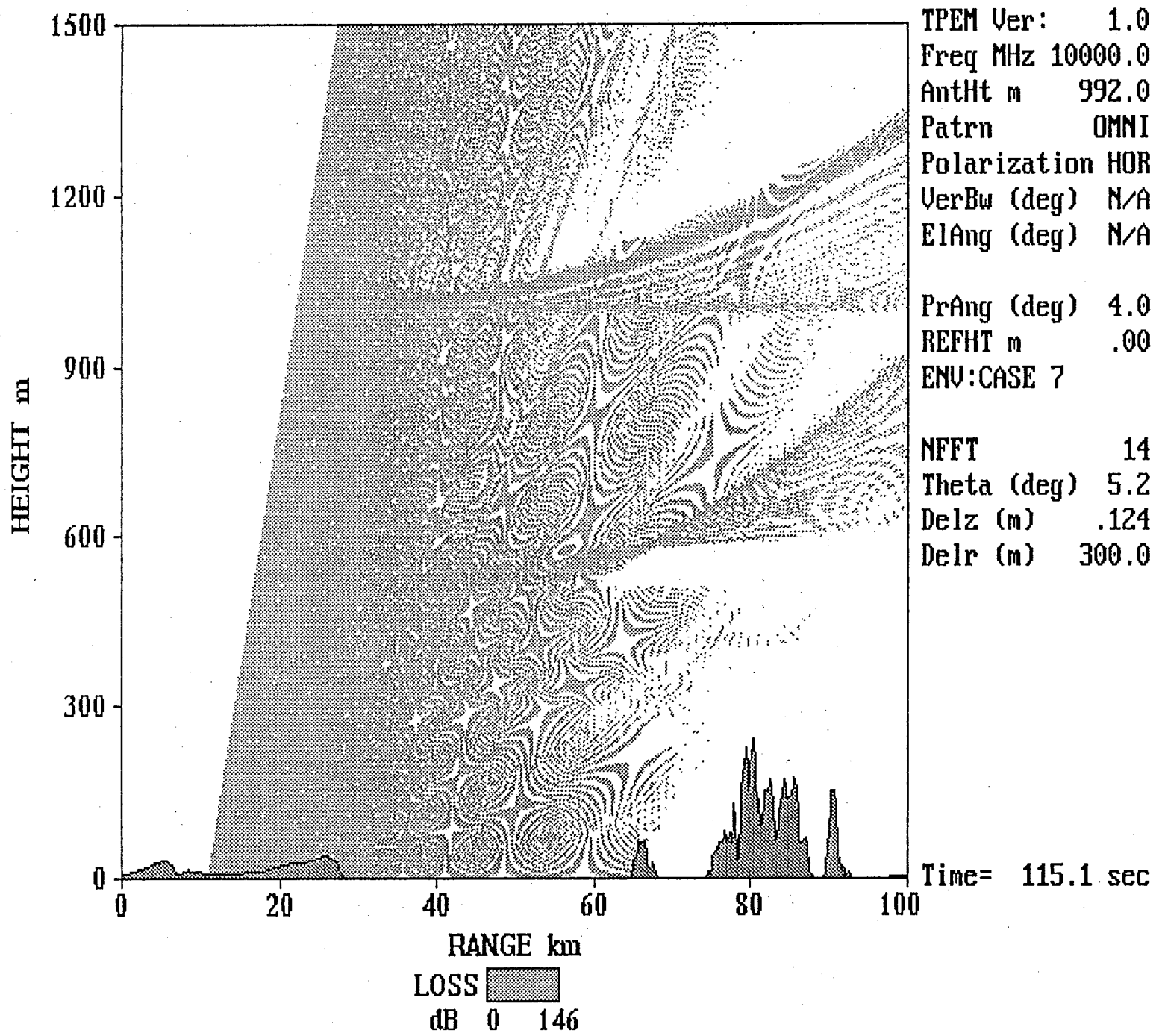
1500
1200
900
600
300
0
HEIGHT m
0
20
40
60
80
100
RANGE km
LOSS
dB 0 146
TPEM Ver: 1.0
Freq MHz 10000.0
AntHt m 992.0
Patrn OMNI
Polarization HOR
VerBw (deg) N/A
ElAng (deg) N/A
PrAng (deg) 4.0
REFHT m .00
ENV:CASE 7
NFFT 14
Theta (deg) 5.2
Delz (m) .124
Delr (m) 300.0
Time= 115.1 sec

CASE #7, TEMPER VERSION 2.01

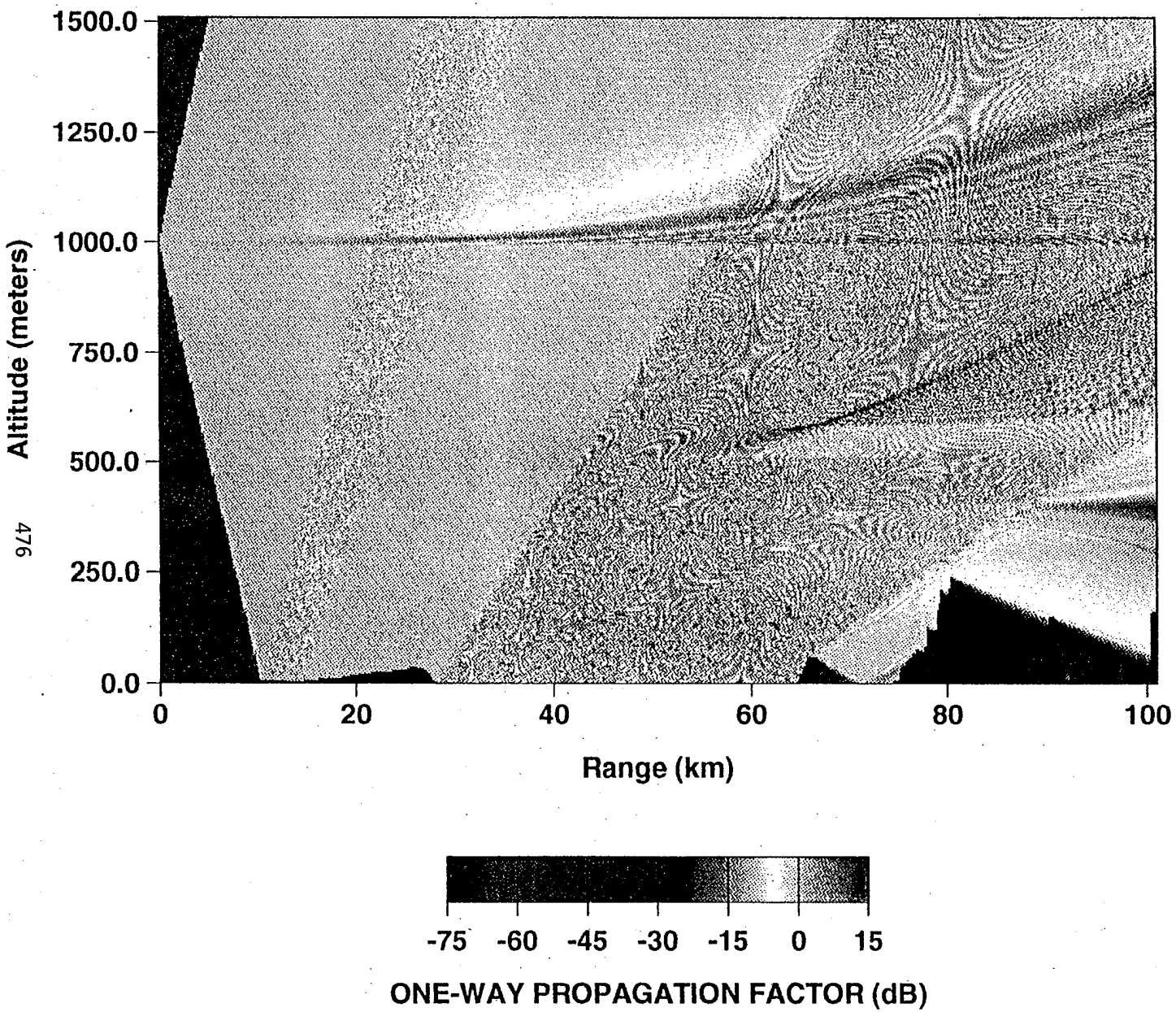

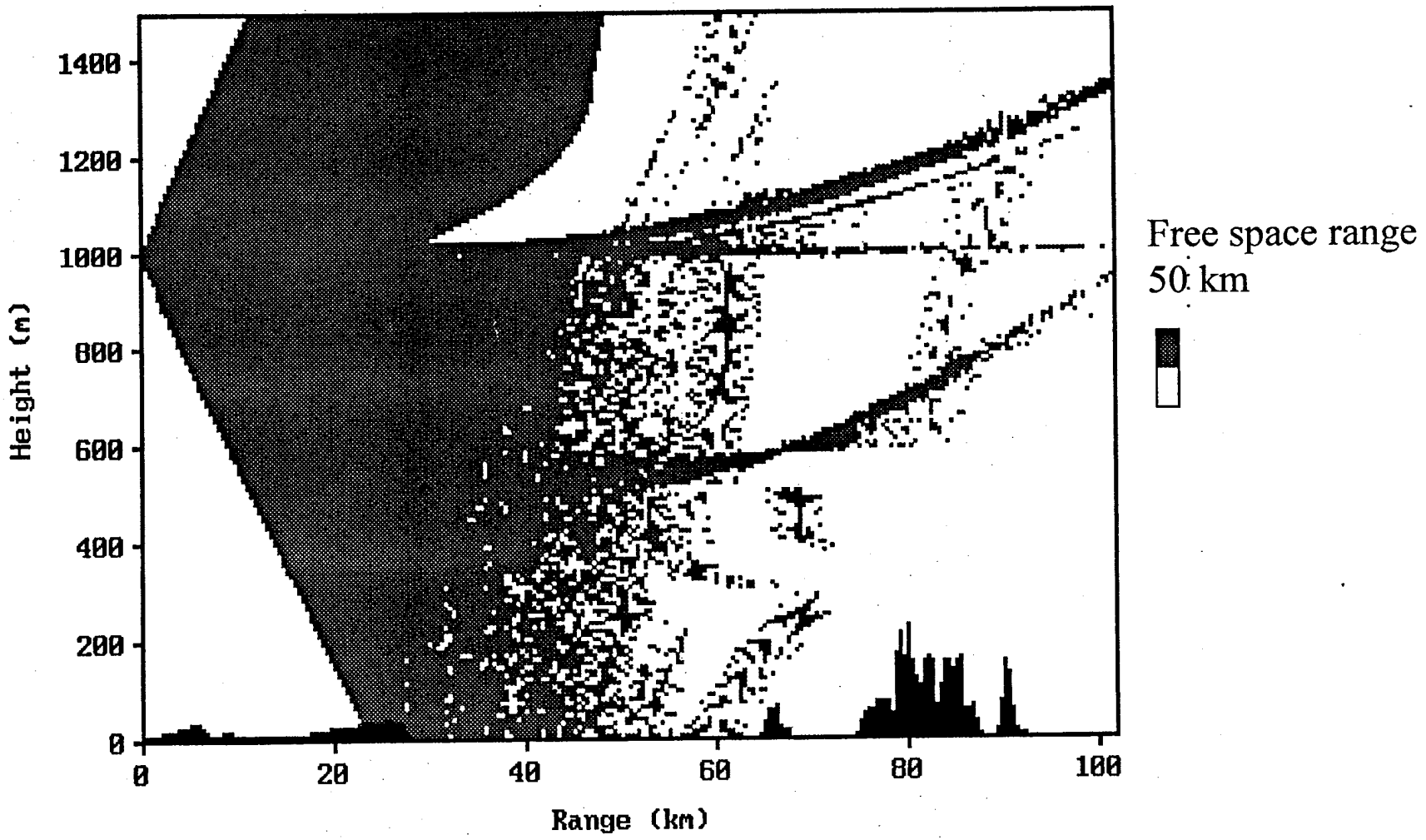

EEMS 1.0 Sample case 7

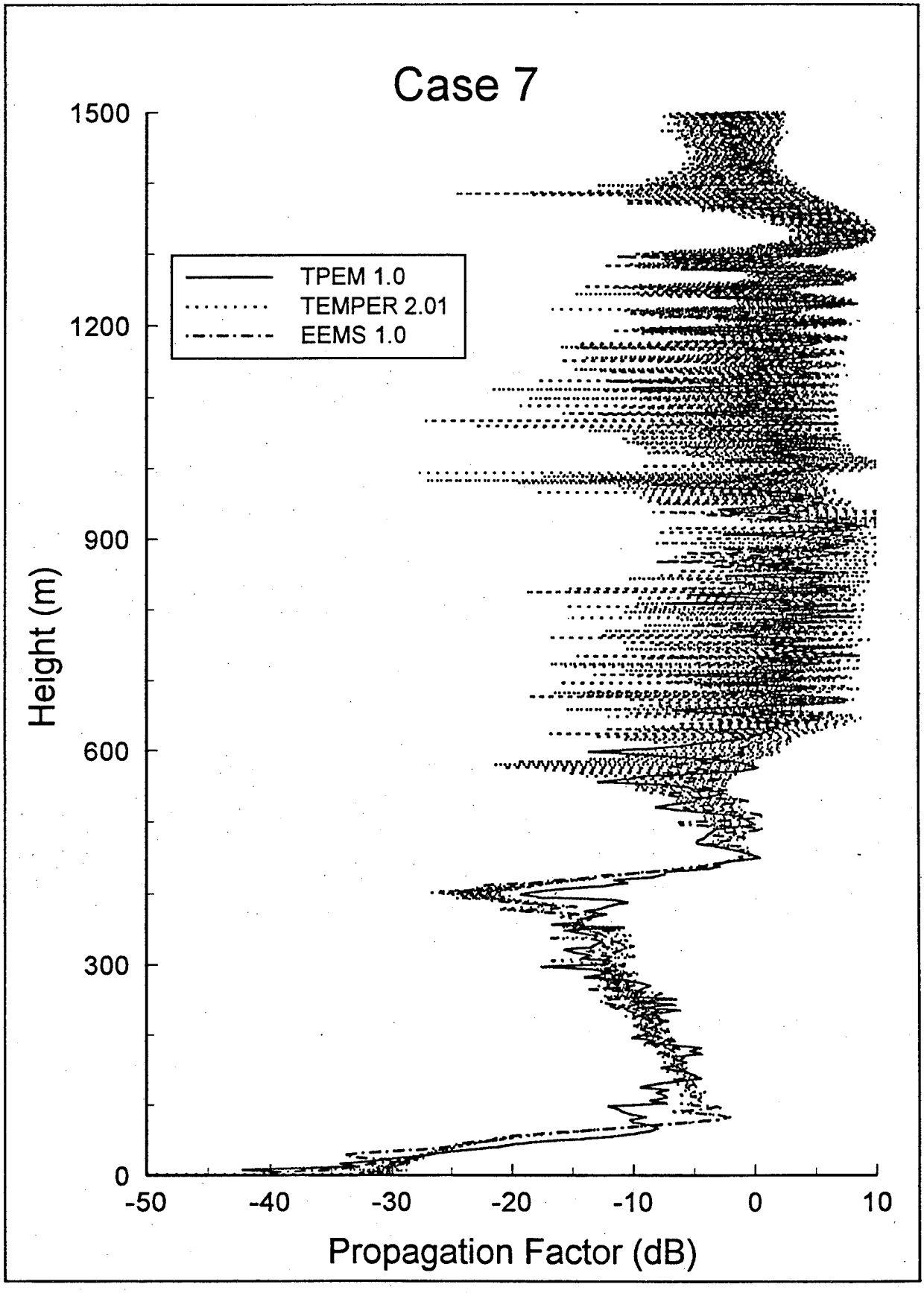
Case 7
1500
1200
900
600
300
0
Height (m)
TPEM 1.0
TEMPER 2.01
EEMS 1.0
-50
-40
-30
-20
-10
0
10
Propagation Factor (dB)

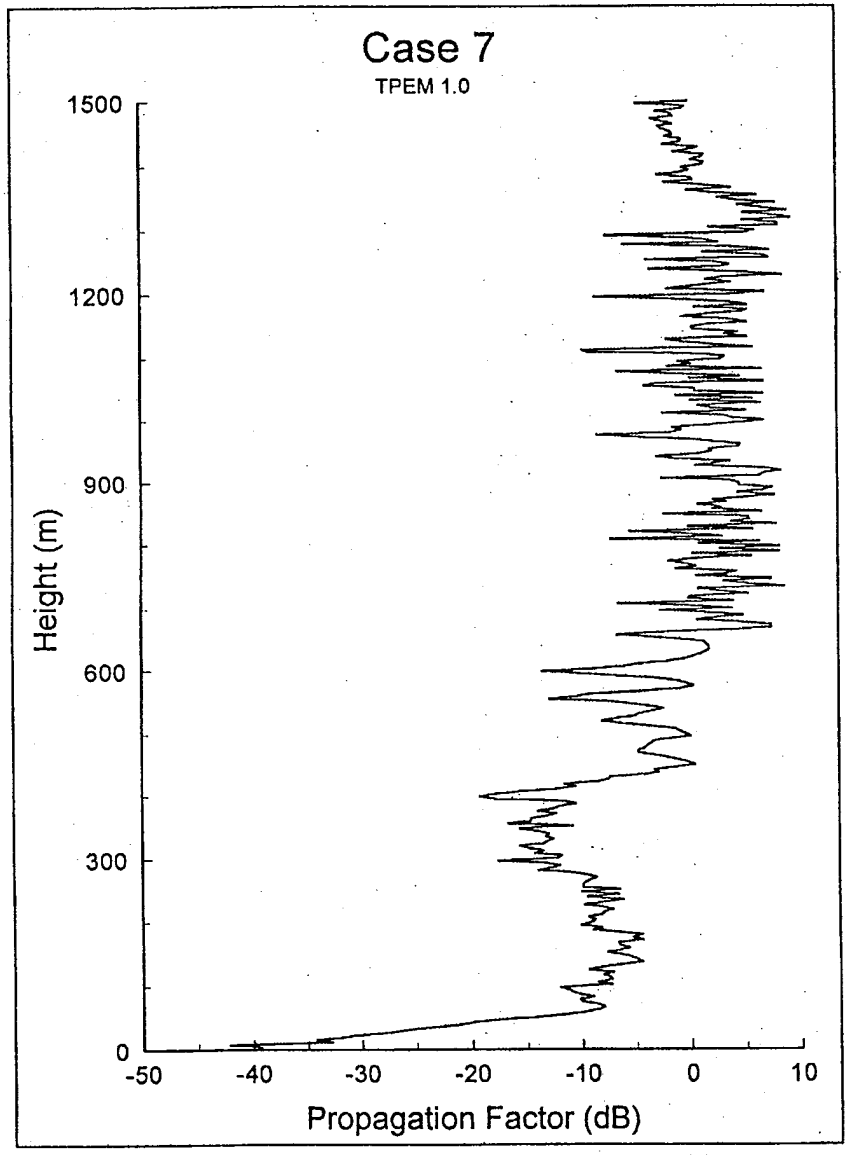
Case 7
TPEM 1.0
1500
1200
900
600
300
0
Height (m)
-50
-40
-30
-20
-10
0
10
Propagation Factor (dB)

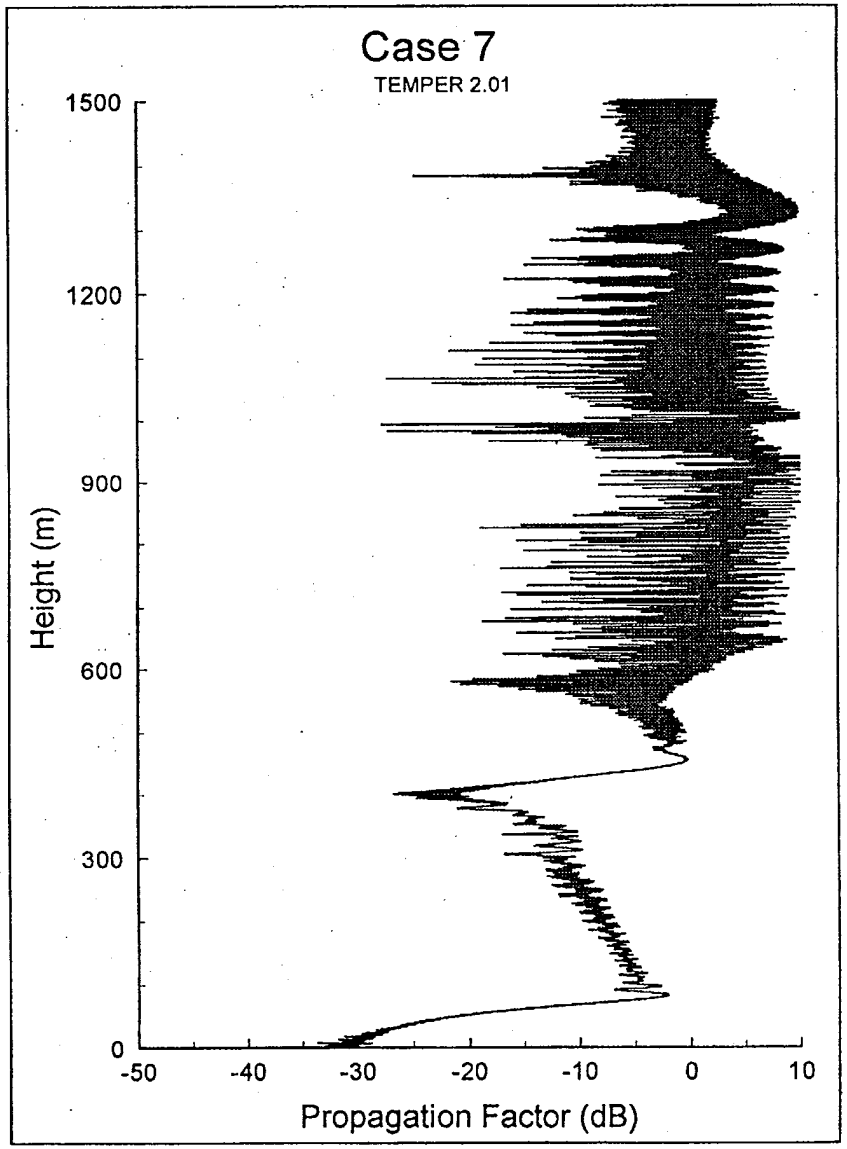
Case 7
TEMPER 2.01
1500
1200
900
600
300
0
Height (m)
-50
-40
-30
-20
-10
0
10
Propagation Factor (dB)

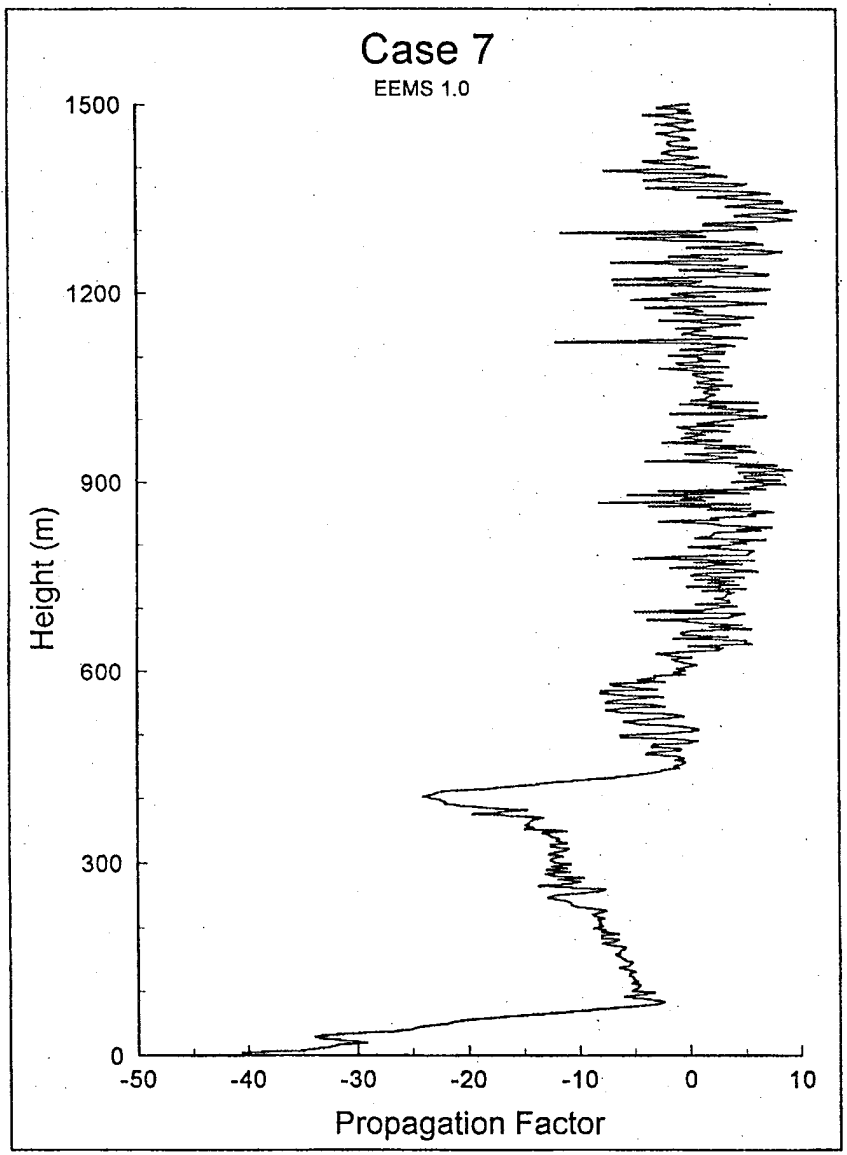
Case 7
EEMS 1.0
1500
1200
900
600
300
0
Height (m)
-50
-40
-30
-20
-10
0
10
Propagation Factor

Sample Case 8.

This case considers propagation over terrain assuming a standard atmosphere refractivity profile. The frequency is 3 GHz and the transmitter antenna is 10 m above the local terrain at Long Beach. The standard atmosphere refractivity profile is specified in Table 7. A coverage diagram is desired for receiver heights from the local ground height to 500 m above sea level for ranges from 0 to 100 km, based on a free space range of 100 km. Propagation factor is required at 100 km range for receiver heights from the local ground height to 500 m above sea level.

Height (m)	Refractivity (M units)
0	340
1000	458

Table 7. Standard atmosphere modified refractivity profile.

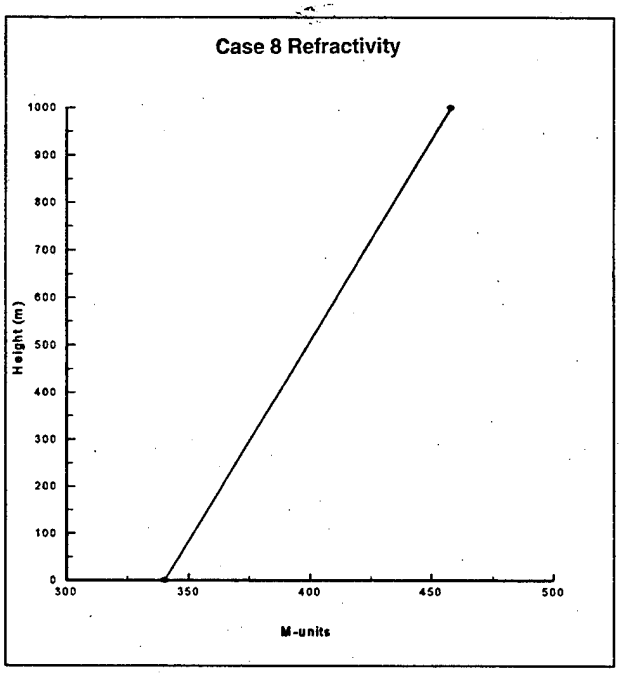

Figure 7. Plot of data of Table 7.

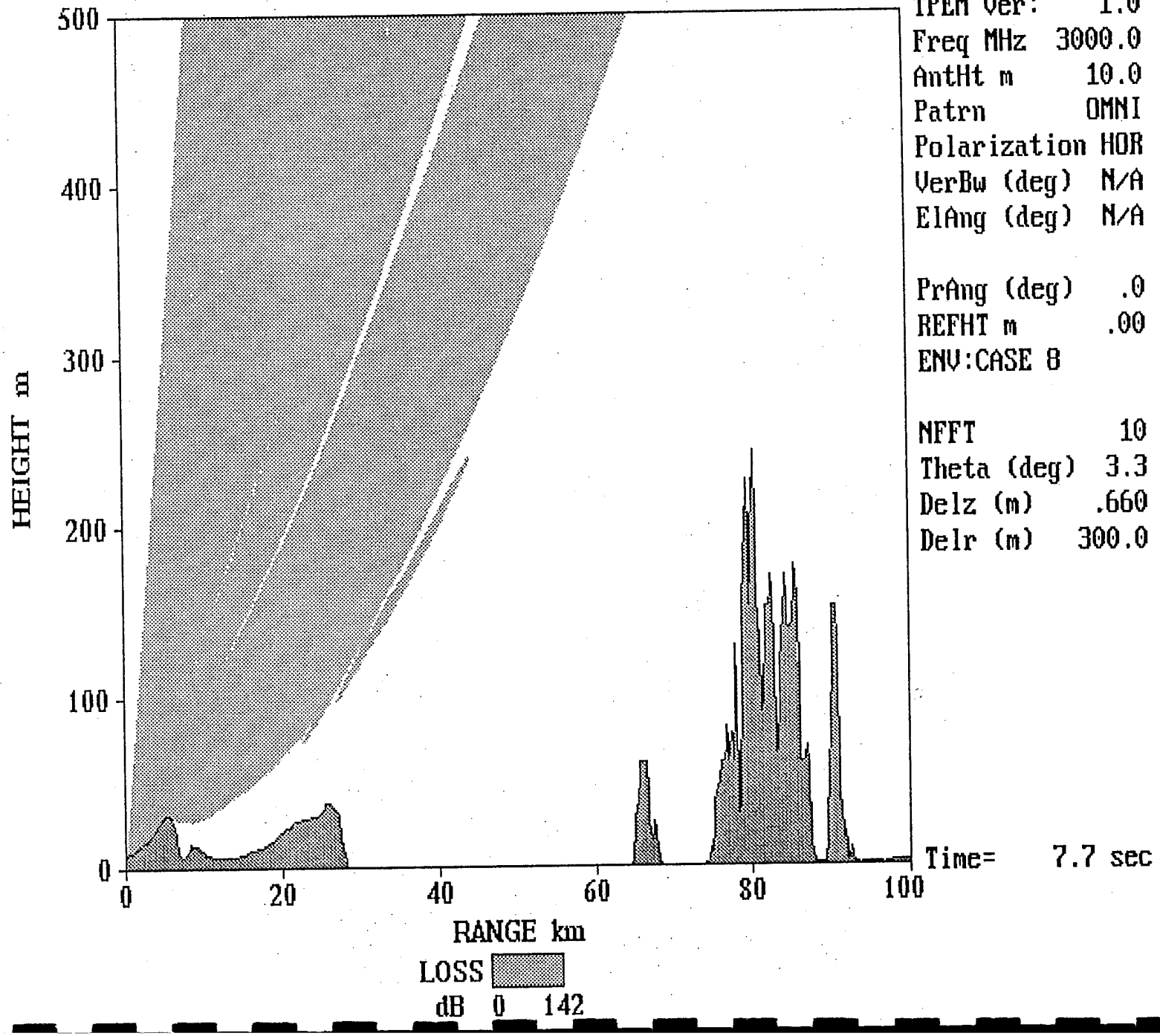
500
400
300
200
100
0
HEIGHT m
0
20
40
60
80
100
RANGE km
LOSS
dB 0 142
TPEM Ver: 1.0
Freq MHz 3000.0
AntHt m 10.0
Patrn OMNI
Polarization HOR
VerBw (deg) N/A
ElAng (deg) N/A
PrAng (deg) .0
REFHT m .00
ENV:CASE 8
NFFT 10
Theta (deg) 3.3
Delz (m) .660
Delr (m) 300.0
Time= 7.7 sec

Case #8, TEMPER VERSION 2.01

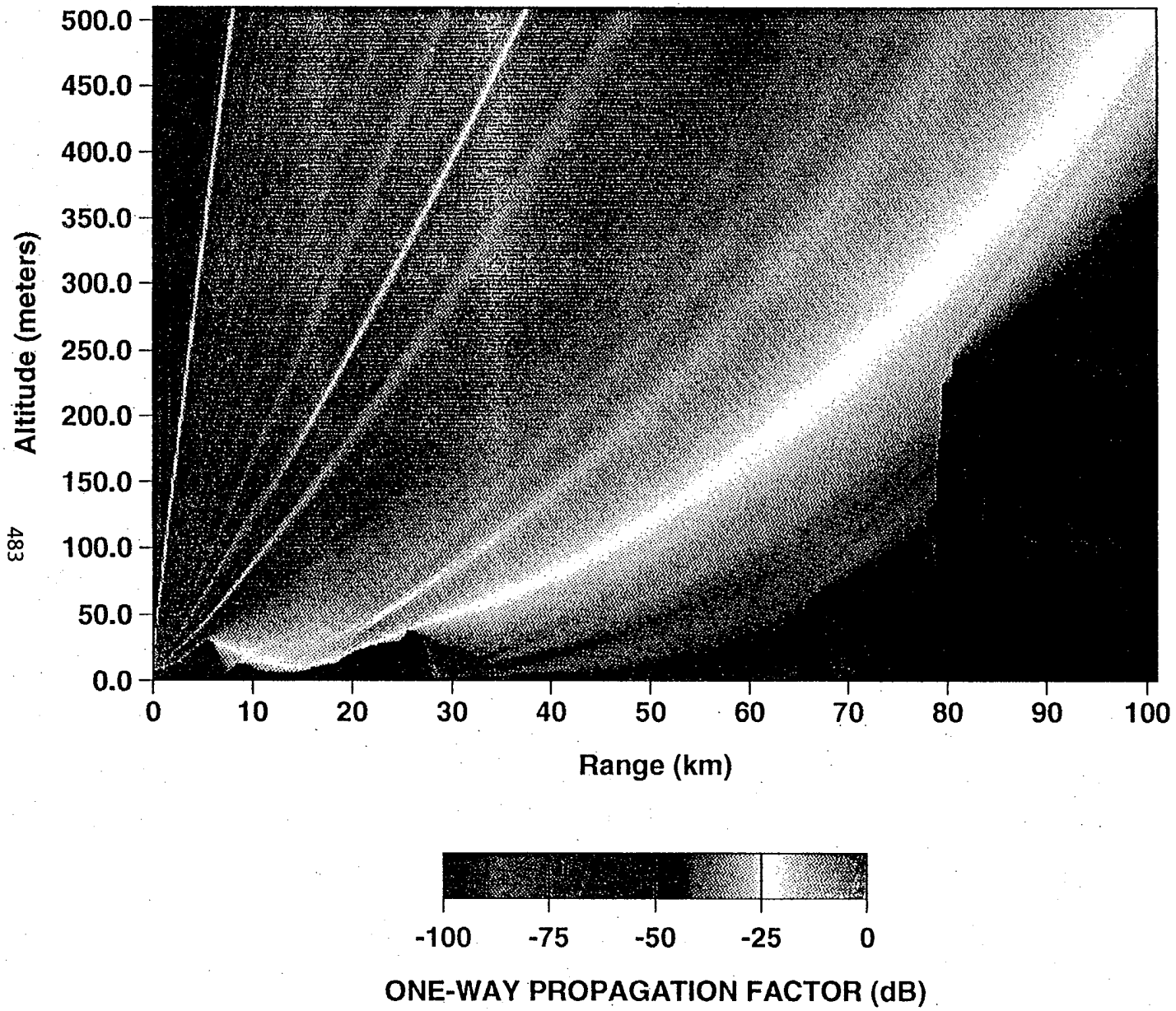

SAMPLE CASE 8 – model : DIF–CERT

freq=3 GHz, ht=10m, standard atmosphere, smooth sea surface

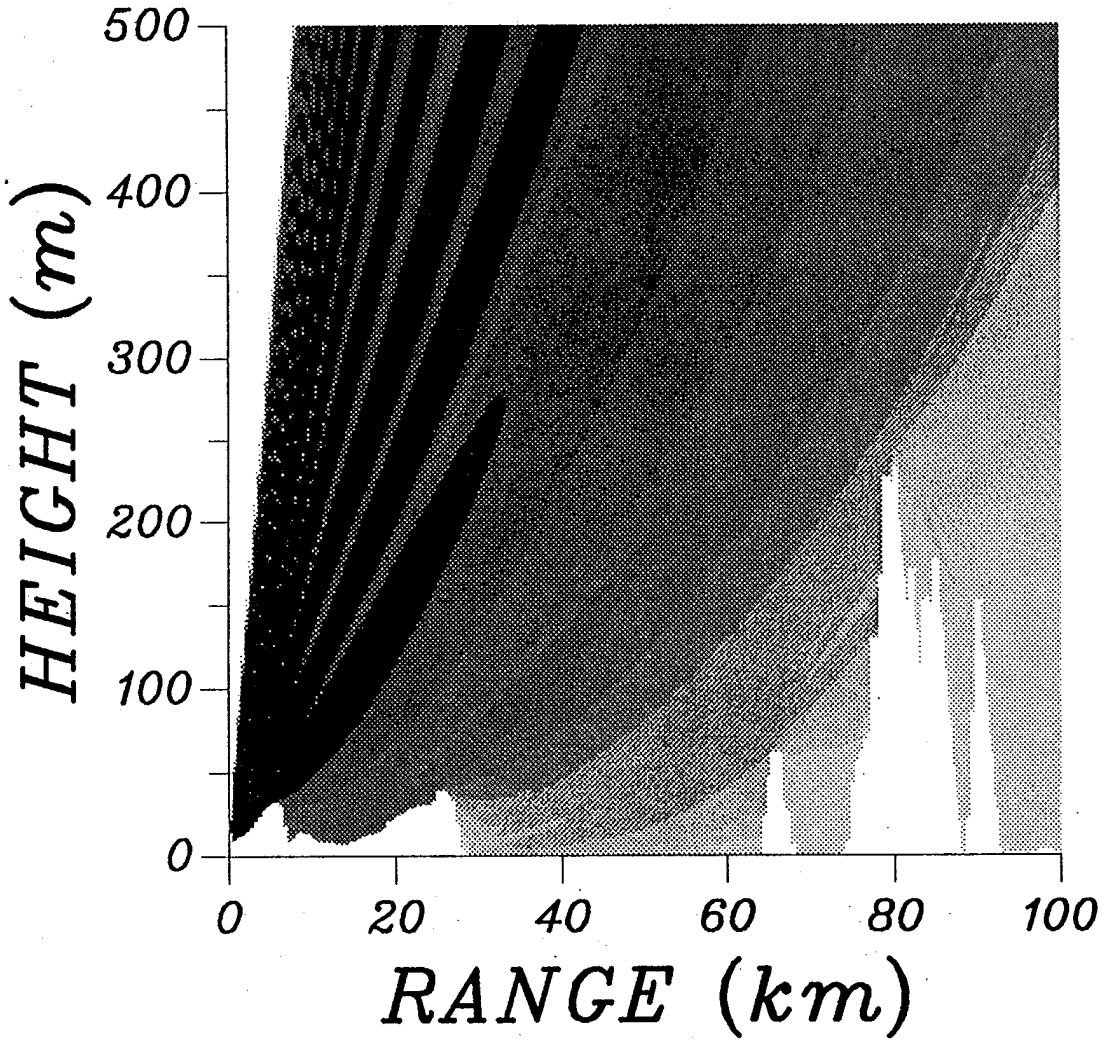

PROPAGATION LOSS
(dB)

ABOVE	300
200 –	300
190 –	200
180 –	190
170 –	180
160 –	170
150 –	160
140 –	150
130 –	140
BELOW	130

CERT/DERMO

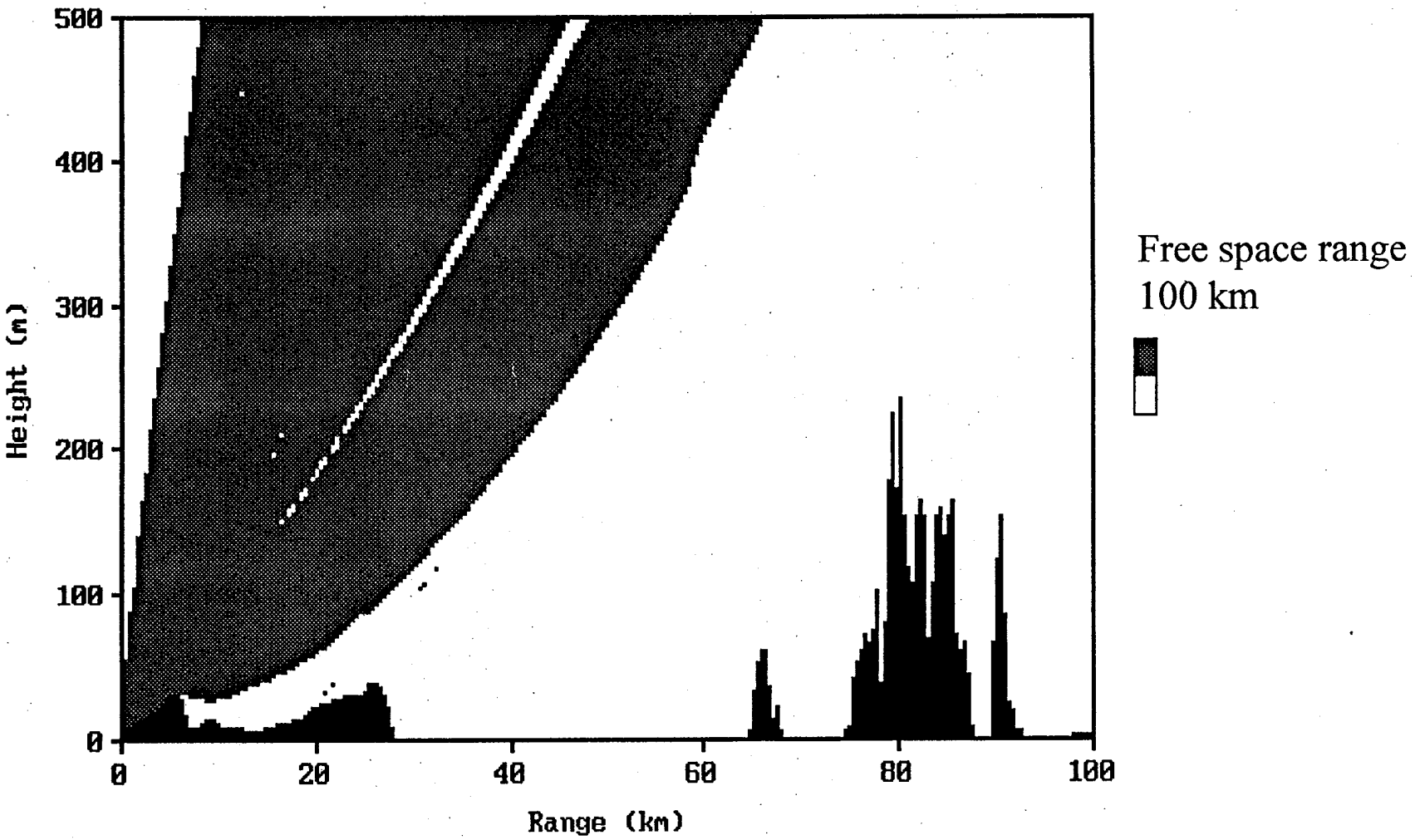

EEMS 1.0 Sample case 8

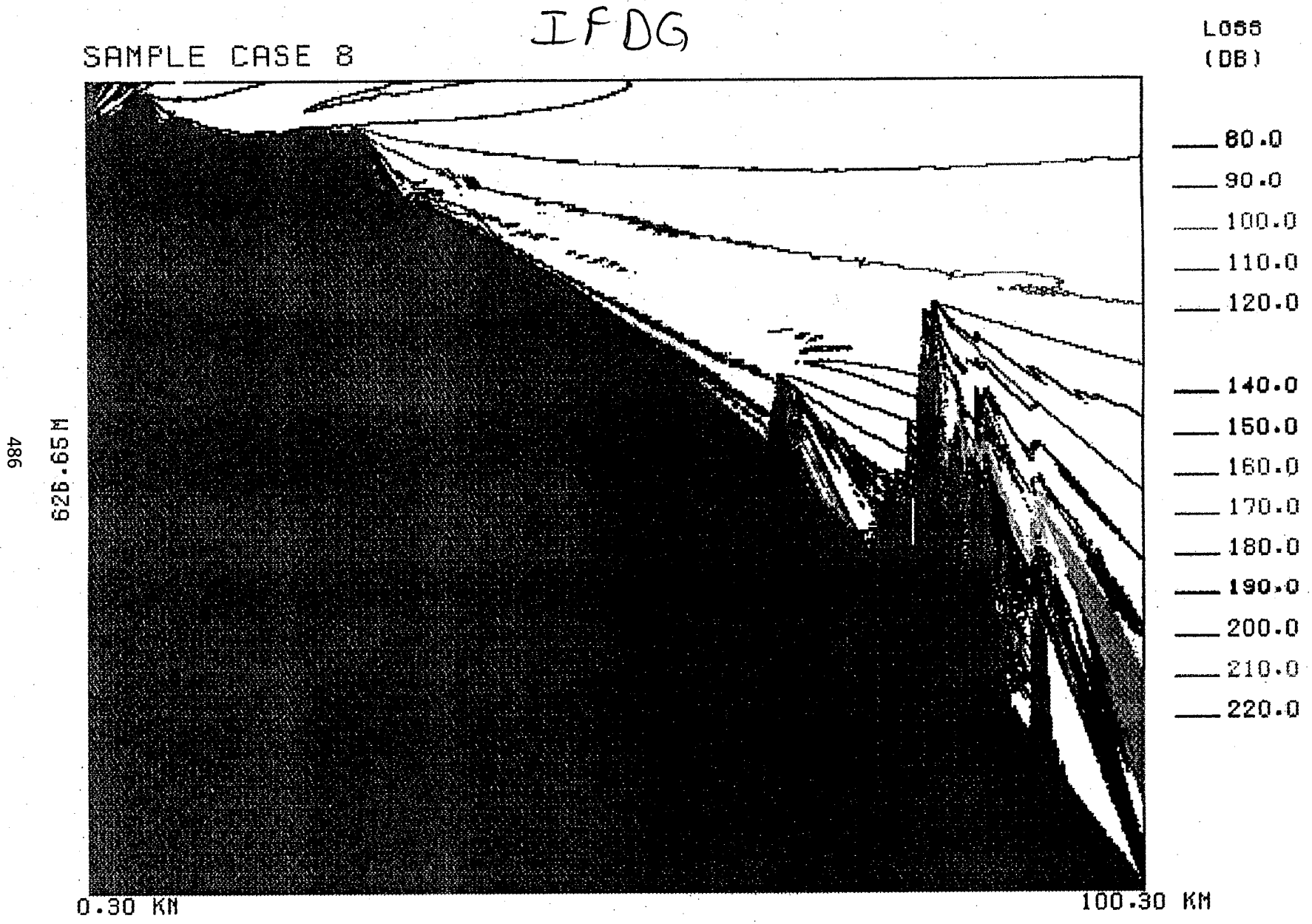
IfDG
SAMPLE CASE 8
LOSS
(DB)
80.0
90.0
100.0
110.0
120.0
140.0
150.0
160.0
170.0
180.0
190.0
200.0
210.0
220.0
626.65 M
486
0.30 KM
100.30 KM

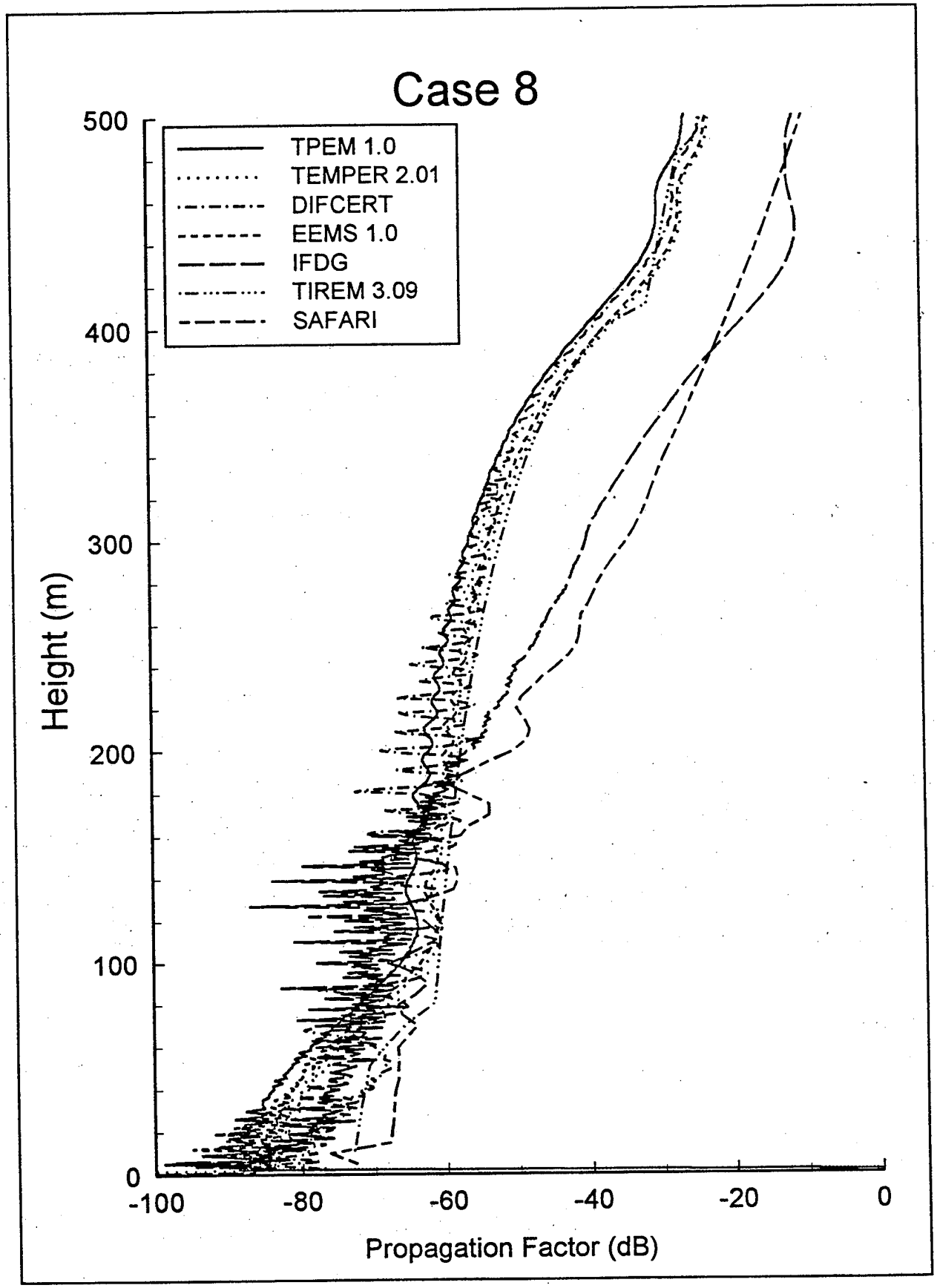
Case 8
TPEM 1.0
TEMPER 2.01
DIFCERT
EEMS 1.0
IFDG
TIREM 3.09
SAFARI
500
400
300
200
100
0
Height (m)
-100
-80
-60
-40
-20
0
Propagation Factor (dB)

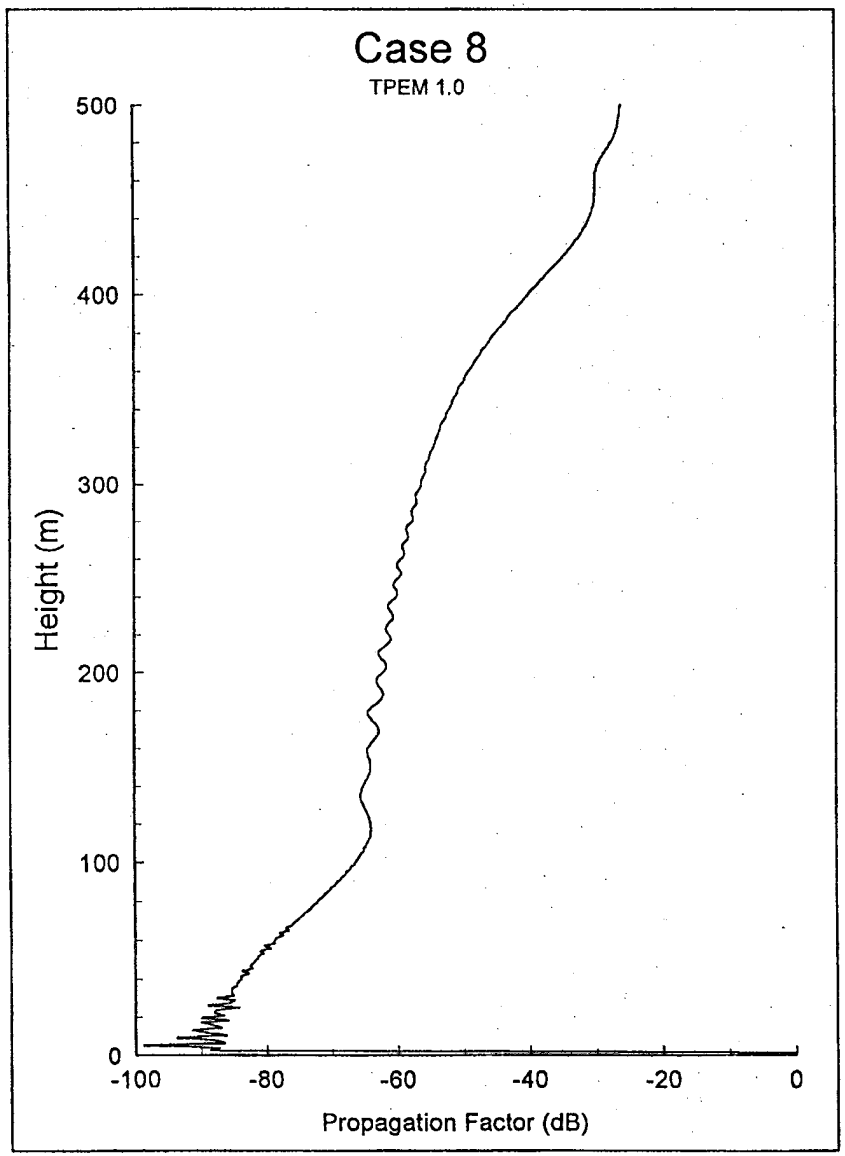
Case 8
TPEM 1.0
Height (m)
500
400
300
200
100
0
-100
-80
-60
-40
-20
0
Propagation Factor (dB)

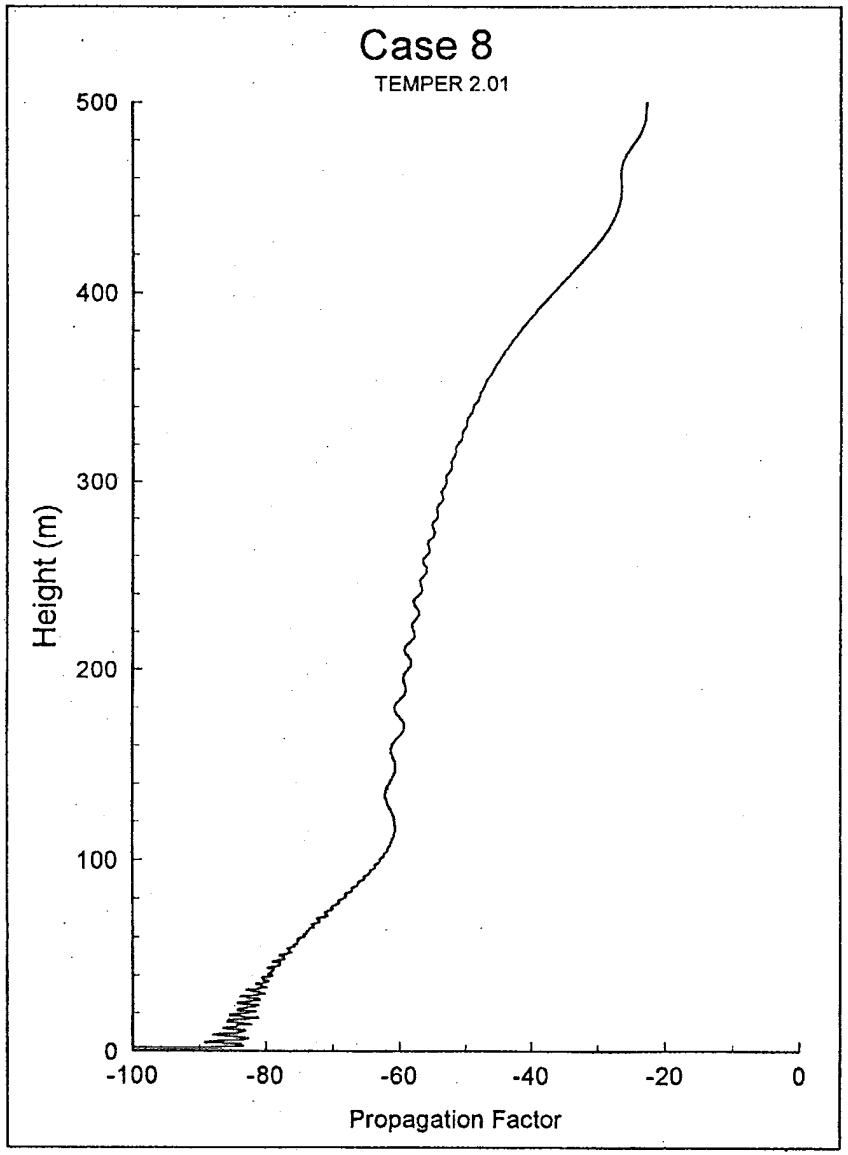
Case 8
TEMPER 2.01
Height (m)
500
400
300
200
100
0
-100
-80
-60
-40
-20
0
Propagation Factor

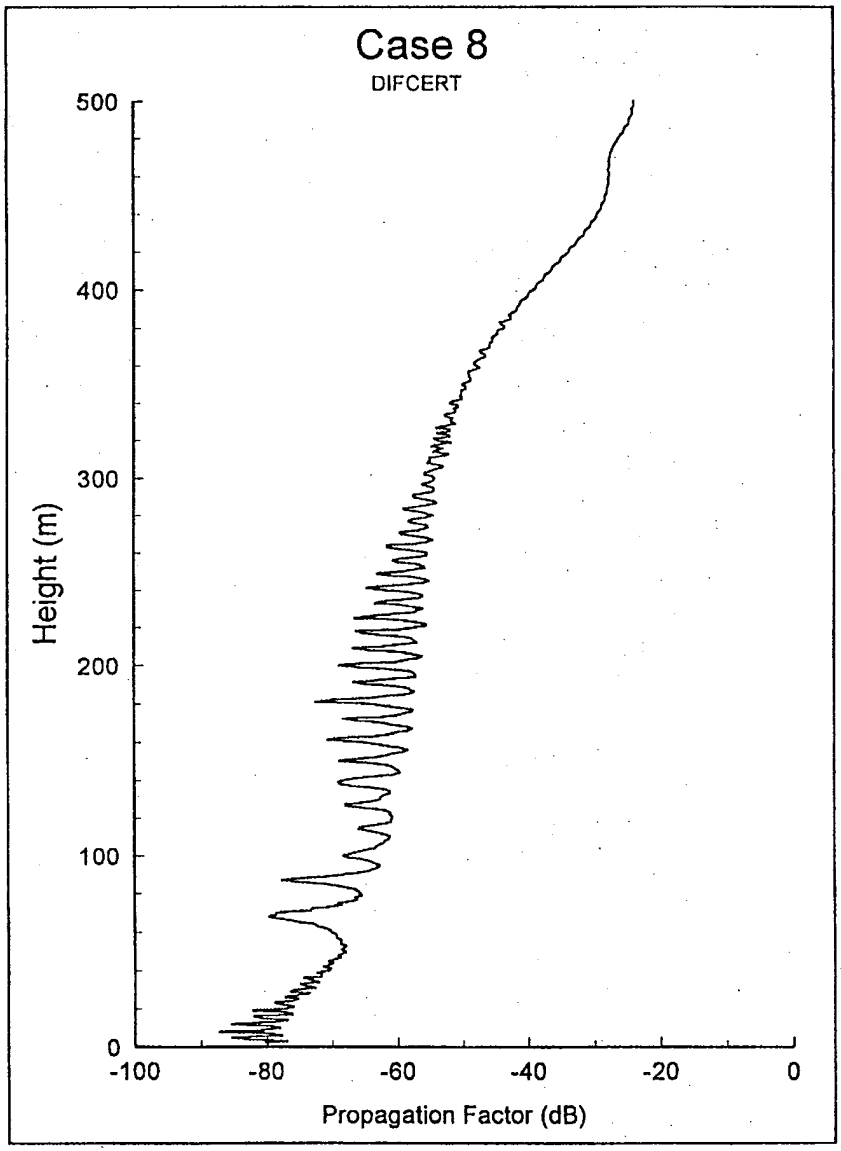
Case 8
DIFCERT
Height (m)
500
400
300
200
100
0
-100
-80
-60
-40
-20
0
Propagation Factor (dB)

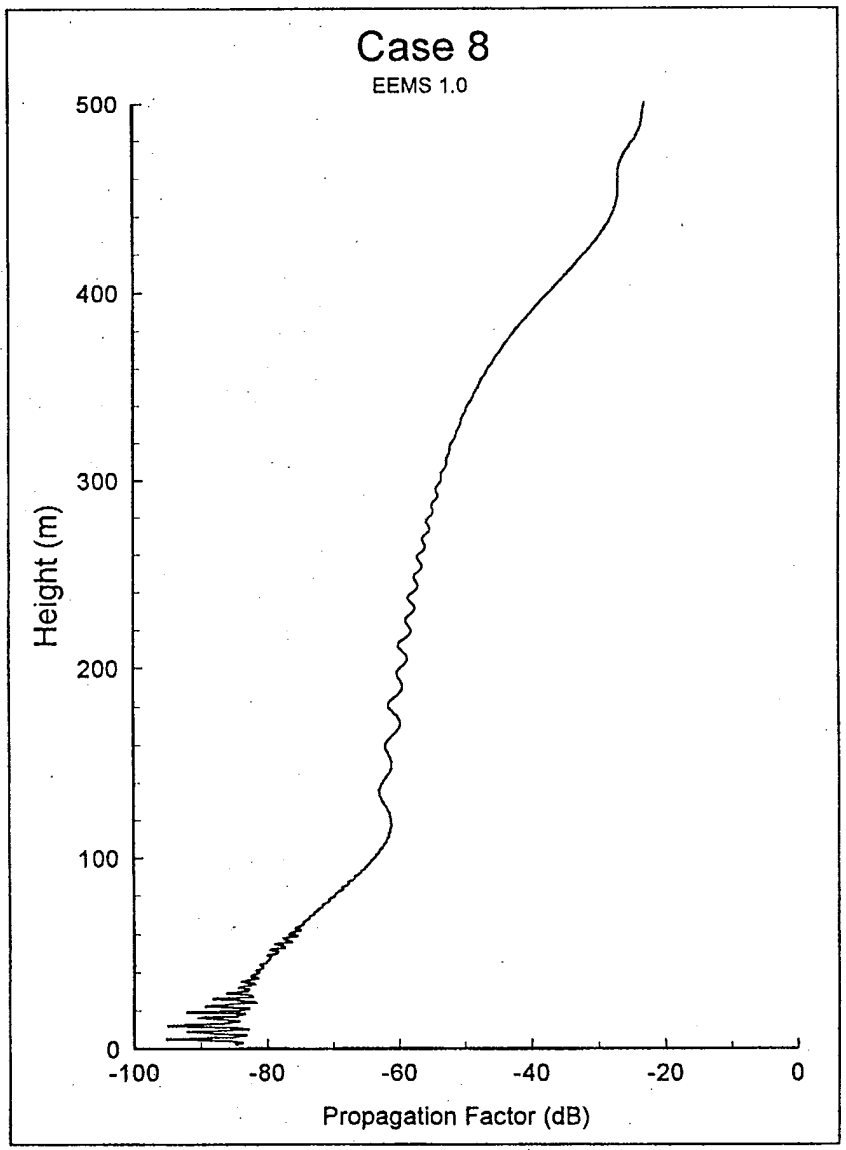
Case 8
EEMS 1.0
Height (m)
500
400
300
200
100
0
-100
-80
-60
-40
-20
0
Propagation Factor (dB)

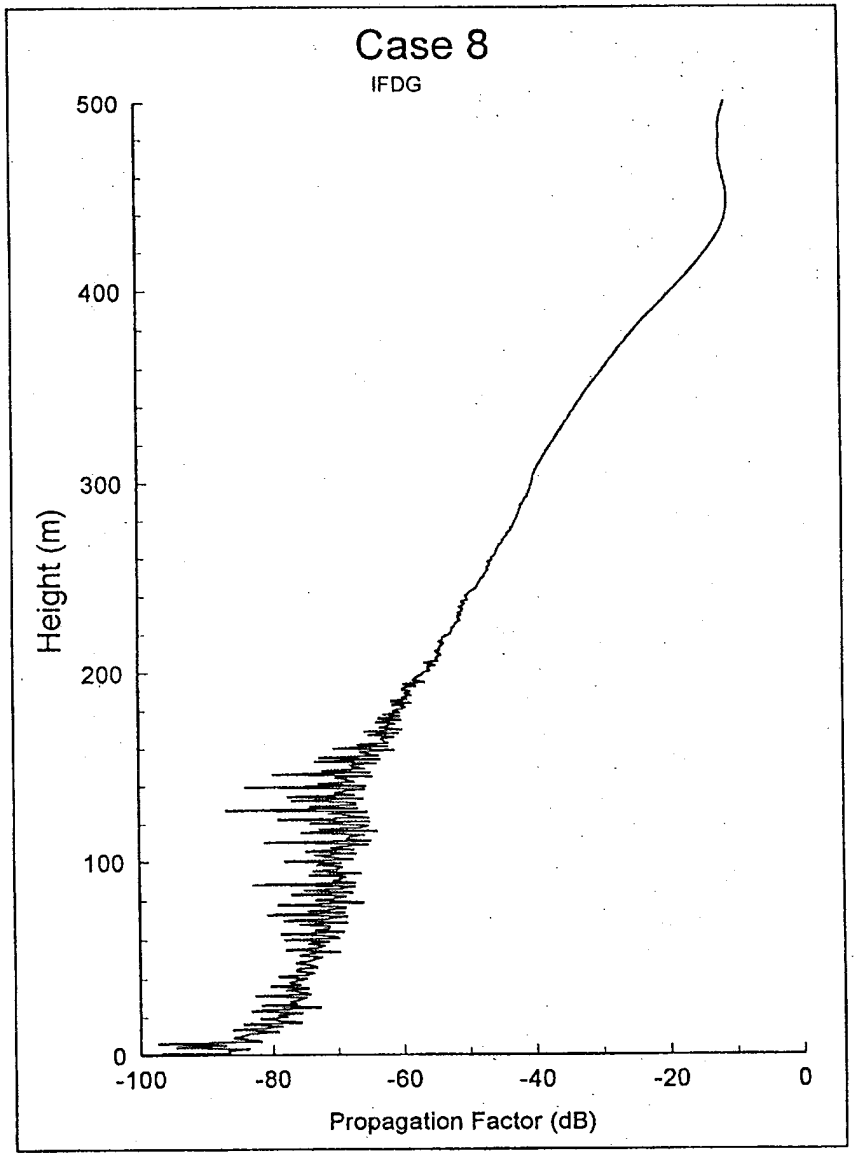
Case 8
IFDG
Height (m)
500
400
300
200
100
0
-100
-80
-60
-40
-20
0
Propagation Factor (dB)

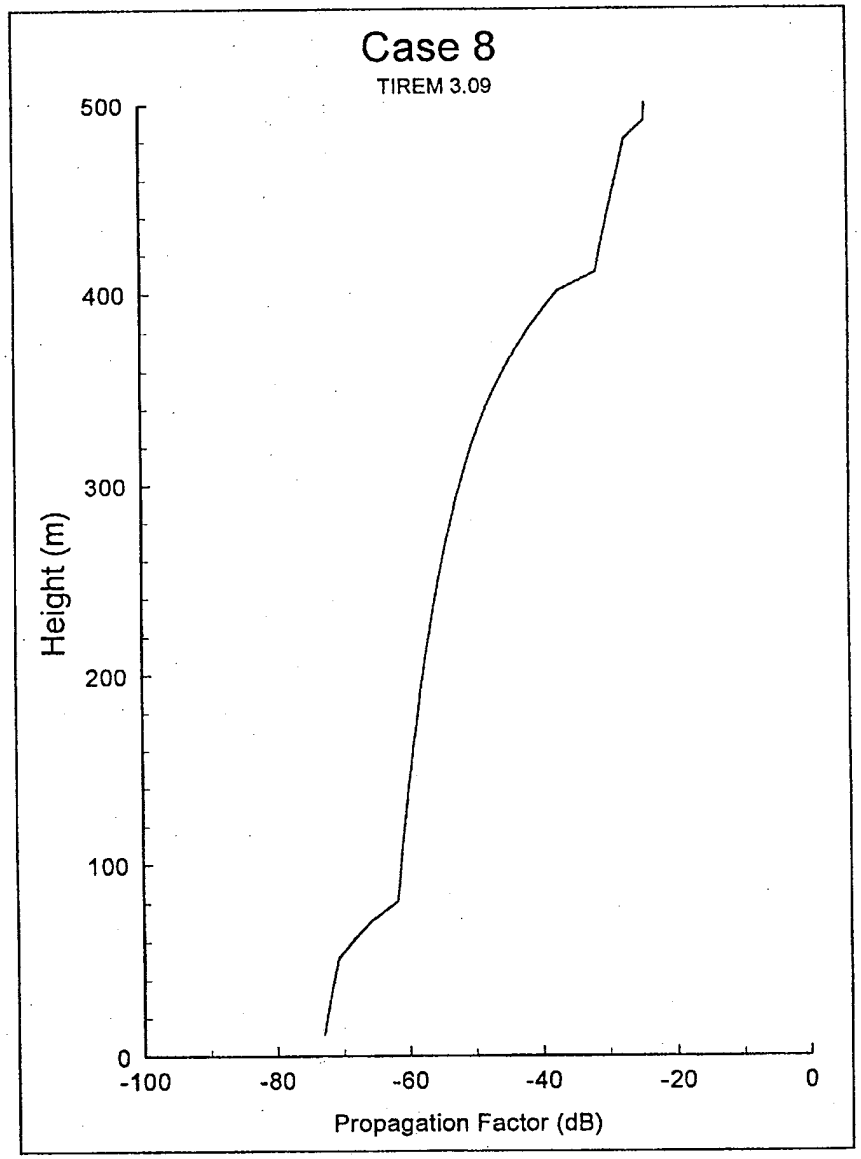
Case 8
TIREM 3.09
Height (m)
500
400
300
200
100
0
-100
-80
-60
-40
-20
0
Propagation Factor (dB)

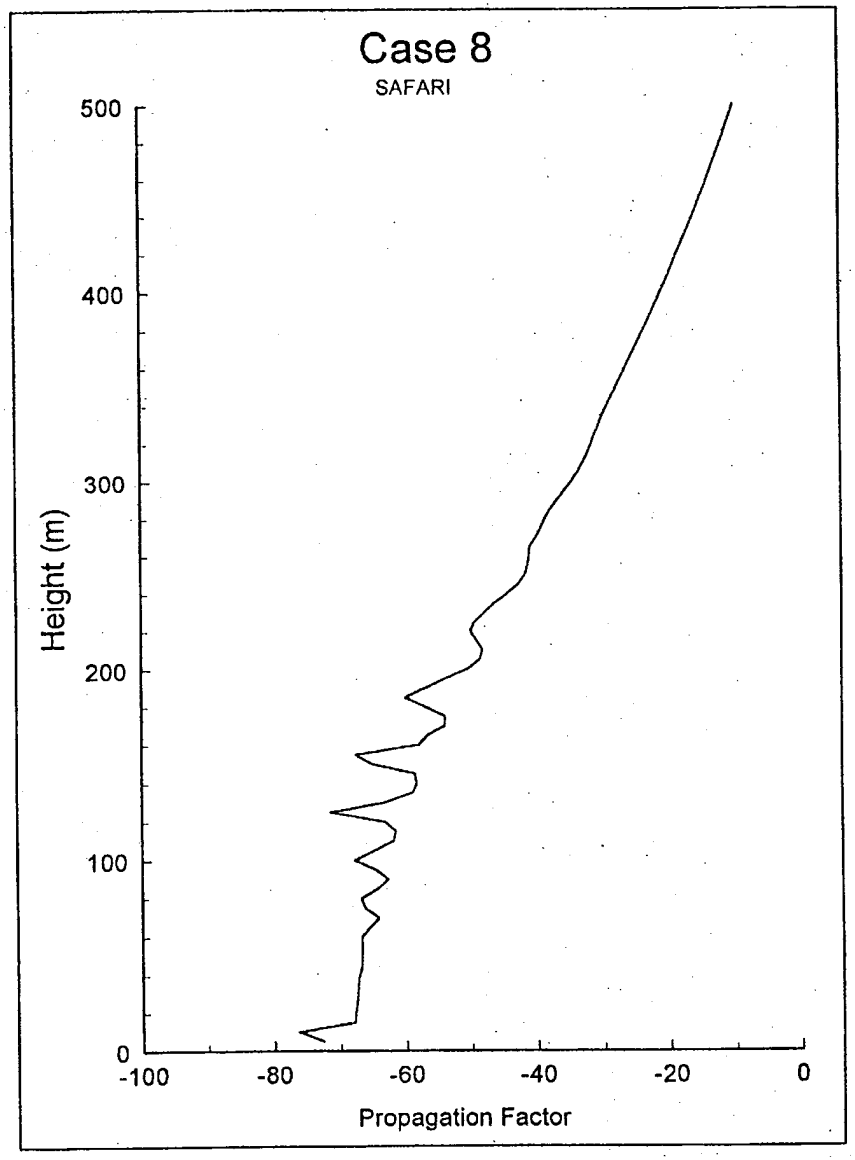
Case 8
SAFARI
500
400
300
200
100
0
Height (m)
-100
-80
-60
-40
-20
0
Propagation Factor

Sample Case 9.

This case considers propagation over terrain in a surface based duct. The frequency is 3 GHz and the transmitter antenna is 10 m above the local terrain at Long Beach. The refractivity profile is specified in Table 2. A coverage diagram is desired for receiver heights from the local ground height to 500 m above sea level for ranges from 0 to 100 km, based on a free space range of 100 km. Propagation factor is required at 100 km range for receiver heights from the local ground height to 500 m above sea level.

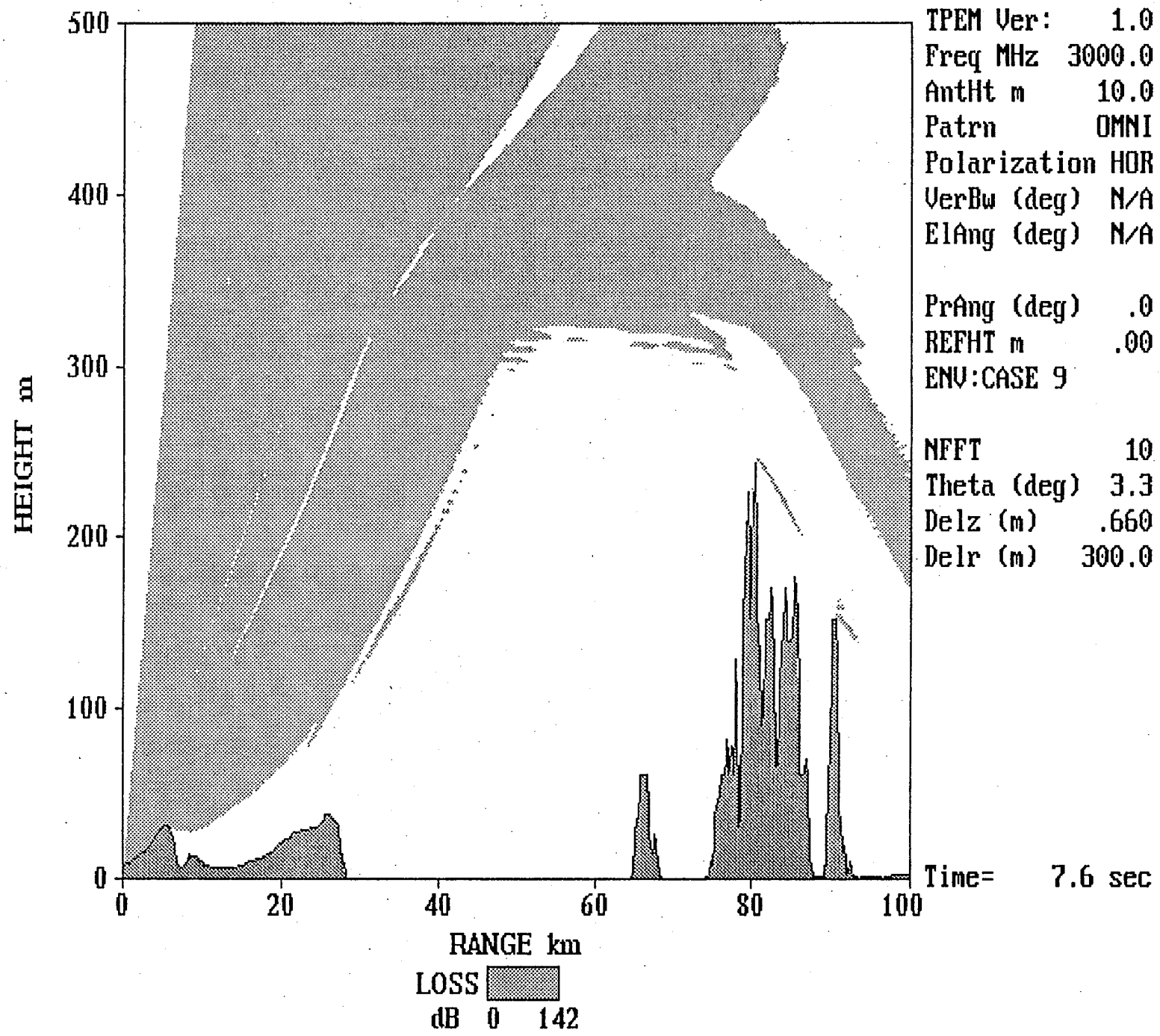
500
400
300
200
100
0
HEIGHT m
0
20
40
60
80
100
RANGE km
LOSS
dB 0 142
TPEM Ver: 1.0
Freq MHz 3000.0
AntHt m 10.0
Patrn OMNI
Polarization HOR
VerBw (deg) N/A
ElAng (deg) N/A
PrAng (deg) .0
REFHT m .00
ENV:CASE 9
NFFT 10
Theta (deg) 3.3
Delz (m) .660
Delr (m) 300.0
Time= 7.6 sec

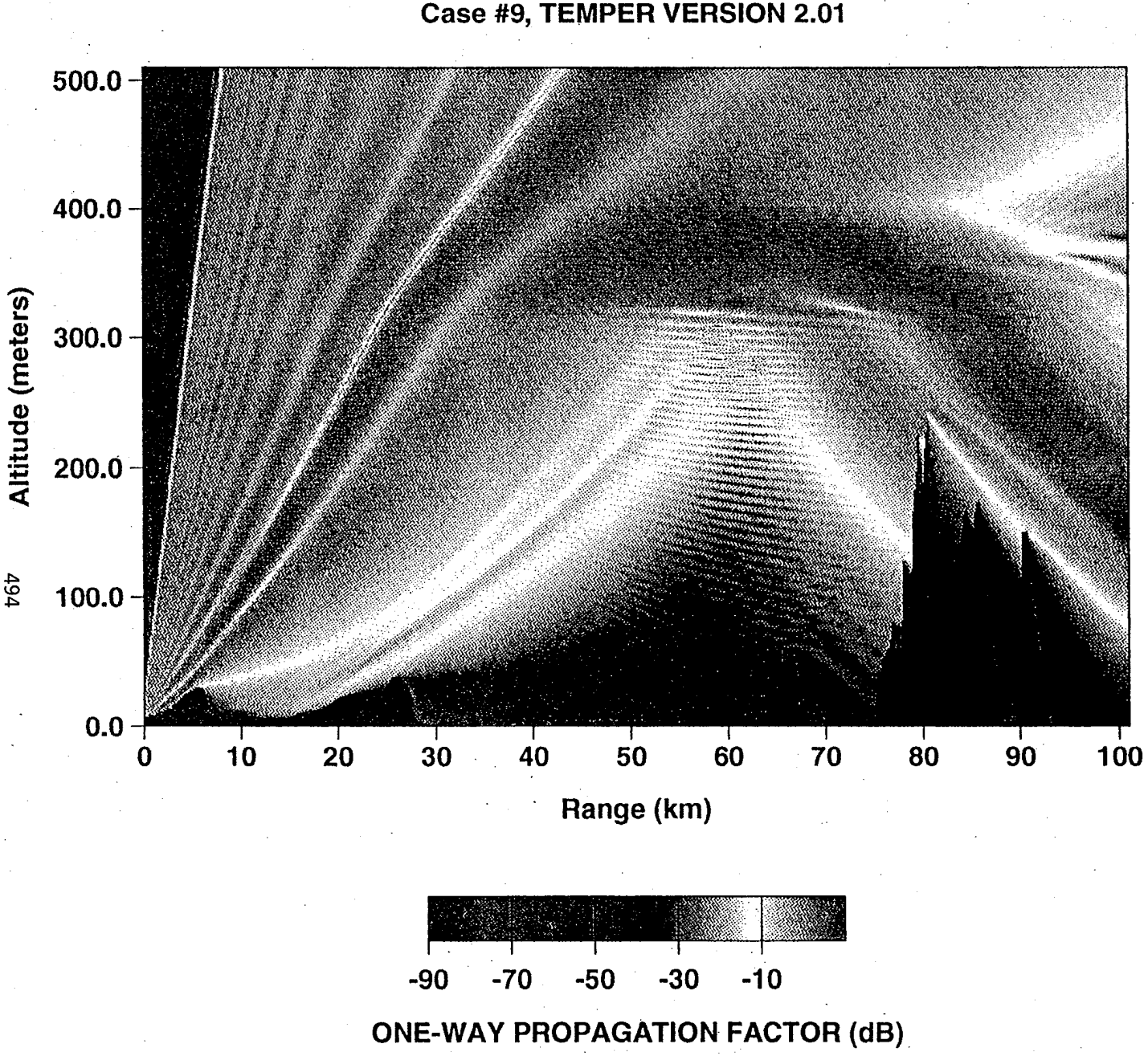
Case #9, TEMPER VERSION 2.01
500.0
400.0
300.0
200.0
100.0
0.0
Altitude (meters)
0
10
20
30
40
50
60
70
80
90
100
Range (km)
-90
-70
-50
-30
-10
ONE-WAY PROPAGATION FACTOR (dB)

SAMPLE CASE 9 – model : DIF–CERT

freq=3 GHz, ht=10m, surface based duct, smooth sea surface

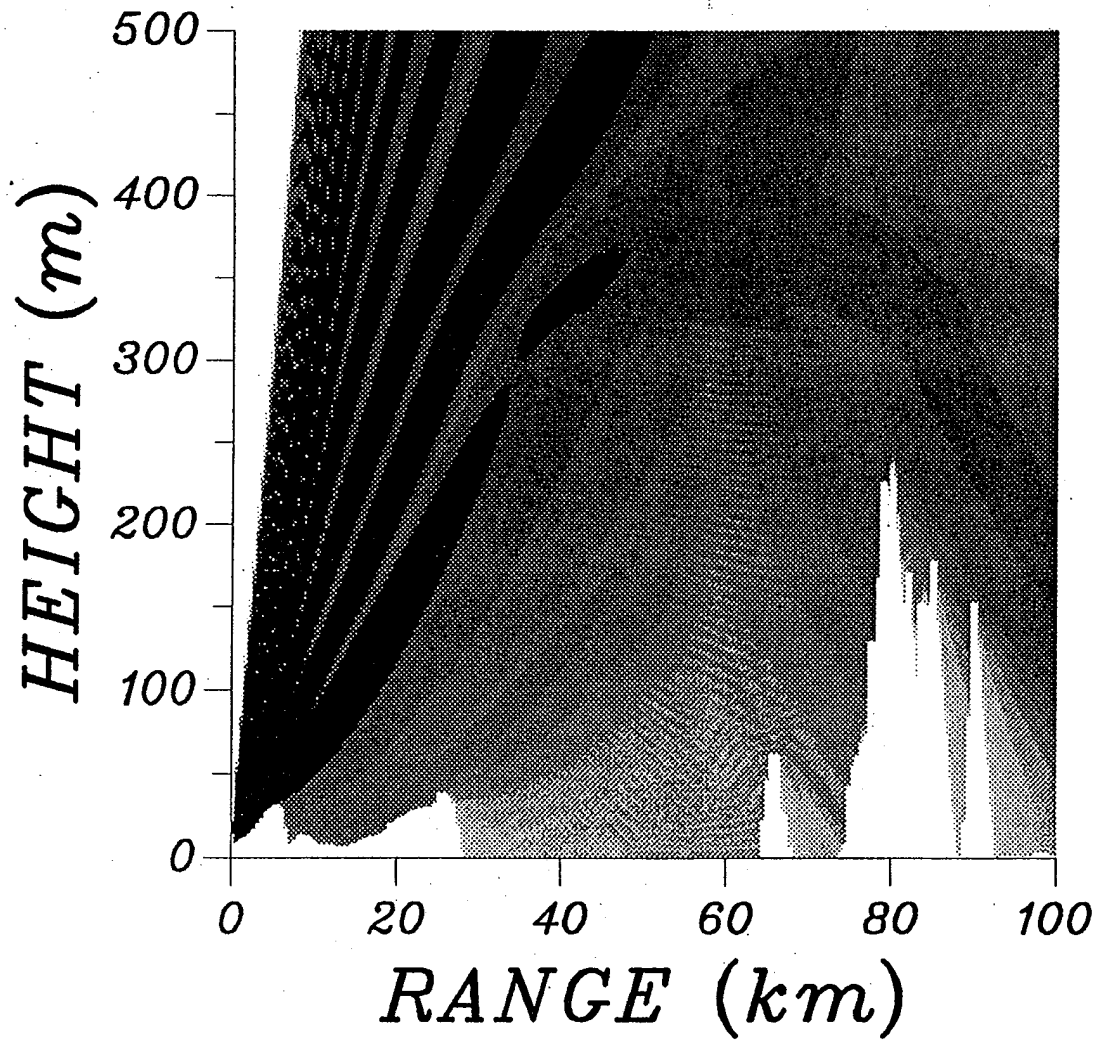

PROPAGATION LOSS
(dB)

ABOVE	300
200 –	300
190 –	200
180 –	190
170 –	180
160 –	170
150 –	160
140 –	150
130 –	140
BELOW	130

CERT/DERMO

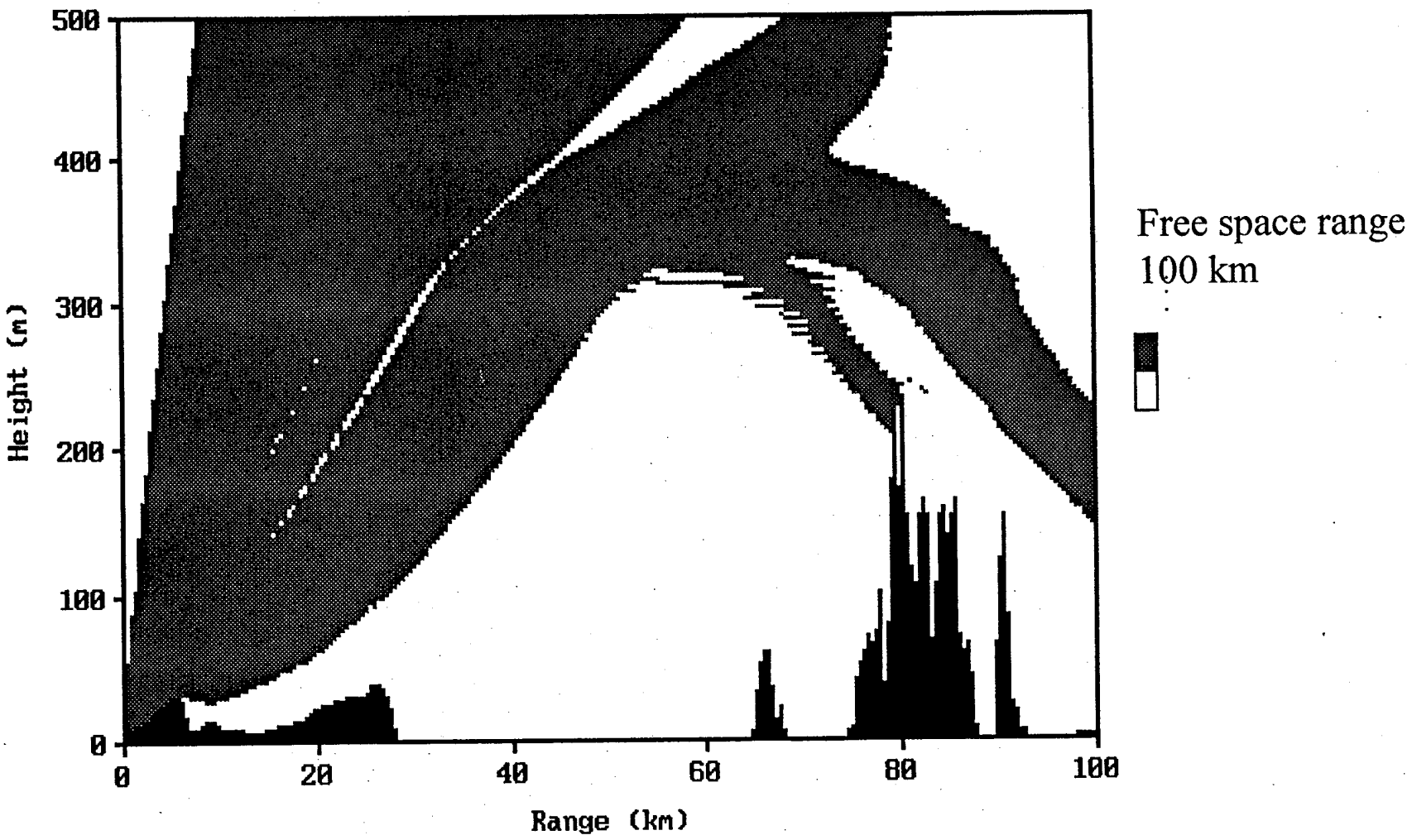

EEMS 1.0 Sample case 9

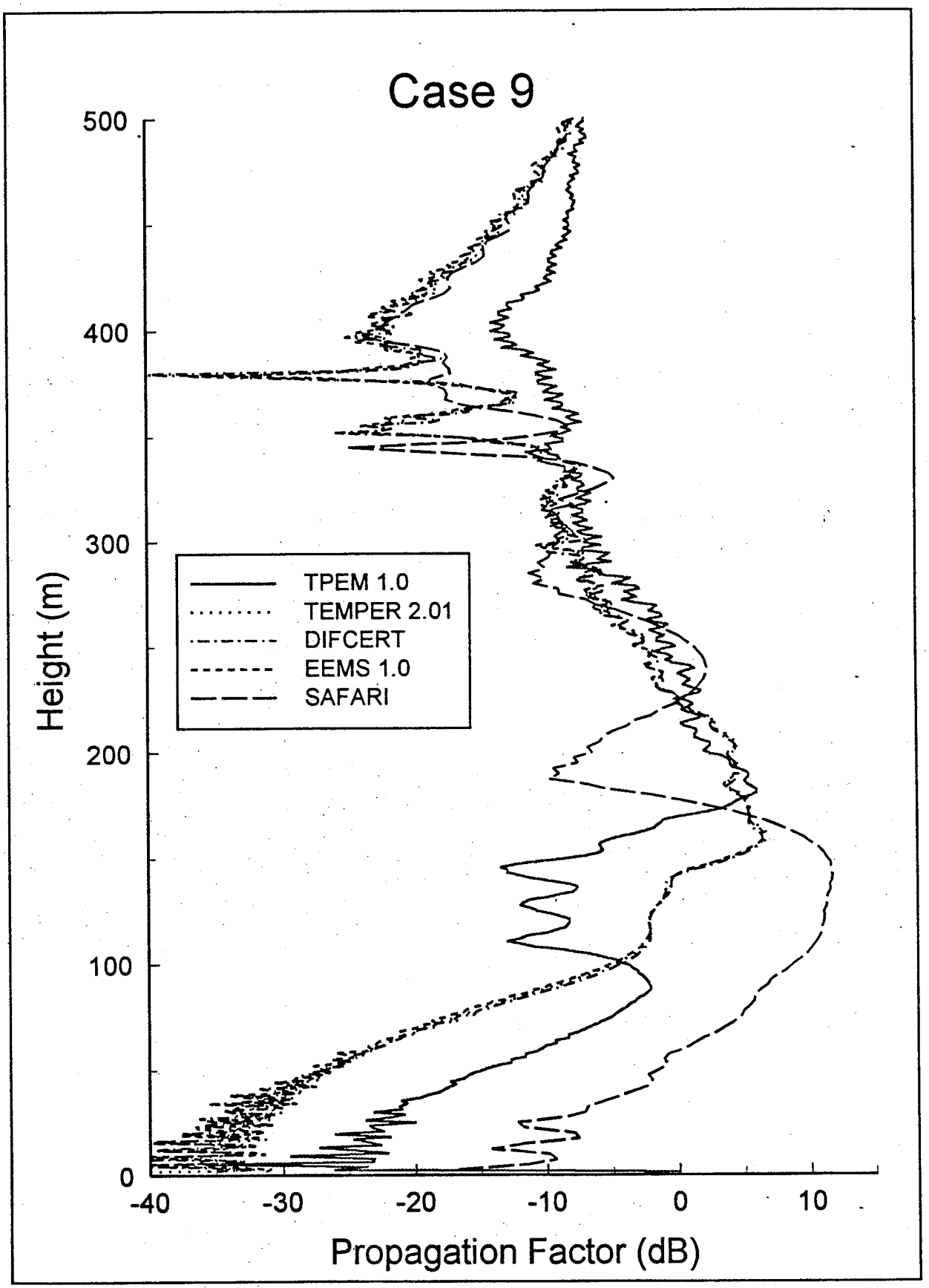
Case 9
500
400
300
200
100
0
Height (m)
TPEM 1.0
TEMPER 2.01
DIFCERT
EEMS 1.0
SAFARI
-40
-30
-20
-10
0
10
Propagation Factor (dB)

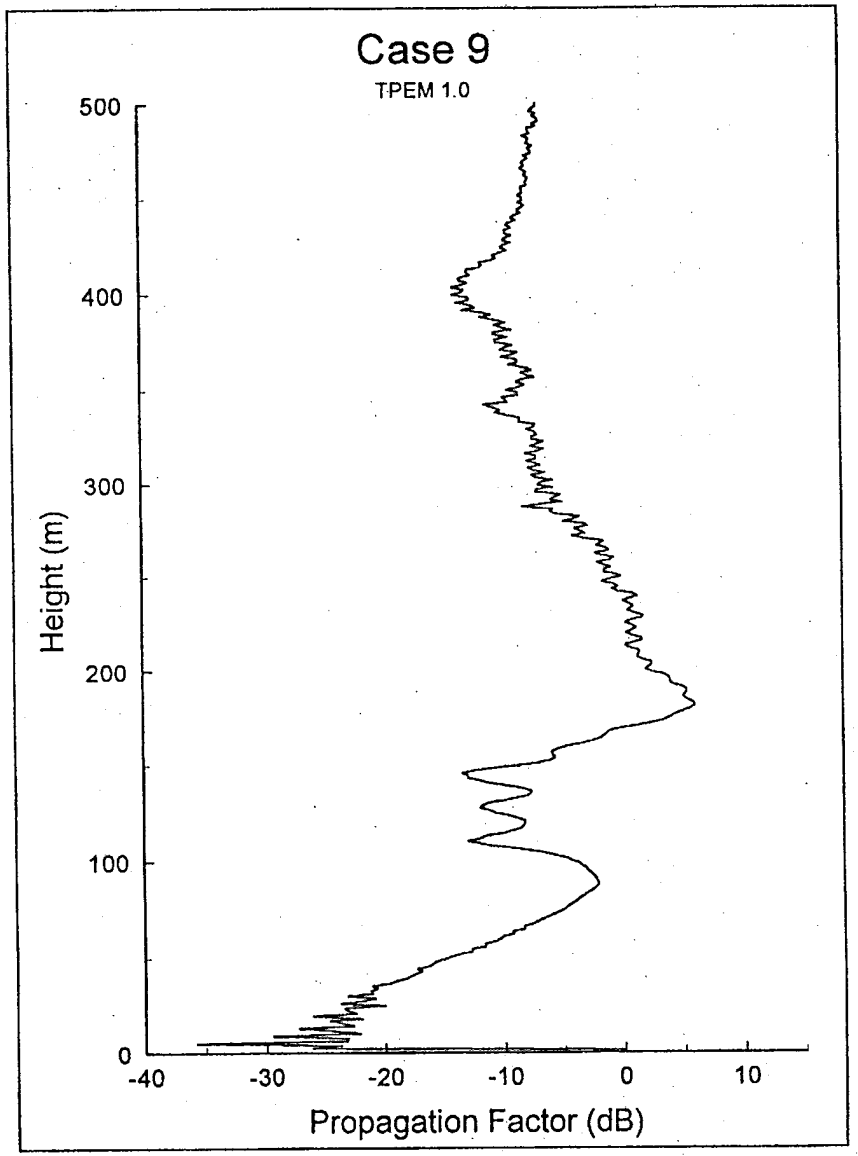
Case 9
TPEM 1.0
Height (m)
500
400
300
200
100
0
-40
-30
-20
-10
0
10
Propagation Factor (dB)

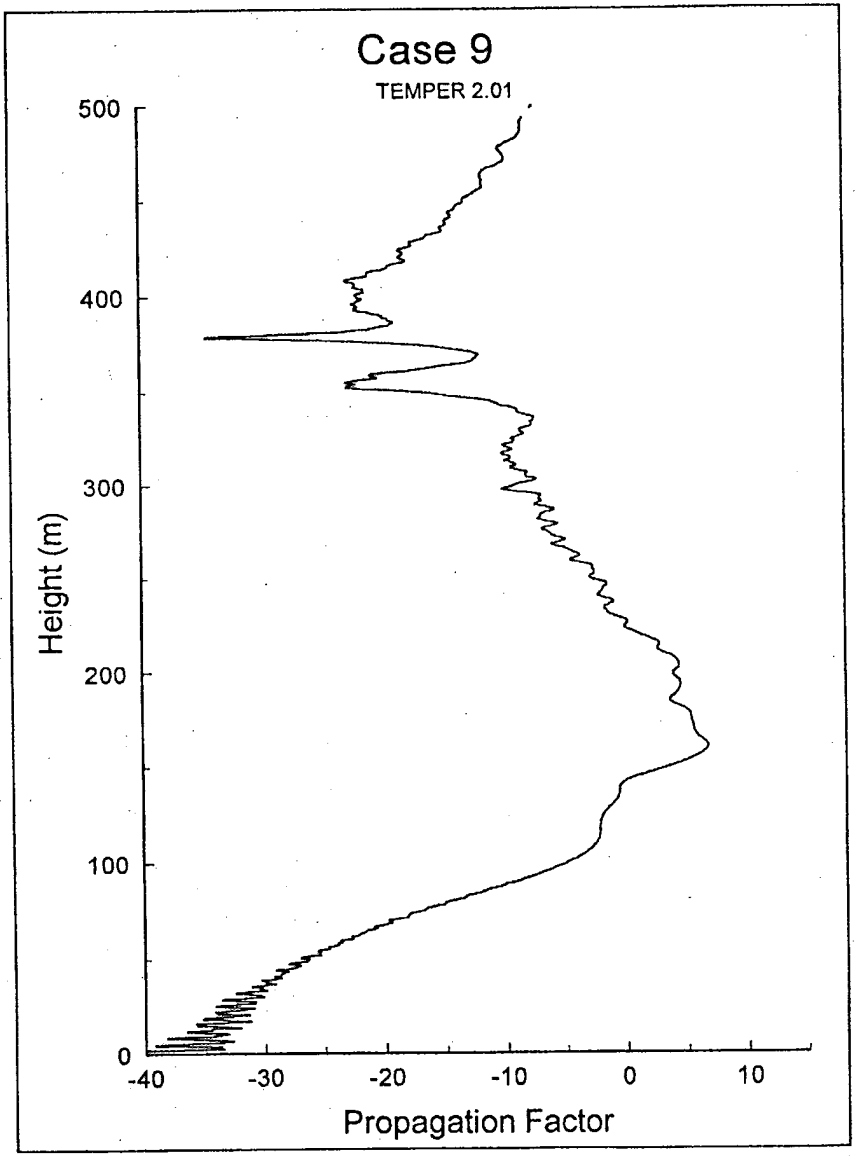
Case 9
TEMPER 2.01
Height (m)
500
400
300
200
100
0
-40
-30
-20
-10
0
10
Propagation Factor

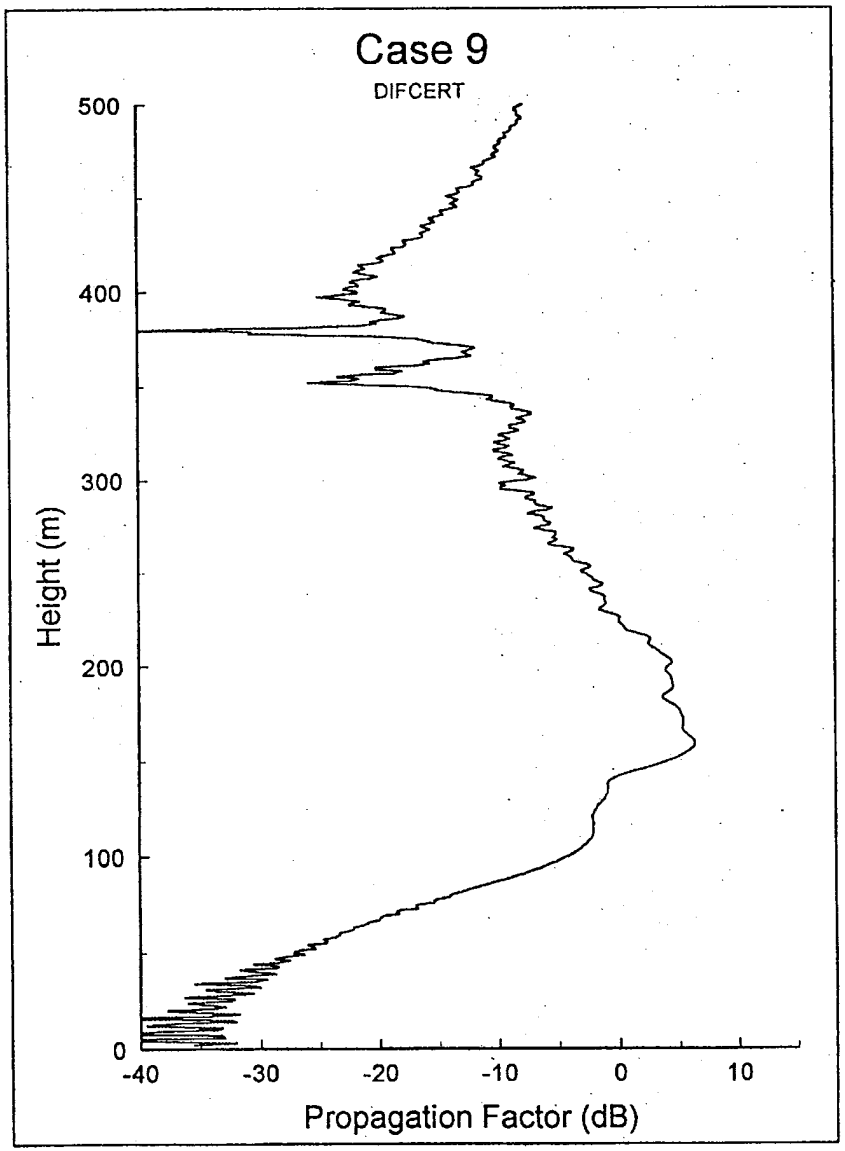
Case 9
DIFCERT
500
400
300
200
100
0
Height (m)
-40
-30
-20
-10
0
10
Propagation Factor (dB)

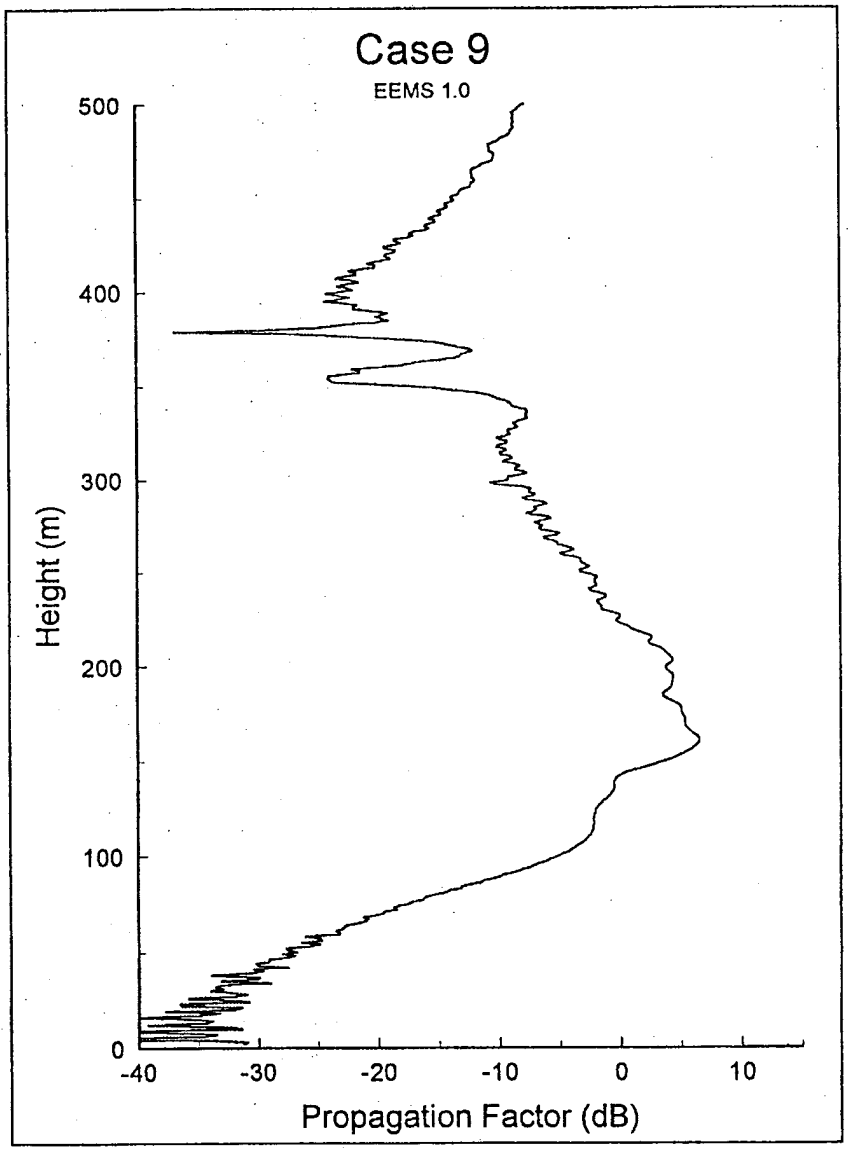
Case 9
EEMS 1.0
500
400
300
200
100
0
Height (m)
-40
-30
-20
-10
0
10
Propagation Factor (dB)

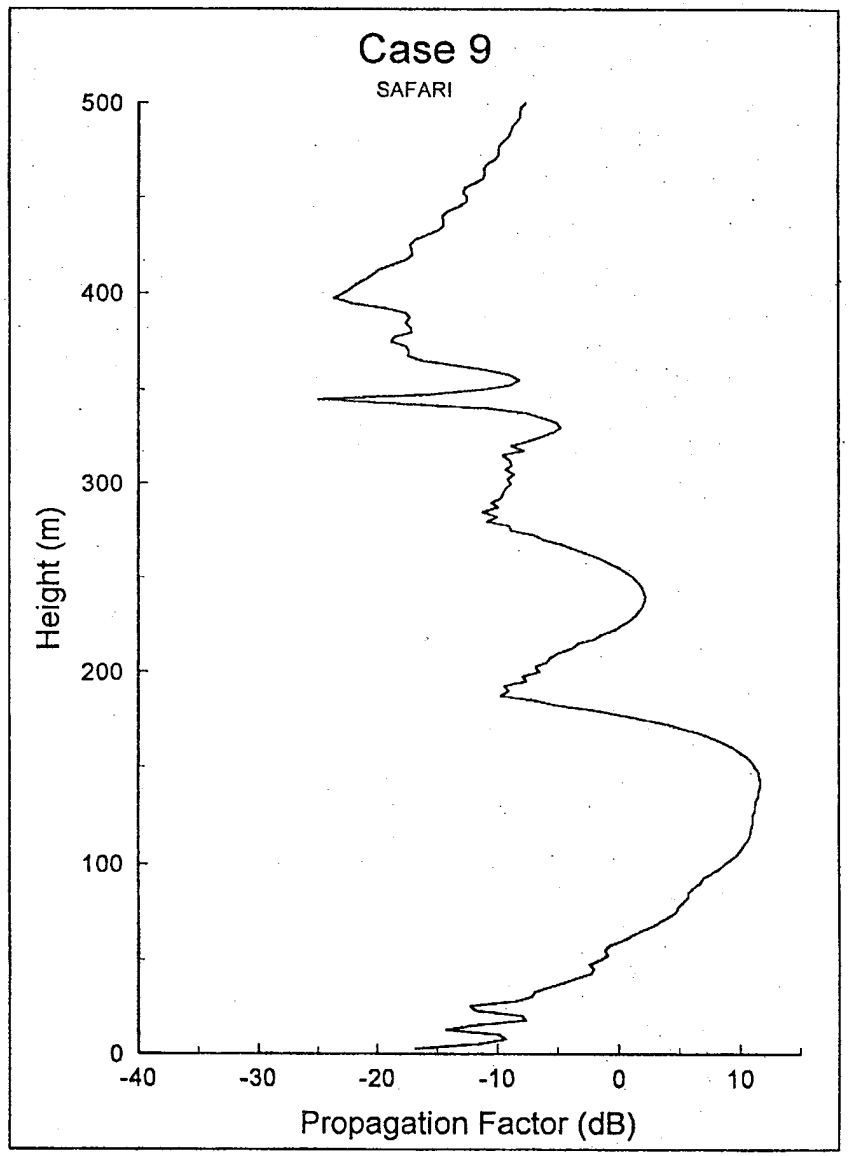
Case 9
SAFARI
500
400
300
200
100
0
Height (m)
-40
-30
-20
-10
0
10
Propagation Factor (dB)

Sample Case 10.

This case considers model ability to assess propagation effects at 127.75 MHz versus time on a propagation path that is partially over land and partially over water. The dominant propagation mechanisms are surface-based and low-elevated ducts from elevated trapping layers. The transmitter is located at Long Beach and the receiver is at Point Mugu, which is a path length of 100.35 km. The transmitter antenna is 9.1 m above the local ground level and the receiver antenna is 30.5 m above mean sea level. The polarization is vertical and an omnidirectional antenna pattern is assumed. 43 modified refractivity profiles were measured by radiosonde at Point Mugu from 23 Aug. 93 1558 U to 2 Sep. 93 1955 U. These profiles are plotted in Figure 8 and were available to participants in digital form. Coverage diagrams are not desired. Measured radio data were available for this case.

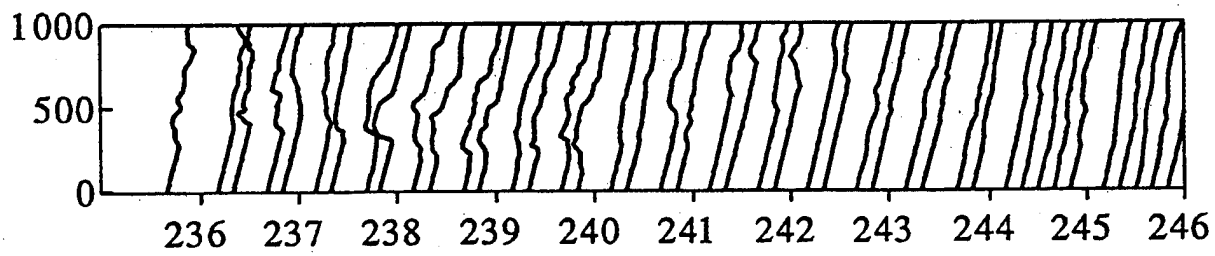

Figure 8. Modified refractivity profiles vs. Julian Day of 1993 (day 236 is 24 Aug.). Vertical axis is height in meters.

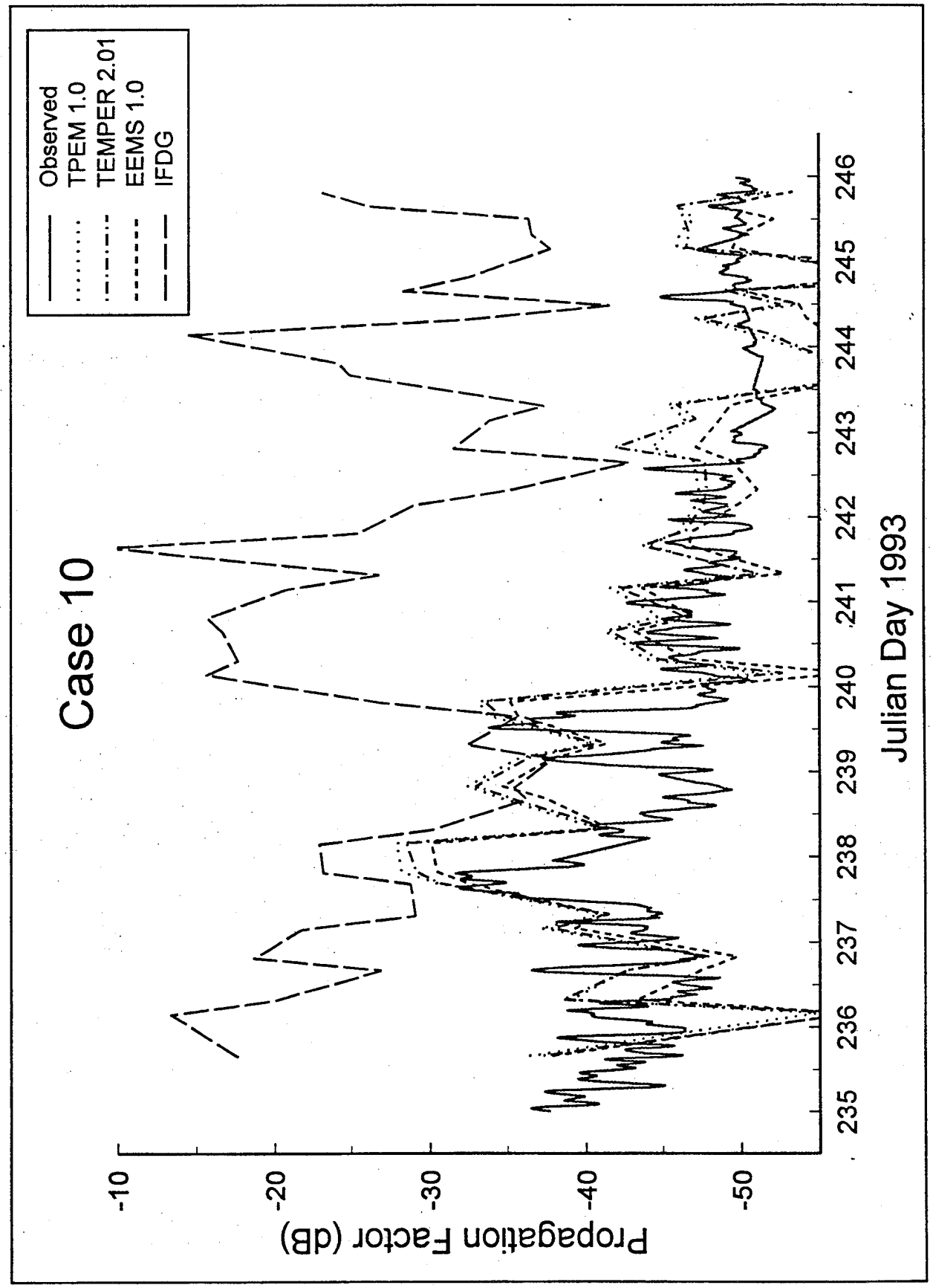
Case 10
Observed
TPEM 1.0
TEMPER 2.01
EEMS 1.0
IFDG
Propagation Factor (dB)
-10
-20
-30
-40
-50
235
236
237
238
239
240
241
242
243
244
245
246
Julian Day 1993

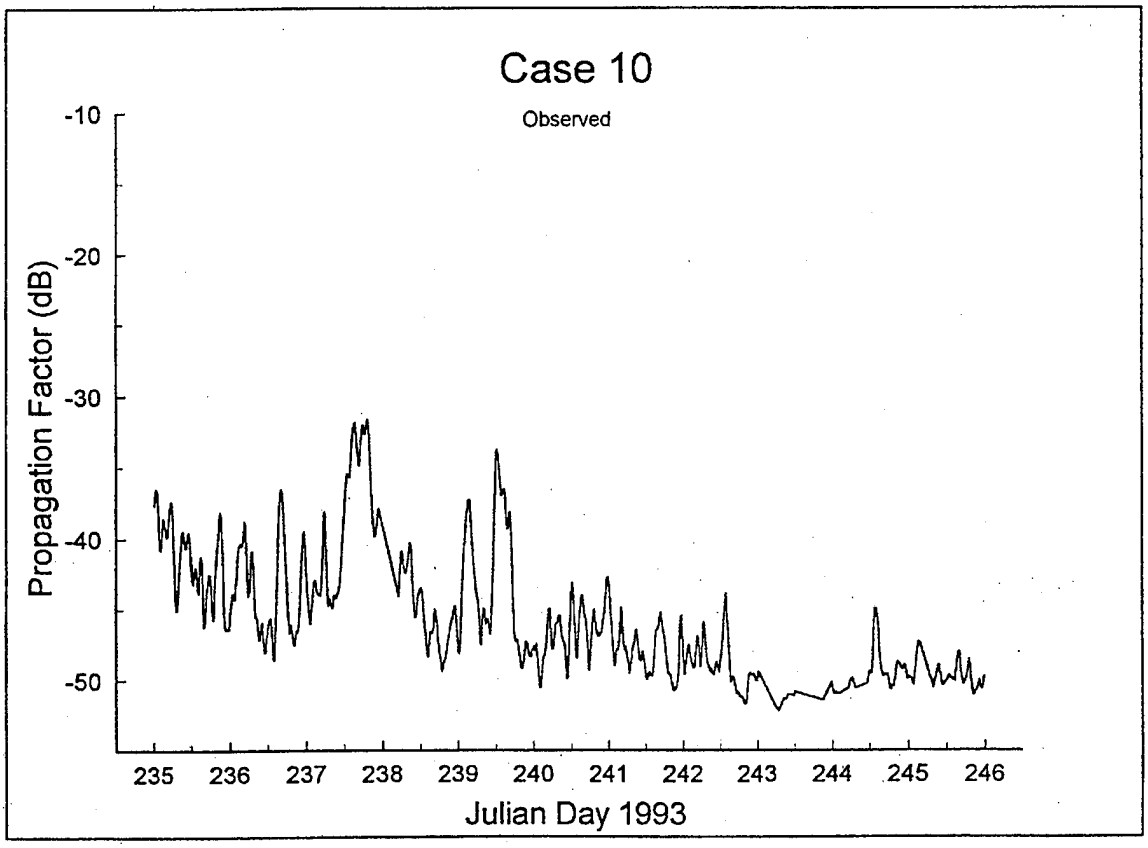
Case 10
Observed
-10
-20
-30
-40
-50
Propagation Factor (dB)
235
236
237
238
239
240
241
242
243
244
245
246
Julian Day 1993

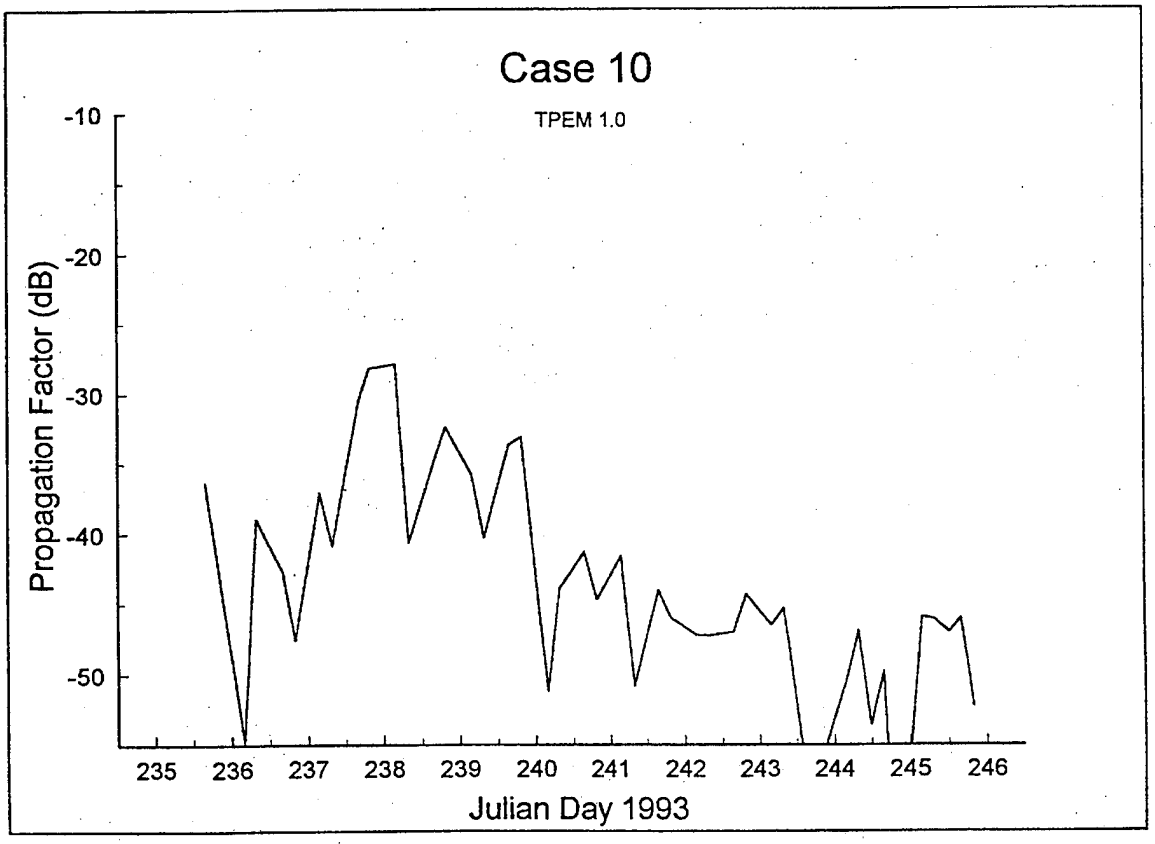
Case 10
TPEM 1.0
-10
-20
-30
-40
-50
Propagation Factor (dB)
235
236
237
238
239
240
241
242
243
244
245
246
Julian Day 1993

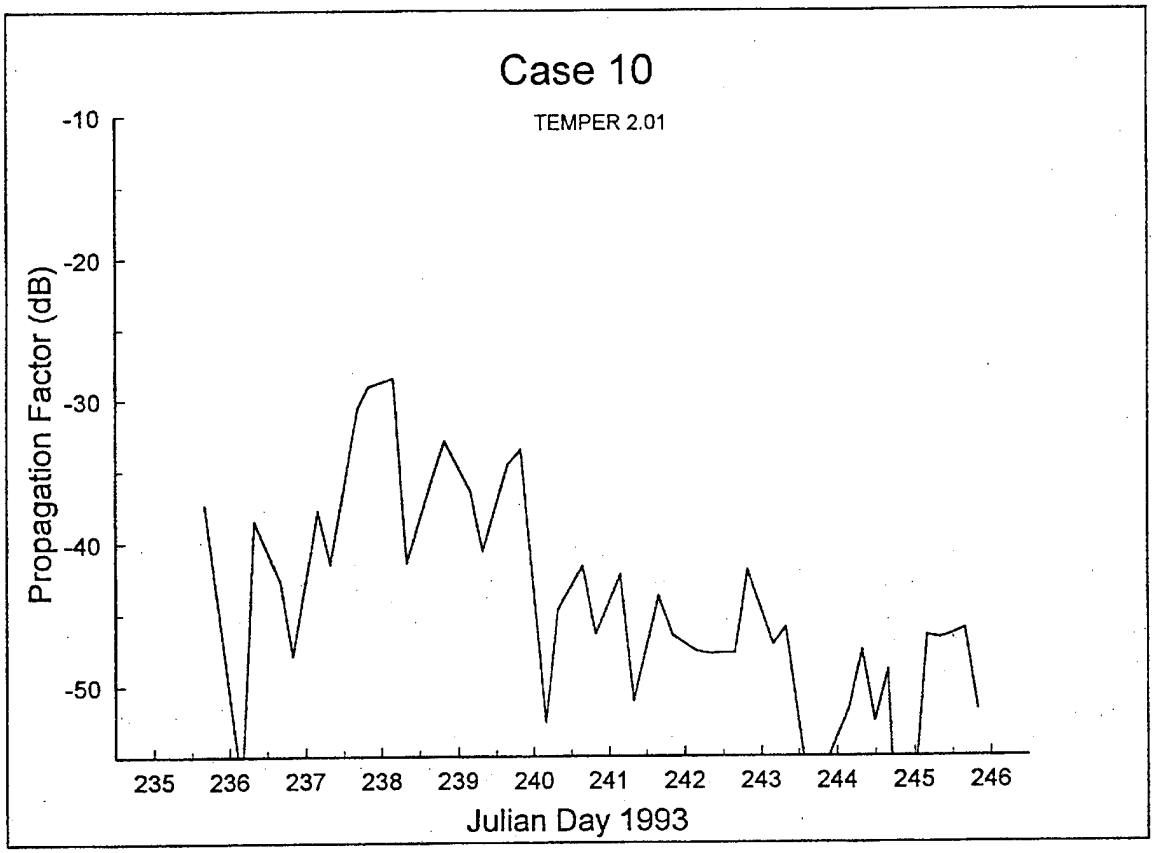
Case 10
TEMPER 2.01
Propagation Factor (dB)
-10
-20
-30
-40
-50
235
236
237
238
239
240
241
242
243
244
245
246
Julian Day 1993

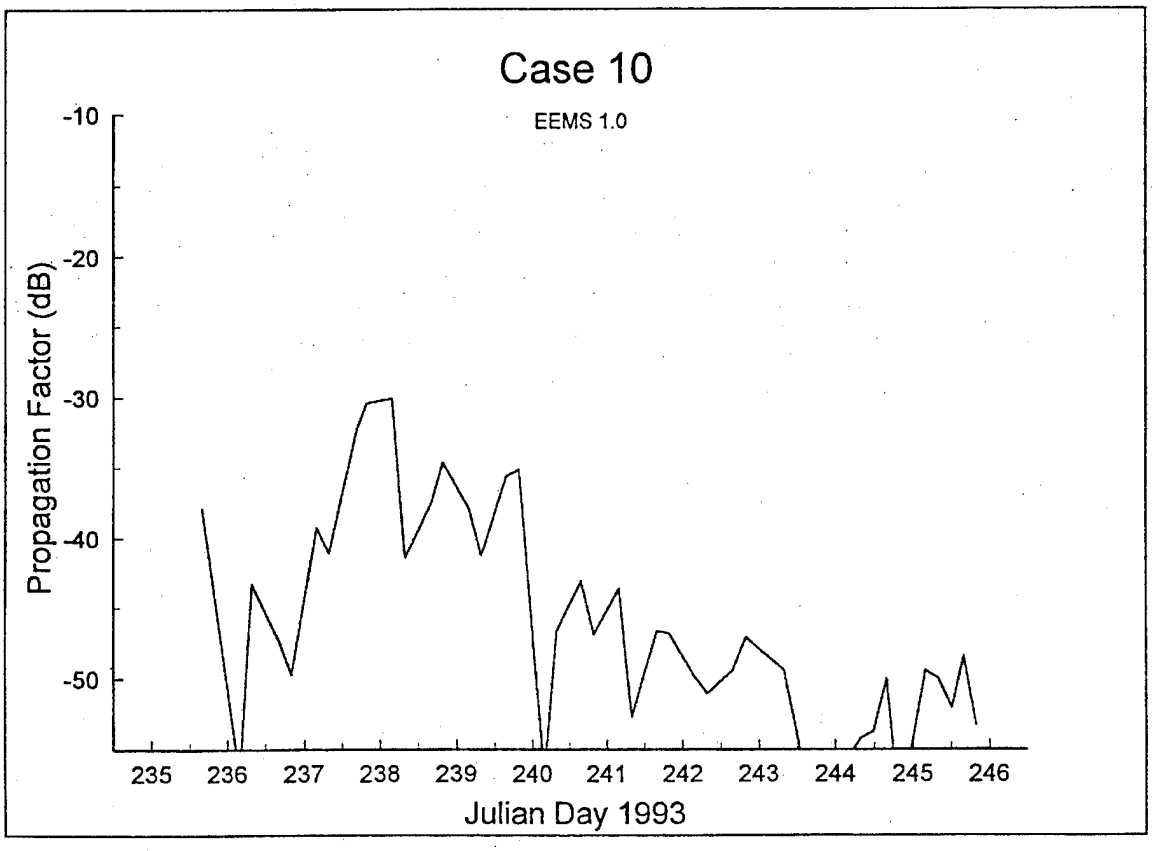
Case 10
EEMS 1.0
Propagation Factor (dB)
-10
-20
-30
-40
-50
235
236
237
238
239
240
241
242
243
244
245
246
Julian Day 1993

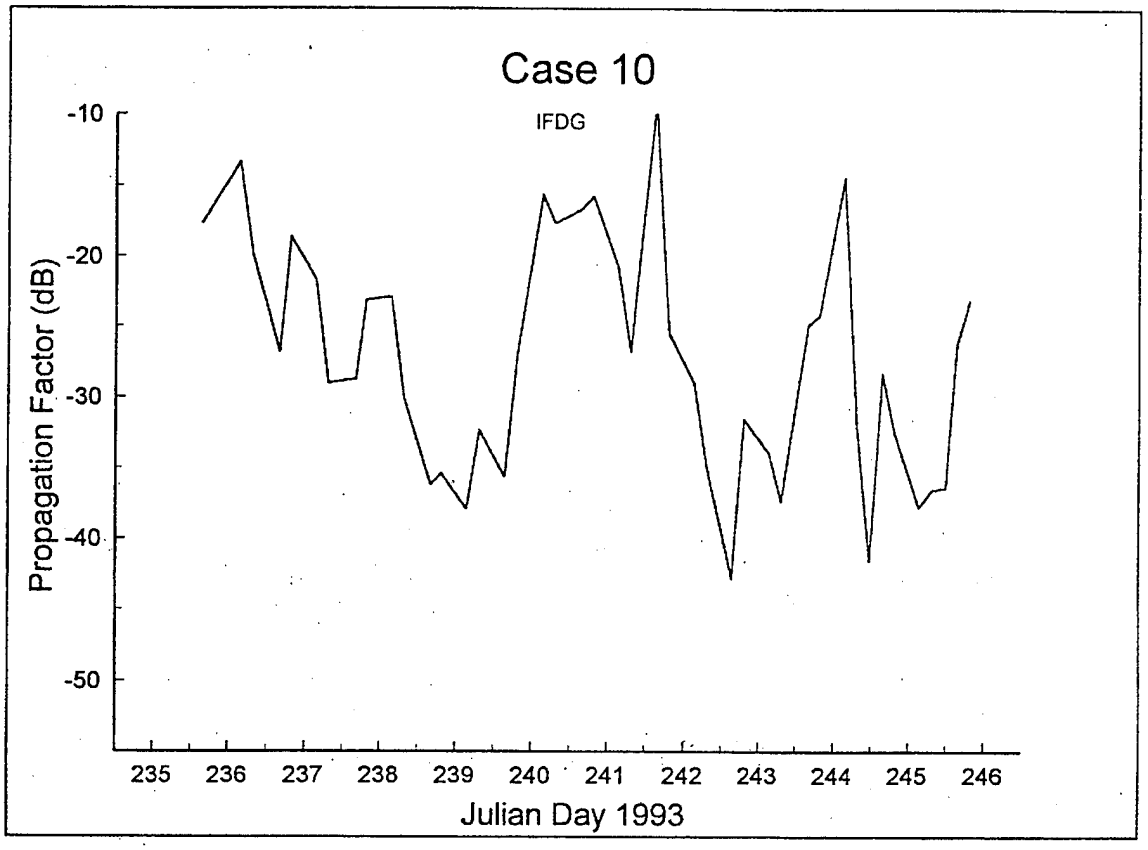
Case 10
IFDG
-10
-20
-30
-40
-50
Propagation Factor (dB)
235
236
237
238
239
240
241
242
243
244
245
246
Julian Day 1993

REFERENCES

1. Paulus, R.A., "VOCAR: An Experiment in Variability of Coastal Atmospheric Refractivity," in *"IGARSS '94" Symposium Digest*, IEEE Catalog No. 94CH3378-7, pp. 386-388.
2. Rogers, L.T., "Statistical Assessment of the Variability of Atmospheric Propagation Effects in the Southern California Coastal Area," in *"IGARSS '94" Symposium Digest*, IEEE Catalog No. 94CH3378-7, pp. 389-393.
3. Recommendation 527-2, "Electrical characteristics of the surface of the Earth," in "Recommendations and Reports of the CCIR, Volume V, Propagation in Nonionized Media," ITU XVIIth Plenary Assembly, Düsseldorf, 1990.
4. Barrios, A.E., "Parabolic Equation Modeling in Horizontally Inhomogeneous Environments," *IEEE Trans. Antennas Propagat.*, 40, 7, July 1992, pp. 791-797.

SESSION VI. SUMMARY AND FUTURE DIRECTIONS

Panel: CDR D. Markham, G. Brooke, S. Burk, J. Kuttler, and R. Paulus

PANEL DISCUSSION

The final session of the workshop was a panel discussion organized to address three issues with approximately one half hour time allotted to each. The following summarizes the comments and points made by panel members and workshop attendees.The comments have been paraphrased from audio tapes of the discussion and do not represent quotations of the speaker.

Issue 1: What features/characteristics are needed in an operational assessment system and how does that differ from a research system?

CDR D. Markham It's become apparent to me throughout this workshop that there is in different people's minds different definitions for operational versus research. I'd like to throw open for discussion what features/characteristics would one want to have in an operational system and how would that differ from a research system? Keep in mind that that system includes, but is not necessarily limited to an electromagnetic propagation model. The model is a key component but it is not the entire system. As far as an operator is concerned, if you saw Rich Paulus's presentation of the system chart, the operator is concerned with the end result which is how effectively is he going to be able to deliver a weapon on target or to sense the enemy in the passive case. The propagation model, which is a component of that system, has to perform to a certain level. If it has fallacies, it is not necessarily going to doom the system. If it has significant fallacies, obviously the system is not going to be able to perform and the user is not going to be able to perform his mission.

R. Paulus: The architecture of TESS as it exists now is a good starting point. With respect to electromagnetic propagation assessment:

- The environmental input data, can be either climatological for mission planning or real time. Real time can be in situ observations or forecasts from 24 hours ago. The power of the predictive models is to show the tendencies where you will be tomorrow.
- Propagation models (have been discussed here in detail)
- Radar/system models, emphasized by Pete Econ at an earlier meeting, may need to be upgraded, particularly for assessing the performance of your own system. That's not so critical for assessing someone else's system because you just don't know all the details for that system.
- Information displays have been addressed by the British as evident by their presentation at the Propagation Assessment in Coastal Regions, AGARD Symposium last September. We need to take into account what is displayed to whom and in what form. Research systems are not as concerned with information displays.

G. Brooke: From a research modeler's point of view, there has to be an agreement among operational and research modelers that they are not competing. The research modelers are there to assist the operational modelers in making their models better. The objective is to produce a better operational model.

J. Kuttler: Here at APL we work all sides of this problem with the goal of something for the Navy to take and put to sea. We work generally a systems engineering concept with the idea that the end product is going to be a deployable system that is user friendly, works in real time, and gives accurate and useful results. At the same time, we're doing research with models such as TEMPER to find "what is truth". Then we try and transition that into a product and we work all stages of the problem down the line. You heard presentations by Gerry Konstanzer and John Rowland regarding system test and evaluation. Of interest is the meteorological data that in some instances minor fluctuations in the data and their presentation can result in dramatic effects in the output and in other cases vast differences in the treatment of the data have only small effects in the output. These are some of the questions that need to be understood.

J. Richter: I do not go along with the differentiation between research and operational models. Using the example of a head of the NSF, an engineer by education, when asked if he favored engineering science or basic science replied that there was only good science and bad science. Similarly, don't differentiate between research and operational models, either they are correct or not correct.

J. Kuttler: Of course when one says correct, there is always an epsilon, an error in there. For the operational side, the question is how big an epsilon can we tolerate and how fast can we get to it.

R. Philbrick. In follow on to the system view mentioned earlier, a point about the future more than the present. In the future, one would expect these kind of model applications to be applied in a predictive sense - the mission planning aspect for 4 hours, 8 hours, 24 hours ahead. That is, taking real time sensor data and the past history in mesoscale modeling to predict the RF conditions at some point in the future.

S. Burk: This is a little different than the traditional NWP way. You're stating it as taking remotely sensed data taken now and coupling that directly with the model forecast to give a forecast 24 hours from now. Currently, observations and remotely sensed data (satellite) get into the models through data assimilation cycles. This is not in the sense of taking a profile at a site and evolving it with time.

R. Philbrick: The point I was trying to get to is that in a mission sense, frequently the weather observer is asked to say what's the condition going to be to support this mission that's going to be 6 hours into the future. The thing of the future is a mesoscale model coupling that information back in to where you're making a prediction of the RF conditions.

S. Burk: That's along the lines of my workshop presentation. Meteorologically, the numerical forecasts during VOCAR were quite good - we forecast the temperature and structure of the marine boundary layer quite well. However, a good meteorological forecast may not translate to good RF predictions. This requires taking a predicted temperature and moisture field, creating a refractivity field to drive a PE model and

comparing that with measured propagation. After going through this chain of events, the results may not be as good as you would like. The gradients at the top of the boundary layer do not make or break a meteorology forecast but may be very significant to propagation. The most encouraging thing about mesoscale modeling in the propagation arena is the capability to forecast the trends in the structures that affect RF propagation.

K. Craig: Are we as propagation modelers to assume that in the very near future that we are going to be able to take numerical model output and use it or should we still be trying to do pseudo-meteorological modeling? By the latter I mean, for example, adapting profiles in the littoral.

S. Burk: I don't know of any model currently that can give high enough fidelity boundary layer profiles to rely on a great deal of the time. In VOCAR, for the period of the first 3 or 4 days, the model results were excellent and the data could be run through RPO with good agreement. In the middle of the VOCAR period, there was a lot of moisture advection outside of the boundary layer that was not picked up by the modeling system and the results were not in good agreement. I don't think there are any other models that are going to do a lot better.

CDR D. Markham: Something that the EM propagation community can do to help the NWP modelers is to define what the temporal and spatial data requirements are to support the current high-fidelity propagation models. Ted Rogers pointed out with VOCAR results that in order to realize a significant gain in using range-dependent propagation models, you need to take observations more frequently than every two hours. That kind of temporal and spatial information would be useful in developing the NWP models to support EM propagation and system assessment. Referring to the earlier comment by R. Philbrick, 4 to 6 hours for a tactical planner is reasonable. But we like to think of 3 echelons of decisions to be made on board ship, the tactical planner is only one of them. The operational decision maker, the admiral or general in charge of the operation, has to make more top level decisions so he needs information that is more long range and broader in scope. At the other end is the pilot, the person on the ground, or the person aboard ship that needs information right now. So we need to do not only mid- and long-range forecasts but also nowcasts.

M. Levy: Going back to the issue of research versus operational models, the operational models that we have are high fidelity models and agree pretty well with each other. The research is to speed them up, not to do new models. The EM community is happy with our models and the research is to make them faster. It is not true any more that accuracy is lost to gain speed.

G. Brooke: The acoustics community separates research and operational models; there does not appear to be this division in the EM community. Whether this is right or wrong I don't know. A research model does provide a system of checks and balances. The models presented do compare quite well. Is this related to the sample cases that were

proposed? How do we know that if we change the sample cases the models will agree as well?

M. Levy: The people who chose the sample cases tried to cover a very wide variety. There are ongoing comparisons of a much wider variety than covered in this workshop and we get the same agreement.

S. Fast: An operational model needs to provide a sufficient tolerance so that bad decisions do not result. A research model is an aid in understanding the physics of the problem.

K. Anderson: The EM community does have research models, TEMPER is one. MLAYER is another that is clearly only a research model. Modelers make comparisons to these models.

J. Richter: Checks and balances do exist in the EM community. The modelers have extensively published in the peer reviewed literature. That, for me, is still the best criterion to judge the science aspects. Publishing serves the checks and balances role.

G. Bust: A research model should keep the full vector field, amplitude and phase as a function of time; 3-dimensional information on the environment to investigate the physical phenomena in detail. The presentations here have not really been concerned with phase or temporal information. With regards to accuracy, comparison of model predictions to real world data seems to yield a variance of 8-10 dB. That leaves a lot of room for improvement. There are a lot of missions today that work with a 3 or 4 dB variance at the edge of a region.

D. McCammon: Operational models need to portray the entire scope of the problem to the operator quickly. In a variable environment that can never be sampled in time and space as well as needed, the operational model needs to be broader based and less accurate in order to display the possible range of performance.

H. Hitney: Operational and research models have the same goal, to be as accurate as possible. On the operational side one might try to limit the complexity of the model or improve its efficiency but you still want it to be as good as it can be. It is not a given that faster is less accurate.

M. Pastore: The models as described during the workshop have a very broad range of applicability. Is there any value in tuning the model to a specific application, like the close-in ranges?

M. Levy. In response to G. Bust, the models do include phase. It was not shown during the workshop because the operators don't want it. The 10 dB difference you mentioned is due to measurement problems and knowing the environment, not the models. The models are accurate and it is not sure that we can ever measure the environment well enough.

G. Bust: On that environmental question, in the ionospheric community, ionospheric tomography is giving real-time 2- and 3-D slices of the medium so saying we will never be able to measure the environment accurately enough is not necessarily true.

Issue 2. Do models need to be improved?

D. Williams: One concern is a small target like a periscope or rubber boat, with 3-dimensional motion of its own, protruding above a wavy ocean surface in a clutter intensive environment. More attention to target physics is needed. Also, detection to operational people usually means classification, that is, a radar operator has to recognize that a blip on his screen is a target and not clutter. There is a probability of detection and a false alarm rate associated with this process. Data on this needs to be collected.

J. Kuttler: This is indeed an area where we have to look at improving our models, that is, right down on the deck. Most of these models agree quite well, at least in major respects. One of the primary Navy concerns today is littoral warfare where you have shallow water, terrain, and clutter that you would like to quantify. If you want your model to be able to predict backscatter, you forward propagate over obstacles, terrain, waves, whatever and get a very reliable estimate of the field right down to the surface. Then you need to do a scattering formulation to predict the amount of backscatter from that terrain or water and propagate back to the receiver. This will require very accurate predictions in a difficult area for these codes to operate, that is right on the surface in the presence of obstacles.

R. Paulus: Characterizing a periscope should fall into a target modeling class. Similar to an aircraft coming in that is always moving and changing aspect, the RCS is fluctuating. There has to be a cross section model of that. An operational system would take this into account as a given RCS with a POD based on the fluctuations. This is not a propagation modeler's problem but these two models must be put together.

J. Kuttler: You need to know the power on the periscope and then you factor in the RCS of the periscope.

CDR D. Markham: There is no question, as was pointed out on the first day of this workshop, that from the Navy and Marine Corps standpoint, the submarine periscope, low flying aircraft, and cruise missiles are our biggest threats and something that EM assessment and system performance abilities that we have in the fleet today do not adequately treat.

J. Kuttler: There is no question that the most stressing case for most of these radar problems is at grazing incidence and most of the time this problem is not well done.

LCDR R. Dees: It's not the operational EM propagation model that is the difficulty, its what is done with the answer. The answer should be input to a system model that answers "Where is the best place to do my surveillance mission?" or "Am I going to get

shot because I'm not tuning my radar properly?" I need to pose these kind of questions and have the answers come out of the system model. The EM models have to feed the system models with enough fidelity that I get a good answer. A lot of models now give a very pessimistic answer and all can cause me to make mistakes because I plan on that pessimistic answer. I need something fairly close to the best possible prediction. Operationally, I need it to take into account what the environment has for temporal change and recommend that, although the measurements may be exact, here's how good the answer is based on what the environment will do over minutes or hours; I need it to represent when it breaks down. I need a system model to answer the questions on what my system can do.

G. Konstanzer: In terms of fleet training and sensitivity, SEAWASP represents probability of firm track versus range.

T. Rogers: A lot of the questions that are asked require stochastic processes to answer. It is interesting that there is a real demand for these answers and they are being based on deterministic propagation models. There is a whole area here that is underexplored.

R. Paulus: One of the things from the French presentation (Mandine) is they are looking at a mean profile, making a scale separation between the mean profile and the fluctuating part, and determining the effects with the propagation model.

S. Burk: In addition to taking mean profiles and adding turbulence, Roger Helvey's presentation of up-down radiosonde data showed ~100 m differences in depth of the boundary layer between when the radiosonde went up and when it came down. That kind of variability on short spatial scales would be interesting to input into PE codes as well and explore the sensitivity of PE codes to a boundary layer that is oscillating the way you see boundary layers oscillate in SODAR returns.

K. Craig: Some years ago, we had an AGARD paper which did look the problem of random features (not oscillatory). Putting in typical values of randomness, the errors were not that great over most of the coverage; the errors were greatest where expected — in the nulls. More simulations of that sort ought to be done.

S. Burk: Molly Barrios, in her presentation, showed small ripples in the vertical on the M-profile lead to large differences. There is a whole range of things that can happen that is confusing to someone outside the PE modeling community as to what level of accuracy the meteorological model is expected to provide to be satisfactory to a PE code.

H. Hitney: It is not really a question of satisfactory to PE codes but rather to the end user for the application he has in mind. That may be quite different in strike warfare in going against a radar whose parameters are not well known when all you want is the gross features (in a duct or out of the duct) or if comparing measurements made in an experimental campaign where you are looking at a few dB difference.

S. Burk: If forecasting the existence of an elevated duct is what is considered successful, NWP models did very well in VOCAR. It was at the level of comparing against propagation loss that was not as successful.

H. Hitney: Following earlier comments, the weak spots are not in the propagation models but in characterizing the environment and making the application to the system in question. We have gone beyond the point of keeping the propagation model in balance with the expected inputs on the meteorology and the expected use of it in the application.

P. Econ: Not a lot has been said about land clutter during the workshop, we've heard a lot about propagation models and demonstrated field uses of propagation models. There seems to be a lot to be done in determining and predicting land clutter to optimize radar systems in real time. This seems like a direction we need to move.

M. Levy: That strikes me as a new demand. For years, people asked us to predict path loss, just forward propagation so they could use that; and for years it was not possible to do that quickly. And now that it's possible, we've just gone on to the next thing! People should reflect and be thankful for what they can do with forward scatter!

J. Kuttler: We always have to have something to aspire to!

Issue 3. Are Benchmarks Needed?

R. Paulus: Gary Brooke raised the pro side of benchmark models in his presentation. We would like to investigate this further. As has been previously expressed by several people and as was obvious from the model comparisons, most of the model plots lie over each other. If that's the case, what is the use of the benchmark? There is coordination within the community through the scientific exchanges (AGARD, URSI, IEEE). People have published their results in these articles. Those results are taken by others and compared to their models. What can be gained by a formal panel to determine benchmarks?

E. Holmes: The earlier statements that we are happy with our models, with doing refraction, with doing one-way proploss is about to change in that we need to do clutter. This is a place where an awful lot of the talks this week talked about problems with polarization, not being able to do anything too near the surface, to terrain. It's a perfect opportunity to get some benchmarks ready for those kinds of cases in which I guarantee your models aren't going to over lay each other and they won't get the right answer.

R. Paulus: That's a presumption that's not supported.

E. Holmes: It's my feeling.

M. Pastore: Are we talking about the results that were shown during the model comparisons?

R. Paulus: We are talking about benchmarks. The distinction between sample cases and benchmarks is that the sample cases were intended to show how the models compare without saying which was right or more accurate. The idea of benchmarks, as I understand them, is that there is a right answer to a given problem and then models are judged against that right answer based on some criteria which is yet to be established.

M. Pastore: Can all model results be compared on one page so that differences can be seen?

H. Hitney: Can the model output data files be shared?

K. Craig: If data files are shared, the comments of the model developers must be included.

[*Editors note: Gary Brooke has made the data files and comments provided by the model developers available by anonymous ftp at farside@atinc.com in the /pub/EMEO directory. The data has been zipped with PKZIP and there are subdirectories for each contributor.*]

R. Paulus: The ultimate military user is not interested in the propagation models, he is interested in the final information display upon which he bases his tactical decision as Bob Dees has said. Since we are dealing with a system which has several components, among them a propagation model, if we benchmark the propagation model, then necessarily we need to benchmark the environmental models, the radar models, the target models. Is that a reasonable and realistic thing to do?

P. Econ: Why do you want to do this? What would be the purpose? I can see benchmarking the propagation model to select the best features of a propagation model. Why would you do radar models? What is it you're trying to accomplish?

R. Paulus: For a system, you would want to have the most accurate output for the specific application. For example, IREPS assumes horizontal homogeneity; sometimes that's good and sometimes it's not. If access to environmental data is a limiting factor, then no matter how good the propagation model is and the money you spend to improve it, there is no end payoff for the user. Radar models are probably not a large source of error; I suspect that, and agree with what others have expressed, environmental characterization is the limiting factor.

P. Econ: I agree with that also but radar models are not a trivial effort. I don't see where benchmarking a SPQ-9, SPS-49, or SPY-1 radar model is going to have any payoff.

CDR D. Markham: I think the point is that each of the components of the system contributes to the cumulative error that results in your ability to perform an accurate assessment. If any one component is put under the microscope to determine what its

contribution to the error budget is, then the others must be done also. Otherwise, you could make EM propagation models perfect and still have a bad answer on the end because one of the other components has a large contribution to the error budget.

H. Hitney: Is it likely there will be more than one radar model? We've been talking about benchmarking and comparing propagation models; is there more than one AEGIS detection model?

Several replies: Yes.

S. Burk: I would like to clarify what is meant by benchmarking. If none of the ten workshop sample cases are considered candidates for bench marking, then what is considered a candidate?

CDR D. Markham: Extending that, is it proper to benchmark using a model given that no one has the market on understanding all the physics involved in any process be it acoustics or electromagnetic propagation or should you use real data.

LCDR R. Dees: From the operational side, you have to take it out into the real world to see if it works. We do continual testing to see if equipment works, if systems models give the answer. Once we've seen it works in post analysis, we want to go to the future. I don't see a need for a benchmark at all for fleet models. The answer is when you take it out into the real world and compare to what you see.

G. Brooke: The point of a benchmark model is to tell you whether you didn't get all the input right or the physics right. In comparing to real data, what do you do if you don't get the right answer or the answer you expect?

LCDR R. Dees: It is very tough. Having done a lot of experiments, if something affected you that you didn't measure, then you may have wasted time. You have to oversample so you've got everything you think could affect the outcome.

S. Burk: I would be very skeptical that there is such a thing as a benchmark model separate from real data comparisons unless you have analytical solutions. Otherwise, it is just a matter of saying I put a lot of physics into this model, more physics than someone else. Therefore my model is the benchmark. That would be a never ending game.

D. Alessio: A benchmark doesn't necessarily have to be the best model. It should be freely available so that everyone can compare their models to it.

T. Rogers: Based on examining a lot of experimental data and comparing to models, I would expect to see the models to be unbiased in any particular regime in representing the propagation loss that is measured. If there is no bias, this means that you did the measurements right and the models and measurements agree well.

E. Holmes: There is a lot of confusion about what a benchmark model even is. We are not looking for a single model to answer every test case problem. Steve Fast showed a certain solution to terrain problems with no refraction. Lloyd's mirror is a benchmark model for a perfectly reflecting surface and no refraction. For any particular case that's tough, like the periscope detection or clutter problem, you want to do propagation to a surface, maybe to a rough surface. There may or may not be a benchmark model right now. But when you come upon that problem, the development of an operational model that can solve that problem will move along a lot more quickly if you can find a benchmark solution and design a test case that says whether or not your model can meet that.

M. Levy: The measurements presented by NRL showed very, very good results. I think it would be nice to do more of that sort of thing but it's very, very expensive. I think that's the reason it's not done. I think that's what the operational people want to give them confidence in the models. That's still needed.

LCDR R. Dees: From the AEGIS point of view, we have events during the year. As we build a new ship, we take it out and run it through its paces to make sure that the combat system is operating up to design specification. Which means we do a lot of the events that are going to explore a lot of different ranges and a lot of different environments. It provides, to a limited extent, a recurring opportunity to get some of the measurements. If the measurement requirements can be provided that define the experiment, it can happen. That's an event we still want to make open to people.

REPORT DOCUMENTATION PAGE

Form Approved
OMB No. 0704-0188

Public reporting burden for this collection of information is estimated to average 1 hour per response, including the time for reviewing instructions, searching existing data sources, gathering and maintaining the data needed, and completing and reviewing the collection of information. Send comments regarding this burden estimate or any other aspect of this collection of information, including suggestions for reducing this burden, to Washington Headquarters Services, Directorate for Information Operations and Reports, 1215 Jefferson Davis Highway, Suite 1204, Arlington, VA 22202-4302, and to the Office of Management and Budget, Paperwork Reduction Project (0704-0188), Washington, DC 20503.

1. AGENCY USE ONLY *(Leave blank)*	2. REPORT DATE	3. REPORT TYPE AND DATES COVERED
	December 1995	Final

4. TITLE AND SUBTITLE

PROCEEDINGS OF THE ELECTROMAGNETIC PROPAGATION WORKSHOP

5. FUNDING NUMBERS

6. AUTHOR(S)

R. Paulus

7. PERFORMING ORGANIZATION NAME(S) AND ADDRESS(ES)

Naval Command, Control and Ocean Surveillance Center (NCCOSC)
RDT&E Division
San Diego, California 92152–5000

8. PERFORMING ORGANIZATION REPORT NUMBER

TD 2891

9. SPONSORING/MONITORING AGENCY NAME(S) AND ADDRESS(ES)

SPAWAR (PMW–175),
NAVSEA (PED USW ASTD–E),
and the Office of the Director, Defense Research & Engineering (ODDRE)

10. SPONSORING/MONITORING AGENCY REPORT NUMBER

11. SUPPLEMENTARY NOTES

12a. DISTRIBUTION/AVAILABILITY STATEMENT

Approved for public release; distribution is unlimited.

12b. DISTRIBUTION CODE

13. ABSTRACT *(Maximum 200 words)*

14. SUBJECT TERMS

15. NUMBER OF PAGES

520

16. PRICE CODE

17. SECURITY CLASSIFICATION OF REPORT	18. SECURITY CLASSIFICATION OF THIS PAGE	19. SECURITY CLASSIFICATION OF ABSTRACT	20. LIMITATION OF ABSTRACT
UNCLASSIFIED	UNCLASSIFIED	UNCLASSIFIED	SAME AS REPORT

21a. NAME OF RESPONSIBLE INDIVIDUAL	21b. TELEPHONE *(include Area Code)*	21c. OFFICE SYMBOL
R. Paulus	(619) 553-1424	Code 883

INITIAL DISTRIBUTION

Code 0012	Patent Counsel	(1)
Code 0271	Archive/Stock	(6)
Code 0274	Library	(2)
Code 712	F. Ryan	(1)
Code 88	J. H. Richter	(1)
Code 883	R. Paulus	(25)
Code 883	K. Anderson	(1)
Code 883	A. Barrios	(1)
Code 883	C. Hattan	(1)
Code 883	H. Hitney	(1)
Code 883	W. Patterson	(1)
Code 883	T. Rogers	(1)

Defense Technical Information Center
Fort Belvoir,.VA 22060–6218 (4)

NCCOSC Washington Liaison Office
Washington, DC 20363–5100

Center for Naval Analyses
Alexandria, VA 22302–0268

Navy Acquisition, Research and Development
Information Center (NARDIC)
Arlington, VA 22244–5114

GIDEP Operations Center
Corona, CA 91718–8000

Naval Research Laboratory
Washington, DC 20375–5336 (12)

Naval Research Laboratory
Monterey, CA 93943–5502 (5)

Naval Research Laboratory
Stennis Space Center, MS 39529–5004

Chief of Naval Operations
Washington, DC 20392–5421

Space & Naval Warfare Systems Command
Arlington, VA 22245–5200 (2)

Naval Sea Systems Command
Arlington, VA 22242–5169 (2)

Naval Air Warfare Center
China Lake, CA 93555–6001

Naval Air Warfare Center
Point Mugu, CA 93042–5001 (2)

Naval Air Systems Command
Arlington, VA 22243–5120

Naval Surface Warfare Center
Dahlgren, VA 22448–5100 (4)

Naval Surface Warfare Center
Silver Spring, MD 20903–5000

Naval Undersea Warfare Center
Newport, RI 02841–1708

Naval Undersea Warfare Center
New London, CT 06320

Naval Oceanographic Office
Stennis Space Center, MS 39522–5001

DoD Joint Spectrum Center
Annapolis, MD 21402–5064 (2)

Naval Information Warfare Activity
Washington, DC 20393

Office of Naval Research
Arlington, VA 22217–5660

NAVLANTMETOCCEN
Norfolk, VA 23511–2394

CNMOC
Stennis Space Center, MS 39529–5005

Pennsylvania State University
University Park, PA 16801

Pennsylvania State University
Applied Research Laboratory
State College, PA 16804 (9)

University of Texas at Austin
Applied Research Laboratories
Austin, TX 78713–8029 (3)

Johns Hopkins University
Applied Physics Laboratory
Laurel, MD 20723–6099 (22)

IIT Research Institute
Annapolis, MD 21401 (5)

Army Research Laboratory
Aberdeen Proving Ground, MD 21005–5068 (2)

USARL/SLAD/EWD
White Sands Missile Range, NM 88002–5513

HQ U.S. Special Operations Command
MacDill AFB, FL 33621–5323

Air Force Information Warfare Center
San Antonio, TX 78243–7020

HQ, Air Weather Service
Scott AFB, IL 62225–5206

Computer Sciences Corporation
Arlington, VA 22202–4016

Integrated Performance Decisions (IPD)
Monterey, CA 93940

Lockheed Martin–Government Electronic Systems
Moorestown, NJ 08057–3075

MIT Lincoln Laboratory
Lexington, MA 01273–9108 (3)

Planning Systems Incorporated (PSI)
Slidell, LA 70458

Science & Engineering Services, Inc.
Burtonsville, MD 20866 (2)

SWL, Inc.
Albuquerque, NM 87111–3984

Technology Service Corporation
Silver Spring, MD 20910